National Water-Quality Assessment Program

Hydrogeologic Settings and Ground-Water Flow Simulations for Regional Studies of the Transport of Anthropogenic and Natural Contaminants to Public-Supply Wells—Studies Begun in 2001

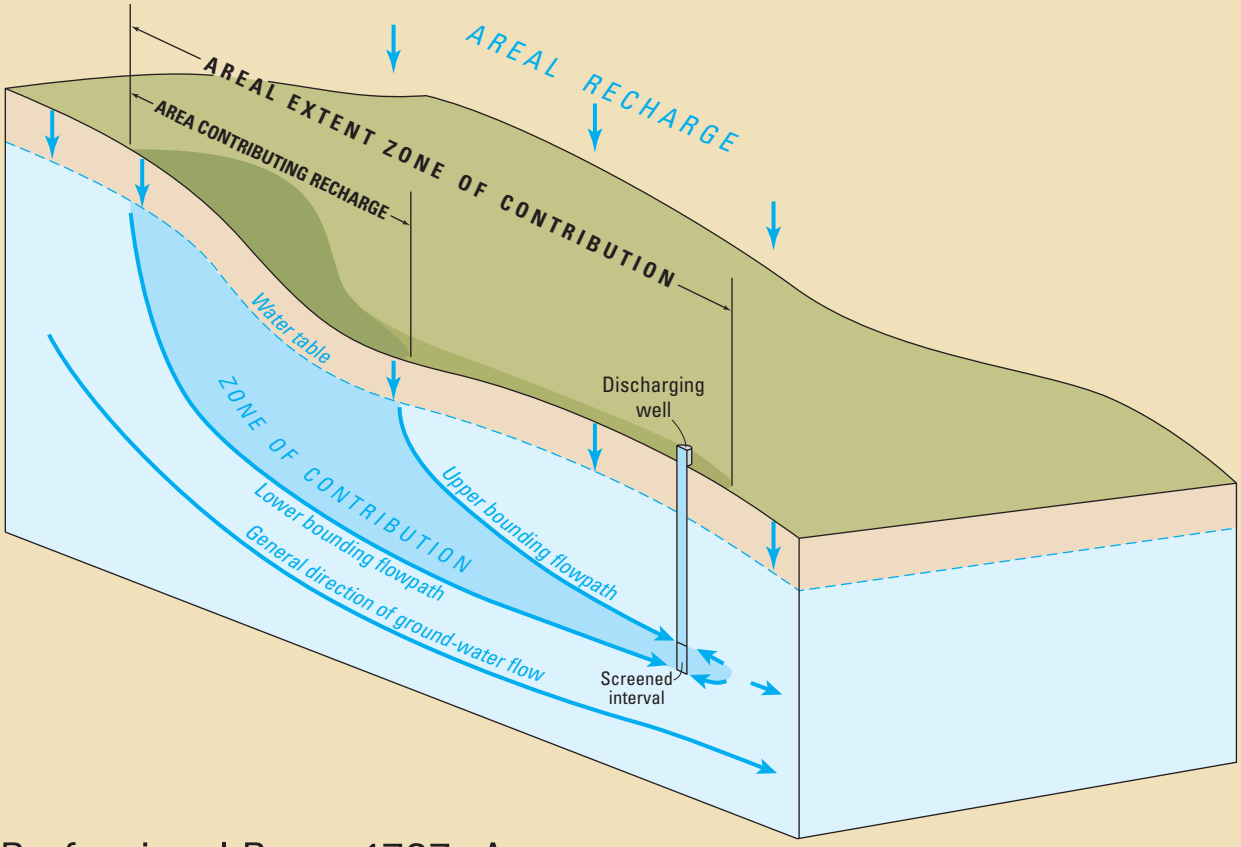

Professional Paper 1737–A

U.S. Department of the Interior
U.S. Geological Survey

Hydrogeologic Settings and Ground-Water Flow Simulations for Regional Studies of the Transport of Anthropogenic and Natural Contaminants to Public-Supply Wells—Studies Begun in 2001

Edited by Suzanne S. Paschke

National Water-Quality Assessment Program

Professional Paper 1737–A

U.S. Department of the Interior
U.S. Geological Survey

U.S. Department of the Interior
DIRK KEMPTHORNE, SECRETARY

U.S. Geological Survey
Mark D. Myers, Director

U.S. Geological Survey, Reston, Virginia: 2007

For product and ordering information:
World Wide Web: http://www.usgs.gov/pubprod
Telephone: 1-888-ASK-USGS

For more information on the USGS--the Federal source for science about the Earth, its natural and living resources, natural hazards, and the environment:
World Wide Web: http://www.usgs.gov
Telephone: 1-888-ASK-USGS

Any use of trade, product, or firm names is for descriptive purposes only and does not imply endorsement by the U.S. Government.

Although this report is in the public domain, permission must be secured from the individual copyright owners to reproduce any copyrighted materials contained within this report.

Suggested citation:
Paschke, Suzanne S., ed., 2007, Hydrogeologic settings and ground-water flow simulations for regional studies of the transport of anthropogenic and natural contaminants to public-supply wells—studies begun in 2001: U.S. Geological Survey, Professional Paper 1737–A, 244 p.

Foreword

The U.S. Geological Survey (USGS) is committed to providing the Nation with accurate and timely scientific information that helps enhance and protect the overall quality of life and that facilitates effective management of water, biological, energy, and mineral resources *(http://www.usgs.gov/)*. Information on the quality of the Nation's water resources is critical to assuring the long-term availability of water that is safe for drinking and recreation and suitable for industry, irrigation, and habitat for fish and wildlife. Population growth and increasing demands for multiple water uses make water availability, now measured in terms of quantity and quality, even more essential to the long-term sustainability of our communities and ecosystems.

The USGS implemented the National Water-Quality Assessment (NAWQA) Program in 1991 to support national, regional, and local information needs and decisions related to water-quality management and policy *(http://water.usgs.gov/nawqa)*. Shaped by and coordinated with ongoing efforts of other Federal, State, and local agencies, the NAWQA Program is designed to answer: What is the condition of our Nation's streams and ground water? How are the conditions changing over time? How do natural features and human activities affect the quality of streams and ground water, and where are those effects most pronounced? By combining information on water chemistry, physical characteristics, stream habitat, and aquatic life, the NAWQA Program aims to provide science-based insights for current and emerging water issues and priorities.

From 1991–2001, the NAWQA Program completed interdisciplinary assessments in 51 of the Nation's major river basins and aquifer systems, referred to as Study Units (*http://water.usgs.gov/nawqa/studyu.html*). Baseline conditions were established for comparison to future assessments, and long-term monitoring was initiated in many of the basins. During the next decade, 42 of the 51 Study Units will be reassessed so that 10 years of comparable monitoring data will be available to determine trends at many of the Nation's streams and aquifers. The next 10 years of study also will fill in critical gaps in characterizing water-quality conditions, enhance understanding of factors that affect water quality, and establish links between *sources* of contaminants, the *transport* of those contaminants through the hydrologic system, and the potential *effects* of contaminants on humans and aquatic ecosystems.

The USGS aims to disseminate credible, timely, and relevant science information to inform practical and effective water-resource management and strategies that protect and restore water quality. We hope this NAWQA publication will provide you with insights and information to meet your needs, and will foster increased citizen awareness and involvement in the protection and restoration of our Nation's waters.

The USGS recognizes that a national assessment by a single program cannot address all water-resource issues of interest. External coordination at all levels is critical for a fully integrated understanding of watersheds and for cost-effective management, regulation, and conservation of our Nation's water resources. The NAWQA Program, therefore, depends on advice and information from other agencies—Federal, State, interstate, Tribal, and local—as well as nongovernmental organizations, industry, academia, and other stakeholder groups. Your assistance and suggestions are greatly appreciated.

Robert M. Hirsch
Associate Director for Water

Contents

Section 1.
Overview of Regional Studies of the Transport of Anthropogenic and Natural Contaminants to Public-Supply Wells, by S.S. Paschke, L.J. Kauffman, S.M. Eberts, and S.R. Hinkle

Section 2.
Hydrogeologic Setting and Ground-Water Flow Simulations of the Salt Lake Valley Regional Study Area, Utah, by B.J. Stolp

Section 3.
Hydrogeologic Settings and Ground-Water Flow Simulations of the Eagle Valley and Spanish Springs Valley Regional Study Areas, Nevada, by D.H. Schaefer, J.M. Green, and M.R. Rosen

Section 4.
Hydrogeologic Settings and Ground-Water Flow Simulations of the San Joaquin Valley Regional Study Area, California, by S.P. Phillips, K.R. Burow, D.L. Rewis, J.J. Shelton, and Bryant Jurgens

Section 5.
Hydrogeologic Setting and Ground-Water Flow Simulations of the Northern Tampa Bay Regional Study Area, Florida, by C.A. Crandall

Section 6.
Hydrogeologic Setting and Ground-Water Flow Simulations of the Pomperaug River Basin Regional Study Area, Connecticut, by F.P. Lyford, Carl S. Carlson, Craig J. Brown, and J. Jeffrey Starn

Section 7.
Hydrogeologic Setting and Ground-Water Flow Simulations of the Great Miami River Basin Regional Study Area, Ohio, by R.A. Sheets

Section 8.
Hydrogeologic Setting and Ground-Water Flow Simulations of the Eastern High Plains Regional Study Area, Nebraska, by M.K. Landon and M.J. Turco

Appendix 1.
Database Dictionary for the Study of Anthropogenic and Natural Contaminants

Conversion Factors, Datum, Abbreviations, and Definitions

Multiply	By	To obtain
	Length	
centimeter (cm)	0.3937	inch (in.)
millimeter (mm)	0.03937	inch (in.)
meter (m)	3.281	foot (ft)
kilometer (km)	0.6214	mile (mi)
kilometer (km)	0.5400	mile, nautical (nmi)
meter (m)	1.094	yard (yd)
	Area	
square meter (m^2)	0.0002471	acre
hectare (ha)	2.471	acre
square hectometer (hm^2)	2.471	acre
square kilometer (km^2)	247.1	acre
square centimeter (cm^2)	0.001076	square foot (ft^2)
square meter (m^2)	10.76	square foot (ft^2)
square centimeter (cm^2)	0.1550	square inch (ft^2)
square hectometer (hm^2)	0.003861	section (640 acres or 1 square mile)
hectare (ha)	0.003861	square mile (mi^2)
square kilometer (km^2)	0.3861	square mile (mi^2)
	Volume	
liter (L)	0.2642	gallon (gal)
cubic meter (m^3)	264.2	gallon (gal)
cubic meter (m^3)	0.0002642	million gallons (Mgal)
cubic centimeter (cm^3)	0.06102	cubic inch (in^3)
cubic meter (m^3)	1.308	cubic yard (yd^3)
cubic kilometer (km^3)	0.2399	cubic mile (mi^3)
cubic meter (m^3)	0.0008107	acre-foot (acre-ft)
cubic hectometer (hm^3)	810.7	acre-foot (acre-ft)
	Flow rate	
cubic meter per second (m^3/s)	70.07	acre-foot per day (acre-ft/d)
cubic meter per year (m^3/yr)	0.000811	acre-foot per year (acre-ft/yr)
cubic hectometer per year (hm^3/yr)	811.03	acre-foot per year (acre-ft/yr)
meter per second (m/s)	3.281	foot per second (ft/s)
meter per minute (m/min)	3.281	foot per minute (ft/min)
meter per hour (m/hr)	3.281	foot per hour (ft/hr)
meter per day (m/d)	3.281	foot per day (ft/d)
meter per year (m/yr)	3.281	foot per year ft/yr)
cubic meter per second (m^3/s)	35.31	cubic foot per second (ft^3/s)
cubic meter per second per square kilometer [$(m^3/s)/km^2$]	91.49	cubic foot per second per square mile [$(ft^3/s)/mi^2$]
cubic meter per day (m^3/d)	35.31	cubic foot per day (ft^3/d)
liter per second (L/s)	15.85	gallon per minute (gal/min)
cubic meter per day (m^3/d)	264.2	gallon per day (gal/d)
cubic meter per day per square kilometer [$(m^3/d)/km^2$]	684.28	gallon per day per square mile [$(gal/d)/mi^2$]
cubic meter per second (m^3/s)	22.83	million gallons per day (Mgal/d)
cubic meter per day per square kilometer [$(m^3/d)/km^2$]	0.0006844	million gallons per day per square mile [$(Mgal/d)/mi^2$]
cubic meter per hour (m^3/h)	39.37	inch per hour (in/h)
millimeter per year (mm/yr)	0.03937	inch per year (in/yr)
kilometer per hour (km/h)	0.6214	mile per hour (mi/h)

Multiply	By	To obtain
	Mass	
gram (g)	0.03527	ounce, avoirdupois (oz)
kilogram (kg)	2.205	pound avoirdupois (lb)
	Hydraulic conductivity	
meter per day (m/d)	3.281	foot per day (ft/d)
	Hydraulic gradient	
meter per kilometer (m/km)	5.27983	foot per mile (ft/mi)
	Transmissivity	
meter squared per day (m^2/d)	10.76	foot squared per day (ft^2/d)

Overview of Regional Studies of the Transport of Anthropogenic and Natural Contaminants to Public-Supply Wells

By Suzanne S. Paschke, Leon J. Kauffman, Sandra M. Eberts, and Stephen R. Hinkle

Section 1 of

Hydrogeologic Settings and Ground-Water Flow Simulations for Regional Studies of the Transport of Anthropogenic and Natural Contaminants to Public-Supply Wells—Studies Begun in 2001

Edited by Suzanne S. Paschke

Professional Paper 1737–A

U.S. Department of the Interior
U.S. Geological Survey

U.S. Department of the Interior
DIRK KEMPTHORNE, SECRETARY

U.S. Geological Survey
Mark D. Myers, Director

U.S. Geological Survey, Reston, Virginia: 2007

For product and ordering information:
World Wide Web: http://www.usgs.gov/pubprod
Telephone: 1-888-ASK-USGS

For more information on the USGS--the Federal source for science about the Earth, its natural and living resources, natural hazards, and the environment:
World Wide Web: http://www.usgs.gov
Telephone: 1-888-ASK-USGS

Any use of trade, product, or firm names is for descriptive purposes only and does not imply endorsement by the U.S. Government.

Although this report is in the public domain, permission must be secured from the individual copyright owners to reproduce any copyrighted materials contained within this report.

Suggested citation:
Paschke, S.S., Kauffman, L.J., Eberts, S.M., and Hinkle, S.R., 2007, Overview of regional studies of the transport of anthropogenic and natural contaminants to public-supply wells, *section 1 of* Paschke, S.S., ed., Hydrogeologic settings and ground-water flow simulations for regional studies of the transport of anthropogenic and natural contaminants to public-supply wells—studies begun in 2001: Reston, Va., U.S. Geological Survey Professional Paper 1737–A, pp. 1–1 –1–18.

Contents

Abstract 1–1
Introduction 1–1
Purpose and Scope 1–2
Study Area Locations 1–2
Basin and Range Basin-Fill Aquifers 1–5
Central Valley Aquifer System 1–5
Floridan Aquifer System 1–7
Glacial Aquifer System 1–8
High Plains Aquifer 1–9
Methods 1–9
Retrospective Data Compilation 1–10
Source Water-Quality Assessment Sample Collection 1–10
Ground-Water Flow Simulation 1–10
Oxidation-Reduction and pH Classification and Mapping 1–12
Database Development 1–14
References Cited 1–14

Figures

Maps showing:
1.1. The 19 principal aquifers selected as the primary focus of ground-water studies during Cycle II of the National Water-Quality Assessment program. 1–4
1.2. Locations of principal aquifers, National Water-Quality Assessment program study-unit boundaries, and 2001-start regional study areas for the transport of anthropogenic and natural contaminants. 1–6
1.3. Schematic diagram of area contributing recharge and zone of contribution for a single discharging well in a simplified hypothetical ground-water system. 1–11

Tables

1.1. The 19 principal aquifers selected as the primary focus of ground-water studies during Cycle II of the National Water-Quality Assessment Program 1–3
1.2. Effects of weak sinks on the determination of contributing areas 1–12
1.3. Oxidation-reduction classification scheme 1–13

Overview of Regional Studies of the Transport of Anthropogenic and Natural Contaminants to Public-Supply Wells

By Suzanne S. Paschke, Leon J. Kauffman, Sandra M. Eberts, and Stephen R. Hinkle

Abstract

This study of the Transport of Anthropogenic and Natural Contaminants to public-supply wells (TANC study) is being conducted as part of the U.S. Geological Survey National Water Quality Assessment (NAWQA) Program and was designed to increase understanding of the most important factors to consider in ground-water vulnerability assessments. The seven TANC studies that began in 2001 used retrospective data and ground-water flow models to evaluate hydrogeologic variables that affect aquifer susceptibility and vulnerability at a regional scale. Ground-water flow characteristics, regional water budgets, pumping-well information, and water-quality data were compiled from existing data and used to develop conceptual models of ground-water conditions for each study area. Steady-state regional ground-water flow models were used to represent the conceptual models, and advective particle-tracking simulations were used to compute areas contributing recharge and traveltimes from recharge to selected public-supply wells. Retrospective data and modeling results were tabulated into a relational database for future analysis. Seven study areas were selected to evaluate a range of hydrogeologic settings and management practices across the Nation: the Salt Lake Valley, Utah; the Eagle Valley and Spanish Springs Valley, Nevada; the San Joaquin Valley, California; the Northern Tampa Bay region, Florida; the Pomperaug River Basin, Connecticut; the Great Miami River Basin, Ohio; and the Eastern High Plains, Nebraska. This Professional Paper Chapter presents the hydrogeologic settings and documents the ground-water flow models for each of the NAWQA TANC regional study areas that began work in 2001. Methods used to compile retrospective data, determine contributing areas of public-supply wells, and characterize oxidation-reduction (redox) conditions also are presented. This Professional Paper Chapter provides the foundation for future susceptibility and vulnerability analyses in the TANC study areas and comparisons among regional aquifer systems. The report is organized in sections. In addition to the introductory section (Section 1) are seven sections that present the hydrogeologic characterization and ground-water flow model documentation for each TANC regional study area (Sections 2 through 8). Abstracts in Sections 2 through 8 provide summaries and major findings for each regional study area.

Introduction

About one-third of the population of the United States obtains drinking water from public-supply systems that rely on ground water generating interest in the quality of ground water pumped by public-supply wells (Franke and others, 1998). The occurrence and concentration of anthropogenic and natural contaminants in public-supply wells is controlled by many factors intrinsic and extrinsic to a ground-water system. Aquifer and public-supply well susceptibility to contamination is determined by the intrinsic conditions of an aquifer such as depth to water, flow-system confinement, recharge rate, hydraulic conductivity, and porosity (Focazio and others, 2002). Factors extrinsic to the aquifer include land use and the presence and location of potential contaminant sources overlying or within the area contributing recharge to a public-supply well. Aquifer vulnerability is determined by considering both the intrinsic and extrinsic factors affecting water quality (Focazio and others, 2002). This study of the Transport of Anthropogenic and Natural Contaminants to supply wells (TANC) also considers public-supply well pumping rates and aquifer geochemical conditions when determining aquifer vulnerability.

The TANC study is part of the U.S. Geological Survey National Water-Quality Assessment (NAWQA) Program. The long-term goals of the NAWQA Program are to describe the status and trends in the quality of a large representative part of the Nation's surface- and ground-water resources and to provide a sound, scientific understanding of the major natural and human factors affecting the quality of those resources (Gilliom and others, 1995). The first cycle (Cycle I) of the NAWQA Program was implemented from 1991 to 2000, and a second investigative cycle (Cycle II) began in 2001. During Cycle II (2001 to 2011), 42 NAWQA study units will be

revisited in three groups of 14 on a rotational schedule. Each group is intensively studied for 4 years, followed by 6 years of low-intensity assessment. The primary emphasis of Cycle II is to assess long-term trends in water quality and to improve understanding of the factors and processes governing water quality. The TANC study is one of several Cycle II NAWQA studies designed to aid understanding of our Nation's water quality.

Purpose and Scope

The TANC study was designed to increase understanding of anthropogenic and natural contaminants detected in public-supply wells in support of ground-water susceptibility and vulnerability assessments by examining answers to the question: "What are the primary anthropogenic and natural contaminant sources, aquifer processes, and well characteristics that control the transport and transformation of contaminants along flow paths to public-supply wells in representative water-supply aquifers?"

Seven TANC studies began in 2001 using retrospective data and ground-water flow models to evaluate hydrogeologic variables that affect aquifer susceptibility and vulnerability at a regional scale. Ground-water flow characteristics, regional water budgets, pumping-well information, and water-quality data were compiled from existing data and used to develop conceptual models of ground-water conditions for each study area. Steady-state regional ground-water flow models were used to represent the conceptual models, and advective particle-tracking simulations were used to compute areas contributing recharge and traveltimes from recharge to selected public-supply wells. Retrospective data, ground-water traveltimes from recharge to discharge areas, oxidation-reduction (redox) conditions along flow paths, and the presence of potential contaminant sources in areas contributing recharge to public-supply wells were tabulated into a relational database for future use in analyzing aquifer vulnerability. The 5-year period from 1997 to 2001 was selected for data compilation and modeling exercises in order to facilitate comparisons among study areas and to use large recently collected water-quality data sets.

The purpose of this report is to present the hydrogeologic settings, including regional redox and pH conditions, of the seven NAWQA TANC regional study areas that began work in 2001. The report also documents the ground-water flow models for each regional study area. This report provides the foundation for further susceptibility and vulnerability analyses in the TANC study areas, comparisons among regional aquifer systems, and future local-scale field and modeling investigations. The report is organized into sections. In addition to this introductory section (Section 1), there are seven sections that present the hydrogeologic characterization and ground-water flow model documentation for each TANC regional study area (Sections 2 through 8). Abstracts in Sections 2 through 8 provide summaries and major findings for each regional study area.

Study Area Locations

The U.S. Geological Survey has identified 62 principal aquifers in the United States (Miller, 1999). A principal aquifer is defined as a regionally extensive aquifer or aquifer system that has potential to be used as a source of potable water (U.S. Geological Survey, 2003; Maupin and Barber, 2005). An aquifer is a geologic formation, a group of formations, or a part of a formation that contains sufficient saturated permeable material to yield significant amounts of water to wells and springs. Aquifers are often combined into aquifer systems. The NAWQA Program has designated 19 of the Nation's 62 principal aquifers as the primary focus of Cycle II studies by considering the factors of aquifer areal extent, water use for drinking-water supply, lithology, and widespread geographic coverage of the United States (table 1.1). The 19 principal aquifers account for about 75 percent of the water used for domestic plus public drinking-water supply in the United States in 1990 (Lapham and others, 2005) and provide a good spatial coverage of aquifer systems across the country (fig 1.1).

Aquifers in different parts of the Nation differ in their susceptibility and vulnerability to contamination because of varying hydrogeologic settings and ground-water management practices. Of the NAWQA Cycle II study units that began investigations in 2001, 7 regional study areas located in 5 of the 19 principal aquifers were selected for TANC studies to evaluate a range of hydrogeologic conditions and management practices (fig. 1.2). Additional areas will be selected for TANC studies as NAWQA Cycle II proceeds through its rotational schedule. The NAWQA TANC 2001-start regional study areas and their associated principal aquifers are:

- Salt Lake Valley, Utah, in the Basin and Range basin-fill aquifers,
- Eagle Valley and Spanish Springs Valley, Nevada, in the Basin and Range basin-fill aquifers,
- San Joaquin Valley, California, in the Central Valley aquifer system,
- Northern Tampa Bay, Florida, in the Floridan aquifer system,
- Pomperaug River Basin, Connecticut, in the glacial aquifer system,
- Great Miami River Basin, Ohio, in the glacial aquifer system, and
- Eastern High Plains, Nebraska, in the High Plains aquifer.

A hydrogeologic description of each TANC 2001-start regional study area and its associated principal aquifer follows with additional details of each study provided in subsequent sections of this report.

Table 1.1. The 19 principal aquifers selected as the primary focus of ground-water studies during Cycle II of the National Water-Quality Assessment Program.

[km^2, square kilometers; Mm^3/d, millions of cubic meters per day; NAWQA, National Water-Quality Assessment Program]

Principal aquifer or aquifers	Primary lithologies of the principal aquifer	Approximate area of principal aquifer (km^2)	Number of NAWQA Cycle II study units overlying principal aquifer	Principal aquifer rank by 2000 drinking-water use[1]	Estimated withdrawals for public supply[3] (Mm^3/d)
Glacial aquifer system	Sand and gravel	2,470,655	18	1	7.38
Mississippi Embayment—Texas Coastal Uplands aquifer system	Semiconsolidated sandstone	511,191	7	8	2.74
Cambrian-Ordovician aquifer system	Sandstone	459,722	5	10	2.23
High Plains aquifer	Sand and gravel	457,594	4	14	1.47
Basin and Range basin-fill and carbonate aquifers	Sand and gravel, carbonates	423,513	4	4	4.09
Floridan aquifer system and overlying Surficial aquifer system[2]	Carbonate	292,088	5	3	5.89
Coastal Lowlands aquifer system	Semiconsolidated sandstone	255,975	4	5	3.82
Piedmont and Blue Ridge aquifers	Carbonate and crystalline	227,449	8	24	0.42
Edwards-Trinity aquifer system	Sandstone and carbonate	194,439	2	12	1.56
New England crystalline-rock aquifers	Crystalline	183,158	4	31	0.28
North Atlantic Coastal Plain aquifer system (NACPAS)[3]	Semiconsolidated sandstone	114,542	4	7	3.00
Columbia Plateau basin-fill and basaltic-rock aquifers	Sand and gravel, basalt	112,811	1	18	0.84
Central Valley aquifer system	Sand and gravel	52,633	2	6	3.18
California Coastal basins aquifers	Sand and gravel	26,367	1	2	6.0
Denver Basin aquifer system	Sandstone	17,595	1	49	0.10
Hawaiian volcanic-rock aquifers	Basalt	16,691	1	16	0.92
Biscayne aquifer	Carbonate	9,259	1	9	2.64
Snake River basin-fill and basaltic-rock aquifers	Sand and gravel, basalt	5,060	1	23	0.57

[1]Rank 1 is largest water use; use was estimated for 62 principal aquifers.

[2]Includes that part of the Coastal Plain surficial aquifer that overlies the Floridan.

[3]From Maupin and Barber, 2005

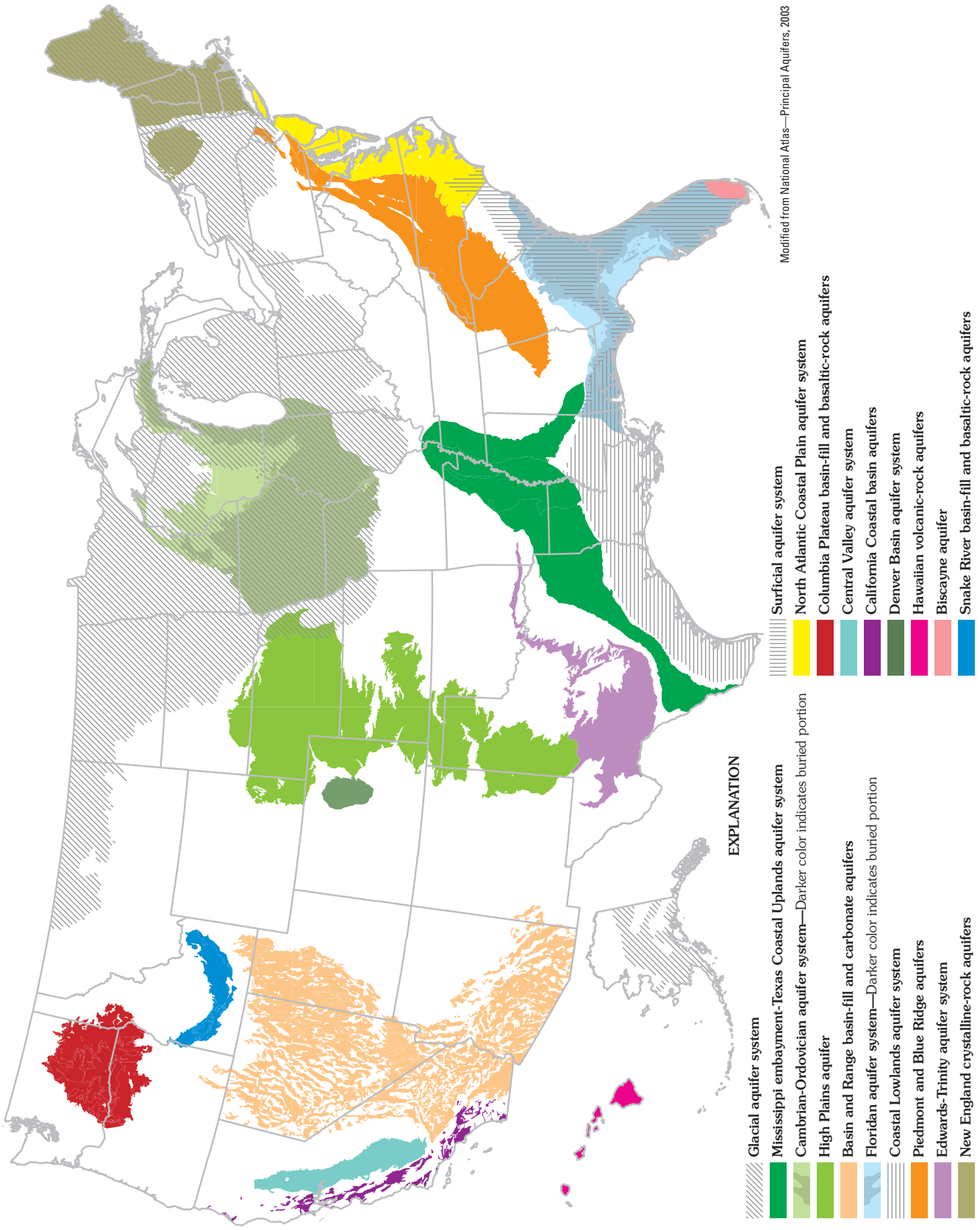

Figure 1.1. The 19 principal aquifers selected as the primary focus of ground-water studies during Cycle II of the National Water-Quality Assessment program.

Basin and Range Basin-Fill Aquifers

The Basin and Range basin-fill aquifers are a primary source of water in the arid West extending through about 423,513 square kilometers (km^2) of the Southwestern United States and underlying most of Nevada and parts of eastern California, southern Oregon and Idaho, western Utah, southern Arizona, and southwestern New Mexico (fig. 1.2). The Basin and Range basin-fill aquifers are thick deposits of alluvial materials in valleys bounded by bedrock mountain ranges. Basin fill primarily consists of unconsolidated to moderately consolidated, poorly- to well-sorted beds of gravel, sand, silt, and clay deposited on alluvial fans, pediments, flood plains, and playas. Basin-fill thickness is not well known in some basins but ranges from about 305 to 1,525 m in many basins and may exceed 3,050 m in a few deep basins in Utah and south-central Arizona (Robson and Banta, 1995).

Recharge to the Basin and Range basin-fill aquifers primarily is derived from stream runoff (mountain-front recharge) and subsurface flow (mountain-block recharge) from mountains surrounding the basins (Robson and Banta, 1995). The generally arid climate of the area causes almost all precipitation in the basins and most of the precipitation in the mountains to be lost to evapotranspiration; only about 5 percent of precipitation recharges the basin-fill aquifers (Robson and Banta, 1995). In extensively developed parts of the aquifers, agricultural and urban irrigation return flow percolates into the basin fill and ultimately recharges the aquifers. Discharge from the aquifers is by evapotranspiration, discharge to streams and springs, underflow, interbasin flow, and withdrawal by wells (Robson and Banta, 1995; Planert and Williams, 1995). Basin-fill aquifers generally are not connected to other basins although underflow and interbasin flow can be significant components of recharge or discharge in some basins where the surrounding bedrock is composed of cavernous carbonate rocks (Robson and Banta, 1995; Planert and Williams, 1995). Ground-water withdrawal from wells is the largest component of discharge from Basin and Range basin-fill aquifers and supplies water for agricultural irrigation and public water supply (Robson and Banta, 1995). Evapotranspiration is the largest natural component of ground-water discharge and can decrease when the water table is lowered by ground-water withdrawal (Robson and Banta, 1995). Although agricultural irrigation is still a principal ground-water use in the area, population increases since the 1960s have decreased the percentage of ground water used for irrigation and increased the percentage of ground water used for public water supply (Robson and Banta, 1995).

Ground water in the basin-fill aquifers generally is of suitable chemical quality for most uses; most ground water has a dissolved-solids concentration of less than 1,000 milligrams per liter (mg/L). However, the dissolved-solids concentration of water in parts of some basins can be as large as 300,000 mg/L (Robson and Banta, 1995). Water that has small dissolved-solids concentration generally is present near the margins of the basins, where recharge from the nearby mountains enters the aquifers; and water with larger dissolved-solids concentrations is present in topographically low parts of some basins, where ground water is discharged by evaporation and transpiration (Robson and Banta, 1995). In basins that have no discharge by underflow or streamflow, salts can accumulate over long periods of time in the fine-grained sediments near the center of the basin or can form extensive surface deposits of salt, such as the salt flats of the Great Salt Lake Desert in western Utah (Robson and Banta, 1995).

The Salt Lake Valley and Eagle Valley and Spanish Springs Valley regional study areas, which are within the Basin and Range basin-fill aquifers, are characterized by the occurrence of ground water in deep sediment-filled graben basins between mountain ranges. The Salt Lake Valley regional study area encompasses the Great Salt Lake Valley west of the Wasatch Range where ground water is used extensively for water supply in and around Salt Lake City, Utah. The basin-fill aquifer of the Salt Lake Valley study area is unconfined on the valley margins and transitions to confined conditions near the center of the valley where an overlying confining layer is present. Section 2 of this report presents the hydrogeologic setting, model setup, and modeling results for the Salt Lake Valley regional study area.

The Eagle Valley and Spanish Springs Valley regional study includes two alluvial basins—Eagle Valley near Carson City, Nevada, in the Carson River basin, and Spanish Springs Valley north of Sparks, Nevada, in the Truckee River basin. Rapid urban development in both the Eagle Valley and the Spanish Springs Valley regional study areas has resulted in reliance on ground water for water supply. Differing population stresses and rates of ground-water movement make the two study areas unique. The Eagle Valley is more urbanized and receives more recharge from precipitation than the Spanish Springs Valley. Section 3 of this report presents the hydrogeologic setting, model setup, and modeling results for the Eagle Valley and Spanish Springs regional study areas.

Central Valley Aquifer System

The Central Valley aquifer system of California (fig. 1.2) contains the largest basin-fill aquifer system in the Western United States. The Central Valley is one of the most important agricultural areas in the World, having more than 28,000 km^2 of agricultural land under irrigation in 1995 (Planert and Williams, 1995). During 1985, crop irrigation accounted for 96 percent of the surface water and 89 percent of the ground water withdrawn in the Central Valley (Planert and Williams, 1995).

The Central Valley is in a structural trough about 644 km long and from 32 to 113 km wide and extends over more than 52,633 km^2 (Planert and Williams, 1995). The trough is filled by marine and continental sediments up to 10 km thick (Gronberg and others, 1998), which form an important aquifer system. The Central Valley is bounded on the west by the Coast Ranges and on the east by the Cascade Range and the Sierra Nevada. The valley floor, which consists primarily of alluvial

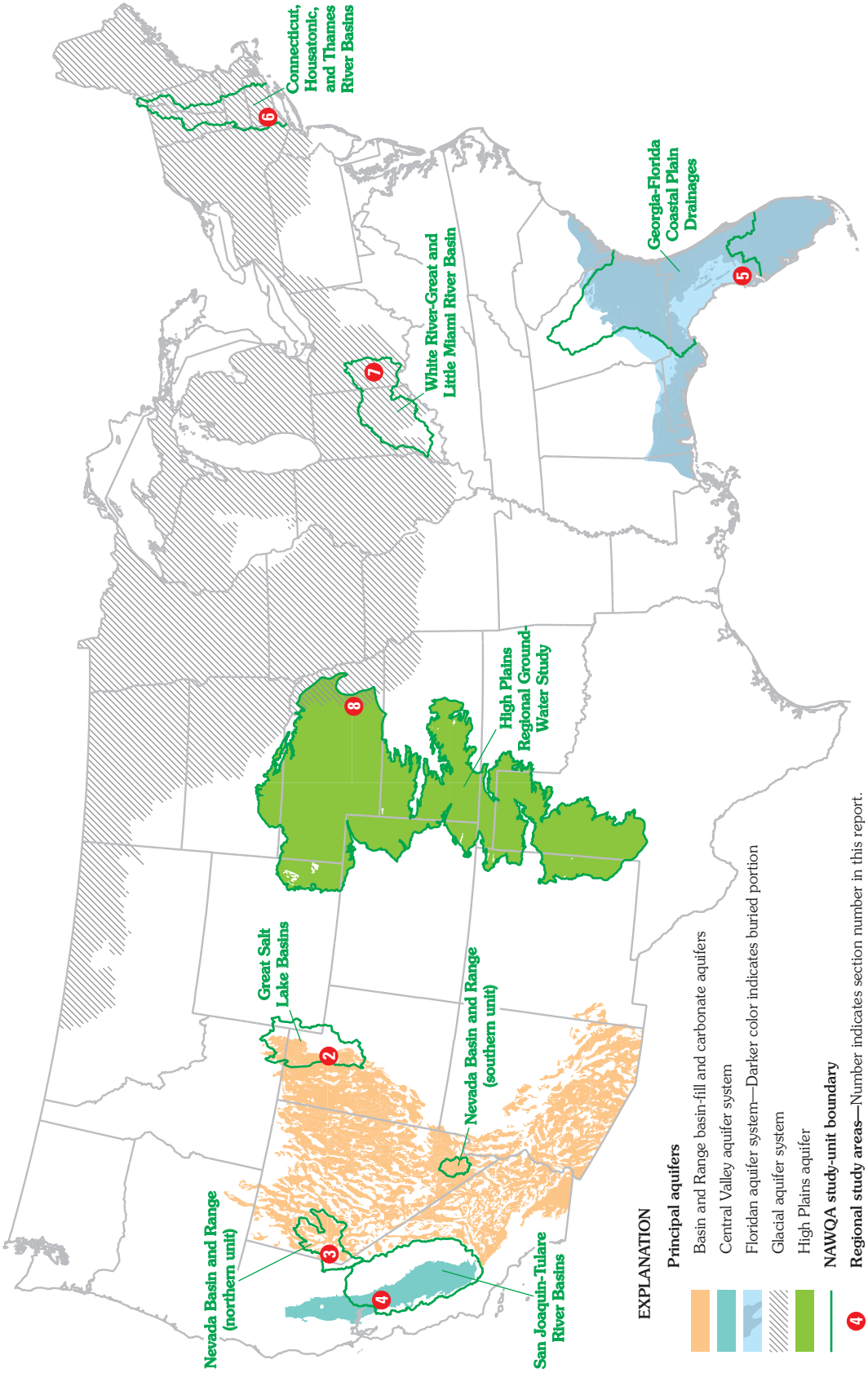

Figure 1.2. Locations of principal aquifers, National Water-Quality Assessment program study-unit boundaries, and 2001-start regional study areas for the transport of anthropogenic and natural contaminants.

and flood-plain deposits of the major rivers, is relatively flat to gently rolling and is generally below an altitude of 152 m. The Sacramento River drains the northern end of the Central Valley, and the San Joaquin River drains much of the middle one-third. The two rivers join in the Sacramento-San Joaquin Delta and empty into the upper end of San Francisco Bay. The southern end of the valley is occupied by the Tulare Basin, in which drainage is internal and the inflowing water is removed by evapotranspiration (Gronberg and others, 1998).

The climate of the Central Valley is Mediterranean and Steppe, characterized by hot summers and mild winters with about 85 percent of the precipitation falling from November to April (Planert and Williams, 1995). Annual precipitation decreases from north to south, with an average of about 58.4 cm in the northern part of the Sacramento Valley to about 15.2 cm in the southern part of the San Joaquin Valley (Planert and Williams, 1995). Runoff from the Coast Ranges is principally on the western slopes to the Pacific Ocean.

Under natural conditions, ground water in the Central Valley aquifer system flowed from areas of higher altitude at the valley margins toward rivers and marshes near the valley axis (Davis and others, 1959). The aquifer was recharged primarily by streams emanating from the Cascade Range and the Sierra Nevada (average of 30.5 cm/yr) (Planert and Williams, 1995). Ground water that was not evaporated or transpired by plants discharged either into the Sacramento and the San Joaquin Rivers or into the Tulare Basin, from which it was eventually removed by evaporation or transpiration. By the early 1960s, intensive ground-water development for agricultural irrigation had substantially lowered water levels and altered ground-water flow patterns in the Central Valley aquifer system (Planert and Williams, 1995). The most striking effect of development on water levels was in the San Joaquin Valley, where water-level declines in the confined part of the aquifer system were locally more than 122 m (Planert and Williams, 1995). Large withdrawals from deep wells in the San Joaquin Valley diverted ground-water flow toward the wells and away from the San Joaquin River and reversed vertical hydraulic gradients over much of the San Joaquin Valley to the point that water in the upper unconfined aquifer leaked downward into the lower confined aquifer (Planert and Williams, 1995). Well construction also affected vertical flow in the valley as many deep wells were perforated across confining units, allowing unrestricted vertical flow through the well bores. Ground-water withdrawals have decreased since the late 1960s as additional surface water was imported to the valley (Planert and Williams, 1995).

Water quality in the Central Valley aquifer system is affected by natural geologic and hydrologic factors as well as agricultural land use. The thickness of aquifers saturated with freshwater (water with less than 1,000 mg/L dissolved solids) varies greatly within the basin, but in general, freshwater is contained in continental fluvial deposits, and dissolved-solids concentrations increase with depth (Gronberg and others, 1998). Selenium, nitrate, and pesticide concentrations are elevated in ground water of some areas of the Central Valley as the result of agricultural irrigation. The pesticide dibromochloropropane (DBCP) is particularly problematic and is present in ground water in every county in the San Joaquin Valley (Planert and Williams, 1995).

The San Joaquin Valley regional study area is located in the northeastern San Joaquin Valley and centered around the city of Modesto, California, which relies heavily on ground water for public water supply. The study area is about 2,700 km^2 in area, bounded on the west by the San Joaquin River, on the north by the Stanislaus River, on the south by the Merced River, and on the east by the Sierra Nevada foothills. The San Joaquin Valley occupies the southern two-thirds of the Central Valley principal aquifer system. Unconfined ground water is present in the Pleistocene sediments of the San Joaquin Valley above a thick confining unit known as the Corcoran Clay member of the Tulare Formation. Confined ground water occurs primarily in Pleistocene and Tertiary sediments below the Corcoran Clay. Section 4 of this report presents the hydrogeologic setting, model setup, and modeling results for the San Joaquin Valley regional study area.

Floridan Aquifer System

The Floridan aquifer system, one of the most productive aquifers in the World, underlies an area of about 292,088 km^2 in southern Alabama, southeastern Georgia, southern South Carolina, and all of Florida (Miller, 1990). The Floridan aquifer system provides water for several large cities, including Savannah and Brunswick in Georgia and Jacksonville, Gainsville, Tallahassee, Orlando, Tampa, and St. Petersburg in Florida. An average of about 15,230,000 m^3/d of freshwater was withdrawn from the Floridan aquifer system for all purposes during the year 2000 (Marella and Berndt, 2005).

A thick sequence of carbonate rocks (limestone and dolomite) of Tertiary age constitutes the Floridan aquifer system (Miller, 1990). In most places, the system can be divided into the Upper and Lower Floridan aquifers, separated by a less permeable confining unit (Miller, 1986). Because it is a prolific aquifer with acceptable water quality, the Upper Floridan is the primary water supply for the area, and its geology and hydraulic properties have been extensively studied. The Upper Floridan is highly permeable in most places and includes the Suwannee and Ocala Limestones and the upper part of the Avon Park Formation (Miller, 1986). Where the Tampa Limestone is highly permeable, it also is included in the Upper Floridan; however, aquifer-system boundaries do not necessarily conform to formational boundaries (Miller, 1990). In most areas, the limestones are highly fractured and dissolved to form secondary porosity and karst features. Sinkholes, springs, and conduits are numerous in the Floridan aquifer in northern and central Florida. The Floridan aquifer system generally thickens seaward from a thin edge near its northern limit to about 914 m in thickness in southern Florida (Miller, 1986).

Prior to extensive ground-water development in the 1960s, ground water generally moved coastward from the outcrop area of the aquifer in Georgia and South Carolina

and outward in all directions from a potentiometric high in central Florida. Although recharge to the aquifer takes place throughout more than one-half of its area, recharge tends to be concentrated in outcrop areas and at potentiometric highs. Recharge rates range from less than 2.54 cm/yr to more than 51 cm/yr depending on local geologic and hydrologic conditions (Miller, 1990). Before development, nearly 90 percent of the discharge from the Floridan aquifer system was to springs and streams supplying base flow to the Suwannee, Flint, Sante Fe, Withlacoochee, Hillsborough, and other rivers, which are important water supply and recreational resources (Bush and Johnson, 1988). The Floridan aquifer also discharged to offshore springs both on the Gulf of Mexico and Atlantic Ocean sides of the northern part of peninsular Florida (Bush and Johnson, 1988).

Following development of the Upper Floridan aquifer, deep cones of depression developed near some major pumping centers, regional water-level declines were noted in some areas, and predevelopment potentiometric gradients were reversed in some coastal areas, creating the potential for encroachment of saltwater from the Gulf of Mexico (Miller, 1990). However, the major characteristics of the predevelopment flow system have not been greatly altered, and the dominant form of discharge remains springflow and discharge to streams (Miller, 1990).

Water quality and dissolved-solids concentrations of water in the Floridan aquifer system are related to (1) the ground-water flow system and (2) the proximity to saltwater. Water in the Floridan aquifer system is predominantly calcium-bicarbonate type water with dissolved-solids concentrations ranging from 10 to 30,000 mg/L and averaging 250 mg/L (Katz, 1992). In places where the aquifer system is unconfined or thinly confined, large volumes of water move quickly in and out of the aquifer system, and dissolved-solids concentrations are generally less than 250 mg/L (Katz, 1992). In areas where the aquifer system is confined, water travels along longer flow paths and has greater dissolved-solids concentrations. Near the east and west coasts of Florida, and locally in coastal areas of South Carolina and Georgia, large dissolved-solids concentrations result from mixing of fresh ground water with deeper saltwater that migrates into the aquifer from the ocean (Miller, 1990).

The Northern Tampa Bay regional study area is located in west-central peninsular Florida in the Tampa Bay metropolitan area. The study area overlies the karst Floridan aquifer system of the Southeastern United States. This study area was chosen because of the extensive water use from the Floridan aquifer system, because the aquifer is shallow, susceptible, and vulnerable to contamination, and because it represents a range of hydrogeologic and land-use conditions found throughout areas overlying the Floridan aquifer system. The Tampa Bay metropolitan area relies heavily on the Floridan aquifer system for drinking water, and the Floridan aquifer system is the primary source of water for domestic, irrigation, and industrial supplies. The study area includes public water-supply systems for the cities of Tampa, St. Petersburg, and Clearwater, Florida, and numerous smaller cities. Section 5 of this report compares the study area characteristics to those of the Floridan principal aquifer system and presents the hydrogeologic setting, model setup, and modeling results for the Northern Tampa Bay regional study area.

Glacial Aquifer System

The glacial aquifer system is present in 21 States from Maine to Washington, and covers more than 27 percent or approximately 2.5 billion km^2 of the continental United States (fig. 1.2) (U.S. Geological Survey, 2003). The glacial sand and gravel aquifers were ranked first in withdrawals for domestic plus public drinking-water supply among the approximately 62 principal aquifers in the United States.

The glacial aquifer system is generally composed of unconsolidated sand, gravel, and clay commonly deposited as individual valley-fill deposits of outwash and ice-contact materials in bedrock valleys when large continental glaciers covered parts of Canada and the northern United States between approximately 1.6 million and 10,000 years ago (Olcott, 1995). The glacial sand and gravel deposits range from a few meters to more than 300 m in thickness and are highly heterogeneous across the North-Central and Northeastern United States. The glacial sand and gravel aquifers are generally unconfined and in hydraulic connection with valley streams and are the most productive aquifers throughout the glaciated area of the country. The glacial aquifer system in the Northeastern United States is located in humid climatic regions with precipitation ranging from 91 to 127 cm/yr (Randall, 1996), and ground-water recharge is primarily from local precipitation and stream runoff from surrounding bedrock uplands. The bedrock surrounding glacial aquifers is usually less permeable than the valley-fill sediments, and ground-water underflow from bedrock uplands is minimal (Randall, 2001). Ground-water discharge in the glacial aquifers is generally to streams and wells with ground-water pumping accounting for about 15 percent of ground-water discharge (Morrissey, 1983).

Ground-water quality in the glacial aquifers is generally characterized as calcium-bicarbonate type water with dissolved-solids concentrations less than 150 mg/L and pH values in the range of 6 to 8 (Rogers, 1989). However, water quality varies regionally, depending on ground-water flow conditions, valley-fill sediment size, and sediment source area (Randall, 2001). Source area of glacial deposits determines the mineral composition of valley-fill deposits, and rock/water interaction and changing redox conditions in an aquifer can mobilize many constituents that affect natural water quality (Warner and Arnold, 2006). For example, high iron concentrations are detected in some parts of glacial aquifers where geochemical reducing conditions cause dissolution of iron oxides present in sediment. The glacial aquifer system also is vulnerable to anthropogenic contaminants such as nitrates and pesticides in agricultural areas because of the unconfined ground-water flow conditions and short ground-water flow paths.

The Pomperaug River Basin and Great Miami River Basin regional study areas are both within the glacial aquifer system. The Pomperaug River Basin study area is located in west-central Connecticut and represents glacial aquifers in the Northeastern United States. Characteristics of the aquifer system selected for this study are similar to many valley-fill-aquifer systems in the Eastern Hills and Valley Fills hydrophysiographic region (Randall, 2001), which encompasses much of the most populated parts of New England, northern New Jersey, and eastern New York. Public water supply in the Pomperaug River Basin is obtained from ground water in the glacial valley-fill aquifer. Section 6 of this report presents the hydrogeologic setting, model setup, and modeling results for the Pomperaug River Basin regional study area.

The Great Miami River Basin regional study area is in the east-central portion of the White River-Great and Little Miami River Basin NAWQA study unit and is centered on the city of Dayton, Ohio. Ground water in the study area occurs in the valley-fill glacial aquifer underlying the Great Miami River, and the study area represents the glacial aquifer system in the North-Central United States. The glacial aquifer in the study area is heavily used by industry and municipalities, and pumping often causes induced infiltration from nearby rivers or artificial recharge lagoons. Section 7 of this report presents the hydrogeologic setting, model setup, and modeling results for the Great Miami River Basin regional study area.

High Plains Aquifer

The High Plains aquifer underlies 457,594 km^2 in parts of eight States (fig. 1.2) and is primarily composed of Tertiary sand and gravel deposits of the Ogallala Formation (Gutentag and others, 1984). Ground water also occurs in Quaternary sand and gravel deposits overlying the Ogallala Formation in some areas. Approximately 27 percent of the irrigated land in the United States is in the High Plains, and about 30 percent of the ground water used for irrigation in the United States is pumped from the High Plains aquifer (Dennehy, 2000). The High Plains aquifer also provides drinking water to 82 percent of the 2.3 million people (1990 census) who live within the aquifer boundary.

The Ogallala Formation, which underlies about 80 percent of the High Plains, is the principal geologic unit forming the aquifer. The Ogallala Formation is a heterogeneous sequence of gravel, sand, silt, and clay deposited by braided streams flowing eastward from the ancestral Rocky Mountains during the Tertiary period. Younger unconsolidated alluvial deposits of Quaternary age in hydraulic connection with the Tertiary deposits make up the High Plains aquifer in eastern and central Nebraska and Kansas. These Quaternary alluvial deposits are derived from erosion and redeposition of sediments from the Ogallala Formation (Gutentag and others, 1984). The Quaternary alluvial deposits directly overlie the Ogallala Formation in many areas of the High Plains.

Regionally, the High Plains aquifer is considered an unconfined aquifer, but confined conditions can exist locally (Gutentag and others, 1984). The average saturated thickness of the aquifer is about 61 m with a maximum of about 366 m (Gutentag and others, 1984; McGuire and others, 2003). Pumping from more than 130,000 wells (Sharon Qi, U.S. Geological Survey, oral commun., 2004) is the largest component of ground-water discharge. Ground water generally flows from west to east and discharges naturally to streams and springs and by evapotranspiration in areas where the water table is near land surface. Irrigation return flows, precipitation, and seepage from canals and reservoirs are the principal sources of recharge to the aquifer (Luckey and others, 1986; Dennehy and others, 2002). Substantial pumping of the High Plains aquifer for irrigation since the 1940s has resulted in water-level declines of nearly 46 m in some parts of the aquifer (McGuire and others, 2003).

Ground-water quality in the High Plains aquifer is characterized as calcium- bicarbonate type water with dissolved-solids concentrations generally less than 500 mg/L (Dennehy and others, 2002). Ground water is generally oxidized with dissolved-oxygen concentrations greater than 5.4 mg/L and pH ranges from 7 to 8 (Dennehy and others, 2002). Naturally occurring constituents in the ground-water system, which are derived from the water interaction with the sedimentary materials and are considered contaminants, include salinity, iron, manganese, fluoride, radon, uranium, and arsenic (Dennehy and others, 2002). Anthropogenic contaminants are the results of agricultural practices and include nitrate, pesticides, salinity, and carbon tetrachloride (Dennehy and others, 2002).

The Eastern High Plains regional study area is near York, Nebraska, in the eastern part of the High Plains aquifer. Ground water in the Eastern High Plains study area is present in Quaternary sand and gravel deposits, is used extensively for public water supply by the city of York, Nebraska, and is vulnerable to contamination because of the shallow depth to water and high permeability. Section 8 of this report presents the hydrogeologic setting, model setup, and modeling results for the Eastern High Plains regional study area.

Methods

TANC regional studies consisted of implementing the following tasks:

- Compilation of retrospective water-quality, well-construction, water-use, and geologic data.
- Collection of ground-water samples from public-supply wells in each study area in association with the NAWQA Source Water-Quality Assessment (SWQA) project.
- Development of a steady-state regional ground-water flow model to represent conditions for 1997–2001.
- Use of the regional ground-water flow model and advective particle tracking to compute the extent of the

steady-state contributing recharge area and the zone of contribution for as many as 15 public-supply wells within each quartile of pumping for each modeled study area.

- Mapping of regional redox and pH conditions using the retrospective and newly collected SWQA water-quality data.
- Development of a TANC database to store retrospective data and modeling results.

The following sections present details of each task.

Retrospective Data Compilation

Existing water-quality, well-construction, water-use, and geologic data were compiled for each study area from the U.S. Geological Survey National Water Information System (NWIS), the U.S. Environmental Protection Agency STORET database, and State and local agencies. Data compilation focused on information for public-supply wells, but information from monitoring and domestic wells was included where available. Parameters within each data set were cross-checked and stored in a consistent manner to allow the data to be jointly evaluated. To support understanding of recent water-quality and water-use conditions, the period 1997–2001 was selected as the focus for the water-quality and water-use data compilation. If more than one water-quality analysis was available for a well, the most recent and complete analysis for the period 1997–2001 was saved in the database developed for the TANC study (discussed in "Database Development" section). In some instances, a well was not sampled for all water-quality parameters on any given date, and for these cases, the complete analysis stored in the database is a composite of the most recent analysis for each parameter.

Source Water-Quality Assessment Sample Collection

NAWQA Source Water-Quality Assessments (SWQA) consisted of sampling public-supply wells. In 2003 and 2004, SWQA studies were implemented in 10 NAWQA study units including the 7 TANC regional study areas discussed in this report. Between 8 and 31 public-supply wells were sampled in each study area, and samples were analyzed for a suite of natural and anthropogenic constituents including major ions (Fishman, M.J., and Friedman, 1989), nutrients (Fishman, 1993), trace elements (Faires, 1993; Garbarino and others, 2006), volatile-organic compounds (Connor and others, 1998; Rose and Sandstrom, 2003), pesticides (Zaugg and others, 1995; Furlong and others, 2001; Sandstrom and others, 2001), and waste-water compounds (Zaugg and others, 2002). Results from the SWQA sampling are stored in the U.S. Geological Survey NWIS database (*http://waterdata.usgs.gov/nwis,* accessed January 31, 2007) and the NAWQA Data Warehouse (*http://infotrek.er.usgs.gov/travers/f?p=NAWQA:HOME:9108424999420775073*, accessed January 31, 2007).

Ground-Water Flow Simulation

As a process-based tool for understanding ground-water vulnerability, a steady-state ground-water flow model was developed or updated from existing models for each TANC regional study area. Ground-water flow was simulated using the U.S. Geological Survey's modular finite-difference ground-water flow simulation code MODFLOW-2000 (Harbaugh and others, 2000; Hill and others, 2000). Models were calibrated following the guidelines of Hill (1998) using water-budget estimates and water-level data for the period 1997–2001 to facilitate comparisons of modeling results among study areas. Steady-state regional models and the particle-tracking program MODPATH (Pollock, 1994) were used to delineate areas contributing recharge and to compute advective traveltime through the aquifers for as many as 143 public-supply wells within each study area. For study areas with more than 60 public-supply wells, at least 15 public-supply wells were selected for particle tracking from each quartile percentage of pumping. Model conceptualization, boundary conditions, calibration, and particle-tracking simulations for each regional study area are presented in Sections 2 through 7 of this report.

MODPATH uses the cell-by-cell flow values calculated by MODFLOW to calculate the ground-water flow velocity distribution throughout the ground-water system, which is then used to determine flow paths of water particles moving through the aquifer (Pollock, 1994). Traveltimes along flow paths are computed by MODPATH using the magnitude of the cell-by-cell flows, porosity of the aquifer, and the model cell dimensions. MODPATH calculates advective ground-water flow only; the effects of mechanical dispersion and chemical reaction on ground-water transport are not included in the analysis.

Particle-tracking simulations can outline the aquifer area contributing recharge to a pumping well and the aquifer volume composing the zone of contribution to a pumping well (fig. 1.3). The "area contributing recharge" is defined as the surface area of the ground-water system that delineates the location of water entering the ground-water system that eventually flows to the well and discharges. This area must provide an amount of recharge that balances the amount of water being discharged from the well (Franke and others, 1998). Thus, lower areal recharge rates result in larger contributing areas (Franke and others, 1998). The "zone of contribution" is the three-dimensional volumetric part of the aquifer through which ground water flows to the discharging well from the area contributing recharge. If the zone of contribution intercepts a surface-water body, the area contributing recharge is reduced and its size is a function of areal recharge rate and surface-water leakage (Franke and others, 1998). Depending on the screen placement of the well and local ground-water

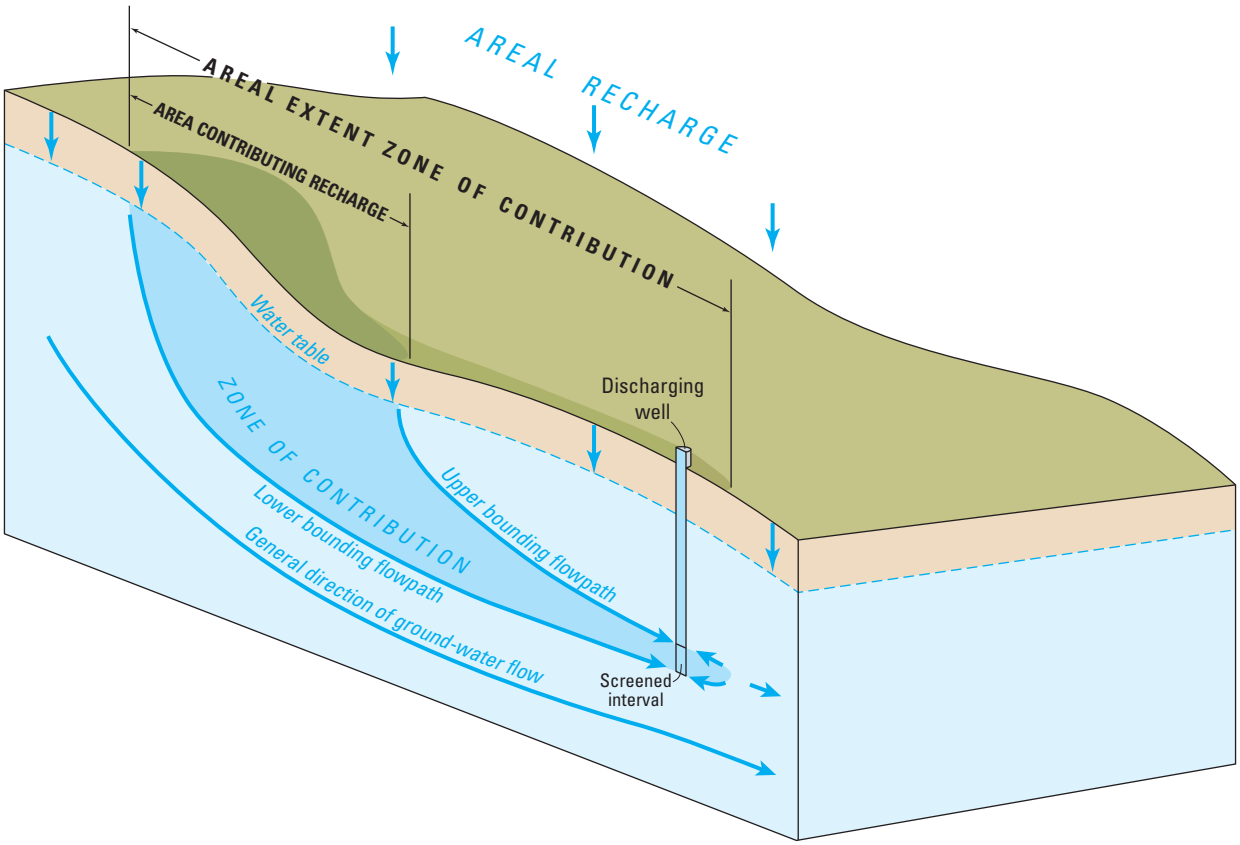

Figure 1.3. Area contributing recharge and zone of contribution for a single discharging well in a simplified hypothetical ground-water system.

flow conditions, the area contributing recharge to a well does not necessarily have to include the location of the well. The vertical projection of the zone of contribution to the land surface is termed the "areal extent of the zone of contribution" (USGS Office of Ground Water Technical Memorandum No. 2003.02, *http://water.usgs.gov/admin/memo/GW/gw03.02.html*, accessed June 15, 2004). Zones of contribution and their areal extents will always include the location of the well.

Because of the regional scale of the models used in this study, special consideration was given to the treatment of weak sinks in the determination of contributing areas. A weak sink is a model cell (representing a well, for example) with an insufficient discharge rate to capture all ground-water flow entering the cell; thus, some of the flow leaves the cell across one or more cell faces. Particle flow paths calculated for a weak-sink cell cannot be uniquely defined because it is impossible to know whether a specific water particle discharges to the weak sink or passes through the cell (Spitz, 2001).

Weak sinks cause problems with associating a given amount of water with each particle. MODPATH offers three options for dealing with weak sinks. Particles can be stopped when they reach a weak sink, allowed to pass through weak sinks, or stopped if the percentage of flow entering the model cell that is captured by the weak sink exceeds a user-supplied threshold (Pollock, 1994). Table 1.2 shows the effects of the first two options. Effects of the third option would be some combination of the other two options.

The approach of grid refinement described by Spitz (2001) was used in TANC particle-tracking simulations to better represent particle movement through weak sinks (see discussions on weak sinks in preceding paragraphs and table 1.2). The grid-refinement approach creates a MODFLOW model of the weak-sink cell (fine model) so the cell containing the well becomes a strong sink. The boundaries of this fine model are set to a constant flux equal to the flow across each face as simulated in the original (coarse) model. The FORTRAN programs described by Spitz (2001) were altered to allow particles to be transferred from the coarse model to the fine model (to allow for forward particle tracking) and to allow the fine model to represent multiple layers from the coarse model (for the case where a well screen spans several model layers).

A forward particle-tracking approach was used in the MODPATH simulations together with a grid-refinement program (Spitz, 2001) to delineate areas contributing recharge to public-supply wells (see discussions on weak sinks and grid-refinement approach). Particles were started on model-boundary cell faces for cells representing sources of water, forward tracked along path lines, and then were stopped when

they reached a weak-sink cell. A fine model was constructed for each weak sink cell, particles were transferred from the coarse model to the fine model and tracked through the model, and then the particles that did not terminate in the fine model were transferred back to the coarse model. The remaining particles then were forward tracked again in the coarse model. This process was repeated until all particles reached a strong sink either in the coarse model or one of the fine models. MODPATH simulations of areas contributing recharge were initially run by starting particles on every boundary cell face of the model with a positive flux of water and tracking particles as previously described. For the final calculation of areas contributing recharge, the particle density for each well was adjusted so that between 100 and 1,500 particles were used to represent the contributing area.

Contributing area results were used to create GIS datasets, which were subsequently used to determine a variety of attributes for each contributing area. The starting locations of particles on a given model-cell face were evenly distributed so a flow could be assigned to each particle equal to the total flow associated with the face divided by the number of particles started on the face. A traveltime also was associated with each particle. For particles associated with recharge from irrigation and(or) precipitation, properties of the landscape (data on land use, census, soils, and potential contaminant sources) were assigned to the particles. Path-line information was combined with descriptions of redox conditions, pH, and geology to determine the environments "experienced" by each particle on the way to the well. To determine average statistics for the entire contributing area, the properties for each particle were weighted by the percentage of the total flow to the well that they represented. A full list of the attributes calculated for the contributing areas is presented in Appendix 1.

Oxidation-Reduction and pH Classification and Mapping

The oxidation-reduction (redox) state of ground water is an important geochemical control on the solubility and mobility of anthropogenic contaminants and naturally occurring trace elements. In aquifers where redox chemistry controls chemical reactions in the system, it is sometimes possible to define redox zones where a dominant redox couple controls the redox potential of the system (Domenico and Schwartz, 1990). Numerous studies have deduced redox conditions in ground water on the basis of concentrations of electron acceptors, intermediate products, and accumulations of final products from terminal electron-accepting processes. However, the lack of an electron acceptor or final product accumulation does not always define the distribution of redox processes and is an admitted limitation of inferring redox state from redox indicator species. For example, a decrease in sulfate concentration and an increase in sulfide concentration would indicate a sulfate-reducing redox zone. However, a decrease in sulfate concentration may not be observed during sulfate reduction if there is a continuous source of sulfate to a system such as gypsum dissolution (Plummer and others, 1990). Similarly, an increase in sulfide concentration may not be observed if metal sulfides are precipitated during sulfate reduction. The measurement of hydrogen concentrations in ground water can be used in conjunction with patterns of electron-acceptor consumption and final-product accumulation to more accurately identify the distribution of terminal electron-accepting processes in ground-water systems (Chapelle and others, 1995).

The TANC regional studies inferred aquifer redox conditions by using concentrations of redox-indicator species from the retrospective water-quality data. A redox-classification system was developed as discussed below, and a "redox environment consistent with redox indicator species" was assigned to each well location based on concentrations of dissolved oxygen, nitrate, manganese, iron, and sulfate (table 1.3). The

Table 1.2. Effects of weak sinks on the determination of contributing areas.

	Water particles stop at weak sink	Water particles pass through weak sink
Forward tracking	First weak sinks encountered can have too many particles, resulting in areas contributing recharge that are too large. Sinks (weak or strong) farther along the flow path may intercept too few particles, resulting in areas contributing recharge that are too small.	No particles associated with weak sink cells. Too many particles reach strong sinks, resulting in areas contributing recharge that are too large. Particles passing through weak sinks effectively lose flow.
Backward tracking	Difficulty in assigning starting particles for weak sinks. Particles that pass back through weak sinks are effectively gaining flow; the resulting area contributing recharge will be too large.	

TANC redox classification system used five general categories to assign redox conditions to individual wells in the TANC regional study areas:

- Conditions consistent with oxygen reduction
- Conditions consistent with nitrate reduction
- Conditions consistent with manganese reduction
- Conditions consistent with iron reduction with high sulfate
- Conditions consistent with iron reduction with low sulfate

Concentration data for these redox-indicator species were commonly available in the retrospective data, and concentration significance levels were used to infer redox conditions for each well location. Hydrogen data were generally not available in the regional retrospective data set. Concentration significance levels for the redox-indicator species followed those presented by Chapelle and others (1995) for dissolved oxygen and nitrate, the Geological Survey of Sweden (*http://www.internat.environ.se/index.php3?main=/documents/legal/assess/assedoc/gndwdoc/aqui.htm*, accessed June 15, 2004) for manganese and iron, and Chapelle and others (2002) for sulfate. The sulfate significance level (4 mg/L) was chosen because Chapelle and others (2002) suggested the threshold sulfate concentration for sulfate reduction may be on the order of 4 mg/L. Thus, once iron-reducing conditions have been achieved and sulfate concentrations drop below 4 mg/L, geochemical conditions likely have progressed well into, if not beyond, sulfate reduction. Such highly-reducing conditions may or may not correspond to methanogenic conditions, but likely do represent a low energy state that may have significance in geochemical investigations.

For this redox classification system, the assumption is made that recharge water contains dissolved oxygen and nitrate at concentrations greater than the significance levels discussed above. Furthermore, the assumption is made that oxidized forms of manganese and iron are available in the aquifer matrix so that manganese and iron are available for reduction. No assumptions are made about initial sulfate concentrations. In this classification system, oxygen-, nitrate-, and manganese-reducing conditions do not depend on sulfate concentrations. This allowance arises from the expectation that sulfate concentrations in recharge water commonly may be either greater than or less than the significance level for sulfate. However, the assumption is made that by the time that redox conditions progress to iron-reducing conditions, sulfate will have become available from either recharge area sources or from various aquifer sources (e.g. Hem, 1985). This assumption facilitates the creation of high-sulfate and low-sulfate iron-reducing conditions.

Examples of how the redox classification system was applied follow. If dissolved-oxygen and nitrate concentrations were greater than their respective significance levels, and manganese and iron concentrations were less than or equal to their respective significance levels, a redox classification was assigned consistent with oxygen reduction. If dissolved-oxygen, manganese, and iron concentrations were less than or equal to their respective significance levels, and nitrate concentrations were greater than its respective significance level, a redox classification was assigned consistent with nitrate reduction. For the case of dissolved-oxygen, nitrate, and iron concentrations less than or equal to their respective significance levels, and manganese concentrations greater than its respective significance level, a redox classification was assigned consistent with manganese reduction. With dissolved-oxygen and nitrate concentrations less than or equal to their respective significance levels, and manganese, iron, and sulfate concentrations greater than their respective significance levels, a redox classification was assigned consistent with iron reduction, high sulfate. Similar water, but with sulfate concentrations less than or equal to its significance level, would be assigned a redox classification consistent with iron reduction,

Table 1.3. Oxidation-reduction classification scheme.

[DO, dissolved oxygen; NO_3, nitrate; Mn, manganese; Fe, iron; SO_4, sulfate; mg/L, milligrams per liter; mg N/L, milligrams nitrogen per liter: µg/L, micrograms per liter; >, greater than; ≤, less than or equal to; —, not applicable]

Redox category assigned—consistent with indicator species concentrations	Redox indicator species significance level				
	DO 0.5 mg/L	NO_3 0.5 mg N/L	Mn 50 µg/L	Fe 100 µg/L	SO_4 4 mg/L
Oxygen reduction	>	>	≤	≤	—
Nitrate reduction	≤	>	≤	≤	—
Manganese reduction	≤	≤	>	≤	—
Iron reduction with high sulfate	≤	≤	>	>	>
Iron reduction with low sulfate	≤	≤	>	>	≤

low sulfate. If more than one redox category was assigned to a sample, the sample was categorized as having a "mixed" redox state.

Redox conditions were mapped at a regional scale using the redox categories assigned to each well, and the maps were discretized using the MODFLOW model grids to calculate traveltime through various redox environments. A wide range of available redox data and redox conditions was observed among TANC study areas, and the redox classification was reduced to two categories in the final particle-tracking analysis: 1) conditions consistent with oxygen or nitrate reduction, and 2) conditions consistent with manganese or iron reduction. The redox classification using retrospective data proved effective for delineating regional redox patterns in all study areas except the Northern Tampa Bay. Redox zones were not mapped for the Northern Tampa Bay regional study area because complex ground-water flow patterns in this karst aquifer resulted in no discernable redox pattern.

The pH of ground water can be another important geochemical control on the mobility of naturally occurring trace elements and anthropogenic contaminants. For example, the adsorption of trace elements onto iron oxides is often a pH-dependent reaction. For the TANC regional study areas, ground-water pH values were grouped into two categories: pH values less than 8 (circumneutral), and pH greater than 8 (high pH). A pH of 8 was chosen, in part, on the basis of the zero point of charge for iron oxide being roughly 8 (Stumm and Morgan, 1981).

Database Development

To conduct a more process-oriented national assessment of the susceptibility and vulnerability of aquifers and public-supply wells than has been previously possible and to complement earlier work such as the U.S. Environmental Protection Agency's review of contaminant occurrence in public-water systems (U.S. Environmental Protection Agency, 1999), TANC data and results were organized using relational-database software. Information in the TANC database includes retrospective water-quality data, well-construction data, water-use data, geologic data, SWQA water-quality data, ground-water flow model and particle-tracking results, potential contaminant sources within the area contributing recharge of selected public-supply wells, and geochemical classifications of redox and pH. Many of the data-field definitions in the TANC database follow those in the U.S. Geological Survey NWIS database. However, several additional data tables and fields were added to accommodate modeling results, which cannot be stored in NWIS. The TANC database structure is such that additional tables can be added as data collection and analyses proceed.

The database currently (2006) consists of 10 data tables generally linked by a combination of NAWQA TANC Study Unit code and U.S. Geological Survey Site Identification (ID) number, which forms a unique identification number assigned to each well location. Appendix 1 contains data dictionaries for the TANC data tables. The TANC_STUDIES table contains summary information about each TANC study area such as its start date, overall location, area, and general aquifer characteristics. The SITES table contains information specific to each sampling location such as U.S. Geological Survey Site ID, local station name, location, altitude, and site use, and the WELL_INFO table contains well-completion details. The RESULTS_RGNL table contains water-quality analysis results for the regional study areas, and the PARAMETERS table contains parameter-code definitions for the RESULTS_RGNL table. The PUMPING_RGNL table stores information about all pumping centers simulated in each of the TANC regional ground-water flow models. Four tables contain ground-water particle-tracking results and geochemical interpretations. The ANCILLARY table includes the geochemical interpretations of redox conditions as previously discussed in the "Redox and pH Classification and Mapping" section. The CAREASUM_RGNL table contains contributing area and traveltime information for each well calculated from the regional ground-water flow models, as previously discussed in the "Ground-Water Flow Simulation" section, and the CAREARDXPH_RGNL table contains tabulations of ground-water traveltime through redox and pH zones. The CAREASRCE_RGNL table contains a tabulation of the land use, population density, and potential contaminant sources overlying contributing areas.

At the completion of initial data compilation (2003), nearly 196,000 water-quality records from 2,242 sampling locations were included in the TANC database; 129 of these locations had new water-quality data collected as part of the NAWQA SWQA project. Contributing areas were calculated for 405 public-supply wells, and water-quality data were stored in the TANC database for 321 of the 405 public-supply wells with calculated contributing areas.

References Cited

Bush, P.W., and Johnston, R.H., 1988, Ground-water hydraulics, regional flow, and ground-water development of the Floridan aquifer system in Florida and in parts of Georgia, South Carolina, and Alabama: U.S. Geological Survey Professional Paper 1403–C, 80 p.

Chapelle, F.H., Bradley, P.M., Lovley, D.R., O'Neill, K., and Landmeyer, J.E., 2002, Rapid evolution of redox processes in a petroleum hydrocarbon-contaminated aquifer: Ground-water, v. 40, no. 4, p. 353–360.

Chapelle, F.H., McMahon, P.B., Dubrovsky, N.M., Fujii, R.F., Oaksford, E.T., and Vroblesky, D.A., 1995, Deducing the distribution of terminal electron-accepting processes in hydrologically diverse groundwater systems: Water Resources Research, v. 31, no. 2, p. 359–371.

Connor, B.F., Rose, D.L., Noriega, M.C., Murtagh, L.K., and Abney, S.R., 1998, Methods of analysis by the U.S. Geological Survey National Water Quality Laboratory—Determination of 86 volatile organic compounds in water by gas chromatography/mass spectrometry, including detections less than reporting limits: U.S. Geological Survey Open-File Report 97–829, 86 p.

Davis, G.H., Green, J.H., Olmsted, F.H., and Brown, D.W., 1959, Ground-water conditions and storage capacity in the San Joaquin Valley, California: U.S. Geological Survey Water-Supply Paper 1469, 287 p.

Dennehy, K.F., 2000, High Plains Regional Ground-Water Study: U.S. Geological Survey Fact Sheet FS 091–00, 6 p.

Dennehy, K.F., Litke, D.W., and McMahon, P.B., 2002, The High Plains aquifer, USA—Groundwater development and sustainability, *in* Hiscock, K.M., Rivett, M.O., and Davison, R.M., eds., Sustainable groundwater development: London, Geological Society Special Publications, 193, p. 99–119.

Domenico, P.A., and Schwartz, F.W., 1990, Physical and chemical hydrogeology: NewYork, John Wiley & Sons, 824 p.

Faires, L.M., 1993, Methods of analysis by the U.S. Geological Survey National Water Quality Laboratory—Determination of metals in water by inductively coupled plasma-mass spectrometry: U.S. Geological Survey Open-File Report 92–634, 28 p.

Fishman, M.J., ed., 1993, Methods of analysis by the U.S. Geological Survey National Water Quality Laboratory—Determination of inorganic and organic constituents in water and fluvial sediments: U.S. Geological Survey Open-File Report 93–125, 217 p.

Fishman, M.J., and Friedman, L.C., 1989, Methods for determination of inorganic substances in water and fluvial sediments: U.S. Geological Survey Techniques of Water-Resources Investigations, book 5, chap. A1, 545 p.

Focazio, M.J., Reilly, T.E., Rupert, M.G., and Helsel, D.R., 2002, Assessing ground-water vulnerability to contamination—Providing scientifically defensible information for decision makers: U.S. Geological Survey Circular 1224, 33 p.

Franke, O.L., Reilly, T.E., Pollock, D.W., and LaBaugh, J.W., 1998, Estimating areas contributing recharge to wells: U.S. Geological Survey Circular 1176, 14 p.

Furlong, E.T., Anderson, B.D., Werner, S.L., Soliven, P.P., Coffey, L.J., and Burkhardt, M.R., 2001, Methods of analysis by the U.S. Geological Survey National Water Quality Laboratory—Determination of pesticides in water by graphitized carbon-based solid-phase extraction and high-performance liquid chromatography/mass spectrometry: U.S. Geological Survey Water-Resources Investigations Report 01–4134, 73 p.

Garbarino, J.R., Kanagy, L.K., and Cree, M.E., 2006, Determination of elements in natural-water, biota, sediment and soil samples using collision/reaction cell inductively coupled plasma-mass spectrometry: U.S. Geological Survey Techniques and Methods, book 5, sec. B, chap.1, 88 p.

Gilliiom, R.J, Alley, W.M., and Gurtz, M.E., 1995, Design of the National Water-Quality Assessment Program—Occurrence and distribution of water-quality conditions: U.S. Geological Survey Circular 1112, 33 p.

Gronberg, J.M., Dubrovsky, N.M., Kratzer, C.K., Domagalski, J.L., Brown, L.R., and Burow, K.R., 1998, Environmental setting of the San Joaquin-Tulare Basins, California: U.S. Geological Survey Water-Resources Investigations Report 97–4205, 45 p.

Gutentag, E.D., Heimes, F.J., Krothe, N.C., Luckey, R.R., and Weeks, J.B., 1984, Geohydrology of the High Plains aquifer in parts of Colorado, Kansas, Nebraska, New Mexico, Oklahoma, South Dakota, Texas, and Wyoming: U.S. Geological Survey Professional Paper 1400–B, 63 p.

Harbaugh, A.W., Banta, E.R., Hill, M.C., and McDonald, M.G., 2000, MODFLOW-2000, The U.S. Geological Survey modular ground-water model—User guide to modularization concepts and the ground-water flow process: U.S. Geological Survey Open-File Report 00–92, 121 p., *http://water.usgs.gov/nrp/gwsoftware/modflow2000/modflow2000.html*

Hem, J.D., 1985, Study and interpretation of the chemical characteristics of natural water (3rd ed.): U.S. Geological Survey Water-Supply Paper 2254, 263 p.

Hill, M.C., 1998, Methods and guidelines for effective model calibration: U.S. Geological Survey Water-Resources Investigations Report 98–4005, 90 p.

Hill, M.C., Banta, E.R., Harbaugh, A.W., and Anderman, E.R., 2000, MODFLOW-2000, The U.S. Geological Survey modular ground-water flow model—User guide to the observation, sensitivity, and parameter-estimation processes and three post-processing programs: U.S. Geological Survey Open-File Report 00–184, 209 p.

Katz, B.G., 1992, Hydrochemistry of the upper Floridan Aquifer System, Florida: U.S. Geological Survey Water-Resources Investigations Report 91–4196, 37 p., 10 pls.

Lapham, W.W., Hamilton, P.A., and Myers, D.N., 2005, National Water-Quality Assessment Program—Cycle II Regional Assessment of Aquifers: U.S. Geological Survey Fact Sheet 2005–3013, 4 p.

Luckey, R.R., Gutentag, E.D., Heimes, F.J., and Weeks, J.B., 1986, Digital simulation of ground-water flow in the High Plains aquifer in parts of Colorado, Kansas, Nebraska, New Mexico, Oklahoma, South Dakota, Texas, and Wyoming: U.S. Geological Survey Professional Paper 1400–D, 63 p.

Marella, R.L., and Berndt, M.P., 2005, Water withdrawals and trends from the Floridan aquifer system in the Southeastern United States, 1950–2000: U.S. Geological Survey Circular 1278, 20 p.

Maupin, M.A., and Barber, N.L., 2005, Estimated withdrawals from principal aquifers in the United States, 2000: U.S. Geological Survey Circular 1279, 47 p.

McGuire, V.L., Johnson, M.R., Schieffer, R.L., Stanton, J.S., Sebree, S.K., and Verstraeten, I.M., 2003, Water in storage and approaches to ground-water management, High Plains aquifer, 2000: U.S. Geological Survey Circular 1243, 51 p.

Miller, J. A., 1986, Hydrogeologic framework of the Floridan Aquifer System—Regional Aquifer System in Florida and in parts of Georgia, Alabama, and South Carolina: U.S. Geological Survey Professional Paper 1403–B, 91 p.

Miller, J.A., 1990, Ground Water Atlas of the United States—Alabama, Florida, Georgia, and South Carolina: U.S. Geological Survey Hydrologic Atlas HA 730–G.

Miller, J.A., 1999, Ground Water Atlas of the United States—Introduction and National summary: *http://capp.water.usgs.gov/gwa/gwa.html*

Morrissey, D. J., 1983, Hydrology of the Little Androscoggin River valley aquifer, Oxford County, Maine: U.S. Geological Survey Water-Resources Investigations 83–4018, 79 p.

Olcott, P.G., 1995, Ground water atlas of the United States—Connecticut, Maine, Massachusetts, New Hampshire, New York, Rhode Island, Vermont: U.S. Geological Survey Hydrologic Atlas HA 730–M.

Planert, Michael, and Williams, J.S., 1995, Ground-water atlas of the United States—California and Nevada: U.S. Geological Survey Hydrologic Atlas HA 730–B.

Plummer, L.N., Busby, J.F., Lee, R.W., and Hanshaw, B.B., 1990, Geochemical modeling of the Madison aquifer in parts of Montana, Wyoming, and South Dakota: Water Resources Research, v. 26, p. 1981–2014.

Pollock, D.W., 1994, User's guide for MODPATH/MODPATH-PLOT, Version 3—A particle tracking post-processing package for MODFLOW, the U.S. Geological Survey finite-difference ground-water flow model: U.S. Geological Survey Open-File Report 94–464, *http://water.usgs.gov/nrp/gwsoftware/modpath41/modpath41.html*

Randall, A.D., 1996, Mean annual runoff, precipitation, and evapotranspiration in the glaciated Northeastern United States, 1951–1980: U.S. Geological Survey Open-File Report 96–395, 2 pls.

Randall, A.D., 2001, Hydrogeologic framework of stratified-drift aquifers in the glaciated northeastern United States: U.S. Geological Survey Professional Paper 1415–B, 179 p.

Robson, S.G., and Banta, E.R., 1995, Ground Water Atlas of the United States—Arizona, Colorado, New Mexico, and Utah: U.S. Geological Survey Hydrologic Atlas HA 730–C.

Rogers, R.J., 1989, Geochemical comparison of ground water in areas of New England, New York, and Pennsylvania: Ground Water, v. 27, no. 5, p. 690–712.

Rose, D.L., and Sandstrom, M.W., 2003, Methods of analysis by the U.S. Geological Survey National Water Quality Laboratory—Determination of gasoline oxygenates, selected degradates, and BTEX in water by heated purge and trap/gas chromatography/mass spectrometry: U.S. Geological Survey Water-Resources Investigations Report 03–4079, 39 p.

Sandstrom, M.W., Stroppel, M.E., Foreman, W.T., and Schroeder, M.P., 2001, Methods of analysis by the U.S. Geological Survey National Water Quality Laboratory—Determination of moderate-use pesticides and selected degradates in water by C-18 solid-phase extraction and gas chromatography/mass spectrometry: U.S. Geological Survey Water-Resources Investigations Report 01–4098, 70 p.

Spitz, F.J., 2001, Method and computer programs to improve pathline resolution near weak sinks representing wells in MODFLOW and MODPATH ground-water-flow simulations: U.S. Geological Survey Open-File Report 00–392, 41 p.

Stumm, Werner, and Morgan, J.J., 1981, Aquatic chemistry: New York, Wiley-Interscience, 780 p.

U.S. Environmental Protection Agency, 1999, A review of contaminant occurrence in public water systems: EPA 816–R–99–006, 78 p., *http://www.epa.gov/safewater/occur/occur.html*

U.S. Geological Survey, 2003, Principal aquifers of the 48 conterminous United States, Hawaii, Puerto Rico, and the U.S. Virgin Islands: *http://nationalatlas.gov/mld/aquifrp.html*, 1 sheet.

Warner, K.L., and Arnold, T.L., 2006, Framework for regional systhesis of water-quality data for the glacial aquifer system of the United States: U.S. Geological Survey Scientific Investigations Report 2005–5223, 6 p.

Zaugg, S.D., Sandstrom, M.W., Smith, S.G., and Fehlberg, K.M., 1995, Methods of analysis by the U.S. Geological Survey National Water Quality Laboratory—Determination of pesticides in water by C-18 solid-phase extraction and capillary-column gas chromatography/mass spectrometry with selected-ion monitoring: U.S. Geological Survey Open-File Report 95–181, 60 p.

Zaugg, S.D., Smith, S.G., Schroeder, M.P., Barber, L.B., and Burkhardt, M.R., 2002, Methods of analysis by the U.S. Geological Survey National Water Quality Laboratory—Determination of wastewater compounds by polystyrene-divinylbenzene solid-phase extraction and capillary-column gas chromatography/mass spectrometry: U.S. Geological Survey Water-Resources Investigations Report 01–4186, 37 p.

Hydrogeologic Setting and Ground-Water Flow Simulations of the Salt Lake Valley Regional Study Area, Utah

By Bernard J. Stolp

Section 2 of

Hydrogeologic Settings and Ground-Water Flow Simulations for Regional Studies of the Transport of Anthropogenic and Natural Contaminants to Public-Supply Wells—Studies Begun in 2001

Edited by Suzanne S. Paschke

Professional Paper 1737–A

U.S. Department of the Interior
U.S. Geological Survey

U.S. Department of the Interior
DIRK KEMPTHORNE, SECRETARY

U.S. Geological Survey
Mark D. Myers, Director

U.S. Geological Survey, Reston, Virginia: 2007

For product and ordering information:
World Wide Web: http://www.usgs.gov/pubprod
Telephone: 1-888-ASK-USGS

For more information on the USGS--the Federal source for science about the Earth, its natural and living resources, natural hazards, and the environment:
World Wide Web: http://www.usgs.gov
Telephone: 1-888-ASK-USGS

Any use of trade, product, or firm names is for descriptive purposes only and does not imply endorsement by the U.S. Government.

Although this report is in the public domain, permission must be secured from the individual copyright owners to reproduce any copyrighted materials contained within this report.

Suggested citation:
Stolp, B.J., 2007, Hydrogeologic setting and ground-water flow simulations of the Salt Lake Valley Regional Study Area, Utah, *section 2 of* Paschke, S.S., ed., Hydrogeologic settings and ground-water flow simulations for regional studies of the transport of anthropogenic and natural contaminants to public-supply wells—studies begun in 2001: Reston, Va., U.S. Geological Survey Professional Paper 1737–A, pp. 2–1 – 2–22.

Contents

Abstract 2–1
Introduction 2–1
Purpose and Scope 2–1
Study Area Description 2–4
Topography and Climate 2–6
Surface-Water Hydrology 2–6
Land Use 2–6
Water Use 2–6
Conceptual Understanding of the Ground-Water System 2–6
Geology 2–6
Ground-Water Occurrence and Flow 2–7
Aquifer Hydraulic Properties 2–9
Water Budget 2–9
Recharge 2–9
Discharge 2–10
Ground-Water Quality 2–11
Ground-Water Flow Simulations 2–11
Modeled Area and Spatial Discretization 2–11
Boundary Conditions and Model Stresses 2–14
Recharge 2–14
Discharge 2–14
Model Calibration and Sensitivity 2–16
Model-Computed Hydraulic Heads 2–16
Model-Computed Water Budget 2–16
Simulation of Areas Contributing Recharge to Wells 2–17
Limitations and Appropriate Use of the Model 2–17
References Cited 2–22

Figures

Maps showing:
2.1. Location of the Salt Lake Valley regional study area within the Basin and Range basin-fill aquifers. 2–2
2.2. Topography, hydrologic features, and location of public-supply wells, Salt Lake Valley regional study area, Utah. 2–3
2.3. Generalized block diagram showing the basin-fill ground-water flow system, Salt Lake Valley regional study area, Utah. 2–7
Maps showing:
2.4. Elevation of model-computed basin-fill aquifer potentiometric surface for 1997–2001 average conditions, Salt Lake Valley regional study area, Utah. 2–8

2.5. Generalized oxidation-reduction classification zones, Salt Lake Valley regional study area, Utah..... 2–12
2.6. Ground-water flow model grid and selected boundary conditions, Salt Lake Valley regional study area, Utah..... 2–13
2.7. Distribution of basin-fill aquifer transmissivity for the calibrated ground-water flow model, Salt Lake Valley regional study area, Utah..... 2–18
2.8. Water-level observation well locations and head residuals, Salt Lake Valley regional study area, Utah..... 2–19

Graphs showing

2.9. Relation between model-computed and measured hydraulic head, Salt Lake Valley regional study area, Utah.....2–20
2.10. Relation between head residual and measured hydraulic head, Salt Lake Valley regional study area, Utah. 2–20
2.11. Map showing model-computed areas contributing recharge to public-supply wells, Salt Lake Valley regional study area, Utah. 2–21

Tables

2.1. Summary of hydrogeologic and ground-water quality characteristics for the Basin and Range basin-fill aquifers and the Salt Lake Valley regional study area, Utah. 2–4
2.2. Model-computed water budget for 1997–2001 average conditions, Salt Lake Valley regional study area, Utah. 2–15

Hydrogeologic Setting and Ground-Water Flow Simulation of the Salt Lake Valley Regional Study Area, Utah

By Bernard J. Stolp

Abstract

The transport of anthropogenic and natural contaminants to public-supply wells was evaluated in the Salt Lake Valley, Utah, as part of the U.S. Geological Survey National Water-Quality Assessment Program. The valley-fill aquifer in the Salt Lake Valley regional study area is representative of the Basin and Range basin-fill aquifers, is an important source of water for agricultural irrigation and public water supply, and is susceptible and vulnerable to contamination. An existing seven-layer, transient ground-water flow model of the Salt Lake Valley was converted to a steady-state model representative of average conditions for the period 1997–2001. The steady-state model and advective particle-tracking simulations were used to compute ground-water flow paths, areas contributing recharge, and traveltimes from recharge areas for 94 wells. Model results indicate recharge from the surrounding mountain block (43.8 percent of inflow) and precipitation plus irrigation (39.5 percent of inflow) provide the majority of ground-water inflow to the study area. Inflow from rivers and canals provides the remaining inflow. Ground-water discharge is primarily to wells (49.4 percent of outflow) and the Jordan River (28.3 percent of outflow) with the remainder of ground-water outflow going to evapotranspiration, springs, drains, and the Great Salt Lake. The model-computed areas contributing recharge reached to the edges of the modeled area indicating mountain-front and mountain-block recharge from the Wasatch Range on the east and the Oquirrh Mountains on the west contributes water to public-supply wells in the Salt Lake Valley study area. The simulated median traveltime for ground water to flow from its recharge point to a well ranged from 5 to 780 years. The longest traveltimes are associated with contributing areas for wells on the west side of Salt Lake Valley.

Introduction

The Salt Lake Valley regional study area for the transport of anthropogenic and natural contaminants to public-supply wells (TANC) study is on the western edge of the 37,500-km^2 Great Salt Lake Basins study unit of the U.S. Geological Survey National Water-Quality Assessment (NAWQA) program (fig. 2.1). The Salt Lake Valley is located west of the Wasatch Range (fig. 2.2) and is the metropolitan and industrial center of the State of Utah. Ground water exists in the unconsolidated and semiconsolidated basin-fill materials of the valley and is used extensively for water supply in and around Salt Lake City, Utah.

Purpose and Scope

The purpose of this Professional Paper section is to present the hydrogeologic setting of the Salt Lake Valley regional study area. The section also documents a steady-state regional ground-water flow model for the study area. Ground-water flow characteristics, pumping-well information, and water-quality data were compiled from existing data to develop a conceptual understanding of ground-water conditions in the study area. A seven-layer transient ground-water flow model of the Salt Lake Valley basin-fill aquifer was converted to a steady-state model to represent average conditions for the period from 1997 to 2001. The 5-year period 1997–2001 was selected for data compilation and modeling exercises for all TANC regional study areas to facilitate future comparisons between study areas. The steady-state ground-water flow model and associated particle tracking were used to simulate advective ground-water flow paths and to delineate areas contributing recharge to selected public-supply wells. Ground-water traveltimes from recharge to public-supply wells, oxidation-reduction (redox) conditions along flow paths, and presence of potential contaminant sources in areas contributing recharge were tabulated into a relational database described in Section 1 of this Professional Paper. This section provides the foundation for future ground-water susceptibility and vulnerability analyses of the study area and comparisons among regional aquifer systems.

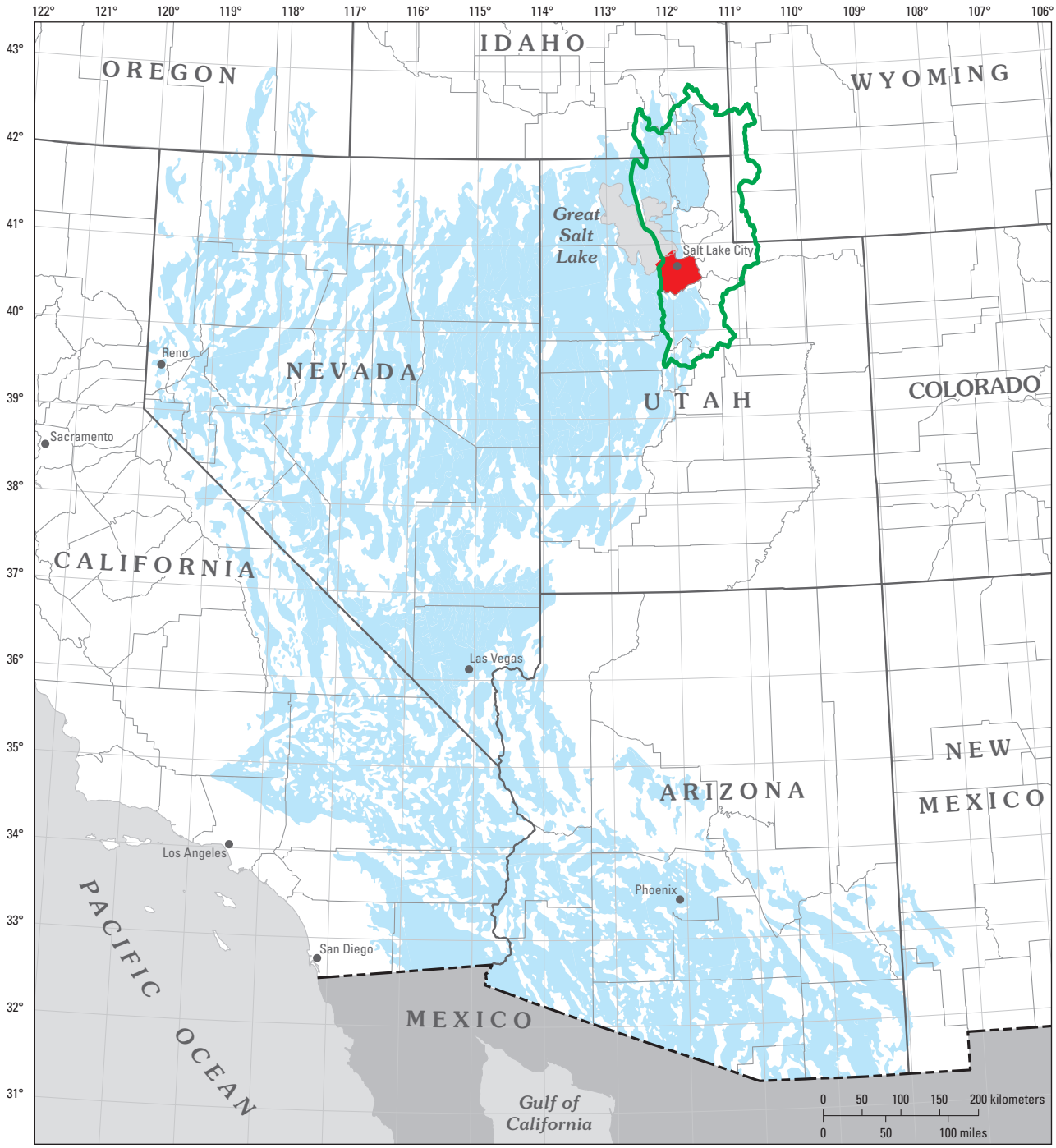

Base from U.S. Geological Survey digital data, 1:2,000,000, 1972, Albers equal-area projection

EXPLANATION

Salt Lake Valley regional study area

Basin and Range aquifer

USGS NAWQA study unit—Great Salt Lake Basins

Figure 2.1. Location of the Salt Lake Valley regional study area within the Basin and Range basin-fill aquifers.

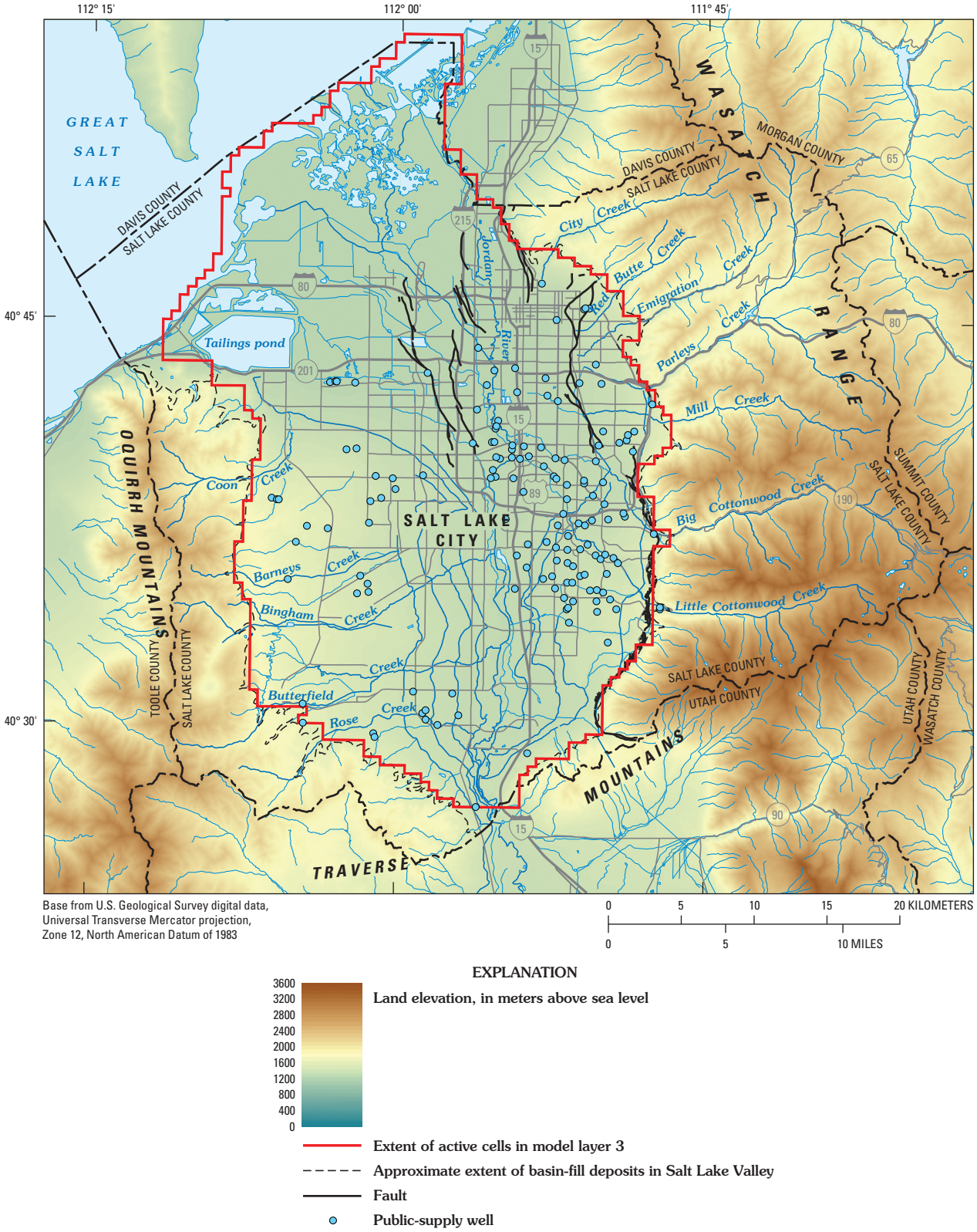

Figure 2.2. Topography, hydrologic features, and location of public-supply wells, Salt Lake Valley regional study area, Utah.

Study Area Description

The Salt Lake Valley regional study area is located in the Basin and Range basin-fill aquifers, which are ranked fourth in total water use of the 62 principal aquifers in the United States (Maupin and Barber, 2005). The Salt Lake Valley regional study area is representative of the Basin and Range basin-fill aquifers (table 2.1) with ground water occurring in the basin-fill deposits of the valley.

Table 2.1. Summary of hydrogeologic and ground-water-quality characteristics for the Basin and Range basin-fill aquifers and the Salt Lake Valley regional study area, Utah.

[m, meters; cm/yr, centimeters per year; hm^3/yr; cubic hectometers per year; m^2/d, squared meters per day; m^3/d, cubic meters per day; m/d, meters per day; ET, evapotranspiration; mg/L, milligrams per liter]

Characteristic	Basin and Range basin-fill aquifers	Salt Lake Valley regional study area
	Geography	
Topography	Altitude ranges from about 46m at Yuma, Arizona to over 3,048 m at the crest of some mountain ranges (Robson and Banta, 1995).	Valley floor altitude slopes from 1,280 m near Great Salt Lake to about 1,580 m on the foothills of Wasatch and Oquirrh Mountains.
Climate	Arid to semi-arid climate. Precipitation ranges from 10 to 20 cm/yr in basins and 40 to 76 cm/yr in mountains (Robson and Banta, 1995).	Semi-arid climate. Precipitation in valley ranges from 30 cm/yr to almost 50 cm/yr. Precipitation exceeds 130 cm/yr in surrounding mountains.
Surface-water hydrology	Streams drain from surrounding mountains into basins. Basins generally slope toward a central depression with a main drainage that is dry most of the time. Many basins have playas in their lowest depressions. Ground-water discharge to streams can occur in basin depressions. (Planert and Williams, 1995)	Jordan River is the major stream in Salt Lake Valley with tributaries originating in the Wasatch Mountains. Diversions on Jordon River supply irrigation water. Small streams originating in Oquirrh Mountains infiltrate before reaching the Jordan River.
Land use	Undeveloped basins are unused, grazing, and rural residential. Developed basins are urban, suburban and agricultural.	Urban, suburban, rural residential, and agricultural.
Water use	Ground-water withdrawals from wells supply water for agricultural irrigation and municipal use. Population increases since the 1960's have increased the percentage of water being used for municipal supply.	Approximately 70 percent of total water use is from ground water and 30 percent from surface water. Total ground-water withdrawal estimated for 1997–2001 is about 500,000 m^3/d with 30 percent applied to household use and 70 percent applied to lawn and agricultural irrigation.
	Geology	
Surficial geology	Tertiary and Quaternary unconsolidated to moderately consolidated fluvial gravel, sand, silt and clay basin-fill deposits include alluvial fans, flood plain deposits, and playas. (Robson and Banta, 1995; Planert and Williams, 1995)	Tertiary and Quaternary unconsolidated fluvial basin-fill sediments consist of gravel, sand, silt, clay, tuff, and lava interbedded with lacustrine deposits of historical Lake Bonneville.
Bedrock geology	Mountains surrounding basins are composed of Paleozoic to Tertiary bedrock formations. Tertiary volcanic and metamorphic rocks are in general impermeable. Paleozoic and Mesozoic carbonate rocks are cavernous allowing inter-basin flow in some areas. (Robson and Banta, 1995; Planert and Williams, 1995)	Wasatch Mountains east of Salt Lake Valley are composed of Paleozoic and Precambrian quartzites and crystalline rocks. Oquirrh Mountains west of Salt Lake Valley are composed of Tertiary volcanic rocks and associated sulfide mineralization.

Table 2.1. Summary of hydrogeologic and ground-water-quality characteristics for the Basin and Range basin-fill aquifers and the Salt Lake Valley regional study area, Utah.—Continued

[m, meters; cm/yr, centimeters per year; hm^3/yr; cubic hectometers per year; m^2/d, squared meters per day; m^3/d, cubic meters per day; m/d, meters per day; ET, evapotranspiration; mg/L, milligrams per liter]

Characteristic	Basin and Range basin-fill aquifers	Salt Lake Valley regional study area
	Ground-water hydrology	
Aquifer conditions	Unconfined basin-fill aquifers surrounded by relatively impermeable bedrock mountains and foothills. Basin ground-water flow systems are generally isolated and not connected with other basins except in some locations where basins are hydraulically connected via cavernous carbonate bedrock.	Unconfined basin-fill aquifer along basin margins, which transitions to confined basin-fill aquifer under the central and northern parts of Salt Lake Valley because of the shallow confining layer. Confined aquifer is composed of interbedded clays, silts, sands, and gravels. Ground-water flow is from valley margins toward central and northern valley and upward toward discharge area along the Jordan River.
Hydraulic properties	Transmissivity ranges from less than 93 m^2/d to greater than 2,790 m^2/d. In general, alluvial fan deposits near basin margins are more conductive than flood plain and lacustrine deposits near basin centers. (Robson and Banta, 1995; Planert and Williams, 1995)	Transmissivity ranges from less than 930 m^2/d to more than 4,600 m^2/d (Lambert, 1995a). Horizontal hydraulic conductivity ranges from 3.05×10^{-4} to 19.8 m/d (Thiros, 1992). Vertical hydraulic conductivity ranges from 1.6×10^{-5} to 6.1×10^{-3} m/d (Thiros, 1992).
Ground-water budget	Recharge to basin fill deposits is from surface-water runoff in mountains where precipitation is highest. Ground-water discharges naturally as evapotranspiration (ET) to playas and stream channels in basin depressions. Ground-water withdrawal from wells is largest component of discharge from Basin and Range aquifers. (Robson and Banta, 1995)	Recharge to basin fill is from subsurface inflow from surrounding mountains, local precipitation, seepage from streams, and infiltration from irrigation. Discharge is to streams (Jordan River), wells, ET, springs, drains, and the Great Salt Lake.
	Ground-water quality	
	Water quality varies between basins. Dissolved solids can range from less than 500 mg/L to over 35,000 mg/L. Generally, low-dissolved solids, oxic water occurs near recharge areas of basin margins. High-dissolved solids anoxic water occurs with depth or near basin centers and playa lakes (Robson and Banta, 1995; Planert and Williams, 1995).	Dissolved solids are lowest along the eastern basin margins (200 to 500 mg/L) where calcium-bicarbonate type water dominates. Dissolved solids along the western margin ranges from 400 to 1,100 mg/L, and the water type is calcium-sulfate because mountains west of valley are volcanic rocks with sulfide mineralization. Dissolved solids concentrations increase and water type transitions to sodium-chloride from south to north in the valley. Water near valley margins is generally oxic with redox conditions transitioning to anoxic near the valley center.

Topography and Climate

The Salt Lake Valley is almost 1,300 km^2 in area, trends from south to north, and terminates on its northern end at the Great Salt Lake. The Wasatch Range bounds the valley on the east, and the Oquirrh and Traverse Mountains bound the valley on the west-southwest (fig. 2.2). The valley floor slopes gradually up from an elevation of 1,280 m near Great Salt Lake to about 1,580 m on the foothills of the Wasatch Range and Oquirrh and Traverse Mountains. Elevations in the Wasatch Range exceed 3,300 m. The Oquirrh and Traverse Mountains are not as extensive as the Wasatch Range, and the upper elevations are around 2,900 m.

The Salt Lake Valley is classified as semiarid, and average annual precipitation ranges from about 35 cm/yr in the northwest and central parts of Salt Lake Valley to about 60 cm/yr along the foothills of the Wasatch Range (Prism Group, Oregon State University, 2006). Precipitation in the surrounding mountain areas can exceed 130 cm/yr and occurs mainly as snowfall during the winter months. March and April are the wettest months of the year. Average daytime temperatures range from 33.6˚C in July to 3.1˚C in January.

Surface-Water Hydrology

The major stream in the Salt Lake Valley is the Jordan River (fig. 2.2), which flows north along the axis of the valley and discharges to the Great Salt Lake. Flow in the Jordan River is diverted through seven major canals as it enters the south end of Salt Lake Valley to feed an extensive surface-water irrigation system. The Jordan River has seven major tributaries, all of which originate in the Wasatch Range. Several small streams originate in the Oquirrh and Traverse Mountains but none reach the Jordan River.

Land Use

Land in the Salt Lake Valley was historically used for agriculture, which included grazing, orchards, dry farming, and irrigated cultivation. As population grew and commercial activities increased, agricultural lands have slowly converted to residential and commercial use. The population in Salt Lake Valley more than doubled between 1963 and 2001. As of 2002, land use in the valley is categorized as 39 percent residential, 29 percent commercial/industrial, 21 percent water/riparian/idle, and 11 percent agricultural (Utah Department of Natural Resources, 2003).

Water Use

Most water use in the Salt Lake Valley in 2000 was for domestic purposes. An estimated 30 percent of the domestic water supply goes toward household uses, and about 70 percent of the domestic water supply is used for lawn watering. About 70 percent of the domestic water supply is from surface water, and the remaining 30 percent comes from public-supply wells located throughout the valley (Lawrence Spangler, U.S. Geological Survey, written commun., September 2005) (fig. 2.2).

Conceptual Understanding of the Ground-Water System

The hydrogeology of the Salt Lake Valley has been closely scrutinized since the middle of the 20th century (Marine and Price, 1964; Hely and others, 1971; Waddell and others, 1987; Thiros, 1992 and 1995; and Lambert, 1995a). Those discussions, particularly Lambert (1995a), are paraphrased and summarized in the following sections.

Geology

The ground-water system underlying the Salt Lake Valley exists in unconsolidated and semiconsolidated basin-fill material. The source of basin fill is the surrounding mountains. The depositional basin was created by a downward rotation of the consolidated-rock base of the valley relative to the Wasatch Range. The thickness of the unconsolidated basin fill averages about 600 m and in some places exceeds 1,200 m.

The basin-fill material consists mostly of Tertiary- and Quaternary-age clay, silt, sand, gravel, tuff, and lava. The depositional history of these sediments is extremely complex (Marine and Price, 1964). In the late Pleistocene (10,000 to 25,000 years ago), changes in regional climate and topography created conditions that led to numerous cycles of inundation and subsequent desiccation of the Salt Lake Valley by a series of ancient lakes. The most extensive and recent ancient lake was Lake Bonneville. As the valley filled with water, lacustrine and deltaic depositional mechanisms dominated. As lakes dried, these sediments were reworked and redeposited by stream erosion. Previously inundated areas were eroded and received stream-channel and flood-plain deposits. Alluvial fans formed along the mountain fronts at canyon mouths; glacial and mud-rock flow deposits also were laid down at the valley margins. As lakes reappeared and filled the valley, lacustrine deposition again predominated. These cyclic changes in the depositional environment resulted in the interlayered lacustrine, alluvial, and glacial sediments that compose the basin fill. Generally, coarse-grained sediments are common near the mountains, and finer grained sediments are dominant in the low-lying areas in the central and northern parts of the valley.

The consolidated rock of the Wasatch Range consists mainly of Precambrian and Paleozoic quartzites, tillites, and carbonates. Where the range borders the southeastern Salt Lake Valley, the consolidated rock is Tertiary-age quartz monzonite. The Oquirrh and Traverse Mountains consist of Paleo-

zoic-age quartzite and limestone. Volcanism occurred during the Oligocene Period and resulted in sulfide mineralization.

Ground-Water Occurrence and Flow

A generalized conceptual model of the saturated basin-fill material consists of (1) a confined aquifer underlying the central and northern parts of the Salt Lake Valley that transitions to unconfined conditions along the margins of the valley (hereinafter called the basin-fill aquifer), (2) a shallow confining layer that overlies the basin-fill aquifer in the center of the valley, and (3) shallow, unconfined ground water above the shallow confining layer (fig. 2.3). The basin-fill aquifer is composed of interbedded clay, silt, sand, and gravel and exists within the discontinuous and interconnected lenses of sand and gravel. The confining layer is composed of finer grained, lower permeability materials than the underlying basin-fill aquifer. The top of the shallow confining layer generally lies within 30 m of land surface. Along the margins of the valley, the higher energy depositional environment deposited coarse-grained sediment, and the ground-water system in these areas is conceptualized as a single, deeper unconfined aquifer without vertical stratification. Ground water is withdrawn from wells completed in both the confined basin-fill aquifer beneath the shallow confining layer and the unconfined basin-fill aquifer near the margins of the valley.

The Salt Lake Valley basin-fill aquifer exists primarily in the Quaternary-age basin-fill material that ranges from 0 to 600 m thick. Quaternary-age material generally overlies relatively impermeable, semiconsolidated sediments of Tertiary and pre-Tertiary age (Arnow and others, 1970, p. D257). In scattered areas, the Tertiary-age basin fill is more permeable and yields small amounts of ground water to wells. Where the Tertiary-age sediments yield water, they are considered part of the basin-fill aquifer.

Ground water flows laterally from the primary recharge areas at the valley margins to the center and northern parts of the valley (fig. 2.4). An upward gradient is established between the confined aquifer and the unconfined aquifer as water moves laterally beneath the confining layer. In the central part of the valley, ground water flows upward in the confined aquifer, through the overlying confining layer and into the shallow unconfined aquifer. From the shallow unconfined aquifer, water discharges primarily into the Jordan River, to drains, and is used by riparian vegetation, or evaporates at land surface. Ground water along the valley margins is generally 30

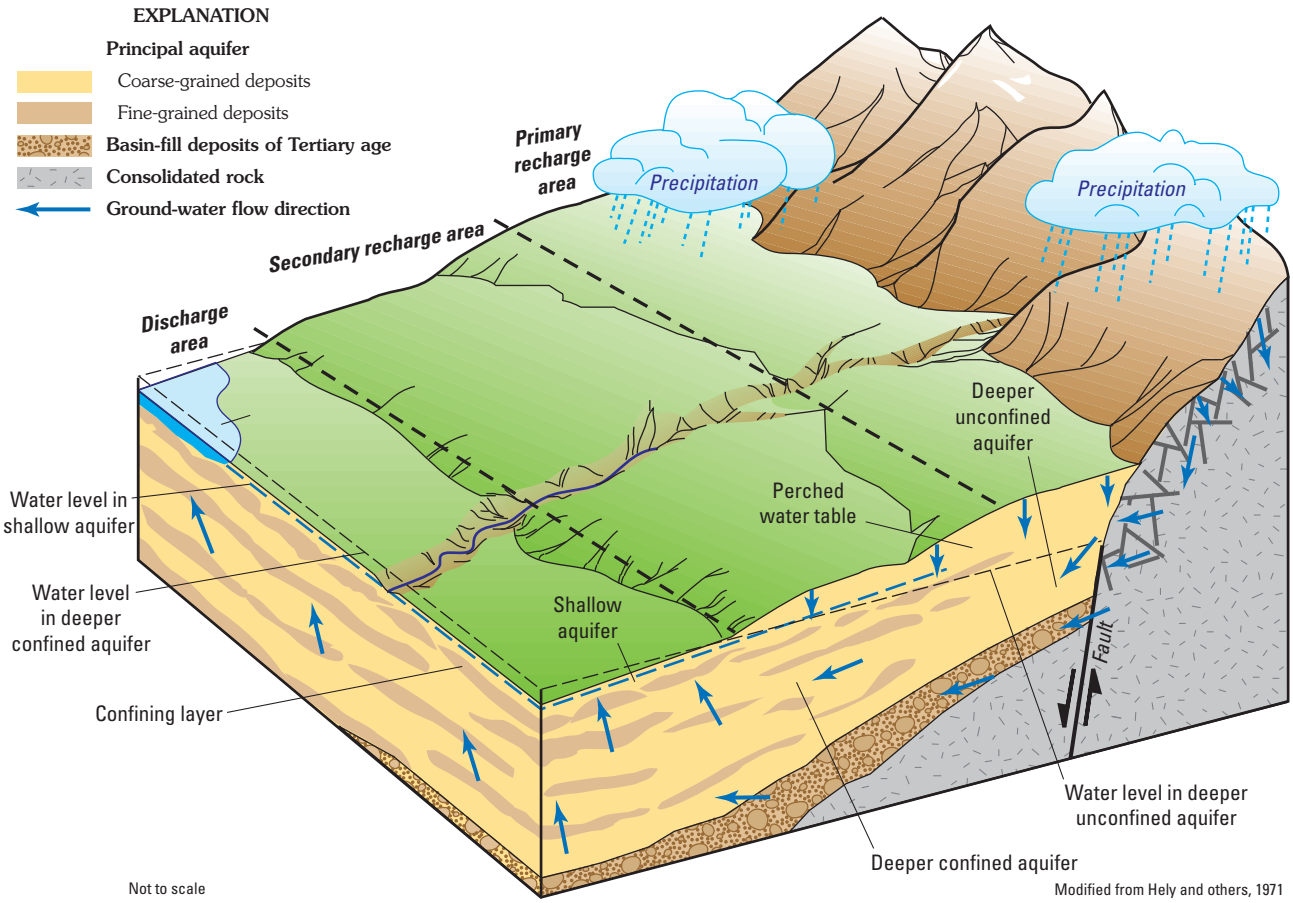

Figure 2.3. Basin-fill ground-water flow system, Salt Lake Valley regional study area, Utah.

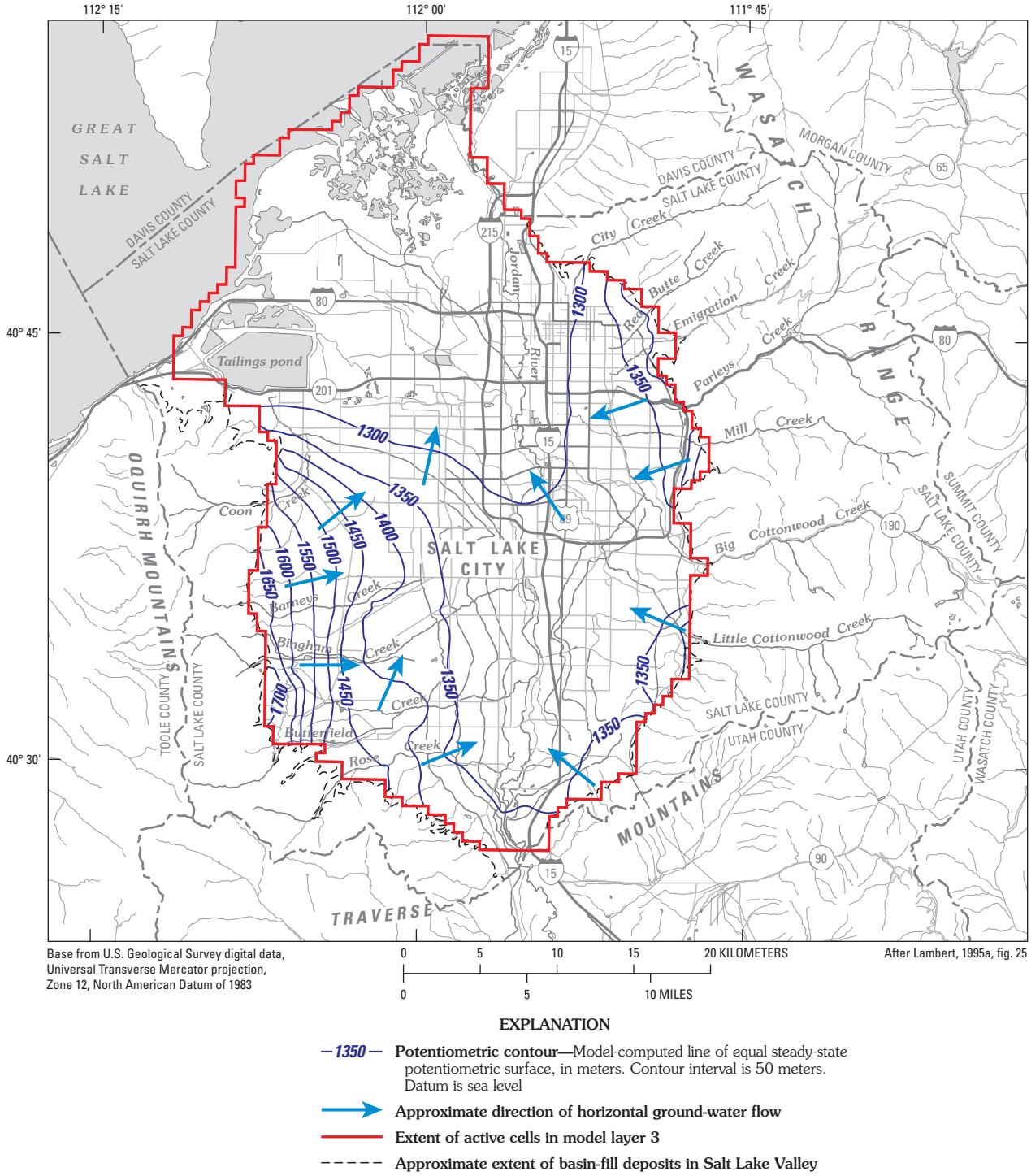

Base from U.S. Geological Survey digital data, Universal Transverse Mercator projection, Zone 12, North American Datum of 1983

0 5 10 15 20 KILOMETERS

0 5 10 MILES

After Lambert, 1995a, fig. 25

EXPLANATION

—1350— **Potentiometric contour**—Model-computed line of equal steady-state potentiometric surface, in meters. Contour interval is 50 meters. Datum is sea level

Approximate direction of horizontal ground-water flow

Extent of active cells in model layer 3

Approximate extent of basin-fill deposits in Salt Lake Valley

Figure 2.4. Elevation of model-computed basin-fill aquifer potentiometric surface for 1997–2001 average conditions, Salt Lake Valley regional study area, Utah.

to 100 m below land surface. In the central and northern areas, water levels are usually 3 to 6 m below land surface.

Aquifer Hydraulic Properties

Hydraulic properties of aquifer materials were determined using a number of standard techniques that include (1) ground-water gradients and discharge, (2) slug tests, (3) laboratory testing of core samples, (4) aquifer tests, and (5) specific-capacity data. Generally, these methods test only small intervals and volumes of the aquifer, and quantification commonly produces results that vary over several orders of magnitude. This range of aquifer hydraulic properties is not surprising and reflects the complex depositional history of the Salt Lake Valley.

Horizontal hydraulic conductivity for the shallow unconfined aquifer is estimated to range from 9.1 X 10^{-4} to 19.8 m/d (Thiros, 1995), and horizontal hydraulic conductivity for the confining layer is estimated to range from 1.2 X 10^{-4} to 0.7 m/d (S.A. Thiros, U.S. Geological Survey, written commun., 1993). Vertical hydraulic conductivity of the shallow confining layer ranges from 1.6 X 10^{-5} to 0.3 m/d (Hely and others, 1971; Waddell and others, 1987; Thiros, 1992; Thiros, 1995). Transmissivity of the basin-fill aquifer is estimated to range from less than 930 to more than 4,600 m^2/d (Lambert, 1995a). Hydraulic conductivity, which equals transmissivity divided by saturated thickness of the aquifer, was given an upper limit of 70 m/d on the basis of reported hydrologic properties for aquifers of the Basin and Range Province (Bedinger and others, 1986). Vertical hydraulic conductivity of the basin-fill aquifer is estimated to range from 0.003 to 1.5 m/d (Lambert, 1995a, p. 17 and fig. 8).

Storage-coefficient values in confined zones of the Salt Lake Valley are estimated to range from 1 X 10^{-3} to less than 1 X 10^{-4} (Hely and others, 1971). The range of probable storage-coefficient values for confined zones of the basin-fill aquifer was assumed also to apply to the storage-coefficient value of the shallow confining layer. Hely and others (1971) estimated that specific yield of the shallow unconfined aquifer ranges from 0.10 to 0.20 and that specific yield of unconfined basin-fill aquifer near the basin margins has an upper limit of 0.3.

Water Budget

Recharge to the ground-water system in the Salt Lake Valley is primarily from (1) subsurface inflow from consolidated rock at the margins of the valley; (2) infiltration of precipitation on the valley floor; (3) seepage from streams and canals; and (4) infiltration from commercial crop fields, lawns, and gardens. Discharge occurs to (1) streams and canals, (2) pumping and flowing wells, (3) evapotranspiration, (4) springs, (5) drains, and (5) Great Salt Lake. Recharge and discharge quantities were originally estimated by Hely and others (1971) for conditions during 1964 through 1968. Since then, components of the water budget have been reevaluated because of additional data collection and interpretation (Herbert and others, 1985; Waddell and others, 1987; Lambert, 1995a). The conceptual water budget presented here is a combination of previously estimated water budgets and scaling of water-budget components determined from the 1969–91 transient ground-water flow model calibration (Lambert, 1995a, p. 21) to 1997–2001 conditions on the basis of precipitation and streamflow ratios. Given the various timeframes, the complexity of the ground-water system, and the density of available data, individual components of the budget are probably only accurate to within +/– 25 percent. Conceding these limitations, the conceptual budget described here is presented as a 1997–2001 average and is considered a steady-state portrayal because ground-water pumping rates and climatic conditions were relatively stable for the time period.

Recharge

The movement of ground water from the fractures, joints, and pore space of the mountain block into the adjacent basin fill (mountain-block recharge) recharges the aquifer at an estimated rate of approximately 402,000 m^3/d for 1997–2001. This rate was computed using a long-term average water balance for the mountains and measured hydraulic gradients at the margins of the valley. It is scaled to 1997–2001 conditions by using the ratio of 1997–2001 average Wasatch Range precipitation to the long-term average Wasatch Range precipitation. Inflow is distributed along the mountain front on the basis of the inferred relative permeability of the different consolidated rock units (Hely and others, 1971, table 21; Waddell and others, 1987, table 1).

Recharge from infiltration of precipitation on the valley floor was estimated to be about 257,000 m^3/d for 1997–2001. The 1997–2001 recharge rate is scaled from a long-term estimate by using the ratio of average 1997–2001 precipitation rate to the long-term precipitation rate in the Salt Lake Valley. The long-term estimate was derived by subtracting the sum of surface runoff and precipitation consumed by evapotranspiration from the total precipitation falling on the valley (Hely and others, 1971, table 21; Waddell and others, 1987, table 1; Lambert, 1995a, table 5).

Mountain-front recharge occurs where mountain streams enter the Salt Lake Valley and lose surface water to the coarser grained basin-fill material at the canyon mouths. Ground water moving laterally through the channel fill beneath the streams (underflow) also contributes recharge to adjoining basin-fill material at canyon mouths. In addition, recharge from underflow occurs where the Jordan River enters the southern end of the Salt Lake Valley. On the basis of data collected by Hely and others (1971, p. 123 and table 5) and modifications by Lambert (1995a, table 5), the annual recharge rate from streams and underflow for 1997–2001 is estimated to be about 60,800 m^3/d. Surface-water seepage losses were established from data collected at multiple streamflow-gaging stations on individual streams. Estimates of underflow were determined using Darcy's law. In addition to streams, there is also seep-

age from the major irrigation canals in the valley. On the basis of gain/loss measurements made in 1983 (Herbert and others, 1985), recharge from the canals is estimated at about 94,500 m^3/d. Total recharge from streams and canals is estimated as 155,300 m^3/d.

Infiltration from agricultural irrigation return flow during 1997–2001 was estimated to be about 108,000 m^3/d on the basis of historical estimates (Hely and others, 1971, p. 126) and modifications by Lambert (1995a, p. 37). Infiltration from irrigation of lawns and gardens is estimated to be about 33,700 m^3/d (Lambert, 1995a, p. 33). Historical estimates (Hely and others, 1971) assumed recharge rates that were about 30 percent of the applied irrigation water and were based on generalized field-application efficiency rates and a series of site-specific farm studies. The more recent recharge estimates are close to 15 percent of the applied irrigation water (Lambert, 1995a).

Discharge

The largest component of natural discharge from the aquifer system in the Salt Lake Valley is seepage to the Jordan River and the lower reaches of its principal tributaries. Based on records from an extensive streamflow-gaging network, Hely and others (1971, p. 83 and 136) estimated annual ground-water discharge from the confined part of the basin-fill aquifer to the Jordan River and its tributaries to be 500,000 m^3/d. The average rate of ground-water discharge to canals in the valley is estimated as 33,700 m^3/d and is based on gain/loss measurements made by Herbert and others (1985) and adjusted to average climatic conditions by Waddell and others (1987,
p. 27). The relation between the aquifer and streams/canals in the central parts of the valley has been fairly stable over time, and the previous analysis of discharge is likely a reasonable estimate of discharge for 1997–2001.

Ground water is withdrawn from wells in the Salt Lake Valley for the purposes of public-supply, irrigation, industrial, and domestic/stock uses. The average withdrawal for all these purposes for 1997–2001 is estimated as 500,000 m^3/d for the Salt Lake Valley regional study area. Withdrawals for public-supply, irrigation, and industrial uses is estimated as about 399,000 m^3/d and is based on annual withdrawal compilations made by the U.S. Geological Survey. The remaining withdrawals, 101,000 m^3/d, are from thousands of small domestic and stock wells scattered throughout the valley and were estimated by Hely and others (1971, p. 140) for the period 1964–68. The domestic/stock withdrawal estimate for 1964-1968 also was used for the period 1997–2001 because it was beyond the scope of this study to inventory all domestic and stock wells in the valley. Some verification of the domestic/stock withdrawals was made in 1992 by examining the number of recorded water rights for domestic and stock uses (Utah Department of Natural Resources, Division of Water Rights, written commun., 1992) and results indicate that the 1964–68 estimate is reasonable for 1997–2001.

Initial estimates of evapotranspiration in the Salt Lake Valley were based on the assumption that evapotranspiration occurred in areas where the average depth to ground water is less than 5 m (Hely and others, 1971, p. 179). To determine an evapotranspiration rate, the area of shallow ground water was divided into five major land categories: bare ground, cultivated land, urban land, waterfowl-management land, and areas of phreatophytes. The phreatophyte area was further subdivided by plant group. Each land category and plant group was assigned a maximum evapotranspiration rate (Hely and others, 1971, p. 179; Blaney and Criddle, 1962). The multiplication of area and rate (adjusted to compensate for an average depth to ground water) resulted in an evapotranspiration rate of 203,000 m^3/d for 1964–1968. Revised evapotranspiration estimates made initially by Waddell and others (1987, p. 29), and later by Lambert (1995a, p. 36), resulted in evapotranspiration rates about 40 percent less than that presumed by Hely and others (1971). The revised evapotranspiration estimates were made by simulating ground-water flow in the valley-fill aquifer of Salt Lake Valley and matching model-computed and measured water levels for the shallow unconfined portion of the aquifer. On the basis of the last stress period of the transient calibration by Lambert (1995a, p. 37), which incorporates land-use changes in Salt Lake Valley from 1968 to 1991, the average evapotranspiration rate estimated for 1997–2001 is 109,000 m^3/d.

Discharge to springs in the Salt Lake Valley from the basin-fill aquifer was originally estimated by Hely and others (1971) on the basis of springflow water-rights records. For the present modeling study, the 1964–1968 estimates of Hely and others (1971) are used to estimate a spring discharge rate of about 64,110 m^3/d for 1997–2001. The estimate assumes springflows have been relatively stable over time because the springs are located near the valley margins and are generally not affected by pumping.

Ground-water discharge from the shallow unconfined aquifer to surface drains is known to occur near the Great Salt Lake and to buried storm drains in Salt Lake City. Data are available to quantify flow to the surface drains near the Great Salt Lake, and a rate of 17,000 m^3/d was estimated by Hely and others (1971 p. 136). The discharge rate to buried drains in the Salt Lake City area is not known. However, a steady discharge to and from storm drains has been observed by the employees of the Salt Lake City Department of Public Utilities (Charles H. Call, Jr., oral commun., 1992) and is assumed by them to be seepage from shallow ground water. Lambert (1995a) simulated 33,700 m^3/d of discharge to surface and buried drains during steady-state simulation, and for lack of additional information, this is the rate assumed for 1997–2001.

Ground-water discharge to Great Salt Lake has been calculated by applying Darcy's law along an arbitrary line parallel to and near the shore of Great Salt Lake (Mower, 1968, p. D71; Hely and others, 1971, p. 136; and Waddell and others, 1987, p. 29). The average discharge rate from previous computations is about 11,800 m^3/d, and this same rate is

assumed for 1997–2001. Discharge to the Great Salt Lake is less than 1 percent of the Salt Lake Valley water budget.

Ground-Water Quality

General ground-water quality in the Salt Lake Valley has identifiable trends along east- west and south-north transects. Dissolved-solids concentrations in ground water are lowest along the margins of the valley where most recharge occurs. Along the eastern margin, dissolved-solids concentrations typically range from 200 to 500 mg/L, and the dominant ions are calcium and bicarbonate. On the western margin, dissolved-solids concentrations are in the range of 400 to 1,100 mg/L, and the dominant ions are calcium, magnesium, and sulfate. The difference in water quality between the eastern and western parts of the valley can be explained by rock type in the recharge source area. Recharge on the eastern valley margin originates in the Wasatch Range, which is predominantly composed of crystalline rock and quartzites, and recharge on the western valley margin originates in the Oquirrh and Traverse mountains, which are predominantly composed of Tertiary-age volcanic rocks and associated sulfide mineralization.

Dissolved-solids concentrations increase and the dominant ions become sodium and chloride as ground water flows from south to north in the Salt Lake Valley. As ground-water residence time increases from south to north, there is more time for ground water to interact with the basin-fill materials and dissolved-solids concentrations increase. Vertically, the best quality water is at intermediate depths within the basin-fill aquifer. Water in the shallow unconfined aquifer and deeper in the basin-fill aquifer have the highest dissolved-solids concentrations.

Oxidation-reduction zones within the Salt Lake Valley (fig. 2.5) have been conceptualized on the basis of recharge and discharge areas using existing water-quality data. The basin-fill aquifer is spatially divided into three areas with respect to recharge/discharge processes (Anderson and others, 1994): (1) the primary recharge area, (2) the secondary recharge area, and (3) the discharge area. These areas are delineated on the basis of lithology reported on drillers' logs and vertical hydraulic-gradient information.

The primary recharge area exists along the valley margins where coarse-grained sediments dominate the basin fill and the vertical hydraulic gradient is downward. Fresh oxygenated water recharges the aquifer in these areas, and ground water is assumed oxygen reducing (oxic). The secondary recharge area occurs where layers of fine-grained sediment are present, but the vertical gradient is still downward. The secondary recharge area is adjacent to and downgradient from the primary recharge area, although a small amount of recharge from land surface does occur. Because ground water in the secondary recharge area has a longer residence time than that in the primary recharge area, the secondary recharge area is conceptualized as a transition zone between oxic and iron-reducing (anoxic) conditions. The discharge zone is defined by extensive fine-grained layering within the aquifer and vertically upward gradients. No recharge occurs in the discharge zone and ground water in these areas has experienced the longest travel and residence times, so it is assumed that all dissolved oxygen has been consumed and ground water is iron-reducing in the discharge zone.

Ground-Water Flow Simulations

The modular ground-water flow simulation code MODFLOW-2000 (Harbaugh and others, 2000) was used to simulate a steady-state condition based on the annual average conditions for the 5-year period from 1997 through 2001. A previously calibrated transient model, which was constructed and calibrated to 1968 steady-state and 1969–91 transient-state conditions by Lambert (1995a), was used by this study to simulate a steady-state stress period representing 1997–2001 average conditions. This study modified specified-flux terms of the Lambert (1995a) model defining (1) inflow from consolidated rock, (2) infiltration of precipitation, (3) inflow from streams, and (4) discharge to pumping wells to reflect 1997–2001 average values. Aquifer parameters of hydraulic conductivity and transmissivity were not recalibrated by this modeling exercise. The steady-state model is considered a reasonable approximation of ground-water flow conditions for 1997–2001 because ground-water pumping rates and climatic conditions were relatively stable for the time period.

Modeled Area and Spatial Discretization

The model grid covers 1,152 km^2 of the Salt Lake Valley and is subdivided into 94 rows, 62 columns (fig. 2.6) and 7 layers. Each model cell represents 0.32 km^2 of surface area. The shallow unconfined aquifer is represented by model layer 1, and the shallow confining layer is represented by model layer 2. The thicknesses of model layers 1 and 2 vary spatially and roughly represent the estimated depth and thickness of the shallow unconfined aquifer and the underlying shallow confining layer, respectively. Layers 1 and 2 are both simulated as convertible between confined and unconfined conditions depending on the elevation of hydraulic head computed by the model. The basin-fill aquifer is simulated by model layers 3 through 7. Layer 3 defines the areal extent of the model domain and is simulated as convertible between confined and unconfined conditions. Model layers 4 to 7 represent deep sediments of the basin-fill aquifer and are simulated as confined. Model layers 3 to 5 are each 46 m thick, and model layer 6 is 61 m thick. Model layer 7 ranges in thickness from 61 m to more than 460 m. The term "vertical column," as used in this report, is the set of model cells with the same row and column index.

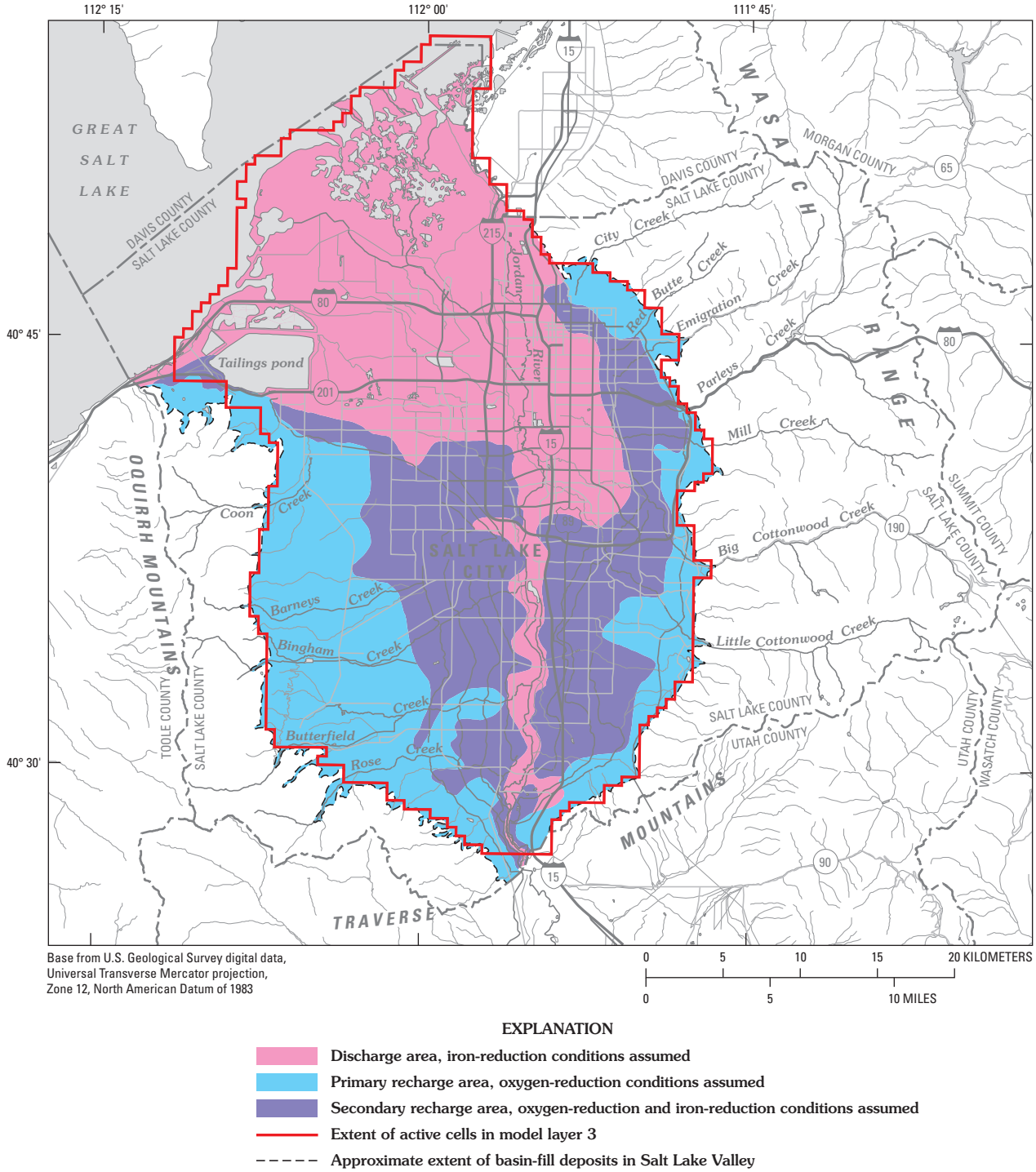

Figure 2.5. Generalized oxidation-reduction classification zones, Salt Lake Valley regional study area, Utah.

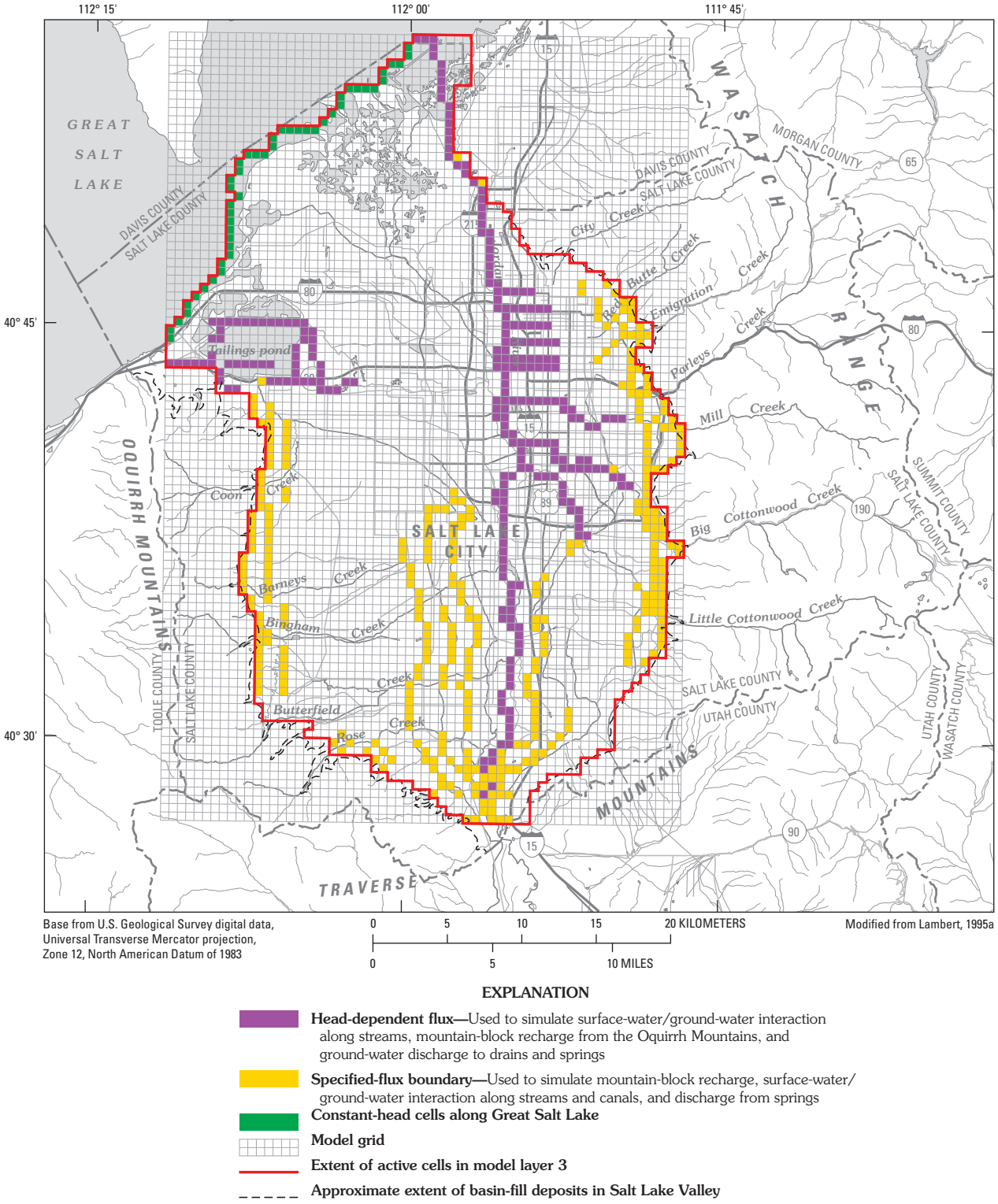

Figure 2.6. Ground-water flow model grid and selected boundary conditions, Salt Lake Valley regional study area, Utah.

Boundary Conditions and Model Stresses

Boundary conditions assigned to the numerical solution are mathematical equations that represent flow at surface boundaries and internal sources and sinks. Boundary types and the specified amounts of recharge and discharge were assigned to reflect the conceptual analysis of the ground-water flow system (table 2.2). Four distinct boundary types are used to simulate recharge, discharge, and the spatial extent of the Salt Lake Valley ground-water system. They are (1) no flow, (2) specified flux, (3) head-dependent flux, and (4) constant head. A no-flow boundary simulates an impermeable hydrologic boundary. Unless specifically noted, the horizontal and vertical extent of the model domain is set by no-flow boundaries. A specified-flux boundary allows a specified rate of flow across a boundary as a function of location and time. A head-dependent boundary allows the flow rate across the boundary surface to change in response to changes in water level in the aquifer adjacent to the boundary. Constant-head boundaries fix the water level in a cell, and flows to or from adjacent cells are computed on the basis of that water level.

No-flow boundaries are assigned at the base of the modeled area. The base corresponds to the contact between consolidated rock of pre-Tertiary age and basin-fill material or to a depth within the basin fill below which sediments were assumed not to contribute substantially to the basin-fill ground-water flow system. The northern border of the modeled area approximates a flow line and was treated as a no-flow boundary.

Recharge

Mountain-block recharge from the consolidated rock of the Wasatch Range and the Oquirrh Mountains is simulated using specified-flux cells with the MODFLOW Well package placed at the lateral edges of the model domain in layers 3 or 4 (Lambert, 1995a, fig. 9; fig. 6). Some mountain-block recharge occurs at the northern end of the Oquirrh Mountains, and that portion is simulated using MODFLOW General-head cells (Lambert, 1995a, fig. 15). The amount of specified flow from mountain-block recharge, which is the conceptualized amount minus the Oquirrh Mountains inflow, is set at 401,918 m^3/d (table 2.2).

Recharge from precipitation on the valley floor is simulated as a specified flux using the MODFLOW Recharge package over the entire modeled area except in areas of dense commercial and residential development (Lambert, 1995a). In dense commercial and residential areas, it is assumed that precipitation was collected as runoff in drain systems and routed directly to surface-water bodies. The total simulated amount of precipitation recharge (256,712 m^3/d) is adjusted from the conceptualized amount of precipitation recharge (257,000 m^3/d) to account for the dense commercial and residential area. The MODFLOW Recharge package applies recharge to the uppermost active cells in a vertical column of cells. The total recharge is spatially distributed across the model grid on the basis of mean annual precipitation isohyets (Hely and others, 1971).

Specified-flux cells using the MODFLOW Recharge package also are used to simulate mountain-front recharge from streams at and near where they enter the Salt Lake Valley from the mountains (Lambert, 1995a, fig. 12) and underflow recharge through stream-channel fill where the Jordan River enters the Salt Lake Valley. The boundaries are placed in the uppermost active cell of the model grid that corresponds to the location of the stream. This recharge encompasses the major streams that flow out of the Wasatch Range. Simulated recharge from the streams draining the Wasatch Range is 54,000 m^3/d, and lateral subsurface flow associated with the Jordan River is set at 6,850 m^3/d. Recharge from the five canals that traverse the west and east sides of the valley is simulated using the MODFLOW Well package to specify flux. Ground-water recharge from canals is simulated approximately 94,500 m^3/d.

Recharge from irrigation of fields, lawns, and gardens is simulated as a specified flux using the MODFLOW Recharge package. The cells where the recharge is applied correspond either to irrigated land use or residential land use (lawns and gardens). Recharge was distributed on the basis of the percentage of cell area that represents irrigated fields or residential land and the irrigation recharge is added to the precipitation recharge. The recharge amount for commercial fields is about 108,200 m^3/d (19.5 cm/yr), and for residential areas the rate is about 33,700 m^3/d (5.5 cm/yr) (Lambert, 1995a, p. 33 and 42).

Discharge

Discharge to streams is simulated as head-dependent boundaries using the MODFLOW River package along the length of the Jordan River and the lower reaches of three of the Wasatch Range streams (Lambert, 1995a, fig. 15; fig. 6). The boundary cells are in model layer 1 and follow the course of the streams. Riverbed altitude and length were determined from 1:24,000 U.S. Geological Survey topographic maps. Riverbed width and thickness were not measured; it was assumed that the riverbed thickness is one tenth of the riverbed width. Hydraulic conductivities of the riverbed range from 0.03 to 3.0 m/d and were determined during model calibration (Lambert, 1995a).

Discharge to canals is simulated as a specified flux using the MODFLOW Well package for four of the major canals in the Salt Lake Valley where ground-water discharge has been measured (Herbert and others, 1985). The boundaries are in the uppermost active cell of the vertical columns that correspond to the canal locations (Lambert, 1995a, fig. 12).

Public-supply, irrigation, and industrial wells that withdrew more than 170 m^3/d for the period 1997–2001 are simulated in the ground-water flow model. The wells are simulated as specified-flux cells using the MODFLOW Well package located in model cells corresponding to actual well locations.

Discharge is disseminated vertically to the appropriate model layer on the basis of well depth and the depth of well-casing perforations (Lambert, 1995a, p. 27). All simulated wells withdraw water from model layers 3 to 7. The discharge quantity associated with individual wells is based on annual-withdrawal data reported by the water user and compiled by the U.S. Geological Survey and the Utah Division of Water Rights. The steady-state model simulates the average withdrawals for 1997–2001, and the total simulated withdrawal in the model is 398,630 m^3/d.

The model also simulates withdrawals from domestic and stock wells. These small-diameter wells are represented as specified-flux cells using the MODFLOW Well package in model layer 3. Areal distribution of withdrawal was determined from individual locations recorded by the Utah Department of Natural Resources, Division of Water Rights (Lambert, 1995a, p. 28). Simulated withdrawals from domestic and stock wells are 101,370 m^3/d.

Evapotranspiration (ET) is simulated as head-dependent flux boundaries using the MODFLOW ET package. The boundary is placed at cells in model layer 1 that correspond to the areas of shallow ground water in the Salt Lake Valley (Lambert, 1995a, fig. 15). The extinction-depth value assigned to the boundary is 4.6 m (Lambert, 1995a). As a generalization, the presence of phreatophytes is limited to areas of the valley where the water table is within 4.6 m of land surface. To capture the variability in water use by different plant species, the evapotranspiration area was subdivided into five major land-use categories. Each category is assigned a maximum evapotranspiration rate. The rate was adjusted to a finalized value during model calibration by Lambert (1995a, p. 36).

Six major freshwater springs exist in the Salt Lake Valley, and they are simulated as specified-flux boundaries using the MODFLOW Well package. The boundaries are assigned to model layer 3 and correspond to the locations of the springs (Lambert, 1995a, fig. 12). Total specified spring discharge is 64,110 m^3/d.

Surface drains near Great Salt Lake and buried drains beneath commercial and residential areas in Salt Lake City are simulated using MODFLOW Drain cells placed in model layer 1 at the location of actual drains. Drain altitudes were specified to be 3.0 m less than land-surface altitude. Drain conductance was not measured, and initial values were arbitrarily selected. Drain conductance was adjusted during model calibration by Lambert (1995a, p. 36) to simulate a conceptually reasonable amount of ground-water discharge (23,562 m^3/d).

The hydrologic connection between the basin-fill aquifers and Great Salt Lake is simulated with a constant-head boundary (fig. 2.6). The boundary is in model layer 1 along the northwestern border of the model domain at cells that represent the shore of Great Salt Lake (Lambert, 1995a, fig. 15). The water level assigned to the constant-head boundary is 1,280 m, which is the approximate average historical water level of the lake.

Table 2.2. Model-computed water budget for 1997–2001 average conditions, Salt Lake Valley regional study area, Utah.

[m^3/d, cubic meters per day]

Water-budget component	Specified flow (m^3/d)	Computed flow (m^3/d)	Total flow (m^3/d)	Percentage of inflow or outflow
Model inflow (recharge)				
Mountain-block recharge	401,918	40,548	442,466	43.8
Precipitation	256,712		256,712	25.4
Irrigation return flow	141,918		141,918	14.1
Mountain-front recharge, rivers, and canals	155,342	13,425	168,767	16.7
TOTAL INFLOW			**1,009,863**	**100**
Model outflow (discharge)				
Jordan River		287,123	287,123	28.3
Wells				
Public supply, irrigation, and industrial	398,630		398,630	39.4
Domestic and stock	101,370		101,370	10.0
Evapotranspiration		104,658	104,658	10.3
Springs and drains	64,110	23,562	87,671	8.7
Canals	30,411		30,411	3.0
Great Salt Lake		3,288	3,288	0.3
TOTAL OUTFLOW			**1,013,151**	**100**

Model Calibration and Sensitivity

The model used to simulate the average conditions for 1997–2001 was calibrated to 1968 steady-state and 1969–91 transient conditions by Lambert (1995a). The model was calibrated by manually adjusting calibration variables (primarily transmissivity) within a prescribed range until a reasonable match between model-computed and observed conditions was achieved. A complete discussion of the calibration process is given in Lambert (1995a). Final values of transmissivity assigned to the basin-fill aquifer by Lambert (1995a) are shown in figure 2.7 and represent the sum of transmissivity values for the basin-fill aquifer (model layers 3 to 7). Calibrated aquifer hydraulic properties presented by Lambert (1995a) were not altered during the present modeling exercise.

As part of the model calibration by Lambert (1995a), a sensitivity analysis was done to determine the response of the model to changes in selected parameters. Calibration parameters were independently adjusted and the effects of these adjustments on simulated water levels and flow rates were noted. Generally, the calibrated model is more sensitive to decreasing parameter values than to increasing values. Specifically, the model is most sensitive to decreasing horizontal hydraulic conductivity in model layer 1; decreasing conductivity caused substantial increases in water levels in model layer 1. The model is relatively insensitive to (1) increasing vertical leakance within model layers 1 to 3, (2) decreasing or increasing vertical leakance within model layers 3 to 7, and (3) increasing riverbed conductance (Lambert, 1995a).

Model-Computed Hydraulic Heads

The ability of the ground-water flow model to simulate the 1997–2001 average conditions was judged by comparing model-computed and measured water levels at 45 wells for the same time period. Measured levels are an average of the February, March, and April 1997–2001 available water-level data for the well. The overall goodness of fit of the model to the observation data was evaluated using summary measures and graphical analyses. The root-mean-squared error (RMSE), the range of head and residuals, the standard deviation, and the standard-mean error of the residuals (SME) were used to evaluate the model calibration. The RMSE is a measure of the variance of the residuals and was calculated as:

$$RMSE = \sqrt{\frac{\sum_{i=1}^{N} (h_{meas} - h_{sim})i^2}{N}}$$

where h_{meas} is the measured hydraulic head, h_{sim} is the model-computed (simulated) hydraulic head, $(h_{meas} - h_{sim})$ is the head residual, and N is the number of wells used in the computation. If the ratio of the RMSE to the total head change in the modeled area is small, then the error in the head calculations is a small part of the overall model response (Anderson and Woessner, 1992).

The SME was calculated as:

$$SME = \frac{\sigma(h_{meas} - h_{sim})i}{\sqrt{N}}$$

where $\sigma(h_{meas} - h_{sim})$ is the standard deviation of the residuals.

A simple method of assessing model fit is to plot the model-computed hydraulic head values against the measured observations. For a perfect fit, all points should fall on the 1:1 diagonal line. Figure 2.8 shows the locations of water-level measurements and the spatial distribution of head residuals and indicates a random spatial distribution of the residuals. A plot of the model-computed heads against the measured hydraulic heads for the Salt Lake Valley regional ground-water flow model (fig. 2.9) indicates reasonable model fit. The mean residual for the entire model is 3.91 m, and residuals range from –18.3 m to 38.4 m. The RMSE for the entire model is 10.7 m, which is about 6 percent of the 183-m range of head observations in the model, and the head residuals appear to be randomly distributed at all values of measured head (fig. 2.10). The standard deviation of the residuals is 10.1 m, and the SME is 1.58 m. The results of these comparisons indicate a reasonable match between model-computed and measured water levels for 1997–2001 average conditions.

Model-Computed Water Budget

The model-computed water budget for 1997–2001 average conditions in the Salt Lake Valley regional study area is presented in table 2.2. Many of the water-budget components simulated by the model were specified values and some components were computed by the model. Mountain-block recharge (43.8 percent of inflow) and recharge from precipitation and irrigation (39.5 percent of inflow) were the primary sources of recharge to the basin-fill aquifer. Recharge from mountain-front recharge, streams, and canals provided the remaining 16.7 percent of ground-water inflow. Discharge to wells (49.4 percent of outflow) and to the Jordan River (28.3 percent of outflow) were the primary ground-water outflows from the Salt Lake Valley. Model-computed ground-water discharge to the Jordan River was less than the conceptual model estimate, but, in general, the model-computed water budget is in reasonable agreement with the conceptual estimates of flow discussed in the Water Budget section of this chapter.

Simulation of Areas Contributing Recharge to Wells

The steady-state regional flow model was used to estimate areas contributing recharge and zones of contribution for 94 wells in the Salt Lake Valley using the MODPATH (Pollock, 1994) particle-tracking post processor and methods outlined in Section 1 of this Professional Paper. The model-computed areas contributing recharge represent advective ground-water flow and do not account for mechanical dispersion. Advection-dispersion transport simulations would likely yield larger areas contributing recharge than advective particle-tracking simulations because the effects of dispersion caused by aquifer heterogeneity would be included.

Along with flux output from the models, the MODPATH simulations require effective porosity values to calculate ground-water flow velocities. An effective porosity value of 0.4 was assigned to model layers 1 and 2, and an effective porosity value of 0.3 was assigned to model layers 3 to 7 based on estimates from Lambert (1995b, p. 21).

The simulated contributing areas can be summarized as long and narrow and truncating at specified-flux boundaries at the edges of the model domain (fig. 2.11). This summarization holds true regardless of the pumping rate at individual wells. The shape of the contributing areas is controlled mainly by the recharge being simulated primarily along the edges of the model domain, which is a direct reflection of the conceptualization of the ground-water system. Truncation of contributing areas at model boundaries indicates mountain-front and mountain-block recharge from the Wasatch Range and Oquirrh Mountains is contributing water to public-supply wells in the Salt Lake Valley.

The simulated median traveltime for water to move from its recharge point to a well ranges from 5 to 780 years based on particle-tracking estimates from MODPATH. The longest traveltimes are associated with contributing areas for wells on the west side of the Salt Lake Valley.

Limitations and Appropriate Use of the Model

The ground-water flow model for the Salt Lake Valley regional study area was designed to evaluate the water budget for 1997–2001 and to delineate areas contributing recharge to public-supply wells. Sources of error in the model may include the steady-state flow assumption and errors in the conceptual model of the system, hydraulic properties, and boundary conditions.

The assumption of steady-state conditions for the Salt Lake Valley regional model is reasonable for the time period of study because sources of recharge and discharge were relatively stable from 1997 to 2001. However, model calibration parameters were taken from an existing model and were not specifically calibrated to match water levels and flow rates during 1997-2001. Further calibration for transient conditions may be needed to accurately represent temporal changes in the system.

Measured water levels, historical water-level changes, and simulated discharge to the Jordan River were not accurately simulated in all areas of the model domain. However, a reasonable match was obtained between simulated and measured hydrologic conditions for the study area.

Sensitivity analysis indicates that increasing vertical hydraulic conductivity relative to calibrated estimates within reasonable limits does not substantially affect model results. Vertical gradients and flows simulated in the model are controlled, in part, by the vertical hydraulic conductivity incorporated in model input. The uncertainty of the final estimates of vertical hydraulic conductivity of the basin fill (and thus, vertical leakance between model layers) should be noted when evaluating simulation results.

The simulation of mountain-block recharge to the basin-fill aquifer is greatly simplified. In the physical system, flow from the consolidated-rock aquifer to the basin-fill aquifer is controlled by the difference in water level between the two aquifers. The head-dependent nature of flow between the two aquifers is not accounted for in the model other than at the northern end of the Oquirrh Mountains. Large declines in basin-fill hydraulic heads near the margins of the valley may increase inflow from consolidated rock, and because the model represents mountain-block recharge using constant-flux boundaries, changes in mountain-block flux resulting from drawdown in the basin fill are not simulated.

Computed areas contributing recharge and traveltimes through zones of contribution are based on a calibrated model and estimated effective porosity values. In a steady-state model, changes to input porosity values do not change the area contributing recharge to a given well. Changes to input porosity values, however, will change computed traveltimes from recharge to discharge areas in direct proportion to changes in porosity because there is an inverse linear relation between ground-water flow velocity and effective porosity and a direct linear relation between traveltime and effective porosity. For example, a one-percent decrease in porosity will result in a one-percent increase in velocity and a decrease in particle traveltime. There are no available porosity data for this, so a reasonable estimated value was chosen. A detailed sensitivity analysis of porosity distributions was beyond the scope of this study, although future work could compare simulated ground-water traveltimes to ground-water ages to more thoroughly evaluate effective porosity values.

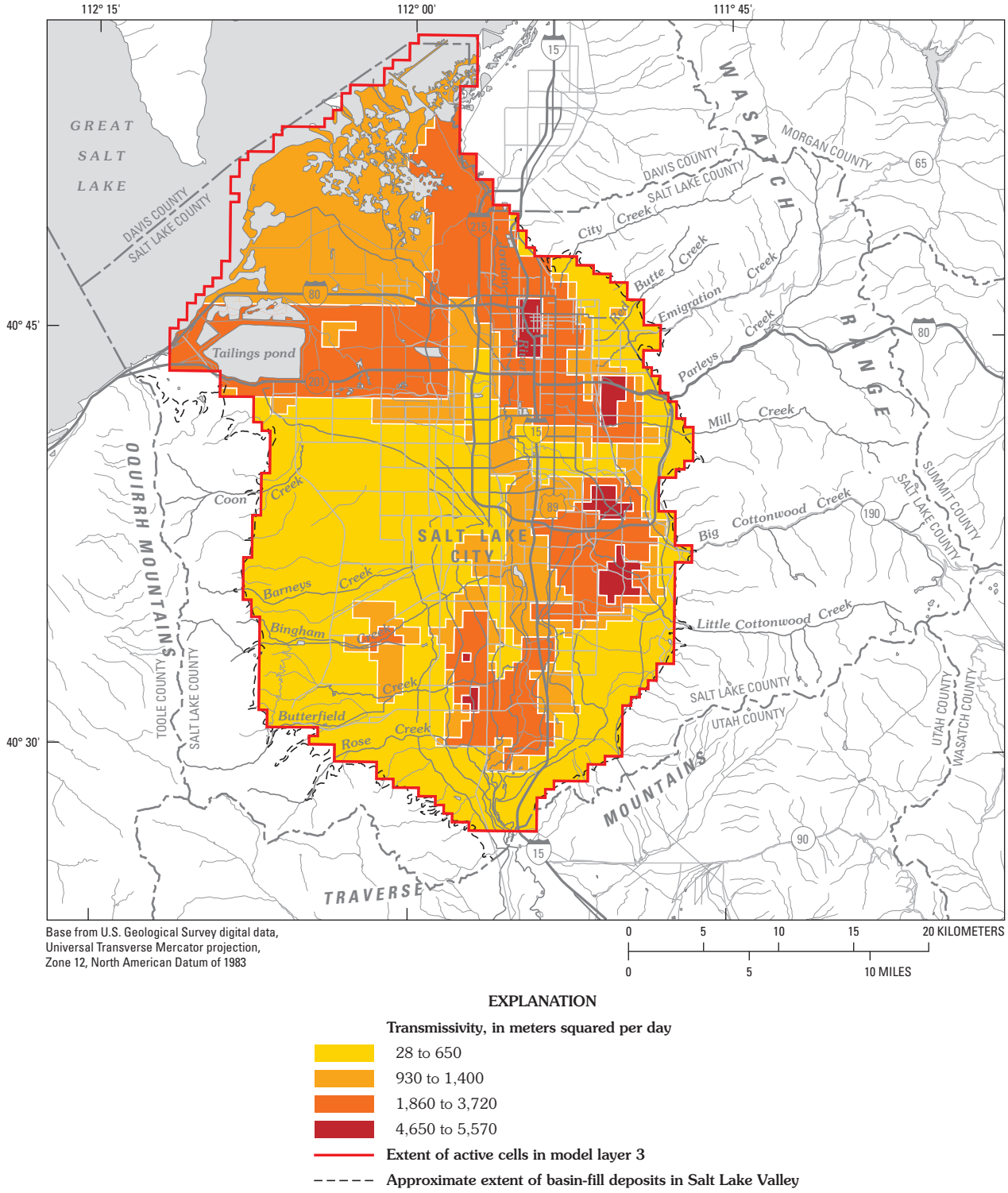

EXPLANATION

Transmissivity, in meters squared per day

- 28 to 650
- 930 to 1,400
- 1,860 to 3,720
- 4,650 to 5,570
- Extent of active cells in model layer 3
- Approximate extent of basin-fill deposits in Salt Lake Valley

Figure 2.7. Distribution of basin-fill aquifer transmissivity for the calibrated ground-water flow model, Salt Lake Valley regional study area, Utah.

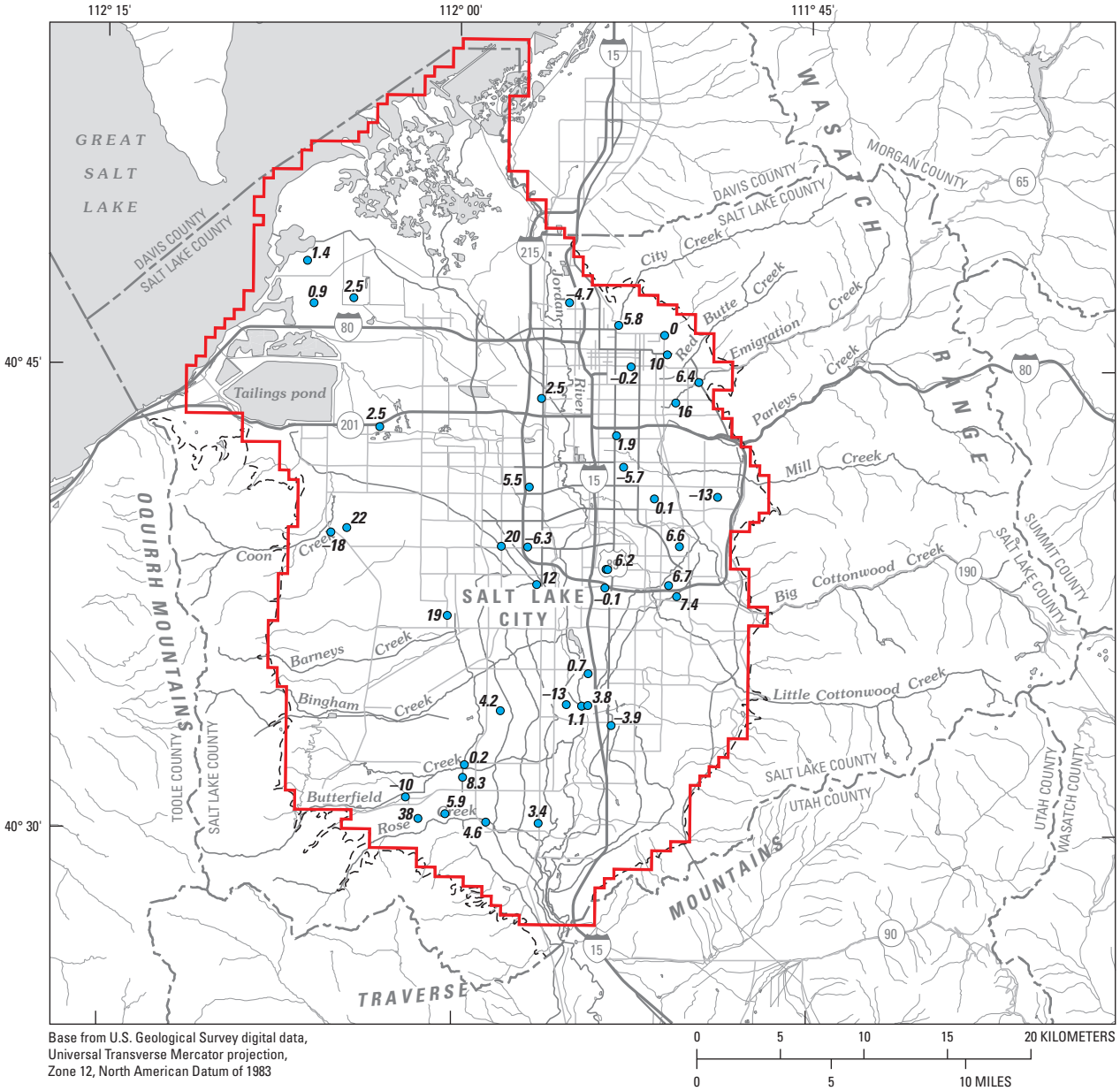

Figure 2.8. Water-level observation well locations and head residuals, Salt Lake Valley regional study area, Utah.

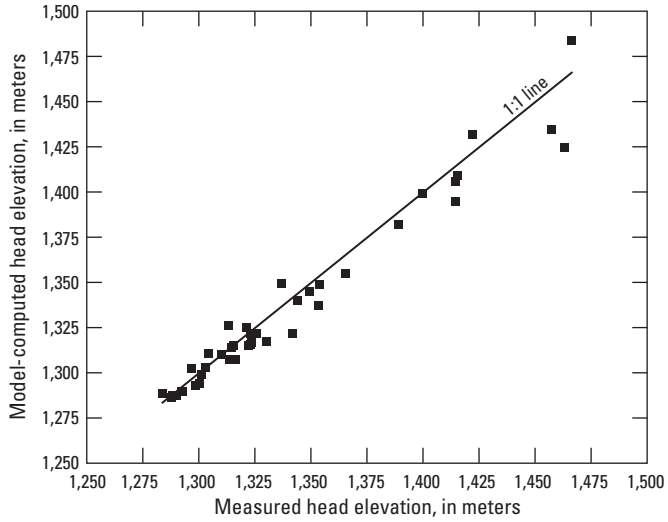

Figure 2.9. Relation between model-computed and measured hydraulic head, Salt Lake Valley regional study area, Utah.

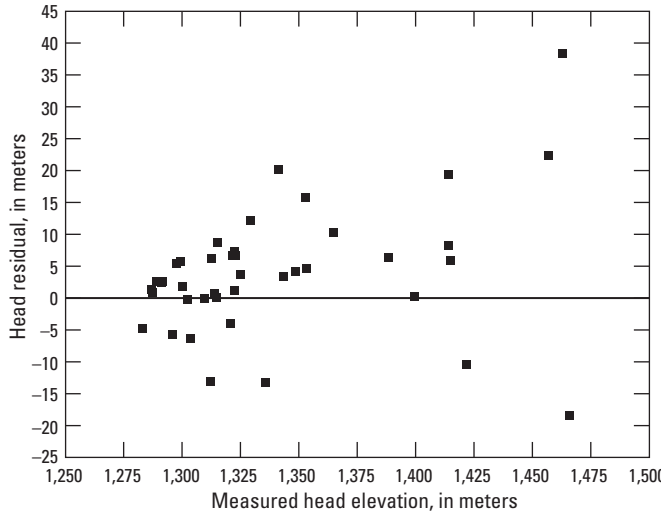

Figure 2.10. Relation between head residual and measured hydraulic head, Salt Lake Valley regional study area, Utah.

The Salt Lake Valley regional ground-water-flow model uses previously calibrated aquifer properties and boundary conditions and provides a reasonable representation of average ground-water flow conditions for 1997–2000. The model is suitable for evaluating regional water budgets and ground-water flow paths in the study area for the time period of interest but may not be suitable for long-term predictive simulations. This regional model provides a useful tool to evaluate aquifer vulnerability at a regional scale, to facilitate comparisons of ground-water traveltime between regional aquifer systems, and to guide future detailed investigations in the study area.

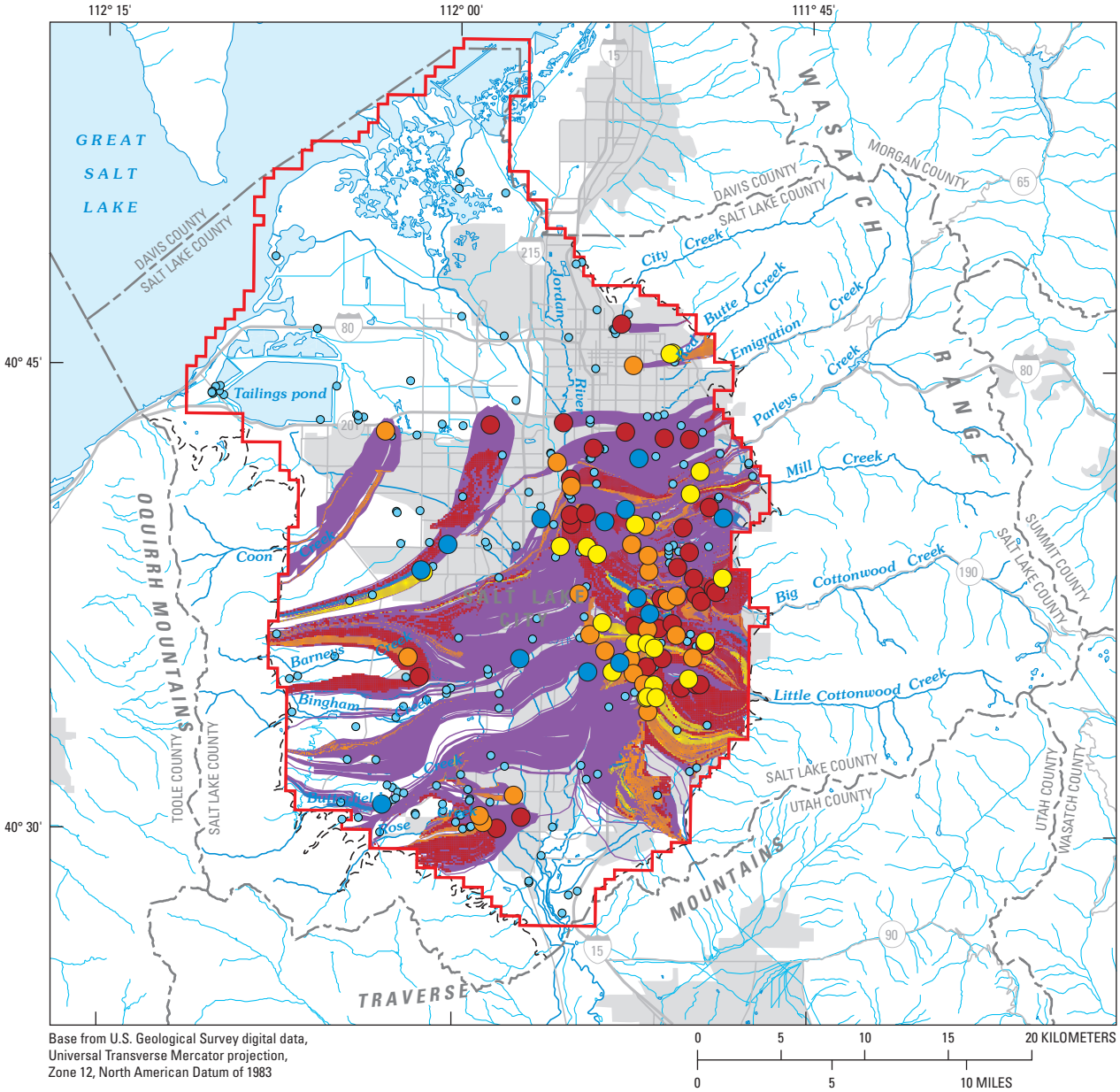

Figure 2.11. Model-computed areas contributing recharge to public-supply wells, Salt Lake Valley regional study area, Utah.

References Cited

Anderson, P.B., Susong, D.D., Wold, S.R., Heilweil, V.M., and Baskin, R.L., 1994, Hydrogeology of recharge areas and water quality of the principal aquifers along the Wasatch Front and adjacent areas, Utah: U.S. Geological Survey Water-Resources Investigations Report 93–4221, 74 p.

Anderson, M.P., and Woessner, W.W., 1992, Applied ground-water modeling: Academic Press, Inc., New York, 381 p.

Arnow, Ted, Van Horn, Richard, and LaPray, Reed, 1970, The pre-Quaternary surface in the Jordan Valley, Utah, *in* Geological Survey Research 1970: U.S. Geological Survey Professional Paper 700–D, p. D257–D261.

Blaney, H.F., and Criddle, W.D., 1962, Determining consumptive use and irrigation requirements: U.S. Agricultural Research Service Technical Bulletin 1275, 59 p.

Bedinger, M.S., Langer, W.H., and Reed, J.E., 1986, Synthesis of hydraulic properties of rocks in the Basin and Range Province, southwestern United States: U.S. Geological Survey Water-Supply Paper 2310, p. 35–43.

Harbaugh, A.W., Banta, E.R., Hill, M.C., and McDonald, M.G., 2000, MODFLOW-2000, the U.S. Geological Survey modular ground-water model—User guide to modularization concepts and the ground-water flow process: U.S. Geological Survey Open-File Report 00–92, 121 p.

Hely, A.G., Mower, R.W., and Harr, C.A., 1971, Water resources of Salt Lake County, Utah: Utah Department of Natural Resources Technical Publication no. 31, 244 p.

Herbert, L.R., Cruff, R.W., and Waddell, K.M., 1985, Seepage study of six canals in Salt Lake County, Utah, 1982–83: Utah Department of Natural Resources Technical Publication no. 82, 95 p.

Lambert, P.M., 1995a, Numerical simulation of ground water flow in basin-fill material in Salt Lake Valley, Utah: Utah Department of Natural Resources Technical Publication no. 110–B, 58 p.

Lambert, P.M., 1995b, Particle–tracking analysis of time-related capture zones for selected public-supply wells in Salt Lake Valley, Utah: Utah Department of Natural Resources Technical Publication no. 110–C, 36 p.

Marine, I.W., and Price, Don, 1964, Geology and ground-water resources of the Jordan Valley, Utah: Utah Geological and Mineralogical Survey Bulletin 7, 68 p.

Maupin, M.A., and Barber, N.L., 2005, Estimated withdrawals from principal aquifers in the United States, 2000: U.S. Geological Survey Circular 1279, 47 p.

Mower, R.W., 1968, Ground-water discharge toward Great Salt Lake through valley fill in the Jordan Valley, Utah, in Geological Survey Research 1968: U.S. Geological Survey Professional Paper 600–D, p. D71–D74.

Pollock, D.W., 1994, User's guide for MODPATH/MODPATH-PLOT, Version 3—A particle tracking post-processing package for MODFLOW, the U.S. Geological Survey finite-difference ground-water flow model: U.S. Geological Survey Open-File Report 94-464, accessed June 15, 2004, at *http://water.usgs.gov/nrp/gwsoftware/modpath41/modpath41.html*

Planert, Michael, and Williams, J.S., 1995, Ground Water Atlas of the United States—California and Nevada: U.S. Geological Survey Hydrologic Atlas 730–B.

PRISM Group, Oregon State University, 2006, Prism products matrix, accessed Feb. 7, 2007, at *http://www.ocs.oregonstate.edu/prism/products/matrix.phtml?vartype=ppt&view=maps*

Robson, S.G., and Banta, E.R., 1995, Ground Water Atlas of the United States—Arizona, Colorado, New Mexico, and Utah: U.S. Geological Survey Hydrologic Atlas 730–C.

Thiros, S.A., 1992, Selected hydrologic data for Salt Lake Valley, Utah, 1990–92, with emphasis on data from the shallow unconfined aquifer and confining layers: U.S. Geological Survey Open-File Report 92–640, duplicated as Utah Hydrologic-Data Report no. 49, 44 p.

Thiros, S.A., 1995, Chemical composition of ground water, hydrologic properties of basin-fill material, and ground-water movement in Salt Lake Valley, Utah: Utah Department of Natural Resources Technical Publication no. 110–A.

Utah Department of Natural Resources, Division of Water Resources, 2003, Agricultural land-use program, AgriculturalUrbanLandUse2003.shp: accessed Sept. 22, 2005, at URL *http://agrc.utah.gov/agrc_sgid/sgidlib/sgid024_agriculturalurbanlanduse2003.htm*

Waddell, K.M., Seiler, R.L., Santini, Melissa, and Solomon, D.K., 1987, Ground-water conditions in Salt Lake Valley, Utah, 1969–83, and predicted effects of increased withdrawals from wells: Utah Department of Natural Resources Technical Publication no. 87, 69 p.

Hydrogeologic Settings and Ground-Water Flow Simulations of the Eagle Valley and Spanish Springs Valley Regional Study Areas, Nevada

By Donald H. Schaefer, Jena M. Green, and Michael R. Rosen

Section 3 of

Hydrogeologic Settings and Ground-Water Flow Simulations for Regional Studies of the Transport of Anthropogenic and Natural Contaminants to Public-Supply Wells—Studies Begun in 2001

Edited by Suzanne S. Paschke

Professional Paper 1737–A

U.S. Department of the Interior
U.S. Geological Survey

U.S. Department of the Interior
DIRK KEMPTHORNE, SECRETARY

U.S. Geological Survey
Mark D. Myers, Director

U.S. Geological Survey, Reston, Virginia: 2007

For product and ordering information:
World Wide Web: http://www.usgs.gov/pubprod
Telephone: 1-888-ASK-USGS

For more information on the USGS--the Federal source for science about the Earth, its natural and living resources, natural hazards, and the environment:
World Wide Web: http://www.usgs.gov
Telephone: 1-888-ASK-USGS

Any use of trade, product, or firm names is for descriptive purposes only and does not imply endorsement by the U.S. Government.

Although this report is in the public domain, permission must be secured from the individual copyright owners to reproduce any copyrighted materials contained within this report.

Suggested citation:
Schaeffer, D.H., and Rosen, M.R., 2007, Hydrogeologic settings and ground-water flow simulations of the Eagle Valley and Spanish Springs Regional Study Areas, Nevada, *section 3 of* Paschke, S.S., ed., Hydrogeologic settings and ground-water flow simulations for regional studies of the transport of anthropogenic and natural contaminants to public-supply wells—studies begun in 2001: Reston, Va., U.S. Geological Survey Professional Paper 1737–A, pp. 3–1 – 3–33

Contents

Abstract 3–1
Introduction 3–1
Purpose and Scope 3–1
Study Area Description 3–3
Topography and Climate 3–3
Surface-Water Hydrology 3–3
Land Use 3–8
Water Use 3–8
Conceptual Understanding of the Ground-Water System 3–8
Geology 3–8
Ground-Water Occurrence and Flow 3–10
Aquifer Hydraulic Conductivity 3–10
Water Budget 3–11
Ground-Water Quality 3–13
Ground-Water Flow Simulations 3–16
Modeled Areas and Spatial Discretizations 3–16
Boundary Conditions 3–16
Recharge 3–16
Discharge 3–17
Aquifer Hydraulic Conductivity 3–17
Model Calibration 3–25
Model-Computed Hydraulic Heads 3–25
Model-Computed Water Budget 3–27
Simulation of Areas Contributing Recharge to Public-Supply Wells 3–28
Limitations and Appropriate Use of the Model 3–28
References Cited 3–32

Figures

Maps showing:
3.1. Location of the Eagle Valley and Spanish Springs Valley regional study areas within the Basin and Range basin-fill aquifers. 3–2
3.2*A*. Topography, hydrologic features, and locations of public-supply wells, Eagle Valley regional study area, Nevada. 3–6
3.2*B*. Topography, hydrologic features, and locations of public-supply wells, Spanish Springs Valley regional study area, Nevada. 3–7
Generalized block diagrams showing:
3.3*A*. Basin-fill ground-water flow system of the Eagle Valley regional study area, Nevada. 3–9
3.3*B*. Basin-fill ground-water flow system of the Spanish Springs Valley regional study area, Nevada. 3–9

Maps showing:

3.4*A*. Basin-fill aquifer potentiometric surface and oxidation-reduction classification zones, Eagle Valley regional study area, Nevada.....3–14

3.4*B*. Basin-fill aquifer potentiometric surface and oxidation-reduction classification zones, Spanish Springs Valley regional study area, Nevada. 3–15

3.5*A*. Ground-water flow model grid, boundary conditions, and location of public-supply wells, Eagle Valley regional study area, Nevada. 3–18

3.5*B*. Ground-water flow model grid, boundary conditions, and location of public-supply wells, Spanish Springs Valley regional study area, Nevada. 3–19

3.6*A*. Distribution of hydraulic conductivity for model layer 1, Eagle Valley regional study area, Nevada. 3–20

3.6*B*. Distribution of hydraulic conductivity for model layer 2, Eagle Valley regional study area, Nevada. 3–21

3.7*A*. Distribution of hydraulic conductivity for model layer 1, Spanish Springs Valley regional study area, Nevada. 3–22

3.7*B*. Distribution of hydraulic conductivity for model layer 2, Spanish Springs Valley regional study area, Nevada. 3–23

3.7*C*. Distribution of hydraulic conductivity for model layer 3, Spanish Springs Valley regional study area, Nevada. 3–24

Graphs showing:

3.8*A*. Relation between residual head and measured hydraulic head, Eagle Valley regional study area, Nevada. 3–26

3.8*B*. Relation between residual head and measured hydraulic head, Spanish Springs Valley regional study area, Nevada. 3–26

Maps showing:

3.9*A*. Model-computed areas contributing recharge to public-supply wells, Eagle Valley regional study area, Nevada. 3–30

3.9*B*. Model-computed areas contributing recharge to public-supply wells, Spanish Springs Valley regional study area, Nevada. 3–31

Tables

3.1. Summary of hydrogeologic and ground-water quality characteristics for the Basin and Range basin-fill aquifers and the Eagle Valley and Spanish Springs Valley regional study areas, Nevada 3–4

3.2. Average ground-water pumping rates for public-supply wells, 1997– 2001, Eagle Valley regional study area, Nevada. 3–12

3.3. Average ground-water pumping rates for public-supply wells, 1997– 2001, Spanish Springs Valley regional study area, Nevada..... 3–13

3.4. Model-computed water budget for 1997–2001 average conditions, Eagle Valley regional study area, Nevada. 3–27

3.5. Model-computed water budget for 1997–2001 average conditions, Spanish Springs Valley regional study area, Nevada..... 3–27

Hydrogeologic Settings and Ground-Water Flow Simulations of the Eagle Valley and Spanish Springs Valley Regional Study Areas, Nevada

By Donald H. Schaefer, Jena M. Green, and Michael R. Rosen

Abstract

The transport of anthropogenic and natural contaminants to public-supply wells was evaluated in the Eagle and Spanish Springs Valleys, Nevada, as part of the U.S. Geological Survey National Water-Quality Assessment Program. The valley-fill aquifers in the Eagle and Spanish Springs Valleys regional study areas are representative of the Basin and Range basin-fill aquifers, are important sources of water for agricultural irrigation and public water supply, and are susceptible and vulnerable to contamination. Three-dimensional, steady-state ground-water flow models were developed for the Basin and Range basin-fill aquifers in each of the valleys and calibrated to average conditions for the period from 1997 to 2001. The calibrated models and advective particle-tracking simulations were used to compute ground-water flow paths, areas contributing recharge, and traveltimes from recharge areas for public-supply wells. The Eagle Valley ground-water flow model is a two-layer, steady-state finite-difference model modified from a previous finite-element model of the basin, and the Spanish Springs Valley ground-water flow model is a three-layer, steady-state finite-difference model modified from a previous two-layer finite-difference model of the basin. Modeling results for the Eagle Valley indicate ground-water recharge is primarily from streams flowing into the basin from the surrounding mountains (mountain-front recharge) and from subsurface flow from the adjacent mountains (mountain-block recharge); ground-water discharge is primarily to public-supply wells and evapotranspiration. Modeling results for the Spanish Springs Valley indicate ground-water recharge is primarily from precipitation, irrigation, and canal leakage; ground-water discharge is primarily to public-supply wells and evapotranspiration. Particle-tracking simulations for all 20 public-supply wells in Eagle Valley indicate that areas contributing recharge extend from the pumping wells in the valley to areas of mountain-block and mountain-front recharge along the edges of the basin with traveltimes from recharge areas on the order of 30 to 50 years. Particle-tracking results for all eight public-supply wells in Spanish Springs Valley were similar to those in the Eagle Valley with areas contributing recharge extending to the mountain front but with slightly greater traveltimes on the order of 50 to 100 years. In both the Eagle and Spanish Springs Valley models, areas contributing recharge extended to the general-head boundary cells along the mountain-front boundary of the alluvial aquifer indicating mountain-front and mountain-block recharge are important sources of water for the public-supply wells.

Introduction

Two regional study areas within the Nevada Basin and Range study unit of the U.S. Geological Survey National Water-Quality Assessment (NAWQA) Program were included in the study of the transport of anthropogenic and natural contaminants to public-supply wells (TANC). The first TANC regional study area is Eagle Valley, which includes Carson City and is part of the Carson River Basin. The second TANC regional study area is Spanish Springs Valley, north of Sparks, which is in the Truckee River Basin. The study areas are within the Basin and Range basin-fill aquifers, which are important water sources for agricultural irrigation and drinking-water supply throughout the region (fig. 3.1).

Purpose and Scope

The purpose of this Professional Paper section is to present the hydrogeologic setting of the Eagle Valley and Spanish Springs Valley regional study areas. The section also documents the setup and calibration of steady-state regional ground-water flow models for the study areas. Ground-water flow characteristics, pumping-well information, and water-quality data were compiled from existing data to develop a conceptual understanding of ground-water conditions in the study area. A two-layer steady-state ground-water flow model of the Eagle Valley basin-fill aquifer and a three-layer steady-state ground-water flow model of the Spanish Springs Valley basin-fill aquifer were developed and calibrated to average conditions for the period from 1997 to 2001. The 5-year

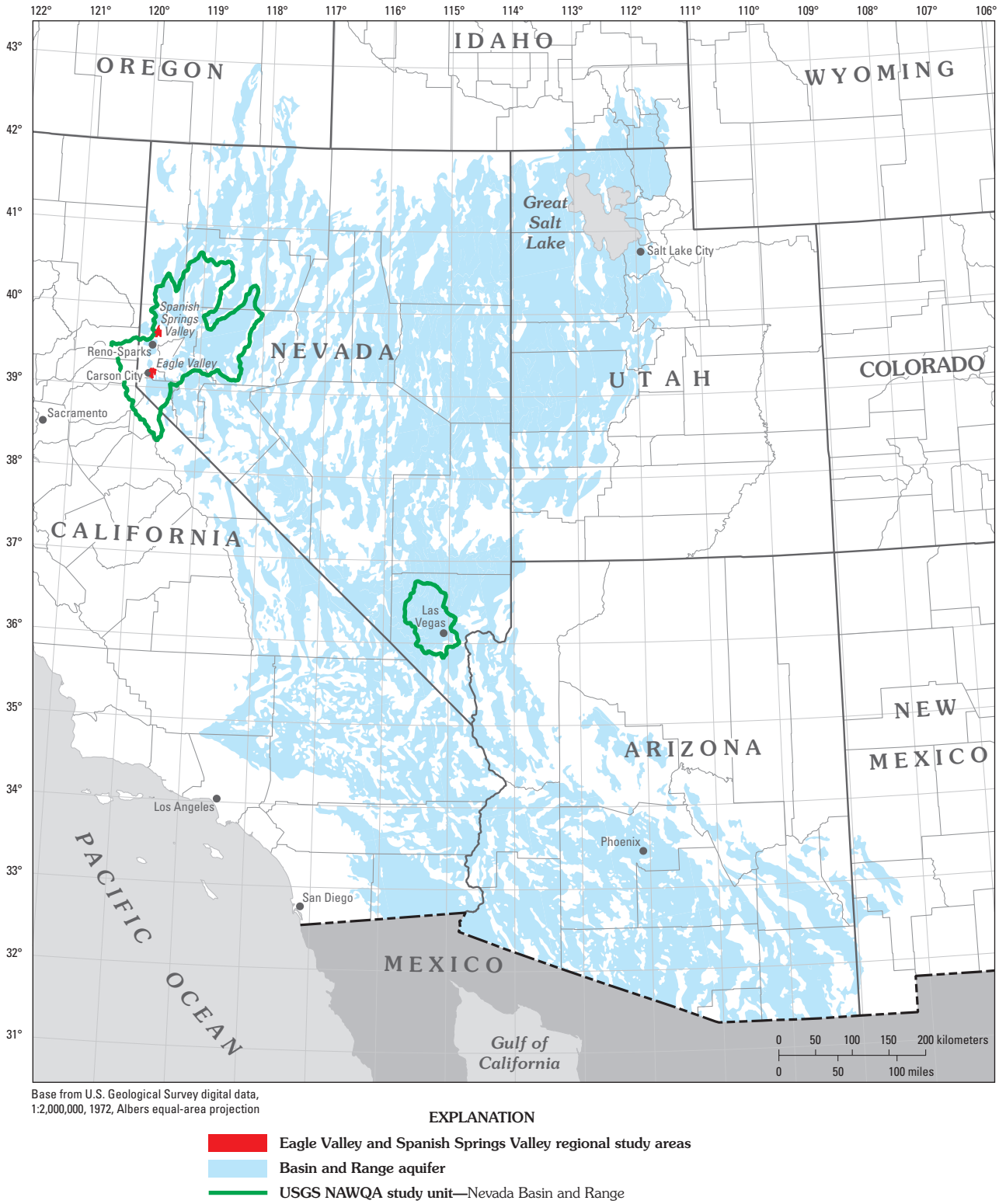

Figure 3.1. Location of the Eagle Valley and Spanish Springs Valley regional study areas within the Basin and Range basin-fill aquifers.

period 1997–2001 was selected for data compilation and modeling exercises for all TANC regional study areas to facilitate future comparisons between study areas. The calibrated ground-water flow models and associated particle tracking were used to simulate advective ground-water flow paths and to delineate areas contributing recharge to selected public-supply wells. Ground-water traveltimes from recharge to public-supply wells, oxidation-reduction (redox) conditions along flow paths, and presence of potential contaminant sources in areas contributing recharge were tabulated into a relational database as described in Section 1 of this Professional Paper. This section provides the foundation for future ground-water susceptibility and vulnerability analyses of the study areas and comparisons among regional aquifers.

Study Area Description

The Nevada Basin and Range NAWQA study unit includes the Truckee and Carson River Basins in northwestern Nevada and northeastern California and the Las Vegas Valley area in southeastern Nevada (fig. 3.1). These two areas represent many of the diverse environments found in the Basin and Range physiographic province, which is characterized by high mountains surrounding valleys underlain by thick, unconsolidated deposits (Covay and others, 1996). The Nevada Basin and Range study unit is located in the Basin and Range basin-fill aquifers, which are ranked fourth in total water use of the 62 principal aquifers in the United States (Maupin and Barber, 2005). The study areas were chosen because the aquifers are used extensively for public water supply, are susceptible and vulnerable to contamination, and are representative of the Basin and Range basin-fill principal aquifer (table 3.1).

Two study areas within the Nevada Basin and Range study unit were included in the TANC regional study. The first regional study area is the Eagle Valley, which includes Carson City and is part of the Carson River Basin (fig. 3.2*A*). The population of Carson City is greater than 50,000 (U.S. Census Bureau, 2003), and the area has experienced a steady population increase since the 1970s. The second regional study area is the Spanish Springs Valley, north of Sparks, which is in the Truckee River Basin (fig. 3.2*B*). The population of the Spanish Springs Valley has grown substantially since the early 1980s, and this growth has affected water quality in the basin (Seiler and others, 1999). The two areas were chosen for TANC regional studies because they have similar hydrologic and geologic characteristics, different rates of population increase, and different potential sources of ground-water contaminants.

Topography and Climate

The Eagle Valley is a semiarid basin in the west-central part of Nevada. The valley is bordered on the west by the Carson Range of the Sierra Nevada, on the north by the Virginia Range, on the east by Prison Hill and the Pine Nut Mountains and on the south by Carson Valley (fig. 3.2*A*). The floor of the Eagle Valley averages about 1,433 m above NAVD88, and the summit of Prison Hill is about 1,737 m. The Virginia Range is about 2,438 m in altitude; and the Carson Range is greater than 2,804 m in altitude (Maurer and others, 1996).

The Spanish Springs Valley is bounded on the west by Hungry Ridge and its unnamed southern extension with summits approaching 1,829 m. The northern boundary separating the Spanish Springs Valley from Warm Springs Valley is a narrow (less than 805 m) topographic divide lying between bedrock outcrops of the Hungry Ridge and the Pah Rah Range to the east (Berger and others, 1997). The southern boundary is bedrock and includes a low alluvial divide where an agricultural ditch (the Orr Ditch) enters and an agricultural drain (the North Truckee drain) exits the study area.

Climate in both valleys is similar, although the differing western boundaries (higher Carson Range and lower Hungry Ridge) affect precipitation in the valleys. Annual precipitation on the floor of the Eagle Valley averages about 25.4 cm (Arteaga and Durbin, 1979). Average annual precipitation along the crest of the Carson Range is about 96.5 cm. The Virginia Range receives much less precipitation than the Carson Range: average annual precipitation is slightly more than 35.6 cm (Arteaga and Durbin, 1979). In both ranges, most precipitation falls as rain or snow during November through April. Snow in the Carson Range accumulates to several meters during most winters and melts in early spring to early summer.

Average annual precipitation on the floor of the Spanish Springs Valley is generally less than 20.0 cm. The surrounding mountains receive 22.9 to 27.9 cm of precipitation in an average year, and as much as 33.0 cm of precipitation may fall in the higher altitudes of the Pah Rah Range (VanDenburgh and others, 1973).

Surface-Water Hydrology

One large river, the Carson River, crosses the Eagle Valley, and several streams discharge into the Carson River within the valley (fig. 3.2*A*). The Carson River acts as both a recharge and discharge boundary to the ground-water system on the south and east sides of the basin. The annual mean flow in the Carson River is 11.7 cubic meters per second (m^3/s) at the Carson City gage and 14.2 m^3/s, 11.3 km downstream at the Deer Run Road gage (periods of record 1940–2001 and 1979–2001, respectively (U.S. Geological Survey, 1939–00 and 1978–00). Streams in Ash and Kings Canyons drain the eastern flank of the Carson Range west of Carson City and provide perennial flow into the Eagle Valley during most years. The stream in Vicee Canyon flows downstream from the canyon mouth only during severe storms or during spring snowmelt in years with above-normal precipitation. The only other perennial stream is Clear Creek, which has the largest drainage area (40 km^2) of any stream entering the Eagle Valley. The remaining streams entering Eagle Valley are ephemeral, flowing only occasionally onto the valley floor.

Surface water in the Spanish Springs Valley consists almost entirely of Truckee River water imported by way of the

Table 3.1. Summary of hydrogeologic and ground-water-quality characteristics for the Basin and Range basin-fill aquifers and the Eagle and Spanish Springs Valleys regional study areas, Nevada.

[m, meters; cm/yr, centimeters per year; m^2/d, squared meters per day; m/d, meters per day; ET, evapotranspiration; mg/L, milligrams per liter]

Characteristic	Basin and Range basin-fill aquifers	Eagle and Spanish Springs Valleys regional study areas
Geography		
Topography	Altitude ranges from about 46 m at Yuma, Arizona to more than 3,048 m at the crest of some mountain ranges (Robson and Banta, 1995).	Eagle Valley floor altitude ranges from 1,410 m to 1,460 m. Spanish Springs Valley floor ranges from about 1,356 m to 1,450 m.
Climate	Arid to semi-arid climate. Precipitation ranges from 10 to 20 cm/yr in basins and 40 to 76 cm/yr in mountains (Robson and Banta, 1995).	Arid climate. Eagle Valley floor precipitation is about 25.4 cm/yr with up to 96.5 cm/yr precipitation in surrounding mountains. Spanish Springs Valley floor precipitation is less than 20.0 cm/yr with up to 33.0 cm/yr in Pah Rah Range.
Surface-water hydrology	Streams drain from surrounding mountains into basins. Basins generally slope toward a central depression with a main drainage that is dry most of the time. Many basins have playas in their lowest depressions. Ground-water discharge to streams can occur in basin depressions. (Planert and Williams, 1995)	Carson River crosses south and east sides of Eagle Valley and is a recharge and discharge boundary. Spanish Springs Valley contains no natural streams, although the Orr Ditch, which imports irrigation water, crosses the valley.
Land use	Undeveloped basins are unused, grazing, and rural residential. Developed basins are urban, suburban and agricultural.	Eagle Valley—Urban, suburban, and rural residential. Spanish Springs Valley—Urban, suburban, rural residential, agricultural.
Water use	Ground-water withdrawals from wells supply water for agricultural irrigation and municipal use. Population increases since the 1960's have increased the percentage of water being used for municipal supply.	Eagle Valley—Approximately 30 percent of public supply provided by ground water and 70 percent provided by surface water. Spanish Springs Valley—Similar to Eagle Valley but with some agricultural irrigation ground-water use.
Geology		
Surficial geology	Tertiary and Quaternary unconsolidated to moderately consolidated fluvial gravel, sand, silt and clay basin-fill deposits include alluvial fans, flood plain deposits, and playas. (Robson and Banta, 1995; Planert and Williams, 1995)	Eagle Valley—Tertiary and Quaternary unconsolidated fluvial basin-fill sediment up to 610 m in thickness. Sediments are coarse grained near the basin margins and finer grained near the basin center. Spanish Springs Valley—Similar to Eagle Valley with greater variation in basin-fill thickness.
Bedrock geology	Mountains surrounding basins are composed of Paleozoic to Tertiary bedrock formations. Tertiary volcanic and metamorphic rocks are in general impermeable. Paleozoic and Mesozoic carbonate rocks are cavernous allowing inter-basin flow in some areas. (Robson and Banta, 1995; Planert and Williams, 1995)	Eagle Valley—Carson Range west of Eagle Valley is composed of Mesozoic granitic and metamorphic rocks overlain by Tertiary volcanic rocks. Spanish Springs Valley—Surrounding ranges are composed of Mesozoic granitic and metamorphic rocks overlain by Tertiary volcanic rocks.

Table 3.1. Summary of hydrogeologic and ground-water-quality characteristics for the Basin and Range basin-fill aquifers and the Eagle and Spanish Springs Valleys regional study areas, Nevada.—Continued

[m, meters; cm/yr, centimeters per year; m^2/d, squared meters per day; m/d, meters per day; ET, evapotranspiration; mg/L, milligrams per liter]

Characteristic	Basin and Range basin-fill aquifers	Eagle and Spanish Springs Valleys regional study areas
Ground-water hydrology		
Aquifer conditions	Unconfined basin-fill aquifers surrounded by relatively impermeable bedrock mountains and foothills. Basin ground-water flow systems are generally isolated and not connected with other basins except in some locations where basins are hydraulically connected via cavernous carbonate bedrock.	Eagle Valley—Unconfined basin-fill aquifer surrounded by bedrock mountains. Recharge originates as precipitation in the mountains. Ground-water flow is generally eastward across the valley because there is greater precipitation in the Carson Range to the west. Spanish Springs Valley—Unconfined basin-fill aquifer surrounded by bedrock mountains.
Hydraulic properties	Transmissivity ranges from less than 93 m^2/d to greater than 2,790 m^2/d. In general, alluvial fan deposits near basin margins are more conductive than flood plain and lacustrine deposits near basin centers. (Robson and Banta, 1995; Planert and Williams, 1995)	Eagle Valley—Transmissivity ranges from 42 to 77 m^2/d (Johnson and others, 1996). Hydraulic conductivity ranges from 0.12 to 1.6 m/d for basin fill (Arteaga, 1986). Spanish Springs Valley—Hydraulic conductivity ranges from 0.15 to 3.6 m/d (Berger and others, 1997).
Ground-water budget	Recharge to basin fill deposits is from surface-water runoff in mountains where precipitation is highest. Ground-water discharges naturally as evapotranspiration (ET) to playas and stream channels in basin depressions. Ground-water withdrawal from wells is largest component of discharge from Basin and Range aquifers. (Robson and Banta, 1995)	Eagle Valley—Recharge to basin fill is from surface-water runoff in mountains. Runoff from Carson Range is largest component of recharge. Discharge to ET, base flow to Eagle Valley Creek, and municipal pumping wells. Pumping has decreased ET. Spanish Springs Valley—Less precipitation than Eagle Valley. Recharge is from imported surface water and local precipitation. Discharge is to ET, ground-water underflow, and pumping wells.
Ground-water quality		
	Water quality varies between basins. Dissolved solids can range from less than 500 mg/L to over 35,000 mg/L. Generally, low-dissolved solids, oxic water occurs near recharge areas of basin margins. High-dissolved solids anoxic water occurs with depth or near basin centers and playa lakes (Robson and Banta, 1995; Planert and Williams, 1995).	Eagle Valley and Spanish Springs Valley exhibit similar water quality of calcium-bicarbonate type water. Dissolved solids range from 100 to more than 3,000 mg/L and averages 250 mg/L. Eagle Valley pH range is 6.5 to more than 8. Spanish Springs pH generally is greater than 8. Eagle Valley redox conditions are generally oxic with some iron and manganese reducing conditions near basin center. Spanish Springs Valley is predominantly oxic.

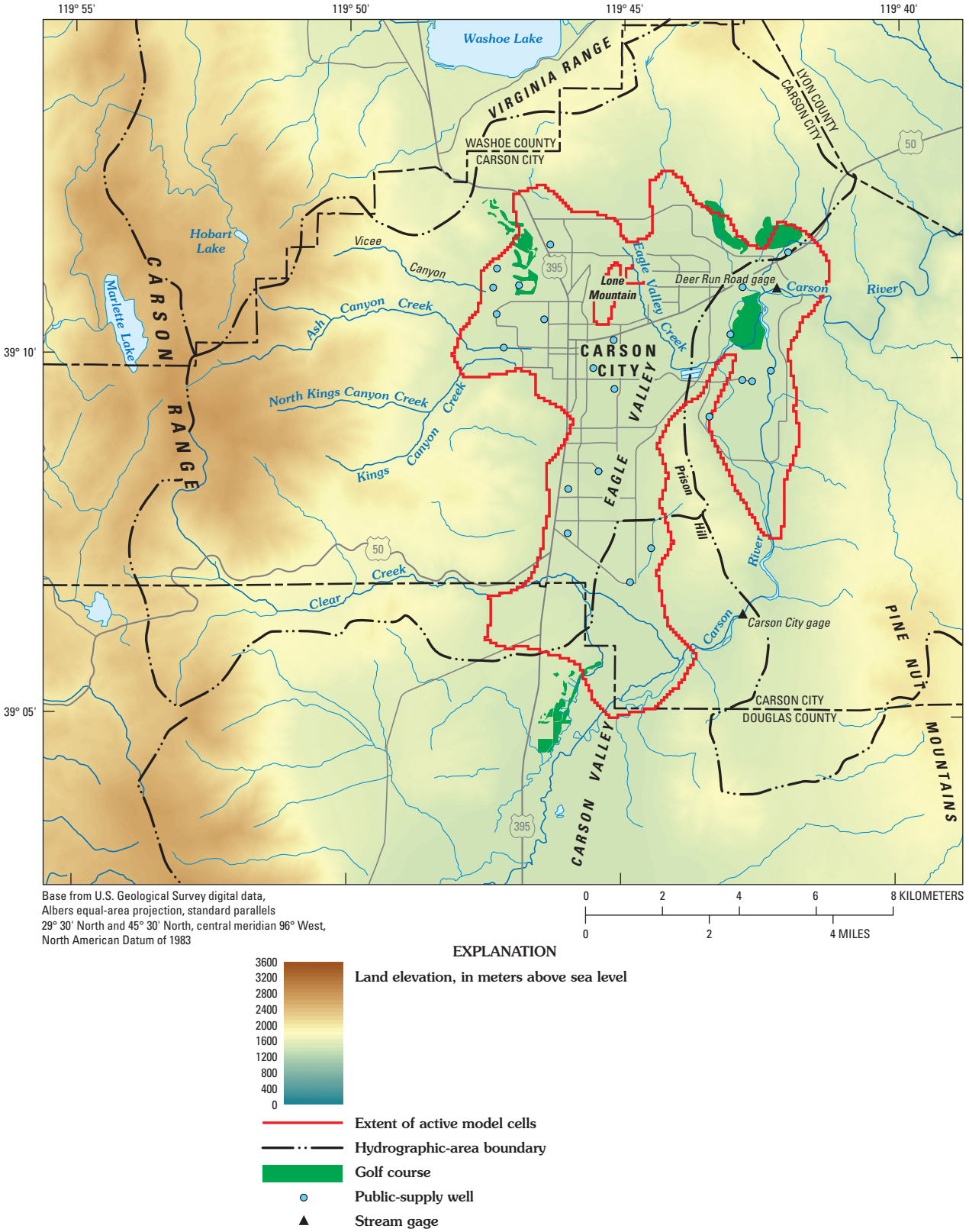

Figure 3.2*A*. Topography, hydrologic features, and locations of public-supply wells, Eagle Valley regional study area, Nevada.

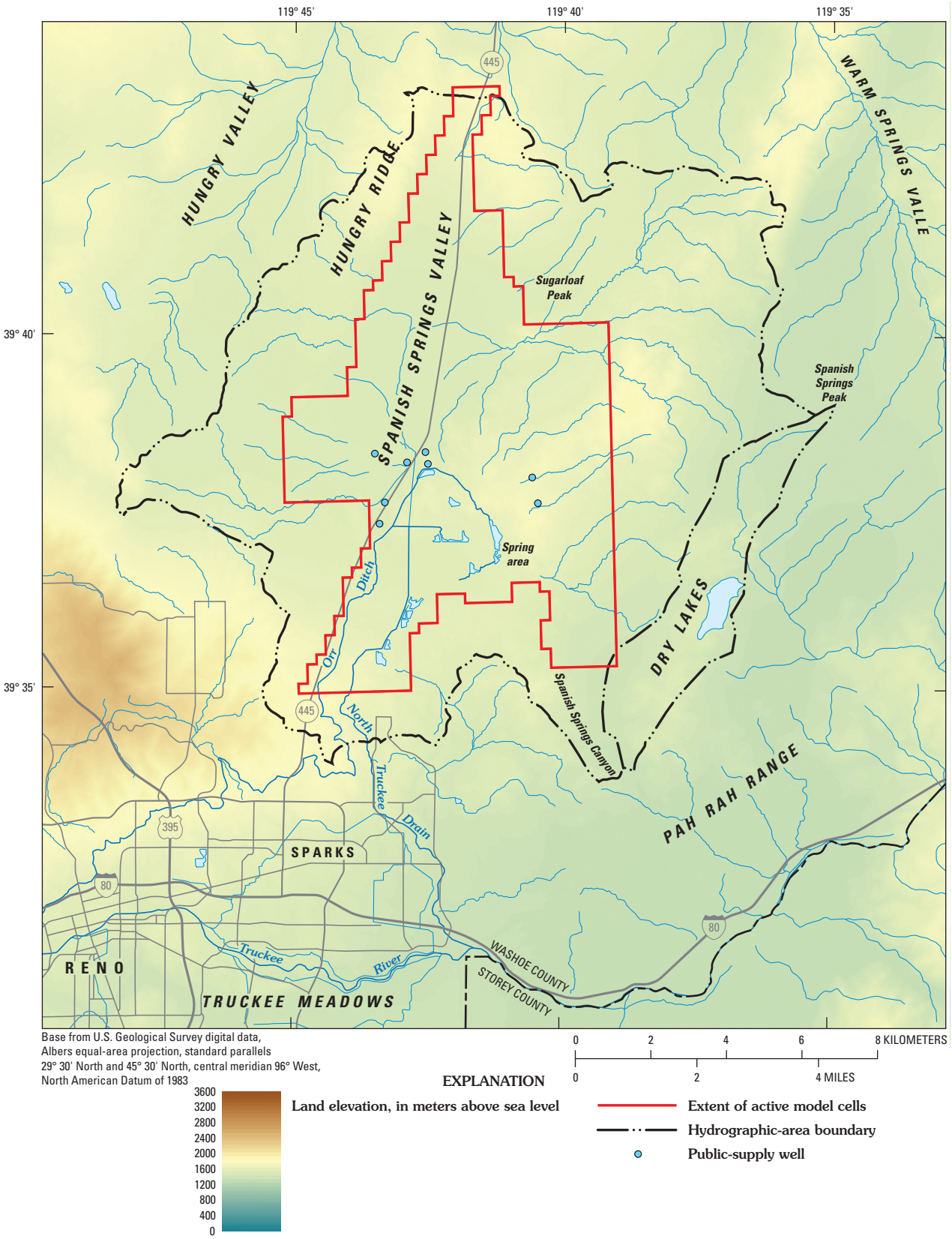

Figure 3.2*B*. Topography, hydrologic features, and locations of public-supply wells, Spanish Springs Valley regional study area, Nevada.

Orr Ditch, which is used to support agriculture in the southern part of the valley (fig. 3.2*B*). Several dry channels throughout the study area, however, indicate sufficient precipitation occasionally falls to produce runoff from surrounding mountains. The Orr Ditch has delivered water from the Truckee River through the southern boundary of the valley since 1878 (Berger and others, 1997). The ditch is unlined throughout its 11.2-km length in the valley and has numerous take-out gates to smaller ditches used for flood irrigation and stock watering. The North Truckee Drain originates near the center of the irrigated lands within the area encompassed by the Orr Ditch. The drain conveys unused irrigation water and, to a lesser extent, ground-water discharge out of the study area.

Land Use

Land use in the Eagle Valley slowly changed from unused scrubland to urban and residential development over the past several decades. The population of Carson City was estimated at 35,000 in 1979 and was more than 50,000 by 2001 (U.S. Census Bureau, 2003). The initial city limits slowly expanded in all directions as urban development progressed, and little land in the valley is currently (2006) used for pasture or agriculture.

Development in the Spanish Springs Valley was virtually nonexistent before about 1960, except for a small number of agricultural homesteads in the southern part of the valley. Based on comparison of aerial photographs taken in 1956, 1977, and 1994 and assessor parcel maps, general agricultural land use within the area serviced by the Orr Ditch has remained relatively unchanged, although some acreage has been developed in the southwest part of the valley. Urban growth and development in the Spanish Springs Valley increased sharply after 1979 when the population increased from less than 800 in 1979 to more than 4,000 in 1990 (Berger and others, 1997). Most subdivisions are located around the northern perimeter of the Orr Ditch with smaller subdivisions in the southern part of the valley. Individual homes also are scattered in the northern part of the basin in and adjacent to the surrounding mountains.

Water Use

Water use in the Eagle Valley is primarily for domestic purposes and is supplied though public water systems. Ground-water pumping provides about 30 percent of the public water supply, and surface-water sources supply the remaining 70 percent (Welch, 1994). Lesser amounts of water are provided by domestic wells. Very little water is used for agriculture or manufacturing. Most of the homes in the Eagle Valley are served by a wastewater-treatment plant that exports effluent out of the basin.

The Spanish Springs Valley has water-use characteristics similar to those in the Eagle Valley, although there is slightly more agricultural water use in the Spanish Springs Valley. As of 1994, more than 3,000 subdivision houses had water supplied by a public utility; however, nearly 1,000 of these received water from a supplier outside of the valley (Berger and others, 1997). Of the total number of houses with public water supply, 1,600 have septic systems and about 1,400 are served by wastewater-treatment facilities located outside the basin. Nearly 200 houses had domestic wells with septic systems. Although no new septic systems are allowed in the basin, there are now approximately 2,300 parcels with septic systems in Spanish Springs Valley (Rosen and others, 2006).

Conceptual Understanding of the Ground-Water System

Unconfined to confined ground water is present in the Eagle Valley Quaternary basin-fill sediments and the surrounding bedrock, although most wells are completed in the basin-fill deposits (fig. 3.3*A*). Ground-water recharge originates as precipitation in the surrounding mountains, and ground water generally flows eastward through the Eagle Valley basin-fill sediments because there is greater precipitation at higher altitudes, especially in the Carson Range (Worts and Malmberg, 1966; Arteaga, 1986; Maurer and Fisher, 1988). Prior to ground-water development in Eagle Valley, ground water discharged by evapotranspiration through phreatophytes and pasture grasses and by subsurface flow to the Carson River flood plain. Ground-water pumping, mostly for municipal supply, has diverted ground water that would have historically discharged through phreatophytes or flowed eastward to the Carson River flood plain.

Similar to Eagle Valley, ground water in the Spanish Springs Valley is present in the Quaternary basin-fill alluvial sediments and the surrounding bedrock both under water-table and confined conditions. However, in contrast to Eagle Valley, ground-water recharge in the Spanish Springs Valley is derived from imported surface water and precipitation falling within the drainage basin (fig. 3.3*B*). Ground water flows generally in an eastward direction toward the North Truckee Drain, irrigated areas, and areas of evapotranspiration (Berger and others, 1997).

Geology

The mountains surrounding the Eagle Valley consist of Mesozoic granitic and metamorphic rocks overlain by Tertiary volcanic rocks (Welch, 1994). The mountains were uplifted and the valley floor was lowered relative to the mountains by extensional tectonics, forming a basin that is partly filled with Quaternary sediments eroded from the surrounding mountains. In this chapter, the consolidated rocks exposed in the mountains and buried beneath the sediments in the valley are collectively called bedrock; the sediments in the valley are collectively called basin-fill sediments. The basin-fill sediments

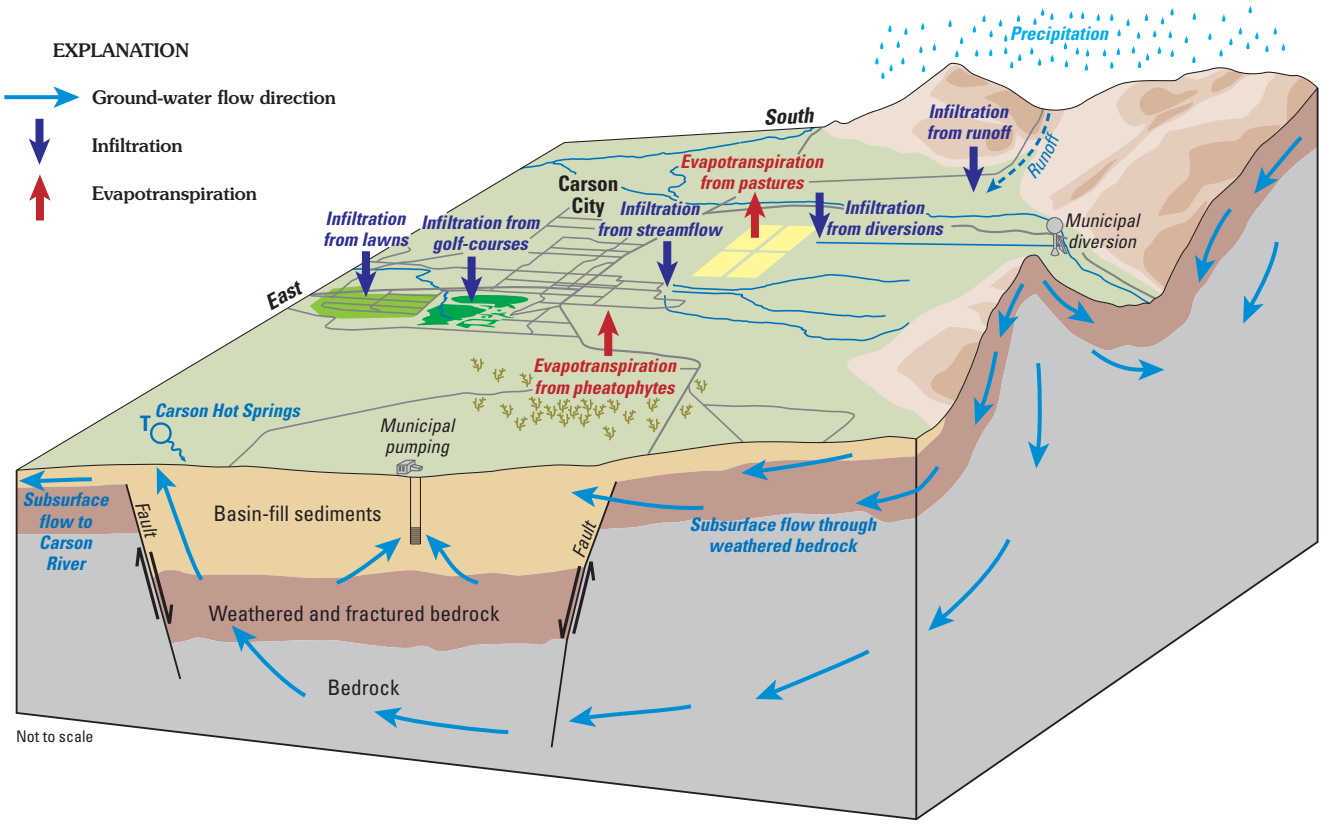

Figure 3.3*A*. Basin-fill ground-water flow system of the Eagle Valley regional study area, Nevada.

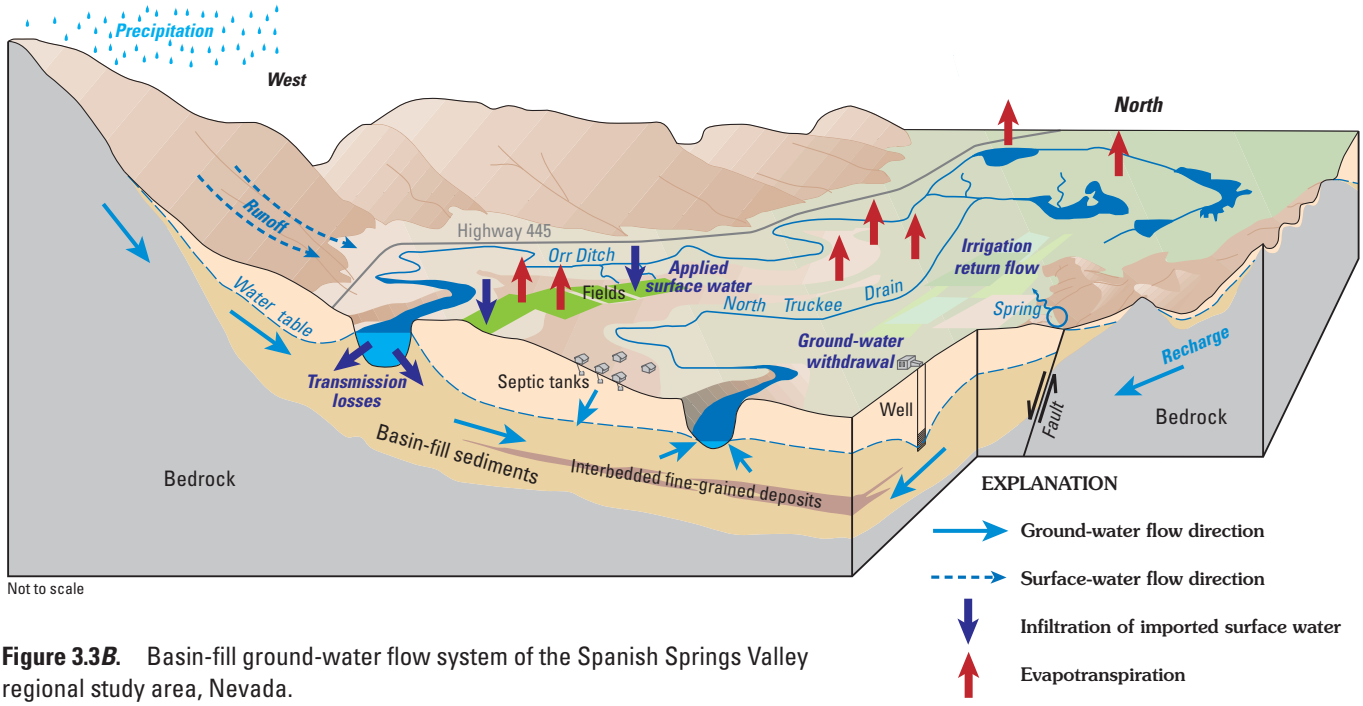

Figure 3.3*B*. Basin-fill ground-water flow system of the Spanish Springs Valley regional study area, Nevada.

consist primarily of poorly sorted sands and gravels with small boulders and intervening clay layers. Basin-fill sediments are generally coarse grained near the base of the mountains and finer grained near the center of the valley. The basin-fill sediments are estimated to be about 366 m thick 2.4 km west of Lone Mountain, about 122 to 244 m thick beneath the northeastern and southern parts of the Eagle Valley, and about 610 m thick about 1.6 km northwest of Prison Hill (Arteaga, 1986). In general, the deepest part of the alluvial basin is in the center of the Eagle Valley.

The geologic setting of the Spanish Springs Valley is similar to that of the Eagle Valley, consisting of basin-fill sediments surrounded by mountains composed of Mesozoic granitic and metamorphic rocks overlain by Tertiary volcanic rocks (Berger and others, 1997). For purposes of this report, the major geologic units identified in the Spanish Springs Valley were subdivided into two general groups on the basis of their hydrogeologic properties: (1) consolidated igneous and metamorphic bedrock, which commonly has low porosity and permeability except where fractured, and (2) basin fill, which is highly porous and transmits water readily. The structural depression occupied by the Spanish Springs Valley is filled in part by interbedded deposits of sand, gravel, clay, and silt derived primarily from adjacent mountains. These deposits form the basin-fill aquifer, which is bounded and underlain by consolidated rock. The areal extent of the basin-fill aquifer is approximated by the contact between consolidated rock and basin fill along the periphery of the valley floor. Total surface area of basin fill is about 88 km^2, or almost 43 percent of the total drainage area of Spanish Springs Valley (Berger and others, 1997). On the north, an alluvium-covered topographic divide exists between the Spanish Springs and Warm Springs Valley. At the southern boundary of the study area the saturated basin fill in the Spanish Springs Valley may be continuous with saturated basin fill of Truckee Meadows (fig. 3.2*B*). This boundary, which is not a topographic divide, is underlain by consolidated rock at depths of less than 6 m. Basin fill also occupies the structurally controlled Dry Lakes area in the southeast part of the Pah Rah Range (Berger and others, 1997).

Wells drilled in the Spanish Springs Valley range in depth from several meters to more than 240 m, and most wells are completed in basin fill (Berger and others, 1997). Discrepancies in basin-fill thickness reported on drillers' logs for several wells limit the use of these logs to estimate areal distribution of basin-fill thickness. Basin-fill sediments are thickest along a northeast-trending trough close to the mountain front of Hungry Ridge, where depth to bedrock reaches a maximum value of about 305 m (Berger and others, 1997). In general, the greatest depth to bedrock is beneath the west part of the Spanish Springs Valley, and the basin-fill sediments thin toward the east. In the southern part of the valley, depth to bedrock is less than 30 m, and basin-fill sediments thin toward the southern boundary (Berger and others, 1997).

Ground-Water Occurrence and Flow

In the northern part of the Eagle Valley, ground water flows eastward and southeastward beneath the topographic divide into Dayton Valley (fig. 3.4*A*) (Worts and Malmberg, 1966; Arteaga, 1986; Maurer, 1997). In the southern part of the Eagle Valley, some ground water flows northeastward around the northern end of Prison Hill and southeastward beneath the topographic divide into the Carson Valley (Worts and Malmberg, 1966; Arteaga, 1986). Figure 3.4*A* shows the potentiometric surface for 2001 as simulated in the upper layer of the Eagle Valley model.

Ground water flows both north and south from the ground-water divide that has developed beneath the center of the Spanish Springs Valley (fig. 3.4*B*). Ground water flows south out of the valley through the basin fill and probably through fractured bedrock to Truckee Meadows. Ground water also flows from the ground-water divide toward the northern part of the study area. Geochemical data from a municipal well, which is screened in more than 37 m of saturated basin fill, indicates the source of ground water is a mixture of local recharge and water from the Truckee River. Stable isotope and chlorofluorocarbon data (Berger and others, 1997) support the conclusion that imported Truckee River water moves northward from the Orr Ditch. Figure 3.4*B* shows the potentiometric surface for 2001 as simulated in the upper layer of the Spanish Springs Valley model.

Aquifer Hydraulic Conductivity

The hydraulic conductivity and transmissivity of basin-fill sediments in the Eagle Valley have been estimated by Arteaga (1986), Johnson and others (1996), and Maurer and others (1996). Values of hydraulic conductivity reported by Arteaga (1986) ranged from 0.12 to 1.6 m/d. Transmissivities of 42, 45, and 77 m^2/d for three wells were reported by Johnson and others (1996). Dividing transmissivity values by aquifer saturated thickness in the perforated interval of the respective wells results in hydraulic conductivities of 0.98, 0.91, and 0.98 m/d, respectively. Maurer and others (1996) estimated hydraulic conductivities of lithologic units in the Eagle Valley basin-fill sediments and in fractured and weathered bedrock from correlations between slug-test analyses and borehole resistivity logs. In the basin-fill sediments, hydraulic conductivity ranged from 0.006 to 0.027 m/d for clay and from 10 to 14 m/d for sand and gravel (Maurer and others, 1996). Hydraulic conductivity of weathered and unweathered granitic bedrock closed fractures ranged from 0.02 to 0.28 m/d, whereas hydraulic conductivity of open-fractured metamorphic rocks was up to 18 m/d (Maurer and others, 1996) indicating that metamorphic rocks with open fractures can be more permeable than basin-fill sediments and weathered granitic rocks.

In the Spanish Springs Valley, hydraulic conductivity was calculated from several aquifer tests completed in the upper 100 m of saturated basin fill and ranged from 0.15 to about 3.6 m/d (Berger and others, 1997). Analyses of geophysical and lithologic logs and grain-size distributions collected from observation wells drilled as part of the study by Berger and others (1997) and Washoe County (1993) provided additional qualitative estimates of the ability of the basin-fill aquifer to transmit water. In general, basin fill derived from volcanic rocks tends to be dominated by fine-grained deposits resulting in an overall lower hydraulic conductivity than basin fill derived from granitic bedrock, which is dominated by sand and gravel. Hydraulic conductivity in the deepest part of the basin fill is unknown but is probably less than that of the upper 100 m owing to sediment compaction and induration. The distribution of hydraulic conductivity within the basin-fill aquifer was refined during ground-water flow model calibration, as discussed in the section "Ground-Water Flow Modeling."

Water Budget

Historical recharge estimates for the Eagle Valley were based on precipitation data. Original estimates of recharge to Eagle Valley (Worts and Malmberg, 1966) used an empirical relation between altitude, precipitation, and recharge (Maxey and Eakin, 1949) to estimate ground-water recharge to basins in eastern Nevada. Worts and Malmberg (1966) estimated 29,300 m^3/d (15 cm/yr over the modeled area of 71 km^2) of potential recharge to the Eagle Valley in 1965. A subsequent recharge estimate of 18,900 m^3/d (9.7 cm/yr over the modeled area) for the period 1967–77 was made for Eagle Valley using a relation between precipitation and surface runoff from Clear Creek and creeks in Ash and Kings Canyons (Arteaga and Durbin, 1979).

Sources of recharge and inflow to the Eagle Valley considered by this study include subsurface inflow from the mountains (mountain-block recharge); infiltration of streamflow from Clear, Kings Canyon, and Ash Canyon Creeks and ephemeral streams (mountain-front recharge); infiltration of precipitation; infiltration of lawn and golf course irrigation; and effluent from septic tanks. Estimates of inflow made for 1997–2001 conditions were made from inflow estimates for the period 1995–1998 (Maurer and Thodal, 2000), which were wet years. Average annual precipitation from the two periods was used to scale the 1995–1998 inflow estimates to the period 1997–2001. Mountain-block recharge was estimated to be about 15,600 m^3/d for 1995–98 (Maurer and Thodal, 2000) and about 12,900 m^3/d for 1997–2001 average conditions, and mountain-front recharge from infiltration of streamflow was about 11,800 m^3/d during 1995–98 (Maurer and Thodal, 2000) and about 8,800 m^3/d for 1997–2001 average conditions. Recharge from precipitation on open areas of the valley floor ranged from 110 to 300 m^3/d (0.06 to 0.15 cm/yr over the modeled area) for 1997–2001 average conditions. Recharge from lawn irrigation is estimated to range from 3,300 to 8,200 m^3/d for 1995–98 (Maurer and Thodal, 2000) and from about 2,700 to 7,700 m^3/d for 1997–2001 average conditions. Recharge from irrigation of golf courses with treated effluent is about 2,000 m^3/d (Maurer and Thodal, 2000). An estimated 900 septic tanks were functioning in the Eagle Valley in 1997 with an estimated use and infiltration rate of 0.95 m^3/d per tank for a total of about 855 m^3/d. (Leanna Stevens, Carson City Public Utilities Department, oral and written communs., 1998). Summing the recharge components results in a total recharge estimate from sources on the valley floor (excluding mountain-block recharge) ranging from 18,000 to 23,200 m^3/d (9.3 to 12 cm/yr over the modeled area) for 1995–98 (Maurer and Thodal, 2000) and from about 14,500 to 19,600 m^3/d (7.5 to 10.1 cm/yr over the modeled area) for 1997–2001 average conditions. Estimates for the total for all sources of ground-water recharge and subsurface inflow to the Eagle Valley basin-fill aquifer range from approximately 27,400 to 32,500 m^3/d for 1997–2001. Estimates of ground- water-budget components are probably within 20 percent of their actual values. Water-budget components of greatest uncertainty are subsurface inflow, recharge from ephemeral streamflow, and recharge from lawn irrigation.

Ground water in the basin-fill aquifer of the Eagle Valley is discharged by evapotranspiration from bare soil and plants, by pumping, and to base flow of Eagle Valley Creek and unnamed creeks. In 1964, about 20 km^2 near the center of the valley were covered with phreatophytes (plants that use ground water) and pasture grasses (Worts and Malmberg, 1966, p. 27). Since that time, many acres of phreatophytes and pasture grasses have been replaced by urban and residential development. Based on indirect evidence, phreatophytes covered about 4.4 km^2 in 1997. In addition, ground-water pumping has caused water levels to decline, further reducing the amount of ground water discharged by phreatophytes. Since 1964, ground-water discharge to public-supply wells has increased and discharge by evapotranspiration has decreased. For this study, evapotranspiration within the Eagle Valley was estimated as about 15,100 m^3/d based on output from the ground-water flow model and a known acreage where evapotranspiration occurs. Ground-water pumping was 25,397 m^3/d from 1997 to 2001 (table 3.2). Where the water table is close to land surface, ground water also discharges as seepage to Eagle Valley Creek and two unnamed creeks and as evapotranspiration from phreatophytes. Base flow in Eagle Valley Creek averaged 21 m^3/d for 1997–2001 (U.S. Geological Survey, 1997–01). Estimated total ground-water discharge for the Eagle Valley basin-fill aquifer is approximately 47,900 m^3/d with about 15,100 m^3/d going to evapotranspiration, 25,400 m^3/d going to pumping, and 7,400 m^3/d going to surface-water base flow based on ground-water flow model results.

Table 3.2. Average ground-water pumping rates for public-supply wells, 1997–2001, Eagle Valley regional study area, Nevada (Nevada State Engineer's office, written commun., 2001).

[m^3/d, cubic meters per day]

Well	Pumping rate (m^3/d)
3	1,740
4	723
5	970
6	2,301
7	668
8	1,397
9	882
10	3,123
11	1,175
24	2,219
33	277
34	932
38	879
40	1,937
43	1,537
44	408
45	1,504
46	2,408
47	304
48	0
Total, all wells	**25,397**

Sources of ground-water recharge and inflow to the Spanish Springs Valley considered by this study include infiltration from the Orr Ditch (canal leakage), infiltration of precipitation, subsurface inflow from the surrounding mountains (mountain-block recharge), infiltration of water from lawn irrigation, and effluent from septic tanks. Ground-water recharge from precipitation takes place in or adjacent to the mountains in the Spanish Springs Valley through weathered or fractured bedrock or when intermittent runoff infiltrates dry channel deposits (fig. 3.3*B*). Precipitation that falls on the valley floor is considered a negligible source of recharge, although some recharge may be generated during heavy and localized rain showers. In eastern and western parts of the valley, ground water in basin-fill deposits generally flows toward the center of the basin, away from recharge-source areas in the mountains. Potential recharge, generated from nearly 11,800 m^3/d of annual precipitation (Berger and others, 1997) estimated to fall within the topographically closed Dry Lakes area (fig. 3.2*B*), may enter the basin fill at depth through fractures within the Pah Rah Range along the southeastern part of the study area.

Berger and others (1997) estimated anthropogenic sources of recharge to the Spanish Springs Valley on the basis of the amount of ground-water recycled from municipal and domestic uses. Water applied to outdoor lawn and shrub watering is mostly consumed by evapotranspiration and was considered an insignificant contributor to ground-water recharge (Berger and others, 1997). Recharge from septic systems (indoor uses) was estimated as 75 percent of the total amount of water delivered to the household during winter months, when outdoor watering is at a minimum. This monthly volume of water was assumed constant and was prorated over an entire year to arrive at an annual estimate of recharge from septic systems, which was approximately 1,600 m^3/d for 1994 (Berger and others, 1997). In Spanish Springs Valley, based on field and empirical techniques, total recharge from all sources is estimated at about 14,800 m^3/d (Berger and others, 1997). An estimated 54 percent of recharge is from canal leakage from the Orr Ditch (Truckee River water that is diverted into the Spanish Springs Valley) with the remainder coming from mountain-block recharge, infiltration of precipitation, infiltration from lawn irrigation, and septic-tank effluent.

Prior to urban development and ground-water withdrawal for water supply, evapotranspiration was the principal mechanism of ground-water discharge from Spanish Springs Valley. In areas where the water table is less than one meter below land surface, ground water can be discharged by evaporation. Under natural conditions, bare-soil evaporation in the Spanish Springs Valley probably took place in the area surrounding the springs, where the water table is near land surface. Transpiration by phreatophytes has been documented in other arid basins in Nevada to consume relatively large quantities of ground water (Robinson, 1970; Harrill, 1973, table 9; Berger, 1995, p. 35). Rush and Glancy (1967) estimated about 7.7 km^2 of phreatophytes discharged nearly 3,000 m^3/d of ground water by evapotranspiration under natural conditions in the Spanish Springs Valley (conditions without the Orr Ditch). Berger and others (1997) estimated 1,200 m^3/d of ground-water discharge from areas surrounding the Orr Ditch. The total estimate of ground-water discharge by evapotranspiration in Spanish Springs Valley is about 8,400 m^3/d.

Similar to the Eagle Valley, ground-water discharge to public-supply wells has increased and discharge by evapotranspiration has decreased as urban development occurred in the Spanish Springs Valley. Average 1997–2001 ground-water pumping rates for public-supply wells in the Spanish Springs Valley are listed in table 3.3 and total approximately 4,850 m^3/d.

Table 3.3. Average ground-water pumping rates for public-supply wells, 1997–2001, Spanish Springs Valley regional study area, Nevada, Nevada (Nevada State Engineer's office, written commun., 2001).

[m^3/d, cubic meters per day]

Well name	Pumping rate (m^3/d)
DS1	838
DS2	27
DS3	1,458
DS4	540
SC2	975
SC3	121
SC4	581
SC5	310
Total	**4,850**

Subsurface outflow from Spanish Springs Valley to the Truckee Meadows was estimated between 330 and 500 m^3/d (Cohen and Loeltz, 1964, p. 23; Rush and Glancy, 1967). These investigators evaluated subsurface outflow through the basin fill and did not attempt to estimate flow volumes through fractured bedrock. However, subsurface flow to the Truckee Meadows probably moves through fractured or weathered bedrock, as indicated from stable isotope data (Berger and others 1997, p. 48). Total discharge from the Spanish Springs Valley from evapotranspiration, pumping, and subsurface outflow is estimated at about 13,750 m^3/d.

Ground-Water Quality

The ground-water quality of the Eagle Valley and Spanish Springs Valley is similar, although there is considerable variability in the major-ion composition of both areas. Calcium and sodium are the predominant cations, and bicarbonate and sulfate are the predominant anions, although most ground water is dominated by calcium and bicarbonate. Dissolved-solids concentrations range from approximately 100 mg/L to more than 3,000 mg/L with a median of about 250 mg/L. The pH within the Eagle Valley Basin ranges from approximately 6.5 to greater than 8 pH units, and the pH of the Spanish Springs Valley ground water is more basic than Eagle Valley ground water, with most values greater than 8 pH units (Welch, 1994; Christian Kropf, Washoe County Department of Water Resources, written commun., 2001).

Oxidation-reduction (redox) conditions in Eagle Valley tend to follow trends that are controlled by the mountain-front and mountain-block recharge (fig. 3.4*A*). The most oxygenated ground water occurs around the edges of the basin near the mountain recharge areas, regardless of depth, and less oxygenated water is located near the center of the basin. Some areas near the basin center exhibit conditions consistent with manganese- and iron-reducing redox conditions, but oxygen and nitrate-reducing conditions predominate in the basin. Depth-related trends in redox conditions are not apparent in the Eagle Valley.

The Spanish Springs Valley aquifer is dominantly oxygen reducing (fig. 3.4*B*), although there are relatively few available water-quality analyses for redox classification. Two wells exhibited concentrations consistent with iron-reducing conditions, but these wells are completed in fractured bedrock and are probably not related to the redox conditions in the basin-fill aquifer (Christian Kropf, Washoe County Department of Water Resources, written commun., 2001).

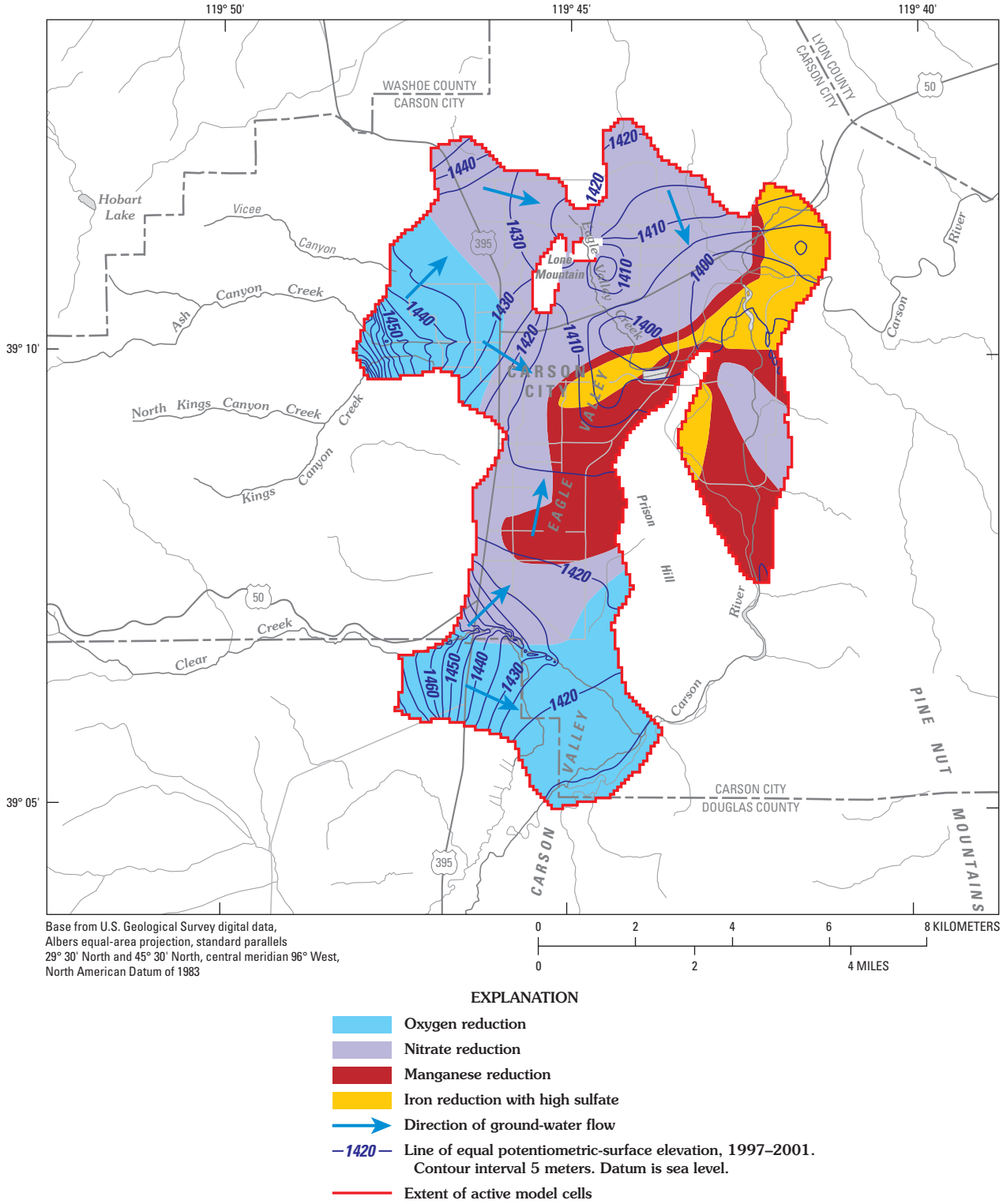

Figure 3.4*A*. Basin-fill aquifer potentiometric surface and oxidation-reduction classification zones, Eagle Valley regional study area, Nevada.

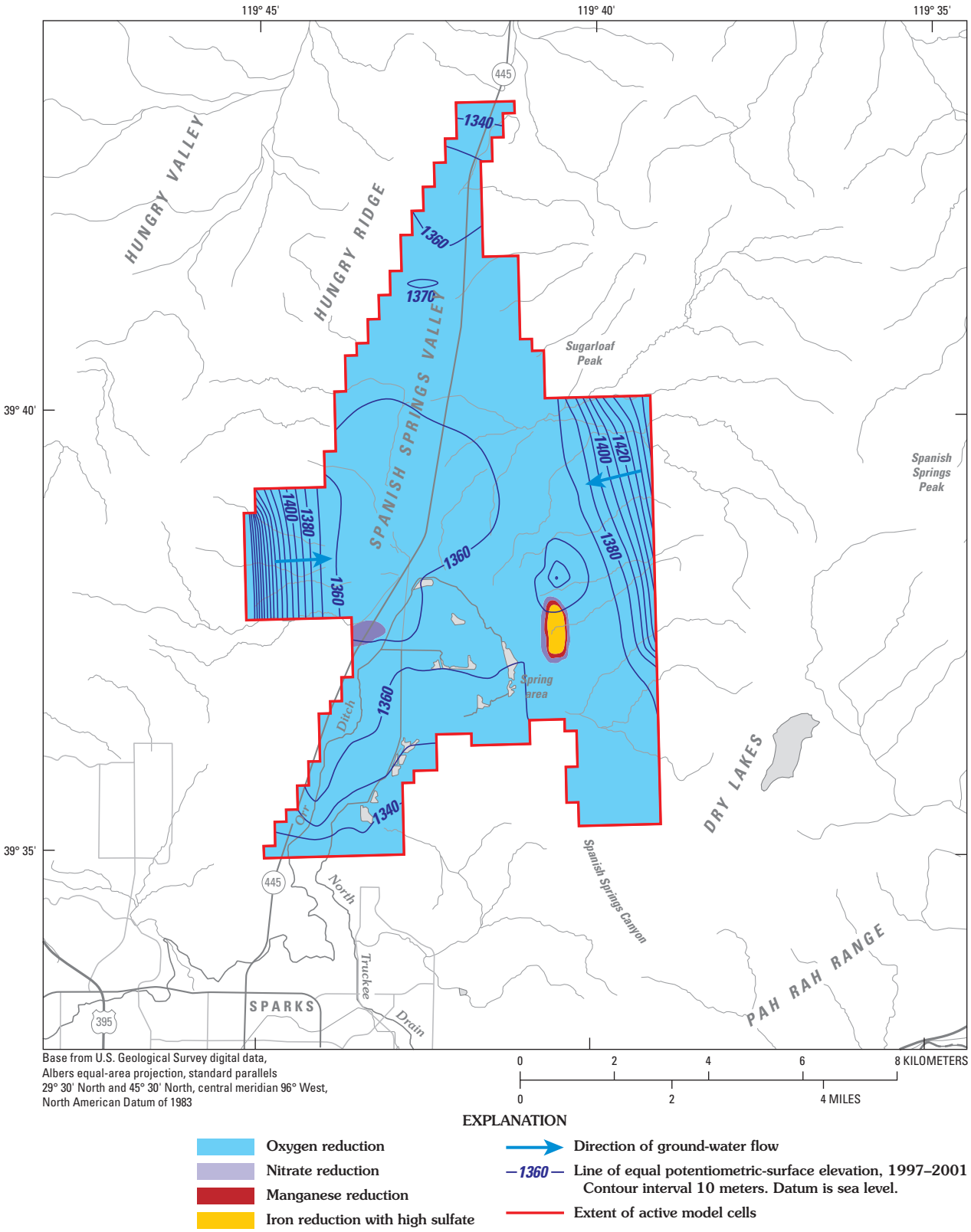

Figure 3.4*B*. Basin-fill aquifer potentiometric surface and oxidation-reduction classification zones, Spanish Springs Valley regional study area, Nevada.

Ground-Water Flow Simulations

The modular ground-water flow simulation code MODFLOW-2000 (Harbaugh and others, 2000) was used to construct steady-state finite-difference ground-water flow models for the Eagle and Spanish Springs Valleys representing average conditions for the 5-year period from 1997 to 2001. Both models were modified from previously existing models and recalibrated to average conditions for 1997–2001. The following sections present details of the modeled areas, model input, model calibration, and particle-tracking simulations.

Modeled Areas and Spatial Discretizations

The Eagle Valley model simulates ground-water flow in the basin-fill deposits. The modeled area covers the entire valley floor of approximately 70 km^2 where basin-fill deposits are exposed at the surface, and the model perimeter coincides with the horizontal extent of the basin-fill aquifer. The model grid (fig. 3.5*A*) contains 186 rows and 130 columns with grid cells 76 m on a side. The model contains 48,360 cells of which 24,356 cells are active. Vertically, the model is discretized into two layers. The top layer (layer 1) represents coarse-grained alluvial material in the upper 30 m of the basin fill, and layer 2 represents the underlying coarse-grained alluvial material. Layer 2 thickness extends to the base of basin-fill sediments as determined from gravity and seismic surveys (Arteaga, 1986) ranging from 50 to 2,160 m. Both layers are simulated as confined. The intervening fine-grained confining layer is simulated by a vertical leakance coefficient, which allows some flow between the two coarse-grained layers. The Eagle Valley MODFLOW finite-difference model was converted from a finite-element model constructed in the late 1970s (Arteaga, 1986) by overlaying the finite-difference grid on the finite-element mesh and interpolating the hydrologic properties to the finite-difference grid.

The Spanish Springs Valley finite-difference ground-water flow model used for this study was originally developed by Berger and others (1997) and later modified by the Washoe County Department of Water Resources (Wyn Ross, Washoe County Department of Water Resources, written commun., 2003). The original Spanish Springs Valley model grid contained 37 rows, 28 columns, and 2 layers that divided the saturated basin fill into discrete three-dimensional model cells. Variable node spacing was used to provide higher resolution in areas of concentrated ground-water recharge and discharge related to the importation of Truckee River water. Model-cell size ranged from a minimum of 62,500 m^2 (250 m by 250 m) to a maximum of 250,000 m^2 (500 m by 500 m). Of the 1,036 cells in each model layer, 625 were active in layer 1 and 282 were active in layer 2. The top 100 m of saturated basin fill was represented as unconfined by layer 1, and the processes of ground-water recharge and discharge were simulated in layer 1. Layer 2 extended from the bottom of layer 1 to the top of consolidated bedrock, functioning as a conduit for deep flow and as a reservoir of stored water. Layer 2 was simulated as convertible from confined to unconfined, which allowed conversion to unconfined conditions if water levels dropped below the bottom of layer 1. The original Spanish Springs Valley model (Berger and others, 1997) was slightly altered by Washoe County Department of Water Resources to facilitate their management of ground-water resources in the valley (Wyn Ross, Washoe County Department of Water Resources, written commun., 2003). The altered model now contains 71 rows, 35 columns, and 3 layers (fig. 3.5*B*). The grid cells throughout the entire model are now 250 m on a side. The altered model contains 7,455 model cells of which 2,917 are active. Layer 3 represents a basalt layer at depth penetrated by several newer supply wells on the east side of the valley. The altered model provides better coverage of the modeled area especially for the purposes of this study.

Boundary Conditions

Model stresses for both modeled areas include areal recharge from precipitation and irrigation, subsurface recharge from the surrounding mountains (mountain-block recharge), recharge from and discharge to streams, discharge to evapotranspiration, and discharge to pumping wells.

Recharge

Recharge boundaries in the Eagle Valley model consist of recharge cells to simulate precipitation and irrigation recharge to the land surface, general-head boundary cells to simulate mountain-block recharge, and river cells to simulate surface-water infiltration (fig. 3.5*A*). The MODFLOW General-Head package is used to simulate the edges of the model where basin-fill deposits lie adjacent to consolidated bedrock and mountain-block recharge of winter snow contributes significant recharge to the basin. General-head cells are located in layer 1, although some mountain-block recharge may occur at greater depths. Precipitation recharge is insignificant in the Eagle Valley, but the MODFLOW Recharge package is used to simulate small amounts of lawn and golf course irrigation with rates on the order of 7.3 cm/yr. The MODFLOW River package cells are used to represent recharge from surface-water flow in the Carson River, and Clear Canyon, Ash Canyon, and Kings Canyon Creeks.

In the Spanish Springs Valley model, ground-water recharge from septic systems, precipitation, and imported surface water were simulated in the model as assigned recharge rates based on either empirical estimates or measured quantities. Recharge rates from precipitation and septic systems were assumed constant. Mountain-block recharge was simulated using 18 recharge nodes. Recharge nodes and rates for the model are shown in figure 3.5*B*. Recharge from septic systems and irrigation return flows were simulated using well nodes with a positive discharge. For cells containing a domestic well (discharge) and a septic system (recharge), values of domestic

pumping were input to the model as the net difference between well discharge and septic-system recharge.

Discharge

Discharge boundaries in the Eagle Valley model included evapotranspiration discharge, river discharge, and public-supply well pumping (fig. 3.5*A*). Evapotranspiration (ET) was the primary discharge component and was simulated using the MODFLOW ET package. Evapotranspiration was simulated as a linear function of depth computed from a maximum rate, which was decreased linearly to the depth at which evapotranspiration is assumed to cease (the evapotranspiration extinction depth). An evapotranspiration extinction depth of 12 m was used in the model and provided a reasonable calculation of evapotranspiration, which generally was simulated for the center portion of the basin where evapotranspiration historically occurred. Discharge to rivers and creeks in the valley was represented using the MODFLOW River package (319 river cells) and public-supply well pumping was represented using the MODFLOW Well package (20 well cells). Average pumping rates for 1997–2001 for public-supply wells in Carson City were used as model input (table 3.2).

The Spanish Springs Valley model also included discharge by evapotranspiration. Ground-water discharge by evapotranspiration was specified in model layer 1 as head-dependent flow boundaries using the ET package and was assigned to selected active cells on the basis of plant distribution from field observations. In Spanish Springs Valley, evapotranspiration is limited to the area encompassed by the Orr Ditch and along the outside of the Orr Ditch near the central and southeast part of the valley. Inside the area encompassed by the Orr Ditch, the depth to water is shallow and vegetation consists of meadow grasses and alfalfa separated by large areas of bare soil (fig. 3.5*B*). A maximum evapotranspiration rate of 0.005 m/d at land surface and an extinction depth of 3 m were used to simulate evapotranspiration inside the area of the Orr Ditch. Assuming evapotranspiration is at a maximum when depth to ground water is 1 m, the maximum evapotranspiration rate used in the model for the area outside the Orr Ditch was 5 X 10^{-4} m/d and the extinction depth was 10 m.

In the Spanish Spring model, the simulation of ground-water discharge to domestic and public-supply wells was accomplished using the MODFLOW Well package. Average pumping rates for 1997–2001 for the eight public-supply wells in the Spanish Springs Valley were input to the model (table 3.3).

Aquifer Hydraulic Conductivity

Aquifer properties used in the Eagle Valley model were taken from the original model done in the late 1970s (Arteaga, 1986). The transmissivity values used by that model ranged from 1 to 940 m^2/d in layer 1 and from 5 to 11,600 m^2/d in layer 2. The areal distribution of transmissivity and hydraulic conductivity values coincides in general with grain size of the alluvial deposits. In layer 1, the coarser, more conductive deposits tend to be near creeks coming from the mountainous areas surrounding the valley (fig. 3.6*A*). The finer, less conductive deposits tend to be in the center of the valley. For layer 1, the aquifer thickness was held constant at 30 m; hydraulic conductivity ranged from 0.01 to 9.4 m/d with an average value of approximately 0.3 m/d. In general, layer 2 was simulated as coarser grained and as more transmissive than layer 1 (fig. 3.6*B*). Hydraulic conductivity of layer 2 ranged from 0.009 to 47.2 m/d with an average value of approximately 2 m/day.

In the Spanish Springs Valley model, transmissivity values determined from several aquifer tests were used to calculate hydraulic conductivities, which ranged from 0.5 to about 4 m/d (Berger and others, 1997). Figure 3.7*A* shows the hydraulic-conductivity distribution for layer 1 where values ranged from less than 0.01 to 15 m/d. Figure 3.7*B* shows the hydraulic-conductivity distribution for layer 2 where values ranged from less than 0.01 to 5 m/d, and figure 3.7*C* shows the hydraulic-conductivity distribution of layer 3 where values also varied from less than 0.01 to 5 m/d.

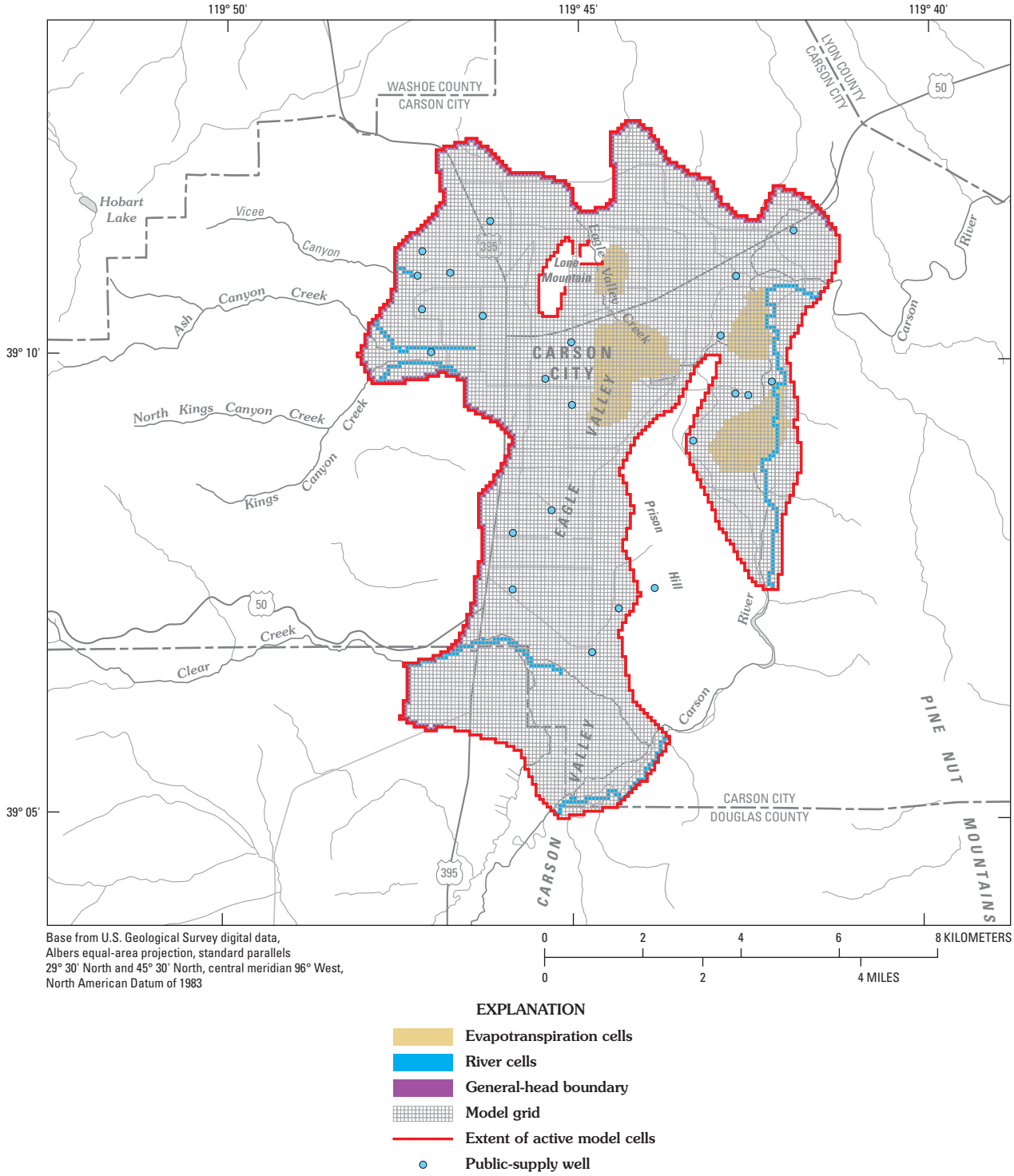

Base from U.S. Geological Survey digital data, Albers equal-area projection, standard parallels 29° 30' North and 45° 30' North, central meridian 96° West, North American Datum of 1983

EXPLANATION

- Evapotranspiration cells
- River cells
- General-head boundary
- Model grid
- Extent of active model cells
- Public-supply well

Figure 3.5*A*. Ground-water flow model grid, boundary conditions, and location of public-supply wells, Eagle Valley regional study area, Nevada.

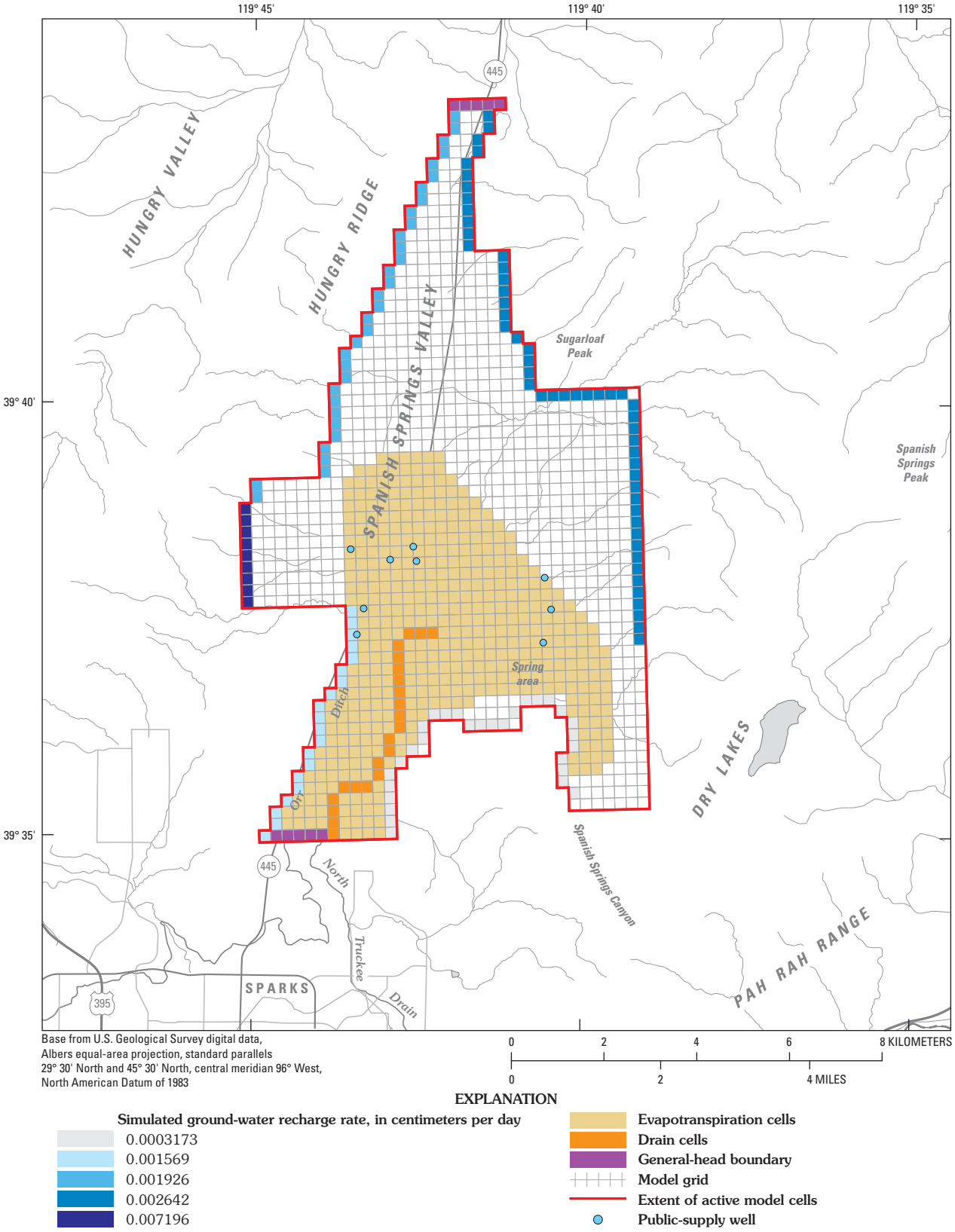

Figure 3.5*B*. Ground-water flow model grid, boundary conditions, and location of public-supply wells, Spanish Springs Valley regional study area, Nevada.

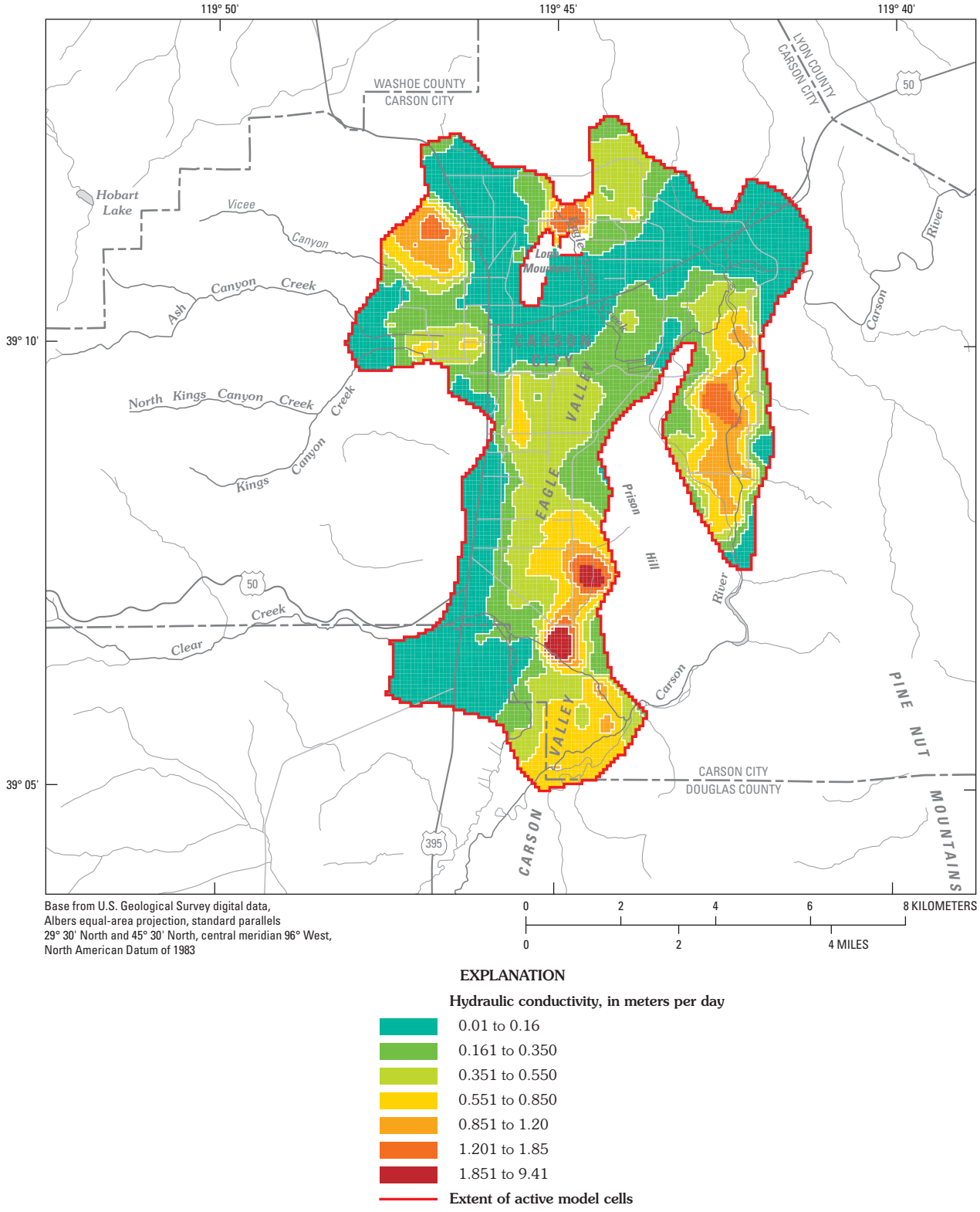

Base from U.S. Geological Survey digital data, Albers equal-area projection, standard parallels 29° 30' North and 45° 30' North, central meridian 96° West, North American Datum of 1983

Figure 3.6*A*. Distribution of hydraulic conductivity for model layer 1, Eagle Valley regional study area, Nevada.

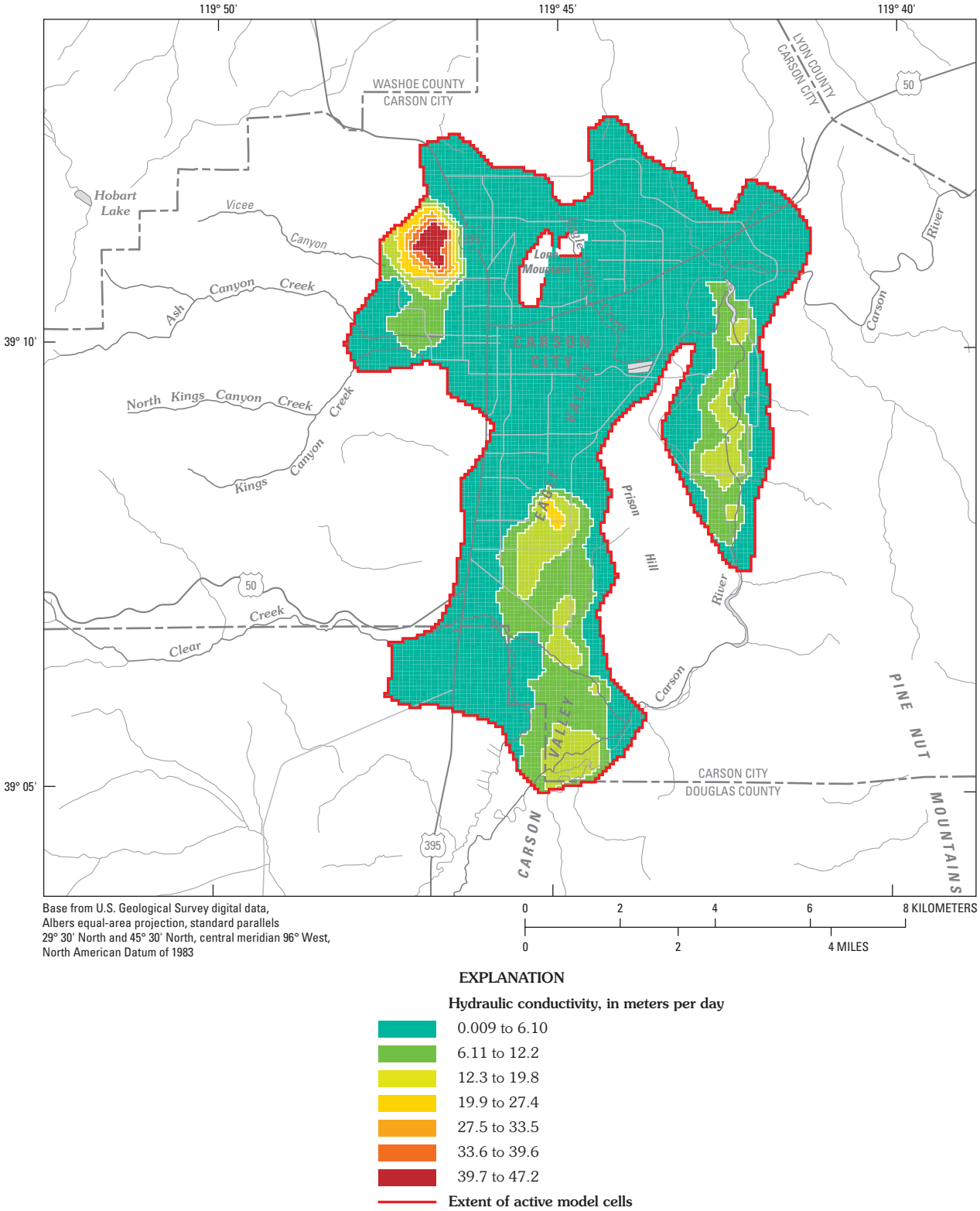

Figure 3.6*B*. Distribution of hydraulic conductivity for model layer 2, Eagle Valley regional study area, Nevada.

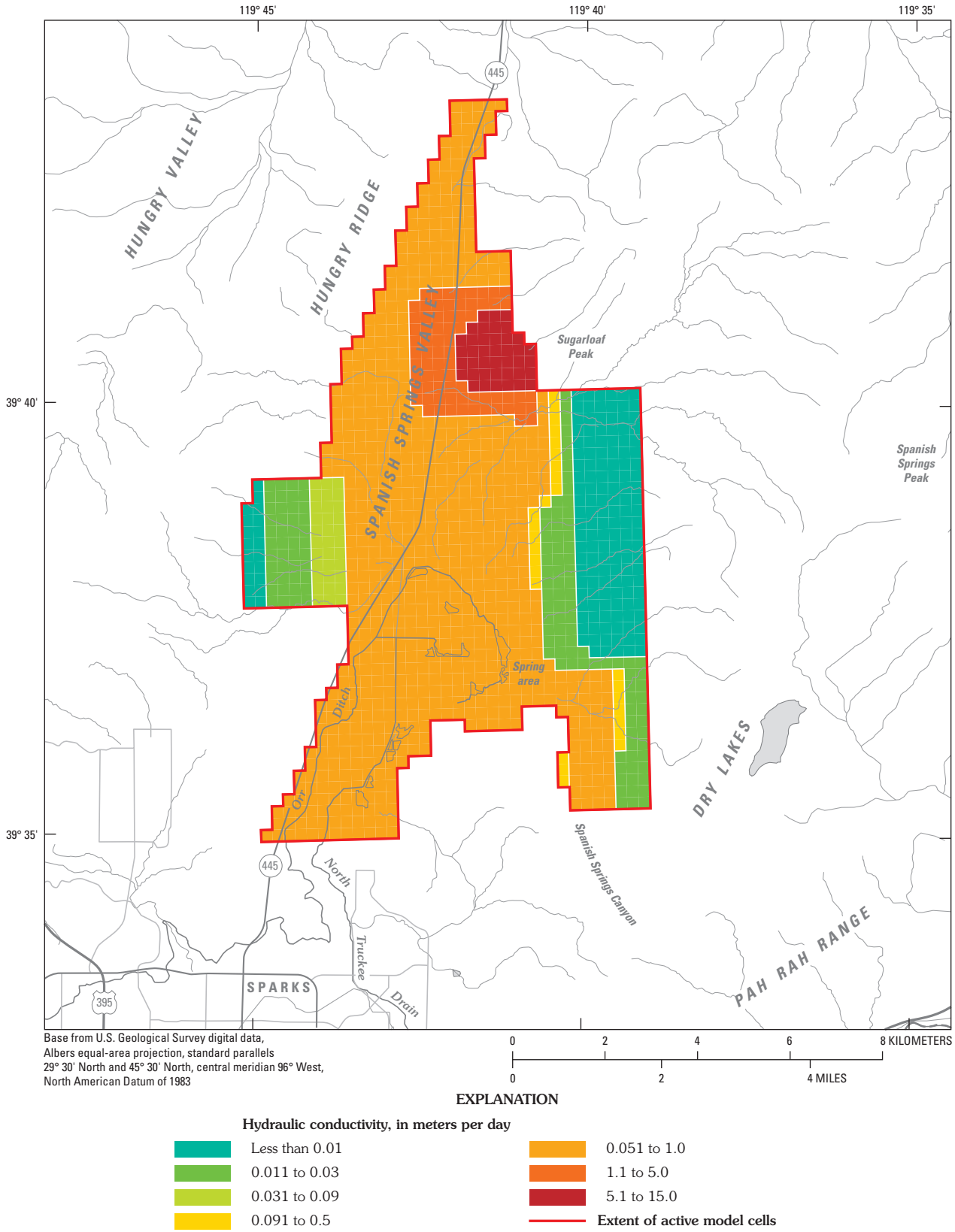

Figure 3.7*A*. Distribution of hydraulic conductivity for model layer 1, Spanish Springs Valley regional study area, Nevada.

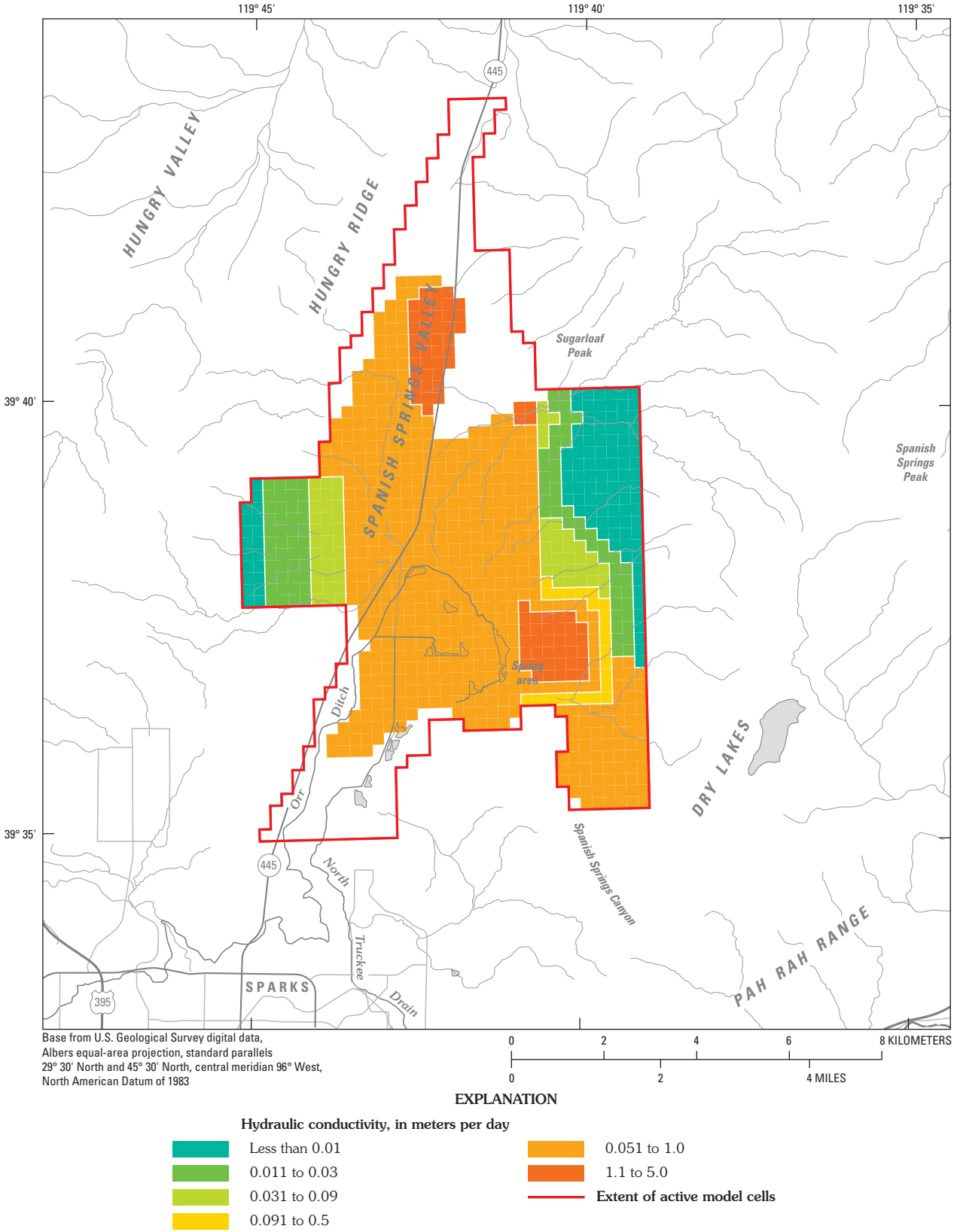

Figure 3.7*B*. Distribution of hydraulic conductivity for model layer 2, Spanish Springs Valley regional study area, Nevada.

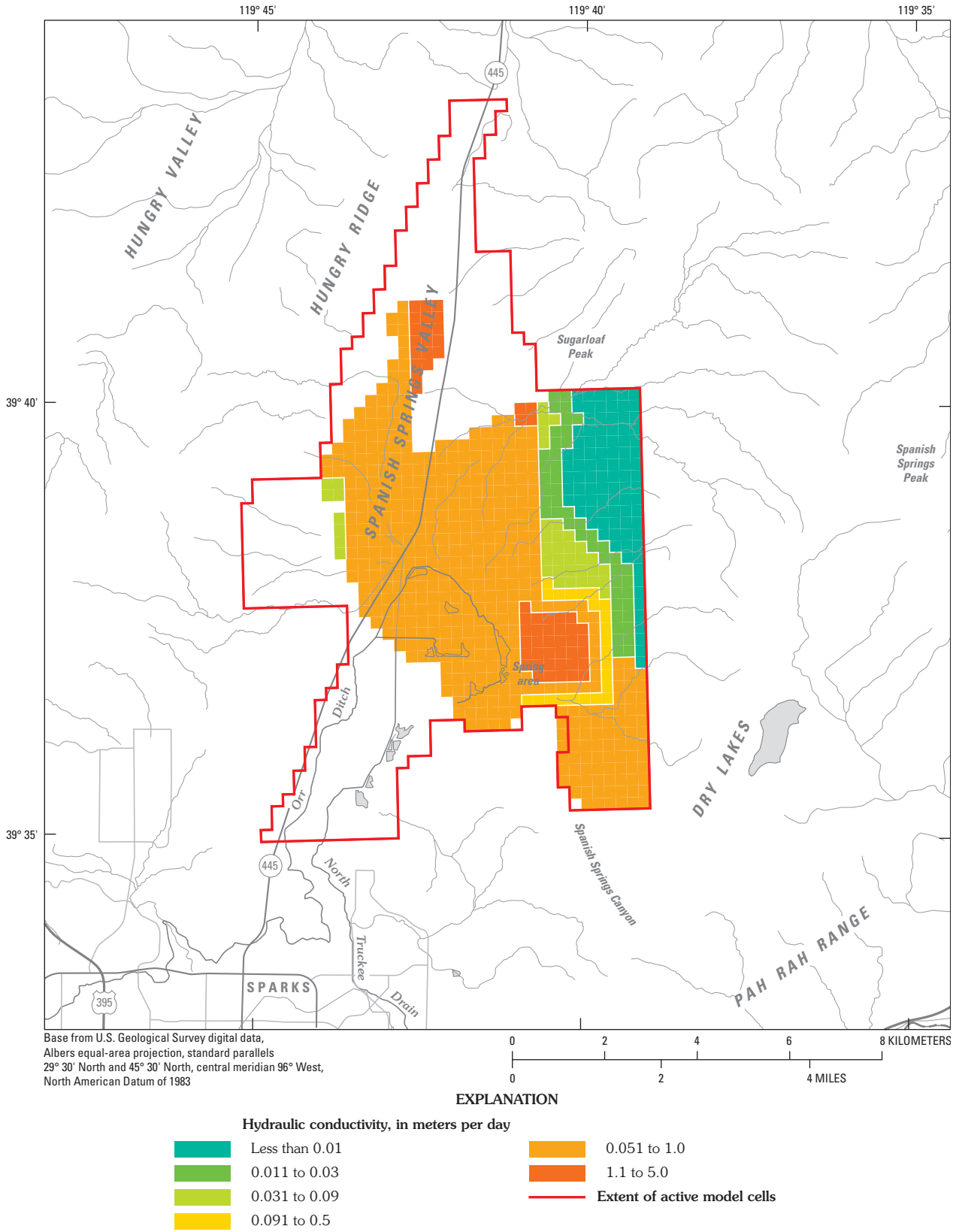

Figure 3.7*C*. Distribution of hydraulic conductivity for model layer 3, Spanish Springs Valley regional study area, Nevada.

Model Calibration

Both the Eagle Valley and Spanish Springs Valley steady-state models were calibrated by comparing model-computed hydraulic heads to measured hydraulic heads for 1997–2001. Hydraulic conductivity and recharge values were manually adjusted within a prescribed range until a reasonable match was obtained between model-computed and measured hydraulic heads. There were no surface-water flow data available for use in model calibration.

The overall goodness of fit of the model to the observation data was evaluated using summary measures and graphical analyses. The root-mean-squared error (RMSE), the range of head and residuals, the standard deviation, and the standard-mean error of the residuals (SME) were used to evaluate the model calibration. The RMSE is a measure of the variance of the residuals and was calculated as:

$$RMSE = \sqrt{\frac{\sum_{i=1}^{N} (h_{meas} - h_{sim})i^2}{N}}$$

where h_{meas} is the measured hydraulic head, h_{sim} is the model-computed (simulated) hydraulic head, $(h_{meas} - h_{sim})$ is the head residual, and N is the number of observations used in the computation. If the ratio of the RMSE to the total head change in the modeled area is small, then the error in the head calculations is a small part of the overall model response (Anderson and Woessner, 1992).

The SME was calculated as:

$$SME = \frac{\sigma(h_{meas} - h_{sim})}{\sqrt{N}}$$

where $\sigma(h_{meas} - h_{sim})$ is the standard deviation of the residuals.

Model-Computed Hydraulic Heads

The model-computed hydraulic heads compared favorably with measured hydraulic heads for the Eagle Valley model. The average residual was 0.14 m and residuals ranged from 13.6 to -18.6 m with the largest errors occurring along the model boundary representing the contact between the basin fill and mountain front. The standard deviation of the residuals is 5.77 m, and the SME is 0.58 m. The root-mean-squared error (RMSE) for the entire model was 5.7 m, which is approximately 6 percent of the 99-m range of measured hydraulic head. Measured hydraulic heads ranged from 1,397 to 1,496 m above NAVD88 and were similar to model-computed hydraulic heads, which ranged from 1,407 to 1,489 m above NAVD88. Figure 3.8*A* shows the relation between the residual head calculated as the difference between model-computed and measured hydraulic heads for both model layers and indicates the head residuals appear to be randomly distributed about zero at all values of measured head.

For the Spanish Springs Valley model, model-computed hydraulic heads also compare favorably with measured hydraulic heads. The average residual was 2.96 m and residuals ranged from -2.58 to 9.38 m with the largest errors generally occurring along the model boundary representing the contact between the basin fill and mountain front. The standard deviation of the residuals is 3.14 m, and the SME is 0.55 m. The RMSE for the entire model was 4.28 m, which is approximately 9 percent of the 50-m range of measured hydraulic head. Measured hydraulic heads ranged from 1,351 to 1,401 m above NAVD88 and were similar to model-computed hydraulic heads, which ranged from 1,352 to 1,396 m above NAVD88. Figure 3.8*B* shows the relation between the residual head calculated as the difference between model-computed and measured hydraulic heads for model layers 1 and 2 and indicates residuals are greatest in areas of highest hydraulic head.

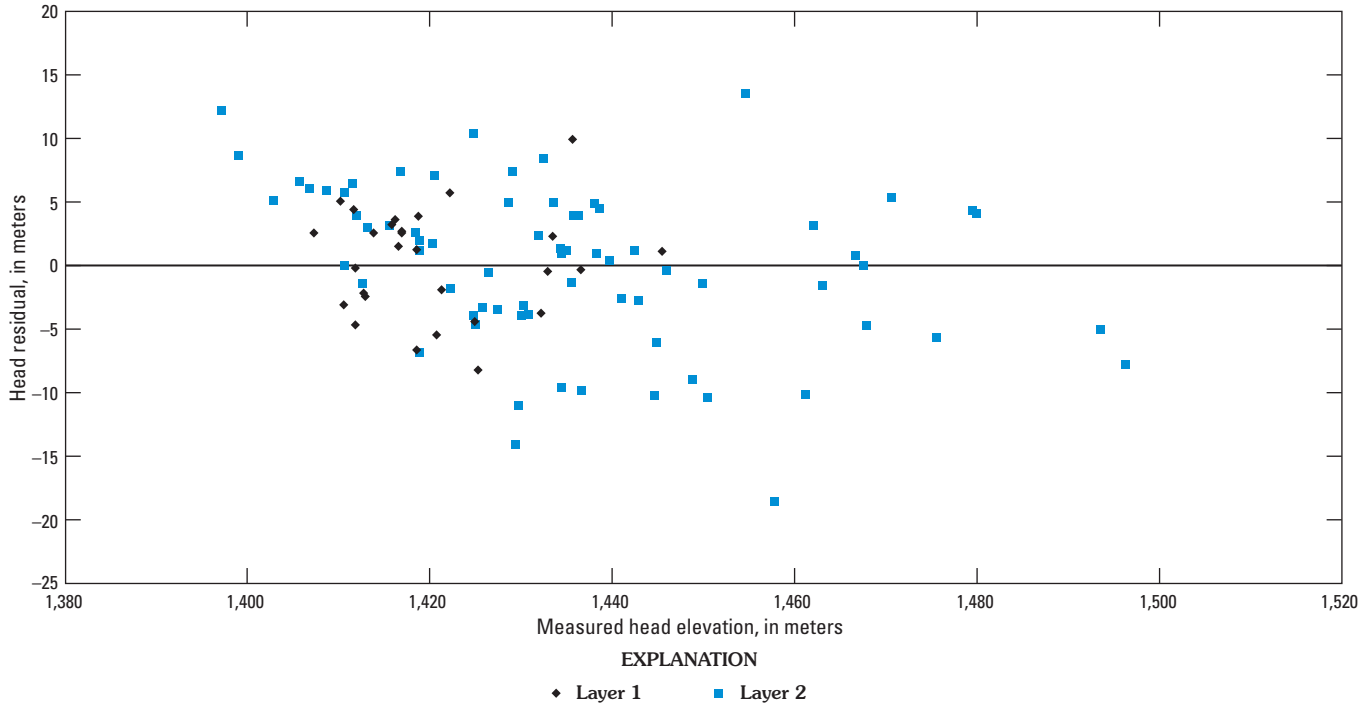

Figure 3.8*A*. Relation between residual head and measured hydraulic head, Eagle Valley regional study area, Nevada.

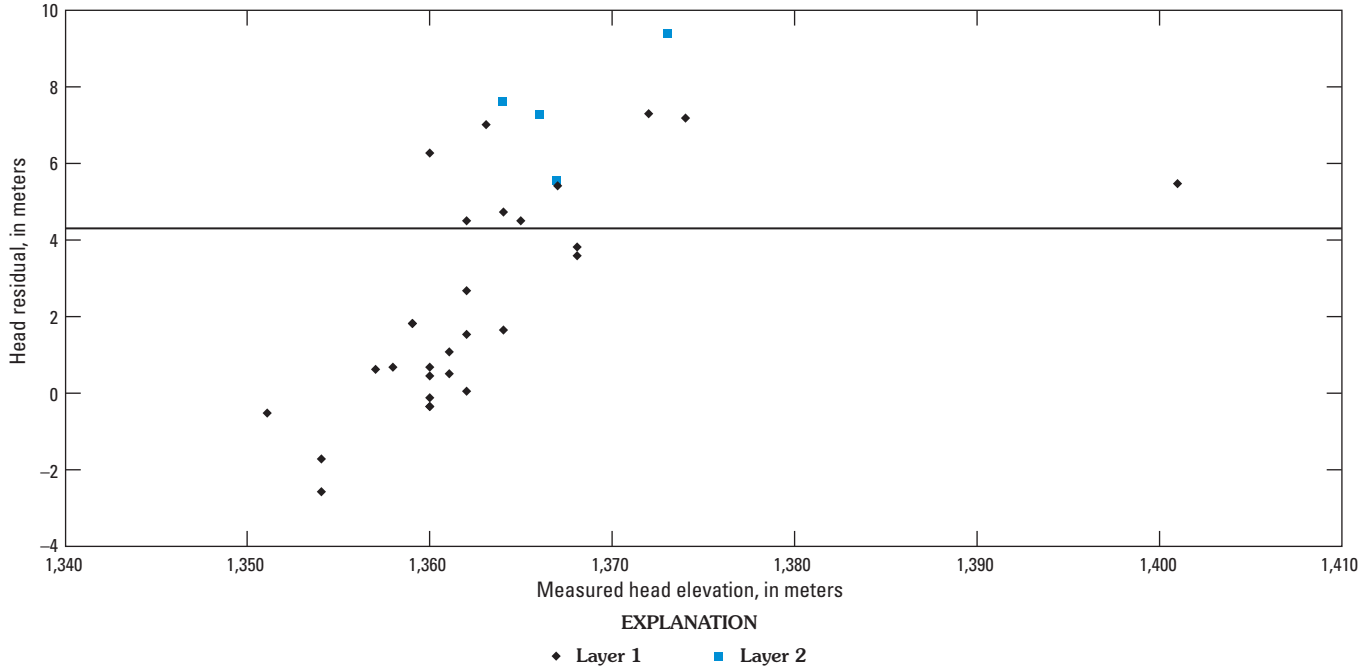

Figure 3.8*B*. Relation between residual head and measured hydraulic head, Spanish Springs Valley regional study area, Nevada.

Model-Computed Water Budget

The model-computed water budget for the Eagle Valley model is presented in table 3.4, and the model-computed water budget for the Spanish Springs Valley model is presented in table 3.5. In the Eagle Valley, infiltration of streamflow from the surrounding mountains (mountain-front recharge—62.9 percent of inflow) and mountain-block recharge (28.1 percent of inflow) were the primary sources of recharge to the basin-fill aquifer. Recharge from precipitation and irrigation provided 9 percent of the ground-water inflow. Discharge to public-supply wells (52.9 percent of outflow) and evapotranspiration (31.9 percent of outflow) were the primary ground-water outflows from the Eagle Valley. In the Spanish Spring Valley, canal leakage from the Orr Ditch (42.7 percent of inflow) and precipitation and irrigation (39.3 percent of inflow) were the primary sources of recharge to the basin-fill aquifer. Mountain-block recharge accounted for 13.3 percent of the ground-water inflow. Similar to the Eagle Valley, discharge to evapotranspiration (56 percent of outflow) and public-supply wells (34.7 percent of outflow) were the primary ground-water outflows from the Spanish Springs Valley. In general, both budgets compare fairly well with the conceptual water budgets discussed in the Water Budget section of this section.

Table 3.4. Model-computed water budget for 1997–2001 average conditions, Eagle Valley regional study area, Nevada.

[m^3/d, cubic hectometers per year]

Water-budget component	Flow (m^3/d)	Percentage of inflow or outflow
Model inflow		
Streams (mountain front recharge)	30,200	62.9
Mountain-block recharge	13,500	28.1
Precipitation, lawn and golf course watering	4,300	9.0
TOTAL INFLOW	**48,000**	**100**
Model outflow		
Wells	25,400	52.9
Evapotranspiration	15,300	31.9
Streams	7,300	15.2
TOTAL OUTFLOW	**48,000**	**100**

Table 3.5. Model-computed water budget for 1997–2001 average conditions, Spanish Springs Valley regional study area, Nevada.

[m^3/d, cubic hectometers per year]

Water-budget component	Flow (m^3/d)	Percentage of inflow or outflow
Model inflow		
Canal leakage	6,400	42.7
Precipitation and lawn irrigation	5,900	39.3
Mountain-block recharge	2,000	13.3
Head-dependent boundaries	700	4.7
TOTAL INFLOW	**15,000**	**100**
Model outflow		
Evapotranspiration	8,400	56.0
Wells	5,200	34.7
Head-dependent boundaries	1,100	7.3
Streams	300	2.0
TOTAL OUTFLOW	**15,000**	**100**

Simulation of Areas Contributing Recharge to Public-Supply Wells

The calibrated steady-state regional flow models were used to estimate areas contributing recharge and zones of contribution for public-supply wells using the MODPATH (Pollock, 1994) particle-tracking post processor and methods outlined in Section 1 of this Professional Paper. The model-computed areas contributing recharge represent advective ground-water flow and do not account for mechanical dispersion. Advection-dispersion transport simulations would likely yield larger areas contributing recharge than advective particle-tracking simulations because the effects of dispersion caused by aquifer heterogeneity would be included.

Along with flux output from the models, the MODPATH simulations require effective porosity values to calculate ground-water flow velocities. There are no porosity data available for the study areas, so a reasonable porosity value of 0.15 from the literature (Fetter, 2001) was used for all layers in both the Eagle Valley and Spanish Springs Valley particle-tracking simulations.

Particle-tracking simulations were used to outline areas contributing recharge for all 20 public-supply wells in the Eagle Valley. Areas contributing recharge are irregular in shape and extend to the mountain front on the north and west sides of the valley because a large amount of water enters the model as mountain-front or mountain-block recharge (fig. 3.9*A*). Traveltimes from recharge areas to public-supply wells were on the order of 5 to 40 years.

Particle-tracking simulations for the eight public-supply wells in the Spanish Springs Valley provided results similar to those for the Eagle Valley. In general, areas contributing recharge were along the mountain front on the east and west sides of the valley (fig. 3.9*B*). Traveltimes from recharge to discharge areas were somewhat longer in the Spanish Springs Valley than in the Eagle Valley, ranging from 10 to 2,600 years.

The areas contributing recharge in both the Eagle and Spanish Springs Valleys models extend to the general-head boundary cells along the mountain-front boundary of the alluvial aquifer indicating mountain-front and mountain-block recharge are the primary source of water for the public-supply wells.

Limitations and Appropriate Use of the Model

The ground-water flow models for the Eagle Valley and Spanish Springs Valley regional study areas were designed to evaluate the water budgets and delineate contributing areas to public-supply wells for hydrologic conditions in 1997–2001. A numerical ground-water model is a simplification of a physical system, and the intent in developing these regional models was not to reproduce every detail of the natural systems, but rather to portray their general characteristics. Sources of error in the model may include the steady-state flow assumption and errors in the conceptual model of the system, hydraulic properties, and boundary conditions.

The assumption of steady-state conditions for these models is a source of model uncertainty because the steady-state model may not be representative of ground-water flow conditions as time progresses and there were limited water-level data with which to evaluate long-term water-level trends. As water continues to be pumped from public-supply wells, water may be removed from aquifer storage especially in this arid climate where recharge is limited. The result may be a considerable delay before land-use practices in contributing areas delineated by this analysis could actually affect water quality in supply wells.

In some cases, model data were derived from sparse data or data of questionable quality (for example some drillers' logs) or by empirical methods that are inherently uncertain (such as estimating recharge as a percentage of precipitation). Other properties of the system had to be estimated without observation or measurement (for example, hydraulic properties of deep basin fill) and are another source of model uncertainty.

Although substantial information exists on some system stresses (for example, public-supply pumping), others such as evapotranspiration rates and septic-system recharge were estimated from literature values. It was not possible to identify the uncertainties, or the magnitude of the uncertainties, in the model data sets that contributed to the lack of complete agreement between simulated and measured hydraulic heads and ultimately to limitations of the results.

Computed areas contributing recharge and traveltimes through zones of contribution are based on a calibrated model and estimated effective porosity values. In a steady-state

model, changes to porosity values do not change the area contributing recharge to a given well. Changes to porosity values will change computed traveltimes from recharge to discharge areas in direct proportion to changes of effective porosity because there is an inverse linear relation between ground-water flow velocity and effective porosity and a direct linear relation between traveltime and effective porosity. For example, a one-percent decrease in porosity will result in a one-percent increase in velocity and a one-percent decrease in particle traveltime. There are no available porosity data for these study areas, so a reasonable estimated value was used. A detailed sensitivity analysis of porosity distributions was beyond the scope of this study, although future work could compare simulated ground-water traveltimes to ground-water ages to more thoroughly evaluate effective porosity values.

Despite their limitations, the Eagle Valley and Spanish Springs Valley regional ground-water flow models use justifiable aquifer properties and boundary conditions and provide reasonable representations of average ground-water flow conditions for 1997-2000. The models are suitable for evaluating regional water budgets and ground-water flow paths in the study area for the time period of interest but may not be suitable for long-term predictive simulations. These regional models provide useful tools to evaluate aquifer vulnerability at a regional scale, to facilitate comparisons of ground-water traveltime between regional aquifer systems, and to guide future detailed investigations in the study areas.

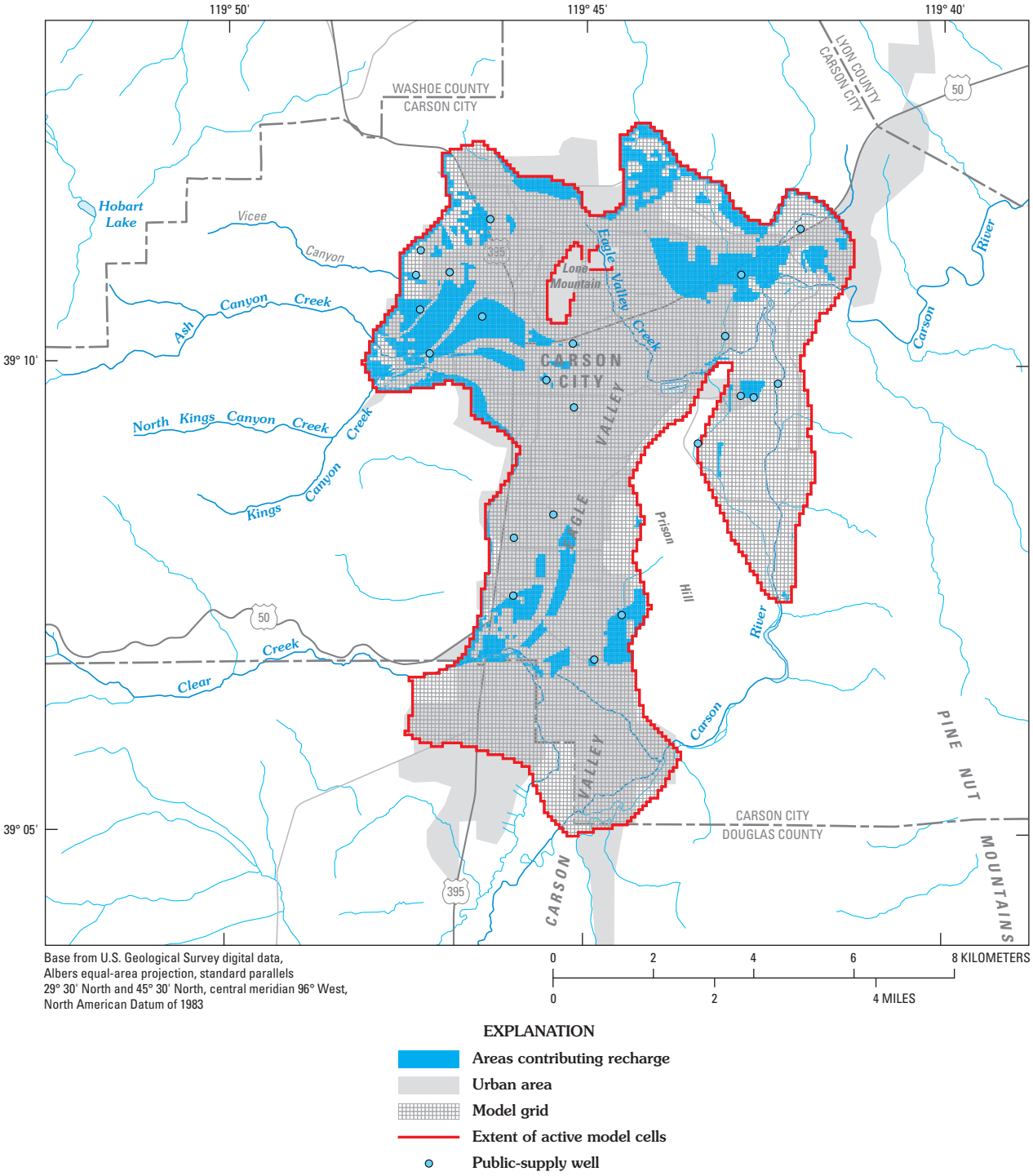

Figure 3.9*A*. Model-computed areas contributing recharge to public-supply wells, Eagle Valley regional study area, Nevada.

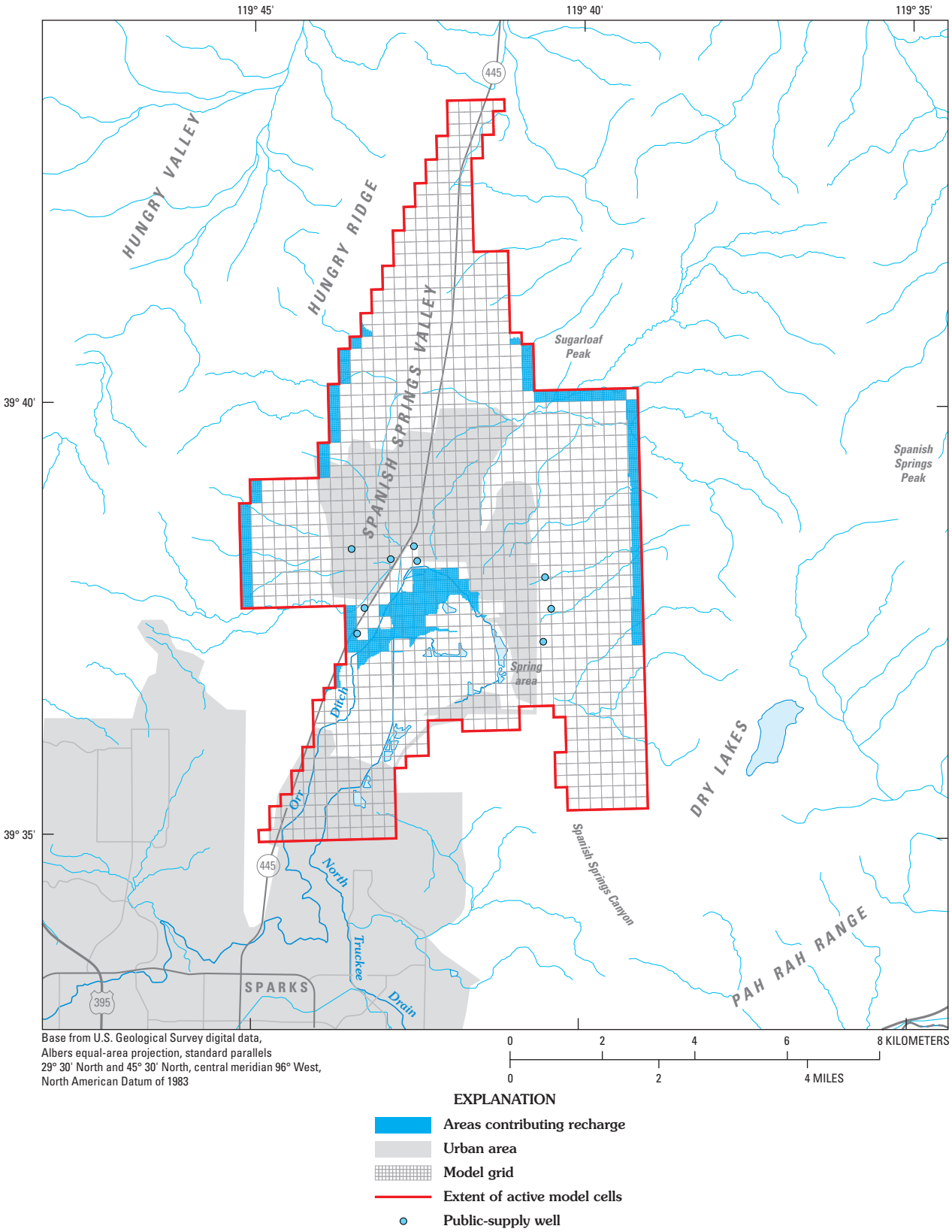

Figure 3.9*B*. Model-computed areas contributing recharge to public-supply wells, Spanish Springs Valley regional study area, Nevada.

References Cited

Anderson, M.P., and Woessner, W.W., 1992, Applied ground-water modeling: New York, Academic Press, Inc., 381 p.

Arteaga, F.E., 1986, Mathematical model analysis of the Eagle Valley ground-water basin, west-central Nevada: Nevada Division of Water Resources Bulletin 45, 53 p.

Arteaga, F.E., and Durbin, T.J., 1979, Development of a relation for steady-state pumping rate for Eagle Valley ground-water basin, Nevada: U.S. Geological Survey Open-File Report 79–261, 44 p.

Berger, D.L., 1995, Ground-water conditions and effects of mine dewatering in Desert Valley, Humboldt and Pershing Counties, northwestern Nevada, 1962–91: U.S. Geological Survey Water-Resources Investigations Report 95–4119, 79 p.

Berger, D.L., Ross, W.C., Thodal, C.E., and Robledo, A.R., 1997, Hydrogeology and simulated effects of urban development on water resources of Spanish Springs Valley, Washoe County, west-central Nevada: U.S. Geological Survey Water-Resources Investigations Report 96–4297, 44 p.

Cohen, P., and Loeltz, O.J., 1964, Evaluation of hydrogeology and hydrogeochemistry of Truckee Meadows area, Washoe County, Nevada: U.S. Geological Survey Water-Supply Paper 1779–S, 62 p.

Covay, K.J., Banks, J.M., Bevans, H.E., and Watkins, S.A., 1996, Environmental and hydrologic settings of the Las Vegas Valley area and the Carson and Truckee River Basins, Nevada and California: U.S. Geological Survey Water-Resources Investigations Report 96–4087, 72 p.

Fetter, C.W., 2001, Applied hydrogeology (4th ed.) Prentice Hall, Upper Saddle River, New Jersey.

Harbaugh, A.W., Banta, E.R., Hill, M.C., and McDonald, M.G., 2000, MODFLOW-2000, the U.S. Geological Survey modular ground-water model—User guide to modularization concepts and the ground-water flow process: U.S. Geological Survey Open-File Report 00–92, 121 p.

Harrill, J.R., 1973, Evaluation of the water resources of Lemmon Valley, Washoe County, Nevada, with emphasis on effects of ground-water development to 1971: Nevada Division of Water Resources, Bulletin 42, 130 p.

Johnson, K.L., Ball, G.W., Jr., and Harrigan, W.A., 1996, Carson City well completion report amendment, Silver Oak, Speedway, Well 11 redrill sites: Carson City Comprehensive Water Program.

Maupin, M.A., and Barber, N.L., 2005, Estimated withdrawals from principal aquifers in the United States, 2000: U.S. Geological Survey Circular 1279, 47 p.

Maurer, D.K., 1997, Hydrology and ground-water budgets of the Dayton Valley Hydrographic Area, west-central Nevada: U.S. Geological Survey Water-Resources Investigations Report 97–4123, 89 p.

Maurer, D.K., Berger, D.L., and Prudic, D.E., 1996, Subsurface flow to Eagle Valley from Vicee, Ash, and Kings Canyons, Carson City, Nevada, estimated from Darcy's Law and the chloride-balance method: U.S. Geological Survey Water-Resources Investigations Report 96–4088, 74 p.

Maurer, D.K., and Fischer, J.M., 1988, Recharge to the Eagle Valley ground-water basin by streamflow in Vicee Canyon, west-central Nevada: U.S. Geological Survey Water-Resources Investigations Report 88-4158, 66 p.

Maurer, D.K., and Thodal, C.E., 2000, Quantity and chemical quality of recharge, and updated water budgets, for the basin-fill aquifer in Eagle Valley, western Nevada: U.S. Geological Survey Water-Resources Investigations Report 99–4289, 46 p.

Maxey, G.B., and Eakin, T.E., 1949, Ground water in White River Valley, White Pine, Nye, and Lincoln Counties, Nevada: Nevada State Engineer, Water-Resources Bulletin 8, 59 p.

Planert, Michael, and Williams, J.S., 1995, Ground Water Atlas of the United States—California and Nevada: U.S. Geological Survey Hydrologic Atlas HA 730–B.

Pollock, D.W., 1994, User's guide for MODPATH/MODPATH-PLOT, Version 3—A particle tracking post-processing package for MODFLOW, the U.S. Geological Survey finite-difference ground-water flow model: U.S. Geological Survey Open-File Report 94–464, accessed Feb. 6, 2007 at *http://water.usgs.gov/nrp/gwsoftware/modpath41/modpath41.html*

Robinson, T.W., 1970, Evapotranspiration by woody phreatophytes in the Humboldt River Valley near Winnemucca, Nevada: U.S. Geological Survey Professional Paper 491–D, 41 p.

Robson, S.G., and Banta, E.R., 1995, Ground Water Atlas of the United States—Arizona, Colorado, New Mexico, and Utah: U.S. Geological Survey Hydrologic Atlas HA 730–C.

Rosen, M.R., Kropf, C., and Thomas, K.A., 2006, Quantification of the contribution of nitrogen from septic tanks to ground water in Spanish Springs Valley, Nevada, U.S. Geological Survey Scientific-Investigations Report 2006–5206, 12 p.

Rush, F.E., and Glancy, P.A., 1967, Water-resources appraisal of the Warm Springs-Lemmon Valley area, Washoe County, Nevada: Nevada Department of Conservation and Natural Resources, Water Resources Reconnaissance Report 43, 70 p.

Seiler, R.L., Zaugg, S.D., Thomas, J.M., and Howcroft, D.L., 1999, Caffeine and pharmaceuticals as indicators of wastewater contamination in wells: Ground Water, v. 37, no. 3, p. 405–410.

U.S Census Bureau, 2003, 2000 Census of population and housing–population and housing unit counts, PHC–3–29, Nebraska: Washington, D.C.

U.S. Geological Survey, 1939-00 and 1978-00, Water resources data, Nevada, water years 1996–2000: U.S. Geological Survey Water-Data Reports NV–39–1 to NV–00–1 and NV–78–1 to NV–00–1 (published annually).

U.S. Geological Survey, 1997–01, Water resources data, Nevada, water years 1996–2000: U.S. Geological Survey Water-Data Reports NV–96–1 to NV–00–1 (published annually).

Van Denburgh, A.S., Lamke, R.D., and Hughes J.L., 1973, A brief water-resources appraisal of the Truckee River Basin, western Nevada: Nevada Division of Water Resources, Reconnaissance Report 57, 122 p.

Washoe County, 1993, Spanish Springs Valley, monitoring well construction, August–October 1993, Reno, Nevada: Washoe County Department of Public Works, Utility Division, 19 p. and appendix.

Welch, A.H., 1994, Ground-water quality and geochemistry in Carson and Eagle Valleys, western Nevada and eastern California, U.S. Geological Survey Open-File Report 93–33, 99 p.

Worts, G.F., Jr., and Malmberg, G.T., 1966, Hydrologic appraisal for Eagle Valley, Ormsby County, Nevada: Nevada Department of Conservation and Natural Resources Reconnaissance Report 39, 55 p.

Hydrogeologic Settings and Ground-Water Flow Simulations of the San Joaquin Valley Regional Study Area, California

By Steven P. Phillips, Karen R. Burow, Diane L. Rewis, Jennifer Shelton, and Bryant Jurgens

Section 4 of

Hydrogeologic Settings and Ground-Water Flow Simulations for Regional Studies of the Transport of Anthropogenic and Natural Contaminants to Public-Supply Wells—Studies Begun in 2001

Edited by Suzanne S. Paschke

Professional Paper 1737–A

U.S. Department of the Interior
U.S. Geological Survey

U.S. Department of the Interior
DIRK KEMPTHORNE, SECRETARY

U.S. Geological Survey
Mark D. Myers, Director

U.S. Geological Survey, Reston, Virginia: 2007

For product and ordering information:
World Wide Web: http://www.usgs.gov/pubprod
Telephone: 1-888-ASK-USGS

For more information on the USGS--the Federal source for science about the Earth, its natural and living resources, natural hazards, and the environment:
World Wide Web: http://www.usgs.gov
Telephone: 1-888-ASK-USGS

Any use of trade, product, or firm names is for descriptive purposes only and does not imply endorsement by the U.S. Government.

Although this report is in the public domain, permission must be secured from the individual copyright owners to reproduce any copyrighted materials contained within this report.

Suggested citation:
Phillips, S.P., Burow, K.R., Lewis, D.L., Shelton, J., and Jurgens, B., 2007, Hydrogeologic settings and ground-water flow simulations of the San Joaquin Valley Regional Study Area, California, *section 4 of* Paschke, S.S., ed., Hydrogeologic settings and ground-water flow simulations for regional studies of the transport of anthropogenic and natural contaminants to public-supply wells—studies begun in 2001: Reston, Va., U.S. Geological Survey Professional Paper 1737–A, pp. 4–1 – 4–31.

Contents

Abstract 4–1
Introduction 4–1
Purpose and Scope 4–1
Study Area Description 4–3
Topography and Climate 4–3
Surface-Water Hydrology 4–3
Land Use 4–3
Water Use 4–3
Conceptual Understanding of the Ground-Water System 4–5
Geology 4–5
Ground-Water Occurrence and Flow 4–7
Aquifer Hydraulic Conductivity 4–7
Water Budget 4–12
Ground-Water Quality 4–13
Ground-Water Flow Simulations 4–18
Modeled Area and Spatial Discretization 4–18
Boundary Conditions and Model Stresses 4–18
Aquifer Hydraulic Properties 4–20
Model Calibration and Sensitivity 4–20
Model-Computed Hydraulic Heads 4–22
Model-Computed Water Budget 4–26
Simulation of Areas Contributing Recharge to Public-Supply Wells 4–26
Particle-Tracking Simulations 4–26
Public-Supply Well Contributing Areas 4–28
Limitations and Appropriate Use of the Model 4–28
References Cited 4–30

Figures

Maps showing:
4.1. Location of the San Joaquin Valley regional study area within the Central Valley aquifer system 4–2
4.2. Topography, hydrologic features, and location of public-supply wells, San Joaquin Valley regional study area, California 4–4
4.3. Physiographic provinces and selected geologic units, San Joaquin Valley regional study area, California. 4–6
4.4 Generalized *A*) map and *B*) hydrogeologic section showing of regional ground-water flow near Modesto, California. 4–8
4.5. Map showing measured hydraulic-head elevations in the unconfined to semi-confined aquifer for spring 2000, San Joaquin Valley regional study area, California. 4–9

4.6. Graph showing measured hydraulic-head elevations from November 1969 to November 2000 for selected irrigation wells, San Joaquin Valley regional study area, California. 4–10

Maps showing:

4.7. Percentage of coarse-grained texture for model layer 4, San Joaquin Valley regional study area, California 4–11

4.8. Ground-water flow model subareas used for water-budget calculations, San Joaquin Valley regional study area, California 4–14

4.9. Water-year 2000 estimated recharge rates for model subareas, San Joaquin Valley regional study area, California. 4–15

4.10 Water-year 2000 estimated ground-water pumping rates for model subareas, San Joaquin Valley regional study area, California 4–16

4.11. Conceptual diagram of oxidation-reduction conditions near Modesto, California..... 4–17

4.12 Map showing ground-water flow modeled area and boundary conditions San Joaquin Valley regional study area, California 4–19

Graphs showing:

4.13 Frequency of estimated horizontal hydraulic conductivity (*Kh*) and estimated vertical hydraulic condivivity (*Kv*) for the eastern and western alluvial fans, San Joaquin Valley regional study area, California 4–21

4.14. Ground-water flow model calibration results, San Joaquin Valley regional study area, California. 4–23–24

4.15. Map showing spatial distribution of hydraulic-head residuals, San Joaquin Valley regional study area, California..... 4–25

Graphs showing:

4.16. Relation between head residual and measured hydraulic head, San Joaquin Valley regional study area, California. 4–26

4.17. Relation between model-computed and measured hydraulic head, San Joaquin Valley regional study area, California. 4–26

4.18. Map showing model-computed areas contributing recharge for 15 public-supply wells in top quartile of pumping, San Joaquin Valley regional study area, California 4–29

Tables

4.1. Summary of water-budget components for water-year 2000 in the Modesto area, San Joaquin Valley regional study area, California..... 4–12

4.2. Model-computed water budget for water-year 2000, San Joaquin Valley regional study area, California. 4–27

4.3. Effective porosity values, by percentage of coarse-grained texture, used for MODPATH simulations, San Joaquin Valley regional study area, California..... 4–27

Hydrogeologic Settings and Ground-Water Flow Simulations of the San Joaquin Valley Regional Study Area, California

By Steven P. Phillips, Karen R. Burow, Diane L. Rewis, Jennifer Shelton, and Bryant Jurgens

Abstract

The transport of anthropogenic and natural contaminants to public-supply wells was evaluated in the northeastern part of the San Joaquin Valley near Modesto, California, as part of the U.S. Geological Survey National Water-Quality Assessment Program. The basin-fill aquifer system in the San Joaquin Valley regional study area is representative of the Central Valley aquifer system, is used extensively for agricultural irrigation and public water supply, and is susceptible and vulnerable to contamination. The Central Valley aquifer system in the study area consists of an unconfined to semi-confined aquifer in the upper sediments of the basin above and east of the Corcoran Clay confining unit. A confined aquifer occurs beneath the Corcoran Clay. Irrigation and public-supply wells are completed in both the unconfined and confined aquifers, and pumping in the valley has altered the natural ground-water flow patterns. A 16-layer, steady-state ground-water flow model of the basin-fill aquifer in an area around Modesto, California, was developed and calibrated to water-year 2000 conditions. The calibrated model and advective particle-tracking simulations were used to compute areas contributing recharge and traveltimes from recharge areas for 60 public-supply wells. Model results indicate agricultural irrigation return flow (41.5 percent of inflow) and precipitation (29.3 percent of inflow) provide most of the ground-water inflow, whereas the majority of ground-water discharge is to pumping wells (54.2 percent of outflow) and evapotranspiration (11.9 percent of outflow). Particle-tracking results indicate the areas contributing recharge to wells generally extend upgradient to the northeast of Modesto beyond the extent of the Corcoran Clay. Minimum traveltime from the water table to a well ranges from 3 to 141 years with a median of about 20 years, and maximum traveltime ranges from 18 to more than 1,600 years with a median of 107 years on the basis of particle-tracking results.

Introduction

The San Joaquin Valley regional study area for the transport of anthropogenic and natural contaminants to public-supply wells (TANC) is in the San Joaquin Valley near Modesto, California, and is part of the San Joaquin-Tulare Basins study unit of the U.S. Geological Survey National Water-Quality Assessment (NAWQA) Program (fig. 4.1).

Purpose and Scope

The purpose of this Professional Paper section is to present the hydrogeologic setting of the San Joaquin Valley regional study area. The section also documents the setup and calibration of a steady-state regional ground-water flow model for the study area. Ground-water flow characteristics, pumping-well information, and water-quality data were compiled from existing data to develop a conceptual understanding of ground-water conditions in the study area. A 16-layer steady-state ground-water flow model of the basin-fill aquifer in an area around Modesto, California, was developed and calibrated to ground-water flow conditions for the water-year 2000. The water-year 2000 was assumed to represent average conditions for the period from 1997 to 2001. The 5-year period 1997–2001 was selected for data compilation and modeling exercises for all TANC regional study areas to facilitate future comparisons between study areas. The calibrated ground-water flow model and associated particle tracking were used to simulate advective ground-water flow paths and to delineate areas contributing recharge to selected public-supply wells. Ground-water traveltimes from recharge to public-supply wells, oxidation-reduction (redox) conditions along flow paths, and presence of potential contaminant sources in areas contributing recharge were tabulated into a relational database as described in Section 1 of this Professional Paper. This section provides the foundation for future ground-water susceptibility and vulnerability analyses of the study area and comparisons among regional aquifer systems.

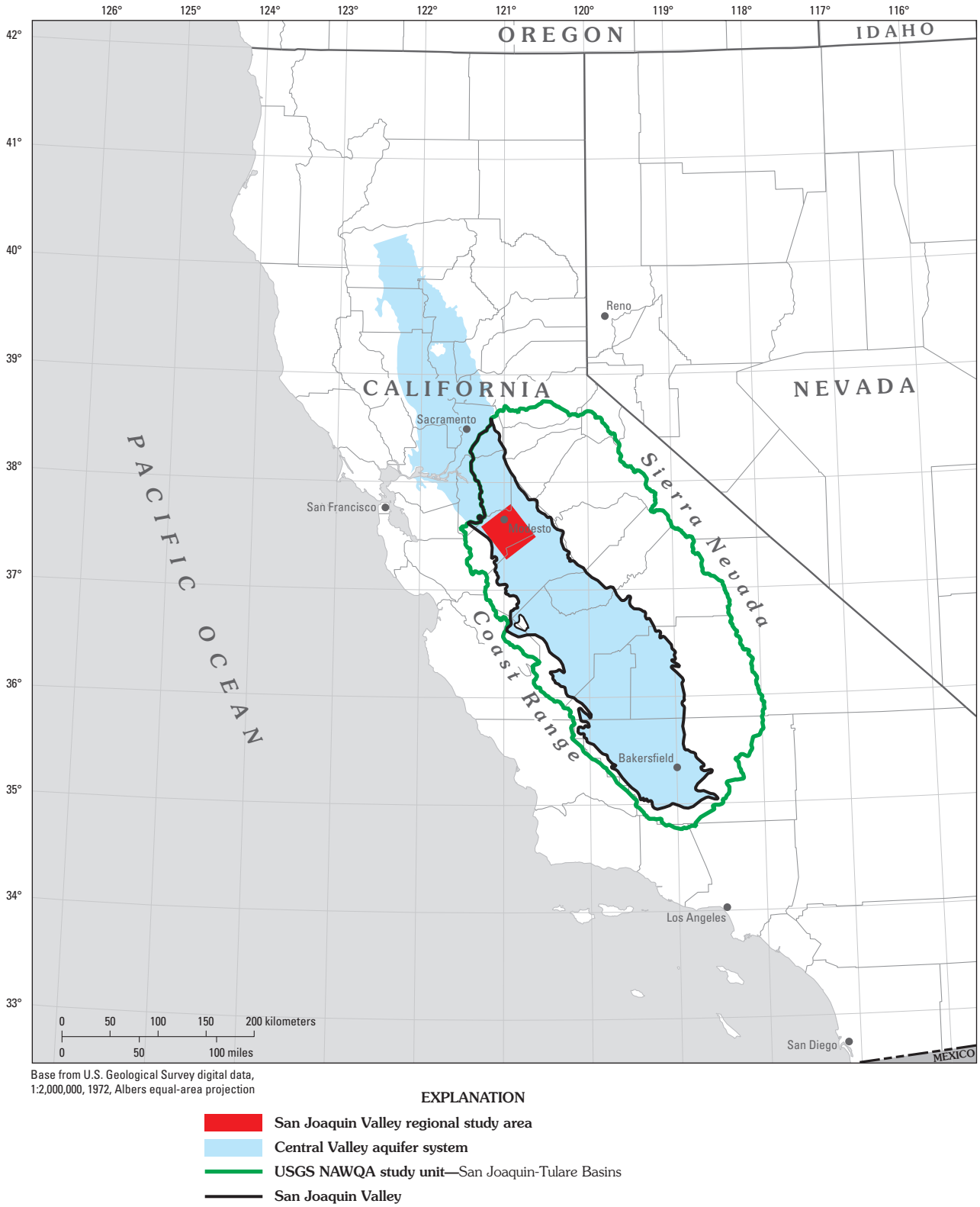

Figure 4.1. Location of the San Joaquin Valley regional study area within the Central Valley aquifer system.

Study Area Description

The San Joaquin Valley regional study area is about 2,700 square kilometers (km^2) centered on the city of Modesto, California, in the San Joaquin Valley. The San Joaquin Valley composes the southern two-thirds of the Central Valley aquifer system of California (fig. 4.1), which is ranked second in total water use of the 62 principal aquifers in the United States (Maupin and Barber, 2005).

Cities in the San Joaquin Valley are among those with the highest growth rates in the Nation, resulting in a gradual urbanization of adjacent farmlands. In Stanislaus County, the estimated population in 2000 was more than 446,000 people, an increase of 20 percent since 1990 (U.S. Census Bureau, 2002). Although more than 90 percent of the 1995 water demands in this region were for irrigation, approximately one-half of the demand for municipal and industrial supply is met by ground water. The increasing population and periods of drought are expected to increase reliance on ground water.

Topography and Climate

The San Joaquin Valley regional study area is bounded on the west by the San Joaquin River, on the north by the Stanislaus River, on the south by the Merced River, and on the east by the Sierra Nevada foothills (fig. 4.2). The Sierra Nevada rise east of the valley to an elevation of more than 4,200 m; the Coast Ranges, of moderate elevations, form the western edge of the valley. Surface topography in the study area slopes downward from the Sierra Nevada foothills to the San Joaquin River with gradients ranging from less than 1 m/km near the river to about 5 m/km near the foothills (fig. 4.2). The climate is semiarid, characterized by hot summers and mild winters, with rainfall (averaging 31.5 cm annually from 1931–1997 [National Oceanic and Atmospheric Administration, 2005]) during late fall through early spring.

Surface-Water Hydrology

The San Joaquin River is the central drainage for the northern San Joaquin Valley; it is the only major surface-water outlet from the valley draining out through San Francisco Bay. The southern San Joaquin Valley is a hydrologically closed basin. The water quality of the San Joaquin River is of critical interest because it flows into the Sacramento-San Joaquin Delta, a key source of drinking water for southern California and irrigation water for the western San Joaquin Valley. The Stanislaus, Tuolumne, and Merced Rivers drain the Sierra Nevada and are tributaries to the San Joaquin River in the study area.

All rivers in the study area have been significantly modified from their natural state. Each has multiple reservoirs for irrigation and power generation, which effectively delays discharge of large amounts of snowmelt runoff. Imprinted over this hydrology is an extensive network of canals used to deliver water for irrigation (fig. 4.2).

Land Use

Agriculture is the primary land use, covering more than 65 percent of the study area, and most of the agricultural land is irrigated. The primary crops are almonds, walnuts, peaches, grapes, grain, corn, pasture, and alfalfa. The towns of Modesto, Turlock, and a number of smaller urban areas composed about 6 percent of the study area in 2000, and the remaining 29 percent of the study area was natural vegetation near the foothills and in riparian areas (Burow and others, 2004).

Water Use

Agricultural irrigation supplied by surface water and ground water accounted for about 95 percent of the total water use in 2000 (Burow and others, 2004). Surface-water supplies originate primarily from a series of reservoirs in the Sierra Nevada foothills, are managed by irrigation districts, and are delivered to agricultural users through hundreds of kilometers of lined canals.

Irrigation districts and private agricultural users pump ground water for irrigation. Some districts also pump ground water to lower the water table in areas where it has risen too close to the land surface to support agriculture without active management. Private agricultural ground-water pumping is not measured in the study area but is estimated as about 32 percent of total agricultural water use in the study area in 2000.

Urban water demand is met by a combination of surface-water and ground-water supplies. Before 1995, the City of Modesto, the largest urban area, used ground water exclusively for public supply. In 1994, a surface-water treatment plant was completed, which, in 2000, provided about one-half of Modesto's municipal and industrial water supplies (Burow and others, 2004). Data from all of the urban areas, as a whole, indicate that about 55 percent of the urban water requirement was met with ground water in 2000 (Burow and others, 2004).

Based on local drillers' logs, about 60 percent of wells in the study area are for domestic use, followed by about 27 percent for irrigation, 4 percent for public supply, and 9 percent for test, stock, industrial, and other uses (Burow and others, 2004). Well depths range from 7 to 368 m below land surface, with a median depth of 59 m. In general, domestic wells tap shallow parts of the aquifer, whereas irrigation and public-supply wells are screened in deeper zones. The wells generally are distributed throughout the region, though fewer wells exist in the older sediments and terraces east of Modesto and Turlock and along the San Joaquin River. The deepest wells generally are in the older sediments in the eastern part of the study area, and the shallowest wells generally are in the western part and along the rivers. Additional clusters of deep wells are in the urban areas (fig. 4.2).

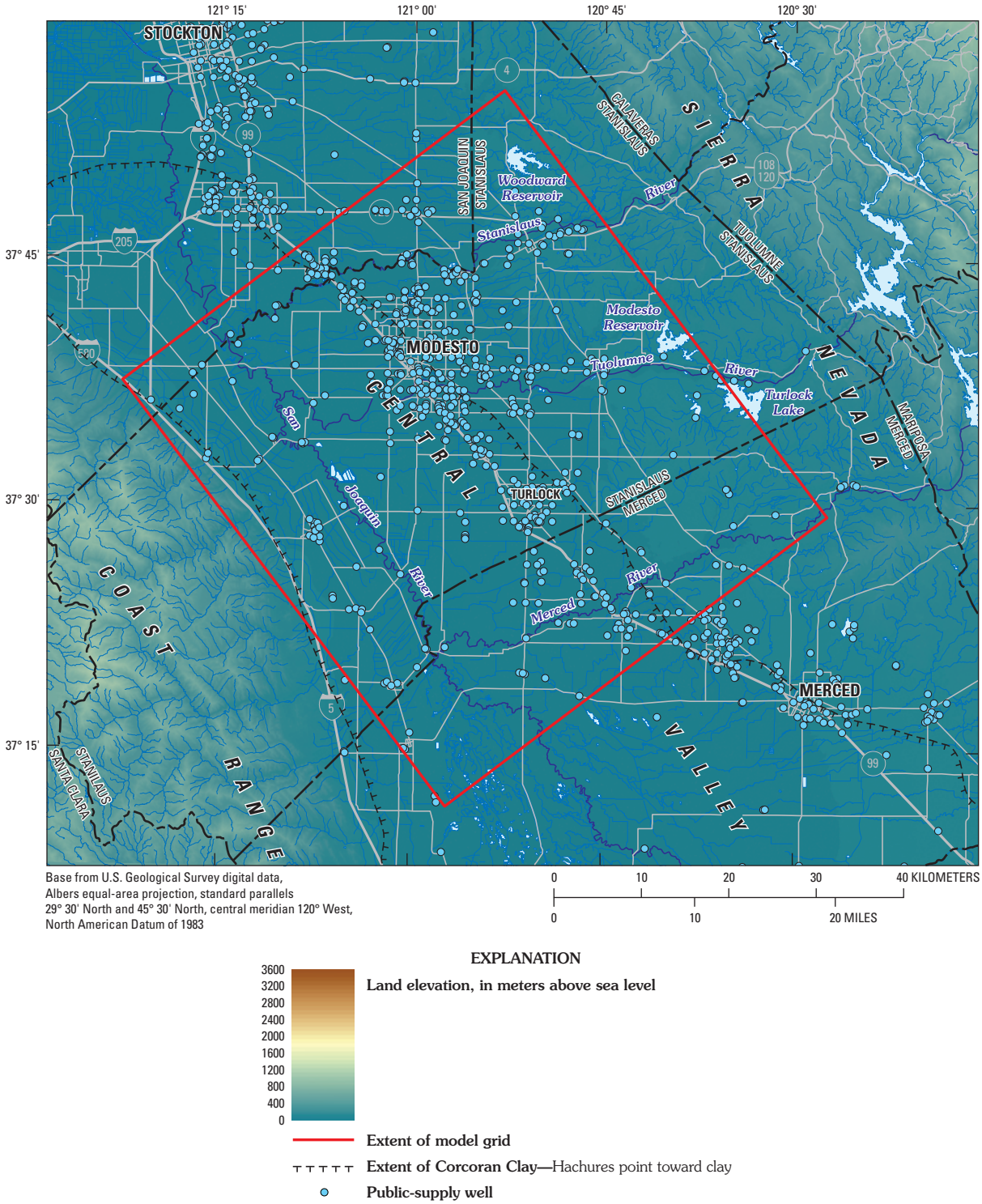

Figure 4.2. Topography, hydrologic features, and location of public-supply wells, San Joaquin Valley regional study area, California.

Conceptual Understanding of the Ground-Water System

The aquifers in the San Joaquin Valley TANC regional study area are composed of Tertiary and Quaternary alluvial deposits shed from the surrounding Sierra Nevada and Coast Ranges. The basin-fill is composed of coalescing alluvial fans, which tend to be coarse grained near the mountains and finer grained toward the center of the basin. The Corcoran Clay, correlated to the Corcoran Clay Member of the Tulare Formation south of the study area, is a lacustrine clay deposit that separates the basin-fill deposits into an upper unconfined aquifer and a lower confined aquifer throughout much of the study area. Under natural conditions, ground-water recharge occurred in the upper parts of the alluvial fans where stream valleys enter the basin, and ground water discharged to the San Joaquin River and surrounding marshlands. However, ground-water pumping in the valley for agricultural irrigation and public water supply has altered ground-water flow patterns. Water flowing laterally toward the center of the basin may be pumped, applied as irrigation, recharge the aquifer, then be pumped and reapplied at the surface several times as it moves toward the San Joaquin River. Ground-water quality is influenced by recharge from the surrounding mountain streams and irrigated agriculture.

Geology

The Central Valley of California is a northwest-trending structural trough filled with Tertiary and Cretaceous continental and marine sediments up to 10 km thick (Gronberg and others, 1998; Bartow, 1991). The Sierra Nevada Range lies on the eastern side of the valley and is composed primarily of pre-Tertiary granitic rocks. In the northern San Joaquin Valley, the Sierra Nevada Range is separated from the Central Valley by a foothill belt of marine and metavolcanic rocks. The Coast Ranges lie on the western side of the valley and are a complex assemblage of rocks, including marine and continental sediments of Cretaceous to Quaternary age (Gronberg and others, 1998).

The San Joaquin Valley can be divided into three physiographic regions (fig. 4.3): the western alluvial fans, the eastern alluvial fans, and the basin (Gronberg and others, 1998) Alluvial fan deposits on both sides of the valley are composed predominantly of coarse-grained sediments near the head of each fan that become finer grained toward the valley trough. The sediments in the eastern alluvial fan region generally are more permeable than sediments in the western alluvial fan region because sediment-source rocks and watershed characteristics are different between the two areas. The basin region is composed of continental (shallow) and marine (deeper) sediments that are overlain by fine-grained, moderately to densely compacted clays. These low-permeability deposits restrict the downward movement of water.

Consolidated rocks and deposits exposed along the margin of the valley floor include Tertiary and Quaternary continental deposits, Cretaceous and Tertiary marine sedimentary rocks, and the pre-Tertiary Sierra Nevada basement complex (Piper and others, 1939; Davis and others, 1959). Most unconsolidated deposits in the study area are contained within the Pliocene-Pleistocene Laguna (not mapped at the surface in study area), Turlock Lake, Riverbank, and Modesto Formations, with minor amounts of Holocene stream-channel and flood-basin deposits (fig. 4.3) (Arkley, 1962, 1964; Davis and Hall, 1959). The Turlock Lake, Riverbank, and Modesto Formations form a sequence of overlapping terrace and alluvial fan systems (Marchand and Allwardt, 1981) indicating cycles of alluviation, soil formation, and channel incision that were influenced by climatic fluctuations and resultant glacial stages in the Sierra Nevada (Bartow, 1991).

The Corcoran Clay Member of the Tulare Formation is a lacustrine deposit that is a key subsurface feature in the San Joaquin Valley. Page (1986) mapped the areal extent of this regional confining unit based on a limited number of well logs and geophysical logs. Additional lithologic data recently were used to modify the extent of this prominent unit in the study area (Burow and others, 2004). The eastern extent of the Corcoran Clay roughly parallels the San Joaquin River valley axis (fig. 4.3). The Corcoran Clay ranges in depth from 28 to 85 m below land surface and in thickness from 0 to 57 m in the study area.

The Mehrten Formation is tapped by wells in the eastern part of the study area. The Mehrten Formation reflects a change in lithology and texture from overlying sediments of primarily unconsolidated coarse-grained sediments of arkosic composition to Mehrten Formation sediments of primarily consolidated sediments of volcanic-derived mafic materials (Burow and others, 2004). The Mehrten Formation outcrops in the eastern part of the study area and lies at depths of at least 120 m below land surface beneath Modesto.

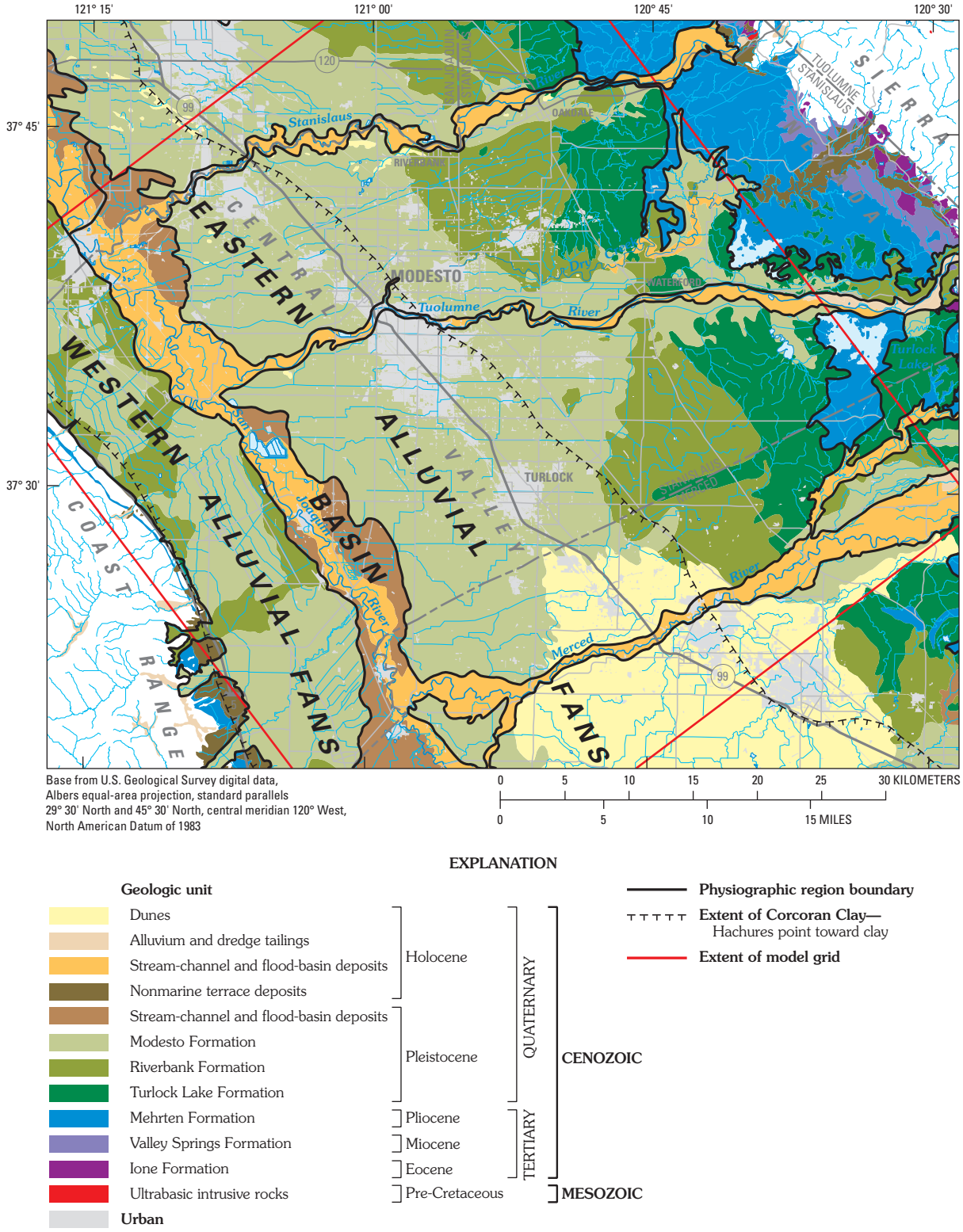

Figure 4. 3. Physiographic provinces and selected geologic units, San Joaquin Valley regional study area, California.

Ground-Water Occurrence and Flow

Ground water in the study area is present in the unconfined to semi-confined aquifer above and east of the Corcoran Clay and in the confined aquifer beneath the Corcoran Clay. The unconfined to semiconfined aquifer above the Corcoran Clay ranges in thickness from about 40 to 70 m. The unconfined to semiconfined aquifer east of the Corcoran Clay is composed primarily of alluvial sediments but includes the upper part of the Mehrten Formation, which is more consolidated than the overlying formations. Coarse-grained gravel and sand layers present in the upper part of the Mehrten are tapped by irrigation and public-supply wells. The confined aquifer is composed of alluvial sediments and upper Mehrten Formation sediments from beneath the Corcoran Clay to the lowermost freshwater. The contribution of ground water from the consolidated rocks beneath the primary aquifers was assumed negligible and was not considered for this study.

Under natural conditions, ground water was primarily recharged at the upper parts of the alluvial fans where the major streams enter the valley (fig. 4.4). Ground-water flow followed the southwest slope of the basement complex and the dip of the overlying sedimentary deposits toward the southwest in the direction of the valley trough. Artesian conditions near the San Joaquin River indicated discharge to the river and surrounding marshlands (Davis and others, 1959).

Ground-water resource development in the basin changed ground-water flow patterns. Pumping for agricultural irrigation and agricultural irrigation return flows are much greater than natural recharge and discharge and caused an increase in vertical flow in the system (fig. 4.4) (Page and Balding, 1973; Londquist, 1981). Ground-water flow direction for 2000 is generally toward the southwest and is somewhat similar to the predevelopment flow regime (fig. 4.5). However, ground water moving along a lateral flow path may be extracted by wells and applied at the surface several times before reaching the valley trough (fig. 4.4), at which point it may cross to the other side of the valley rather than discharge to the river because of pumping on the west side of the valley. South of the Tuolumne River is a centrally located ground-water-flow divide, east of which water flows northeastward toward irrigation wells in an agricultural area with no surface-water supplies. West of the flow divide, water flows southwestward toward the valley trough (fig. 4.5).

The western part of the study area along the San Joaquin River is an area of ground-water discharge where the water table is within 3 m of the land surface. Ground-water pumping is used in this area to keep the water table from affecting crop roots. Depth to the water table increases eastward, particularly south of the Tuolumne River, where depths can exceed 40 m.

Long-term water levels measured in selected wells representing the unconfined to semi-confined aquifer near the city of Modesto indicate water levels generally decreased in the Modesto area until the early 1990s (fig. 4.6). This hydraulic-head decrease likely was caused by increased urban development and associated public-supply pumping punctuated by drought conditions in 1976 and 1987–92. A series of wet years in the early 1990s and completion of a surface-water treatment plant in 1994, which provided an additional source of public-supply and industrial water, resulted in a recovery of ground-water levels near Modesto.

Aquifer Hydraulic Conductivity

The hydraulic properties of the aquifer system were estimated for this study based on the distribution of sediment texture and through calibration of the ground-water flow model. The texture distribution was estimated using the general approach of Laudon and Belitz (1991), which made use of drillers' logs and geophysical logs.

To facilitate this texture-based approach, a database was constructed as part of a cooperative effort between the U.S. Geological Survey and the Modesto Irrigation District to organize information on well construction and subsurface lithology in the study area (Burow and others, 2004). About 10,000 drillers' logs were examined. Because sediment descriptions on drillers' logs can be ambiguous and widely variable, a rating scheme was developed to select a subset of about 3,500 logs for use in this study. In addition to lithologic data, the database contains well-construction information, which was used to vertically distribute ground-water pumping in the flow model.

To visualize subsurface sediment-texture distributions and provide a heterogeneous hydraulic-conductivity field for the flow model, the primary texture of sediments in the study area was characterized using a geostatistical approach (Burow and others, 2004). Lithologic descriptions in the database were expressed as a percentage of coarse-grained sediment. These percentages were then interpolated within each layer of the model grid (using kriging), providing an estimated distribution of sediment texture. The estimated texture distribution for model layer 4 (above the Corcoran Clay) is shown in figure 4.7. The estimated texture distributions are reasonably constrained in the model layers above the Corcoran Clay and in some areas where the deepest wells penetrate the sub-Corcoran part of the system. In deeper parts of the aquifer system, where no data were available, the texture value in the lowest layer estimated was duplicated in all underlying model cells.

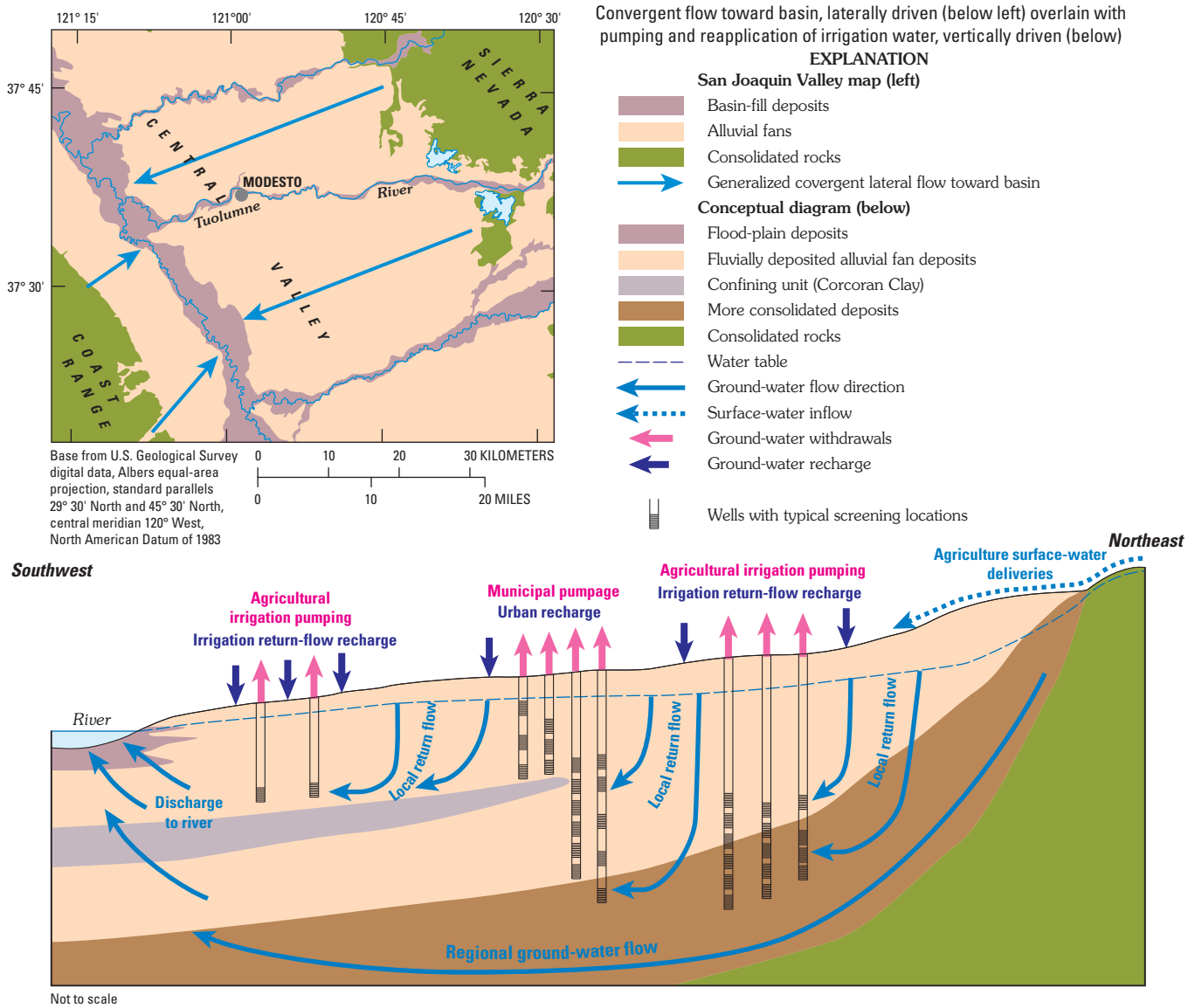

Figure 4. 4. Regional ground-water flow near Modesto, California.

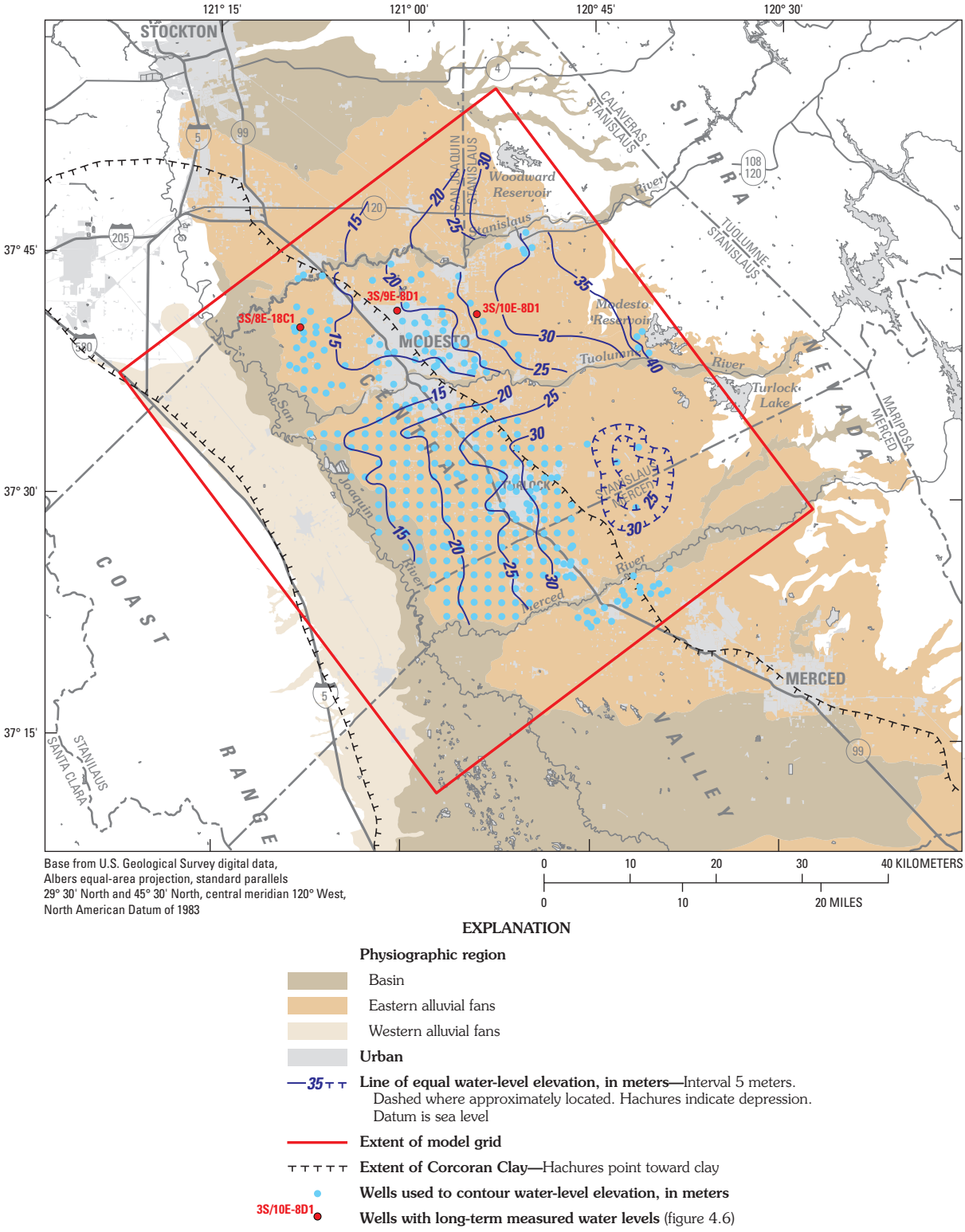

Figure 4. 5. Measured hydraulic-head elevations in the unconfined to semi-confined aquifer for spring 2000, San Joaquin Valley regional study area, California.

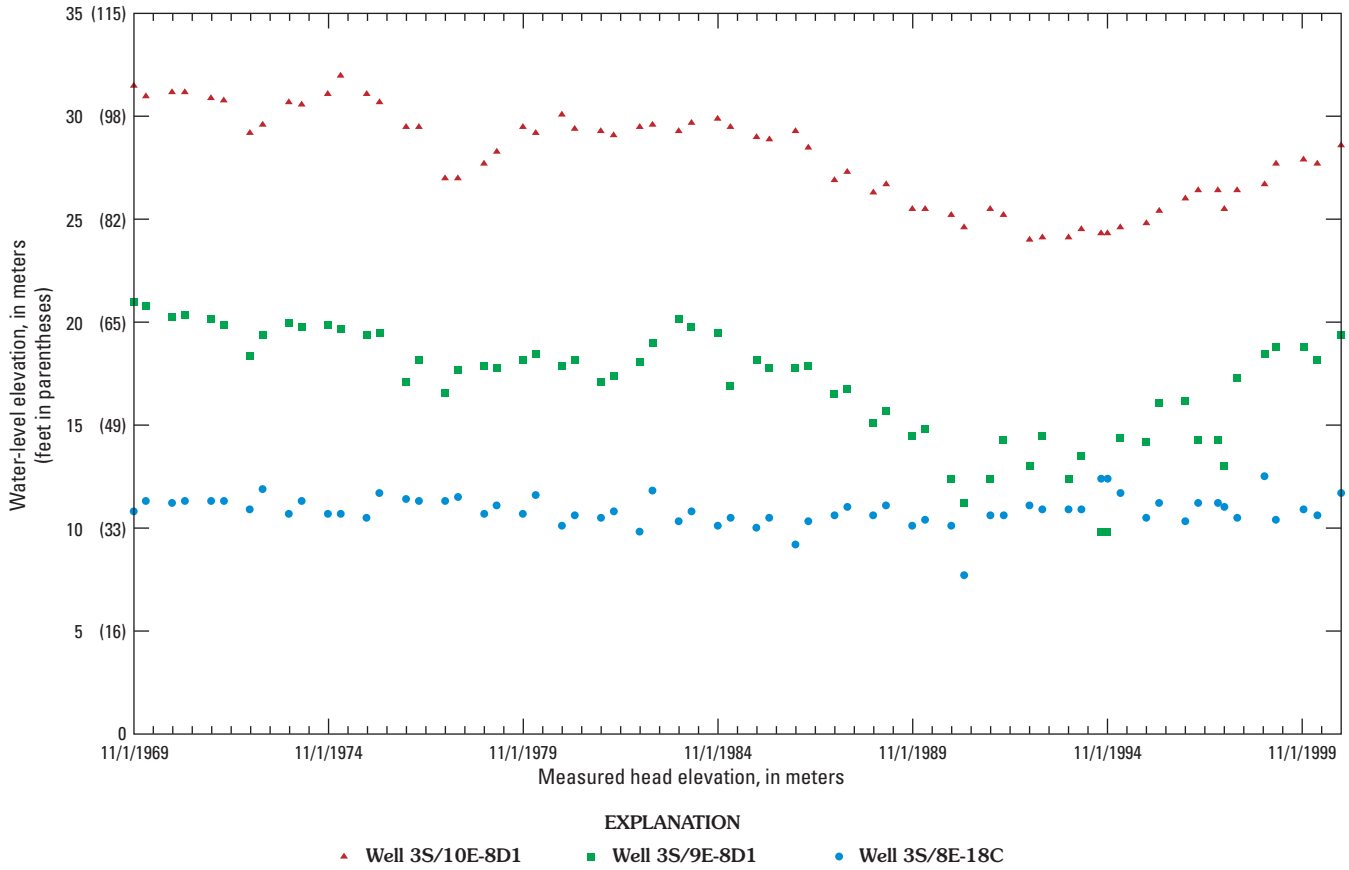

Figure 4. 6. Measured hydraulic-head elevations from November 1969 to November 2000 for selected irrigation wells, San Joaquin Valley regional study area, California. Well locations shown on figure 4.5.

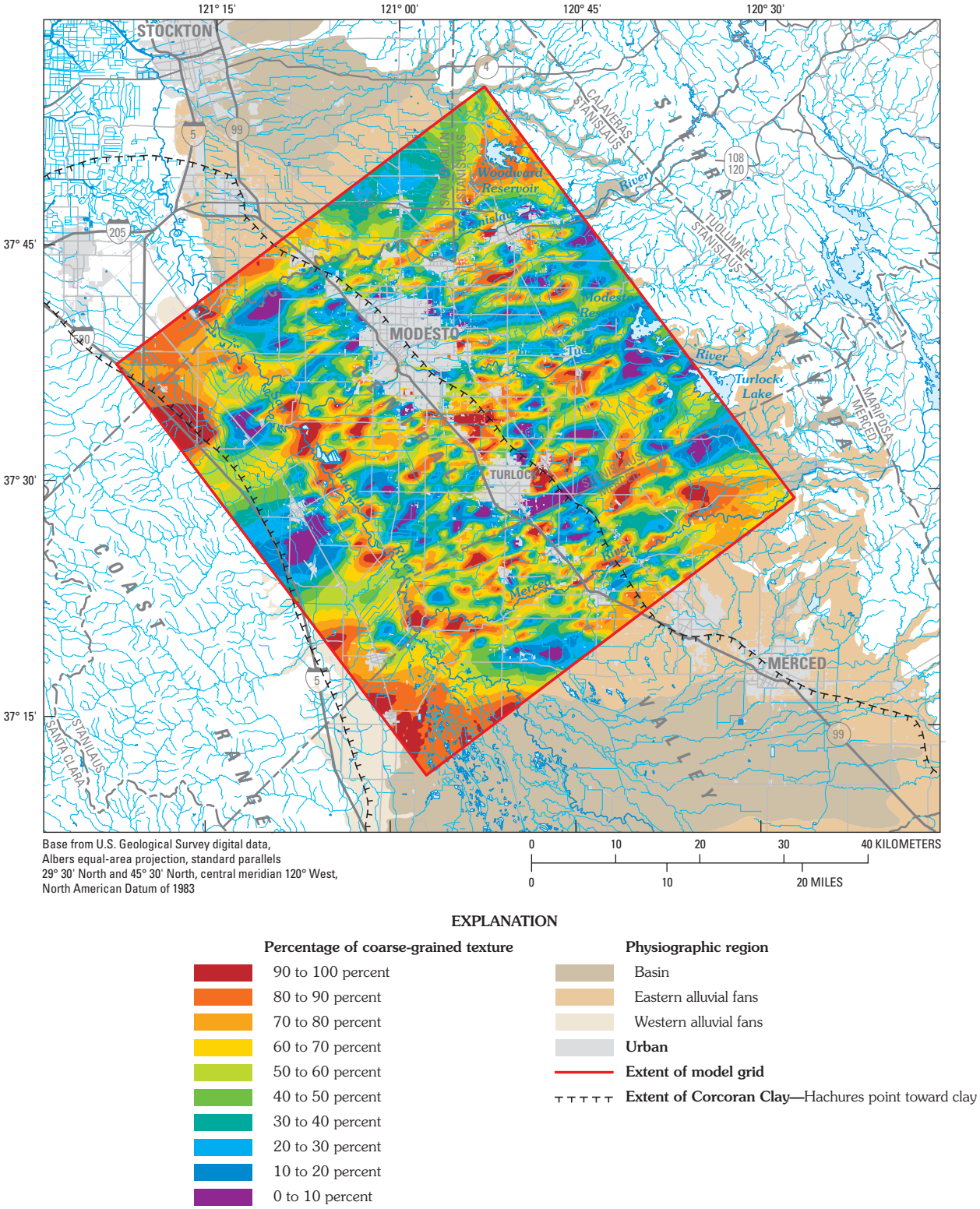

Figure 4. 7. Percentage of coarse-grained texture for model layer 4, San Joaquin Valley regional study area, California

Water Budget

A water-budget approach was used to estimate ground-water pumping and recharge from infiltration of rainfall and irrigation return flow for water-year 2000 (October 1, 1999, through September 30, 2000). Surface water and ground water are used for irrigation in the agricultural areas. Surface-water delivery data were available for most of the water-budget subareas, although private pumping records generally were not. Therefore, the water budget was critical for estimating ground-water use in agricultural areas and was important for estimating areal recharge throughout the model area.

The water budget was derived by dividing the basin into subareas for which surface-water deliveries could be obtained or estimated. A separate water budget was calculated for each of the resulting 47 subareas, which were then grouped into 12 model subareas (table 4.1) (fig. 4.8), which included agricultural and urban settings, foothill areas, riparian areas with natural vegetation and(or) crops, and reservoirs.

A land-use approach (Burow and others, 2004) was used to estimate the water budget for subareas containing primarily nonurban land use. The area of each crop or other vegetation type was determined, a daily crop demand was calculated based on crop or vegetation type and climate, and a daily irrigation demand was estimated for each subarea. The irrigation demand was met by a combination of surface-water deliveries, ground water pumped by irrigation districts, and private ground-water pumping. The total reported or estimated monthly surface-water and ground-water deliveries were subtracted from the estimated monthly irrigation demand to determine the monthly unmet irrigation demand. Private ground-water pumping was then assumed to be the source of unmet irrigation demand.

The consumptive use of applied water, or irrigation efficiency, was estimated at about 63 percent for most of the study area on the basis of irrigation methods used and estimates in subareas with relatively high surface-water deliveries and few known wells. Irrigation efficiency was assumed greater (80 percent) in the older fan deposits in the foothill areas, where the sediments are more indurated and modern and efficient irrigation methods are more commonly used (Burow and others, 2004).

Recharge in the urban areas was estimated using the minimum month method to determine indoor and outdoor

Table 4.1 Summary of water-budget components for water-year 2000 in the Modesto area, San Joaquin Valley regional study area, California.

[m^2, square meters; m^3, cubic meters]

Water-budget subarea	Irrigation demand			Surface-water deliveries	
	Irrigated cropped area, including double and intercropped area (m^2)	Crop demand (m^3)	Irrigation demand (m^3)	Surface-water deliveries (m^3)	Agricultural ground-water pumpage deliveries (m^3)
Eastside Water District (EWD)	214,781,896	192,159,808	240,199,759	—	—
Merced Irrigation District (MER)	134,263,686	118,920,445	188,762,611	85,184,253	2,563,052
Merquin Community Water District (MERQ)	29,744,731	28,761,456	45,653,105	21,909,708	—
Modesto Irrigation District (MID)	252,669,587	236,308,482	375,092,829	172,897,795	25,894,607
Oakdale Irrigation District (OID)	206,238,419	209,521,576	261,901,970	302,202,485	10,274,903
South San Joaquin Irrigation District (SSJID)	127,848,622	119,424,314	189,562,403	157,031,625	—
Stevinson Water District (SWD)	14,464,212	13,809,833	21,920,370	10,654,212	—
Turlock Irrigation District (TID)	603,293,199	529,757,589	840,885,063	554,268,926	94,771,341
Foothills (FOOT)	—	—	—	—	—
Reservoirs (RES)	—	—	—	—	—
Riparian and miscellaneous agricultural areas (RIP)	182,577,869	158,586,562	251,724,701	208,025,236	—
Urban (URB)	—	—	—	38,102,384	—
TOTAL	1,765,882,221	1,607,250,065	2,415,702,811	1,550,276,623	133,503,903

[1] Negative pumpage resulted from excess delivery for calculated crop demand. Pumpage was set to zero in the model.

water use (California Department of Water Resources, 1994). Ten percent of the estimated outdoor use was subtracted from the total to account for leakage from water distribution lines (California Department of Water Resources, 1994). Fifty percent of the remaining outdoor water use was assumed to be consumptive use for landscape irrigation or runoff to streams, and the remainder of outdoor use was assumed to be urban recharge (Burow and others, 2004).

The average areal recharge rate for the study area is about 54 cm/yr, which includes recharge from precipitation and irrigation return flow, with the highest recharge rates occurring in the agricultural areas in the western part of the study area and along the rivers in the eastern part (fig. 4.9). The lowest recharge rates were in the foothills and the urban areas. Similarly, the highest pumping rates were in the agricultural areas in the western part of the study area (fig. 4.10). The relatively high rates of pumping and recharge in the western agricultural areas are related to the irrigation efficiency and supplemental pumping required to manage the shallow water table. No information was available regarding pumping rates from domestic wells. Although domestic wells are common in the study area, they were assumed to represent an insignificant percentage of the water budget and were not included.

Ground-Water Quality

Ground-water quality in the study area is influenced by recharge from streams and surface water imported through canals. This recharge can infiltrate from irrigated fields to the water table and by regional ground-water flow from the alluvial fans on the east and west sides of the valley toward the axial trough (Davis and others, 1959; Bertoldi and others, 1991). Ground water on the east side of the San Joaquin River is fairly uniform in composition, consisting of predominantly sodium-calcium-bicarbonate or calcium-sodium-bicarbonate type water (Davis and Hall, 1959), and has generally low dissolved-solids concentrations (less than 500 mg/L). Ground-water quality east of the San Joaquin River reflects recharge of water originating in the granitic Sierra Nevada to the east (Page, 1973; Bertoldi and others, 1991). Ground water on the west side of the San Joaquin River is predominantly of

and ground-water pumpage			Recharge			
Private agricultural ground-water pumpage (m^3)	Urban ground-water pumpage (m^3)	Total ground-water pumpage (m^3)	Recharge from urban water distribution lines (m^3)	Recharge from irrigation (m^3)	Recharge from precipitation (m^3)	Total recharge (m^3)
240,199,759	—	240,199,759	—	48,039,952	62,028,511	110,068,463
101,015,306	1,858,512	105,436,870	—	69,842,166	37,207,316	107,049,482
23,743,397	—	23,743,397	—	16,891,649	10,573,559	27,465,208
176,300,427	11,636,020	213,831,054	—	138,784,347	66,807,374	205,591,721
[1] –50,575,417	3,591,759	[1] –36,708,755	—	52,380,394	58,648,959	111,029,353
32,530,778	2,107,287	34,638,065	—	70,138,089	33,885,822	104,023,911
11,266,159	—	11,266,159	—	8,110,537	6,738,661	14,849,198
206,059,686	33,568,641	334,399,669	—	311,127,473	161,236,620	472,364,093
—	—	—	—	—	61,362,021	61,362,021
—	—	—	—	—	4,995,484	4,995,484
43,699,465	—	43,699,465	—	93,138,139	69,747,688	162,885,828
—	47,182,527	47,182,527	4,101,222	18,455,497	9,858,789	32,415,508
784,239,561	99,944,746	1,017,688,210	4,101,222	826,908,243	583,090,805	1,414,100,270

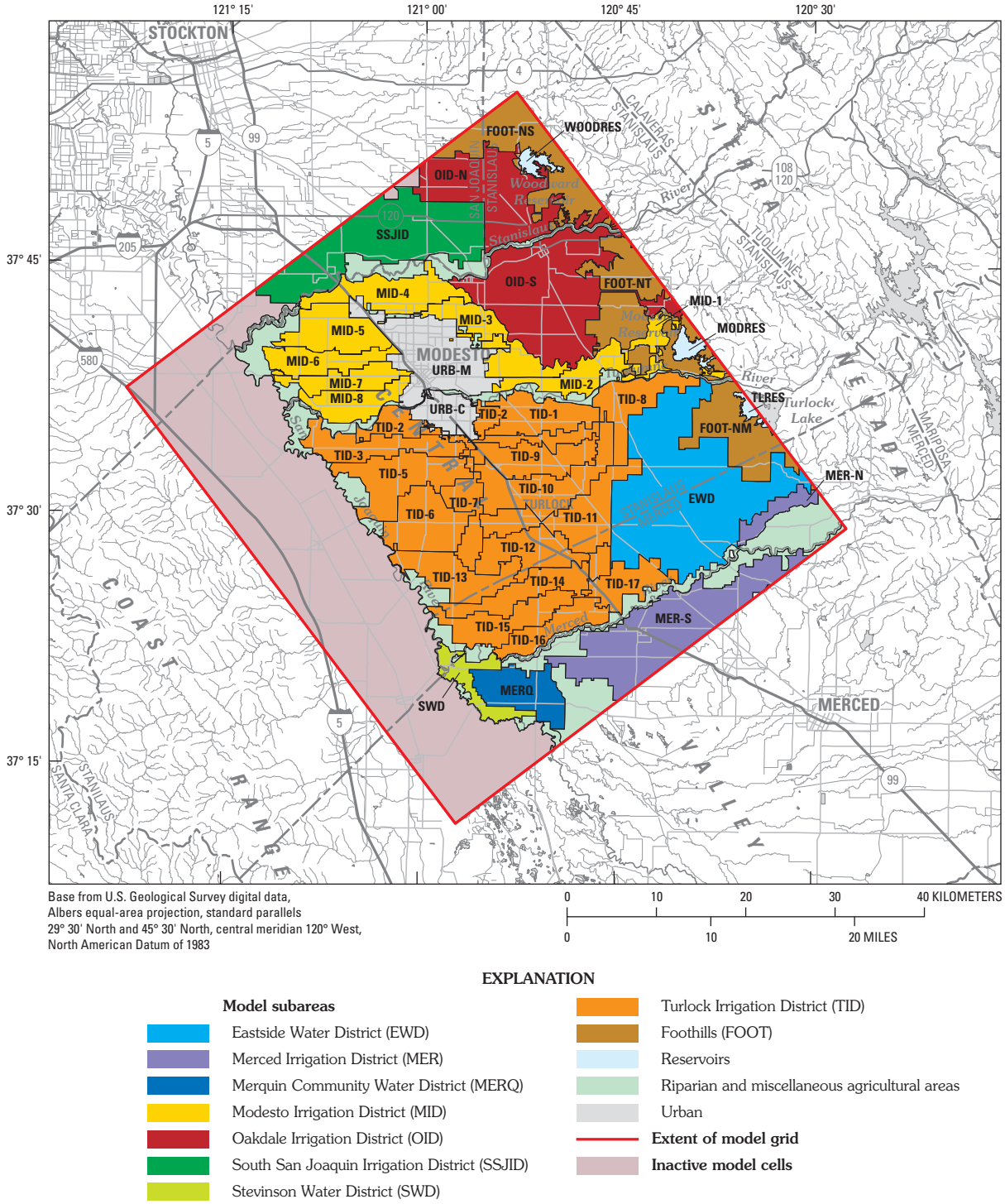

Figure 4. 8. Ground-water flow model subareas used for water-budget calculations, San Joaquin Valley regional study area, California.

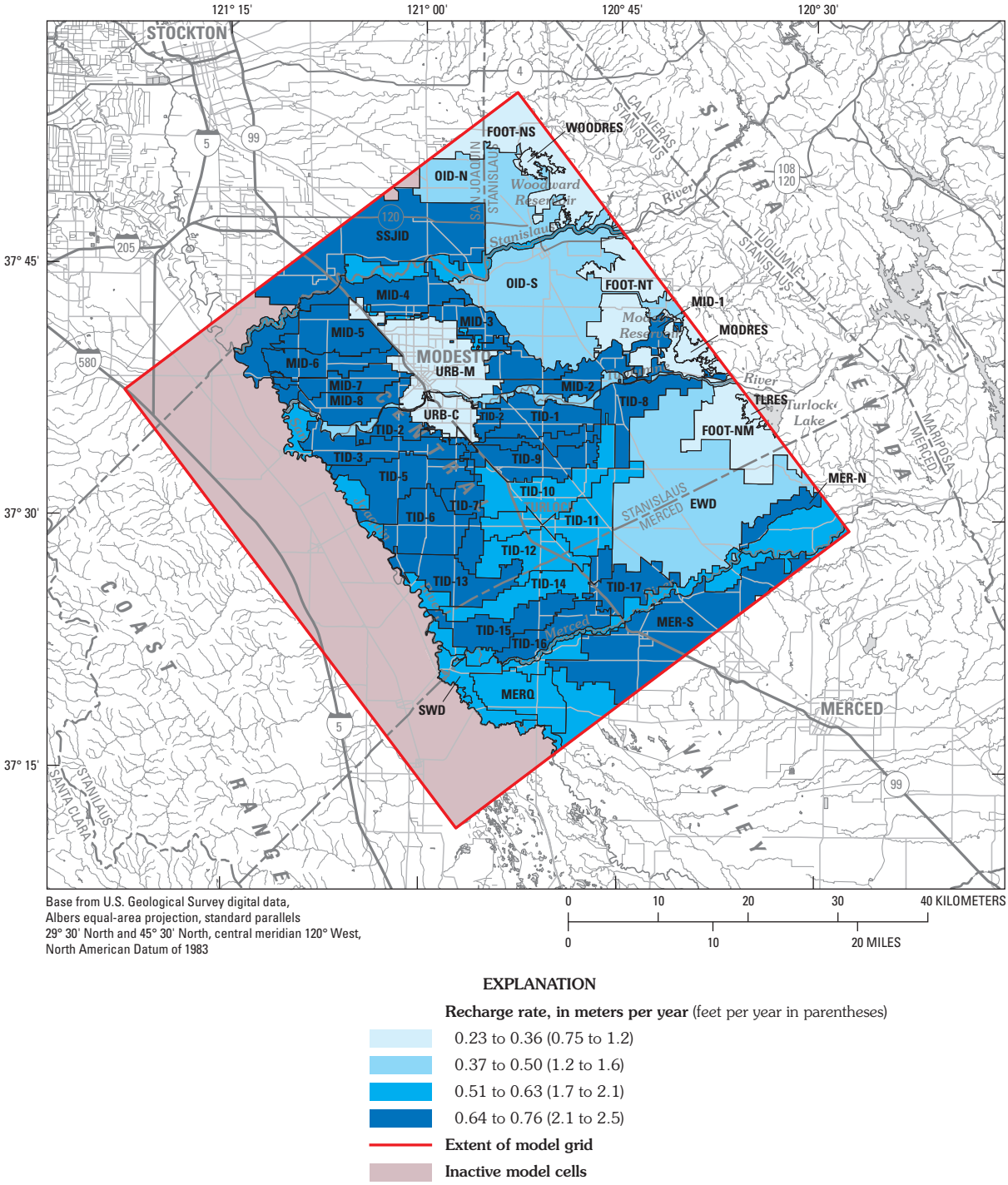

Figure 4. 9. Water-year 2000 estimated recharge rates for model subareas, San Joaquin Valley regional study area, California.

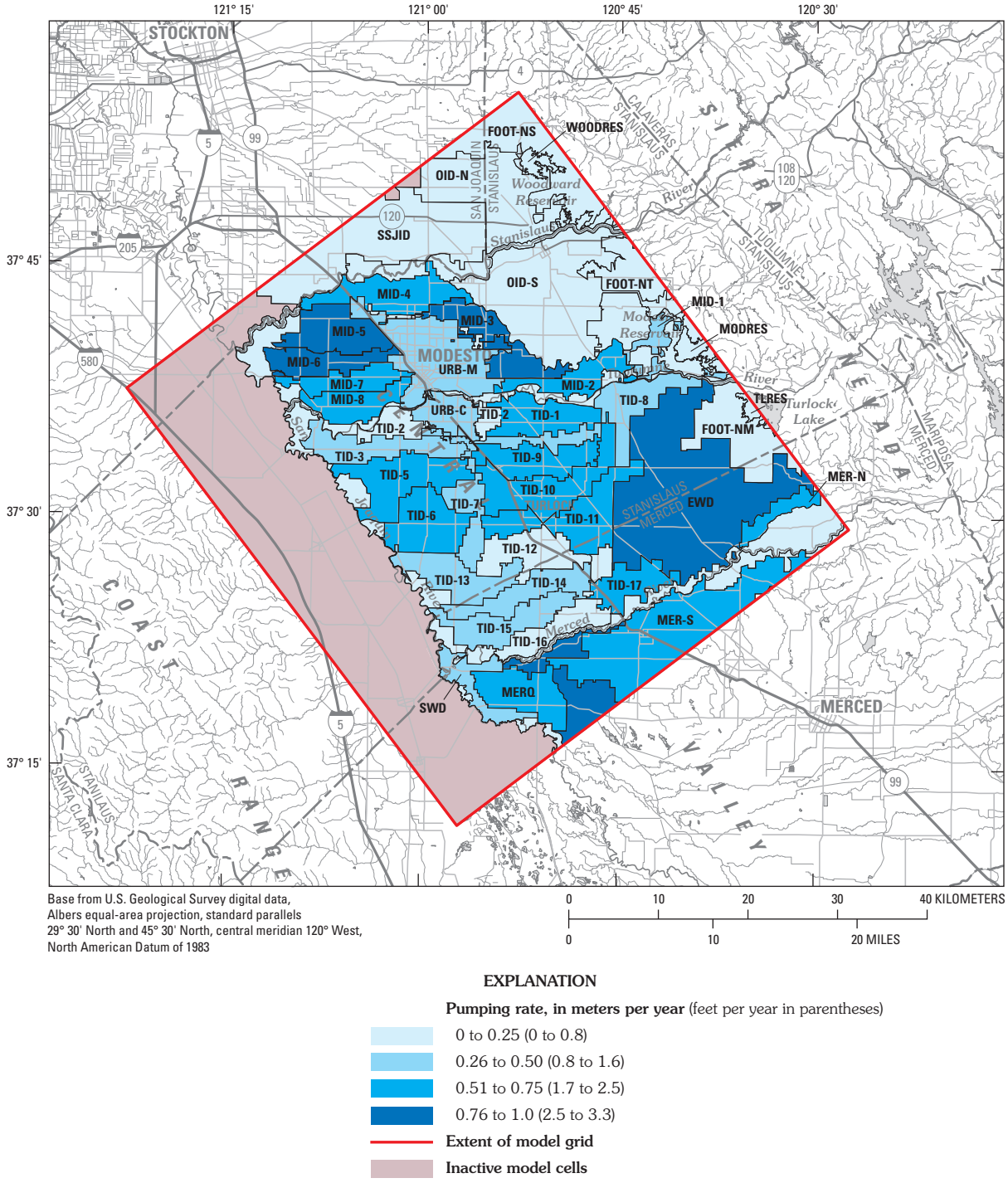

Figure 4. 10. Water-year 2000 estimated ground-water pumping rates for model subareas, San Joaquin Valley regional study area, California.

calcium-sulfate or calcium-bicarbonate type water with dissolved-solids concentrations ranging from 500 to 1,500 mg/L (Davis and others, 1959; Bertoldi and others, 1991), likely reflecting recharge of water originating in the marine and continental sedimentary rocks of the Coast Ranges to the west (Davis and Hall, 1959). Because the axial trough has been the discharge area in the past, ground water in this area is derived from a combination of water from the east and west sides of the valley and varies widely in composition with depth.

The water chemistry is further influenced by an increase in reducing conditions and cation-exchange processes as the water moves through the sediments (Bertoldi and others, 1991). Ground water beneath the alluvial fans in the valley area is largely oxidizing, whereas ground water beneath the axial trough and in discharge areas adjacent to streams typically is geochemically reduced (Gronberg and others, 1998; fig. 4.11). Geochemically reduced water is likely associated with relatively fine-grained sediments of higher organic content, longer residence times of water reaching natural discharge areas, and confined portions of the aquifer. Concentrations of oxidation-reduction- sensitive (redox) species in retrospective ground-water quality data for the study area were used to delineate regional redox patterns. Because of the limited spatial coverage of suitable water-quality samples and the dominantly oxygenated conditions in the aquifer, most of the study area was mapped as conditions consistent with oxygen and nitrate reduction. Areas of manganese reduction and iron reduction with high sulfate were mapped along the axial trough and deep in the more consolidated sediments and confined parts of the aquifer beneath the alluvial fans.

Agricultural water use is the largest nonpoint source of water-quality degradation in the San Joaquin Valley. Irrigation has become the major source of recharge to the ground-water system and can contain elevated concentrations of dissolved solids, nutrients, pesticides, and in some areas, trace elements (Gronberg and others, 1998).

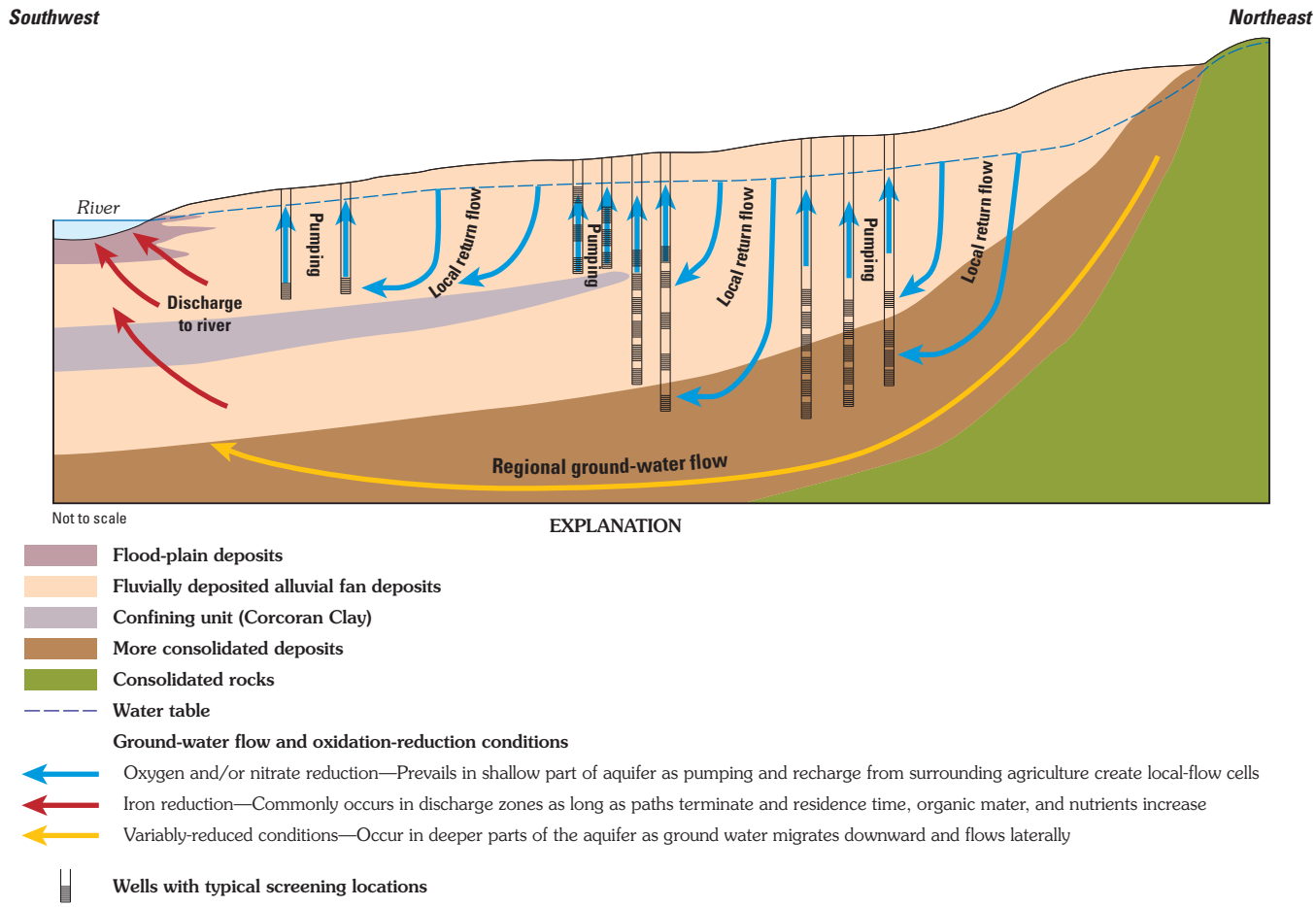

Figure 4. 11. Conceptual diagram of oxidation-reduction conditions near Modesto, California.

Ground-Water Flow Simulations

A steady-state model of ground-water flow in the study area was developed using MODFLOW-2000 (Harbaugh and others, 2000) to estimate aquifer-system properties, delineate areas contributing recharge to public-supply wells in Modesto, and support future local modeling efforts. The model represents the water-year 2000 when the ground-water system was in a quasi-steady-state condition. Measured hydraulic heads in the study area indicate much of the system has been at equilibrium for many years (fig. 4.6), particularly the areas with a shallow water table downgradient from Modesto and Turlock. The two areas where hydraulic heads have recently changed are Modesto and the agricultural area upgradient from Turlock. Water levels recovered rapidly with importation of surface water to the Modesto area in 1995, but the recovery slowed greatly by 2000. Upslope from Turlock, hydraulic heads have declined for about 2 decades due to increased ground-water use associated with new agricultural development. Although water-level data for this area are sparse, they indicate hydraulic heads continue to decline, albeit slowly. Transient conditions cannot be taken into account in a steady-state simulation; therefore, some model error is to be expected in these areas.

Modeled Area and Spatial Discretization

The modeled area for the San Joaquin Valley regional study area extends from the Stanislaus River on the north to the Merced River on the south and bounded on the east by the Sierra Nevada foothills and the west by the San Joaquin River. The model grid is oriented parallel to the valley axis, 37 degrees west of due north (fig. 4.12). The modeled area extends 61.2 km along the valley axis from north of the Stanislaus River to south of the Merced River and 54.8 km from the Coast Ranges to the Sierra Nevada foothills. The model grid is 137 columns and 153 rows and is uniformly spaced; each model cell is 400 m by 400 m in size.

Sixteen model layers were used to represent the geologic materials in the study area with model layers designed as a series of wedges to represent the regional dip of the sediments. The uppermost layer was a constant thickness of 10 m. Layers 2 through 7 represent the unconfined aquifer above and east of the Corcoran Clay. The thicknesses of layers 2 through 7 were assigned as a percentage of the thickness of materials between layer 1 and the top of the Corcoran Clay (10, 10, 15, 20, 20, and 25 percent of that thickness, respectively) and ranged from 1.9 to 18.8 m in thickness. Layer 8 represents the Corcoran Clay, where present, and its specified thickness and presence varies spatially as determined from analysis of drillers' and geophysical logs. A minimum thickness of 10 m was specified for layer 8 where the Corcoran Clay was not present. Layers 9 through 16 represent the confined aquifer beneath the Corcoran Clay, and thickness of layers 9–16 was assigned as a percentage of the thickness of materials between the bottom of the Corcoran Clay and the bottom of the model. Layers 9 through 13 were assigned 10 percent of the total thickness, layers 14 and 15 were assigned 15 percent of the thickness, and layer 16 was assigned 20 percent of the total thickness. Layer thickness below the Corcoran Clay ranged from 17 to 80 m. The bottom of the model was an artificial surface loosely representing topographic variability and the general dip of the Corcoran Clay. The total thickness of the wedge-shaped model ranges from about 230 to 430 m.

Boundary Conditions and Model Stresses

Lateral boundary conditions in the model were no-flow along the Sierra Nevada foothills and general-head elsewhere. The general-head boundaries (fig. 4.12) were specified at a distance of 400 m using a water-level contour map (fig. 4.5) and hydraulic-conductivity estimates for each cell along the boundary. The northwestern and southeastern edges of the model grid were located beyond the Stanislaus and Merced Rivers, respectively, to include these rivers in the modeled area. The southwestern model boundary was coincident with the San Joaquin River, and all cells west of the river were inactive. These general-head boundaries allow for cross-valley flow beneath the San Joaquin River, which is known to occur (Belitz and Phillips, 1995; Phillips and others, 1991), and provide reasonable boundary conditions in the northwest and southeast where no identified hydrologic boundaries exist within a reasonable distance of the study area.

The upper model boundary was simulated as the water table, and the lower model boundary was simulated as no-flow. The lower model boundary was arbitrarily located far below the deepest wells, and significant vertical flow in the lowest model layer is unlikely.

Model stresses included recharge from irrigation return flow; infiltration of precipitation, reservoir leakage, and inflow from rivers; and discharge from ground-water pumping, outflow to rivers, and evaporation from the shallow water table. Irrigation return flow, infiltration of precipitation, and private-agricultural pumping rates were all determined in the water-budget analysis. The two recharge terms were summed for each water-budget subarea and distributed evenly to the uppermost active model layer within each subarea. Private-agricultural pumping was distributed laterally within water-budget subareas assuming an average well spacing of 1,200 m (3 cells). Wells with measured pumping rates (those supplying urban areas or operated by irrigation districts) were placed in the model at their actual locations. The vertical distribution of private-agricultural pumping was estimated using the average screened interval of irrigation wells in each subarea (using the texture data base). Given this average screened interval, the total pumping per well was distributed to the model layers within this interval on the basis of effective transmissivity of these layers. The vertical distribution of measured pumping was distributed using the actual screened intervals (or those of nearby wells of the same type).

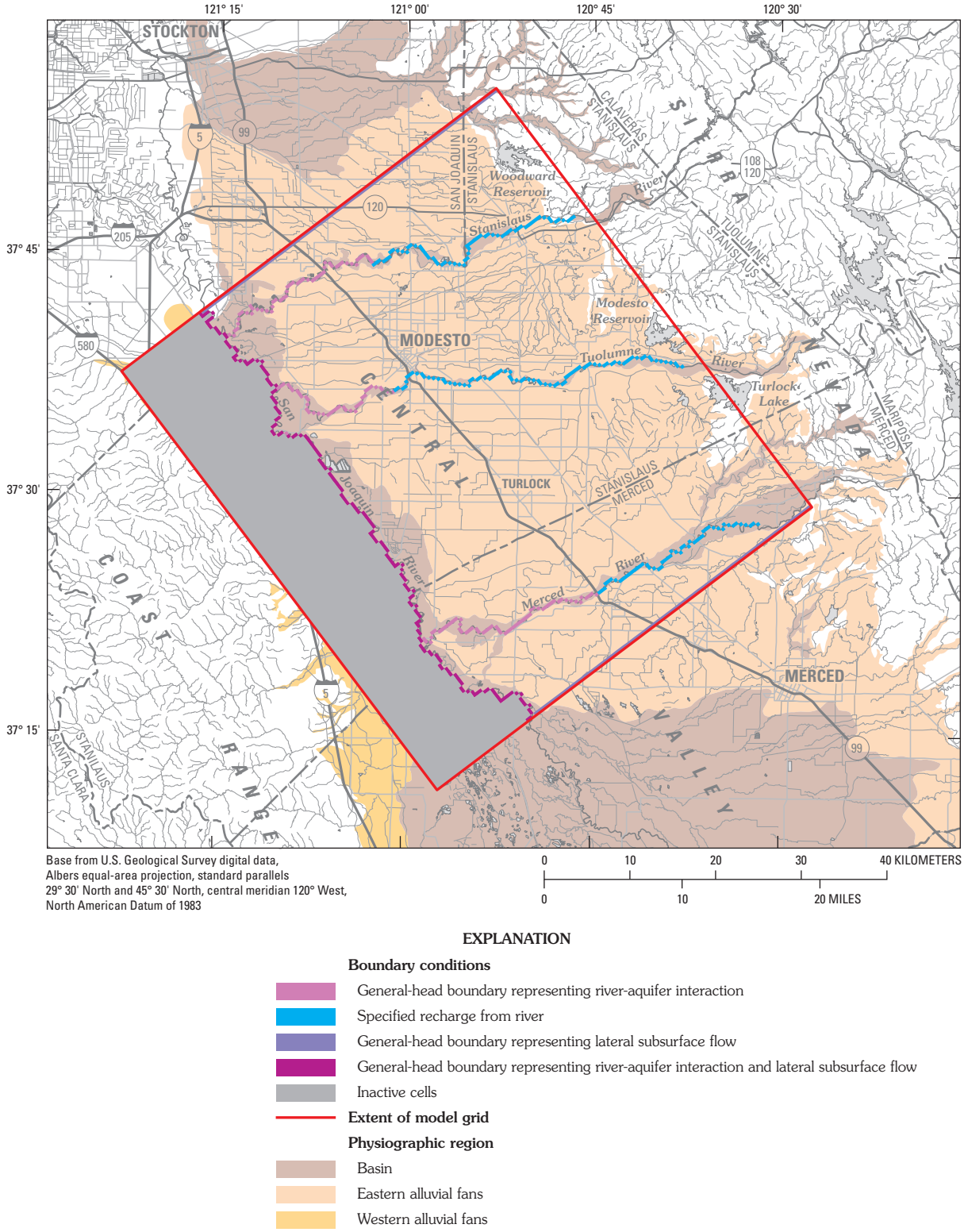

Figure 4.12. Ground-water flow modeled area and boundary conditions, San Joaquin Valley regional study area, California.

The interaction of ground water and surface water is poorly understood in the study area but is incorporated in the model as reservoir leakage and gaining and losing reaches of the four rivers. There are three significant reservoirs along the northeastern model boundary: Woodward and Modesto Reservoirs and Turlock Lake (fig. 4.2). These reservoirs are approximately equal in size, and information on leakage rates was available only for the Modesto Reservoir. Results from a recent short-term study conducted by the Modesto Irrigation District, which manages the reservoir, indicate a leakage rate of about 67,600 to 84,500 m^3/d (Modesto Irrigation District, oral commun., 2001). Leakage rates for the other two reservoirs were assumed to be the same as those for the Modesto Reservoir. The MODFLOW-2000 Reservoir package (Fenske and others, 1996) was used to simulate the reservoirs, which requires specification of reservoir stage and information for calculating the hydraulic conductance of the reservoir bottom. The stage was estimated from U.S. Geological Survey 7.5-minute topographic maps, and the hydraulic conductance terms were adjusted to approximate the assumed leakage rate (the total reservoir leakage in the calibrated model was 207,000 m^3/d).

The four rivers in the study area were represented in the model as a combination of general-head and specified-flux cells. General-head cells were used where the river was directly connected to the water table, which allowed flow into and out of the river. The head term was estimated from streamgage data and topography, and the conductance was calculated using the estimated vertical hydraulic conductivity by cell, the river width, and an assumed riverbed thickness of 1 m. Recharge from the river was specified as a flux where the river was disconnected from the water table. This value (0.005 m/d per river cell) was impossible to estimate with the available data, and its calibration was poorly constrained.

Bare-soil evaporation from the water table was simulated where the water table was within 2.1 m of the land surface. The maximum evaporation rate was 1.6 m/yr at the land surface, and decreased linearly to zero at 2.1 m below land surface.

Aquifer Hydraulic Properties

A method of parameter estimation based on sediment texture, which was used successfully in the development of a transient three-dimensional ground-water flow model of the central western San Joaquin Valley (Belitz and Phillips, 1995; Phillips and Belitz, 1991), was adapted for use in this study. This method uses the estimated sediment texture (as percentage of coarse-grained sediments) for each model cell and several user-specified values of hydraulic conductivity to generate horizontal and vertical hydraulic conductivities throughout the model domain.

The hydraulic-conductivity values specified for the model include that of the Corcoran Clay (K_{corc}) and of the coarse-grained (K_{coarse}) and fine-grained (K_{fine}) lithologic end members of the remaining materials. In the modeled area, the remaining materials were divided into two lithologic subareas during model calibration: the eastern alluvial fans upslope of the Modesto Formation (fig. 4.3) and everywhere else. Horizontal hydraulic conductivity (K_h) was calculated for each cell in these subareas using the arithmetic mean:

$$K_h = K_{coarse} \times F_{coarse} + K_{fine} \times F_{fine} \qquad \text{(eq. 4.1)}$$

where F_{coarse} is the fraction of coarse-grained sediment in a cell, and F_{fine} is the fraction of fine-grained sediment in a cell.

Vertical hydraulic conductivity between model layers (K_v) either was set to K_{corc}, if the Corcoran Clay was present within one of the layers, or was calculated using the geometric mean:

$$K_v = K_{coarse}^{F_{coarsev}} \times K_{fine}^{F_{finev}} \qquad \text{(eq. 4.2)}$$

where $F_{coarsev}$ is the fraction of coarse-grained sediment between layer midpoints, and F_{finev} is the fraction of fine-grained sediment between layer midpoints.

The calibrated value (see next section) of K_{corc} was 4 X 10^{-3} m/d and that for K_{fine} was 4 X 10^{-4} m/d. The calibrated value of K_{coarse} varied by lithologic subarea: 24 m/d for the older fan deposits and 235 m/d for the remaining area. The resulting values of K_h and K_v are summarized in figure 4.13. The distributions of K_h and K_v are the same as those for the sediment texture for the appropriate depth intervals (for example, the distribution of K_h in layer 4 is shown in figure 4.7).

Model Calibration and Sensitivity

Model calibration consisted primarily of a systematic application of the parameter estimation method. K_{coarse} and K_{fine} were varied systematically for a given value of K_{corc}, which was adjusted to roughly match vertical gradients across the Corcoran Clay. Model-computed hydraulic heads were compared to measured water levels in 51 wells representing various parts of the aquifer system. The resulting error distributions constrained the parameter set.

Model-computed and measured hydraulic heads were compared in four areas within the model. The low-lying area where the water table is shallow was represented by 17 wells. The intermediate-depth zone between the water table and the Corcoran clay and the deep zone below the Corcoran were represented by six wells each. The area east of the extent of the Corcoran was represented by 22 wells.

Two statistics were used to quantify model error:

$$RMSE = \sqrt{\sum_{i=1}^{n} \frac{(h_{meas} - h_{sim})_i^2}{n}} \qquad \text{(eq. 4.3)}$$

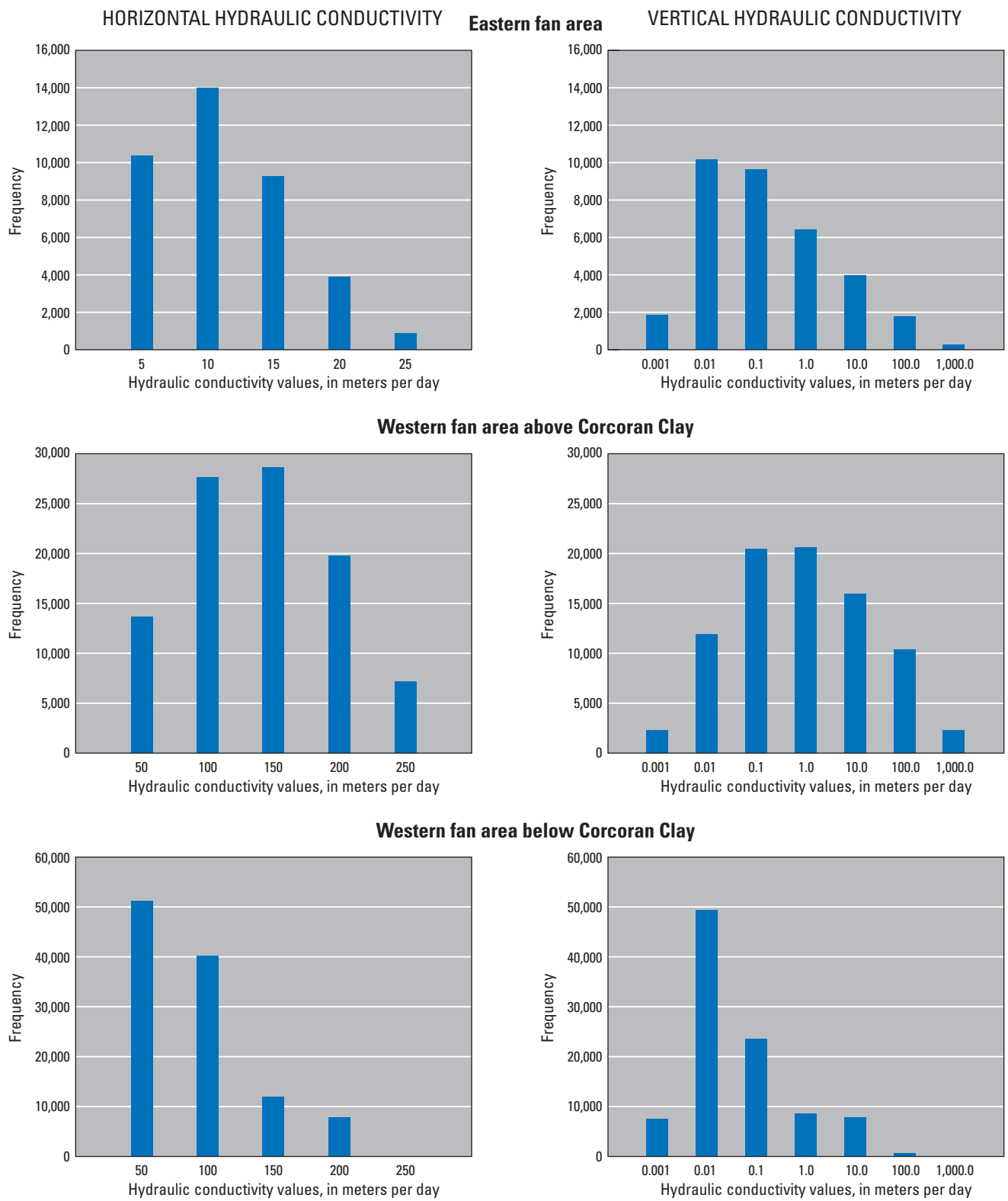

Figure 4. 13. Frequency of estimated horizontal hydraulic conductivity (Kh) and estimated vertical hydraulic conductivity (Kv) for the eastern and western alluvial fans, San Joaquin Valley regional study area, California.

$$BIAS = \sum_{i=1}^{n} (h_{meas} - h_{sim})i \qquad \text{(eq. 4.4)}$$

where *RMSE* is root-mean-square error, h_{meas} is measured hydraulic head, h_{sim} is model-computed hydraulic head, $(h_{meas} - h_{sim})$ is the head residual, *i* is the summation index, *n* is the number of measurements, and *BIAS* is the sum of the residuals. The *RMSE* is a measure of error magnitude, and *BIAS* indicates whether model-computed hydraulic heads were higher or lower than measured hydraulic heads.

Model-computed and measured vertical hydraulic gradients also were compared during model calibration. Measured gradients were calculated using water levels from nearby wells screened at different depths in three areas within the model: from the water table to the intermediate-depth zone above the Corcoran (three well pairs), across the Corcoran (three well pairs), and the area east of the Corcoran extent (five well pairs). *RMSE* and *BIAS* were calculated for vertical gradients in the same way as for hydraulic head by replacing the simulated and measured heads in equations 4.3 and 4.4 with the model-computed and measured vertical hydraulic gradients (change in model-computed or measured hydraulic head divided by the vertical distance between the midpoints of model layers or screened intervals, respectively).

The *RMSE* and *BIAS* calculations were used to estimate the values of K_{coarse} and K_{fine} that generated the best-fit parameter distribution for the conceptual model described herein. *RMSE* and *BIAS* values were calculated for 100 simulations representing K_{coarse} values ranging from 60 to 300 m/d and K_{fine} values ranging from 3 X 10^{-4} to 1 m/d. Results from the 100 simulations were plotted as error surfaces describing model fit with respect to hydraulic heads and gradients for various parts of the aquifer system (fig. 4.14). Each plot in figure 4.14 shows contoured *RMSE* and *BIAS* for hydraulic heads and vertical gradients in a specific part of the aquifer system. Lines of minimum *RMSE* and *BIAS* were drawn where possible. Note the model is numerically stable over a wide range of parameter values, but numerical stability decreased with lower values of K_{coarse} and K_{fine}. Pervasive numerical instability was assumed an indication that such parameter combinations are unlikely to be representative of this aquifer system.

The *RMSE* and *BIAS* values shown in figure 4.14, considered as a whole, constrain K_{coarse} and K_{fine} to the lower left-hand region of the plot and indicate relatively high values of K_{coarse} and low values of K_{fine} provide the best model fit for the given conceptual model. The fact that most of the plots do not contain lines of minimum *RMSE* and zero *BIAS*, and that these lines are not coincident where they do coexist, indicates there is some degree of error in the conceptual model and (or) the calibration criteria. Future modeling efforts can focus on reducing these errors, but current results indicate that K_{coarse} and K_{fine} values of about 235 and 4 X 10^{-4} m/d, respectively, generate the best-fit parameter distribution (K_{corc} was 4 X 10^{-3} m/d).

A hydraulic conductivity of 235 m/d is within the typical range for well-sorted gravel, and a hydraulic conductivity of 4 X 10^{-4} m/d is indicative of clay (Fetter, 1994). Both lithologies are common in the study area and represent the lithologic end members. Permeameter tests of cores from the Corcoran Clay indicate vertical hydraulic conductivities ranging from 1 X 10^{-6} to 3 X 10^{-6} m/d (Page, 1977). Previous investigations, however, indicate wells screened across the Corcoran Clay provide direct vertical connection between the unconfined and confined aquifers and have increased the vertical hydraulic conductivity by orders of magnitude (Williamson and others, 1989; Belitz and Phillips, 1995), which is consistent with the calibrated value of K_{corc} from this study.

Model-Computed Hydraulic Heads

The simulated water table closely resembles that depicted in figure 4.5. In the area overlying the Corcoran Clay, model-computed hydraulic heads in the area with a shallow water table closely match measured heads with an average residual of 0.92 m and *RMSE* of 1.9 m (fig. 4.15). Water levels in wells east of the Corcoran Clay extent that represent the unconfined aquifer also are simulated reasonably well with an average residual of -1.5 m and *RMSE* of 3.6 m, although there is an apparent increase in residuals with increasing measured hydraulic head for the unconfined aquifer east of the Corcoran Clay extent (fig. 4.16). In general, the residuals are randomly distributed around zero for the entire modeled area (fig. 4.16).

A simple method of assessing overall model fit is to plot the model-computed hydraulic head values against the measured observations. For a perfect fit, all points should fall on the 1:1 diagonal line. Figure 4.17 presents a plot of the model-computed heads as compared to measured hydraulic heads for the San Joaquin Valley regional study area and indicates reasonable model fit. The average residual for the entire model is -0.9 m with a standard deviation of 3.67 m, and residuals range from -10.5 m to 6.0 m (range of 16.5 m). The RMSE for the entire model is 3.75 m, which is about 10 percent of the range of head observations in the model (37.7 m).

Measured hydraulic heads in the Modesto area include those in four clusters of piezometers installed for this study (Phillips and others, 2007). The piezometers that represent the water table range in depth from 11 to 14 m, and the deepest piezometer in each cluster ranges from 102 to 108 m deep. The shallow and deep water levels were closely simulated, with an average error of 0.78 m and 0.35 m, respectively. Consequently, the downward vertical gradient, which features an average head difference of 4.4 m, also was simulated well.

Model-computed hydraulic heads between the water table and the Corcoran Clay were greater than the measured heads by an average of 1.8 m. Coupled with the generally low simulated water table, simulated downward gradients above the Corcoran are, on average, too low. Model-computed heads below the Corcoran were generally greater than measured

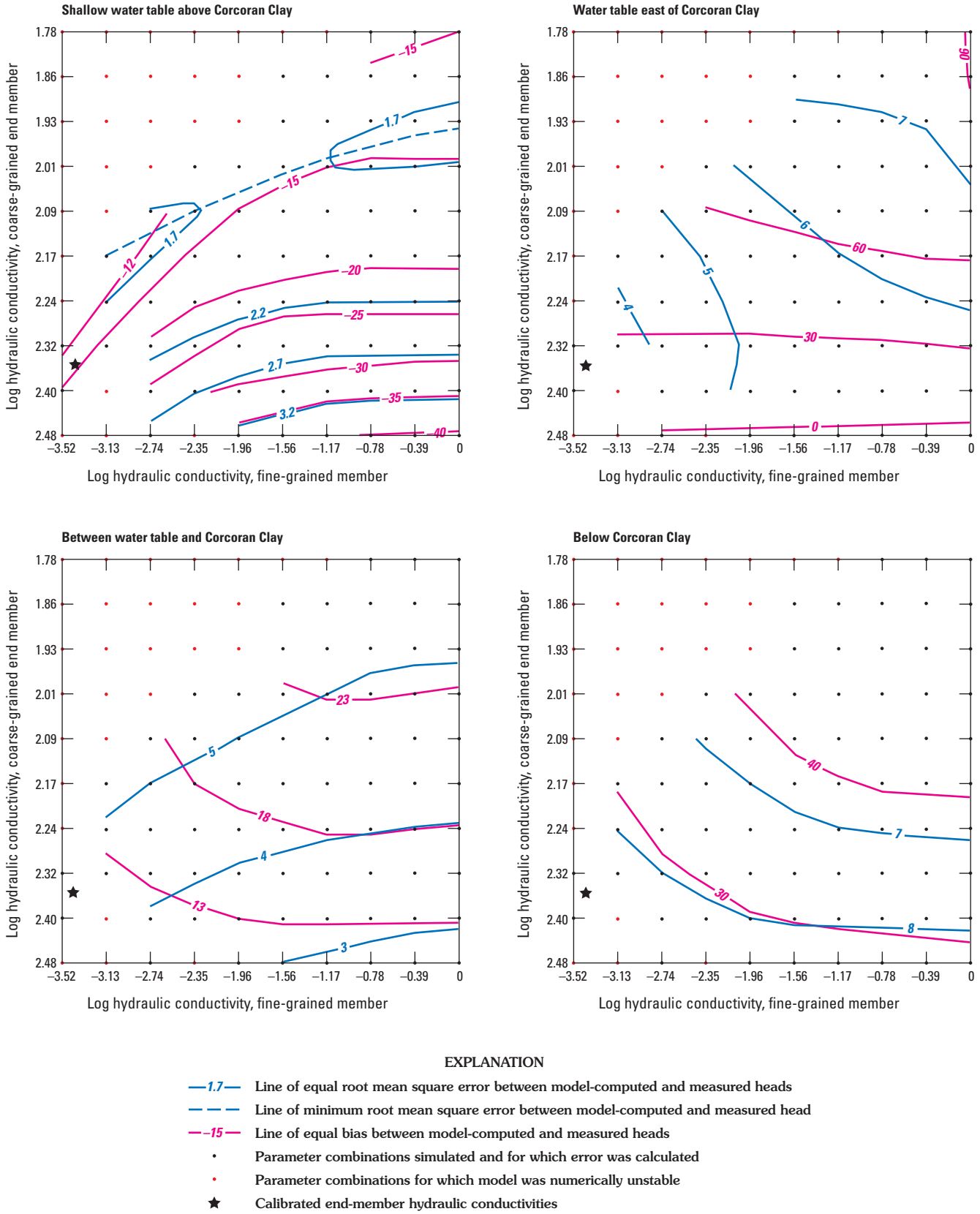

Figure 4. 14. Ground-water flow model calibration results, San Joaquin Valley regional study area, California. (Continued on next page.)

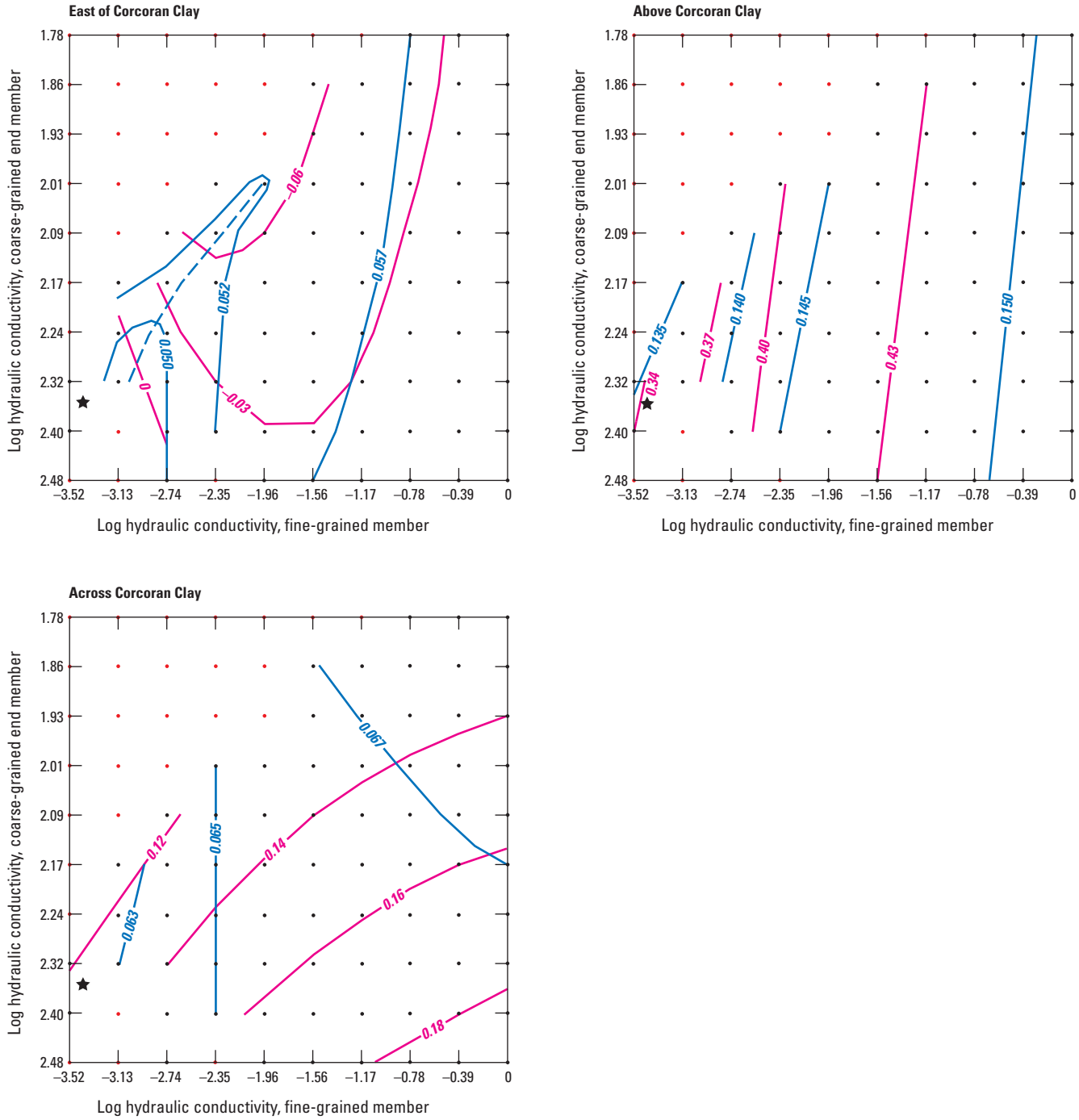

EXPLANATION

—1.7— Line of equal root mean square error between model-computed and measured heads

— — — Line of minimum root mean square error between model-computed and measured head

—–15— Line of equal bias between model-computed and measured heads

• Parameter combinations simulated and for which error was calculated

• Parameter combinations for which model was numerically unstable

★ Calibrated end-member hydraulic conductivities

Figure 4. 14. Ground-water flow model calibration results, San Joaquin Valley regional study area, California.—Continued

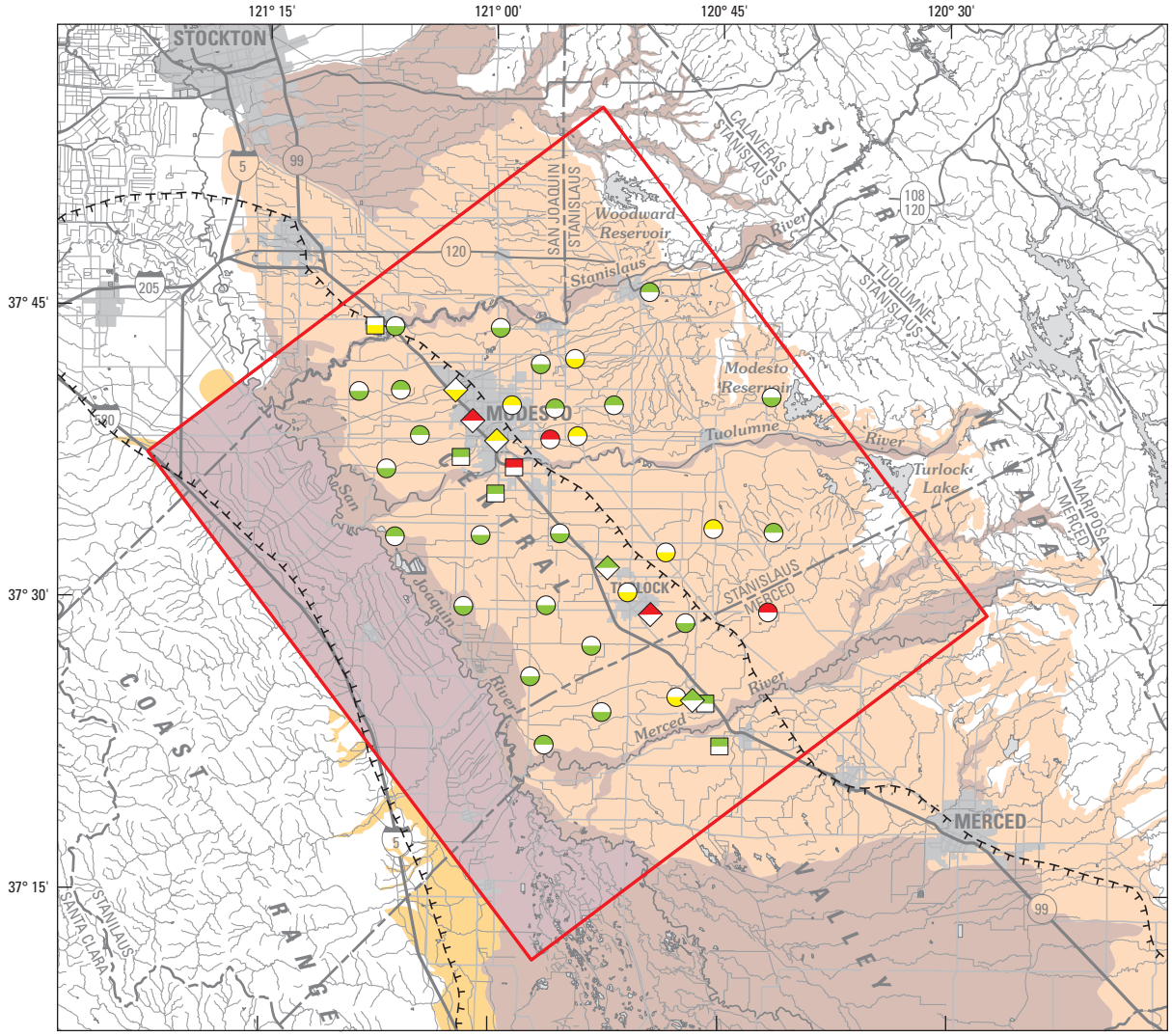

EXPLANATION

Physiographic region

- Basin
- Eastern alluvial fans
- Western alluvial fans
- **Urban**
- **Inactive model cells**
- **Extent of model grid**
- **Extent of Corcoran Clay**—Hachures point toward clay

Model-computed as compared to measured hydraulic heads

Location

- Water table
- Between water table and Corcoran Clay
- Below Corcoran Clay

Model-computed residuals—Difference between model-computed and measured head

- Less than 3 meters
- 3 to 6 meters
- 6.1 to 10.5 meters

Relative difference

- Model-computed head greater than measured water level
- Model-computed head lower than measured water level

Figure 4. 15. Spatial distribution of hydraulic-head residuals, San Joaquin Valley regional study area, California.

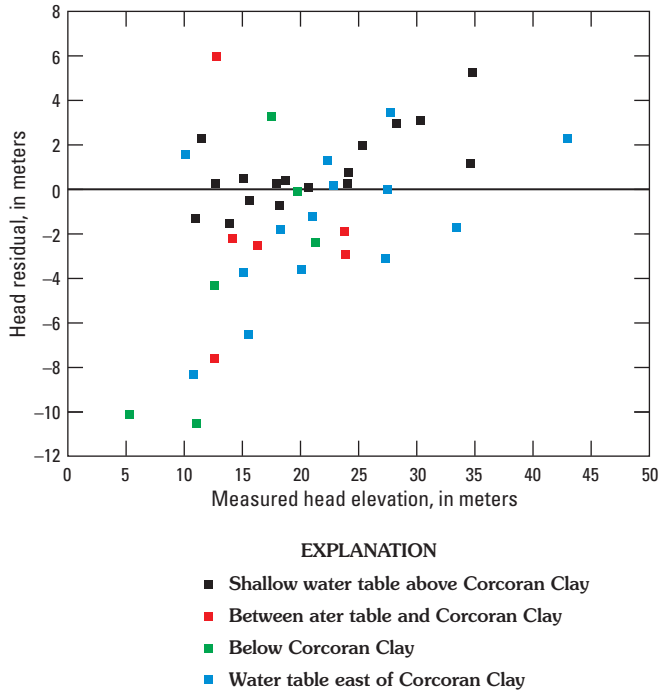

Figure 4. 16. Relation between head residual and measured hydraulic head, San Joaquin Valley regional study area, California.

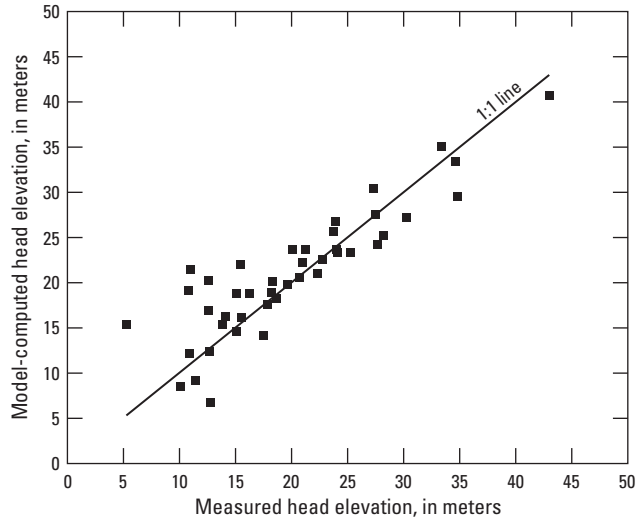

Figure 4. 17. Relation between model-computed and measured hydraulic head, San Joaquin Valley regional study area, California.

heads by an average of 4 m, but the gradient across the Corcoran is simulated reasonably well in the four locations where measurements were available.

Model-Computed Water Budget

Many of the water-budget components simulated by the model were specified values. Areal recharge, which was dominated by agricultural irrigation and precipitation, accounted for about 71 percent of the total recharge (table 4.2). Leakage from reservoirs contributed about 4 percent of the water, and net inflow (inflow minus outflow) from rivers also contributed about 4 percent of the water. Pumping from wells, primarily for agricultural purposes, accounted for about 54 percent of the total discharge. About 12 percent of the discharge was bare-soil evaporation from the shallow water table. The remainder of the model-computed water budget was flow through the lateral head-dependent boundaries, which was a net outflow of about 13 percent. Details of the simulated water budget are listed in table 4.2.

Simulation of Areas Contributing Recharge to Public-Supply Wells

The ground-water flow model was used to simulate capture zones for 60 public-supply wells to aid understanding of the flow system and to elucidate connections between land use and the chemistry of water discharging from public-supply wells. Water extracted from these wells followed various pathways through the aquifer system and is an amalgamation of water that may vary widely in age and origin. Particle tracking was used to approximate the pathway of water particles, associated ages, and points where these particles first entered the aquifer, hereinafter referred to collectively as “the contributing area.” The various land uses overlying the contributing area may be associated with different chemical inputs to the aquifer, which may ultimately reach the public-supply well.

Particle-Tracking Simulations

Sixty public-supply wells with a range of pumping rates were selected for particle-tracking analysis. Pumping rates for 109 wells that supplied the city of Modesto during water-year 2000 were available, and 15 wells from each quartile of pumping rate were selected for particle-tracking analysis. The pumping rates ranged from 131 to 13,381 m^3/d, and the total water extracted from the 60 wells represents about 60 percent of the 57 million cubic meters the city pumped during water-year 2000.

Particle-tracking software, MODPATH (Pollock, 1994), was used in conjunction with flux output from the flow model to calculate flow paths and traveltimes for water particles traveling from the contributing area, through the aquifer system, and to the wells. The model-computed areas contrib-

Table 4.2. Model-computed water budget for water-year 2000, San Joaquin Valley regional study area, California.

[m^3/d, cubic meters per day; —, not applicable]

Water-budget component	Specified flow (m^3/d)	Computed flow (m^3/d)	Total flow (m^3/d)	Percentage of inflow or outflow
Model inflow				
Agricultural irrigation return flow	2,267,000	—	2,267,000	41.5
Precipitation	1,598,000	—	1,598,000	29.3
Rivers	500,000	25,000	525,000	9.6
Reservoir leakage	—	207,000	207,000	3.8
Pipe leakage, urban	11,000	—	11,000	0.2
Flow through lateral boundaries				
Northwest	—	102,000	102,000	1.9
Southeast	—	162,000	162,000	3.0
Southwest	—	584,000	584,000	10.7
TOTAL INFLOW			**5,456,000**	**100**
Model outflow				
Wells				
Agricultural	2,732,000	—	2,732,000	
Public supply	274,000	—	274,000	
Total (smaller due to dry cells in upper part of some well screens)	2,955,000	—	2,955,000	54.2
Evaporation from shallow water table	—	651,000	651,000	11.9
Rivers	—	310,000	310,000	5.7
Flow through lateral boundaries				
Northwest	—	952,000	952,000	17.5
Southeast	—	103,000	103,000	1.9
Southwest	—	480,000	480,000	8.8
TOTAL OUTFLOW			**5,452,000**	**100**

uting recharge represent advective ground-water flow and do not account for mechanical dispersion. Advection-dispersion transport simulations would likely yield larger areas contributing recharge than advective particle-tracking simulations because the effects of dispersion caused by aquifer heterogeneity would be included.

Effective porosity was the only hydraulic parameter entered into the MODPATH input files. Effective porosity values were assigned on the basis of percentage of coarse-grained texture in each model cell (table 4.3). The porosity values are based on literature values for different geologic/textural materials (Domenico and Schwartz, 1990) and previous work in similar geologic formations in the eastern San Joaquin Valley (Burow and others, 1999).

Table 4.3. Effective porosity values, by percentage of coarse-grained texture, used for MODPATH simulations, San Joaquin Valley regional study area, California.

[>, greater than; <=, less than or equal to]

Textural material	Percentage coarse material	Effective porosity
Gravel	> 75	0.25
Coarse sand	51–75	0.28
Fine sand	26–50	0.32
Silt and clay	<= 25	0.35

Public-Supply Well Contributing Areas

Fifteen wells in each quartile of pumping in the Modesto area were selected to delineate areas contributing recharge and compute traveltimes. The resulting contributing areas for the 15 wells in the top quartile pumping rate (fig. 4.18) tend to overlap and generally extend to the northeast of Modesto beyond the extent of the Corcoran Clay. The size of the contributing areas generally is a function of the pumping rate, whereas the shape is influenced by geologic setting and well-construction characteristics. The ground-water flow model incorporates the spatial interpolation model of percentage of coarse-grained texture; therefore, the contributing areas reflect, to a degree, the heterogeneous deposits that are characteristic of these dominantly fluvial sediments. This approach results in uniquely shaped contributing areas that generally do not resemble the tear-shaped areas one would expect in a more homogeneous setting.

Differing well characteristics also account for variability in contributing areas. Shallow wells, which tend to have lower production rates, generally have small contributing areas close to the wells. Traveltimes to shallow wells are relatively short. The larger contributing areas and longer flow paths (and traveltimes) are associated with higher producing wells. These high-producing wells tend to have the longest screened intervals and are relatively deep. Consequently, the contributing areas from these wells commonly have two components: a local area, which may be offset from the well, that represents the source of water flowing to the upper portion of the screened interval; and a distant area that represents the source of water flowing to the lower portion of the screened interval. For example, Well 51 in the northwest part of Modesto has a contributing recharge area immediately east of the well that contributes to the upper portion of the screened interval and a small contributing recharge area more than 6 km to the northeast that contributes to the lower portion of the screened interval.

The minimum traveltime from the water table to the well for all 60 wells ranges from 3 to 141 years with a median of about 20 years. The maximum traveltime ranges from 18 years to more than 1,600 years with a median of 107 years. The zones of contribution outlined by pathlines for the 60 public-supply wells occupy more than 143 km^2 within the modeled area. Agricultural and urban land uses dominate in most of the area contributing recharge to public-supply wells.

Limitations and Appropriate Use of the Model

The ground-water flow model for the San Joaquin Valley regional study area was designed to estimate aquifer-system properties, to delineate contributing areas to public-supply wells in Modesto, to help guide data collection, and to support future local modeling efforts. Limitations of the ground-water flow model, assumptions made during model development, and results of model calibration and sensitivity analysis all are factors that constrain the appropriate use of the model and highlight potential future improvements.

A ground-water flow model is a means for portraying and testing a conceptual understanding of a system. Because ground-water flow systems are inherently complex, simplifying assumptions were made in developing this model (Anderson and Woessner, 1992). Models solve for average conditions within each cell, the parameters for which are interpolated or extrapolated from measurements and(or) estimated during calibration. In light of this, the intent in developing the ground-water flow model was not to reproduce every detail of the natural system, but rather to portray its general characteristics.

Water-level hydrographs indicate the ground-water system in the study area approximated steady-state equilibrium for water-year 2000 (fig. 4.6); however, the data are not conclusive. Long-term hydrographs are not available for some areas, including the southeastern part of the model area, where hydraulic heads may have been changing with time. Errors related to this assumption can be substantial, and care must be taken in interpreting model results and analyses that depend on model output, including particle tracking.

Some of the boundary conditions of the model are poorly constrained, which may be a source of model error. The lateral boundary along the San Joaquin River is based on sparse data, and the spatial distribution of hydraulic head below the river is poorly understood. Similarly, there is little information on river/aquifer interaction in the study area, and none regarding the hydraulic conductivity of riverbed sediments. Simulation results indicate that fluxes across these poorly constrained boundaries (table 4.2) make up a small part of the water budget; however, these boundaries may be more important in the real system.

The accuracy of model results is related strongly to the quality and spatial distribution of input data, and of measurements of system state (for example, measured hydraulic heads) for comparison with simulation results during model calibration. The Modesto area is the only region of the ground-water flow model that has high-quality input data (particularly pumping by well) coupled with a good distribution of measured hydraulic heads. The stresses in other areas of the model are a combination of measured values and those estimated from the water-budget analysis. Accordingly, the user should have higher confidence in simulation results in the Modesto area than in other areas of the model.

The interpolation of sediment texture data within model layers, or two dimensions, may artificially decrease the vertical connectivity of coarse-grained materials in the aquifer system. This potential shortcoming in the parameter-estimation procedure used for the ground-water flow model may affect simulated particle pathways and associated analyses. Applying a three-dimensional interpolation method may provide a significant improvement over the current parameter distribution.

Computed areas contributing recharge and traveltimes through zones of contribution are based on a calibrated

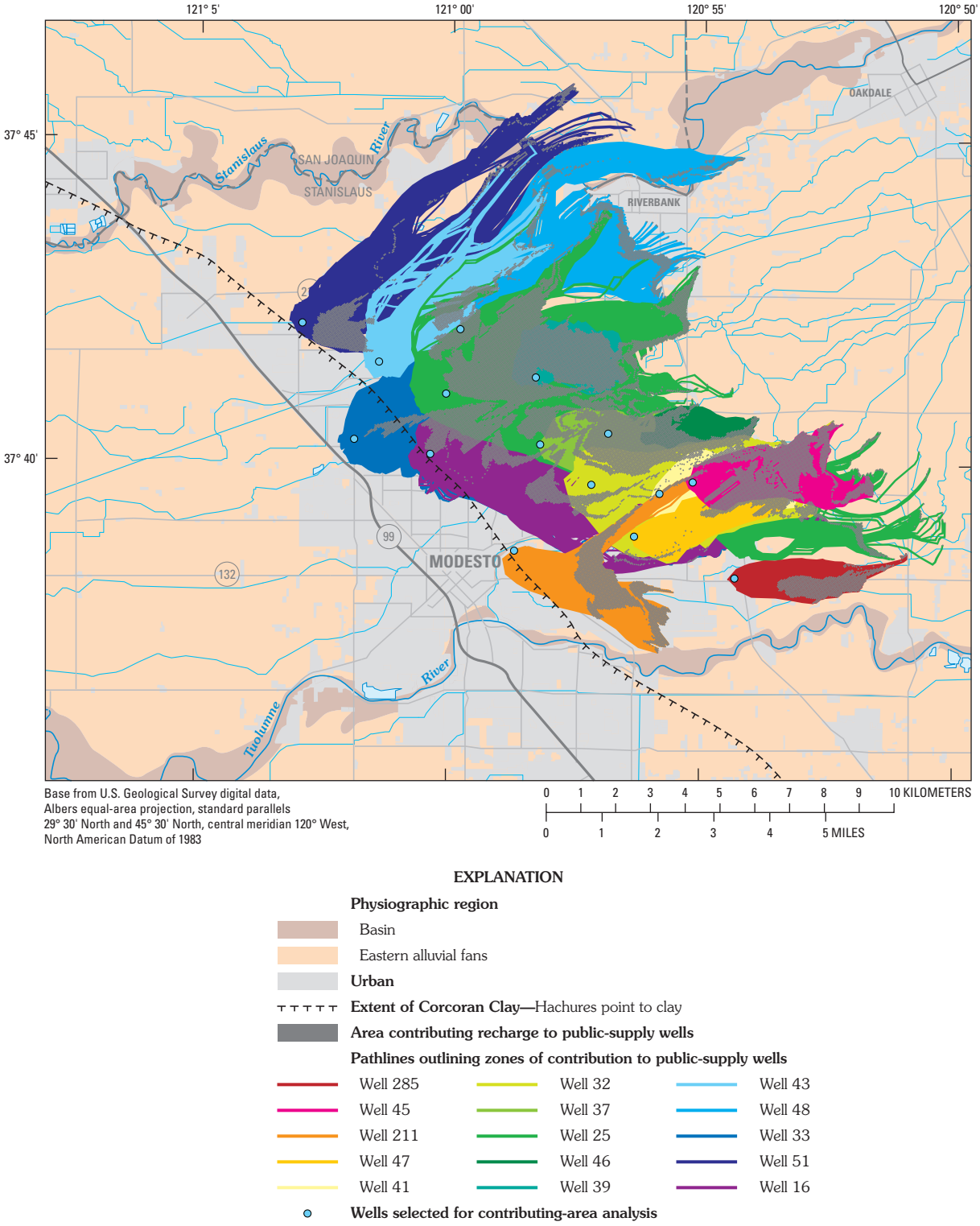

Figure 4. 18. Model-computed areas contributing recharge for 15 public-supply wells in top quartile of pumping, San Joaquin Valley regional study area, California.

model and estimated effective porosity values. In a steady-state model, changes to input porosity values do not change the area contributing recharge to a given well. Changes to input porosity values will change computed traveltimes from recharge to discharge areas in direct proportion to changes of effective porosity because there is an inverse linear relation between ground-water flow velocity and effective porosity and a direct linear relation between traveltime and effective porosity. For example, a one-percent decrease in porosity will result in a one-percent increase in velocity and a one-percent decrease in particle traveltime. A detailed sensitivity analysis of porosity distributions was beyond the scope of this study, although future work could compare simulated ground-water traveltimes to ground-water ages to more thoroughly evaluate effective porosity values.

The San Joaquin Valley regional ground-water flow model uses justifiable aquifer properties and boundary conditions and provides a reasonable representation of ground-water flow conditions in the study area for the year 2000. The model is suitable for evaluating regional water budgets and ground-water flow paths in the study area for the time period of interest but may not be suitable for long-term predictive simulations. This regional model provides a useful tool to evaluate aquifer vulnerability at a regional scale, to facilitate comparisons of ground-water traveltime between regional aquifer systems, and to guide future detailed investigations in the study area.

References Cited

Anderson, M.P. and Woessner, W.W., 1992, Applied ground-water modeling—Simulation of flow and advective transport: San Diego, California, Academic Press, Inc., 381 p.

Arkley, R.J., 1962, Soil survey of Merced area, California: U.S. Department of Agriculture, Soil Conservation Service, Soil Survey series 1950, no. 7, 131 p., 101 pls.

Arkley, R.J., 1964, Soil survey, eastern Stanislaus area, California: U.S. Department of Agriculture, Soil Conservation Service, Soil Survey series 1957, no. 20, 160 p.

Bartow, J.A., 1991, The Cenozoic evolution of the San Joaquin Valley, California: U.S. Geological Survey Professional Paper 1501, 40 p.

Belitz, Kenneth, and Phillips, S.P., 1995, Alternative to agricultural drains in California's San Joaquin Valley—Results of a regional-scale hydrogeologic approach: Water Resources Research, v. 31, no. 8, p. 1845–1862.

Bertoldi, G.L., Johnston, R.H., and Evenson, K.D., 1991, Ground water in the Central Valley, California—A summary report: U.S. Geological Survey Professional Paper 1401–A, 44 p.

Burow, K.R., Panshin, S.Y., Dubrovsky, N.M., VanBrocklin, David, and Fogg, G.E., 1999, Evaluation of processes affecting 1,2-dibromo-3-chloropropane (DBCP) concentrations in ground water in the eastern San Joaquin Valley, California, analysis of chemical data and ground-water flow and transport simulations: U.S. Geological Survey Water-Resources Investigations Report 99–4059, 57 p.

Burow, K.R., Shelton, J.L., Hevesi, J.A., and Weissmann, G.S., 2004, Hydrogeologic characterization of the Modesto area, San Joaquin Valley, California: U.S. Geological Survey Scientific Investigations Report 2004–5232, 54p.

California Department of Water Resources, 1994, Urban water use in California: California Department of Water Resources, Bulletin 166–4, 48 p. plus appendixes.

Davis, G.H., Green, J.H., Olmsted, F.H., and Brown, D.W., 1959, Ground-water conditions and storage capacity in the San Joaquin Valley, California: U.S. Geological Survey Water-Supply Paper 1469, 287 p.

Davis, S.N. and Hall, F.R., 1959, Water quality of eastern Stanislaus and northern Merced counties, California: Palo Alto, California, Stanford University Publications, Geological Sciences, v. 6, no. 1, 112 p.

Domenico, P.A., and Schwartz, F.W., 1990, Physical and chemical hydrogeology: New York, John Wiley and Sons, 824 p.

Fenske, J.P., Leake, S.A., and Prudic, D.E., 1996, Documentation of a computer program (RES1) to simulate leakage from reservoirs using the modular finite-difference ground-water flow model (MODFLOW): U.S. Geological Survey Open-File Report 96–364, 51 p.

Fetter, C.W., 1994, Applied hydrogeology: New York, Macmillan College Publishing Company, 691 p.

Gronberg, J.M., Dubrovsky, N.M., Kratzer, C.K., Domagalski, J.L., Brown, L.R., and Burow, K.R., 1998, Environmental setting of the San Joaquin-Tulare Basins, California: U.S. Geological Survey Water-Resources Investigations Report 97–4205, 45 p.

Harbaugh, A.W., Banta, E.R., Hill, M.C., and McDonald, M.G., 2000, MODFLOW-2000, the U.S. Geological Survey modular ground-water model—User guide to modularization concepts and the ground-water flow process: U.S. Geological Survey Open-File Report 00–92, 121 p.

Laudon, Julie, and Belitz, Kenneth, 1991, Texture and depositional history of late Pleistocene-Holocene alluvium in the central part of the western San Joaquin Valley, California: Bulletin of the Association of Engineering Geologists, v. 28, no. 1, p. 73–88.

Londquist, C.J., 1981, Digital model of the unconsolidated aquifer system in the Modesto Area, Stanislaus and San Joaquin counties, California: U.S. Geological Survey Water-Resources Investigations Report 81–12, 36 p.

Marchand, D.E., and Allwardt, A., 1981, Late Cenozoic stratigraphic units, San Joaquin-Tulare Basins, California: U.S. Geological Survey Bulletin 1470, 70 p.

Maupin, M.A., and Barber, N.L., 2005, Estimated withdrawals from principal aquifers in the United States, 2000: U.S. Geological Survey Circular 1279, 47 p.

National Oceanic and Atmospheric Administration, 2005, Precipitation records for California, Web page accessed Nov. 14, 2005, at *http://lwf.ncdc.noaa.gov/oa/pub/data/coop-precip/california.txt*.

Page, R.W., 1973, Base of fresh ground water (approximately 3,000 micromhos) in the San Joaquin Valley, California: U.S. Geological Survey Hydrologic Investigations Atlas HA–489.

Page, R.W., 1977, Guide for data collection to calibrate a predictive digital ground-water model of the unconfined aquifer in and near the city of Modesto, California: U.S. Geological Survey Water-Resources Investigations Report 76–41, 46 p.

Page, R.W., 1986, Geology of the fresh ground-water basin of the Central Valley, California, with texture maps and sections: U.S. Geological Survey Professional Paper 1401–C, 54 p.

Page, R.W., and Balding, G.O., 1973, Geology and quality of water in the Modesto-Merced area, San Joaquin Valley, California: U.S. Geological Survey Water-Resources Investigations Report 73–6, 85 p.

Phillips, S.P., Beard, Sherrill, and Gilliom, R.J., 1991, Quantity and quality of ground-water inflow to the San Joaquin River, California: U.S. Geological Survey Water-Resources Investigations Report 91–4019, 64 p.

Phillips, S.P. and Belitz, Kenneth, 1991, Calibration of a texture-based model of a ground-water flow system, western San Joaquin Valley, California: Ground Water, v. 29, no. 5, p. 702-715.

Phillips, S.P., Green, C.T., Burow, K.R., Shelton, J.L., and Rewis, D.L., 2007, Simulation of multiscale ground-water flow in part of the northeastern San Joaquin Valley, California: US Geological Survey Scientific Investigations Report 2007–5009, 43 p.

Piper, A.M., Gale, H.S., Thomas, H.E., and Robinson, T.W., 1939, Geology and ground-water hydrology of the Mokelumne area, California: U.S. Geological Survey Water-Supply Paper 780, 230 p.

Pollock, D.W., 1994, User's guide for MODPATH/MODPATH-PLOT, Version 3—A particle tracking post-processing package for MODFLOW, the U.S. Geological Survey finite-difference ground-water flow model: U.S. Geological Survey Open-File Report 94–464, accessed Feb. 6, 2007 at *http://water.usgs.gov/nrp/gwsoftware/modpath41/modpath41.html*

U.S. Census Bureau, 2002, State and county quickfacts, for 1990 and 2000: Web page accessed April 26, 2002, at *http://quickfacts.census.gov/qfd/states/06/06099lk.html*.

Williamson, A.K., Prudic, D.E., and Swain, L.A., 1989, Ground-water flow in the Central Valley, California: U.S. Geological Survey Professional Paper 1401–D, 127 p.

Hydrogeologic Setting and Ground-Water Flow Simulations of the Northern Tampa Bay Regional Study Area, Florida

By Christy Crandall

Section 5 of

Hydrogeologic Settings and Ground-Water Flow Simulations for Regional Studies of the Transport of Anthropogenic and Natural Contaminants to Public-Supply Wells—Studies Begun in 2001

Edited by Suzanne S. Paschke

Professional Paper 1737–A

U.S. Department of the Interior

U.S. Geological Survey

U.S. Department of the Interior
DIRK KEMPTHORNE, SECRETARY

U.S. Geological Survey
Mark D. Myers, Director

U.S. Geological Survey, Reston, Virginia: 2007

For product and ordering information:
World Wide Web: http://www.usgs.gov/pubprod
Telephone: 1-888-ASK-USGS

For more information on the USGS--the Federal source for science about the Earth, its natural and living resources, natural hazards, and the environment:
World Wide Web: http://www.usgs.gov
Telephone: 1-888-ASK-USGS

Any use of trade, product, or firm names is for descriptive purposes only and does not imply endorsement by the U.S. Government.

Although this report is in the public domain, permission must be secured from the individual copyright owners to reproduce any copyrighted materials contained within this report.

Suggested citation:
Crandall, C., 2007, Hydrogeologic settings and ground-water flow simulation of the Northern Tampa Bay Regional Study Area, Florida, *section 5 of* Paschke, S.S., ed., Hydrogeologic settings and ground-water flow simulations for regional studies of the transport of anthropogenic and natural contaminants to public-supply wells—studies begun in 2001: Reston, Va., U.S. Geological Survey Professional Paper 1737–A, pp. 5–1 – 5–30.

Contents

Abstract 5–1
Introduction 5–1
Purpose and Scope 5–1
Study Area Description 5–3
Topography and Climate 5–3
Surface-Water Hydrology 5–3
Land Use 5–3
Water Use 5–3
Conceptual Understanding of the Ground-Water System 5–7
Geology 5–7
Ground-Water Occurrence and Flow 5–7
Surficial Aquifer System 5–7
Floridan Aquifer System 5–9
Aquifer Hydraulic Properties 5–9
Water Budget 5–11
Ground-Water Quality 5–11
Ground-Water Flow Simulations 5–13
Modeled Area and Spatial Discretization 5–13
Boundary Conditions 5–13
Model Stresses 5–15
Recharge 5–15
Pumping 5–15
Rivers 5–15
Drains 5–15
Aquifer Properties 5–15
Model Calibration and Sensitivity 5–19
Model-Computed Hydraulic Heads 5–19
Model-Computed Discharge and Recharge 5–23
Model-Computed Water Budget 5–23
Simulation of Areas Contributing Recharge to Wells 5–27
Limitations and Appropriate Use of the Model 5–27
References Cited 5–29

Figures

Maps showing:
5.1. Location of the Northern Tampa Bay regional study area within the Floridan aquifer system 5–2
5.2. Topography, hydrologic features, and locations of public-supply wells, Northern Tampa Bay regional study area, Florida 5–6
5.3. Generalized hydrologic section showing conceptual ground-water flow and geochemical conditions, Northern Tampa Bay regional study area, Florida. 5–7

Maps showing:

5.4. Year-2000 potentiometric surface and thickness of the Floridan aquifer, Northern Tampa Bay regional study area, Florida 5–10

5.5. Oxidation-reduction classification, Northern Tampa Bay regional study area, Florida 5–12

5.6. Ground-water flow model grid and boundary conditions, Northern Tampa Bay regional study area, Florida. 5–14

5.7. Distribution of hydraulic conductivity for model layer 1, Northern Tampa Bay regional study area, Florida. 5–16

5.8. Distribution of vertical leakance values assigned between model layers 1 and 2, Northern Tampa Bay regional study area, Florida 5–17

5.9. Distribution of transmissivity values assigned to the Floridan aquifer (model layers 2, 3, and 4), Northern Tampa Bay regional study area, Florida. 5–18

5.10. Ground-water flow model calibrated recharge rates, Northern Tampa Bay regional study area, Florida. 5–20

5.11*A*. Distribution of model-computed hydraulic heads for the surficial aquifer system (model layer 1), Northern Tampa Bay regional study area, Florida. 5–21

5.11*B*. Distribution of model-computed hydraulic heads for the uppermost Floridan aquifer system (model layer 2), Northern Tampa Bay regional study area, Florida. 5–22

Graphs showing:

5.12*A*. Relation between model-computed and measured hydraulic head for model layer 1, Northern Tampa Bay regional study area, Florida. 5–23

5.12*B*. Relation between model-computed and measured hydraulic head for model layer 2, Northern Tampa Bay Regional study area, Florida. 5–23

5.13. Map showing distribution of head residuals for model layers 1 and 2, Northern Tampa Bay regional study area, Florida. 5–24

Graphs showing:

5.14*A*. Probability distribution of head residuals for model layer 1, Northern Tampa Bay regional study area, Florida. 5–25

5.14*B*. Probability distribution of head residuals for model layer 2, Northern Tampa Bay regional study area, Florida. 5–25

Maps showing:

5.15. Model-computed ground-water inflows and outflows, Northern Tampa Bay regional study area, Florida. 5–26

5.16. Model-computed areas contributing recharge for selected public-supply wells, Northern Tampa Bay regional study area, Florida. 5–28

Tables

5.1. Summary of hydrogeologic and ground-water quality characteristics for the Floridan aquifer system and the Northern Tampa Bay regional study area, Florida. 5–4

5.2. Geology, hydrogeology, and water-use characteristics, Northern Tampa Bay regional study area, Florida. 5–8

5.3. Model-computed water budget for year 2000, Northern Tampa Bay regional study area, Florida. 5–25

Hydrogeologic Setting and Ground-Water Flow Simulations of the Northern Tampa Bay Regional Study Area, Florida

By Christy Crandall

Abstract

The transport of anthropogenic and natural contaminants to public-supply wells was evaluated for part of the Floridan aquifer system in the vicinity of Tampa Bay, Florida, as part of the U.S. Geological Survey National Water-Quality Assessment Program. The aquifer system in the Northern Tampa Bay regional study area is representative of the karst Floridan aquifer system throughout the Southeastern United States, is used extensively for public water supply, and is susceptible and vulnerable to contamination. The aquifer system in the study area is composed of an unconfined surficial aquifer of sandy deposits underlain by the karst limestone of the Floridan aquifer system. The two aquifers are separated by an intermediate confining zone in some parts of the study area creating confined and unconfined conditions in the Floridan aquifer system. An existing two-layer, steady-state ground-water flow model of the study area was modified to include a finer model grid, two additional layers, and additional boundary conditions and was recalibrated to year-2000 conditions. The calibrated ground-water flow model and advective particle-tracking simulations were used to compute ground-water flow paths, areas contributing recharge, and traveltimes from recharge areas to public-supply wells. Model results indicate precipitation recharge (55.4 percent of inflow) and lateral ground-water flow (35.1 percent of inflow) provide most of the ground-water inflow. Ground-water discharge is to the Gulf of Mexico and Tampa Bay (38 percent of outflow), wells (29.1 percent of outflow), and springs and streams (32.7 percent of outflow). Particle-tracking results indicate minimum traveltimes to public-supply wells ranged from 0.7 to 233 years with an average minimum traveltime of 19 years. Maximum computed traveltimes ranged from 32 to 1,875 years and averaged 600 years. On average, only 3 percent of the flow to a public-supply well was less than 10 years old, about 36 percent of the flow to a public-supply well was less than 50 years old, and about 80 percent of the flow to a public-supply well was less than 200 years old. Simulated traveltimes are probably much longer than actual travel times in the aquifer because the regional ground-water flow model does not accurately represent flow through local karst dissolution features.

Introduction

The Northern Tampa Bay regional study area for the transport of anthropogenic and natural contaminants (TANC) study overlies the karst Floridan aquifer system in west-central peninsular Florida in the Tampa Bay metropolitan area (fig. 5.1). The Floridan aquifer system underlies the Georgia-Florida Coastal Plain drainages National Water-Quality Assessment (NAWQA) study unit and much of the southeastern coast of the United States (fig. 5.1)

Purpose and Scope

The purpose of this Professional Paper section is to present the hydrogeologic setting of the Northern Tampa Bay TANC regional study area. The section also documents the setup and recalibration of a steady-state regional ground-water flow model for the study area. Ground-water flow characteristics, pumping-well information, and water-quality data were compiled from existing data to develop a conceptual understanding of ground-water conditions in the study area. An existing ground-water flow model of the area (Yobbi, 2000) was modified to include a finer model grid, two additional layers, and additional boundary conditions and was recalibrated to year-2000 conditions. The year 2000 was assumed to represent average conditions for the period from 1997 to 2001. The 5-year period 1997–2001 was selected for data compilation and modeling exercises for all TANC regional study areas to facilitate future comparisons between study areas. The updated ground-water flow model and associated particle tracking were used to simulate advective ground-water flow paths and to delineate areas contributing recharge to selected public-supply wells. Ground-water traveltimes from recharge to public-supply wells and presence of potential contaminant sources

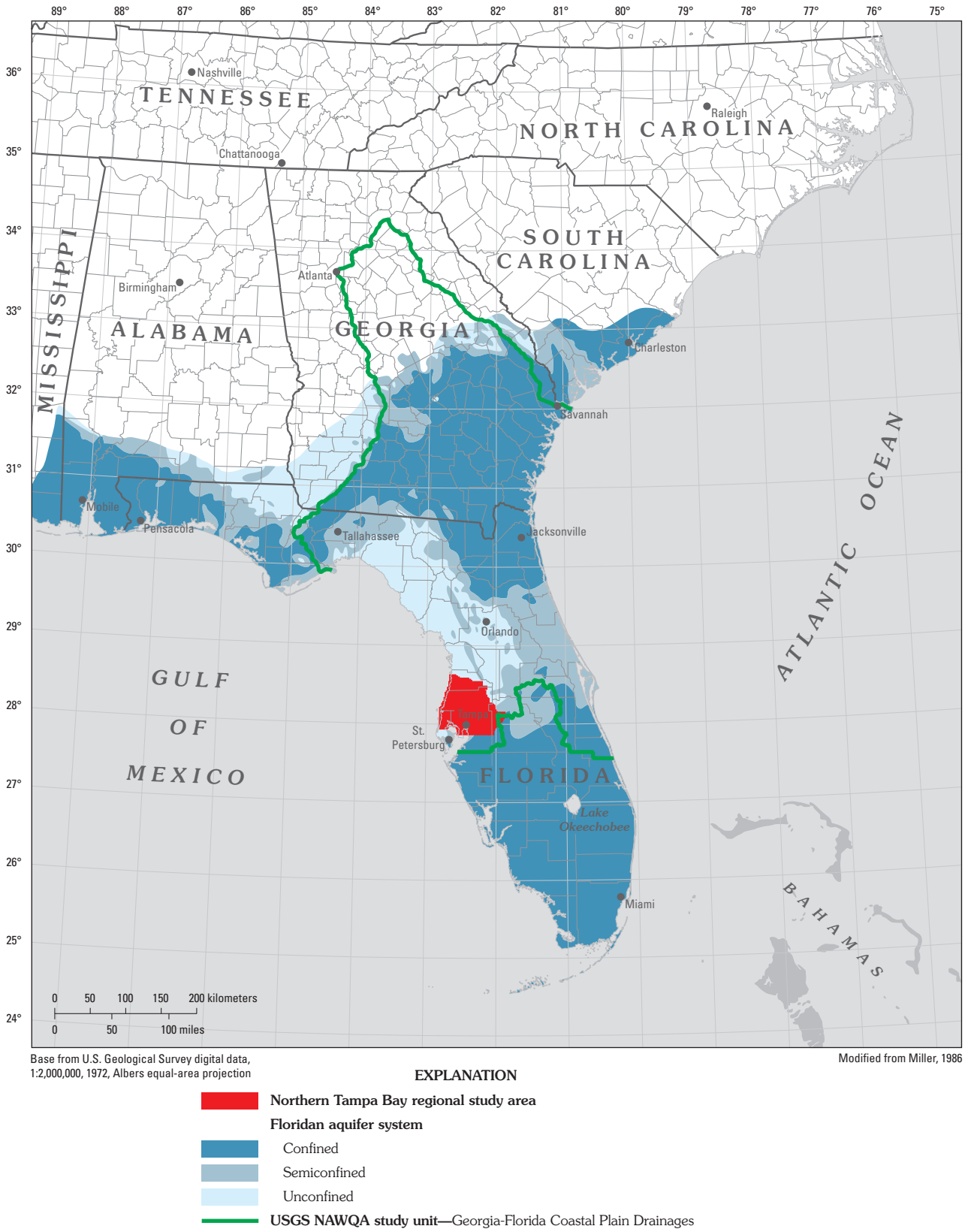

Base from U.S. Geological Survey digital data, 1:2,000,000, 1972, Albers equal-area projection

Modified from Miller, 1986

EXPLANATION

Northern Tampa Bay regional study area

Floridan aquifer system

Confined

Semiconfined

Unconfined

USGS NAWQA study unit—Georgia-Florida Coastal Plain Drainages

Figure 5.1. Location of the Northern Tampa Bay regional study area within the Floridan aquifer system.

in areas contributing recharge were tabulated into a relational database as described in Section 1 of this Professional Paper. This section provides the foundation for future ground-water susceptibility and vulnerability analyses of the study area and comparisons among regional aquifer systems.

Study Area Description

The Northern Tampa Bay regional study area was chosen because the Floridan aquifer system is used extensively for public water supply and is susceptible and vulnerable to contamination. The area also represents the range of hydrogeologic and land-use conditions throughout areas overlying the Floridan aquifer system (table 5.1). For example, variable hydrologic confining conditions and karst features are prevalent in both the Floridan aquifer system and the Northern Tampa Bay regional study area (Miller, 1986).

Topography and Climate

The Northern Tampa Bay regional study area is characterized by relatively flat, marshy lowlands along the coast (Coastal Swamps region), rolling hills of intermediate relief throughout parts of central Pasco County with elevations as high as 30 m above NAVD88 (Gulf Coastal Lowlands), and sand terraces to the northeast and southeast (Brooksville Ridge and Western Highlands, respectively) (White, 1970). The most prominent topographic feature in the study area is the Brooksville Ridge, located in central Hernando and eastern Pasco Counties. Land surface altitudes range from sea level to approximately 90 m above NAVD88 along the Brooksville Ridge (fig. 5.2).

The climate of the study area is subtropical with warm, wet summers and relatively dry, mild winters. Rainfall varies seasonally with more than one-half the total annual rainfall usually occurring between June and September, the result of convective storms. Average annual rainfall in the study area ranges from 125 to 140 cm per year (Metz and Sacks, 2002). Pan evaporation rates are high and average 125 to 150 cm per year (Farnsworth and others, 1982).

Surface-Water Hydrology

Karst features such as sinkholes and springs are prevalent throughout the study area (fig 5.2). Ancient, shallow, stable sinkhole depressions 5 to 8 m below land surface usually contain swamps and cypress domes, whereas deeper depressions infill with water and contain sinkhole lakes. At least 17 major springs are located in the study area. Springs usually discharge to rivers or directly to the Gulf of Mexico. The two largest springs are the Weeki Wachee Springs complex in western Hernando County and Crystal Springs, located along the northern reaches of the Hillsborough River. Weeki Wachee and Crystal Springs provide base flow to the Weeki Wachee and Hillsborough Rivers, respectively (Yobbi, 2000).

Six major rivers and their tributaries are located in the study area (fig. 5.2). The two rivers with the largest discharge are the Hillsborough and Withlacoochee Rivers. Hundreds of lakes, swampy plains, and intermittent ponds ranging in size from 0.001 to 10 km^2 also are dispersed throughout the study area.

Soils covering the Brooksville Ridge and the sand hills (the eastern edge of the study area) are very well drained and have relatively deep water tables, rapid percolation, internal drainage, and high recharge potential (HydroGeoLogic, Inc., 1997). Soils in the lower Gulf Coast Lowlands and Coastal Swamp regions (along river channels and the coast) are moderately to poorly drained with shallow water tables; numerous perched lakes, ephemeral ponds, and wetlands; and high organic contents (Soil Conservation Service, 1976, 1981, 1989). Recharge is relatively low in these areas except in areas with sinkholes and other karst features (HydroGeoLogic, Inc., 1997).

Land Use

Land use in the study area includes urban, residential, new-commercial, suburban, agriculture, wetland, and forests. Land-use change from agriculture and rural forests to residential and commercial is typical of areas overlying the Floridan aquifer system as a whole and the study area. The largest components of land use in the study area are agriculture (28 percent), urban (22 percent), and wetlands (21 percent) (Hitt, 2004). Within these categories, cropland (74 percent) and citrus groves (20 percent) dominate agricultural land uses, whereas residential (77 percent) and commercial (10 percent) land uses account for most of urban land uses. Wetlands are 86 percent forested in the study area. Rangeland (7 percent), forests (10 percent), and waterways (6 percent) account for the remainder of land uses in the study area.

Water Use

Ground-water withdrawals from the entire Floridan aquifer system are 15.4 million cubic meters per day (Mm^3/d) and from the Floridan aquifer system within the study area they are 1.8 Mm^3/d (Marella and Berndt, 2005). The Tampa Metropolitan area relies heavily on the Floridan aquifer system as a drinking-water source. In 2000, Tampa Bay Water, the largest user of the Floridan aquifer system in the study area, withdrew about 0.7 Mm^3/d from the Floridan aquifer system and served 1.2 million people. In addition to public supply, the Floridan aquifer system is the primary source for domestic, irrigation, and industrial wells in the study area. Within the Northern Tampa Bay regional study area, public-supply wells are the basis of community water systems for the cities of Tampa, St. Petersburg, and Clearwater, Florida, and numerous smaller cities.

Table 5.1. Summary of hydrogeologic and ground-water-quality characteristics for the Floridan aquifer system and the Northern Tampa Bay regional study area, Florida.

[m, meters; km, kilometers, cm/yr, centimeters per year; m^3/d, cubic meters per day; m/d, meters per day; Kh, horizontal hydraulic conductivity; Kv, vertical hydraulic conductivity; Sy, specific yield; n, porosity; Mm^3/d, million of cubic meters per day; mg/L, milligrams per liter; O_2, dissolved oxygen; CH_4 methane; Ca, calcium; Mg, magnesium; HCO_3, bicarbonate; SO_4, sulfate; Na, sodium; Cl, chloride]

Characteristic	Floridan aquifer system	Northern Tampa Bay regional study area
	Geography	
Topography	Rolling hills below the Fall Line Hills of Central Georgia (fig. 1); elevations range from 100 to 250 m; sandy terraces with elevations ranging from about 25 to 100 m; Coastal Plains and Wetlands from near sea level to about 25 m. Karst topography, in north through central Florida (Krause and Randolph, 1989).	Sandy hills in the Brooksville Ridge upland (fig. 2); relief generally less than 60 m; eolian deposits and sandy terraces less than 25 m; Coastal Plain and Swamps generally less than 3 m. Karst topography evident (Metz and Sacks, 2002; Ryder, 1985; Yobbi, 2000).
Climate	Temperate to subtropical; humid; precipitation 115 to165 cm/yr; evapotranspiration 115 to165 cm/yr (Bush and Johnston, 1988).	Subtropical; humid; precipitation 125 to150 cm/yr; evapotranspiration 125 to140 cm/yr (Metz and Sacks, 2002).
Land use	Urban, suburban, water, wetland, rural residential/ commercial, woodlands, farmland (Hitt, 2004).	Urban, suburban, rural, water, wetland, residential/ commercial, woodlands, farmland (Hitt, 2004).
	Geology	
Surficial deposits	Eolian sands and clays, gravel, and limestone; more fine-grained deposits further north, sand uplands (Miller, 1986).	Sand and clays; limited clay, mostly fine sand, unconsolidated limestone. Eolian sands discontinuous (Yobbi, 2000).
Bedrock geologic units	Thick carbonate sequence ranging from 30 to 1,000 m in thickness from north to south Florida; fractured with many dissolution features especially in unconfined and semiconfined areas of south Georgia and Peninsular Florida.	Thick carbonate sequence from 200 to 400 m thick; fractured with many dissolution features especially in unconfined and semiconfined areas.
	Ground-water hydrology	
Aquifer conditions	Unconfined; semiconfined; confined (Miller, 1986).	Unconfined; semi-confined, confined (Miller, 1986; Yobbi, 2000).
Hydraulic properties	Floridan: Kh=0.1 to 3,000 m/d; Kv=0.00006 m/d to 0.10 m/d; n=0.02 to 0.50 (Bush and Johnston, 1988; Knochenmus and Robinson, 1996).	Surficial: Kh=0.3 to 5 m/d; n=0.25 Floridan: Kh=0.2 to 2,000 m/d; Kv=0.02 to 2 X 10^{-5} m/d; n=0.15 (Knochenmus and Robinson, 1996; SDI, Inc., 1997)
Ground-water budget	Recharge from precipitation: 12.7 cm/yr or 12.1 Mm^3/d; evaporation: 92 to 102 cm/yr; discharge to springs: approximately 7.8 Mm^3/d; river discharge, offshore springs, and diffuse leakage: 0.73 Mm^3/d; wells: 3.6 Mm^3/d (Bush and Johnston, 1988; Ryder, 1985)	Recharge from precipitation: 23 cm/yr or 3.44 Mm^3/d; recharge from streams: 0.59 Mm^3/d; discharge to springs and rivers: 2.04 Mm^3/d; pumping: 1.8 Mm^3/d. Loss to head-dependent boundaries: 0.30 Mm^3/d (this study).
Lengths of ground-water travel paths	Generally thought short (less than 40 km) (Bush and Johnston, 1988; Knochenmus and Robinson, 1996)	Generally less than 15 km; usually less than 7 km.

Table 5.1. Summary of hydrogeologic and ground-water-quality characteristics for the Floridan aquifer system and the Northern Tampa Bay regional study area, Florida.—Continued

[m, meters; km, kilometers, cm/yr, centimeters per year; m^3/d, cubic meters per day; m/d, meters per day; Kh, horizontal hydraulic conductivity; Kv, vertical hydraulic conductivity; Sy, specific yield; n, porosity; Mm^3/d, million of cubic meters per day; mg/L, milligrams per liter; O_2, dissolved oxygen; CH_4 methane; Ca, calcium; Mg, magnesium; HCO_3, bicarbonate; SO_4, sulfate; Na, sodium; Cl, chloride]

Characteristic	Floridan aquifer system	Northern Tampa Bay regional study area
	Ground-water quality	
Water chemistry (dissolved solids, pH, redox, major water types)	Dissolved solids less than 25 to greater than 1,000 mg/L along the coast and in S. Florida; pH 6.0 to 8.0; varies from O_2 to CH_4 reducing; Ca, and Ca,Mg-HCO_3, Ca-SO_4, and Na-Cl along the coast (Sprinkle,1989)	Dissolved solids less than 200 to greater than 1,000 mg/L along the coast; pH 6.0 to 8.0; varies from O_2 to Fe and SO_4 reducing; Ca, and Ca,Mg-HCO_3, Ca-SO_4, and Na-Cl in Pinellas County (Ryder, 1985).
Contaminants	Nutrients, uranium, radon, arsenic, halogenated volatile organic compounds, including some gasoline and drycleaner free product, triazine and bromated herbicides. Saline water in areas with large pumping wells near the coast (Sprinkle, 1989).	Nutrients, uranium, radon, arsenic, halogenated volatile organic compounds including some gasoline and drycleaner free product, triazine and bromiated herbicides. Saline water in areas with large pumping wells near the coast (Ryder, 1985)

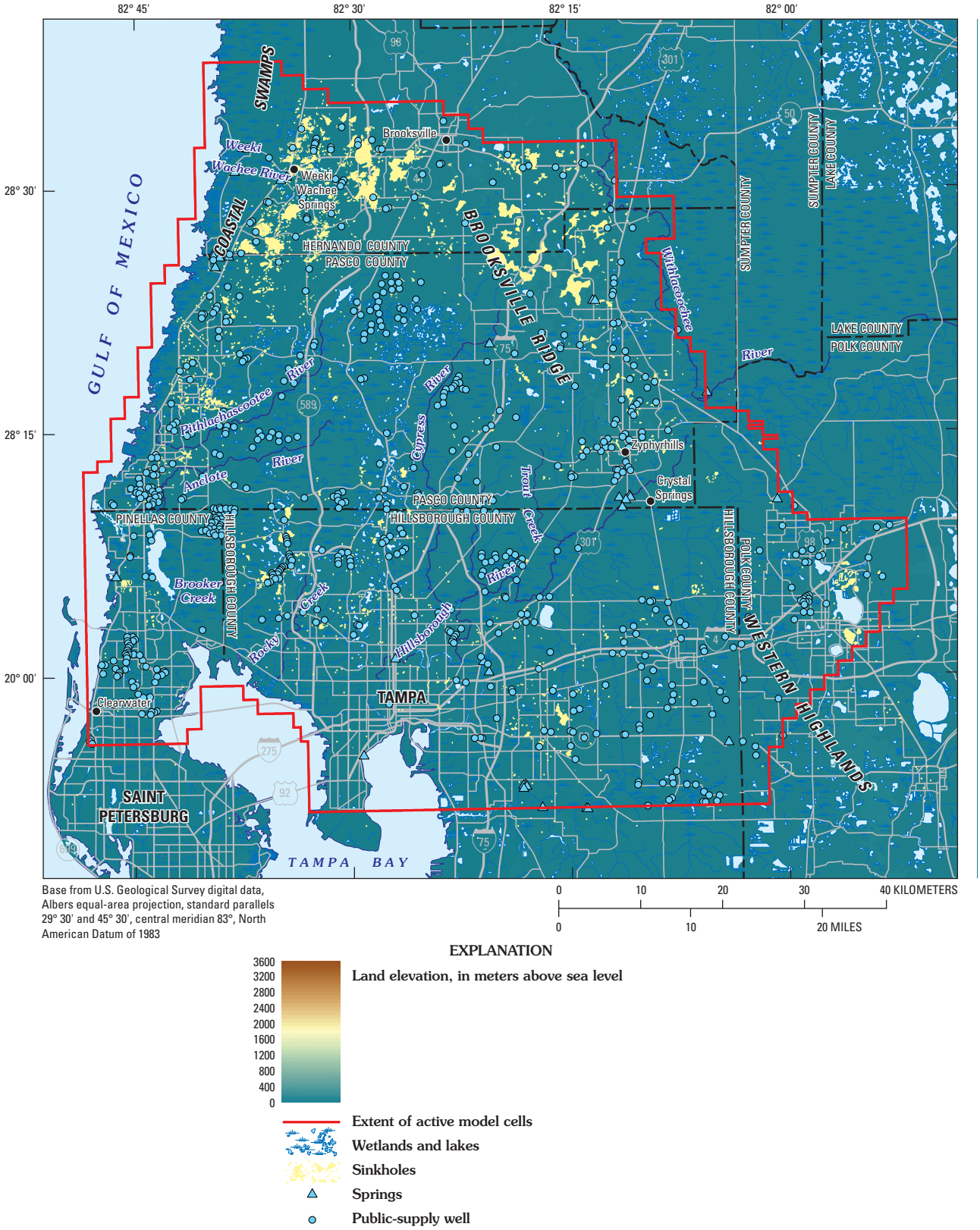

Figure 5.2. Topography, hydrologic features, and locations of public-supply wells, Northern Tampa Bay regional study area, Florida.

Conceptual Understanding of the Ground-Water System

The study area is underlain by a sequence of Paleocene to Miocene carbonate rocks. Karst dissolution features control the ground-water flow, aquifer hydraulic properties, and to a lesser extent, ground-water chemistry (fig. 5.3). Ground-water recharge is greatest where karst sinkholes are present at the land surface. Ground-water discharge occurs to streams by way of karst springs. Aquifer hydraulic properties such as porosity and permeability are greatest where solution-enlarged fissures are present in the subsurface. Ground-water chemistry is controlled by ground-water flow paths and residence time in the carbonate rock aquifer, which are in turn controlled by the presence and location of karst features.

Geology

The ground-water flow system beneath the study area consists of a thick sequence of layered carbonate rocks overlain by surficial clastic deposits (table 5.2). The surficial deposits and carbonate rocks are subdivided into a hydrologeologic framework of two aquifers and one confining unit. The framework includes the unconfined surficial aquifer system, the intermediate confining unit that separates the surficial aquifer system from the Floridan aquifer system, and the Floridan aquifer system. The surficial aquifer system is composed of Pliocene to Holocene undifferentiated sands, clays, and marls. The intermediate confining unit is part of the late Miocene Hawthorn Group sediments and is composed of dense, plastic, green-grey clay, interbedded with varying amounts of chert, sand, clay, marl, shell, and phosphate. The intermediate confining unit is not present or is breached in parts of the study area where the Floridan aquifer system is semiconfined or unconfined (fig. 5.1). The Floridan aquifer system is composed of a thick sequence of limestone, dolomite, and evaporitic dolomite. The formational components of the Floridan aquifer system in the regional study area are as follows (in order of youngest to oldest): the Tampa Member of the Arcadia Formation and Hawthorn Group of early Miocene age, the Suwannee Limestone of Oligocene age, the Ocala Limestone of Oligocene to Eocene age, the Avon Park Formation of middle Eocene age, and the Oldsmar and Cedar Keys Formations of Eocene to Paleocene age (table 5.2) (Miller, 1986; Southeastern Geological Society, 1986). A relatively impermeable layer composed of evaporitic limestone located at the base of the Avon Park Formation forms the middle confining unit at the base of the upper Floridan aquifer system and is considered the base of the freshwater flow system in the study area (Yobbi, 2000; Miller, 1986).

Ground-Water Occurrence and Flow

In general, unconfined ground-water conditions occur in the surficial aquifer system, and confined ground-water conditions occur in the Floridan aquifer system. Ground-water occurrence and flow for each of these aquifer systems are discussed in the following sections.

Surficial Aquifer System

The surficial aquifer system exists throughout most of the study area except where the Floridan aquifer system is exposed at land surface and unconfined (fig. 5.1) (Miller, 1986; Berndt and Katz, 1992). The term surficial aquifer system refers to any permeable material exposed at land surface that contains ground water under water-table conditions and is

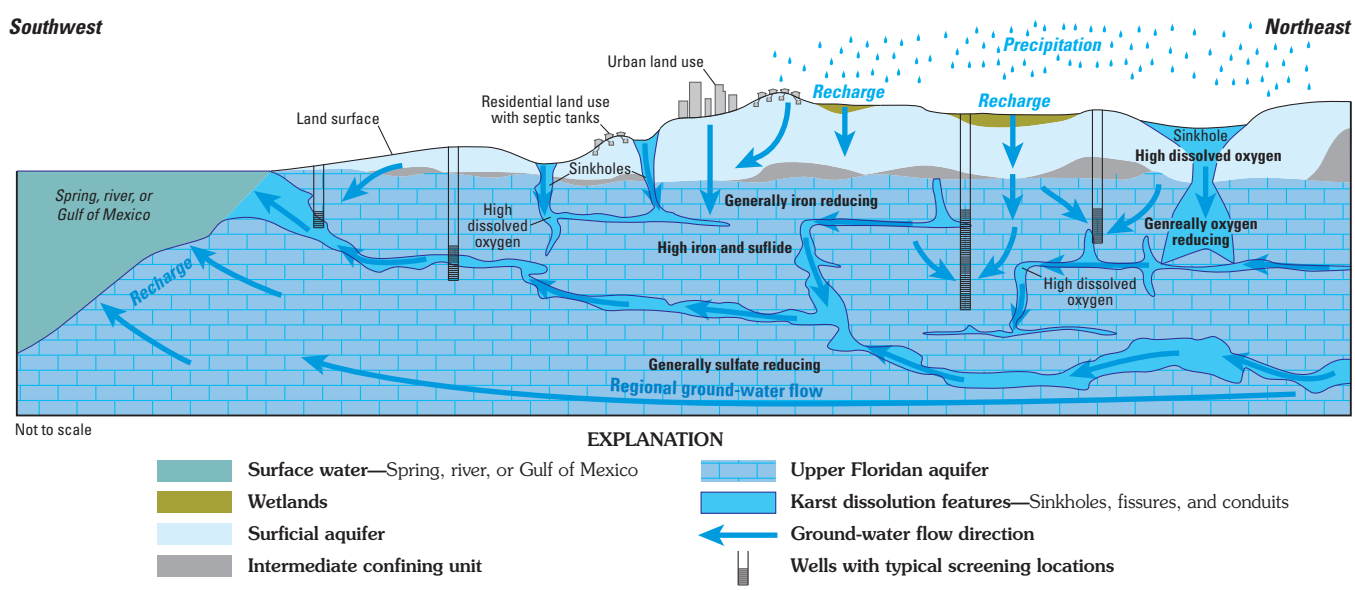

Figure 5.3. Conceptual ground-water flow and geochemical conditions, Northern Tampa Bay regional study area, Florida.

Table 5.2. Geology, hydrogeology, and water-use characteristics of the Northern Tampa Bay regional study area, Florida [adapted from Ryder (1985) and Metz and Sacks (2002)].

[m, meters; SAS, surficial aquifer system; FAS, Floridan aquifer system; m^3/d, cubic meters per day]

Age	Stratigraphic unit	Lithologic descriptions	Range in thickness (m)	Hydrogeologic unit	Aquifer characteristics
Holocene to Pliocene	Undifferentiated surficial deposits, terrace sand, phosphorite	Predominantly fine sand; interbedded clay, marl, shell, limestone, sandy clay.	8 to 15	SAS	Limited use; lawn irrigation; yields less than 27 m^3/d; high iron content.
Miocene	Undifferentiated deposits of the Hawthorn Group	Dense plastic green-grey clay, contains varying amounts of chert, sand; clay, marl, shell, phosphate.	0 to 6	Intermediate Confining bed if present	Semiconfining unit retards downward percolation from the SAS; breaches in clay unit preferentially transmit recharge to the Upper FAS.
	Tampa Member of the Arcadia Formation of the Hawthorn Group	Weathered limestone surface, white to light tan, soft sandy, fossiliferous; clays in lower part in some areas.	6 to 75	FAS—Upper FAS	Many domestic and public-supply wells tap this unit; poor to fair producer of water; yields from a few to 1,100 m^3/d.
Oligocene	Suwannee Limestone	Soft to hard limestone, vuggy, granular, fossiliferous limestone.	30 to 60		Domestic and large capacity public-supply wells tap these units; yields from a 1,100 m^3/d to 11,000 m^3/d.
Oligocene to Eocene	Ocala Limestone	Limestone, chalky, foraminferal, dolomitic near bottom.	50 to 60		
Eocene	Avon Park Formation	Hard brown dolomite and limestone, with intergranular evaporite in lower part.	120 to 200	Middle confining unit at the bottom of the Avon Park Formation	
Eocene to Paleocene	Oldsmar and Cedar Keys Formations	Dolomite and limestone with beds of anhydrite.	180 to 200	Lower FAS	Not used for domestic or public supply—highly mineralized.

not part of the Floridan aquifer system. The surficial aquifer system may be in direct hydraulic contact with the Floridan aquifer system or be separated by confining beds. The base of the surficial aquifer system has been designated as "the top of the laterally extensive and vertically persistent beds of much lower permeability" (Southeastern Geological Society, 1986)—the Hawthorn Group in the study area. The Floridan aquifer system underlies the surficial aquifer system directly where the intermediate confining unit is absent (Berndt and Katz, 1992).

The surficial aquifer system is recharged by rainfall, irrigation, and septic effluent (fig. 5.3). Rainfall easily infiltrates the surficial aquifer system and percolates downward to recharge the Floridan aquifer system by way of downward leakage through the intermediate confining unit. Ground water discharges from the surficial aquifer system through lakes, ditches, streams, evaporatranspiration, pumping, and downward leakage to the Floridan aquifer system (Tibbals and others, 1980). Water levels in the surficial aquifer system fluctuate widely and rapidly in response to rainfall and evaporation (Miller, 1986). The configuration of the top of the water table in the surficial aquifer system is a subdued reflection of the land surface and is generally within 0.1 to 3 m of the land-surface. The surficial aquifer system is not used for water supply (table 5.2) because of low yields (less than 27 m^3/d), high iron content, and its vulnerability to contamination from overlying land use (Metz and Sacks, 2002).

Floridan Aquifer System

The Floridan aquifer system consists of a thick sequence of hydraulically connected carbonate rocks and covers a land area of more than 260,000 km^2. The aquifer underlies coastal regions of southern Mississippi, Alabama, Georgia, and South Carolina and the entire Florida peninsula (fig. 5.1) (Miller, 1986). The Floridan aquifer system is composed of limestones and dolomites of late Paleocene to early Miocene age; however, neither the aquifer boundaries nor its high- and low-permeability zones necessarily conform to either formational boundaries or time-stratigraphic units. Solution-enlarged fissures (channel porosity) in combination with diffuse flow through more uniformly distributed interconnected pores (rock porosity) contribute to flow in the study area. The aquifer ranges in thickness from about 61 m in the north to over 1,000 m in areas of central and south Florida (Miller, 1986). Units that compose the Floridan aquifer system outcrop in west-central-southern Georgia and along the north- to south-central Gulf Coast of Florida (fig. 5.1). The Floridan aquifer system is considered unconfined or semiconfined where it outcrops and the intermediate confining unit is absent or less than 30 m thick and(or) breached. The Floridan aquifer system is considered confined where the intermediate confining unit is present and greater than 30 m thick (Miller, 1986).

Ground-water recharge to and discharge from the Floridan aquifer system are controlled by the prominent karst features and aquifer confinement. Precipitation recharge, which provides most of the recharge to the Floridan aquifer system in the study area, ranges from 25 to 55 cm/yr and occurs primarily in areas considered unconfined and semiconfined (fig. 5.1) (Aucott, 1988). Karst features such as springs, conduits, and sinkholes are common in the study area and elsewhere where the aquifer is unconfined or semiconfined and provide direct pathways for contaminants to travel from land surface to the aquifer (Miller, 1986). Ground-water discharge from the Floridan aquifer system occurs through springs, rivers, and coastal seeps and springs with approximately 75 percent of all Floridan aquifer system discharge flowing to springs (Bush and Johnston, 1988). The Floridan aquifer system in the study area supplies base flow to the Withlacoochee, Hillsborough, and other rivers, which are important water-supply and recreational resources (Bush and Johnston, 1988).

The Floridan aquifer system potentiometric surface is controlled by seasonally influenced recharge and local pumping. The regional ground-water flow direction is from east to west with a slightly southern component (fig. 5.4). Flow is convergent toward springs, rivers, and the Gulf of Mexico, and flow is transmitted vertically and laterally through karst conduits and enlarged fracture planes. The regional potentiometric surface exhibits highs and lows that generally correspond to topographic highs and lows. River and spring discharge features are topographic and potentiometric lows. In the study area, the potentiometric surface ranges from 0 to approximately 40 m in elevation (fig. 5.4).

Aquifer Hydraulic Properties

Hydraulic conductivity of the surficial aquifer system generally ranges from 0.1 to 5 m/d and averages 3 m/d in the modeled area (SDI Environmental Services Inc., 1997; Knochenmus and Robinson, 1996), although hydraulic conductivity may be as large as 30 m/d in some areas (Ryder, 1985). The surficial aquifer system thickness ranges from approximately 0 in the northern part of the study area to more than 30 m in the southeastern part of the study area and averages between 8 and 25 m in the study area (Miller, 1986; Berndt and Katz, 1992). Effective porosity measurements for the surficial aquifer system vary, but an average value of 0.25 based on geophysical measurements has been used in various models (SDI Environmental Services Inc., 1997; Knochenmus and Robinson, 1996).

Horizontal hydraulic conductivity of the Floridan aquifer system in the study area generally is reported to range from 0.2 to 2000 m/d in the literature (Bush and Johnston, 1988; Knochenmus and Robinson, 1996), but it can vary by up to five orders of magnitude where karst features create secondary porosity in the aquifer (Langevin, 1998). Storage coefficients reported in the literature for the Floridan aquifer system range from 1×10^{-5} to 2×10^{-2} (Bush and Johnston, 1988). An average storage coefficient of 2.5×10^{-4} is reported for the study area (Tibbals and Grubb, 1982), and vertical hydraulic conductivity of the Floridan aquifer system ranges from 0.02

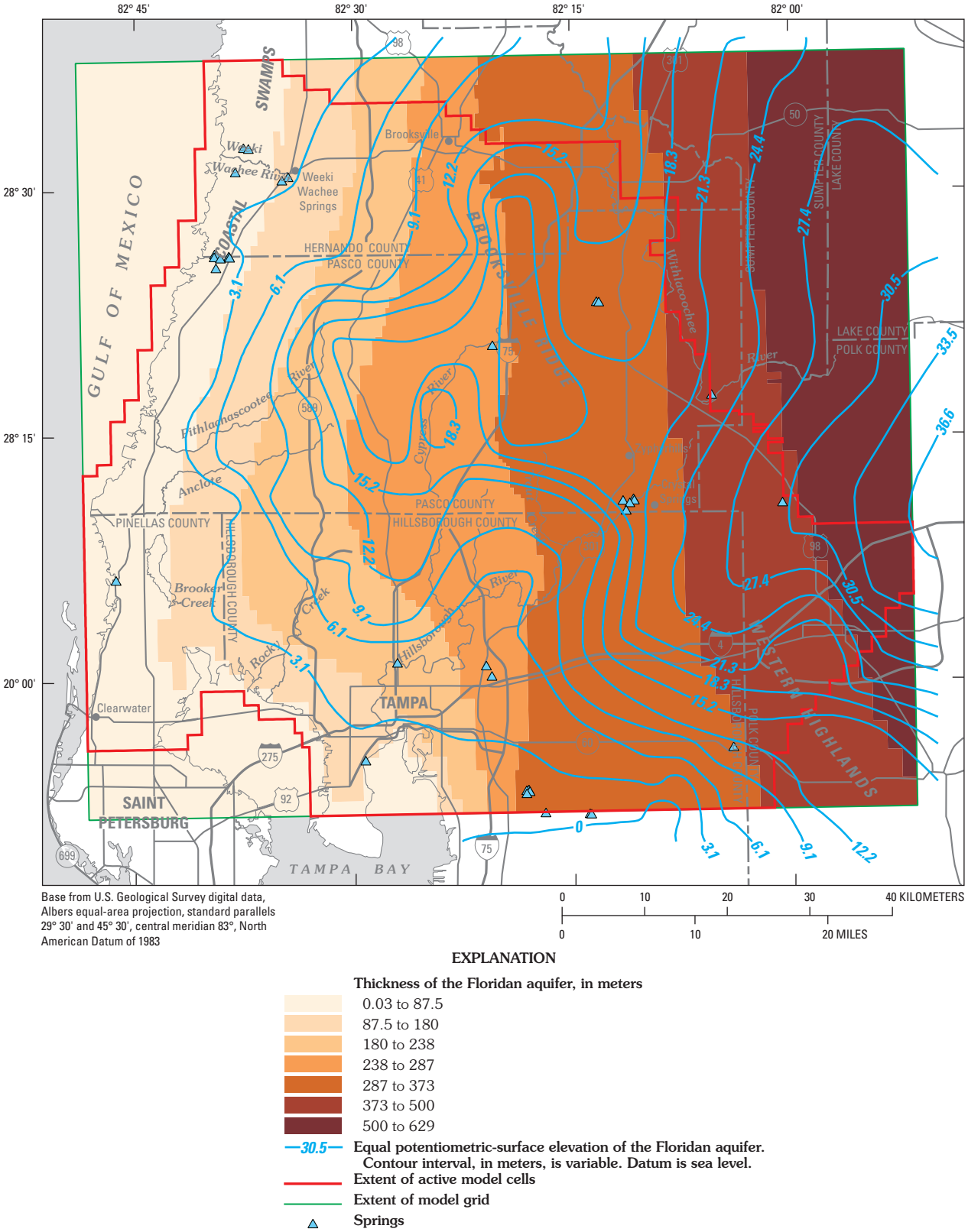

Base from U.S. Geological Survey digital data, Albers equal-area projection, standard parallels 29° 30' and 45° 30', central meridian 83°, North American Datum of 1983

EXPLANATION

Thickness of the Floridan aquifer, in meters

- 0.03 to 87.5
- 87.5 to 180
- 180 to 238
- 238 to 287
- 287 to 373
- 373 to 500
- 500 to 629

—30.5— Equal potentiometric-surface elevation of the Floridan aquifer. Contour interval, in meters, is variable. Datum is sea level.

Extent of active model cells

Extent of model grid

Springs

Figure 5.4. Year-2000 potentiometric surface and thickness of the Floridan aquifer, Northern Tampa Bay regional study area, Florida.

to 2 X 10^{-5} m/d in the study area (Bush and Johnston, 1988; Knochenmus and Robinson, 1996).

Water Budget

Estimates of the water budget in the modeled area for the year 1987 (a representative year) are provided in Yobbi (2000) and are reported here. Recharge estimates for the modeled area vary greatly. A net recharge rate of 23.1 cm/yr from precipitation is considered reasonable, although site-specific values likely vary from 0 to more than 30 cm/yr because of the karst topography. An estimated net discharge rate of 1.05 Mm^3/d was calculated from the total average annual ground-water discharge to 13 major springs in the modeled area. Total base flow to rivers from ground water, determined from hydrograph separation techniques for 21 sites in the modeled area, was 1.37 Mm^3/d. Discharge to wells estimated from year-2000 pumping data is approximately 1.8 Mm^3/d as discussed in the "Model Stresses" section.

Ground-Water Quality

Concentrations of major ions in any aquifer reflect the quality of recharge water, lithology and mineralogy of geologic deposits, residence time of water, and proximity to the coast and(or) other contaminant sources. The most commonly occurring water types in the surficial aquifer system in the study area are mixed and calcium-bicarbonate. Precipitation, which provides most of the recharge to the surficial aquifer system, is generally a sodium-chloride type water; however, water quality rapidly evolves to calcium-bicarbonate or mixed type water owing to water-rock interaction with the carbonate rocks (Berndt and Katz, 1992). Dissolved-solids concentrations are generally low (less than 100 mg/L) (Berndt and Katz, 1992), pH is normally less than 5, and water entering the aquifer through recharge is normally oxic.

The intermediate confining unit overlying the Floridan aquifer system contains many minerals including magnesium-rich clay sediments, uranium, pyrite, and phosphatic minerals (Katz, 1992). Arsenic, uranium, radon, and radium are present as trace elements in the phosphatic and(or) pyrite minerals, and these constituents may leach into the Floridan aquifer system when conditions are favorable. The dominant water type for the intermediate confining unit is mixed, and the pH and dissolved-solids concentration in the intermediate confining unit are generally greater than those of water from the surficial aquifer system.

Ground water in the Floridan aquifer system has a predominantly calcium-bicarbonate to calcium-sulfate, or calcium-magnesium-bicarbonate-sulfate chemical signature (Katz, 1992), although water-chemistry conditions in the Floridan aquifer system can be highly variable because karst features can cause variable residence times. Ground-water pH of the Floridan aquifer system in the study area is generally between 6.0 and 8.0 pH units. Dissolved-solids concentrations range from 10 to 30,000 mg/L and average approximately 250 mg/L depending on the degree of confinement, depth in the aquifer, and mixing with seawater. Calcium concentrations generally increase with depth in the Floridan aquifer system within the study area because aquifer residence times tend to increase with depth. The dissolution of gypsum may also contribute to high concentrations of calcium and sulfate. Pyrite dissolution from the Suwannee Limestone, and possibly the overlying Hawthorn Group, may contribute iron and arsenic to the Florida aquifer (Thomas Pichler, University of South Florida, Tampa, oral commun., 2002). Ground water in discharge areas is commonly mixed or of sodium-chloride type indicating mixing with or evolving to seawater (Katz, 1992).

Oxidation-reduction (redox) conditions in the Floridan aquifer system were difficult to generalize, but several observations came from analysis of retrospective data. Conditions consistent with oxygen reduction generally occurred in ground water from shallow sediments and in the Floridan aquifer system in areas where sinkhole density is highest and(or) the aquifer is unconfined or semiconfined (figs. 5.3, 5.5). Conditions consistent with oxygen reduction in deeper wells were observed almost exclusively in waters from large-capacity public-supply wells and may be the result of high pumping rates oxidizing ground water near the well. Reduced conditions, represented by iron-reducing waters, were more often present in proximity to wetlands, discharge areas, and at greater aquifer depths (fig. 5.3). Iron and sulfate concentrations are high in waters from shallower wells because of the iron- and magnesium-rich clay minerals, pyrite and dolomite dissolution from the Hawthorn Group intermediate confining unit, and gypsum dissolution in the deeper Floridan aquifer system.

Because of the complex karst ground-water flow system within the Floridan aquifer system and the various types of wells used to evaluate redox conditions (public-supply wells with large open intervals compared to monitoring wells with short open intervals), delineation of spatial or vertical redox zones is not possible with the available water-quality data. The ability to delineate redox zones in the Floridan aquifer system may be improved by defining a quantifiable link between the total area of wetlands and/or number of sinkholes (and other karst features) in the contributing areas of wells and the redox conditions of the aquifer.

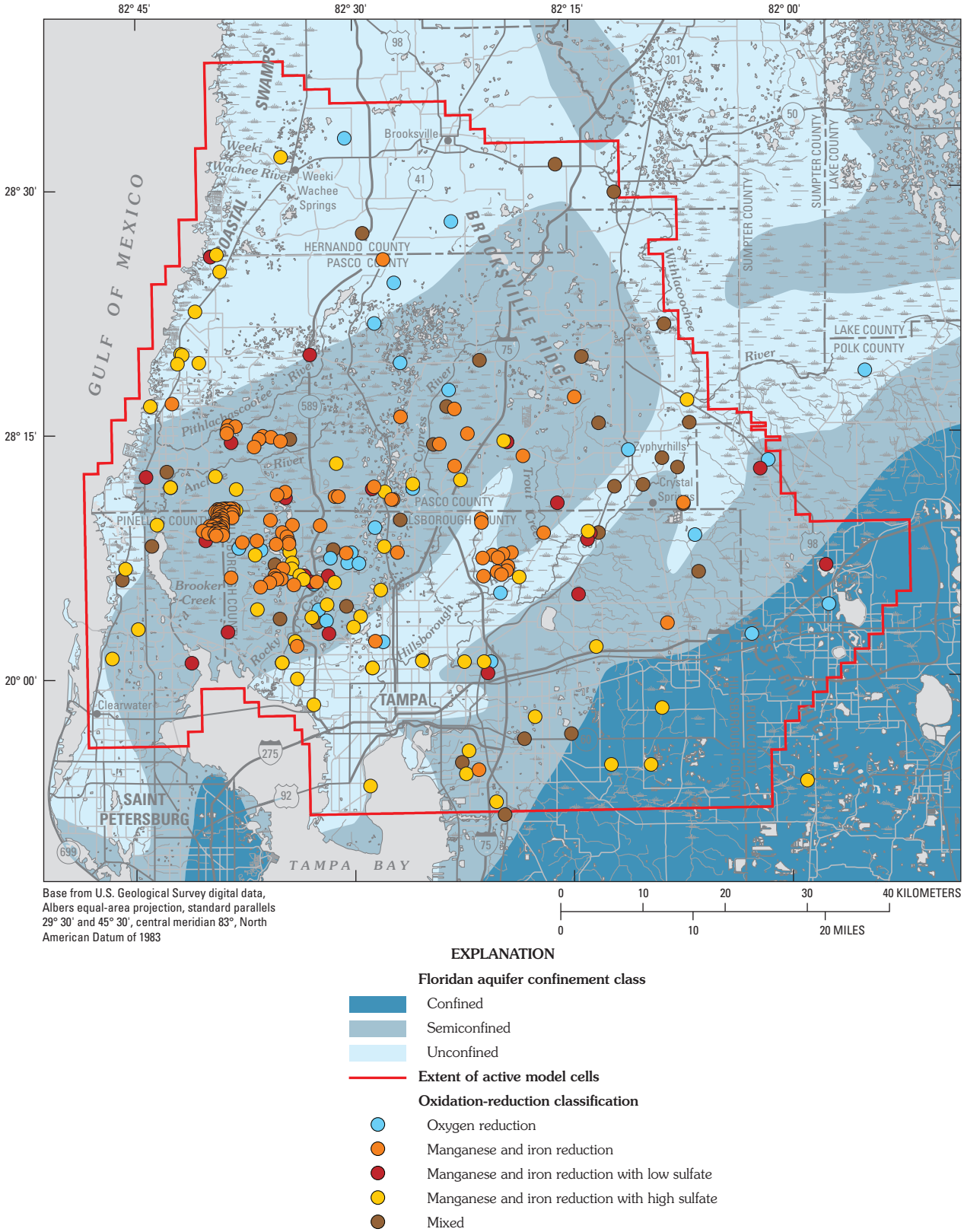

Figure 5.5. Oxidation-reduction classification, Northern Tampa Bay regional study area, Florida.

Ground-Water Flow Simulations

Ground-water flow of the Northern Tampa Bay regional study area was simulated by modifying an existing steady-state ground-water flow model, developed in MODFLOW88 (McDonald and Harbaugh, 1988) of the Central-Northern Tampa Bay area (SDI Environmental Services, Inc., 1997). The Central-Northern Tampa Bay model was originally developed as a tool to evaluate the effects of ground-water withdrawal from specific well fields on aquifer and lake water levels. The Central-Northern Tampa Bay model was a transient, coupled surface-water/ground-water flow model with a simulation period of 1971 through 1993 (SDI Environmental Services, Inc., 1997). In the late 1990's, the ground-water component of the Central-Northern Tampa Bay model was split from the coupled model, converted to a steady-state model, and the hydraulic parameters of the ground-water model were optimized by Yobbi (2000).

The optimized steady-state ground-water flow model of Yobbi (2000) was updated by this study to reflect withdrawal rates for year 2000, rediscretized, converted to MODFLOW-2000 (Harbaugh and others, 2000), and recalibrated. The year 2000 was selected for the steady-state simulations because estimated withdrawal rates for agricultural and industrial wells already existed (Nick Sepulveda, U.S. Geological Survey, Orlando, Florida, written commun., 2002), measured withdrawal rates for public-supply wells are available for year 2000, and because year-2000 withdrawal rates are considered representative of withdrawal conditions for 1997–2001. The steady-state flow assumption is reasonable for the study area for 1997–2001 because the Floridan aquifer system has high transmissivity values, a large volume of water circulates through the system, and pumping rates were relatively stable during the time period of study. Other significant changes made to the Yobbi (2000) ground-water model for this study include:

- The surficial aquifer system and Floridan aquifer system were both modeled as convertible from confined to unconfined aquifers to prevent surficial aquifer system nodes from going dry during steady-state simulations. The model modification did not affect the resulting heads, recharge rates, or other parameters.
- The number of drain cells in layer 2 was reduced to represent only those cells with identified springs.
- All drain cells in layer 1 were removed because it was assumed that the springs emanate from the Floridan aquifer system (layer 2).
- The number of river cells was reduced to better represent model areas actually containing river channels.
- The potentiometric surface of the surficial aquifer system in the north-central portion of the model dropped below the bottom of layer 1. The dry cells in layer 1 were therefore deactivated by this study (fig. 5.6) to correct the problem. Dry cells probably occurred because the surficial aquifer is very thin or not present in the area where the Floridan aquifer system outcrops (fig. 5.1).

Initial conditions for starting heads, hydraulic conductivity, base of the surficial aquifer system, transmissivity, leakance, hydraulic parameter zones, watershed boundaries, and boundary conditions were derived from the original Central-Northern Tampa Bay model and Yobbi's optimized hydraulic parameters (SDI Environmental Services, Inc., 1997; Yobbi, 2000) with those exceptions previously mentioned. Land-surface elevation, thickness of the active freshwater flow system, base of the Floridan aquifer system, and recharge estimates were derived from Sepulveda (2002).

Modeled Area and Spatial Discretization

The Central-Northern Tampa Bay ground-water flow model covers 5,426 km^2 in Hillsborough, Pasco, Hernando, Pinellas, and Polk Counties of Florida (fig. 5.2). The Central-Northern Tampa Bay model had 121 columns, 131 rows, and 2 layers, and cell sizes ranged from about 300 to 1,600 m on a side. The Central-Northern Tampa Bay model simulated flow in the surficial aquifer system as layer 1 and flow in the Floridan aquifer system as layer 2. The updated Northern Tampa Bay regional ground-water flow model has 227 columns, 234 rows, and 4 model layers; cell sizes range from approximately 200 to 1,600 m on a side. Additional rows and columns were added in the middle of the modeled area to improve the simulation in areas where multiple large pumping wells or other stresses are in close proximity to one another (fig. 5.6). In addition, the Floridan aquifer system in the Northern Tampa Bay regional model was divided into three layers (layers 2, 3, and 4) to resolve weak-sink problems in the particle-tracking analysis (see discussion of weak-sink problems in Section 1 of this Professional Paper). The layer spacing in the Floridan aquifer system was computed by dividing the total thickness of the active freshwater zone of the Floridan aquifer system into thirds.

Boundary Conditions

Model layer 1 lateral boundaries are represented by no-flow cells except where the layer 1 boundary coincides with the coastline of the Gulf of Mexico and Tampa Bay, where the boundary is represented with constant heads (fig. 5.6). The surficial aquifer in the central northern portion of the modeled area is very thin if present and created problems with the steady-state potentiometric surface of layer 1 dropping below the bottom of layer 1, so the layer 1 cells in this area are inactive. In layers 2, 3, and 4, the southeastern and most of the northern boundary are no-flow boundaries representing ground-water flow lines in the Floridan aquifer system. The

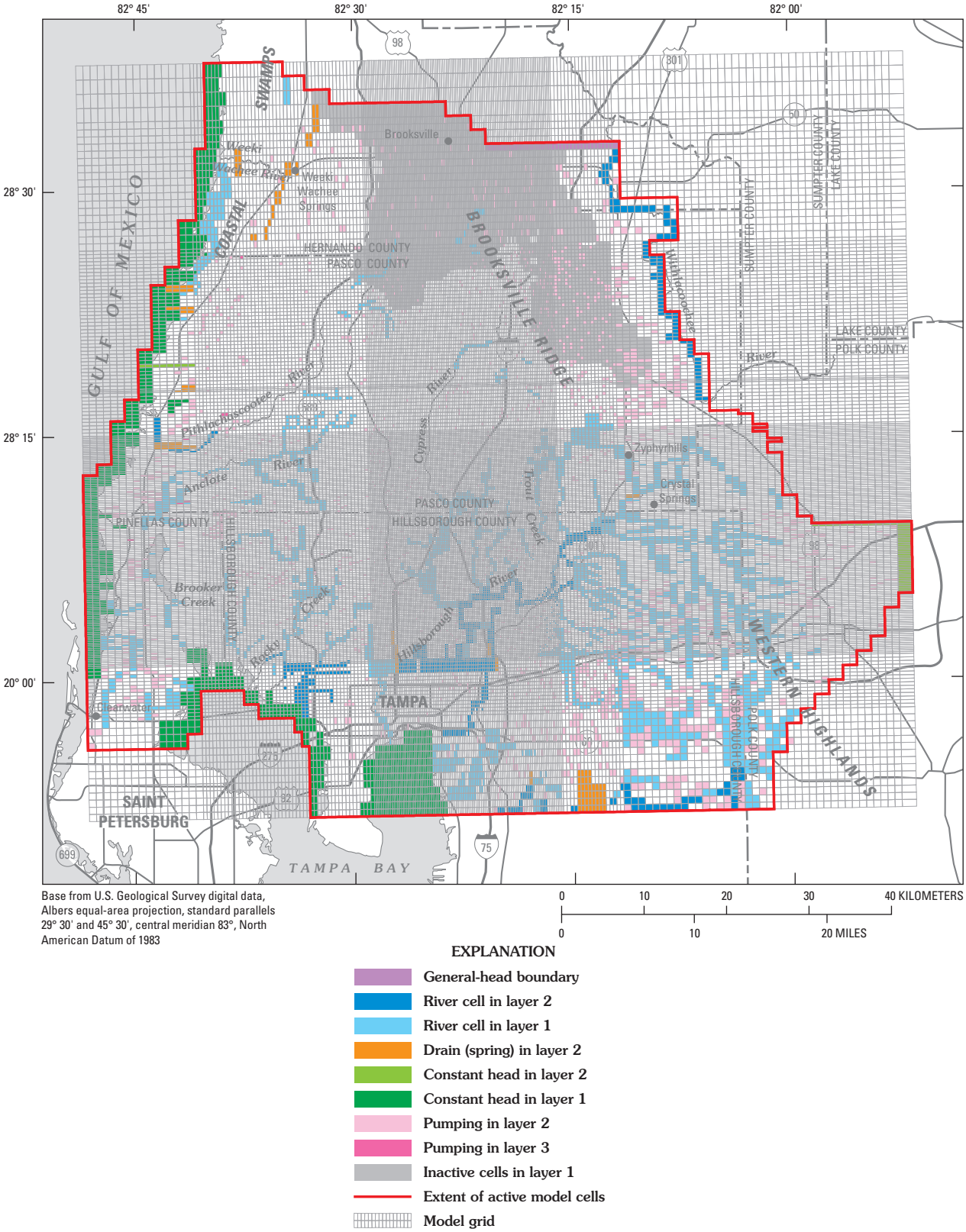

Base from U.S. Geological Survey digital data, Albers equal-area projection, standard parallels 29° 30' and 45° 30', central meridian 83°, North American Datum of 1983

0 10 20 30 40 KILOMETERS

0 10 20 MILES

EXPLANATION

- General-head boundary
- River cell in layer 2
- River cell in layer 1
- Drain (spring) in layer 2
- Constant head in layer 2
- Constant head in layer 1
- Pumping in layer 2
- Pumping in layer 3
- Inactive cells in layer 1
- Extent of active model cells
- Model grid

Figure 5.6. Ground-water flow model grid and boundary conditions, Northern Tampa Bay regional study area, Florida.

extreme part of the northeastern boundary is represented by a general-head boundary in layer 2 (fig. 5.6). The southeastern edge of the study area is represented as a specified-head boundary in layers 2, 3, and 4. The coastline is represented as a no-flow boundary in layers 2, 3, and 4.

Model Stresses

Hydrologic stresses on the Northern Tampa Bay regional ground-water flow system include recharge from precipitation and surface water and discharge to wells, rivers, and springs.

Recharge

Recharge is defined as the amount of water that infiltrates and percolates through the unsaturated zone to reach the aquifer, in this case the surficial aquifer system (layer 1). In the Northern Tampa Bay regional model, the complexities of rainfall, runoff, infiltration, percolation, and evapotranspiration were highly simplified. The MODFLOW Recharge package was used to assign initial values of recharge to the modeled area using watershed by watershed recharge estimates from Aucott (1988). Final recharge values were derived from model calibration as discussed in the “Model Calibration” section.

Pumping

Total pumping withdrawal from the Floridan aquifer system in the modeled area for all public water supply, agricultural, and industrial wells was 1.8 Mm^3/d in 2000. Approximately 1.34 Mm^3/d were withdrawn for public-supply wells; the remaining 0.23 Mm^3/d was the estimated withdrawal for agricultural and industrial purposes. Withdrawal rates for agricultural and industrial wells for 2000 were compiled and estimated by Nicasio Sepulveda of the U.S. Geological Survey in Orlando, Florida, from permit data from the Southwest Florida Water Management District—measured withdrawal rates were not available. Withdrawal rates for public-supply wells for 2000 were computed from average monthly withdrawal rates obtained from the Southwest Florida Water Management District. Domestic-well withdrawals of approximately 45,000 m^3/d are insignificant compared to public-supply withdrawals and were assumed offset by septic-tank-effluent recharge. Withdrawals are spaced throughout the modeled area based on actual well locations, and the largest public-supply withdrawals are concentrated in the southeastern part of the modeled area (fig. 5.6). The MODFLOW Well package was used to simulate ground-water pumping.

Rivers

The MODFLOW River package was used to simulate river/aquifer interaction in the modeled area. Major rivers included in the Northern Tampa Bay regional model were the Hillsborough, Withlacoochee, Anclote, and Pithlachascotee Rivers, and their tributaries. Other surface-water features simulated as rivers include Brooker, Rocky, Trout, and Cypress Creeks. River stage, conductance, bottom elevations, and layer of interaction were obtained from the optimized ground-water flow model (Yobbi, 2000). Most river cells were located in layer 1 (83 percent), but stretches of the Hillsborough and Withlacoochee Rivers and a few small rivers along the Gulf of Mexico (Weeki Wachee) were simulated in layer 2 (17 percent). Discharge to streams from the ground-water system was calculated for calibration purposes, but riverbed conductances were not altered for this study to improve model fit. Lakes and wetlands were assumed to be part of the surficial aquifer system and were not explicitly simulated.

Drains

Sixty-nine springs were simulated in layer 2 to represent discharge from the Floridan aquifer system using the MODFLOW Drain package. Spring stage, drain conductance, and bottom elevations were taken from the optimized model (Yobbi, 2000). Springs in the study emanate from the Floridan aquifer system (not the surficial aquifer system), so drains in the Northern Tampa Bay regional model were simulated only in layer 2. In the optimized model (Yobbi, 2000), drain cells in layer 1 were used to simulate wetlands. The layer 1 drains of Yobbi (2000) were eliminated from the current regional model because they were negatively affecting the models ability to determine flowpaths.

Aquifer Properties

Hydraulic conductivities (K) used for model layer 1 were defined using five different zones and values ranging from 0.3 to 5 m/d (fig. 5.7) (Yobbi, 2000). A hydraulic conductivity of 3.0 m/d or less was used in most of the upland areas of the model (3,500 km^2). Hydraulic conductivity was greatest (4.5 m/d) along the coast and river/wetland areas (1,600 km^2).

Vertical leakance values used to simulate leakage between the surficial aquifer system and the Floridan aquifer system (through the intermediate confining unit) ranged from 1×10^{-6} to 3.5×10^{-1} m/d/m (fig. 5.8) and were based on aquifer-test data reported in Knochenmus and Robinson (1996) and other references (SDI Environmental Services, Inc., 1997). Smaller values were assigned in areas where the intermediate confining unit is thick and(or) not breached and the Floridan aquifer system is confined. Vertical leakance values of 0.35 m/d/m were assigned in areas where the Floridan aquifer system is considered unconfined. Using leakance values greater than 0.35 m/d/m resulted in equal model-computed head values for layers 1 and 2 in the optimized model (Yobbi, 2000).

Transmissivity of the Floridan aquifer system was defined by 23 zones with transmissivity values ranging from 60 to 500,000 m^2/d for each (fig. 5.9) (Yobbi, 2000). Transmissivity values for the Floridan aquifer system were derived from aqui-

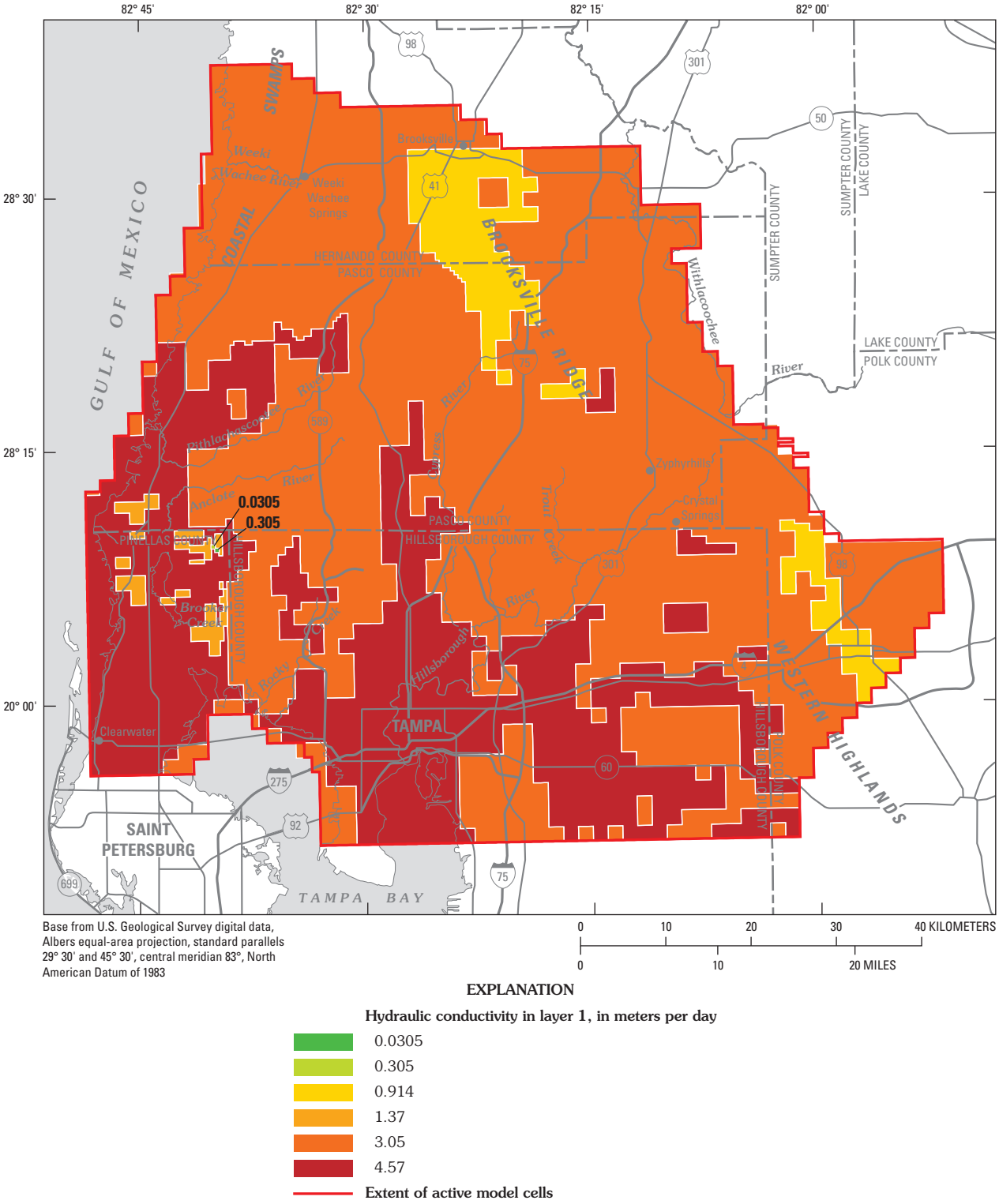

Base from U.S. Geological Survey digital data, Albers equal-area projection, standard parallels 29° 30' and 45° 30', central meridian 83°, North American Datum of 1983

EXPLANATION

Hydraulic conductivity in layer 1, in meters per day

- 0.0305
- 0.305
- 0.914
- 1.37
- 3.05
- 4.57
- **Extent of active model cells**

Figure 5.7. Distribution of hydraulic conductivity for model layer 1, Northern Tampa Bay regional study area, Florida.

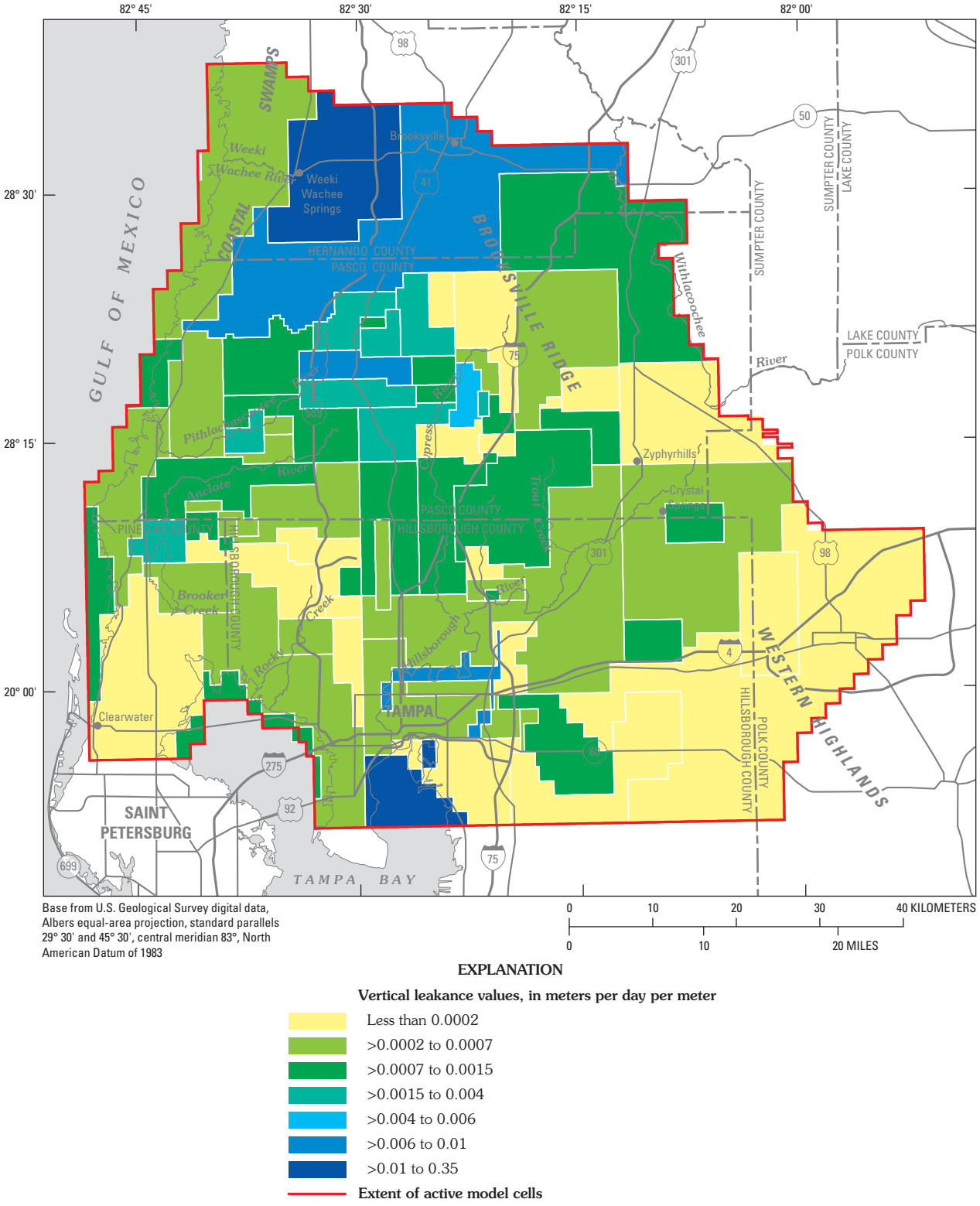

Figure 5.8. Distribution of vertical leakance values assigned between model layers 1 and 2, Northern Tampa Bay regional study area, Florida.

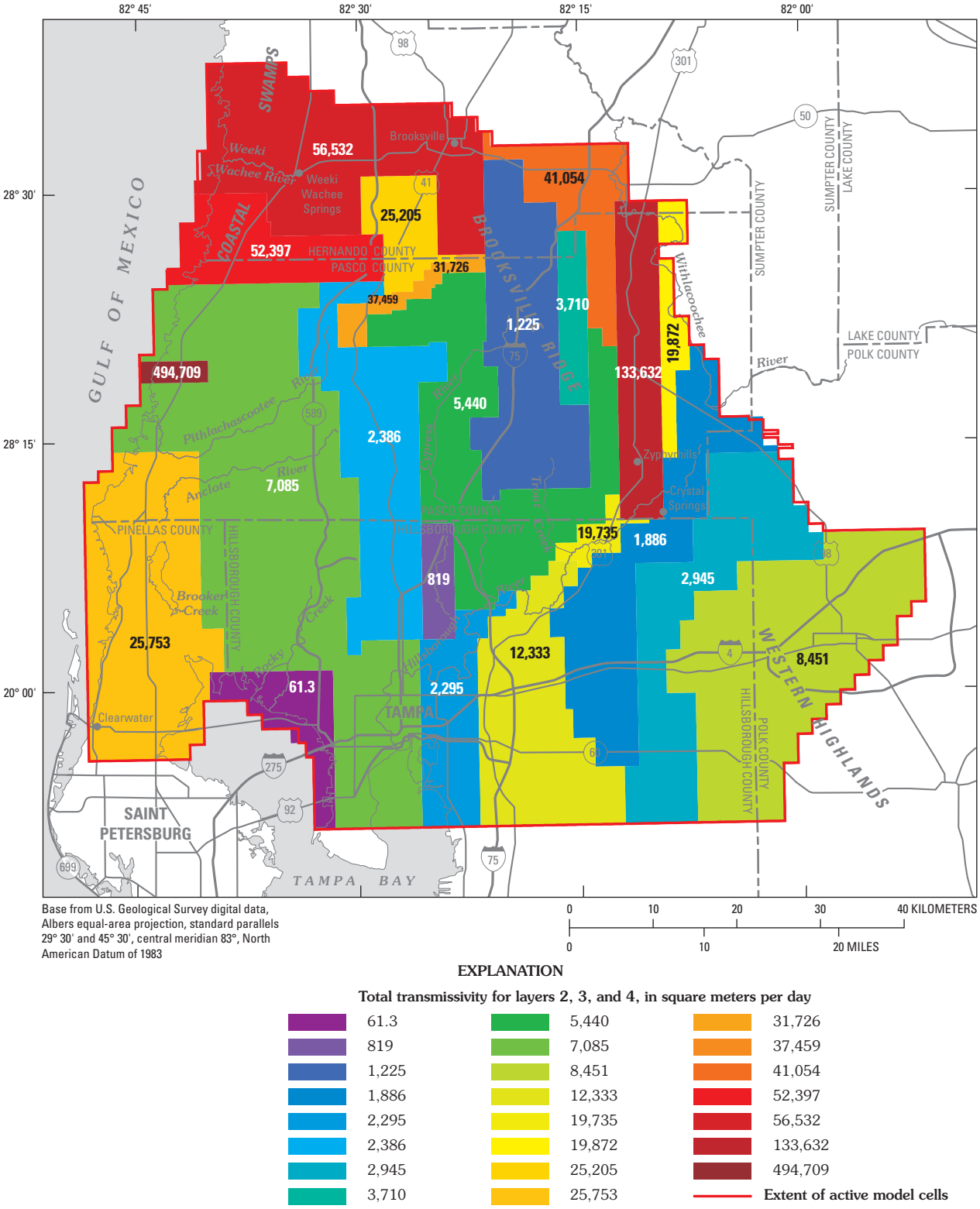

Base from U.S. Geological Survey digital data, Albers equal-area projection, standard parallels 29° 30' and 45° 30', central meridian 83°, North American Datum of 1983

0 10 20 30 40 KILOMETERS

0 10 20 MILES

EXPLANATION

Total transmissivity for layers 2, 3, and 4, in square meters per day

61.3	5,440	31,726
819	7,085	37,459
1,225	8,451	41,054
1,886	12,333	52,397
2,295	19,735	56,532
2,386	19,872	133,632
2,945	25,205	494,709
3,710	25,753	Extent of active model cells

Figure 5.9. Distribution of transmissivity values assigned to the Floridan aquifer (model layers 2, 3, and 4), Northern Tampa Bay regional study area, Florida.

fer tests and published values (SDI Environmental Services, Inc., 1997), and the transmissivity distribution for the Northern Tampa Bay regional model (layers 2, 3, and 4) was the same as that based on parameter-estimation results of Yobbi (2000). Because the total thickness of the Floridan aquifer system was divided into equal thirds when layers 3 and 4 were added to the model, the total transmissivity shown in figure 5.9 was also divided into thirds and an identical transmissivity distribution was assigned to each of layers 2, 3, and 4. Transmissivity values were smallest in areas where the Floridan aquifer system is confined or semiconfined, and transmissivity values were largest in the northern sections of the modeled area, coastal areas, and in the Withlacoochee River Basin (Yobbi, 2000).

Model Calibration and Sensitivity

The Northern Tampa Bay regional model was recalibrated to year-2000 conditions using a trial-and-error approach by adjusting recharge and comparing model-computed (simulated) hydraulic head and ground-water discharge to measured hydraulic head and streamflow and spring-flow data. The optimized hydraulic conductivity, transmissivity, and vertical leakance distributions of Yobbi (2000) were not modified during model calibration.

Initial recharge values were adjusted during model calibration until the difference between model-computed and measured hydraulic heads and ground-water discharge were minimized. Calibrated recharge values in the modeled area ranged between 0 and 63.5 cm/yr (fig. 5.10), and the average recharge rate for the study area (23.1 cm/yr) was kept less than the Yobbi (2000) value of 33 cm/yr. Recharge is greatest in areas where the Floridan aquifer system is unconfined or semiconfined. Zero recharge was specified in discharge areas such as the Hillsborough River and the coastal areas (fig. 5.10).

Model-computed hydraulic head was compared to median head values for the year 2000 from 187 monitoring wells in the Floridan aquifer system and 210 wells in the surficial aquifer system. Model-computed discharge was compared to the increase in base flow to the Hillsborough River between gages on the Hillsbourough River near Zephyrhills, Florida, (station 02301990) and the Hillsborough River above Crystal Springs, near Zephyrhills, Florida, (station 02303000) (Coffin and Fletcher, 2001). The calibration goal was to reduce the difference between simulated and measured head (residual), especially in the Floridan aquifer system.

The overall goodness of fit of the model to the observation data was evaluated using summary measures and graphical analyses. The root-mean-squared error (RMSE), the range, the standard deviation, and the standard-mean error of the residuals (SME), were used to evaluate the model calibration. The RMSE is a measure of the variance of the residuals and was calculated as:

$$RMSE = \sqrt{\frac{\sum_{i=1}^{N} (h_{meas} - h_{sim})i^2}{N}}$$

where h_{meas} is the measured hydraulic head, h_{sim} is the model-computed (simulated) hydraulic head, $(h_{meas} - h_{sim})$ is the head residual, and N is the number of wells used in the computation. If the ratio of the RMSE to the total head change in the modeled area is small, then the error in the head calculations is a small part of the overall model response (Anderson and Woessner, 1992).

The SME was calculated as:

$$SME = \frac{\sigma(h_{meas} - h_{sim})}{\sqrt{N}}$$

where $\sigma(h_{meas} - h_{sim})$ is the standard deviation of the residuals.

Model-Computed Hydraulic Heads

The spatial distribution of model-computed hydraulic heads for model layers 1 and 2 (figs. 5.11*A* and 5.11*B*) present a reasonable representation of potentiometric surfaces for the surficial and Floridan aquifer systems, respectively. Model-computed hydraulic head maps for both layers indicate highest heads in the northern and eastern parts of the modeled area and the lowest heads in the western and southwestern parts of the modeled area along the Gulf of Mexico. The maps of model-computed hydraulic head indicate ground-water flow is from the northern and eastern parts of the modeled area toward the coastal lowlands consistent with land-surface topography and previous maps of hydraulic head (Yobbi, 2000).

A simple method of assessing overall model fit is to plot the model-computed hydraulic head values against the measured observations. For a perfect fit, all points should fall on the 1:1 diagonal line, and a reasonable model fit is indicated in figures 5.12*A* and 5.12*B*. The spatial distribution of the head residuals is shown in figure 5.13 and can be used to understand the geographic distribution of head residuals. Head residual in the surficial aquifer system range from -8.9 to 19.1 m with a mean of 0.6 m (median of 0.3 m) (figs. 5.13 and 5.14*A*). Head residuals in the surficial aquifer system are greatest in the southern parts of the modeled area in locations where there are few water-level measurements and where head values are highest (figs. 5.11*A* and 5.13). Head residuals in the Floridan aquifer system range from –6.6 to 7.9 m and average 0.2 m (median also of 0.2 m) (figs. 5.13 and 5.14*B*). Floridan aquifer system head residuals are smallest in the northern coastal lowlands and center of the model area and largest in northern Pinellas County and southeastern parts of the modeled area (fig. 5.13). The average residual for the entire model is 0.28 m. The RMSE for the entire model is 2.63 m, which is

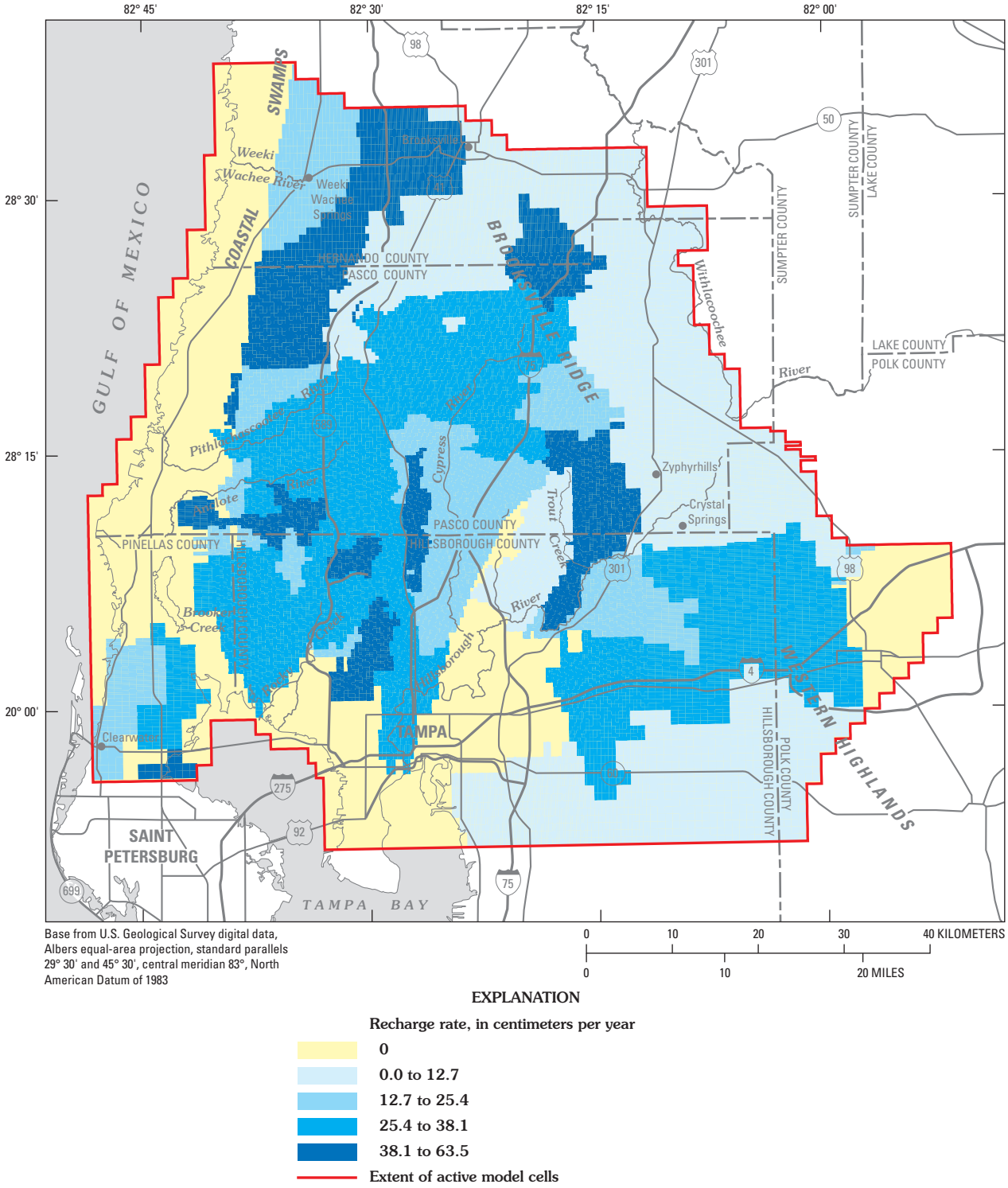

Figure 5.10. Ground-water flow model calibrated recharge rates, Northern Tampa Bay regional study area, Florida.

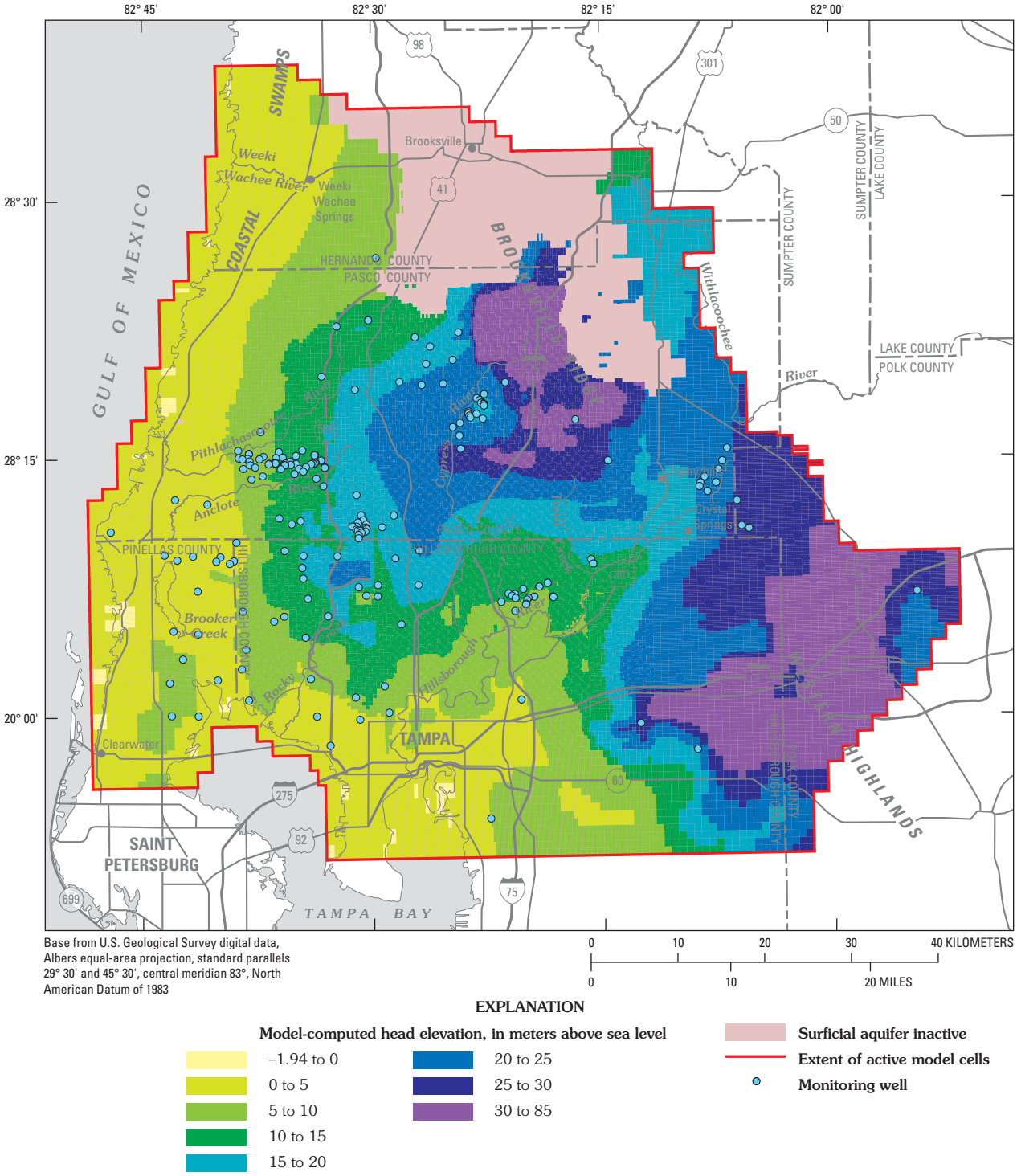

Base from U.S. Geological Survey digital data, Albers equal-area projection, standard parallels 29° 30' and 45° 30', central meridian 83°, North American Datum of 1983

EXPLANATION

Model-computed head elevation, in meters above sea level

- –1.94 to 0
- 0 to 5
- 5 to 10
- 10 to 15
- 15 to 20
- 20 to 25
- 25 to 30
- 30 to 85

- **Surficial aquifer inactive**
- **Extent of active model cells**
- **Monitoring well**

Figure 5.11*A*. Distribution of model-computed hydraulic heads for the surficial aquifer system (model layer 1), Northern Tampa Bay regional study area, Florida.

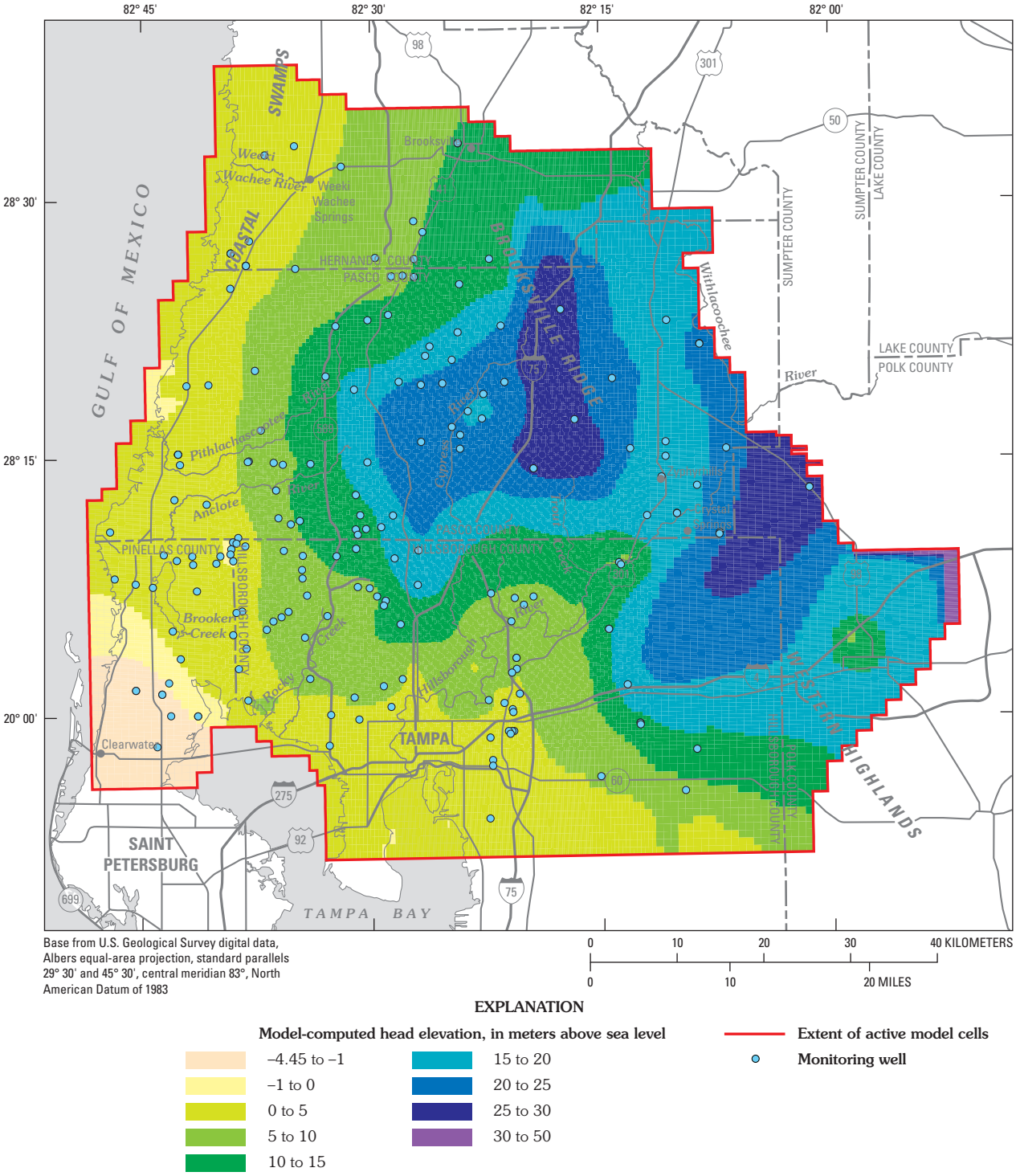

Base from U.S. Geological Survey digital data, Albers equal-area projection, standard parallels 29° 30' and 45° 30', central meridian 83°, North American Datum of 1983

EXPLANATION

Model-computed head elevation, in meters above sea level

- –4.45 to –1
- –1 to 0
- 0 to 5
- 5 to 10
- 10 to 15
- 15 to 20
- 20 to 25
- 25 to 30
- 30 to 50

- **Extent of active model cells**
- **Monitoring well**

Figure 5.11*B*. Distribution of model-computed hydraulic heads for the uppermost Floridan aquifer system (model layer 2), Northern Tampa Bay regional study area, Florida.

approximately 6 percent of the range of head observations for the model (41.3 m) and also indicates a reasonable model fit. The standard deviation of the residuals is 2.62 m, and the SME is 0.13 m. Ultimately, more water-level measurements and more accurate recharge estimates could improve the model fit for the surficial aquifer system. Of all residuals in both the surficial and Floridan aquifer systems, ninety percent are between –1.6 and 1.6 m (figs. 5.14*A* and 5.14*B*).

Model-Computed Discharge and Recharge

Model-computed base-flow and spring discharge were compared to measured discharge as another model-calibration criterion. The segment of the Hillsborough River used to calibrate the model is located between gaging stations 02301990 and 02303000. This segment was chosen because there are no major flow-altering structures between the two gages. The estimated base-flow increase (based on measured values) in the reach is 121,000 m^3/d; the model-computed discharge to the river in the reach was 112,000 m^3/d. The difference of 9,000 m^3/d is considered a good match between simulated and measured discharge along this stream segment. The difference between simulated discharge and measured discharge to springs was calculated for several important springs including the Weeki Wachee Spring as a further check on model calibration. For Weeki Wachee Spring, the measured average discharge is approximately 450,000 m^3/d (Coffin and Fletcher, 2001); however, the model-computed steady-state discharge is 122,000 m^3/d. Model-computed discharge from the aquifer to this and other springs is lower than measured values indicating the model does a poor job of simulating discharge to springs. This regional-scale simulation likely does not include sufficient localized karst features to adequately simulate local springs.

Recharge is the most sensitive parameter in this model according to Yobbi (2000). Simulated hydraulic heads in the surficial aquifer system and Floridan aquifer system can be readily manipulated by adding or subtracting recharge from an area. A complete description of hydraulic-parameter sensitivities is provided by Yobbi (2000).

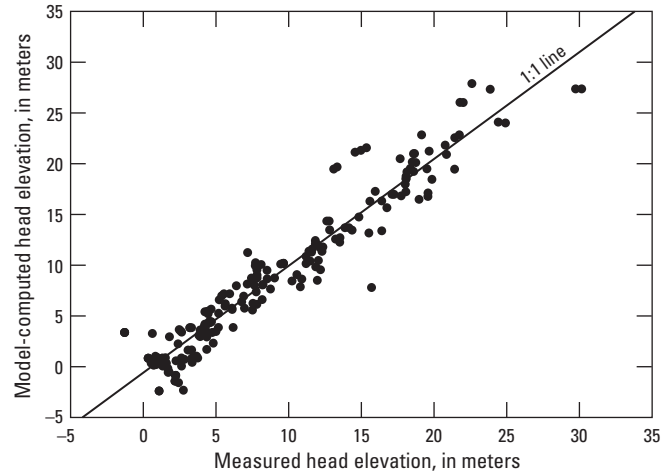

Figure 5.12*A*. Relation between model-computed and measured hydraulic head for model layer 1, Northern Tampa Bay regional study area, Florida.

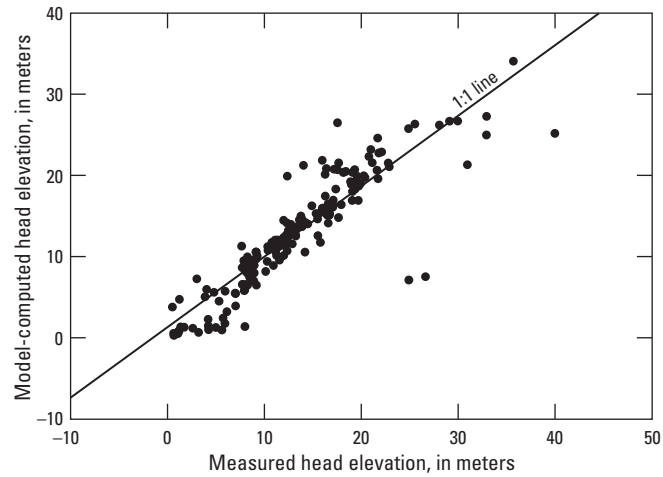

Figure 5.12*B*. Relation between model-computed and measured hydraulic head for model layer 2, Northern Tampa Bay Regional study area, Florida.

Model-Computed Water Budget

The Northern Tampa Bay regional model simulated water budget for the year 2000 is shown in table 5.3. Recharge from precipitation composed most of the inflow of water to the modeled area at 3.44 Mm^3/d (55.4 percent of model inflow). Inflow to the modeled area through constant head cells along the southeastern border composed the second highest amount of inflow to the modeled area (2.17 Mm^3/d or 35.0 percent of model inflow). River inflow to the aquifer was somewhat balanced by river outflow (0.59 Mm^3/d inflow compared to 0.83 Mm^3/d outflow, respectively) (table 5.3; fig. 5.15). Inflow to the aquifer from the rivers occurred mainly in the upper reaches of the Hillsborough and Withlacoochee Rivers and their tributaries and along lower sections of the Hillsborough River. Outflow from the aquifer to rivers was simulated in smaller rivers near the Gulf of Mexico and the mid section of the Hillsborough River among others. Other simulated discharge included outflow at constant-head boundaries along the Gulf of Mexico and Tampa Bay and at the northern general-head boundary to the Withlacoochee River (2.36 Mm^3/d or 38.0 percent of model outflow), wells (1.81 Mm^3/d or 29.1 percent of model outflow—84 percent of which was to public-supply wells), and springs (0.90 Mm^3/d or 14.6 percent of model outflow). There was zero percent error between model-calculated inflows and outflows for this steady-state simulation.

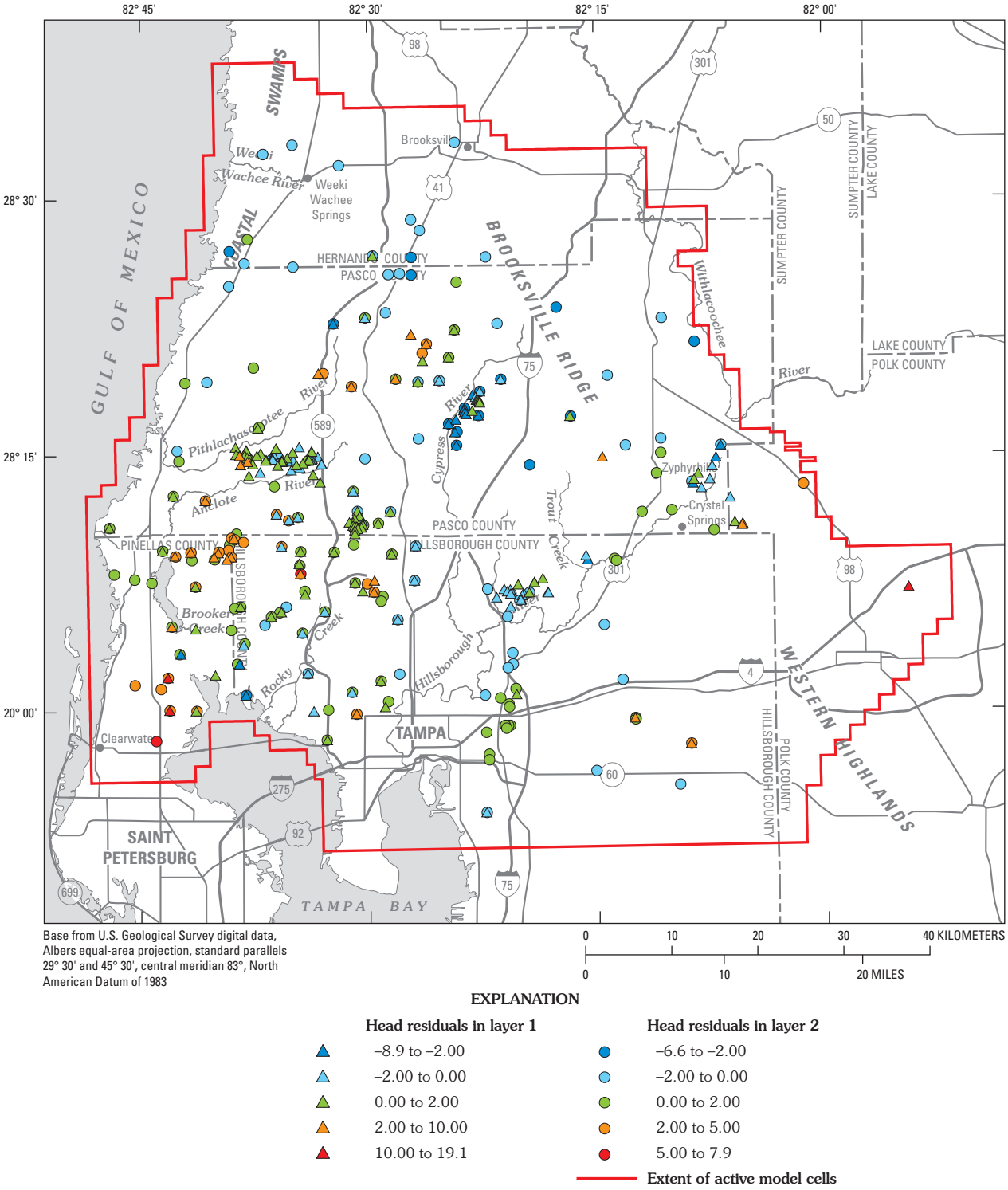

Figure 5.13. Distribution of head residuals for model layers 1 and 2, Northern Tampa Bay regional study area, Florida.

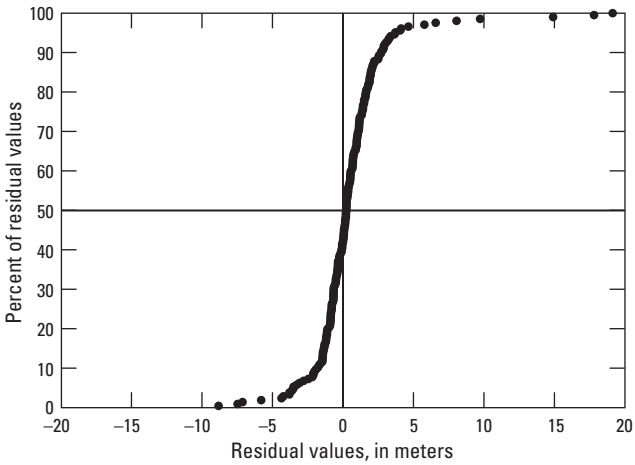

Figure 5.14*A*. Probability distribution of head residuals for model layer 1, Northern Tampa Bay regional study area, Florida.

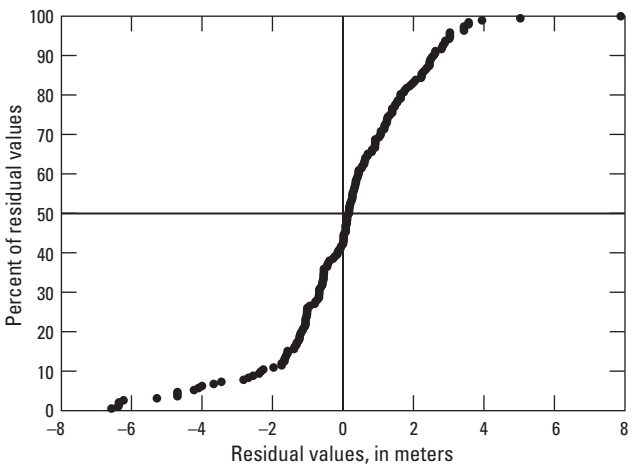

Figure 5.14*B*. Probability distribution of head residuals for model layer 2, Northern Tampa Bay regional study area, Florida.

Table 5.3. Model-computed water budget for year 2000, Northern Tampa Bay regional study area, Florida.

[m^3/d, cubic meters per day]

Water-budget component	Flow (m^3/d)	Percentage of inflow or outflow*
Model inflow		
Precipitation recharge	3,440,000	55.4
Lateral ground-water inflow from constant-head wells	2,173,000	35.0
Rivers	591,000	9.5
TOTAL INFLOW	6,207,000	**100**
Model outflow		
To the Gulf of Mexico, Tampa Bay and the central-northern portion of modeled area	2,360,000	38.0
Wells	1,810,000	29.1
Rivers	830,000	13.4
Springs	904,000	14.6
TOTAL OUTFLOW	6,207,000	**100**

*Total may not equal 100 percent because of rounding.

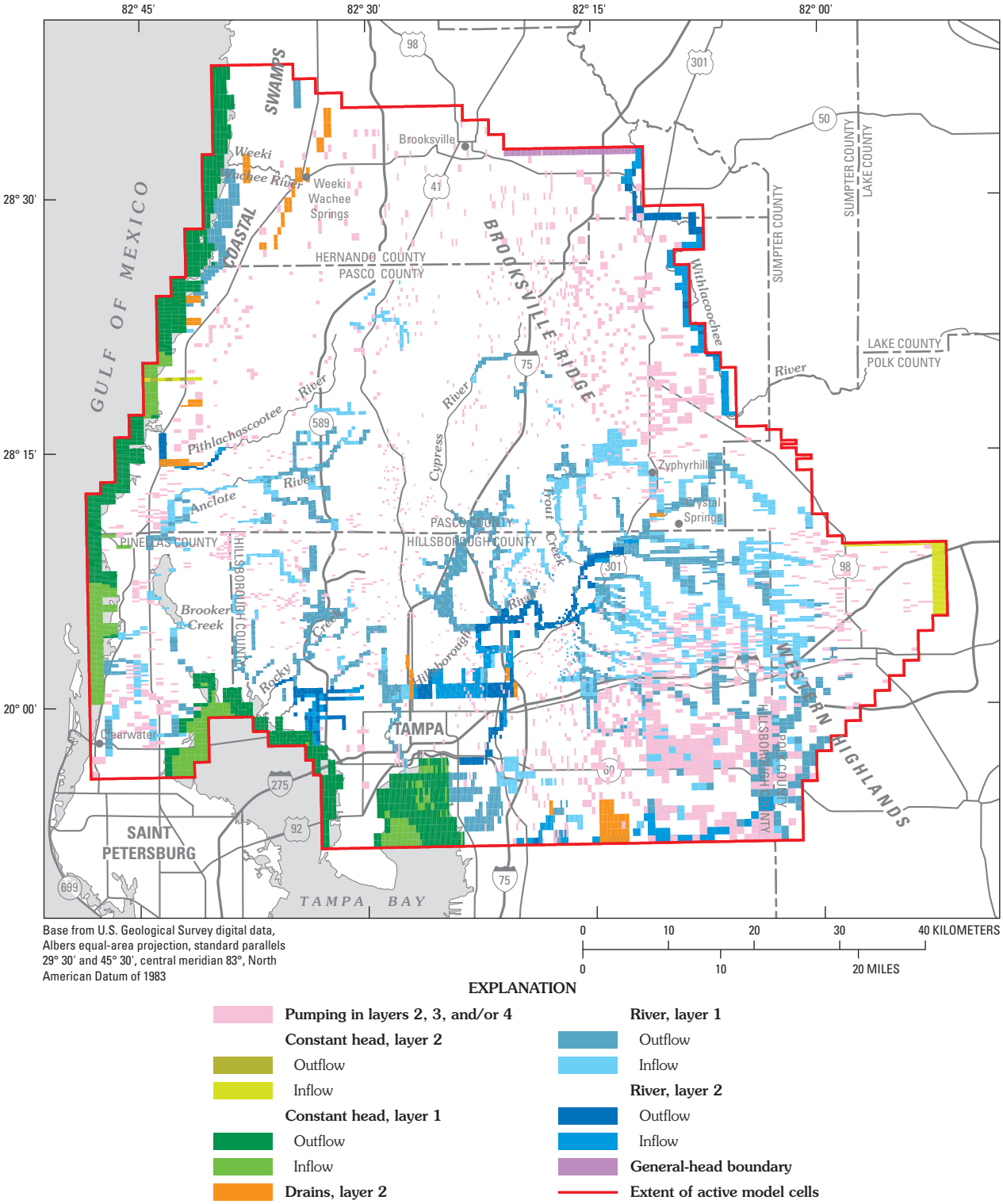

Figure 5.15. Model-computed ground-water inflows and outflows, Northern Tampa Bay regional study area, Florida.

Simulation of Areas Contributing Recharge to Wells

The calibrated steady-state ground-water flow model was used to estimate areas contributing recharge and zones of contribution for approximately 104 public-supply wells from the four quartiles of pumping rates using the MODPATH (Pollock, 1994) particle-tracking post processor and methods outlined in Section 1 of this Professional Paper. The model-computed areas contributing recharge represent advective ground-water flow and do not account for mechanical dispersion. Advection-dispersion transport simulations would likely yield larger areas contributing recharge than advective particle-tracking simulations because the effects of dispersion caused by aquifer heterogeneity would be included.

Along with output from the ground-water flow model, the MODPATH simulation requires effective porosity values to calculate ground-water flow velocities. For the Northern Tampa Bay regional model, porosity values were assumed uniform within each layer based on typical regional values. A porosity of 0.25 was used for the surficial aquifer system (model layer 1), and a porosity of 0.15 was used for the Floridan aquifer system (model layers 2, 3, and 4). Because of the karst nature of ground-water flow in the study area, the porosity values used for this regional simulation would not be applicable to local karst conditions.

Results of the MODPATH simulations used to delineate areas contributing recharge for selected wells are shown on figure 5.16. In general, areas contributing recharge extend upgradient (fig. 5.4) toward the northeast boundary of the modeled area. Summary statistics were computed for the particle-tracking results for wells from all quartiles of pumping rates. Areas contributing recharge ranged from near 0 to 1.25 km^2, and the average area contributing recharge was approximately 0.26 km^2. Minimum computed traveltimes for all wells ranged from 0.7 to 233 years and averaged 19 years. Maximum computed traveltimes ranged from 32 to 1,875 years and averaged 600 years. On the basis of average traveltimes of particles reaching the wells, about 3 percent of the flow to a public-supply well was less than 10 years old, about 36 percent of the flow to a public-supply well was less than 50 years old, and about 80 percent of the flow to a public-supply well was less than 200 years old. Simulated traveltimes are probably much longer than actual traveltimes in the aquifer because the regional ground-water flow model does not accurately represent flow through local karst dissolution features.

Limitations and Appropriate Use of the Model

The ground-water flow model for the Northern Tampa Bay regional study area was designed to delineate areas contributing recharge to public-supply wells, to help guide data collection, and to support future local modeling efforts. Sources of error in the model may include the steady-state flow assumption and errors in the conceptual model of the system, hydraulic properties, and boundary conditions.

The steady-state flow assumption is reasonable for the study area for 1997–2001 because the Floridan aquifer system has high transmissivity values, a large volume of water circulate through the system, and pumping rates were relatively stable during the time period of study. However, errors related to the steady-state assumption can be substantial, and further calibration for transient conditions may be needed to accurately represent temporal changes in the system.

For karst terrains, where a substantial percentage of flow occurs through a series of discrete openings, conduits, and fractures, a porous-media approach at a regional scale cannot accurately predict zones of contribution, areas contributing recharge, and traveltimes to public-supply wells. Secondary porosity created by karst dissolution features contributes to uncertainty in values of hydraulic conductivity, which can vary by up to five orders of magnitude (Langevin, 2003; Bush and Johnston, 1988), and porosity, which also can vary substantially. Knochenmus and Robinson (1996) used very low effective porosities in order to achieve realistic traveltimes in the Floridan aquifer system and Kuniansky and others (2001) found that an effective porosity of 1 to 3 percent was needed for the karst Edwards aquifer system in Texas to match estimated traveltimes derived from geochemical mixing models. Changes to input porosity values will change computed traveltimes from recharge to discharge areas in direct proportion to changes of effective porosity because there is an inverse linear relation between ground-water flow velocity and effective porosity and a direct linear relation between traveltime and effective porosity. For example, a one-percent decrease in porosity will result in a one-percent increase in velocity and a one-percent decrease in particle traveltime. A detailed sensitivity analysis of porosity distributions was beyond the scope of this regional study.

The ground-water flow model for the Northern Tampa Bay regional study area represents a first approximation of ground-water conditions and the areas contributing recharge to public-supply wells in the modeled area. The model is suitable for evaluating regional water budgets and ground-water flow paths in the study area for the time period of interest but may not be suitable for long-term predictive simulations. To improve contributing area delineation, the model could incorporate karst features, possibly using a probabilistic (Monte Carlo) simulation approach over a much smaller area. Additional hydraulic head observations in the surficial aquifer system in the southern part of the modeled area would improve the calibration of the existing model as would additional measurements of recharge and discharge if possible. This regional model does provide a useful tool to evaluate aquifer vulnerability at a regional scale, to facilitate comparisons of ground-water traveltime between regional aquifer systems, and to guide future detailed investigations in the study area.

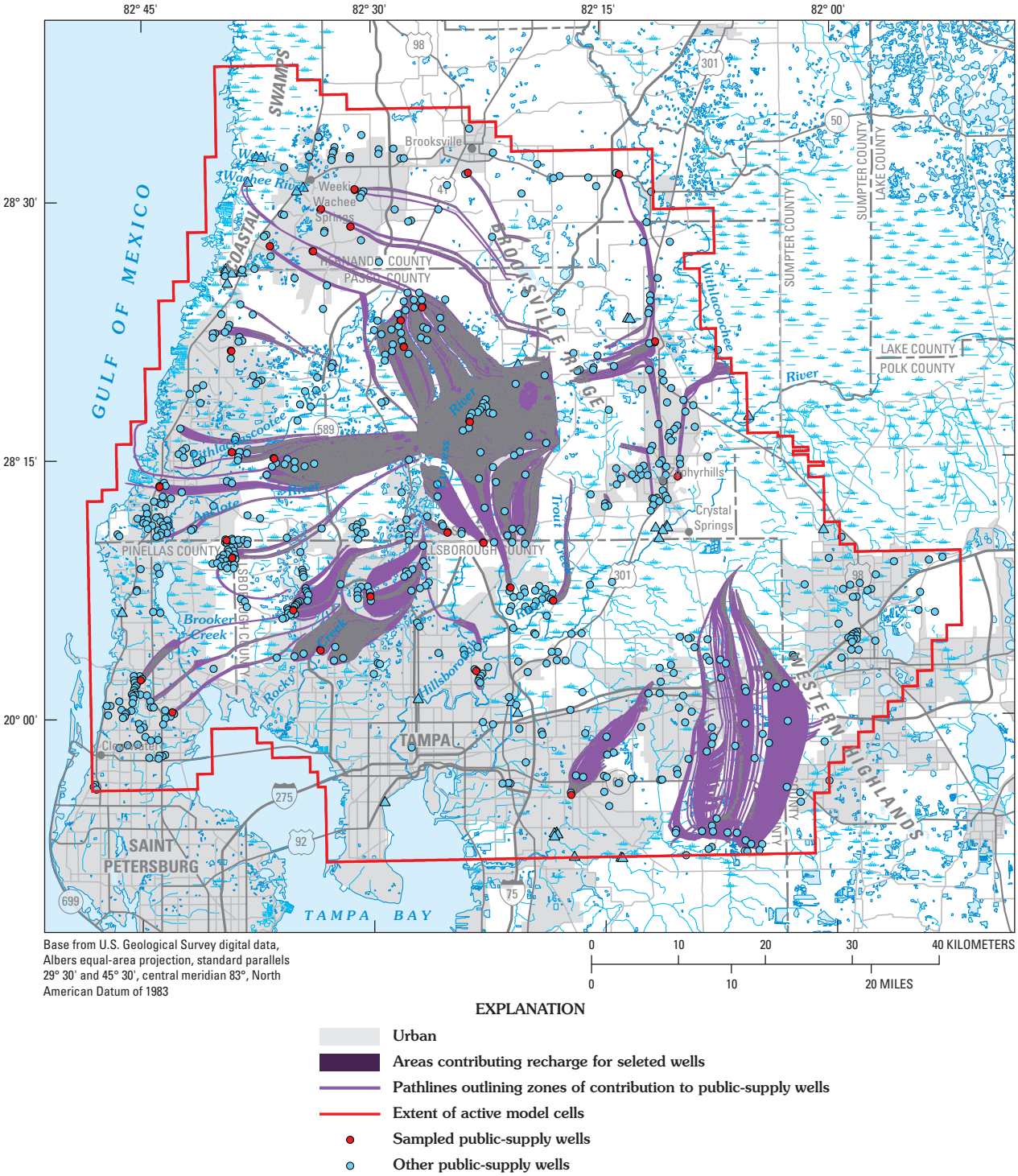

Figure 5.16. Model-computed areas contributing recharge for selected public-supply wells, Northern Tampa Bay regional study area, Florida.

References Cited

Anderson, M.P., and Woessner, W.W., 1992, Applied ground-water modeling: New York, Academic Press, Inc., 381 p.

Aucott, W.R., 1988, Areal variation in recharge to and discharge from the Floridan Aquifer System in Florida: U.S. Geological Survey Water-Resources Investigations Report 88–4057, 1 sheet.

Berndt, M.P., and Katz, B.G., 1992, Hydrochemistry of the surficial and intermediate aquifer systems in Florida: U.S. Geological Survey Water-Resources Investigations Report 91–4186, 24 p.

Bush, P.W., and Johnston, R.H., 1988, Ground-water hydraulics, regional flow, and ground-water development of the Floridan Aquifer System in Florida and in parts of Georgia, South Carolina, and Alabama: U.S. Geological Survey Professional Paper 1403–C, 80 p.

Coffin, J.E. and Fletcher, W.L, 2001, Water Resources Data Florida Water Year 2000, Vol. 3A. Southwest Florida Surface Water: U.S. Geological Survey Water-Data Report FL–00–3A, 359 p.

Farnsworth, R.K., Thompson, E.S., and Peck, E.L., 1982, Evaporation atlas for the contiguous 48 United States: Asheville, N.C., National Oceanic and Atmospheric Administration Technical Report NWS 33, 26 p., 4 sheets.

Harbaugh, A.W., Banta, E.R., Hill, M.C., McDonald, M.G., 2000, MODFLOW-2000, The U.S. Geological Survey modular ground-water model—User guide to modularization concepts and the ground-water flow process: U.S. Geological Survey Open-File Report 00–92, 121 p., accessed Feb. 6, 2007, at *http://water.usgs.gov/nrp/gwsoftware/modflow2000/modflow2000.html*

Hitt, K.J., 2004, Refining 1970's land-use data with 1990 population data to indicate new residential development: U.S. Geological Survey Water-Resources Investigations Report 94–4250, 21 p.

HydroGeoLogic, Inc., 1997, Development of a computer model of the regional groundwater flow system in Hernando County Water Resources Assessment Project, Phase I—Data compilation and analysis: Brooksville, report on file at the Southwest Florida Water Management District, variously paged.

Katz, B.G., 1992, Hydrochemistry of the upper Floridan Aquifer System, Florida: U.S. Geological Survey Water-Resources Investigations Report 91–4196, 37 p., 10 pls.

Knochenmus, L.A., and Robinson, J.L., 1996, Descriptions of anisotropy and heterogeneity and their effect on ground-water flow and areas of contribution to public-supply wells in a karst carbonate aquifer system: U.S. Geological Survey Water-Supply Paper 2475, 43 p.

Krause, R.E., and Randolph, R.B., 1989, Hydrology of the Floridan Aquifer System in southeast Georgia and adjacent parts of Florida and South Carolina: U.S. Geological Survey Professional Paper 1403–D, 65 p.

Kuniansky, E.L., Fahlquist, Lynne, and Ardis, A.F., 2001, Travel times along selected flow paths of the Edwards Aquifer, Central Texas *in* Kuniansky, E.L. ed., 2001, U.S. Geological Survey Karst Interest Group Proceedings, St. Petersburg, Florida, February 13–16, 2001: U.S. Geological Survey Water Resources Investigations Report 01–4011, p. 69–77, accessed Feb. 6, 2007, at *http://water.usgs.gov/ogw/karst/kigconference/proceedings.htm*.

Langevin, C.D., 1998, Stochastic methods for evaluating the potential for wetland rehydration in covered-karst terrains: Tampa University of South Florida dissertation, 133 p.

Langevin, C.D., 2003, Stochastic ground water flow simulation with a fracture zone continuum model: Ground Water, v. 41, no. 5, p. 587–601.

Marella, R.L., and Berndt, M.P., 2005, Water withdrawals and trends from the Floridan aquifer system in the Southeastern United States, 1950–2000: U.S. Geological Survey Circular 1278, 20 p.

McDonald, M.G., and Harbaugh, A. W., 1988, A modular three-dimensional finite-difference ground-water flow model: Techniques of Water-Resources Investigations of the U.S. Geological Survey, book 6, chap. A1, [variously paginated].

Metz, P.A., and Sacks, L.A., 2002, Comparison of the hydrogeology and water quality of a ground-water augmented lake with two nonaugmented lakes in northwest Hillsborough County, Florida: U.S. Geological Survey Water-Resources Investigations Report 02–4032, 74 p.

Miller, J.A., 1986, Hydrogeologic framework of the Floridan Aquifer System in Florida and parts of Georgia, South Carolina, and Alabama: U.S. Geological Survey Professional Paper 1403–B, 91 p.

Pollock, D.W., 1994, User's guide for MODPATH/MODPATH-PLOT, Version 3—A particle tracking post-processing package for MODFLOW, the U.S. Geological Survey finite-difference ground-water flow model: U.S. Geological Survey Open-File Report 94–464, accessed Feb. 6, 2007 at *http://water.usgs.gov/nrp/gwsoftware/modpath41/modpath41.html*

Ryder, P.D., 1985**,** Hydrology of the Floridan Aquifer System in West Central Florida: U.S. Geological Survey Professional Paper 1403–F, 63 p.

SDI Environmental Services, Inc., 1997, Water resources evaluation and integrated hydrologic model of the northern Tampa Bay region: Consultant's report on file at Tampa Bay Water, Clearwater, Florida., 146 p.

Sepulveda, Nicasio, 2002, Simulation of ground-water flow in the intermediate and Florida aquifer systemss in Peninsular Florida: U.S. Geological Survey Water-Resources Investigations Report 02–4009, 130 p., accessed Feb. 6, 2007, at *http://pubs.er.usgs.gov/usgspubs/wri/wri024009*

Soil Conservation Service, 1976, General soil map, Hernando County, Florida: Soil Conservation Service, 1 sheet.

Soil Conservation Service, 1981, General soil map, Pasco County, Florida: Soil Conservation Service, 1 sheet.

Soil Conservation Service, 1989, General soil map, Hillsborough County, Florida: Soil Conservation Service, 1 sheet.

Southeastern Geological Society, 1986, Hydrogeological units of Florida: Tallahassee, Florida Bureau of Geology Special Publication 28, 9 p.

Sprinkle, C.L., 1989, Geochemistry of the Floridan Aquifer System in Florida and in parts of Georgia, South Carolina, and Alabama: U.S. Geological Survey Professional Paper 1403–I, 105 p.

Tibbals, C.H., Anderson, W., and Laughlin, C.P., 1980, Ground-water hydrology of the Dade City area, Pasco County, Florida, with emphasis on the hydrologic effects of pumping from the FAS: U.S. Geological Survey Water-Resources Investigations 80–33, 64 p.

Tibbals, C.H., and Grubb, H.F., 1982, Aquifer test results, Green Swamp area, Florida: U.S. Geological Survey Water-Resources Investigations Report 82–35, 29 p.

White, W.A., 1970, The geomorphology of the Florida Peninsula: Tallahassee, Florida Bureau of Geology Bulletin 51, 164 p.

Yobbi, D.K., 2000, Application of nonlinear least-squares regression to ground-water flow modeling, west-central Florida: U.S. Geological Survey Water-Resources Investigations 00–4094, 58 p., accessed Feb. 6, 2007, at *http://pubs.er.usgs.gov/usgspubs/wri/wri004094.*

Hydrogeologic Setting and Ground-Water Flow Simulations of the Pomperaug River Basin Regional Study Area, Connecticut

By Forest P. Lyford, Carl S. Carlson, Craig J. Brown, and J. Jeffrey Starn

Section 6 of

Hydrogeologic Settings and Ground-Water Flow Simulations for Regional Studies of the Transport of Anthropogenic and Natural Contaminants to Public-Supply Wells—Studies Begun in 2001

Edited by Suzanne S. Paschke

Professional Paper 1737–A

U.S. Department of the Interior

U.S. Geological Survey

U.S. Department of the Interior
DIRK KEMPTHORNE, SECRETARY

U.S. Geological Survey
Mark D. Myers, Director

U.S. Geological Survey, Reston, Virginia: 2007

For product and ordering information:
World Wide Web: http://www.usgs.gov/pubprod
Telephone: 1-888-ASK-USGS

For more information on the USGS--the Federal source for science about the Earth, its natural and living resources, natural hazards, and the environment:
World Wide Web: http://www.usgs.gov
Telephone: 1-888-ASK-USGS

Any use of trade, product, or firm names is for descriptive purposes only and does not imply endorsement by the U.S. Government.

Although this report is in the public domain, permission must be secured from the individual copyright owners to reproduce any copyrighted materials contained within this report.

Suggested citation:
Lyford, F.P., Carlson, C.S., Brown, C.J., and Starn, J.J., 2007, Hydrogeologic setting and ground-water flow simulation of the Pomperaug River Basin Regional Study Area, Connecticut, *section 6 of* Paschke, S.S., ed., Hydrogeologic settings and ground-water flow simulations for regional studies of the transport of anthropogenic and natural contaminants to public-supply wells—studies begun in 2001: Reston, Va., U.S. Geological Survey Professional Paper 1737–A, pp. 6–1 – 6–26.

Contents

Abstract 6–1
Introduction 6–1
Purpose and Scope 6–1
Study Area Description 6–1
Topography and Hydrography 6–3
Land Use 6–3
Water Use 6–3
Conceptual Understanding of the Ground-Water System 6–8
Geologic Units and Hydraulic Properties 6–8
Bedrock 6–8
Surficial Materials 6–9
Ground-Water Occurrence and Flow 6–11
Water Budget 6–11
Ground-Water Quality 6–13
Ground-Water Flow Simulations 6–14
Modeled Area and Spatial Discretization 6–14
Boundary Conditions and Model Stresses 6–14
Aquifer Hydraulic Properties 6–18
Model Calibration 6–18
Model-Computed Hydraulic Heads 6–20
Model-Computed Water Budget 6–20
Simulation of Areas Contributing Recharge to Public-Supply Wells 6–22
Model Limitations and Uncertainties 6–22
References Cited 6–24

Figures

Maps showing:
6.1. Location of the Pomperaug River Basin regional study area within the glacial aquifer system. 6–2
6.2. Topography, hydrologic features, and locations of public-supply wells, Pomperaug River Basin regional study area, Connecticut. 6–7
6.3. Generalized hydrogeologic section showing conceptual ground-water flow patterns, representative hydraulic properties, and recharge rates, Pomperaug River Basin regional study area, Connecticut 6–8
Maps showing:
6.4. Bedrock and surficial geologic units, Pomperaug River Basin regional study area, Connecticut 6–10
6.5. Wells sampled, oxidation-reduction classification zones, and directions of ground-water flow, Pomperaug River Basin regional study area, Connecticut. 6–12

6.6. Ground-water flow model grid and simulated streams and wells, Pomperaug River Basin regional study area, Connecticut. 6–16
6.7. Ground-water recharge zones, Pomperaug River Basin regional study area, Connecticut. 6–17
6.8. Hydraulic-conductivity and porosity zones for model layer 1, Pomperaug River Basin regional study area, Connecticut. 6–19
6.9. Graph showing relation between model-computed and measured hydraulic head, Pomperaug River Basin regional study area, Connecticut. 6–20

Maps showing:

6.10. Observation points and head residuals, Pomperaug River Basin regional study area, Connecticut. 6–21
6.11. Model-computed flow paths, areas contributing recharge to public-supply wells, and gaining and losing stream reaches, Pomperaug River Basin regional study area, Connecticut..... 6–23

Tables

6.1. Summary of hydrogeologic and ground-water quality characteristics for the glacial aquifer system and the Pomperaug River Basin regional study area, Connecticut. 6–4
6.2. Public-supply wells and pumping rates, Pomperaug River Basin regional study area, Connecticut. 6–6
6.3. Summary of aquifer-system and model characteristics, Pomperaug River Basin regional study area, Connecticut..... 6–15
6.4. Model-computed water budget for 1997–2001 average conditions, Pomperaug River Basin regional study area, Connecticut..... 6–20

Hydrogeologic Setting and Ground-Water Flow Simulations of the Pomperaug River Basin Regional Study Area, Connecticut

By Forest P. Lyford, Carl S. Carlson, Craig J. Brown, and J. Jeffrey Starn

Abstract

The transport of anthropogenic and natural contaminants to public-supply wells was evaluated for the glacially derived valley-fill aquifer in the Pomperaug River Basin, Connecticut, as part of the U.S. Geological Survey National Water-Quality Assessment Program. The glacial valley-fill aquifer in the Pomperaug River Basin regional study area is representative of the glacial aquifer system in the Northeastern United States, is used extensively for public water supply, and is susceptible and vulnerable to contamination. A two-layer, steady-state ground-water flow model of the study area was developed and calibrated to average conditions for the period from 1997 to 2001. The calibrated model and advective particle-tracking simulations were used to compute areas contributing recharge and traveltimes from recharge areas for selected public-supply wells. Model results indicate areal recharge provides approximately 87 percent of the ground-water inflow and streams provide approximately 13 percent of ground-water inflow. Ground-water discharge from the model area is to streams (96 percent) and wells (4 percent). Particle-tracking results indicate traveltimes from recharge areas to wells range from less than 1 year to more than 275 years, the median traveltime to wells range from 0.2 to 25 years. Approximately 73 percent of the traveltimes are less than 10 years indicating water quality in the glacial valley-fill aquifer is susceptible to the effects of overlying land use.

Introduction

The Pomperaug River Basin regional study area for the transport of anthropogenic and natural contaminants to public-supply wells (TANC) study is located in the northeast glacial aquifer system (Warner and Arnold, 2005) within the Connecticut, Housatonic, and Thames River Basins study unit of the U.S. Geological Survey National Water-Quality Assessment (NAWQA) program (fig. 6.1).

Purpose and Scope

The purpose of this Professional Paper section is to present the hydrogeologic setting of the Pomperaug River Basin regional study area. The section also documents the setup and calibration of a steady-state regional ground-water flow model for the study area. Ground-water flow characteristics, pumping-well information, and water-quality data were compiled from existing data to develop a conceptual understanding of ground-water conditions in the study area. A two-layer steady-state ground-water flow model of the glacial aquifer of the Pomperaug River Basin was developed and calibrated to average conditions for the period from 1997 to 2001. The 5-year period 1997–2001 was selected for data compilation and modeling exercises for all TANC regional study areas to facilitate future comparisons between study areas. The ground-water flow model and associated particle tracking were used to simulate advective ground-water flow paths and to delineate areas contributing recharge to selected public-supply wells. Ground-water traveltimes from recharge to public-supply wells, oxidation-reduction (redox) conditions along flow paths, and presence of potential contaminant sources in areas contributing recharge were tabulated into a relational database as described in Section 1 of this Professional Paper. This section provides the foundation for future ground-water susceptibility and vulnerability analyses of the study area and comparisons among regional aquifer systems.

Study Area Description

The Pomperaug River Basin regional study area encompasses the glacially derived, valley-fill aquifer of the Pomperaug River Basin. The study area was chosen because the aquifer is used extensively for public water supply, is susceptible and vulnerable to contamination, and is representative of the glacial aquifer system in the Northeastern United States. Characteristics of the Pomperaug River Basin aquifer system are similar to many valley-fill aquifer system in the Eastern

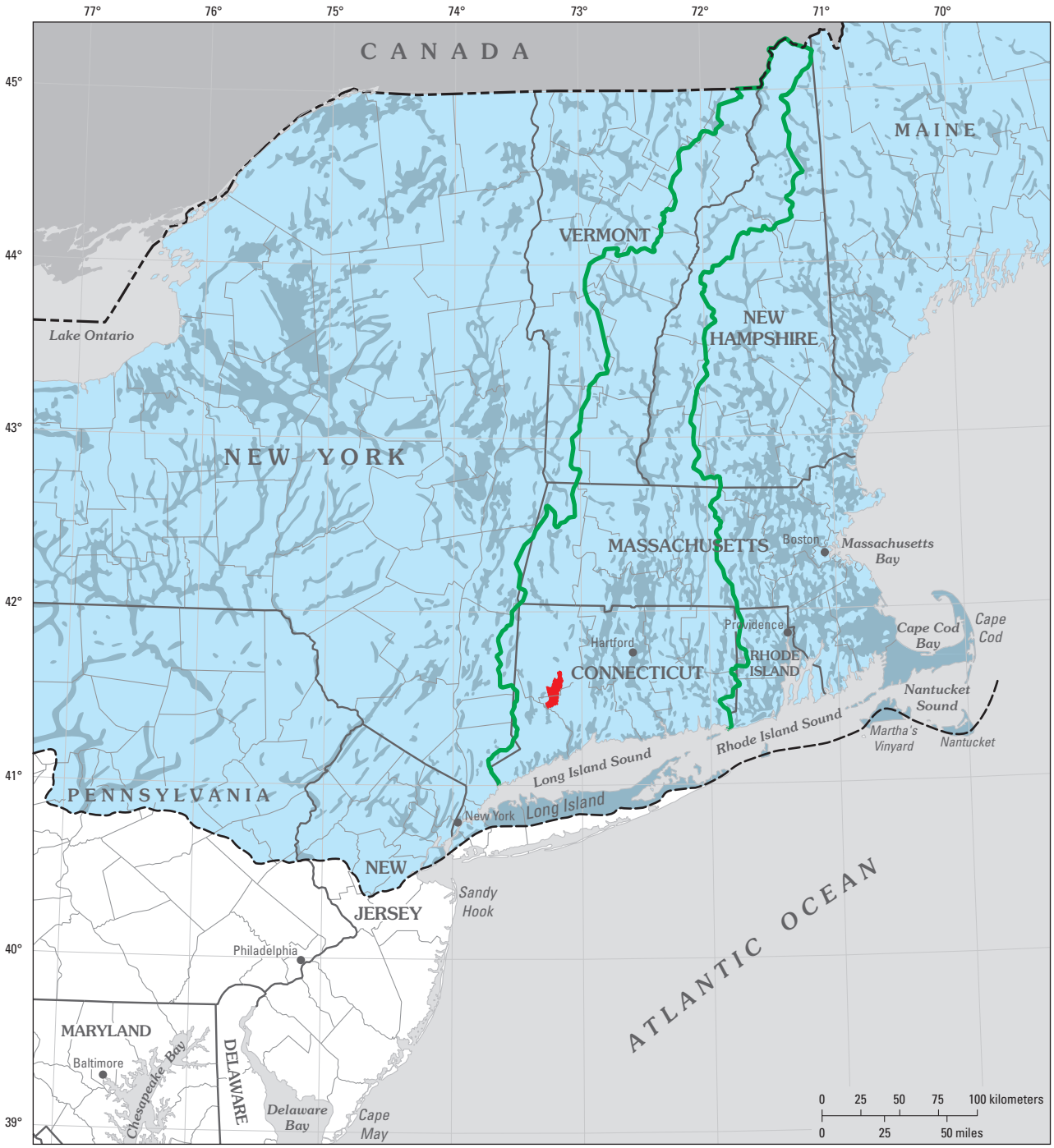

Base from U.S. Geological Survey digital data, 1:2,000,000, 1972, Albers equal-area projection

EXPLANATION

- **Pomeraug River Basin regional study area**
- **Glacial deposits aquifer**—Darker areas represent sand, gravel, and valley-fill aquifers locally
- **USGS NAWQA study unit**—Connecticut, Housatonic, and Thames River Basins
- **Southern limit of Pleistocene continental glaciation**

Figure 6.1. Location of the Pomperaug River Basin regional study area within the glacial aquifer system.

Hills and Valley Fills hydrophysiographic region of Randall (2001), which encompasses much of the most populated parts of New England, northern New Jersey, and eastern New York within the glacial aquifer system (table 6.1).

Topography and Hydrography

The Pomperaug River Basin regional study area covers about 128 km^2 of the Pomperaug River Basin in west-central Connecticut and includes parts of the towns of Southbury, Woodbury, Roxbury, Watertown, Bethlehem, and Middlebury (fig. 6.2). The upper part of the basin is drained by the Nonnewaug and Weekeepeemee Rivers, which join in Woodbury to form the Pomperaug River. Most of the study area is in the Nonnewaug River and Pomperaug River drainage areas. Subbasins of the Pomperaug River Basin that are not in the study area are Transylvania Brook, East Spring Brook, and most of the Weekeepeemee River (fig. 6.2). The major valleys trend north to south and are bounded on the east and west by till-covered bedrock uplands drained by numerous perennial streams. Streams in upland areas are oriented mostly from east to west on the east side and northwest to southeast on the north and west sides. Hesseky Brook flows northward through an area underlain by sand and gravel and joins the Pomperaug River near its origin at the confluence of the Nonnewaug and Weekeepeemee Rivers. Manmade ponds are present on several tributary streams. Altitudes range from about 30 m near the confluence of the Pomperaug River with the Housatonic River to about 300 m at places on the basin divide.

Precipitation in the Pomperaug Basin averages about 117 cm/yr (Randall, 1996). Basin runoff measured in the Pomperaug River at Southbury, Connecticut, averaged 61 cm/yr during 1933–2001 (Morrison and others, 2002; table 1). The balance of about 56 cm/yr is lost mainly to evapotranspiration (Randall, 1996).

Land Use

Land use in the Pomperaug River watershed has changed over the past 50 years from primarily undeveloped or agricultural lands to expanded residential, commercial, and light industrial areas. Most residential areas are served by individual septic disposal systems (ISDS) and are characterized by low-density housing. Agricultural lands are located mostly within flood plains and produce silage corn, hay, and berries. Industrial uses are limited and include small, modern, high-tech industries. Upland areas are largely forested with scattered residences on 0.16-km^2 (40-acre) or larger lots.

Water Use

Most water for public supply is obtained from wells completed in valley fill. Mazzaferro (1986a) estimated that as much as 33,300 m^3/d could be withdrawn from valley-fill materials. Public-supply systems distribute water from wells completed in valley-fill deposits at six locations (fig. 6.2; table 6.2). Three of the locations (WF, WT, and HV) include several closely spaced wells, and two locations (UW1 and UW2) each include a single well. One condominium complex (WP) obtains water from a single well completed in valley fill, and four additional condominium complexes obtain water from wells completed in bedrock (fig. 6.2). Pumping rates at WF, UW1, UW2, HV, and WT wells (table 6.2) are based on several months to 5 years of measurements. Pumping rates for other wells are based on the population served, assuming a per-capita consumption of 0.38 m^3/d. This rate is reasonable for household use (John Mullaney, U.S. Geological Survey, written commun., 2003) but may be somewhat higher than rates for condominium residents where grounds are not irrigated as heavily and for the NHS (Nonnewaug High School) and for the RM (Romatic Manufacturing Company) wells. Numerous residents in the valley and uplands obtain water from private wells for domestic uses, including lawn irrigation.

All of the water pumped from the WF wells and approximately 30 percent of the water pumped from the HV wells is transported out of the basin. Water pumped from other supply wells is used within the basin. Wastewater at the HV facility is treated in a wastewater-treatment plant south of the supply wells and then discharged to the Pomperaug River. Elsewhere, wastewater is disposed to ground water through private septic systems and local treatment facilities.

Table 6.1. Summary of hydrogeologic and ground-water-quality characteristics for the glacial aquifer system and the Pomperaug River Basin regional study area, Connecticut.

[m, meters; cm/yr, centimeters per year; m^3/s, cubic meters per second; m^3/d, cubic meters per day; km, kilometers; Kh, horizontal hydraulic conductivity; Kz, vertical hydraulic conductivity; Sy, specific yield; n, porosity; mg/L, milligrams per liter]

Characteristic	Glacial aquifer system	Pomperaug River Basin regional study area
	Geography	
Topography	Relief generally less than 300 m (Randall, 2001).	Relief approximately 300 m.
Climate	Precipitation 91 to 127 cm/yr; evapotranspiration 46 to 58 cm/yr (Randall, 1996).	Precipitation 117 cm/yr; evapotranspiration 53 to 56 cm/yr (Randall, 1996).
Surface-water hydrology	Runoff 41 to 76 cm/yr (Randall, 1996); streamflow varies widely with the size of drainage basin. Water-supply reservoirs and former mill ponds are common in upland and valley settings.	Runoff 61 cm/yr; flow in Pomperaug River at Southbury averages 71 m^3/s (Morrison and others, 2002). Ponds and former water-supply reservoirs are present in uplands. A mill pond, largely silted, forms behind a dam on the Pomperaug River at Pomperaug.
Land use	Urban, suburban, rural residential, woodlands, farmland.	Suburban, rural residential, woodlands, farmland.
Water use	Potential aquifer yields generally less than 60,500 m^3/d (Kontis and others, 2004).	Pumpage for public supply about 7,570 m^3/d (this study). Potential aquifer yield of 33,300 m^3/d (Mazzaferro, 1986a).
	Geology	
Surficial geology	Glacially-derived sand and gravel in valleys that slope away from retreating ice sheets; limited fine-grained deposits; till prevalent in uplands but discontinuous under valley fill (Randall and others, 1988; Randall, 2001).	Mainly sand and gravel in a southward sloping valley (Stone and others, 1998); till covers uplands and underlies valley fill (Mazzaferro, 1986a).
Bedrock geology	Crystalline granitic and metamorphic rocks and sedimentary rocks; limited carbonate rocks (Randall, 2001; Randall and others, 1988).	Metamorphic crystalline rocks, granite, sedimentary rocks, and volcanics, mainly basalts.
	Ground-water hydrology	
Aquifer conditions	Valley-fill aquifers that are generally less than 2.5 km wide and are unconfined; valley fill generally less than 67 m thick; depth to water generally less than 15 m. Streams that cross valley fill from upland areas are commonly sources of recharge; pumping near surface water commonly induces infiltration (Kontis and others, 2004).	A valley-fill aquifer that is generally less than 1.6 km wide and unconfined; valley fill generally less than 67 m thick; depth to water generally less than 15 m (Mazzaferro, 1986a; 1986b). Several tributary streams are likely sources of recharge. Pumping induces infiltration from streams in at least two areas.
Hydraulic properties	Valley fill: Kh= 1.5 to150 m/d; Kh/Kz = 10:1 (commonly); n = 0.3 to 0.4; Sy = 0.2 to 0.3 Till: Kh = 0.003 to 3 m/d; Kh/Kz = 1; n = 0.1to 0.3; Sy = 0.04 to 0.28 Bedrock: Kh = 0.003–0.3 m/d; Kh/Kz (limited information); n = 0.005–0.02; Sy = 0.0001–0.005 (Randall and others, 1988; Bradbury and others, 1991; Melvin and others, 1992; Gburek and others, 1999).	Valley fill: Kh = 1.5 to 76 m/d; n = 0.3 to 0.45. Till: Kh = 0.003to 3 m/d; n = 0.2 to 0.3 Bedrock: K = 0.003 to1.5 m/d; n = 0.005 to 0.02. Sy values not used for current study; Kh/Kz estimated at 1:1. (Mazzaferro, 1986a; Grady and Weaver, 1988; Starn and others, 2000).

Table 6.1. Summary of hydrogeologic and ground-water-quality characteristics for the glacial aquifer system and the Pomperaug River Basin regional study area, Connecticut.—Continued

[m, meters; cm/yr, centimeters per year; m^3/s, cubic meters per second; m^3/d, cubic meters per day; km, kilometers; Kh, horizontal hydraulic conductivity; Kz, vertical hydraulic conductivity; Sy, specific yield; n, porosity; mg/L, milligrams per liter]

Characteristic	Glacial aquifer system	Pomperaug River Basin regional study area
	Ground-water hydrology—Continued	
Ground-water budget	Recharge to valley fill from infiltration of precipitation, 36 to 76 cm/yr. Recharge to valley fill from upland runoff often exceeds recharge from precipitation (Kontis and others, 2004; Morrissey and others, 1988). Pumpage generally less than 15 percent of water budget; most discharge is to streams (Morrissey, 1983; Tepper and others, 1990; Dickerman and others, 1990; Dickerman and others, 1997; Mullaney and Grady, 1997; Starn and others, 2000; Barlow and Dickerman, 2001; DeSimone and others, 2002.)	Recharge to valley fill from infiltration of precipitation, 48 to 61 cm/yr. Recharge to valley fill from upland runoff at least 50 percent of total recharge. Pumpage for public supply less than 5 percent of water budget; most ground water discharges to streams (Mazzaferro, 1986a; this study)
	Ground-water quality	
	Dissolved solids less than 150 mg/L in crystalline-rock terrains and greater than 150 mg/L in sedimentary-rock terrains; pH, 6–8; oxic. Calcium and bicarbonate are the principal ions (Rogers, 1989). Redox conditions not defined regionally.	Dissolved solids generally less than 200 mg/L. Calcium and bicarbonate are the principal dissolved ions. Redox conditions are typically oxic in valley fill and suboxic to anoxic in bedrock (Grady and Weaver, 1988; this study).

Table 6.2. Public-supply wells and pumping rates, Pomperaug River Basin regional study area, Connecticut.

[m, meters; m^3/d, cubic meters per day]

Map name (fig. 2)	Well name	Number of wells	Depth or depth range (m)	Geologic unit (model layer in parenthesis)	Combined pumping rate (m^3/d)	Basis for pumping rate
HV	Heritage Village	5	17–21	Sand and gravel (1)	3,544	1997 – 2001; well owner's records[1]
WF	Watertown Fire District	10	9–12	Sand and gravel (1)	2,450	1997 – 2001; well owner's records[2]
UW1	United Water Company	1	38 (screened 35–38)	Sand and gravel (1)	334	June – December 2001; well owner's records[3]
UW2	United Water Company	1	19 (screened 12–16)	Sand and gravel (1)	392	June – December 2001; well owner's records[3]
WT	Woodlake Tax District	3	9–12	Sand and gravel (1)	264	October 2001 – September 2002; well owner's records[4]
WP	Woodbury Place Condominiums	1	12	Sand and gravel (1)	27	Population served: 72
WK	Woodbury Knolls Condominiums	1	38 (screened 9–38)	Crystalline bedrock (1)	98	Population served: 258
TC	Town in Country Condominiums	2	43 (screened 9–33) and 85	Crystalline bedrock (1 and 2)	91	Population served: 240
HH	Heritage Hill Condominiums	1	84	Crystalline bedrock (2)	45	Population served: 120
QH	Quassuk Heights Condominiums	3	61–107	Crystalline bedrock (2)	41	Population served: 108
RM	Romatic Manufacturing Co.	1	Unknown	Crystalline bedrock (2)	45	Population served: 120
NHS	Nonnewaug High School	1	Unknown	Crystalline bedrock (2)	322	Population served: 850

[1] Roy Adamitis, Heritage Village, written commun., 2003

[2] Ernie Coppock, Watertown Fire District, written commun., 2003

[3] Kevin Moran, United Water, written commun., 2003

[4] Woodlake Tax District, written commun., 2003

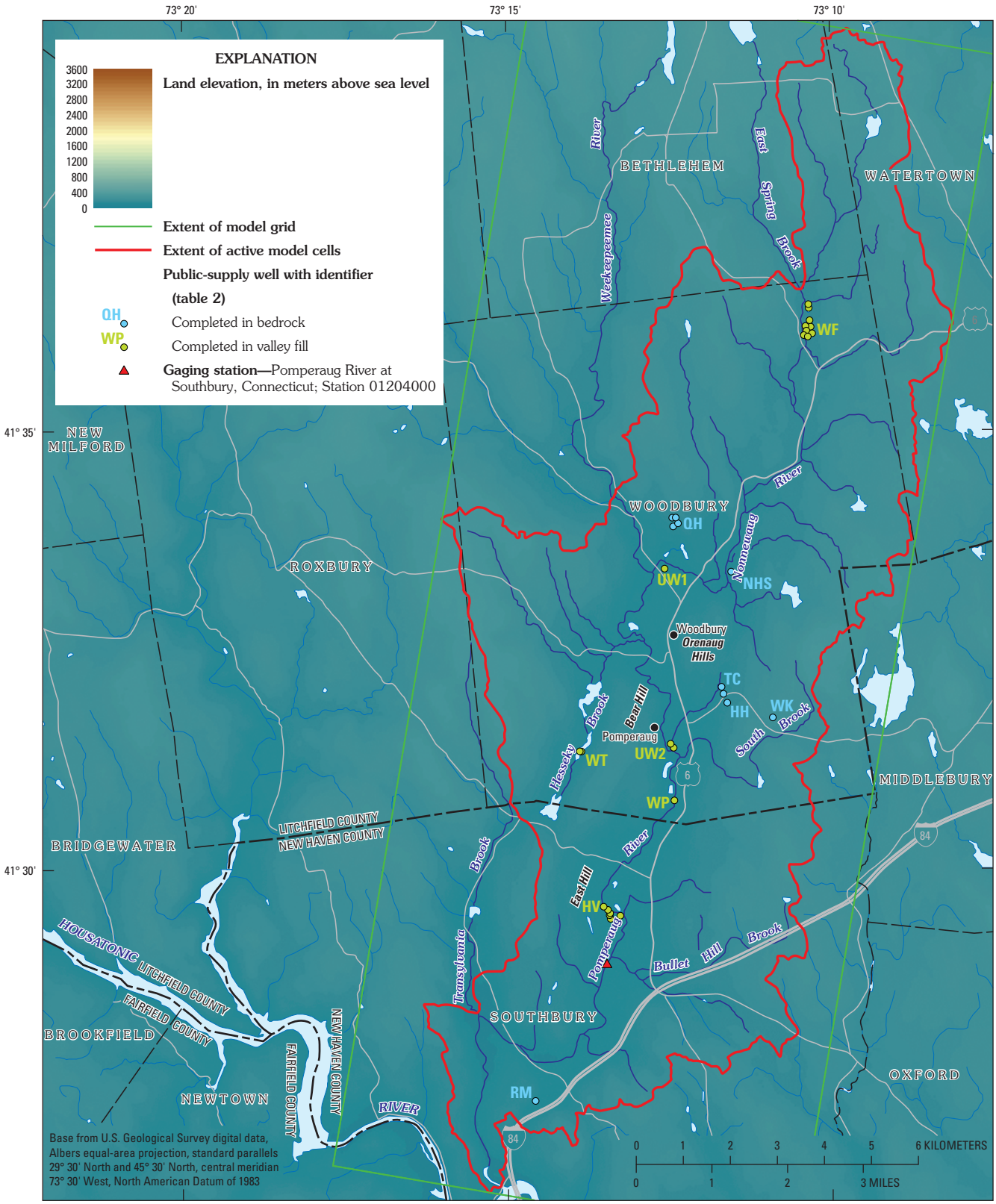

Figure 6.2. Topography, hydrologic features, and locations of public-supply wells, Pomperaug River Basin regional study area, Connecticut.

Conceptual Understanding of the Ground-Water System

Ground water beneath the Pomperaug River Basin regional study area occurs in the glacial valley-fill deposits of the Pomperaug River valley and the underlying Mesozoic and Paleozoic bedrock (fig. 6.3). Recharge to the valley-fill aquifer is from infiltration of precipitation, surface-water flow from upland areas, and ground-water inflow from underlying bedrock. Ground water discharges to wells and surface-water features.

Geologic Units and Hydraulic Properties

Geologic units in the Pomperaug River valley consist of Mesozoic sedimentary and volcanic bedrock within a structural basin in the central and western parts of the study area, surrounded by Paleozoic crystalline bedrock in upland areas; these consolidated units are overlain by Pleistocene-age glacial till and valley-fill surficial deposits. The geologic setting and hydraulic properties of the bedrock and surficial deposits are presented in the following sections.

Bedrock

The Pomperaug River valley in Woodbury and Southbury lies partly within a partial graben (Gates, 1954, 1959; Scott, 1974; Stanley and Caldwell, 1976) composed of Mesozoic-age sedimentary and volcanic rocks. The Pomperaug fault extends north to south through the study area (fig. 6.4) and marks the eastern limit of Mesozoic-age rocks. East Hill, Bear Hill, and the Orenaug Hills (fig. 6.2) are topographically high areas in the Pomperaug River valley underlain by erosion-resistant basalts. Highlands east and west of the valley and structural basin are underlain by crystalline bedrock (Rodgers, 1985).

The Mesozoic-age sequence consists of three basalt layers interbedded with shale, arkosic sandstone, and conglomerate, which dip eastward at various angles but average about 40° (Scott, 1974). The Mesozoic bedrock in the structural

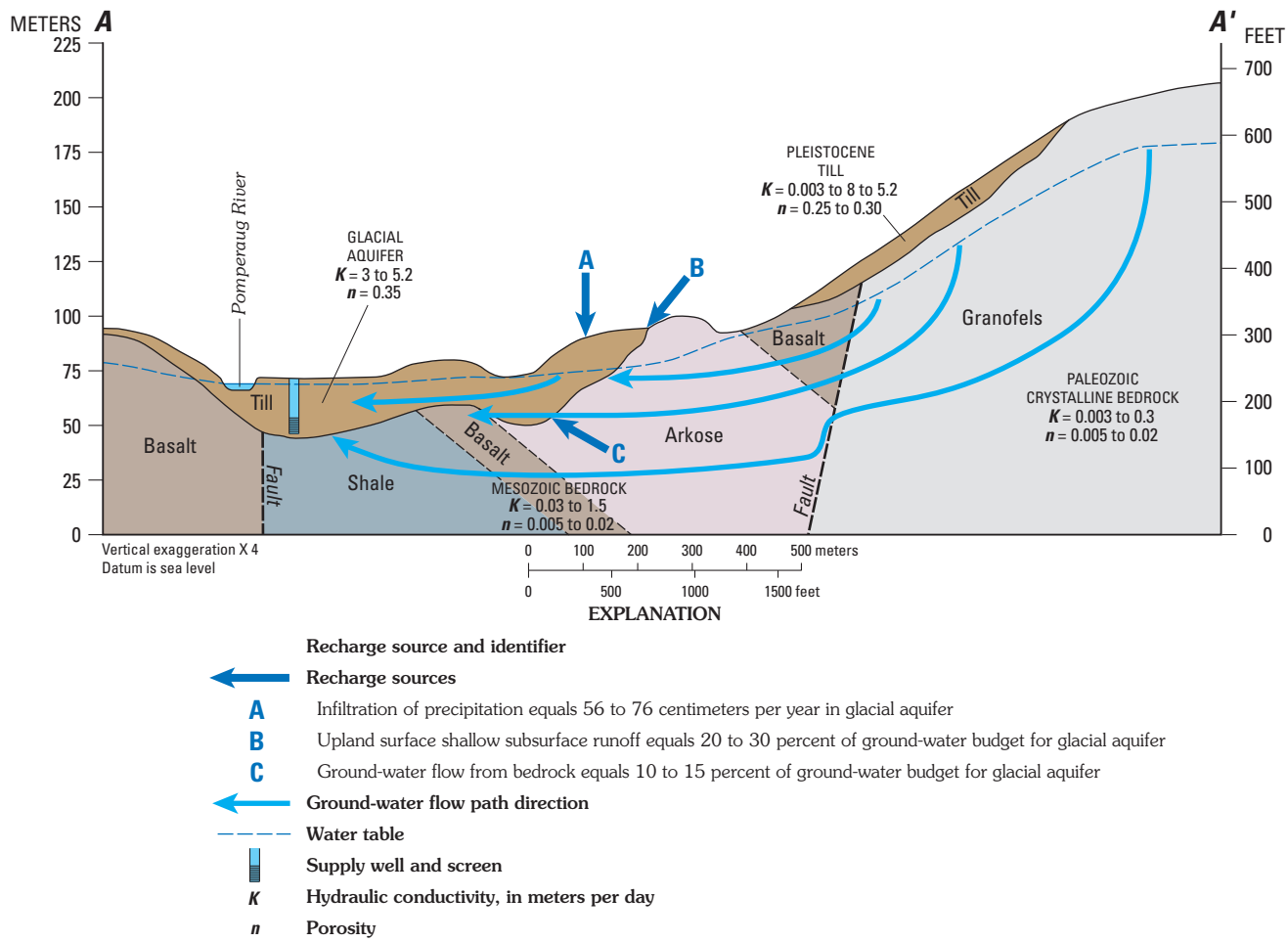

Figure 6.3. Conceptual ground-water flow patterns, representative hydraulic properties, and recharge rates, Pomperaug River Basin regional study area, Connecticut.

basin was fully penetrated at a depth of 376 m in an oil test well drilled in the late 1800s near Southbury (fig. 6.2) (Hovey, 1890). Thicknesses elsewhere are unknown. Faults, which are too numerous to show at the scale on figure 6.4, cause offsets of beds. Mapped faults are oriented approximately northeast to southwest in the southern part of the study area and north to south in the northern part of the study area (Scott, 1974; Rodgers, 1985).

Paleozoic-age crystalline rocks underlying the western part of the study area include granite, quartzite, schist, and gneiss (Scott, 1974; Gates, 1954). Numerous folds have been mapped in the crystalline rocks. Foliation planes typically dip steeply at angles exceeding 45°. Foliation strike varies widely, but a north-northwest to south-southeast trend appears to dominate in much of the study area (Scott, 1974; Gates, 1954).

Wells completed in bedrock obtain most of their water from fractures. Aquifer-test data are not available for bedrock wells in the study area, but driller-reported yields and water levels during pumping are indicators of transmissive properties. Average yields from numerous wells completed in Paleozoic-age crystalline rocks and Mesozoic-age rocks are similar, but wells completed in Paleozoic crystalline rocks are typically deeper than those completed in Mesozoic rocks. A sample of driller's reports for 60 domestic wells was summarized for this study. Yields reported for 14 wells completed in Mesozoic rocks average about 37m^3/d and depths average 83 m. Yields for 46 wells completed in Paleozoic crystalline rocks average about 49 m^3/d and depths average 99 m. Starn and others (2000) report an average hydraulic conductivity of 0.18 m/d for Paleozoic rocks and 1.43 m/d for Mesozoic rocks in the Transylvania Brook Basin, a tributary to the Pomperaug River west of the study area (fig. 6.2). Lower values of 0.006 to 0.03 m/d for crystalline rocks in northern New Hampshire were determined by model calibration (Tiedeman and others, 1997). Lyford and others (2003) report hydraulic conductivity values that range from 0.006 to 4.3 m/d near public-supply wells completed in metamorphic rocks in eastern Massachusetts.

Bedrock transmissivities estimated by applying the Cooper-Jacob formula (Cooper and Jacob, 1946; Fetter, 1994) for driller-reported yields, drawdowns, and pumping times average about 1.9 m^2/d for Mesozoic rocks and about 1.0 m^2/d for Paleozoic rocks. For the average thicknesses of rocks penetrated by wells, hydraulic conductivity values average about 0.03 m/d for Mesozoic rocks and 0.01 m/d for Paleozoic rocks. Because of uncertainties associated with the data, method of analysis, and small data set, these estimates are presented as "order-of-magnitude" values and support the concept that Mesozoic rocks are more transmissive than Paleozoic rocks.

Water-bearing fractures commonly are found along foliation planes in metamorphic rocks and bedding planes in Mesozoic rocks (Janet Stone, U.S. Geological Survey, oral commun., 2002; Walsh, 2001a, 2001b, 2002). A dominant high-angle foliation in metamorphic rocks and numerous high-angle fractures in Mesozoic rocks (Gates, 1954; Scott, 1974) indicate the rocks are well connected vertically, but values of vertical hydraulic conductivity are not available. Lyford and others (2003) report vertical conductance (vertical hydraulic conductivity divided by thickness) values of 0.0015 to 0.04 1/d for two areas where high-angle fractures are present and metamorphic rocks are well connected vertically to surficial materials. Porosity values reported for crystalline bedrock range from 0.005 to 0.02 (Ellis, 1909; Heath, 1989; Barton and others, 1999).

Surficial Materials

Surficial materials are largely glacially derived and include till deposited on bedrock and glacial sand and gravel outwash deposited in valleys (fig. 6.4). Also present but not shown separately on figure 6.4 are Holocene alluvial materials, typically less than 3 m thick, which were deposited by streams after glaciers receded. The alluvial materials commonly include organic matter (Pessl, 1970).

Till includes a surface till unit (also called thin till) deposited by the last glacial ice sheet and a thick till unit (also called drumlin till) deposited during an earlier glacial epoch and compacted by the last ice sheet (Melvin and others, 1992). The surface till unit is fairly continuous and typically less than 5 m thick. The thick till unit typically is found in stream-lined hills, exceeds a thickness of 15 m in places, and is covered by surface till. The depth to bedrock reported by drillers for 60 wells completed in bedrock, mostly in upland areas, ranges from 0.9 to 46 m and averages 12 m. The surface till averages 75 percent sand or coarser and 25 percent silt and clay and typically is not oxidized except in places along sand and gravel lenses. The thick till typically is finer grained, averaging 60 percent sand or coarser and 40 percent silt and clay and is oxidized throughout (Pessl, 1970).

The hydraulic properties of till described by Melvin and others (1992) for Connecticut are reasonable for the study area. They report an average hydraulic conductivity of 0.8 m/d for loose surface till and 0.02 m/d for compact drumlin till derived from crystalline rocks. Horizontal hydraulic- conductivity values for surface and drumlin tills range from 0.0009 to 20 m/d, and vertical hydraulic-conductivity values range from 0.004 to 29 m/d. Porosity ranges from 0.2 for compact drumlin till to 0.35 for surface till (Melvin and others, 1992).

Stratified, glacially derived sediments underlie about 33 km^2 of the valley, or about 26 percent of the study area. The valley-fill deposits include sand and gravel deposited by glacial streams, usually in contact with stagnant ice masses, and silt, sand, and gravel deposited in glacial Lake Pomperaug. The distribution of valley-fill sediments is consistent with the morphosequence depositional model for glacial sediments (Stone and others, 1998; Randall, 2001). A morphosequence is defined as "a body of stratified drift that was laid down by meltwater when deposition was controlled by a specific base level such as a proglacial lake or spillway; the deposits become generally finer distally and their upper surface (where not collapsed) slopes smoothly in the same distal direction" (Randall, 2001, p. 178). Several glacial-lake stages are appar-

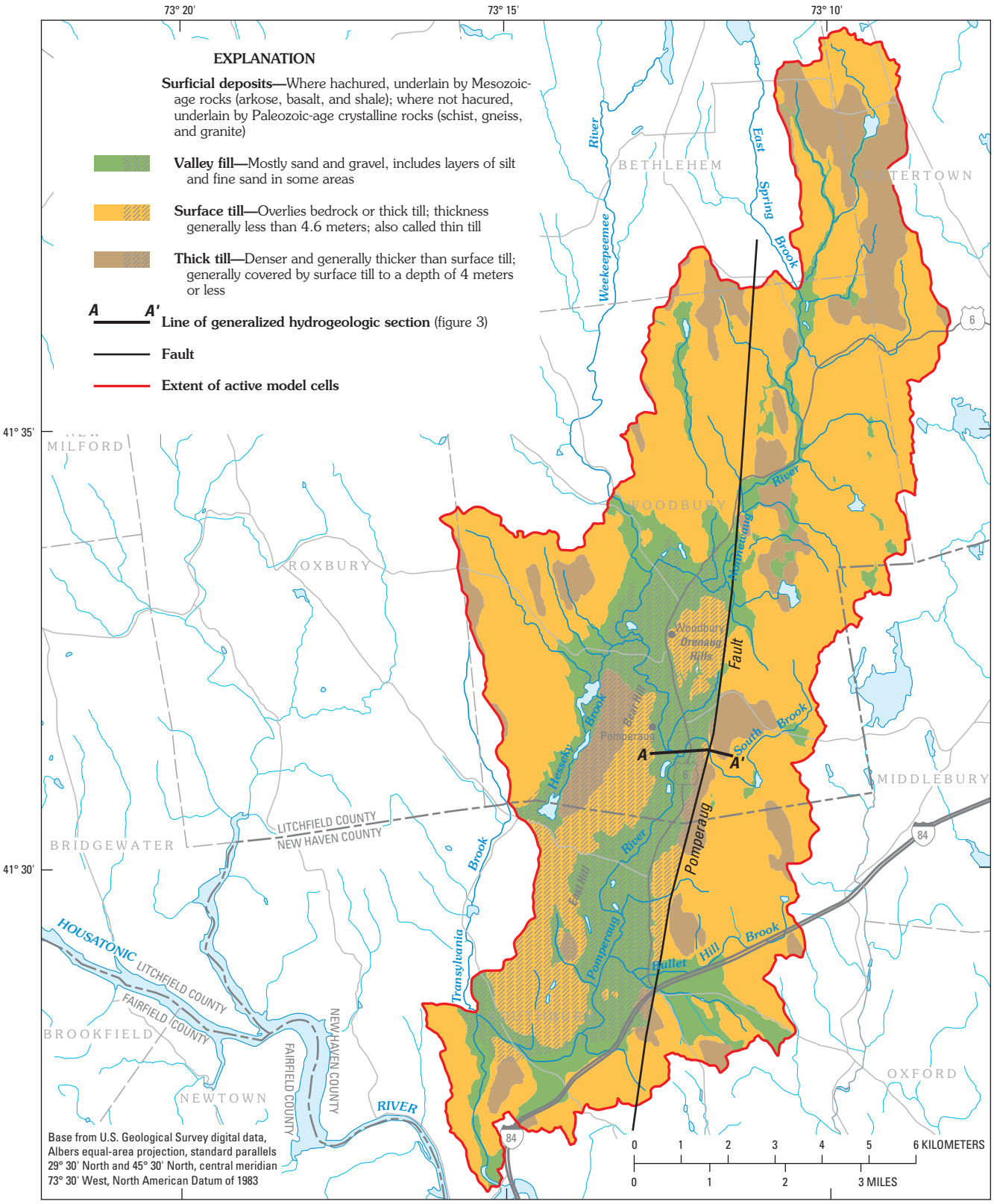

Figure 6.4. Bedrock and surficial geologic units, Pomperaug River Basin regional study area, Connecticut.

ent in relative altitudes of deposits. The last stage of the lake drained when a dam consisting of sand and gravel at Pomperaug (fig. 6.2) was breached (Pessl, 1970). Coarse-grained materials predominate at the land surface, but as much as 47 m of fine-grained sand, silt, and clay has been identified in the subsurface in some parts of the Pomperaug Valley (Mazzaferro, 1986a).

The hydraulic conductivity of outwash deposits, which was determined on the basis of aquifer tests and specific-capacity tests, ranges from 1.5 m/d for fine materials to 76 m/d or more for gravel (Mazzaferro, 1986a; Starn and others, 2000). The greatest hydraulic conductivity areas are mapped near the towns of Woodbury, Pomperaug, and Southbury (Grady and Weaver, 1988). The vertical hydraulic conductivity for sand and gravel has not been determined, but a ratio of 10 for horizontal to vertical commonly is assumed (Kontis and others, 2004). The porosity of sand and gravel typically ranges from 0.3 to 0.45 (Morris and Johnson, 1967; Masterson and others, 1997; Mullaney and Grady, 1997).

Ground-Water Occurrence and Flow

Ground water generally is unconfined and within 15 m of the land surface throughout much of the Pomperaug River Basin regional study area. Depths to water exceed 15 m for some areas of sand and gravel near valley walls and in an area of deltaic sediments near Woodbury (Mazzaferro, 1986b). The valley-fill saturated thickness ranges from zero near the contact with upland till to 37 m near Woodbury (Grady and Weaver, 1988).

Ground-water flow in upland areas includes shallow subsurface flow through surface till and soil to nearby wetlands and stream channels and deep flow through thick till and fractured bedrock to more distant discharge points, including tributaries to the Pomperaug River and valley fill. During periods of high recharge, when the water table is near the land surface, the shallow flow and short flow paths predominate. However, water levels are lower during extended dry periods, and deep flow along longer flow paths predominates. Meinzer and Stearns (1929) report numerous dug wells and ground-water depths generally less than 9 m in upland areas of the Pomperaug River Basin. Driller-reported water levels that average 7.3 m in depth for wells completed in Paleozoic rocks also support the concept of a water table generally less than 9 m deep.

Ground-water flow directions shown in figure 6.5 are based on a water-table map for the valley fill presented by Mazzaferro (1986a) and basin-wide flow paths simulated as part of this study. In general, ground-water flow is from upland recharge areas toward discharge areas along the Pomperaug River and its tributaries. Pumping from public-supply wells may affect ground-water flow locally, but depressions in the water table caused by pumping are not apparent at the 3-m contour interval used to map the water table in valley fill (Mazzaferro, 1986a). Conceptually, pumping has a minimal effect on area-wide flow patterns.

Water Budget

Recharge in upland areas is largely by infiltration of precipitation. Other minor sources include wastewater return from septic systems and leakage from ponds and streams. Recharge rates in upland areas are not well understood in New England, but controlling factors appear to include the distribution of surface till and topography. Areas of shallow ground water can be extensive during wet periods, particularly during the spring. In these areas, a major control on recharge rates is the depth to the water table and the rate at which ground water at the water table drains vertically or laterally. The vertical and lateral flow of ground water varies widely in upland areas and relates to the transmissivity of till and bedrock, topographic relief, and hydraulic gradient at the water table. Annual recharge rates, therefore, can vary widely from near zero in wetland discharge areas where the water table is perennially at or near the land surface to rates that approach annual runoff rates.

Numerous streamflow records in Connecticut have been analyzed for the ground-water runoff component, which is an approximation of ground-water recharge. For basins underlain principally by till, data presented by Mazzaferro and others (1979) indicate ground-water runoff is approximately 33 percent of total runoff. Ground-water runoff from uplands in the Pomperaug River Basin would average about 20 cm/yr on the basis of the statewide analysis. Mazzaferro (1986a) estimated long-term effective recharge rates (ground-water recharge minus ground-water evapotranspiration) of about 18 cm/yr. Analysis of streamflow data in similar upland settings using the programs of Rutledge (1993, 1997, 1998) typically yield higher recharge rates of 38 cm/yr or more (Bent, 1995, 1999; Robert Flynn and Gary Tasker, U.S. Geological Survey, written commun., 2003). Starn and others (2000) determined area-averaged recharge rates of 56 cm/yr for areas underlain by Mesozoic rocks and 20 cm/yr for areas underlain by crystalline rocks on the basis of the statewide analysis of ground-water runoff and numerical modeling of ground-water flow near Transylvania Brook. A water-budget study of the Pomperaug River Basin by Meinzer and Stearns (1929) for 1913–1916 indicated basin-wide ground-water recharge averaged 39.5 cm/yr and precipitation averaged 113 cm/yr. They stated that nearly one-half of the ground-water recharge was lost to evapotranspiration.

Major recharge sources in areas underlain by valley fill include direct infiltration of precipitation, ground-water inflow from bedrock, runoff from bordering hillslopes, and infiltration from tributary streams (Lyford and Cohen, 1988; Randall and others, 1988). Other sources include induced infiltration from streams near wells and disposal of wastewater from septic systems. Direct infiltration of precipitation to valley fill probably approaches annual runoff rates (precipitation

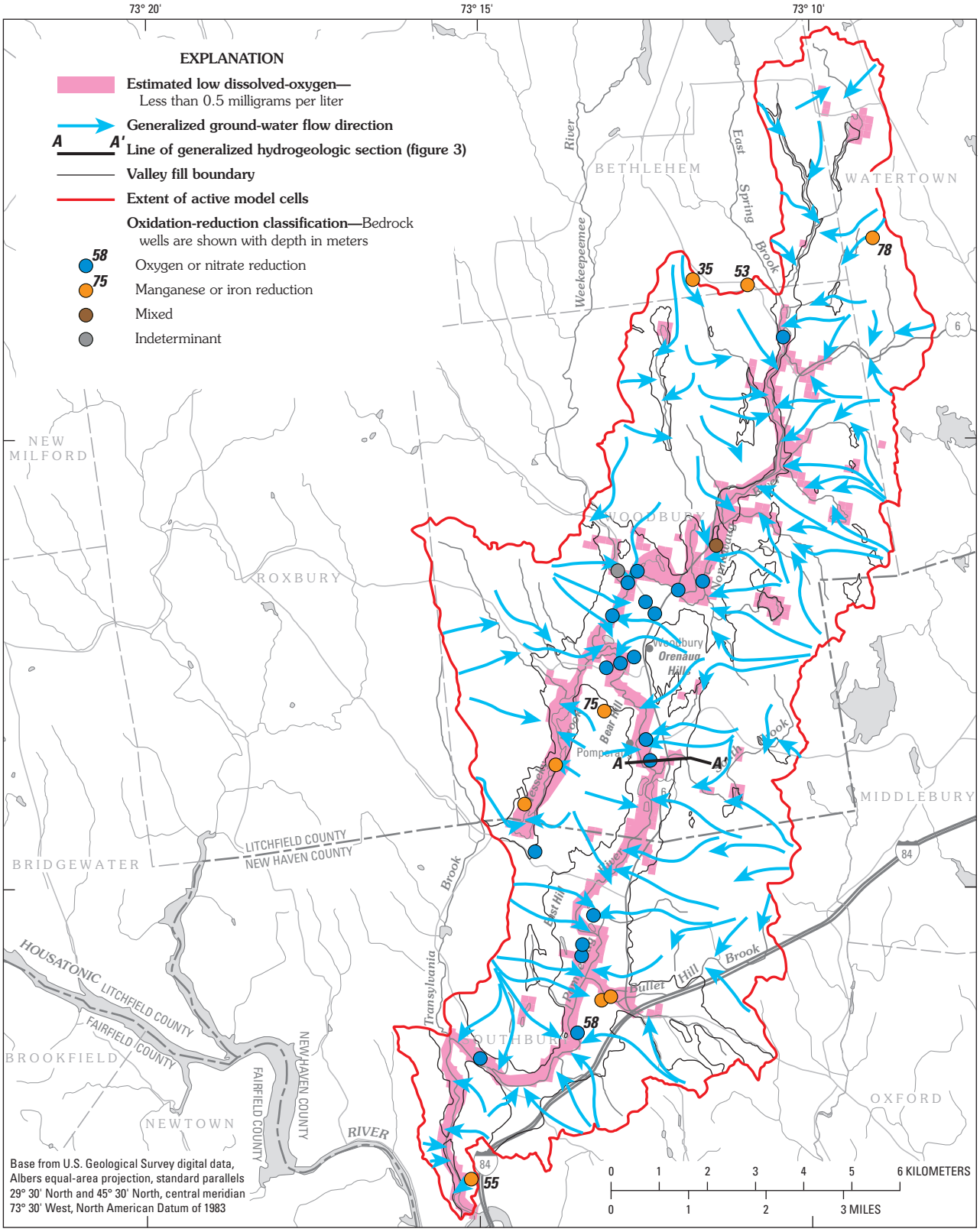

Figure 6.5. Wells sampled, oxidation-reduction classification zones, and directions of ground-water flow, Pomperaug River Basin regional study area, Connecticut.

minus evapotranspiration) or about 61 cm/yr (Randall, 1996; Morrison and others, 2002). Mazzaferro (1986a) estimated long-term effective recharge rates of 48 to 51 cm/yr for areas underlain by sand and gravel. Starn and others (2000) simulated rates of 56 cm/yr for sand and gravel in the Transylvania Brook area. Inflow rates from crystalline rocks typically are small relative to other sources, but inflow rates from Mesozoic rocks, which potentially receive more recharge from precipitation and are more transmissive than crystalline rocks, may be a major source of recharge to valley fill in some areas. Recharge rates from upland hillslopes that border valley-fill materials vary with the size of the hillslope contributing area and can account for 50 percent or more of the total recharge to valley-fill materials (Williams and Morrissey, 1996; Morrissey and others, 1988). Water-budget summaries, which were compiled from ground-water flow models in New England, indicated that from 30 to 60 percent of the inflow to valley fill is from upland sources. Natural infiltration from streams that cross valley fill from upland areas also can be a major component of recharge to valley-fill aquifers in some settings (Williams and Morrissey, 1996). An analysis of streamflow data for the Pomperaug River at Southbury, using the programs of Rutledge (1993, 1997, 1998), indicated that for 1995–96, a period when total runoff was about 5 cm above long-term average runoff, basin-wide recharge was 70 to 80 percent of total runoff, or 46 to 53 cm/yr (J.J. Starn, U.S. Geological Survey, written commun., 2002).

Ground-Water Quality

Ground-water quality data for wells completed in the valley-fill aquifer of the study area indicate dissolved-solids concentrations are generally less than 200 mg/L (Mazzaferro and others, 1979; Mazzaferro, 1986a; Grady and Weaver, 1988). Ground water generally is of the calcium-sodium-magnesium-bicarbonate-chloride type, and the pH typically ranges from 6.0 to 7.5 (Mazzaferro and others, 1979; Mazzaferro, 1986a; Grady and Weaver, 1988). Some water samples in the study area indicate contamination from anthropogenic sources, including road salt, agricultural chemicals, petroleum hydrocarbons, chlorinated compounds, and septic systems. A study by Grady and Weaver (1988) of the effects of land use on ground-water quality in shallow monitoring wells found several contaminants associated with human activities in residential, commercial, light industrial, and agricultural land-use settings. Concentrations of natural contaminants, including radionuclides (Thomas and McHone, 1997) and arsenic (Brown and Chute, 2002), can be high in fractured bedrock aquifers in parts of Connecticut and potentially migrate to community water supplies in adjacent stratified-drift aquifers. High concentrations of radon have been associated with crystalline rocks (the Nonnewaug Granite and the Collinsville and Taine Mountain Formations) (Thomas and others, 1988; Thomas and McHone, 1997).

Ground water in most of the stratified glacial aquifer is oxygen and nitrate reducing, but in some areas near the central part of the valley, manganese- and iron-reducing conditions are present where water along longer flow paths discharge to surface-water bodies (fig. 6.5). In these waters, concentrations of dissolved oxygen typically are low, dissolved iron and manganese concentrations are high, and nitrate concentrations generally are low or below detection. Organic-rich sediments beneath surface-water bodies and in wetlands also can consume dissolved oxygen and create manganese- and iron-reducing shallow ground water, as observed in a flow-path study by Mullaney and Grady (1997) in a glacial aquifer in north-central Connecticut. Ground water in the fractured bedrock generally is older than water from the glacial aquifer, and tends to be manganese and iron reducing. Ground water that has flowed through rocks of Mesozoic or Paleozoic age before passing into the glacial aquifer could reflect chemical characteristics of the bedrock.

Ground-Water Flow Simulations

A steady-state model of ground-water flow in the study area was developed using MODFLOW-2000 (Harbaugh and others, 2000) to estimate aquifer-system properties, delineate areas contributing recharge to public-supply wells, and support future local modeling efforts. The model represents average ground-water flow conditions from 1997 to 2001. Model input includes boundary conditions, model stresses, and hydraulic properties. The preprocessor Argus ONE (Argus Interware, 1997) with the graphical interface for MODFLOW (Winston, 2000), using MODFLOW-2000 (Harbaugh and others, 2000), provided flexibility for setting up model grids, layer thicknesses, and stream characteristics. Aquifer-system and model characteristics are summarized in table 6.3.

Modeled Area and Spatial Discretization

The Pomperaug River Basin regional ground-water flow model encompasses an area of 128 km^2 (fig. 6.6). A no-flow (zero-flux) boundary surrounds the modeled area, which assumes that ground-water divides are coincident with topographic divides, that inflow to the modeled area as underflow from three tributary basins is negligible, and that underflow at the mouth of the Pomperaug River is negligible.

Experiments with uniform model grid sizes consisting of 30.5-m- and 152.4-m-square cells indicated simulated water budgets, flow paths, and contributing recharge areas were nearly identical for the two cell sizes. The calibrated model discussed here is for the 152.4-m cell size because the larger spacing was more numerically stable, computer simulation times were shorter, and output data were easier to manage than those for the 30.5-m cell size. The 30.5-m cell size was later used for particle-tracking simulations to delineate areas contributing recharge to public-supply wells. Two layers that parallel the land surface were selected to represent the vertical dimension. Layer 1 is 46 m thick and represents till and shallow bedrock in upland areas and stratified, glacially derived sediments and shallow bedrock in the valleys. Layer 2 represents a 107-m- thick section of bedrock. It is assumed that most ground water flows through a total thickness of about 152 m. Early attempts to use a uniform 15-m thickness for layer 1 and four layers resulted in numerical instabilities that could not be resolved. The two-layer model was generally stable for a layer 1 thickness of 46 m. Layer 1 was specified as convertible to unconfined where heads were below the top of the layer, and layer 2 was specified as confined.

Boundary Conditions and Model Stresses

Model stresses include streams, recharge, and extraction wells. Perennial streams were simulated using the MODFLOW stream package (Prudic, 1989). The stream package accounts for gains and losses in the simulated streams and routes flow from upstream reaches to downstream reaches. The ends of stream segments were placed at mapped stream origins in headwater areas, at stream intersections, and at major changes in stream-channel slope. The stream altitudes were interpolated linearly within a segment. This approach closely matched actual stream altitudes at stream reaches for low-gradient, uniformly sloped main stems but was less accurate for tributary streams with high-gradient, nonuniform slopes. The top of the streambed was placed 0.9 m below the stream stage, and the bottom of the streambed was placed 1.2 m below the stream stage. The Nonnewaug, Weekeepeemee, and Pomperaug Rivers were assumed 15 m wide except near the Watertown Fire District Wells (WF) where a 30-m width was assigned to account for diversions from the Nonnewaug River through recharge ponds. All other streams were assumed to be 3 m wide. A streambed hydraulic conductivity of 0.3 m/d was assumed for all streams on the basis of literature-reported values (Kontis and others, 2004).

Recharge was applied in five zones defined by geology (fig. 6.7), and recharge rates were assigned so basin runoff approximated 70 to 80 percent of long-term average runoff measured for the Pomperaug River at Southbury. Evapotranspiration of ground water was accounted for in the recharge estimates but was not modeled explicitly. A recharge rate of 56 cm/yr was used for the valley fill by Starn and others (2000) for the Transylvania Brook area and was also applied to areas underlain by valley fill in this study. Surface runoff is limited in areas underlain by valley-fill materials, thus the recharge rate should approximate runoff rates (Lyford and Cohen, 1988). A rate less than the basin runoff rate of about 61 cm/yr accounts for some storm runoff from impermeable surfaces. A recharge rate of 61 cm/yr was applied on hillslopes that adjoin the valley fill to account for water that runs off of these areas and recharges the valley fill near the valley edges. Most areas underlain by Mesozoic rocks form hillslopes adjacent to valley fill, so a recharge rate of 61 cm/yr also was applied in this zone. This rate is similar to a rate of 56 cm/yr used be Starn and others (2000) in the Transylvania Brook area. A rate of 38.1 cm/yr was applied in thick till and thin till areas underlain by crystalline rocks.

Discharge wells were placed at locations of public-supply wells completed in sand and gravel and bedrock. Wells completed in valley fill were placed in layer 1. Wells in upland areas that service condominium units and the Romatic Manufacturing Company (RM) are completed in bedrock. All but two of the bedrock wells were placed in layer 2. A well 43 m deep at the Town in Country Condominiums (TC) and a well 38 m deep at the Woodbury Knolls Condominiums (WK) were placed in layer 1 because of depths less than the thickness of layer 1. A well completed to an unknown depth in bedrock at Nonnewaug High School (NHS) is in a valley setting but also was placed in layer 2. Extraction rates were set to measured or estimated average rates (combined pumping rate; table 6.2).

Screened intervals for wells in sand and gravel and producing intervals for wells in bedrock were available for only United Water Company Wells #1 and #2 (UW1 and UW2),

Table 6.3. Summary of aquifer-system and model characteristics, Pomperaug River Basin regional study area, Connecticut

[m, meters; m/d, meters per day; cm/yr, centimeters per year]

Characteristic	Measured or estimated range	Simulated value
	Thickness	
Valley fill	0 to 61 m	Total thickness of layer 1 is 46 m, which may include any of the following: valley fill, till, and bedrock
Thick till	5 to 46 m	
Surface till	0 to 5 m	
Bedrock	Less than 152 m	107 m
	Hydraulic conductivity	
Valley fill	1.5 to 76 m/d	Less than 3 m thick: 0.12 m/d
		3 to 15 m: 6.28 m/d
		Greater than 15 m thick: 5.7 m/d
		Gravel over fines: 2.8 m/d
Thick till	0.003 to 0.3 m/d	0.12 m/d
Surface till	0.003 to 3 m/d	0.09 m/d
Crystalline bedrock	0.003 to 0.3 m/d	0.03 m/d
Mesozoic bedrock	0.03 to 1.5 m/d	0.09 m/d
Ratio of horizontal to vertical hydraulic conductivity	1.0 to 10	1
	Porosity	
Valley fill	0.3 to 0.45	Less than 3 m thick: 0.01
		3 to 15 m: 0.07
		Greater than 15 m thick: 0.23
		Gravel over fines: 0.23
Thick till	0.25	0.08
Surface till	0.2 to 0.35	0.035
Crystalline bedrock	0.005 to 0.02	0.02
Mesozoic bedrock	0.005 to 0.02	0.02
	Stream characteristics	
Width	3 to 30 m	Near Watertown Fire District wells: 30 m; Main stems: 15 m; tributaries: 3 m
Hydraulic conductivity of streambed	0.1 to 3 m/d	0.3 m/d
Thickness of streambed	0.3 to 1.5 m	0.3 m
	Recharge rates	
Hillslope	38 to 66 cm/yr	61 cm/yr
Valley fill	48 to 61 cm/yr	56 cm/yr
Mesozoic rocks	38 to 66 cm/yr	61 cm/yr
Surface till	20 to 6 cm/yr	38 cm/yr
Thick till	20 to 56 cm/yr	38 cm/yr

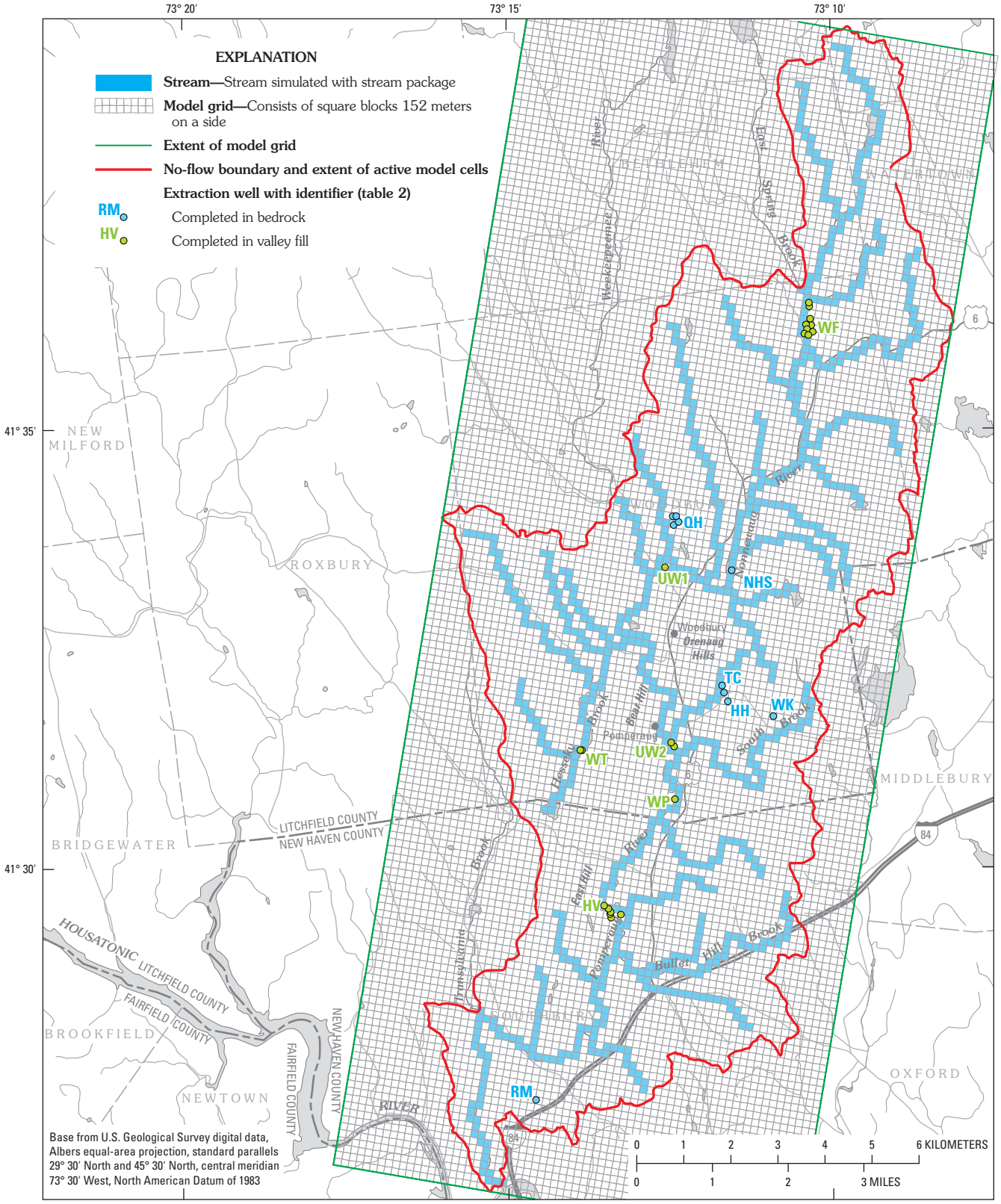

Figure 6.6. Ground-water flow model grid and simulated streams and wells, Pomperaug River Basin regional study area, Connecticut.

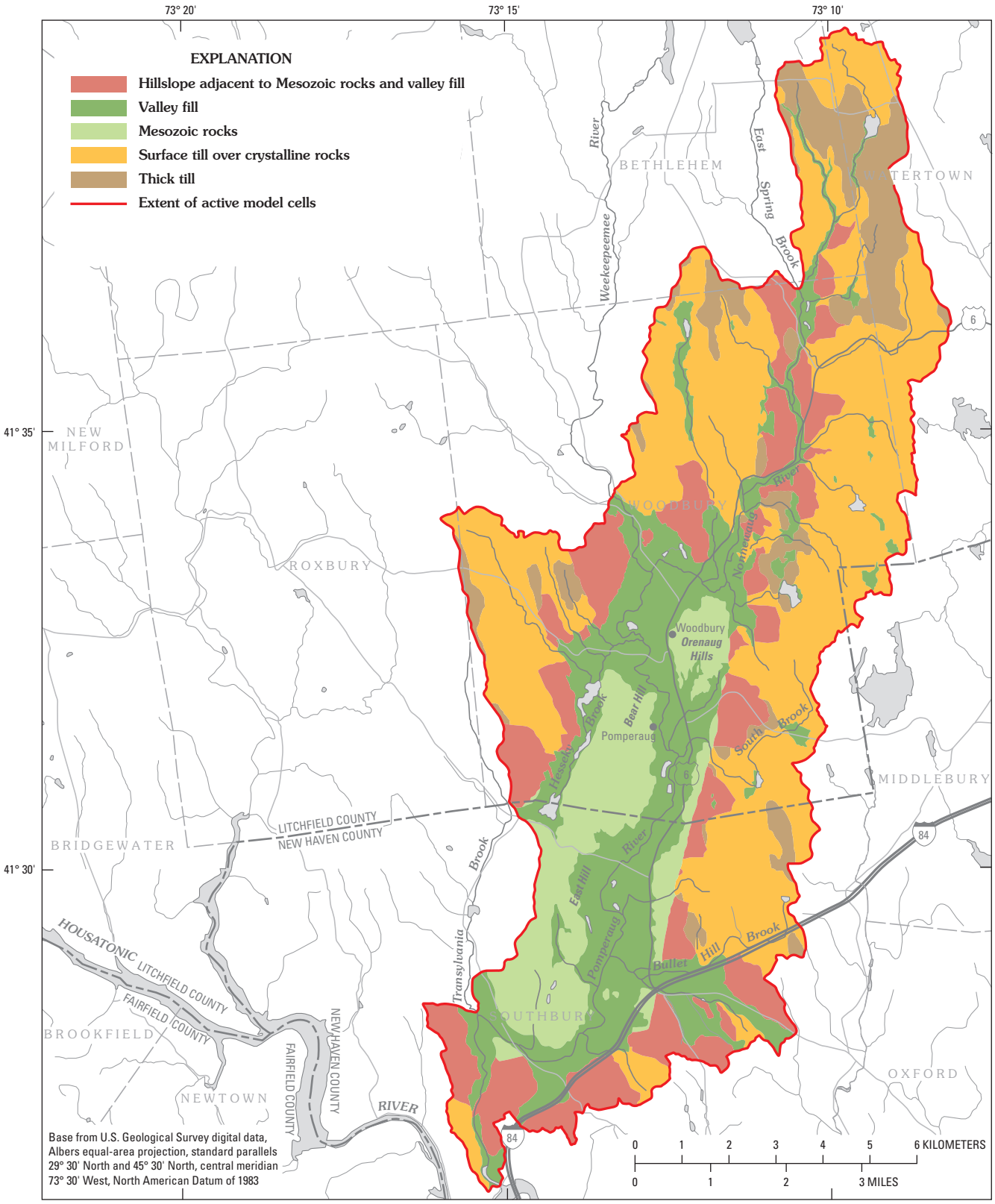

Figure 6.7. Ground-water recharge zones, Pomperaug River Basin regional study area, Connecticut.

Woodbury Knoll Condominium (WK), and Town in Country Condominium (TC) (table 6.2). For purposes of tracking particles, a screen length of 6.1 m at the bottom of the well was assumed for wells completed in valley fill, and a producing interval from the top of layer 2 to the bottom of the well was assumed for bedrock wells. For Romatic Manufacturing Company (RM) and Nonnewaug High School (NHS), where well depths are unknown, the producing interval was assumed to be the thickness of layer 2.

Aquifer Hydraulic Properties

Hydraulic-conductivity zones for each layer were defined on the basis of the mapped distribution of geologic units and saturated thicknesses presented by Grady and Weaver (1988). Layer-1 zones included surface till and thick till zones in uplands and four zones in valley fill (fig. 6.8). The zones for valley-fill materials are defined largely on the basis of saturated thickness of sand and gravel and are best visualized as transmissivity zones rather than hydraulic-conductivity zones because layer-1 thickness generally is greater than actual geologic-unit thickness. These zones include (1) areas along the valley wall where the saturated thickness is less than 3 m, (2) areas where the saturated thickness is 3 to 15 m, (3) areas where the saturated thickness is greater than 15 m, and (4) a fairly extensive area near North Woodbury where coarse materials overlie fine materials. The hydraulic-conductivity values summarized in table 6.3 for valley-fill zones were refined somewhat from initial estimates by the parameter-estimation option in MODFLOW-2000. The hydraulic-conductivity zones for layer 2 include one for Paleozoic crystalline rocks and a second for the more transmissive Mesozoic rocks (fig. 6.4).

Porosity values for layer 1 were adjusted for thickness to simulate approximate cross-sectional pore areas in surficial materials and, thereby, more accurately simulate lateral traveltimes through surficial materials. Model porosities were calculated by multiplying estimated actual porosities by the ratio of saturated thickness to the thickness of layer 1 (46 m). For example, a saturated thickness of 4.6 m for thin till divided by a layer 1 thickness of 46 m and multiplied by an estimated porosity of 0.35 yields a model porosity of 0.035. Estimated and simulated porosity values for layer 1 zones are summarized in table 6.3. A uniform porosity of 0.02 was used for layer 2 to represent fracture porosity in bedrock.

Model Calibration

The Pomperaug River Basin regional ground-water flow model was calibrated by manually adjusting model-input parameters for hydraulic conductivity and comparing model-computed to measured hydraulic heads. Data used for model calibration include average water levels reported by Mazzaferro (1986a) for January 1979 to February 1980 and for one USGS observation well (SB-39) for 1991 to 2002. Water-level data from driller's logs for upland areas indicated a shallow water table but were not used explicitly for model calibration. The calibration goal was to approximately simulate observed heads in valley fill with a uniform distribution of residuals (measured minus model-computed heads) and a shallow water table that approximated the land-surface configuration in upland areas. Streamflow data were not available for model calibration.

The overall goodness of fit of the model to the observation data was evaluated using summary measures and graphical analyses. The root-mean-squared error (RMSE), the range, the standard deviation, and the standard-mean error of the residuals (SME), were used to evaluate the model calibration. The RMSE is a measure of the variance of the residuals and was calculated as:

$$RMSE = \sqrt{\frac{\sum_{i=1}^{N} (h_{meas} - h_{sim})i^2}{N}}$$

where h_{meas} is the measured hydraulic head, h_{sim} is the model-computed (simulated) hydraulic head, $(h_{meas} - h_{sim})$ is the head residual, and N is the number of wells used in the computation. If the ratio of the RMSE to the total head change in the modeled area is small, then the error in the head calculations is a small part of the overall model response (Anderson and Woessner, 1992).

The SME was calculated as:

$$SME = \frac{\sigma(h_{meas} - h_{sim})}{\sqrt{N}}$$

where $\sigma(h_{meas} - h_{sim})$ is the standard deviation of the residuals.

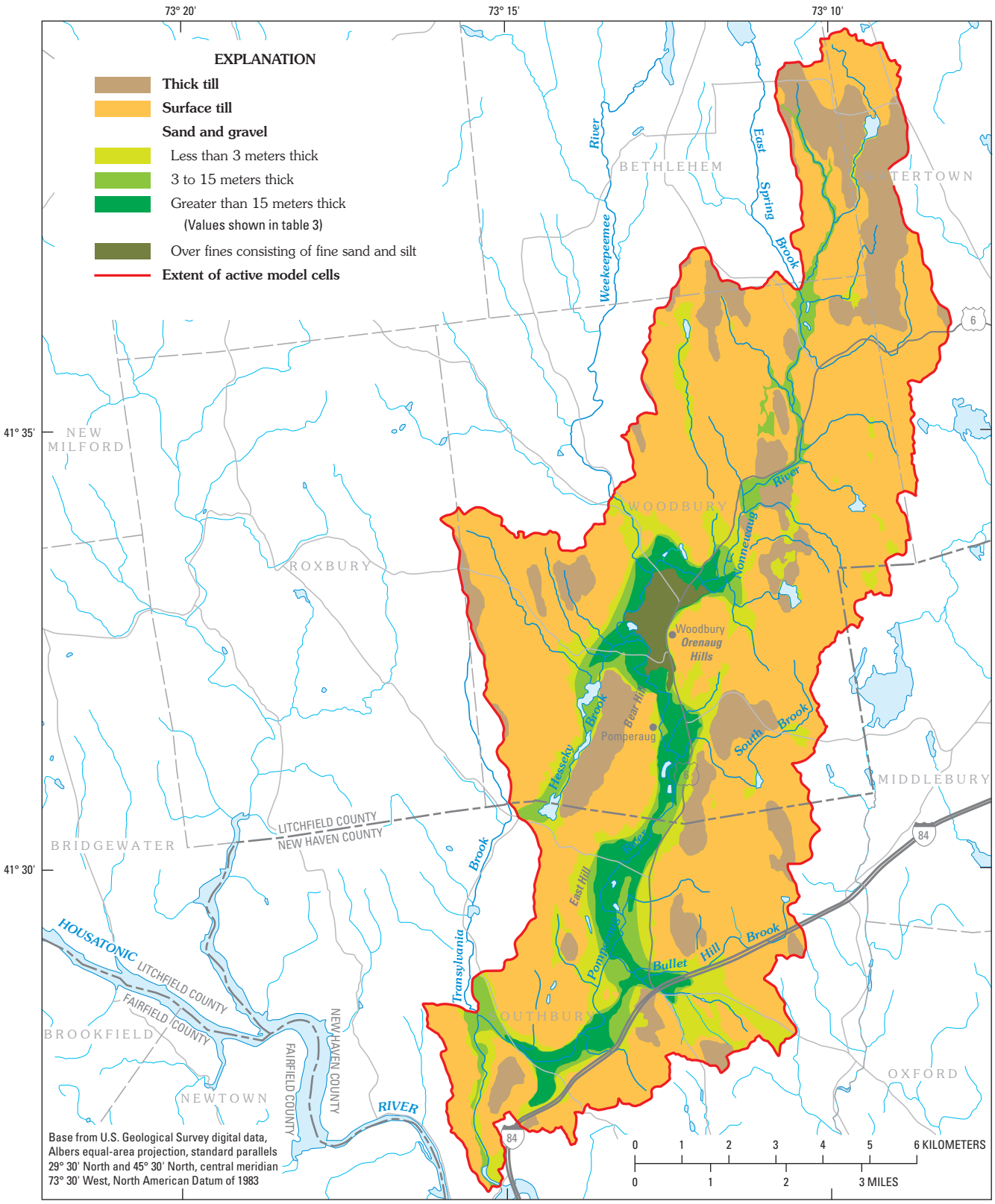

Figure 6.8. Hydraulic-conductivity and porosity zones for model layer 1, Pomperaug River Basin regional study area, Connecticut.

Model-Computed Hydraulic Heads

A simple method of assessing model fit is to plot the model-computed hydraulic head values against the measured observations. For a perfect fit, all points should fall on the 1:1 diagonal line. Figure 6.9 presents a plot of the model-computed compared to the measured hydraulic heads for the study area and indicates a reasonable model fit. The average residual for the entire model is 0.43 m, and residuals range from -10.1 m to 8.2 m (range of 18.1 m). The RMSE for the entire model is 4.43 m, which is 11 percent of the range of head observations in the model (40.8 m). The standard deviation of the residuals is 4.50 m, and the SME is 0.88 m. The spatial distribution of model-computed hydraulic heads in layer 1 approximately parallels the land surface in upland areas, with the largest differences between model-computed and measured heads occurring near the contact between valley-fill sediments and bedrock (fig. 6.10). Factors that may cause differences between model-computed and measured heads include imprecise measuring-point elevations determined from topographic maps, spatial variation in saturated thicknesses and hydraulic conductivity not accounted for in the model, and imprecise recharge rates near the edge of the valley.

The simulated potentiometric surface for valley fill and analysis of basin-wide flow patterns indicate most ground water flows from upland areas toward the Pomperaug River at approximately right angles to the Pomperaug River consistent with the potentiometric surface for valley fill presented by Mazzaferro (1986a). For Bullet Hill Brook and its tributaries, potentiometric-surface data and model results indicate that ground-water flow approximately parallels the stream channels.

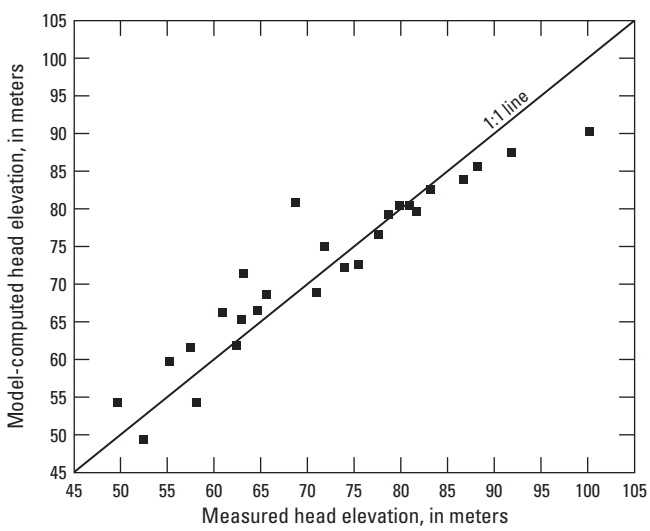

Figure 6.9. Relation between model-computed and measured hydraulic head, Pomperaug River Basin regional study area, Connecticut.

Model-Computed Water Budget

The modeled-area water budget (table 6.4) indicates that areal recharge provides approximately 87 percent of the ground-water inflow, and about 13 percent of the ground-water inflow is from streams. Stream recharge is mostly from tributary streams where they cross valley-fill sediments (fig. 6.11). Stream losses also are apparent near the HV and WF wells. About 96 percent of ground-water discharge is to rivers, and about 4 percent of ground-water discharge is to wells. Recharge of wastewater discharged to ground water from septic tanks was not simulated but could account for an additional 1 percent of the inflow. Simulated streamflow at the outflow point for the basin is 161,000 m^3/d, which is 46.2 cm/yr for the modeled area, or about 77 percent of average basin runoff of 59.9 cm/yr, as measured in the Pomperaug River at Southbury, Connecticut (Morrison and others, 2002).

A water budget for layer 1 in the area underlain by valley fill was determined using the program ZONEBUDGET (Harbaugh, 1990). This analysis indicated that more than one-half of the inflow to the valley-fill aquifer can be attributed

Table 6.4. Model-computed water budget for 1997–2001 average conditions, Pomperaug River Basin regional study area, Connecticut.

[m^3/d, cubic meters per day]

Water-budget component	Flow rate (m^3/d)	Percentage of inflow or outflow
Modeled-area inflow		
Recharge	169,000	87.2
Rivers	24,800	12.8
TOTAL	**193,800**	**100**
Modeled-area outflow		
Wells	7,650	3.9
Rivers	187,000	96.1
TOTAL	**194,650**	**100**
Valley-fill aquifer inflow		
Precipitation	45,500	34.2
Rivers	20,200	15.2
Lateral flow from layer 1	36,400	27.4
Vertical flow from layer 2	30,800	23.2
TOTAL	**132,900**	**100**
Valley-fill aquifer outflow		
Wells	7,100	5.3
Rivers	117,800	88.7
Lateral flow to layer 1	4,800	3.6
Vertical flow to layer 2	3,200	2.4
TOTAL	**132,900**	**100**

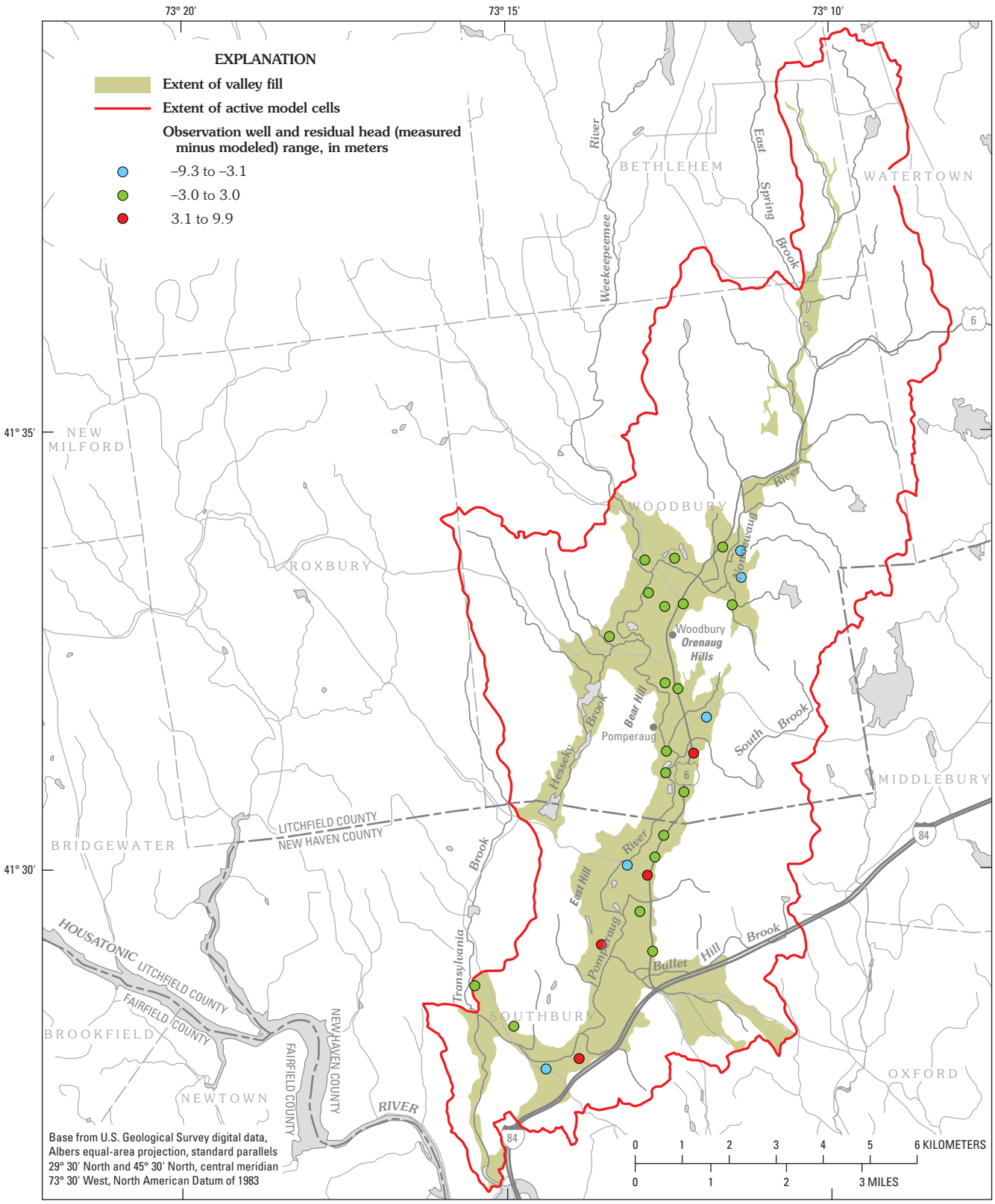

Figure 6.10. Observation points and head residuals, Pomperaug River Basin regional study area, Connecticut.

to upland runoff, which includes river leakage from tributary streams, lateral flow from layer 1 upland areas, and vertical leakage from layer 2 (table 6.4). The net contribution from uplands to valley fill is about 60 percent of the inflow, after adjusting for lateral and vertical outflows to layers 1 and 2 that eventually reenter the valley-fill aquifer. Discharge to wells is about 5 percent of the outflow for the valley-fill aquifer (table 6.4).

Simulation of Areas Contributing Recharge to Public-Supply Wells

Areas contributing recharge to eight public-supply wells or well fields and traveltimes from recharge to discharge areas were simulated by particle-tracking using MODPATH (Pollock, 1994) and methods as described in Section 1 of this Professional Paper (fig. 6.11). A grid spacing of 30.5 m was used for the analysis of contributing areas to better identify flow paths for individual wells. Properties from the calibrated model were used for the finer grid. Porosity values were assigned as discussed in the section "Aquifer Hydraulic Properties." The model-computed areas contributing recharge represent advective ground-water flow and do not account for mechanical dispersion. Advection-dispersion transport simulations would likely yield larger areas contributing recharge than advective particle-tracking simulations because the effects of dispersion caused by aquifer heterogeneity would be included.

Several features of areas contributing recharge and zones of contribution that appear in figure 6.11 are considered noteworthy:

- For all wells completed in valley fill, the areas contributing recharge and zones of contribution extend upgradient into upland areas.
- Areas contributing recharge extend perpendicularly away from the Pomperaug River and its major tributaries reflecting that ground-water flow direction is perpendicular from upland areas toward the rivers.
- Areas contributing recharge can extend large distances from some wells. For example, the contributing area for WP extends approximately 3 km to the eastern model boundary and topographic divide.
- The contributing areas for WF and HV are larger than for other well sites because of larger pumping rates, as expected.
- Simulated losing reaches of streams occur within several of the contributing areas (fig. 6.11) indicating streams contribute recharge to public-supply wells.

An area-wide analysis indicated that traveltimes from recharge areas to wells ranged from less than 1 year to more than 275 years. The median traveltime to wells ranged from 0.2 to 25 years indicating the valley-fill aquifer is susceptible and vulnerable to contamination from overlying land uses. Approximately 73 percent of the traveltimes were less than 10 years, 92 percent of the traveltimes were less than 25 years, 98 percent of the traveltimes were less than 45 years, and about 1 percent of the traveltimes were greater than 60 years.

Model Limitations and Uncertainties

The ground-water flow model for the Pomperaug River Basin regional study area was designed to delineate areas contributing recharge to public-supply wells, to help guide data collection, and to support future local modeling efforts. The model represents the general ground-water flow characteristics of the study area with some limitations including representation of steady-state conditions and the spatial distribution of aquifer parameters.

Water-level hydrographs and computed water budgets indicate the Pomperaug River valley-fill aquifer was generally in steady-state equilibrium for 1997–2001, although the data are not conclusive. Other uses of the model, such as assessing water-management alternatives or transient simulation of flow paths and water budgets, may not be appropriate without further calibration for transient conditions. Also, the model may not be appropriate for local-scale delineation of flow paths and rates, such as near local areas of ground-water contamination.

Particle-tracking simulations were done routinely during model calibration and indicated the contributing areas to wells did not change appreciably for the ranges of adjusted properties. Also, reduction of the grid size had a limited effect on contributing areas to wells except for the UW1 well, which received some water from the southeast for the finer grid (fig. 6.10) but not for the coarser grid. The observation that contributing areas did not change appreciably with variations in model characteristics adds support to the areas shown in figure 6.10. A formal uncertainty analysis, such as one described by Starn and others (2000), however, would be appropriate for delineation of wellhead-protection zones. The contributing areas to bedrock wells could change appreciably with refinements in bedrock properties and, particularly, recharge rates to till (Lyford and others, 2003).

Uncertainty is associated with simulated traveltimes because of uncertain porosity values and hydraulic conductivities of individual geologic units and the geometry of highly conductive zones, which were generalized in the model. In a steady-state model, changes to input porosity values do not change the area contributing recharge to a given well. Changes to input porosity values will, however, change computed traveltimes from recharge to discharge areas in direct proportion to changes of effective porosity because there is an inverse linear relation between ground-water flow velocity and effective porosity and a direct linear relation between traveltime and effective porosity. For example, a one-percent decrease in porosity will result in a one-percent increase in velocity and a one-percent decrease in particle traveltime. A detailed sensitivity analysis of porosity distributions was beyond the scope of this study, although future work could compare simulated

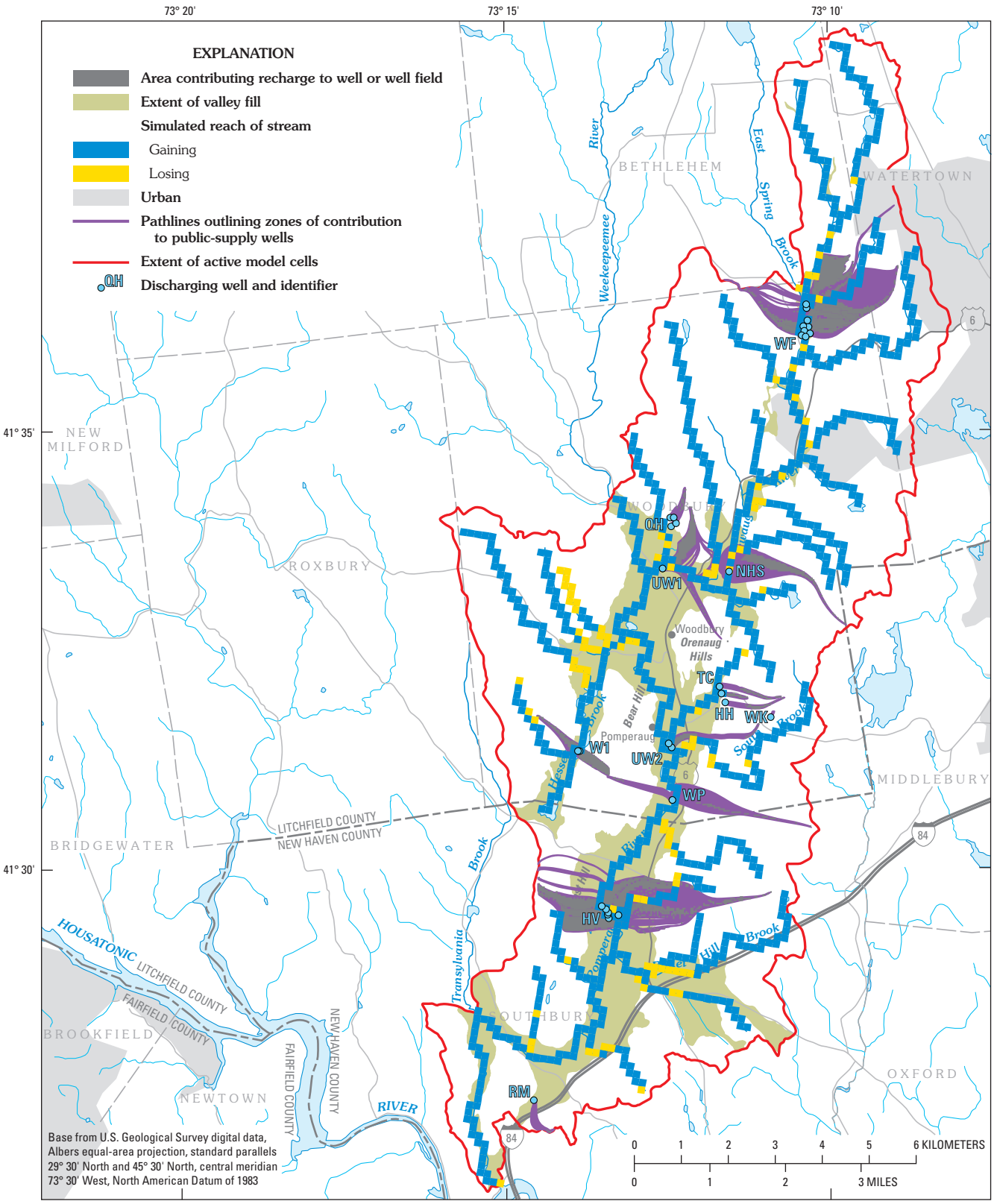

Figure 6.11. Model-computed flow paths, areas contributing recharge to public-supply wells, and gaining and losing stream reaches, Pomperaug River Basin regional study area, Connecticut.

ground-water traveltimes to ground-water ages to more thoroughly evaluate effective porosity values.

The Pomperaug River Basin regional ground-water flow model uses justifiable aquifer properties and boundary conditions and provides a reasonable representation of ground-water flow conditions in the study area for 1997–2001. The model has been helpful for refining concepts about area-wide ground-water flow patterns and water budgets in the study area for the time period of interest but may not be suitable for long-term predictive simulations. This regional model provides a useful tool to evaluate aquifer vulnerability at a regional scale, to facilitate comparisons of ground-water traveltime between regional aquifer systems, and to guide future detailed investigations in the study area.

References Cited

Anderson, M.P., and Woessner, W.W., 1992, Applied ground-water modeling: New York, Academic Press, Inc., 381 p.

Argus Interware, 1997, Argus Numerical Environments and Mesh Maker User's Guide: Jericho, N.Y., 463 p.

Barlow, P.M., and Dickerman, D.C., 2001, Numerical-simulation and conjunctive-management models of the Hunt-Annaquatucket-Pettaquamscutt stream-aquifer system, Rhode Island: U.S. Geological Survey Professional Paper 1636, 88 p.

Barton, G.J., Risser, D.W., Galeone, D.G., and Conger, R.W., 1999, Case study for delineating a contributing area to a water-supply well in a fractured crystalline-bedrock aquifer, Stewartstown, Pennsylvania: U.S. Geological Survey Water-Resources Investigations Report 99–4047, 38 p.

Bent, G.C., 1995, Streamflow, ground-water recharge and discharge, and characteristics of surficial deposits in Buzzards Bay Basin, southeastern Massachusetts: U.S. Geological Survey Water-Resources Investigations Report 95–4234, 56 p.

Bent, G.C., 1999, Streamflow, base flow, and ground-water recharge in the Housatonic River Basin, western Massachusetts and parts of eastern New York and northwestern Connecticut: U.S. Geological Survey Water-Resources Investigations Report 98–4232, 68 p.

Bradbury, K.R., Muldoon, M.A., Zaporozec, A., and Levy, J., 1991, Delineation of wellhead protection areas in fractured rocks: U.S. Environmental Protection Agency, EPA 570/9–91–009, 144 p.

Brown, C.J., and Chute, S.K., 2002, Arsenic concentrations in bedrock wells in Colchester, East Hampton, and Woodstock, Connecticut: U.S. Geological Survey Water-Resources Investigations Report 02–4135, 23 p.

Cooper, H.H., Jr., and Jacob, C.E., 1946, A generalized graphical method for evaluating formation constants and summarizing well-field history: American Geophysical Union Transactions, v. 27, no. 4, p. 526–534.

DeSimone, L.A., Walter, D.A., Eggleston, J.R., and Nimiroski, M.T., 2002, Simulation of ground-water flow and evaluation of water-management alternatives in the Upper Charles River Basin, eastern Massachusetts: U.S. Geological Survey Water-Resources Investigations Report 02–4234, 94 p.

Dickerman, D.C., Kliever, J.D., and Stone, J.R., 1997, Hydrogeology, water quality, and simulation of ground-water development alternatives in the Usquepaug-Queen ground-water reservoir, Southern Rhode Island: U.S. Geological Survey Water-Resources Investigations Report 97–4126, 48 p.

Dickerman, D.C., Trench, E.C.T., and Russell J.P., 1990, Hydrogeology, water quality, and ground-water development alternatives in the lower Wood River ground-water reservoir, Rhode Island: U.S. Geological Survey Water-Resources Investigations Report 89–4031, 109 p.

Ellis, E.E., 1909, Ground water in crystalline rocks of Connecticut, *in* Gregory, H.E., ed., Underground water resources of Connecticut: U.S. Geological Survey Water-Supply Paper 232, p. 54–103.

Fetter, C.W., 1994, Applied hydrogeology (3rd ed.): Englewood Cliffs, N.J., Prentice-Hall, Inc., 691 p.

Gates, R.M., 1954, Bedrock geology of the Woodbury quadrangle: Connecticut Geological and Natural History Survey Quadrangle Report 3, 23 p., scale 1:31,680.

Gates, R.M., 1959, Bedrock geology of the Roxbury quadrangle, Connecticut: U.S. Geological Survey Geologic Quadrangle Map GQ-121, scale 1:24,000.

Gburek, W.J., Folman, G.J., and Urban, J.B., 1999, Field data and ground-water modeling in a layered fractured aquifer: Ground Water, v. 37, no. 2, p. 175–184.

Grady, S.J., and Weaver, M.F., 1988, Preliminary appraisal of the effects of land use on water quality in stratified-drift aquifers in Connecticut—U.S. Geological Survey Toxic Waste-Ground-Water Contamination Program: U.S. Geological Survey Water-Resources Investigations Report 87–4005, 41 p.

Harbaugh, A.W., 1990, A computer program for calculating subregional water budgets using results from the U.S. Geological Survey modular three-dimensional ground-water flow model: U.S. Geological Survey Open-File Report 90–392, 46 p.

Harbaugh, A.W., Banta, E.R., Hill, M.C., McDonald, M.G., 2000, MODFLOW-2000, the U.S. Geological Survey modular ground-water models—User guide to modularization concepts and the ground-water flow process: U.S. Geological Survey Open-File Report, 00–92, p. 121.

Heath, R.C., 1989, Basic ground-water hydrology: U.S. Geological Survey Water-Supply Paper 2220, 84 p.

Hovey, E.O., 1890, The oil well of Southbury, Connecticut: Scientific American, v. 62, p. 275.

Kontis, A.L., Randall, A.D., and Mazzaferro, D.L., 2004, Regional hydrology and simulation of flow of stratified drift aquifers in the glaciated Northeastern United States: U.S. Geological Survey Professional Paper 1415–C, 156 p.

Lyford, F.P., Carlson, C.S., and Hansen, B.P., 2003, Delineation of water sources for public-supply wells in three fractured-bedrock aquifer systems in Massachusett: U.S. Geological Survey Water- Resources Investigations Report 02–4290, 113 p.

Lyford, F.P., and Cohen, A.J., 1988, Estimation of water available for recharge to sand and gravel aquifers in the glaciated Northeastern United States, *in* Randall, A.D., and Johnson, A.I., eds., 1988, Regional aquifer systems of the United States—The northeast glacial aquifers: American Water Resources Association Monograph Series no. 11, p. 37–61.

Masterson, J.P., Walter, D.A., and Savoie, Jennifer, 1997, Use of particle tracking to improve numerical model calibration and to analyze ground-water flow and contaminant migration, Massachusetts Military Reservation, western Cape Cod, Massachusetts: U.S. Geological Survey Water-Supply Paper 2482, 50 p.

Mazzaferro, D.L., 1986a, Ground-water availability and water quality in Southbury and Woodbury, Connecticut: U.S. Geological Survey Water-Resources Investigations Report 84–4221, 105 p.

Mazzaferro, D.L., 1986b, Depth to bedrock, depth to the water table, and classification of unconsolidated materials above the water table in stratified-drift areas of part of the Pomperaug River valley, Southbury and Woodbury, Connecticut: U.S. Geological Survey Miscellaneous Investigations Series Map I-1690, scale 1:24,000.

Mazzaferro, D.L., Handman, E.H., and Thomas, M.P., 1979, Water resources inventory of Connecticut, part 8, Quinnipiac River basin: Connecticut Water Resources Bulletin, no. 27, 88 p.

Meinzer, O.E., and Stearns, N.D., 1929, A study of ground water in the Pomperaug basin, Connecticut, with special reference to intake and discharge: U.S. Geological Survey Water-Supply Paper 597–B, p. 73-146.

Melvin, R.L., Stone, B.D., Stone, J.R., and Trask, J.J., 1992, Hydrogeology of thick till deposits in Connecticut: U.S. Geological Survey Open-File Report 92–43, 49 p.

Morris, D.A., and Johnson, A.I., 1967, Summary of hydrologic and physical properties of rock and soil materials, as analyzed by the Hydrologic Laboratory of the U.S. Geological Survey, 1948-60: U.S. Geological Survey Water-Supply Paper 1839–D, 42 p.

Morrison, Jonathan, Provencher, P.L., Martin, J.W., and Norris, J.R., 2002, Water resources data, Connecticut, water year 2001: U.S. Geological Survey Water-Data Report CT–01–1, 353 p.

Morrissey, D. J., 1983, Hydrology of the Little Androscoggin River valley aquifer, Oxford County, Maine: U.S. Geological Survey Water-Resources Investigations 83–4018, 79 p.

Morrissey, D.J., Randall, A.D., and Williams, J.H., 1988, Upland runoff as a major source of recharge to stratified-drift aquifers in the glaciated Northeast, *in* Randall, A.D., and Johnson, A.I., eds., 1988, Regional aquifer systems of the United States—The northeast glacial aquifers: American Water Resources Association Monograph Series no. 11, p. 17–36.

Mullaney, J.R., and Grady, S.J., 1997, Hydrogeology and water quality of a surficial aquifer underlying an urban area, Manchester, Connecticut: U.S. Geological Survey Water-Resources Investigations Report 97–4195, 40 p.

Pessl, Fred, Jr., 1970, Surficial geologic map of the Woodbury quadrangle, Litchfield and New Haven Counties, Connecticut: U.S. Geological Survey Geologic Quadrangle Map GQ-896.

Pollock, D.W., 1994, User's guide for MODPATH/MODPATH-PLOT, Version 3—A particle tracking post-processing package for MODFLOW, the U.S. Geological Survey finite-difference ground-water flow model: U.S. Geological Survey Open-File Report 94–464, accessed Feb. 6, 2007 at *http://water.usgs.gov/nrp/gwsoftware/modpath41/modpath41.html*

Prudic, D.E., 1989, Documentation of a computer program to simulate stream-aquifer relations using a modular, finite-difference, ground-water flow model: U.S. Geological Survey Open-File Report 88–729, 113 p.

Randall, A.D., 1996, Mean annual runoff, precipitation, and evapotranspiration in the glaciated Northeastern United States, 1951–1980: U.S. Geological Survey Open-File Report 96–395, 2 plates.

Randall, A.D., 2001, Hydrogeologic framework of stratified-drift aquifers in the glaciated Northeastern United States: U.S. Geological Survey Professional Paper 1415–B, 179 p.

Randall, A.D., Francis, R.M., Frimpter, M.H., and Emery, J.M., 1988, Region 19, Northeastern Appalachians, *in* Back, W., Rosenshein, J.S., and Seaber, P.R., eds., Hydrogeology: Boulder, Colorado, Geological Society of America, The geology of North America, v. O–2, p. 177–187.

Rodgers, John (compiler), 1985, Bedrock geological map of Connecticut: Connecticut Geological and Natural History Survey, Natural Resources Atlas Series Map, 2 sheets, scale 1:125,000.

Rogers, R.J., 1989, Geochemical comparison of ground water in areas of New England, New York, and Pennsylvania: Ground Water, v. 27, no. 5, p. 690–712.

Rutledge, A.T., 1993, Computer programs for describing the recession of ground-water discharge and for estimating mean ground-water recharge and discharge from streamflow records: U.S. Geological Survey Water-Resources Investigations Report 93–4121, 45 p.

Rutledge, A.T., 1997, Model-estimated ground-water recharge and hydrograph of ground-water discharge to a stream: U.S. Geological Survey Water-Resources Investigations Report 97–4253, 29 p.

Rutledge, A.T., 1998, Computer programs for describing the recession of ground-water discharge from streamflow records-update: U.S. Geological Survey Water-Resources Investigations Report 98–4148, 43 p.

Scott, R.B., 1974, The bedrock geology of the Southbury quadrangle, Connecticut: Connecticut Geological and Natural History Survey Quadrangle Report 30, 63 p., scale 1:24,000.

Stanley, R.S., and Caldwell, K.G., 1976, The bedrock geology of the Newtown Quadrangle; Connecticut Geological and Natural History Survey, Quadrangle Report 33, 43 p., scale 1:24,000.

Starn, J.J., Stone, J.R., and Mullaney, J.R., 2000, Delineation and analysis of uncertainty of contributing areas to wells at the Southbury Training School, Southbury, Connecticut: U.S. Geological Survey Water-Resources Investigations Report 00–4158, 53 p.

Stone, J.R, Schafer, J.P. London, E.H., DeGiacome-Cohen, Mary, Lewis, R.S., and Thompson, W.B., 1998, Quaternary geologic map of Connecticut and Long Island Sound Basin: U.S. Geological Survey Open-File Report 98–371, 69 p.

Tepper, D.H., Morrissey, D.J., and Johnson, C.D., 1990, Hydrogeology, water quality, and effects of increased municipal pumpage of the Saco River valley glacial aquifer—Bartlett, New Hampshire to Fryeburg, Maine: U.S. Geological Survey Water-Resources Investigations Report 88–4179, 113 p., 6 pls.

Tiedeman, C.R., Goode, D.J., and Hsieh, P.A., 1997, Numerical simulation of ground-water flow through glacial deposits and crystalline bedrock in the Mirror Lake area, Grafton County, New Hampshire: U.S. Geological Survey Professional Paper 1572, 50 p.

Thomas, M.A., Hollis, J.N., Rothney, L.M., Toal, B.F., and Dupuy, C.J., 1988, Correlating radon distribution with geology and areal radioactivity in Connecticut: Northeastern Environmental Science, v. 7, p. 10.

Thomas, M.A. and McHone, N.W., 1997, Indoor radon potential map of Connecticut: Connecticut Departmental of Environmental Protection.

Walsh, G.J., 2001a, Bedrock geology in the vicinity of the Rockland Avenue Well Site, Maynard, Massachusetts: U.S. Geological Survey Open File Report 01–354, 15 p.

Walsh, G.J., 2001b, Bedrock geology in the vicinity of the Knowles and Andreas Well Sites, West Newbury, Massachusetts: U.S. Geological Survey Open File Report 01–353, 14 p.

Walsh, G.J., 2002, Bedrock geology in the vicinity of the Leicester well site, Paxton, Massachusetts: U.S. Geological Survey Open-File Report 02–433, 19 p.

Warner, K.L., and Arnold, T.L., 2005, Framework for regional synthesis of water-quality data for the glacial aquifer system in the United States: U.S. Geological Survey Scientific-Investigations Report 2005–5223, 6 p.

Williams, J.H., and Morrissey, D.J., 1996, Recharge of valley-fill aquifers in the glaciated northeast from upland runoff *in* Subsurface fluid-flow (ground-water and vadose zone) modeling, Joseph D. Ritchey and James O. Rumbaugh, eds.: ASTM STP 1288, , American Society for Testing and Materials, p. 97–113.

Winston, R.B., 2000, Graphical user interface for MODFLOW, version 4: U.S. Geological Survey Open-File Report 00–315, 27 p.

Hydrogeologic Setting and Ground-Water Flow Simulations of the Great Miami River Basin Regional Study Area, Ohio

By Rodney A. Sheets

Section 7 of

Hydrogeologic Settings and Ground-Water Flow Simulations for Regional Studies of the Transport of Anthropogenic and Natural Contaminants to Public-Supply Wells—Studies Begun in 2001

Edited by Suzanne S. Paschke

Professional Paper 1737–A

U.S. Department of the Interior
U.S. Geological Survey

U.S. Department of the Interior
DIRK KEMPTHORNE, SECRETARY

U.S. Geological Survey
Mark D. Myers, Director

U.S. Geological Survey, Reston, Virginia: 2007

For product and ordering information:
World Wide Web: http://www.usgs.gov/pubprod
Telephone: 1-888-ASK-USGS

For more information on the USGS--the Federal source for science about the Earth, its natural and living resources, natural hazards, and the environment:
World Wide Web: http://www.usgs.gov
Telephone: 1-888-ASK-USGS

Any use of trade, product, or firm names is for descriptive purposes only and does not imply endorsement by the U.S. Government.

Although this report is in the public domain, permission must be secured from the individual copyright owners to reproduce any copyrighted materials contained within this report.

Suggested citation:
Sheets, R.A., 2007, Hydrogeologic setting and ground-water flow simulations of the Great Miami Basin Regional Study Area, Ohio, *section 7 of* Paschke, S.S., ed., THydrogeologic settings and ground-water flow simulations for regional studies of the transport of anthropogenic and natural contaminants to public-supply wells—studies begun in 2001: Reston, Va., U.S. Geological Survey Professional Paper 1737–A, pp. 7–1 – 7–23.

Contents

Abstract 7–1
Introduction 7–1
Purpose and Scope 7–1
Study Area Description 7–3
Conceptual Understanding of the Ground-Water System 7–3
Geology 7–3
Ground-Water Occurrence and Aquifer Properties 7–5
Recharge and Discharge 7–5
Ground-Water Flow Directions, Depth to Water, and Hydraulic Gradients 7–5
Ground-Water Quality 7–9
Ground-Water Flow Simulations 7–9
Modeled Area and Spatial Discretization 7–11
Boundary Conditions and Model Stresses 7–11
Aquifer Hydraulic Properties 7–12
Model Calibration 7–12
Comparison of Models 7–12
Model Zonation, Sensitivity Analysis, and Parameter Estimation 7–13
Model-Computed Water Budget 7–18
Simulation of Areas Contributing Recharge to Public-Supply Wells 7–19
Model Limitations and Uncertainties 7–19
References Cited 7–21

Figures

Maps showing:
7.1. Location of the Great Miami River Basin regional study area within the glacial aquifer system. 7–2
7.2. Topograpy, hydrologic features, and locations of public-supply wells, Great Miami River Basin regional study area, Ohio. 7–4
7.3. Generalized geologic and hydrogeologic sections showing (*A*) geology, (*B*) ground-water flow directions, and (*C*) geochemical conditions within the buried valleys around Dayton, Ohio. 7–8
7.4. Map showing location of ground-water flow model grid and parameter-estimation zones, Great Miami River Basin regional study area, Ohio. 7–10
Graphs showing:
7.5. Composite scaled sensitivity of ground-water flow model parameters, Great Miami River Basin regional study area, Ohio. 7–15
7.6. Relation between model-computed and measured hydraulic heads, Great Miami River Basin regional study area, Ohio. 7–16
7.7. Weighted residuals plotted against weighted simulated equivalents, Great Miami River Basin regional study area, Ohio. 7–17
7.8. Map showing model-computed areas contributing recharge for 60 public-supply wells, Great Miami River Basin regional study area, Ohio. 7–20

Tables

7.1. Summary of hydrogeologic and ground-water quality characteristics for the glacial aquifer system and the Great Miami River Basin regional study area, Ohio. 7–6
7.2. Comparison of root-mean-squared error and mean-absolute difference of model-computed and measured hydraulic heads between the original ground-water flow model and the revised parameter-estimation model, Great Miami River Basin regional study area, Ohio. 7–13
7.3. Comparison of model-computed and measured streamflow gains or losses between the original ground-water flow model and the revised parameter-estimation model, Great Miami River Basin regional study area, Ohio. 7–14
7.4. Parameters used in construction of the revised parameter-estimation ground-water flow model, Great Miami River Basin regional study area, Ohio. 7–14
7.5. Root-mean-squared error and mean-absolute difference between model-computed and measured hydraulic heads in the revised parameter-estimation ground-water flow model, Great Miami River Basin regional study area, Ohio. 7–17
7.6. Comparison of model-computed and measured streamflow gains or losses between the original ground-water flow model and the revised parameter-estimation model, Great Miami River Basin regional study area, Ohio. 7–18
7.7. Water budget computed by the revised parameter-estimation model for 1997–2001 average conditions, Great Miami River Basin regional study area, Ohio. 7–18

Hydrogeologic Setting and Ground-Water Flow Simulations of the Great Miami River Basin Regional Study Area, Ohio

By Rodney A. Sheets

Abstract

The transport of anthropogenic and natural contaminants to public-supply wells was evaluated for the glacially derived valley-fill aquifer underlying the Great Miami River and its tributaries near Dayton, Ohio, as part of the U.S. Geological Survey National Water-Quality Assessment Program. The glacial valley-fill aquifer in the Great Miami River regional study area is representative of the glacial aquifer system in the North-Central United States. Water needs in the study area for industry, agriculture, and public water supply are met almost entirely by pumping from the glacial aquifer, and the aquifer is susceptible and vulnerable to contamination. An existing three-layer, steady-state ground-water flow model of the study area was modified to include some bedrock islands within the glacial valleys and recalibrated with parameter estimation to represent average ground-water flow conditions for the period from 1997 to 2001. The calibrated model and advective particle-tracking simulations were used to compute areas contributing recharge and traveltimes from recharge areas to 60 public-supply wells. Model results indicate streamflow loss from streams (39 percent of inflow) and precipitation (39 percent of inflow) provide most of the ground-water inflow, while the majority of ground-water discharge is to pumping wells (53 percent of outflow) and gaining stream reaches (40 percent of outflow). Median simulated traveltimes from recharge areas to wells ranged from 21 days to 184 years. Approximately 73 percent of the traveltimes were less than 25 years indicating water quality in the aquifer is susceptible to the affects of overlying land use.

Introduction

The Great Miami River Basin regional study area for the transport of anthropogenic and natural contaminants to public-supply wells (TANC) study is located in the east-central portion of the White River-Great and Little Miami River Basin National Water-Quality Assessment (NAWQA) study unit (fig. 7.1). Nationwide, the glacial aquifer system is the largest in areal extent of any principal aquifer and is an important source of water for public water supply providing public and domestic water for approximately 41 million people in 2000 (Warner and Arnold, 2005).

Purpose and Scope

The purpose of this Professional Paper section is to present the hydrogeologic setting of the Great Miami River Basin regional study area. The section also documents the setup and calibration of a steady-state regional ground-water flow model for the study area. Ground-water flow characteristics, pumping-well information, and water-quality data were compiled from existing data to develop a conceptual understanding of ground-water conditions in the study area. An existing ground-water flow model was modified to include some bedrock islands within the glacial valleys and was recalibrated with parameter estimation to represent average conditions for the period from 1997 to 2001. The 5-year period 1997–2001 was selected for data compilation and modeling exercises for all TANC regional study areas to facilitate future comparisons between study areas. The recalibrated ground-water flow model and associated particle tracking were used to simulate advective ground-water flow paths and to delineate areas contributing recharge to selected public-supply wells. Ground-water traveltimes from recharge to public-supply wells, oxidation-reduction (redox) conditions along flow paths, and the presence of potential contaminant sources in areas contributing recharge were tabulated into a relational database as described in Section 1 of this Professional Paper. This section provides the foundation for future ground-water susceptibility and vulnerability analyses of the study area and comparisons among regional aquifer systems.

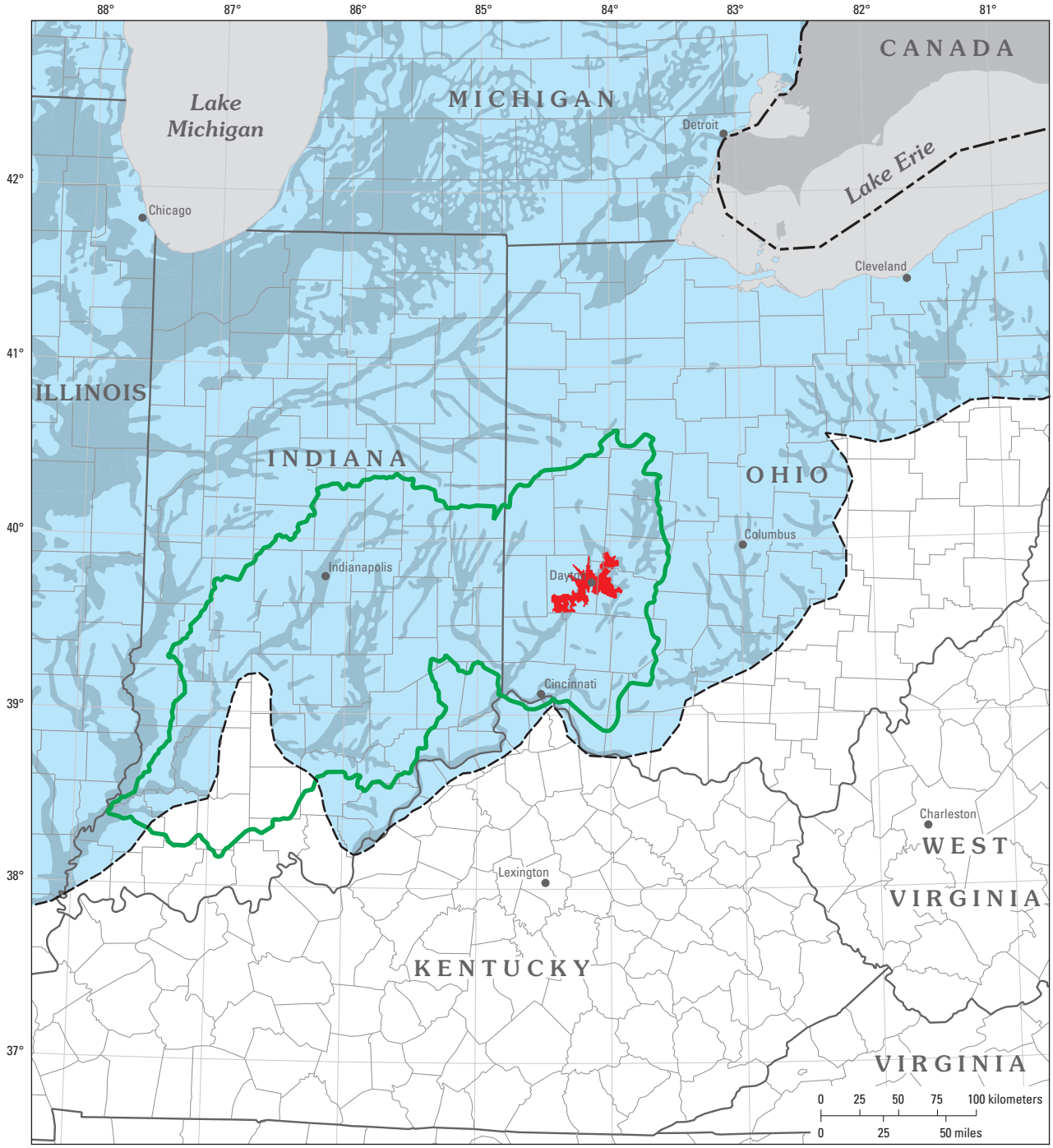

Base from U.S. Geological Survey digital data, 1:2,000,000, 1972, Albers equal-area projection

EXPLANATION

- **Great Miami River Basin regional study area**
- **Glacial deposits aquifer**—Darker areas represent sand, gravel, and valley-fill aquifers locally
- **USGS NAWQA study unit**—White River-Great and Little Miami River Basins
- **Southern limit of Pleistocene continental glaciation**

Figure 7.1. Location of the Great Miami River Basin regional study area within the glacial aquifer system.

Study Area Description

The study area is centered on the city of Dayton, Ohio (fig. 7.2), and examines the effects of pumping unconfined ground water from the unconsolidated, glacially derived valley-fill aquifer underlying the Great Miami River and its tributaries. The Great Miami River Basin regional study area represents the glacial aquifer system (Warner and Arnold, 2005) in the North-Central United States (table 7.1) with ground water occurring in the valley-fill glacial aquifer underlying the Great Miami River and its tributaries. The study area includes the confluence of the Great Miami River and Mad River at Dayton (1,700 km^2) and several tributaries to the Great Miami River, including the Stillwater River (1,750 km^2). The study area also includes the parts of the upper Little Miami River drainage basin. In the Great Miami River Basin regional study area, water needs for industry, agriculture, and public water supply are met almost entirely by pumping from the glacial aquifer.

The primary aquifer within the study area consists of Quaternary glacial deposits overlying Ordovician and Silurian bedrock (Dumouchelle, 1998). The glacial deposits are primarily a result of glacial meltwater or outwash deposits left by retreating continental glaciers. The most productive aquifers in the White-Miami study unit are those that were deposited in buried-valley settings underlying the Great Miami River (fig. 7.2). The buried-valley aquifer in the study area is heavily used by industry and municipalities with well yields commonly greater than 5,300 m^3/d (Dumouchelle, 1998). These high pumping rates often induce infiltration from nearby rivers or artificial recharge lagoons. The buried-valley aquifer has been designated a Sole-Source Aquifer by the U.S. Environmental Protection Agency (Debrewer and others, 2000). Low permeability Ordovician shale with well yields less than approximately 6 m^3/d underlies the buried-valley aquifer beneath most of the study area; Silurian limestone and dolomite form a thin carbonate aquifer that underlies the buried-valley aquifer in the higher elevations of the study area (Dumouchelle, 1998).

The study area is in the Till Plains section of the Central Lowland Physiographic Province. The topography of the till plains was formed by several continental glaciations resulting in a flat to gently rolling land surface (Fenneman, 1938). Bedrock features formed by pre- and periglacial drainage systems were buried under the glacial deposits (Dumouchelle, 1998). In areas where modern rivers dissect the land surface, topographic relief is low to moderate, with steep-walled valleys formed by the river drainages. Surface drainage through the study area is from north to south, toward the Ohio River. Average annual precipitation is 96.5 cm (Harstine, 1991).

Even though Dayton lies near the center of the study area (fig. 7.2), approximately 44 percent of the land use in the study area (2001) is agricultural (row crops, pasture, and so forth); about 41 percent of the land use in the study area is developed. Primarily, the upper reaches of the subbasins are agricultural, and the areas along the main drainages are suburban to urban. The remaining land uses are forested or grasslands (13 percent) and wetlands, quarries, or open water (2 percent) (Homer and others, 2004).

Water use in the study area consists almost entirely of ground-water supplies for domestic, agricultural, industrial and public-supply users. In 1993, Dayton supplied approximately 285,000 m^3/d of water to the areas in and around the city with two well fields (Dumouchelle, 1998). The Dayton Rohrers' Island well field lies along the Mad River, just south of Wright Patterson Air Force Base, and supplied approximately 190,000 m^3/d. The Miami River well field, the second Dayton well field, is located along the Great Miami River and consists of about 50 wells that pumped ground water at the rate of approximately 95,000 m^3/d in 1993. The remaining water use in the study area, approximately 245,000 m^3/d, is provided by other public ground-water supplies (for example, Wright Patterson Air Force Base, smaller cities, and hospitals), industrial ground-water supplies, and agricultural ground-water supplies (Dumouchelle, 1998).

Conceptual Understanding of the Ground-Water System

Ground-water flow is controlled by the geology and the hydraulic properties of the geologic materials. Areal recharge and discharge to streams in this system are the primary inputs and outputs to this system; the ground-water chemistry seems to be controlled by the residence time (from recharge to discharge) and geology. The generalized geologic section in figure 7.3 illustrates features of the conceptual model for the Dayton study area.

Geology

Surficial geology of the study area is dominated by Wisconsinan glacial deposits. Glacial till (ground moraine) covers most of the bedrock in upland areas. The clay-rich tills are unstratified and poorly sorted; grain size ranges from clay size to boulders. Some thin gravel deposits can be found interspersed within the till cover.

Glacial deposits cover the bedrock in the buried river valleys. Illinoian glacial deposits may underlie the Wisconsinan deposits in the deepest areas of the buried valleys (Dumouchelle, 1998). The glacial deposits range from fine-grained sand to gravel with some glacial till interspersed within as sheets that sometimes extend across the buried valleys (Dumouchelle, 1998).

The buried-valley floor and walls consist of Late Ordovician interbedded shale and limestone and form the base of the buried-valley aquifer. The limestone beds typically are thin—from less than a centimeter to several centimeters thick, and typically account for about 25 percent of the Ordovician rocks (Eberts and George, 2000). In upland areas, the Brassfield Formation (Early Silurian) overlies the Ordovician rocks

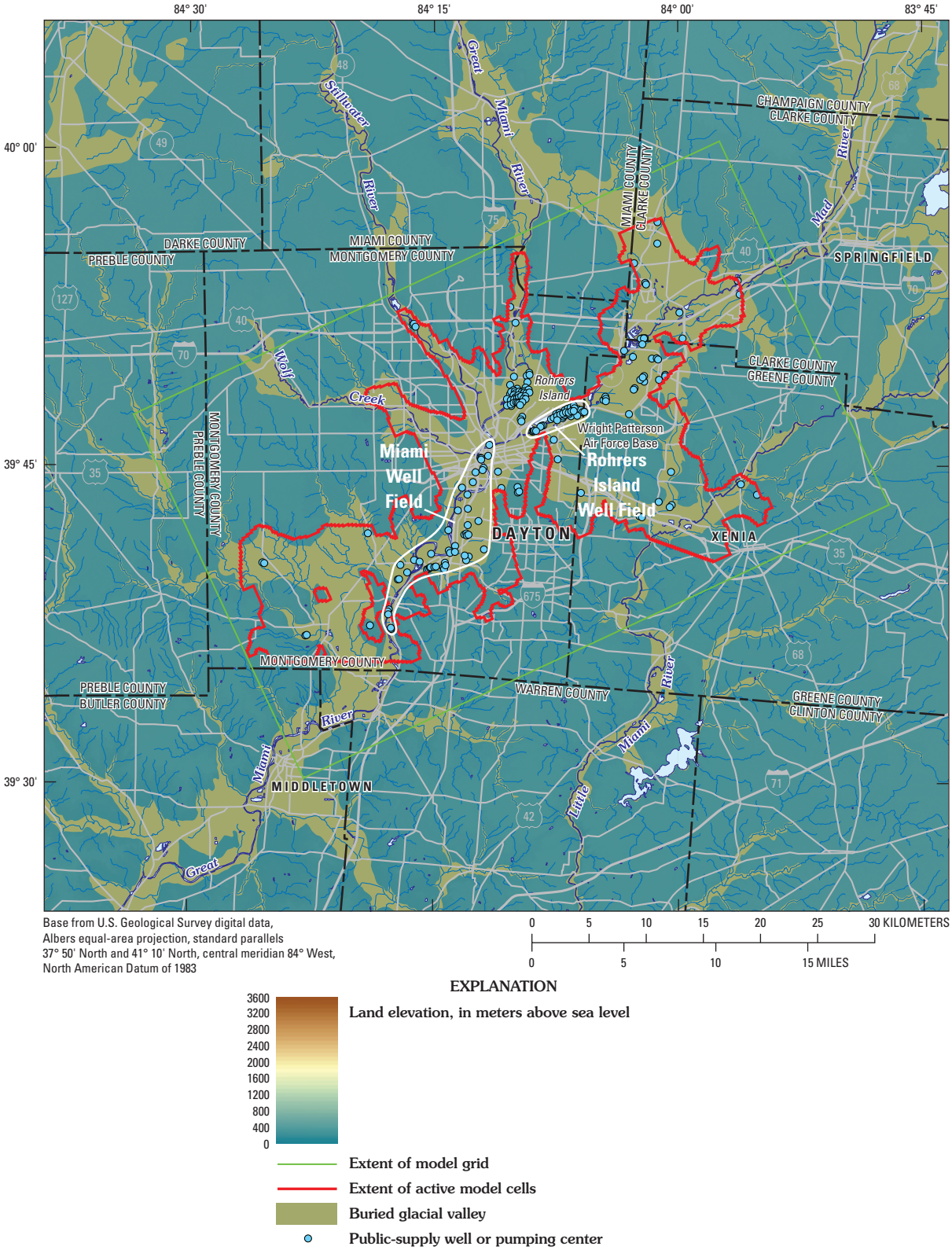

Figure 7.2. Topography, hydrologic features, and locations of public-supply wells, Great Miami River Basin regional study area, Ohio.

(Dumouchelle, 1998). The Brassfield Formation consists of fossiliferous, fine-grained limestone beds that range from massive to irregularly bedded (Sheets and Yost, 1994). Overlying the Brassfield Formation in the study area are thinly bedded Silurian shale and limestone formations.

The study area lies over the axis of the Cincinnati arch, a bedrock high formed between the Appalachian and Illinois Basins (Casey, 1994, 1997). The bedrock at the axis of the arch essentially has zero dip.

Ground-Water Occurrence and Aquifer Properties

The clay-rich tills that cover the upland areas in the study area are generally thin (less than 9 m) and poorly permeable–wells completed in these units yield from 11 to 65 m^3/d (Norris and others, 1948, 1950; Schmidt, 1986, 1991). Vertical hydraulic conductivity of the till ranges from approximately 4 $X10^{-3}$ to 43 m/d (Dumouchelle, 1998). Typically, wells in the upland unconsolidated deposits are completed in sand "stringers." Ground-water flow in the upland unconsolidated deposits is toward small streams or local pumping centers.

The coarse sand and gravels in the glacial deposits are as much as 90 m thick in the center of the valleys and yield as much as 11,500 m^3/d of water to wells (Norris and others, 1950). Hydraulic conductivities range from 860 to $1.X10^6$ m/d (Dumouchelle, 1998, table 2) based on more than 30 multiple-well aquifer tests. Transmissivities have been reported as much as 65,000 m^2/d but generally range from 280 to 6,500 m^2/d (Dumouchelle, 1998). Where laterally continuous tills are present within the glacial deposits, the outwash deposits are separated into two or more aquifers, and the lower aquifers may be confined or semiconfined by the till layers (Norris and Spieker, 1966). Porosity in the glacial deposits has been estimated from 0.15 to 0.25 (Cunningham and others, 1994; Sheets and others, 1998). In the absence of pumping, ground-water flow in the glacial deposits is lateral and upward toward the major streams in the valleys. Ground-water flow can be reversed and streams can lose water to the aquifer near areas such as Dayton where pumping rates are large.

Generally, the Ordovician bedrock is not considered an aquifer—most wells drilled into these rocks yield less than 6 m^3/day and drawdown is generally very large (Dumouchelle, 1998). Only near the subcrop of the Ordovician units, where weathering has created some secondary permeability in fractures and bedding planes, is the permeability high enough to support localized domestic water supplies (hydraulic conductivity of approximately 430 m/d; Dumouchelle and others, 1993). Sheets and others (1998) showed that excess radiogenic helium found in ^{3}Hydrogen-^{3}Helium samples might indicate some ground-water flow from the Ordovician bedrock through the valley walls and into the glacial deposits (fig. 7.3). Wells in the Brassfield Formation and overlying formations ordinarily yield about 30 to 90 m^3/d, which is generally adequate for domestic water supplies in the uplands (Sheets and Yost, 1994). Springs occur at the base of the Brassfield Formation and at the top of the shale units above the Brassfield (Sheets and Yost, 1994).

Recharge and Discharge

Recharge to the Great Miami River Basin regional study area is primarily through direct precipitation and infiltration, but recharge also occurs from surface-water infiltration and inflow from bedrock (Dumouchelle, 1998). Recharge estimates for the glacial deposits are from water-budget analyses (31.5 cm/yr; Walton and Scudder, 1960), recession-curve analyses (31.5 to 40.0 cm/yr; Dumouchelle and others, 1993) and ground-water flow modeling (8 to 31 cm/yr; Dumouchelle and others, 1993; Dumouchelle, 1998). Recharge estimates for the upland areas (2.5 to 15 cm/yr) are lower than estimates for the glacial deposits because of lower permeability soils and till (Sheets, 1994). Particle-tracking analyses show the majority of recharge to the ground-water system is from direct precipitation and infiltration to the glacial deposits and from the upland areas (Cunningham and others, 1994). Additional sources of recharge are induced infiltration from streams near pumping wells and, to a much lesser extent, inflow from the Ordovician bedrock. Some recharge to the ground-water flow systems occurs at the boundary between the valleys and the bedrock hills, where surface-water runoff flows from the low-permeability tills to much higher permeability glacial deposits (Sheets, 1994; Dumouchelle, 1998). Recharge to the glacial deposits from bedrock is generally considered negligible, relative to the amount of recharge from other sources (Dumouchelle, 1998).

Under natural flow conditions, the major streams and rivers within the glacial deposits are the primary discharge areas for the regional ground-water flow system (Yost, 1995; Dumouchelle, 1998; Sheets, 1994). However, ground water in the study area is heavily pumped for water supply, and this pumping locally alters natural ground-water flow conditions in the glacial deposits. Because most of the large pumping centers are near the major cities and rivers (for example, Dayton), induced infiltration from streams lessens the effect of pumping on regional ground-water flow.

Ground-Water Flow Directions, Depth to Water, and Hydraulic Gradients

Dumouchelle (1998) compiled water-level data from 678 wells to assess ground-water levels and flow directions in the buried-valley aquifer for September 1993. Wells were completed at varying depths within the glacial deposits. Ground-water flow directions in the buried-valley aquifer are generally toward the major rivers and downvalley toward the south/southwest. Horizontal hydraulic-head gradients in the center part of the buried valley and away from the discharge areas (rivers, pumping centers) are approximately 0.0006 m/m; in pumping areas (Miami Well Field, for example) horizon-

Table 7.1. Summary of hydrogeologic and ground-water-quality characteristics for the glacial aquifer system and the Great Miami River Basin regional study area, Ohio.

[m, meters; cm/yr, centimeters per year; m^3/s, cubic meters per second; m^3/d, cubic meters per day; km, kilometers; Kh, horizontal hydraulic conductivity; Kz, vertical hydraulic conductivity; Sy, specific yield; n, porosity; mg/L, milligrams per liter]

Characteristic	Glacial aquifer system	Great Miami River Basin regional study area
	Geography	
Topography	Relief generally less than 300 m. (Randall, 2001).	Relief approximately 200 m.
Climate	Precipitation 91 to 127 cm/yr; evapotranspiration 46 to 58 cm/yr (Randall, 1996).	Precipitation 100 cm/yr; evapotranspiration up to 67 cm/yr (Harstine, 1991; Debrewer and others, 2000).
Surface-water hydrology	Runoff 41 to 76 cm/yr (Randall, 1996); streamflow varies widely with the size of drainage basin. Water-supply reservoirs and former mill ponds are common in upland and valley settings.	Runoff 31 cm/yr (Debrewer and others, 2000); average flow in Great Miami River at Dayton is 96 m^3/s (Shindel, and others, 2002). Some water-supply reservoirs are present in upper reaches.
Land use	Urban, suburban, rural residential, woodlands, farmland.	Urban, suburban, rural residential, woodlands, farmland.
Water use	Potential aquifer yields generally less than 60,500 m^3/d (Kontis and others, 2004).	Pumpage for public supply about 510,000 m^3/d. Aquifer yields range from 300 to as much as 11,000 m^3/d (Dumouchelle, 1998).
	Geology	
Surficial geology	Glacially-derived sand and gravel in valleys that slope away from retreating ice sheets; limited fine-grained deposits; till prevalent in uplands but discontinuous under valley fill (Randall and others, 1988; Randall, 2001).	Mainly glacial alluvial sand and gravel in buried bedrock valleys; till covers uplands and is interspersed in valley fill (Dumouchelle, 1998).
Bedrock geology	Crystalline granitic and metamorphic rocks and sedimentary rocks; limited carbonate rocks (Randall, 2001; Randall and others, 1988).	Uplands underlain by limestone/dolomite; buried valleys underlain by shales and limestones (Dumouchelle, 1998).
	Ground-water hydrology	
Aquifer conditions	Valley-fill aquifers that are generally less than 2.5 km wide and are unconfined; valley fill generally less than 67 m thick; depth to water generally less than 15 m. Streams that cross valley fill from upland areas are commonly sources of recharge; pumping near surface water commonly induces infiltration (Kontis and others, 2004).	A valley-fill aquifer that is generally less than 3 km wide and unconfined; valley fill generally less than 100 m thick; depth to water generally less than 15 m. Areal recharge dominates with some leakage in from bedrock. Induced infiltration from streams where pumping is nearby.

Table 7.1. Summary of hydrogeologic and ground-water-quality characteristics for the glacial aquifer system and the Great Miami River Basin regional study area, Ohio.—Continued

[m, meters; cm/yr, centimeters per year; m^3/s, cubic meters per second; m^3/d, cubic meters per day; km, kilometers; Kh, horizontal hydraulic conductivity; Kz, vertical hydraulic conductivity; Sy, specific yield; n, porosity; mg/L, milligrams per liter;]

Characteristic	Glacial aquifer system	Great Miami River Basin regional study area
Hydraulic properties	Valley fill: Kh=6 to 150 m/d; Kh/Kz=10:1 (commonly); n=0.3 to 0.4; Sy=0.2 to 0.3 Till: Kh=0.003 to 3 m/d; Kh/Kz=1; n=0.1 to 0.3; Sy=0.04 to 0.28 Bedrock: Kh=0.003 to 0.3 m/d; Kh/Kz (limited information); n=0.005 to 0.02; Sy=0.0001 to 0.005 (Randall and others, 1988; Bradbury and others, 1991; Melvin and others, 1992; Gburek and others, 1999).	Valley fill: Kh=0.1 to 150 m/d; n=0.15 to 0.25; Kh/Kz estimated at10:1. Till: Kh=0.02 to 3 m/d; n=0.15 to 0.25 Bedrock: K=0.001–1.5 m/d. (Dumouchelle, 1998; Sheets and others, 1998).
Ground-water hydrology—Continued		
Ground-water budget	Recharge to valley fill from infiltration of precipitation, 36 to 76 cm/yr. Recharge to valley fill from upland runoff often exceeds recharge from precipitation. (Kontis and others, 2004; Morrissey and others, 1988). Pumpage generally less than 15 percent of water budget; most discharge is to streams (Morrissey, 1983; Tepper and others, 1990; Dickerman and others, 1990; Dickerman and others, 1997; Mullaney and Grady, 1997; Starn and others, 2000; Barlow and Dickerman, 2001; DeSimone and others, 2002.)	Recharge to valley fill from infiltration of precipitation, 8 to 40 cm/yr. Recharge increases along valley walls from upland runoff. Pumpage for public supply greater than 25 percent of water budget; where induced infiltration doesn't occur, most ground water discharges to streams. (Dumouchelle, 1998).
Ground-water quality		
	Dissolved solids less than 150 mg/L in crystalline-rock terrains and greater than 150 mg/L in sedimentary-rock terrains; pH, 6–8; oxic. Calcium and bicarbonate are the principal ions (Rogers, 1989). Redox conditions not defined regionally.	Calcium and bicarbonate are the principal dissolved ions. Redox conditions are typically oxic in shallow valley fill, suboxic to anoxic in deep valley fill and in bedrock (Rowe and others, 1999; this study).

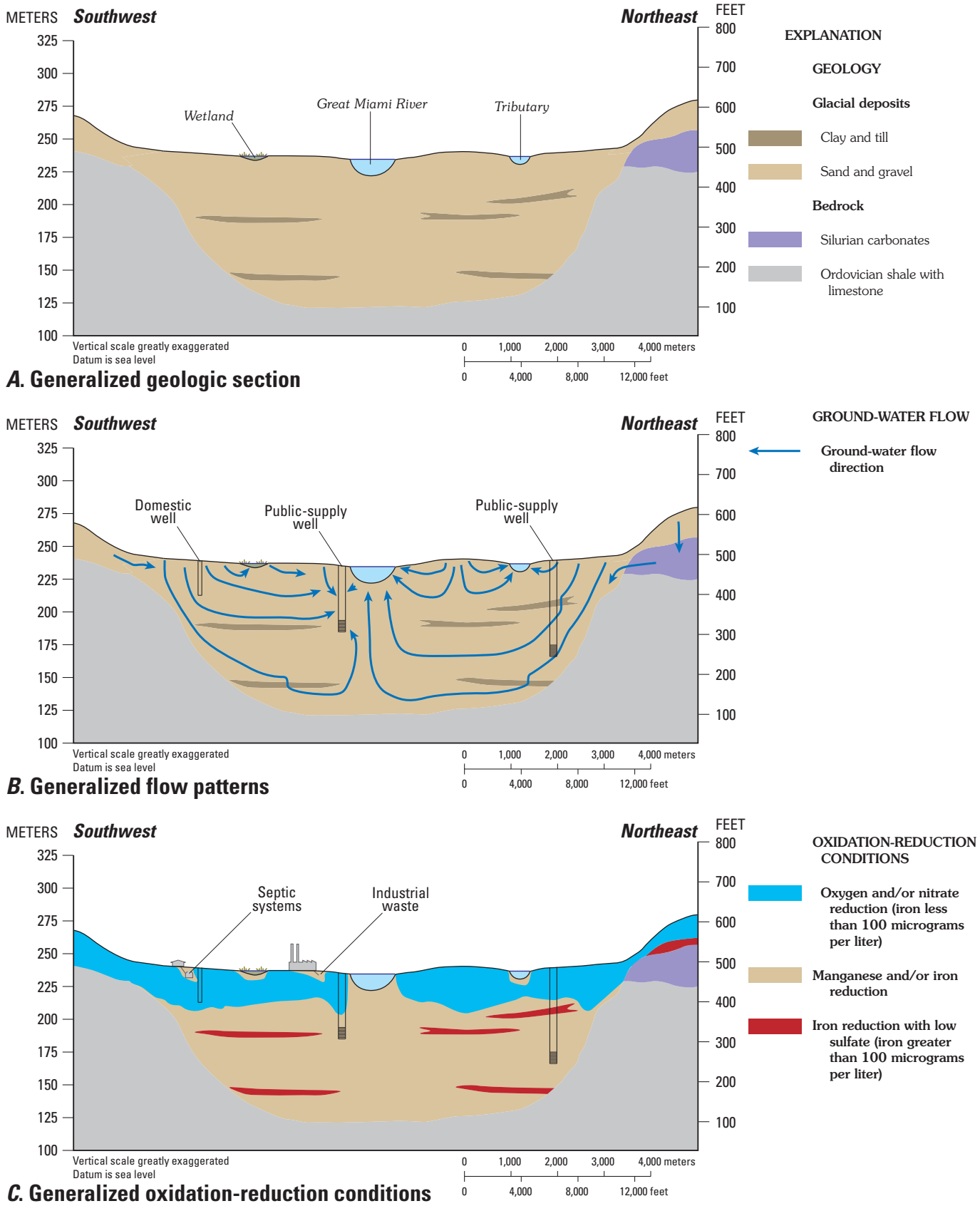

Figure 7.3. (*A*) geology, (*B*) ground-water flow directions, and (*C*) geochemical conditions within the buried valleys around Dayton, Ohio.

tal hydraulic-head gradients are about 0.001 m/m. Near the edge of the buried valley, adjacent to the uplands, horizontal hydraulic-head gradients commonly are greater than 0.0003 m/m.

Water levels for the uplands were not measured by Dumouchelle (1998), but previous work at Wright Patterson Air Force Base indicates the ground-water potentiometric-head surface mimics land-surface topography in the uplands (Schalk, 1992). Ground water flows roughly radial off of upland highs and toward the center of the major river valleys (Dumouchelle, 1998).

Because the ground-water and surface-water systems are generally connected in the study area, depth to ground water often is directly related to land-surface topography. Near the rivers and streams, depth to ground water commonly is just a few feet. Away from the rivers, as elevation increases, depth to ground water generally increases; maximum depth to water away from the river is approximately 15 m, under natural conditions. In areas of heavy pumping, depth to water can be greater than 30 m. The saturated thickness of the buried-valley aquifer also varies in relation to proximity to the axis of the buried valley and in relation to pumping centers. Near the axis of the valley, the maximum depth to bedrock is approximately 90 m; therefore, the maximum buried-valley aquifer saturated thickness is about 80 m. Depth to water in the upland bedrock aquifer is generally between 6 and 9 m (Schalk, 1992). Saturated thickness of the upland bedrock aquifer also varies in relation to topography but generally is about 15 m.

Ground-Water Quality

Ground-water quality in the study area has been divided into two compositional groups—calcium-magnesium-bicarbonate (Ca-Mg-HCO_3) and sodium-chloride (NaCl) type waters (Lloyd and Lyke, 1995; Dumouchelle and others, 1993; Debrewer and others, 2000). Water from the unconsolidated deposits is predominantly Ca-Mg-HCO_3, and water from the bedrock ranges from NaCl to Ca-Mg-HCO_3 type water.

Within the unconsolidated deposits, only subtle variations in major cation concentrations were observed between shallow, intermediate, and deep wells (Dumouchelle and others, 1993). Shallow ground water (less than 18 m below land surface) had higher mean temperatures, specific conductances, and dissolved-solids concentrations than ground water from deep (20 to 70 m below land surface) wells. Median ground-water pH from the unconsolidated deposits was 7.3.

Ground water from the bedrock deposits in the study area varies greatly in its composition. Ordovician shale produces exclusively NaCl-type water with highly variable calcium, magnesium, and bicarbonate concentrations. Median pH of bedrock ground water from Ordovician shale was 7.4. Ground-water quality in the Brassfield limestone, however, is similar to ground-water quality in the glacial deposits consisting of Ca-Mg-HCO_3 type water with a similar pH range of 7.1 to 7.6 (Dumouchelle and others, 1993).

Dissolved oxygen is typically present only in ground water from the shallow glacial deposits (Dumouchelle and others, 1993). Bedrock wells rarely yield water with any measurable dissolved oxygen (greater than 0.1 mg/L). The dissolved oxygen in the shallow aquifers tends to react quickly with organic material in glacial sediments and causes reducing conditions that promote dissolution of iron and manganese oxyhydroxide minerals. Under these low-oxygen and circumneutral pH conditions that are typical of the buried-valley sediments, iron or manganese concentrations can increase in excess of several milligrams per liter (Debrewer and others, 2000). Ground-water concentrations of nitrate greater than a few milligrams per liter are present in shallow, oxygenated parts of the buried-valley aquifers (Debrewer and others, 2000; fig. 7.3), which also are characterized by relatively short ground-water residence times (less than 5 to 10 years) (Rowe and others, 1999). Nitrate in the shallow parts of aquifers in the study area can be reduced to nitrogen gas by denitrification processes as ground-water flows from the oxygenated recharge areas to iron-reducing parts of the buried-valley aquifer (Rowe and others, 1999; fig. 7.3).

Ground-Water Flow Simulations

A numerical ground-water flow model was developed for the glacial deposits in the Great Miami River Basin regional study area by Dumouchelle (1998) (fig. 7.4). Revisions to the steady-state model were made during this study. The following is a brief description of the previously developed model including the original modeled area, boundary conditions, aquifer properties, model stresses, modifications to the original model, and rationale for the changes.

The original model was developed using MODFLOW88 (McDonald and Harbaugh, 1988), MODFLOWARC (Orzol and McGrath, 1992), and ARC/INFO (Environmental Systems Research Institute, 1987). For this study, the model input parameters were translated into files compatible with MODFLOW-2000 (Harbaugh and others, 2000; Hill and others, 2000) using MODFLOW-GUI (Shapiro and others, 1997; Winston, 2000), a graphical user interface for MODFLOW-2000 (Argus Interware, 1997).

The original conceptual model was largely based on previous hydrogeologic investigations and analysis of modeling performed at Wright Patterson Air Force Base (Dumouchelle, 1998). The original model simulated ground-water flow only in the buried-valley aquifer because the underlying Ordovician bedrock and bedrock uplands were not considered significant sources of water to the buried-valley aquifer. The buried-valley aquifer was simulated using three model layers of varying thickness, and the till layers within the aquifer were represented implicitly by reducing horizontal and vertical hydraulic conductivity in locations where tills are present (Dumouchelle, 1998).

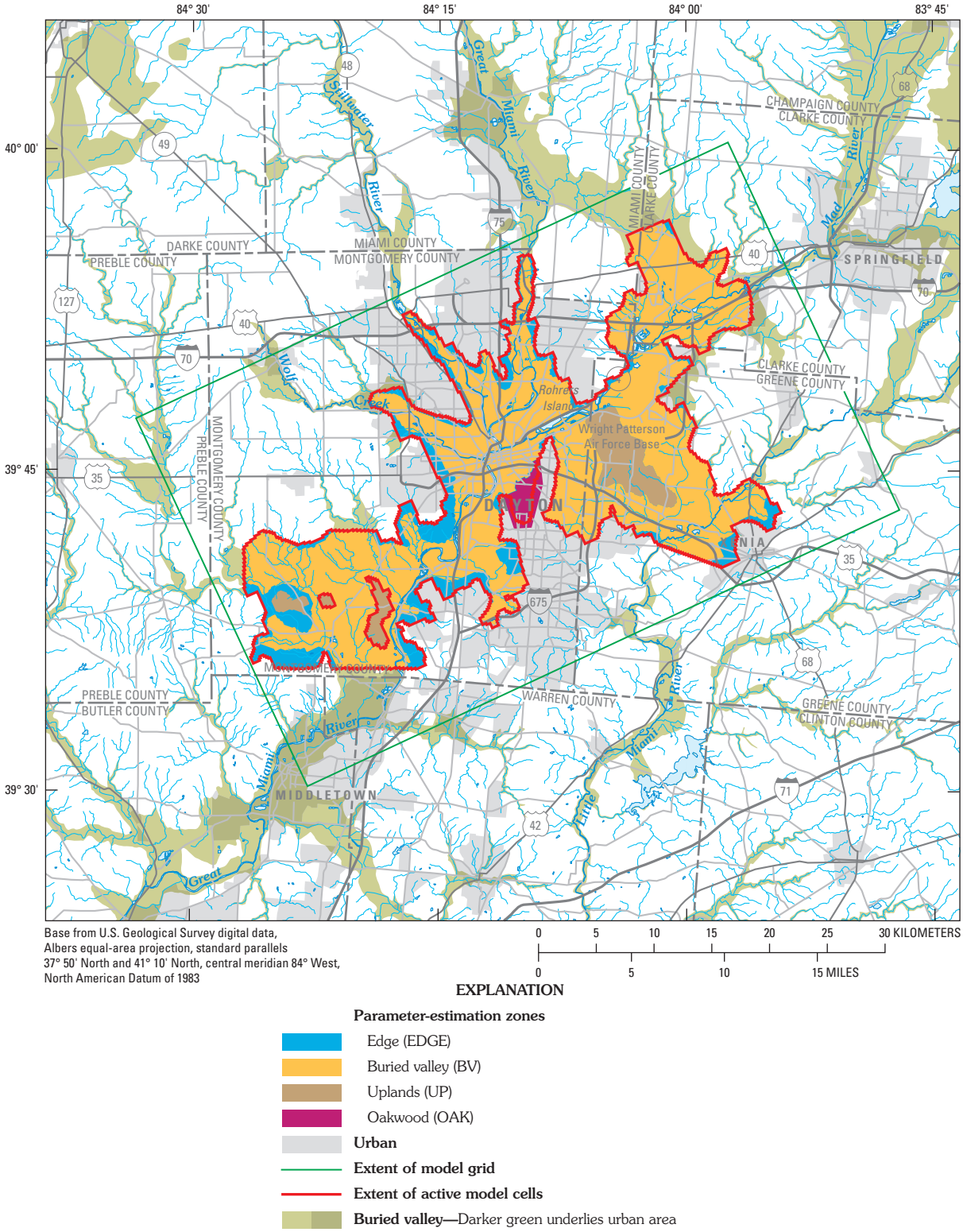

Figure 7.4. Location of ground-water flow model grid and parameter-estimation zones, Great Miami River Basin regional study area, Ohio.

The original model extended laterally to the 800-ft topographic contour around the valley because this contour roughly approximates the knick point between the land surface of the river valleys and the uplands. In some areas, the model was extended into the uplands to account for substantial (greater than 15 m) thickness of sand and gravel deposits (Dumouchelle, 1998). Bedrock islands within the active area of the model (see "Uplands" parameter-estimation zones, fig. 7.4) were not represented in the original model.

The original model simulates steady-state conditions, as observed from water-level and streamflow gain/loss data for late 1993. The revised TANC model simulates these same conditions, as well as those from 1997 through 2001, using water-level data taken from various sources for 1997–2001. The revised model includes two steady-state stress periods with the same model stresses (recharge, river stage and conductance, and so forth) as the original model, except that pumping rates were updated for 1997–2001.

Modeled Area and Spatial Discretization

The original active modeled area covers approximately 620 km^2 and is shown in figure 7.4. The original finite-difference model grid was spatially discretized into 230 rows and 370 columns, corresponding to cells 152.4 m on each side. The model grid was oriented 25 degrees north of east. The original model grid spacing and orientation were not changed by this study.

The ground-water flow system was simulated using three model layers. Layer 1 is simulated as unconfined, with the top representing the ground-water surface and bottom set to the altitude of the uppermost clay layer, an equivalent altitude to the clay layer, or the bedrock surface. Layers 2 and 3 were simulated as confined. The bottom of layer 2 was set to approximately 46 m below the estimated water level or the bedrock altitude. The bedrock valley floor defined the bottom of layer 3 (Dumouchelle, 1998). The vertical connection between model layers was simulated by a vertical leakance parameter.

Boundary Conditions and Model Stresses

No-flow boundaries were used to simulate the Ordovician bedrock-valley walls and floor (Dumouchelle, 1998). The steepness of the valley walls created some numerical instabilities in the original (and revised) model, as narrow or very thin model layers were created during the automatic population of the model grid using MODFLOWARC. Numerical instabilities occurred at the junction between the buried-valley aquifer and uplands or near the four upland "islands" within the modeled area (see "Uplands" parameter estimation zones in fig. 7.4). Similar problems occurred after transferring the model to Argus (Argus Interware, 1997). To decrease numerical instability, the four bedrock islands were simulated using hydraulic conductivities and recharge rates comparable to those given by Sheets and others (1998), who demonstrated that changing the conceptualization of bedrock hills in the Dayton area can improve calibration of numerical ground-water flow models.

Numerical instability in the original model also occurred in the vicinity of the city of Oakwood (fig. 7.4). The Oakwood wells are located in a "hanging valley"—a glacially formed valley that is higher in altitude than the primary buried valley. This area was originally simulated as two layers, with pumping primarily in the second (lower) layer. In the revised model, the Oakwood area was modified to include only one active model layer, and hydraulic conductivity of the layer was assigned as a composite of the original two layers.

At several locations along the edge of the active model layers, specified-head boundaries were used to represent downvalley flow into or out of the modeled area. Specified-head boundaries were typically located in narrow sections of bedrock valleys and far away from the pumping areas, to minimize the effect of boundaries on the simulations (Dumouchelle, 1998). The specified-head boundaries remained unchanged in the revised model.

Stresses on the aquifer system consisted of recharge, rivers, drains, and pumping/recharging wells. The original and revised models are nearly identical in terms of how recharge (except for the bedrock islands), rivers, and drains are simulated. After calibration, recharge in the original model ranged from 15 to 31.0 cm/yr. During the transfer from ARC/INFO to Argus in the revised model, recharge was increased by a small percentage (less than 10 percent) in some model cells near the valley walls to increase numerical stability.

Rivers and larger streams were simulated with the MODFLOW River package (McDonald and Harbaugh, 1988). River stage and river-bottom altitude were obtained by surveying, supplied survey data, U.S. Geological Survey (USGS) topographic maps, or estimates from Geographic Information Systems (GIS) (Dumouchelle, 1998) and were unchanged in the revised model. Values of riverbed hydraulic conductivity for the rivers and streams in the model ranged from 0.09 to 4.3 m/d (Dumouchelle, 1998, p. 20). Drains were used to simulate many streams in the study area, specifically those marked as intermittent on USGS topographic maps. Drains can only remove water from the system, using a drain conductance value (McDonald and Harbaugh, 1988). Drain conductance was not altered from the original model and ranged from 0.0007 to 21.5 m^2/d (most values were 0.003 m^2/d).

In 1993, pumping data were collected for 281 nonresidential pumping wells and 3 recharge wells. As a result of adjustments for model grid size, area, and layering, 187 pumping wells were simulated in the original model at 138 model-cell locations. The total pumping for the original model was approximately 500,000 m^3/d.

Ground-water pumping data for wells in the study area were collected for 1997–2001 from State of Ohio files. Most of these wells were the same as wells simulated in the original model, and well locations, screen lengths, and model grid cells in the revised model were the same as in the original model. Some of the wells in the 1997–2001 data set were previously

unused wells, and the locations and screen lengths were taken from either USGS water-use files (on file at USGS Ohio Water Science Center, Columbus) or Ohio Department of Natural Resource-Division of Water well-log files. In a few cases where inadequate information was obtained from the water-use files, location and screen-length information was obtained from the well owner or a State or local agency. Ground-water pumping data for well fields (for example, Rohrer's Island Well Field) was reported as a single value; the pumping rate for an individual well in the well field was apportioned pumping on a weighted basis of flow, relative to the specific capacity reported. To obtain the pumping rate for a particular well, the total volume reported for the well field was multiplied by the specific capacity of the well divided by the sum of specific capacity for all wells in the well field.

Pumping-rate data for all the wells for 1997–2001 were averaged to obtain average pumping rates representative of the time period. In the revised model, 309 pumping centers were simulated (fig. 7.2); the number of pumping nodes simulated in model layers 1, 2, and 3 were 131, 153, and 25, respectively. The total pumping for the second steady-state stress period of the revised model was approximately 500,000 m^3/d, which is the same as the pumping rate used for the first steady-state stress period, although the spatial distribution of pumping was slightly different for the two different stress periods.

Aquifer Hydraulic Properties

Layer 1 in the original model was simulated as an unconfined layer, and horizontal hydraulic-conductivity values in the original calibrated model ranged from 1.6×10^{-3} to 140 m/d (Dumouchelle, 1998). The lowest values were near the edge of the buried valley near the bedrock subcrop, and the highest values were concentrated in the main valleys (Dumouchelle, 1998). The original model uses the Block-Centered Flow (BCF) package in MODFLOW-96 (Harbaugh and McDonald, 1996). The revised model uses the Layer Property Flow (LPF) in MODFLOW-2000 (Harbaugh and others, 2000). The LPF package requires that an unconfined layer be simulated as convertible between unconfined and confined flow conditions. This does not make an effectual change in the internal solutions to the ground-water flow equation, as the top of layer 1 in the revised model was assigned to the land-surface elevation, and water levels in layer 1 did not rise above land surface.

In the original model, layers 2 and 3 were simulated as confined layers using the BCF package. Assigned transmissivities ranged from 0.09 m^2/d to approximately 3,900 m^2/d in layer 2 and from 0.09 m^2/d to 2,800 m^2/d in layer 3. These transmissivity values represent hydraulic-conductivity values ranging from approximately 1.2×10^{-3} to 1.6×10^{-2} m/d (Dumouchelle, 1998). In the revised model, the LPF package requires that hydraulic conductivity and thickness, not transmissivity, are assigned to grid cells. The original GIS layers of hydraulic conductivity and thickness (tops and bottoms of model layers) were available and were used to assign the appropriate values in the revised model.

A vertical conductance value was used to simulate hydraulic connection between model layers in the original model; the discontinuity of the clay layers did not allow for direct simulation of confining units. In areas where clay layers were present, vertical hydraulic conductivity was set to 3.5×10^{-5} m/d (Dumouchelle, 1998). In areas where no clay layer was present, vertical conductance was calculated using one-tenth of the horizontal hydraulic conductivity, weighted for the thickness of grid cells above and below. In the revised model, the LPF package allowed use of a vertical hydraulic-conductivity value, and vertical hydraulic conductivity was set to one-tenth of the horizontal hydraulic conductivity.

Model Calibration

Calibration of the revised model consisted of several steps including evaluation and reevaluation of input values of hydraulic parameters (as previously discussed), comparisons of original model to revised model output heads and flows, sensitivity analysis, and parameter estimation. With each step of the calibration process, hypotheses about the hydrologic system were tested. Some of these hypotheses tested were local scale (well field) and some were regional scale (buried valley), with the goal of calibrating the model to represent average conditions for 1997–2001.

Comparison of Models

Upon reconstruction of the original model, including modifying the isolated bedrock hills and changing the flow package to accommodate MODFLOW-2000, the model was recalibrated to 1993 conditions. The model calibration to 1993 conditions was evaluated by comparing model-computed and measured hydraulic heads for each layer and comparing model-computed ground-water discharge to gain-loss data collected from selected river reaches. The root-mean-squared error (RMSE) and the mean-absolute difference (MAD), which are statistical measures of the variance and bias, respectively, were used to evaluate the model calibration. The RMSE was calculated as:

$$RMSE = \sqrt{\frac{\sum_{i=1}^{N} (h_{meas} - h_{sim})i^2}{N}}$$

where h_{meas} is the measured hydraulic head, h_{sim} is the model-computed (simulated) hydraulic head, $(h_{meas} - h_{sim})$ is the head residual, and N is the number of wells used in the computation.

The MAD was calculated using:

$$MAD = \frac{\sum_{i=1}^{N} abs(h_{meas} - h_{sim})i}{N}$$

where *abs* indicates the absolute value of the expression. The heads calculated by the ground-water flow model were interpolated to their relative position within the grid cell.

Table 7.2 shows the total number of measured hydraulic-head values changed in all three layers during reconstruction of the original model. In an attempt to isolate the numerical instability in the original model, slight changes were made to the bottom of layer 1, especially in the uplands, which changed the layer in which some head observations and pumping wells were located. In a few locations, observations and wells originally in layer 2 were reassigned to layer 1. In one case, a layer 3 well was reassigned to layer 2. Four pumping wells in the city of Oakwood were changed from layer 2 to layer 1.

The RMSE and MAD values for the revised model are higher for layer 1, nearly the same for layer 2, and somewhat lower for layer 3 than for the original model, and the overall (average) RMSE and MAD are slightly higher for the revised model than for the original model. Differences between model-computed and measured hydraulic heads in the vicinity of the Oakwood pumping wells affected the MAD and RMSE for layer 1 and the entire model. In the original model, the Oakwood measured hydraulic heads were in layer 2, but the measured hydraulic heads were in layer 1 of the revised model; inclusion of these points in layer 1 of the revised model produces a higher RMSE and MAD than the original model. There also was a large difference between model-computed and measured hydraulic heads for the Oakwood well field in the original model, which Dumouchelle (1998) attributed to (1) error in spatial distribution of pumping, (2) large grid size (measured hydraulic heads and pumping well within same cell), (3) measured hydraulic-head location near the pumping wells, or (4) a combination of these and other factors. The same factors likely affected model-computed hydraulic heads in the revised model.

Table 7.3 presents a comparison of model-computed and measured streamflows for the two versions of the model for the first steady-state period. The revised parameter-estimation model-computed streamflow gains and losses were roughly equivalent to those computed by the original model, although the model-computed flow from the original model more closely matched the measured streamflow than the revised model for the Great Miami River from Needmore Road to Railroad and for Little Beaver Creek.

Model Zonation, Sensitivity Analysis, and Parameter Estimation

Because the revised model was constructed with MODFLOW-2000, parameter estimation (Hill and others, 2000) was used to assess and improve performance of the revised model. An additional 34 measured hydraulic-head values were available for 1997–2001, so a second steady-state stress period was added to the model for that period. Some water-level measurements were averaged over the period and some were single measurements. All water-level measurements from both stress periods were weighted according to the range and accuracy of water levels and confidence in measuring average conditions. Some wells were within the immediate influence of drawdown from pumping wells, and water levels from these wells were weighted lower than wells distal from pumping because the distal wells were more representative of regional conditions. Streamflow measurements from 1993 were weighted with a coefficient of variation according to the error in consecutive downstream measurements (based on subjective estimates by the measurement taker; for example, Excellent, 2 percent;

Table 7.2. Comparison of root-mean-squared error and mean-absolute difference of model-computed and measured hydraulic heads between the original ground-water flow model (Dumouchelle, 1998) and the revised parameter-estimation model, Great Miami River basin regional study area, Ohio.

[N, number of observations; RMSE, root-mean-squared error in meters; MAD, mean absolute difference in meters; —, not applicable]

Layer	N (original)	N (modified)	RMSE (original)	RMSE (revised)	MAD (original)	MAD (revised)
1	303	311	2.23	4.88	1.37	2.07
2	259	252	3.08	3.01	1.98	2.10
3	17	16	2.69	2.03	2.07	1.46
Total[1]	579	579	—	—	—	—
Weighted* averages	—	—	2.62	3.99	1.66	2.07

*Total RMSE and MAD values are weighted averages.

Good, 5 percent; Fair, 8 percent; Poor, more than 8 percent [Rantz and others (1982)].

The modeled area was divided into four zones representing different hydrologic conditions to evaluate each area's sensitivity to model input parameters. The four parameter-estimation zones in the revised model are (1) the main buried valley (BV); (2) the edge of the main buried valley, next to the upland areas (EDGE); (3) the newly modified upland areas (UP); and (4) the Oakwood area (OAK) (fig. 7.4). Model sensitivity to the input parameters of horizontal hydraulic conductivity, recharge, river conductance, and vertical hydraulic conductivity are compared among the four parameter-estimation zones.

After reconstructing the original model in MODFLOW-2000 as described in the "Initial Calibration" section, the model input parameters of horizontal and vertical hydraulic conductivity, recharge, and riverbed conductance were parameterized within the MODFLOW-2000 framework. MODFLOW-2000 multiplier arrays were created for each parameter in each layer for each of the two stress periods. The original model output was recreated by using a multiplier value of 1.0 for horizontal hydraulic conductivity in layers 1, 2, and 3 and for recharge in all parameter-estimation zones. A multiplier value of 0.1 was used for vertical hydraulic conductivity to represent vertical hydraulic conductivity as one-tenth of horizontal hydraulic conductivity. The riverbed hydraulic conductivity was also parameterized using the same conductance values as in the original model. A list of parameters used for each parameter-estimation zone is in table 7.4.

Table 7.3. Comparison of model-computed and measured streamflow gains or losses between the original ground-water flow model (Dumouchelle, 1998) and the revised parameter-estimation model, Great Miami River Basin regional study area, Ohio.

[units in m^3/d, cubic meters per day; WPAFB, Wright Patterson Air Force Base]

Stream reach	Streamflow gain or loss (1993)		
	Measured	Model computed (original)	Model computed (revised)
Great Miami River, Taylorsville Dam to Needmore Road	+0.481	–0.139	–0.033
Great Miami River, Needmore Road to Railroad	–0.983	–0.949	+0.0006
Mad River, Huffman Dam to Harshman Road	–2.24	–1.55	–1.45
Little Miami River from Dayton-Xenia Road to Narrows Park	+0.439	+0.425	–0.405
Hebble Creek, WPAFB to Mad River	–0.008	–0.006	–0.006
Little Beaver Creek, Research Road to Factory Road	–0.062	+0.042	+0.031

Table 7.4. Parameters used in construction of the revised parameter-estimation ground-water flow model, Great Miami River Basin regional study area, Ohio.

Parameter	Layer	Main buried valley	Edge of main buried valley	Uplands	Oakwood
Horizontal hydraulic conductivity	1	HK1_BV	HK1_EDGE	HK1_UP	HK1_OAK
	2	HK2	HK2	HK2	HK2
	3	HK3	HK3	HK3	HK3
Vertical hydraulic conductivity	1	VK1	VK1	VK1	VK1
	2	VK2	VK2	VK2	VK2
	3	VK3	VK3	VK3	VK3
Recharge*		RCH_BV	RCH_EDGE	RCH_UP	RCH_OAK
River conductance		RIV_BV		RIV_UP	

*Recharge also was parametized separately for stress period 2 (1997–2001); parameters have a suffix of 2 (for example, RCH_UP2).

The revised model was run in sensitivity mode to determine the relative effect a parameter might have on the weighted residuals (difference between model-computed and measured heads and flows). Figure 7.5 shows the composite scaled sensitivities of all parameters for the two steady-state stress periods. Composite scaled sensitivities are used to evaluate whether the available observations provide enough information for parameter estimation (Hill and others, 2000). The most sensitive parameters in the modified model are shown in red on figure 7.5 and include the horizontal hydraulic conductivity in layer 1 of the main part of the buried valley (HK1_BV), recharge to the buried valley (RCH_BV) and the edges of the buried valley (RCH_EDGE), and the river conductance of that part of the river which overlies the buried valley (RIV_BV). The range of composite scaled sensitivities indicates that parameter estimation should be able to estimate all of the parameters. If the composite scaled sensitivities ranged over an order of magnitude or more, the optimization procedure may have difficulty estimating values for the least sensitive parameters.

All parameters were input to the parameter-estimation mode of MODFLOW-2000 to determine which parameters of the nonlinear regression are highly correlated. Highly correlated parameter pairs are problematic in parameter estimation because of the difficulty in determining unique values for these parameters (Hill and others, 2000). Preliminary results of the nonlinear regression indicate that a few of the values chosen for regression are highly correlated to each other (r^2>0.85). The highly correlated pairs are as follows: HK1_EDGE and RCH_EDGE, and RCH_OAK and HK1_OAK. HK1_EDGE was fixed using an interim value obtained during preliminary model runs; this value was used in the final parameter estimation and was not allowed to vary with the parameter estimation, whereas RCH_EDGE was estimated because it had a somewhat higher composite scaled sensitivity than HK1_EDGE. RCH_OAK and HK1_OAK had relatively low composite scaled sensitivities (fig. 7.5) and were fixed using values obtained during preliminary model runs.

Based on relative sensitivity and correlation of parameters, six parameters (HK1_BV, HK2, RCH_BV, RCH_UP, RCH_EDGE, and RIV_BV) were chosen for final parameter estimation, where the least-squares objective function (derived from the sum of squared, weighted residuals between model-computed and measured values) is minimized using

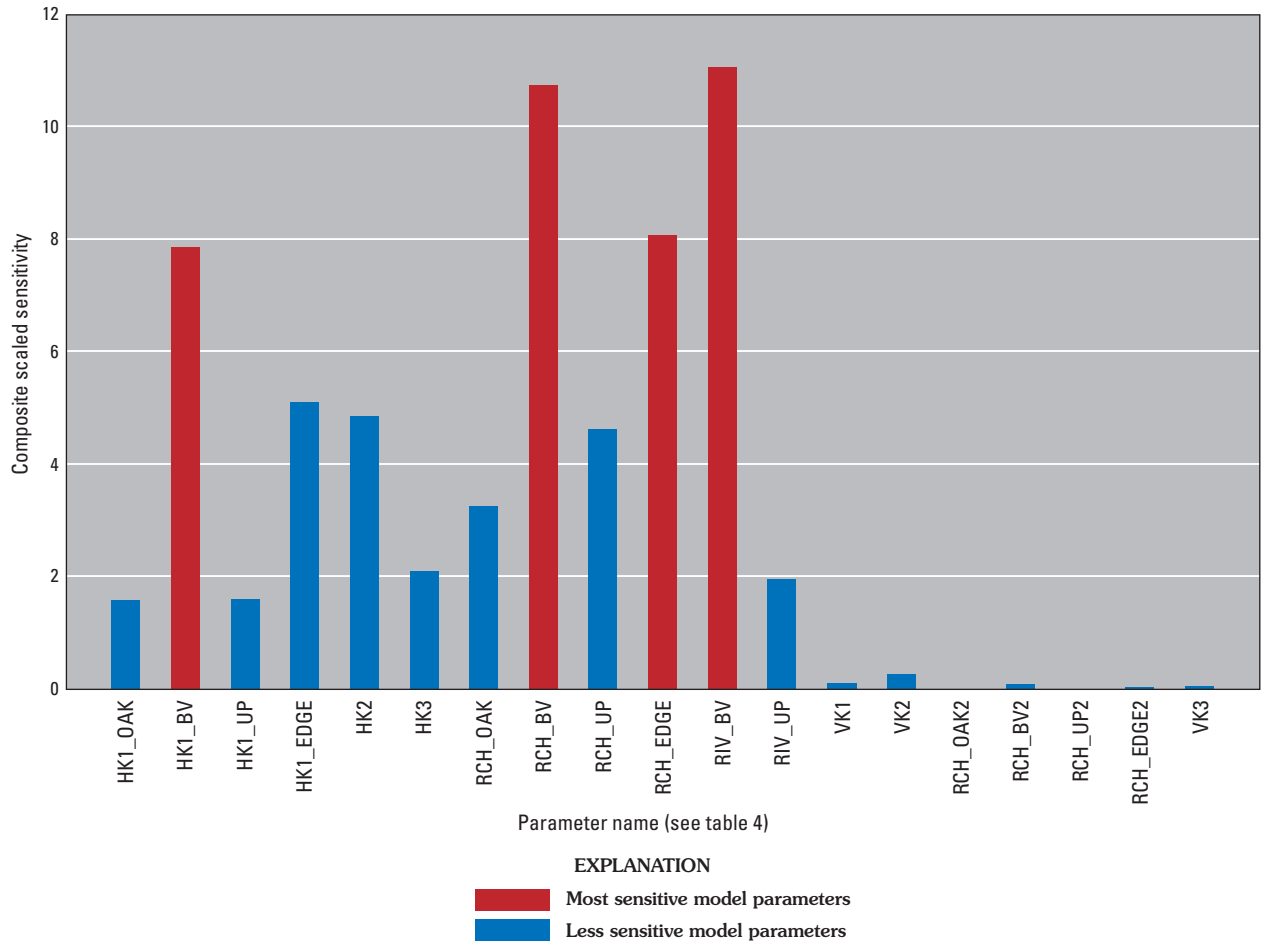

Figure 7.5. Composite scaled sensitivity of ground-water flow model parameters, Great Miami River Basin regional study area, Ohio.

the modified Gauss-Newton method (Hill, 1998). During each parameter-estimation model simulation, each parameter value is modified by MODFLOW-2000 by using their sensitivities, and new parameter values are input to the model to calculate a new objective function. No prior information was used in the nonlinear regression. Parameter estimation was run with a low primary convergence criterion (0.01) and a low convergence criterion (0.001).

Figure 7.6 shows graphs comparing model-computed and measured hydraulic heads for both stress periods, by layer, for the results of the parameter-estimation simulations. The 1:1 line shows where the results would plot if the model-computed heads exactly matched the measured heads for the stress periods. The correlation coefficient between model-computed and measured hydraulic heads is 0.865, which indicates a reasonable model fit. Figure 7.7 presents the weighted residuals compared to the weighted simulated equivalents for both head and streamflow observations and shows that the two variables are independent and that the weighted residuals are scattered evenly about 0.0 (Hill, 1998).

The calculated error variance and standard error for the final calibrated model are 152.6 and 12.4, respectively. A standard deviation of 0.22 m (variance = 0.15 m) was used to calculate weights for the majority of head observations, so the fitted standard error is 2.7 m and represents the overall fit achieved for these hydraulic heads. A calculation of the RMSE and MAD for each layer for stress period 1 (1993) and stress period 2 (1997–2001) is shown in table 7.5. When the results of stress period 1 are compared to the original and revised model (from table 7.2), a slight decrease in the overall MAD and RMSE can be seen, indicating the parameter-estimation resulted in a slightly improved model with respect to hydraulic heads. A coefficient of variation of 0.10 (10 percent) was used to calculate the weights associated with streamflow measurements (1993), so the fitted coefficient of variation of 1.24 (124 percent) represents the overall fit with streamflow measurements. Table 7.6 shows the model-computed and measured streamflow from the calibrated parameter-estimation model. The coefficient of variation and direct comparisons with measurements indicate streamflow is not well represented by this model, and the representation of streamflow is not as good as in the original Dayton-area model (Dumouchelle, 1998). Low weights were applied to streamflow data in the parameter-estimation simulations, which indicates confidence in these measurements is low, and likely resulted in the poorer representation of streamflow in the revised model.

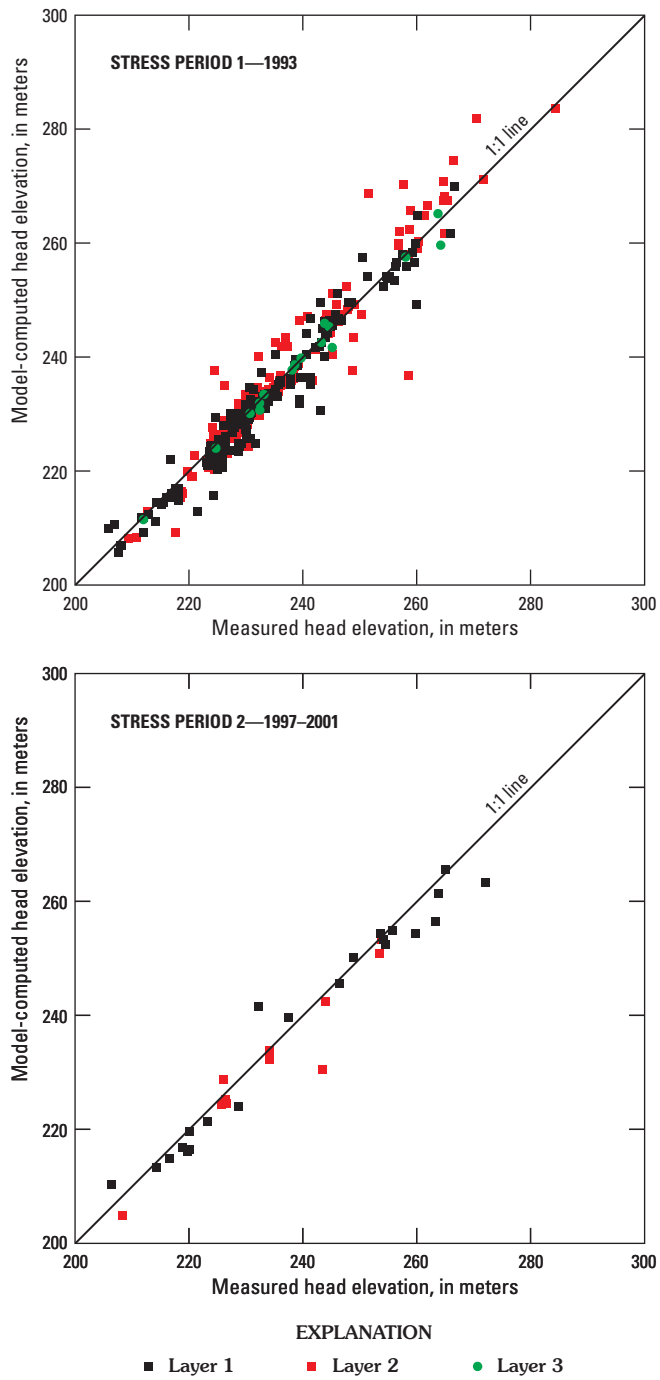

Figure 7.6. Relation between model-computed and measured hydraulic heads, Great Miami River Basin regional study area, Ohio.

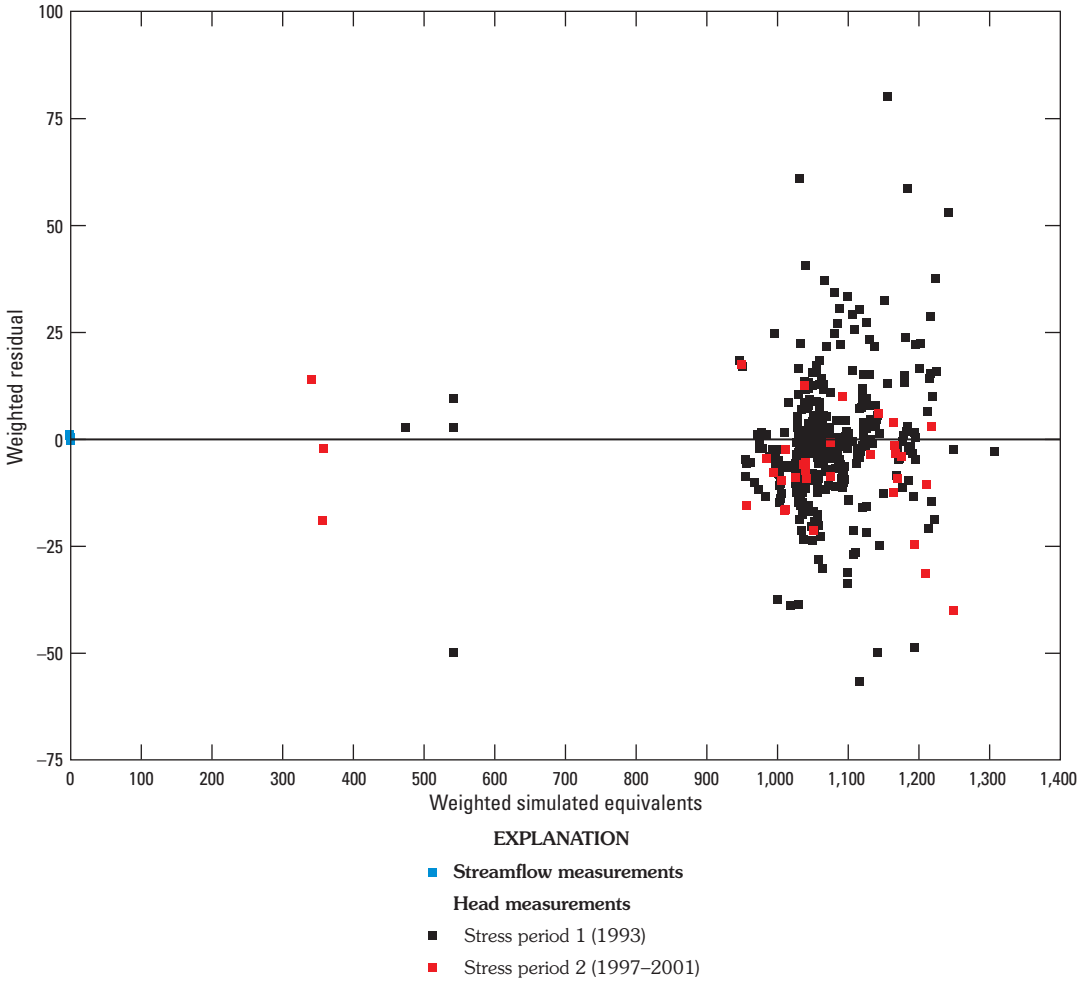

Figure 7.7. Weighted residuals plotted against weighted simulated equivalents, Great Miami River Basin regional study area, Ohio.

Table 7.5. Root-mean-squared error and mean-absolute difference between model-computed and measured hydraulic heads in the revised parameter-estimation ground-water flow model, Great Miami River Basin regional study area, Ohio.

[N, number of observations; RMSE, root-mean-squared error in meters; MAD, mean absolute difference in meters; SP1—Stress period 1 (1993 measurements); SP2—Stress period 2 (1997–2001 measurements); —, not applicable]

Layer	N (SP1)	N (SP2)	RMSE (SP1)	RMSE (SP2)	MAD (SP1)	MAD SP2)
1	311	22	3.04	3.90	1.63	2.96
2	252	12	2.58	4.18	1.73	2.62
3	16	—	1.67	—	1.14	—
Total	579	34	—	—	—	—
Weighted* averages	—	—	2.80	4.00	1.66	2.84

*Total RMSE and MAD values are weighted averages.

Table 7.6. Comparison of model-computed and measured streamflow gains or losses between the original ground-water flow model (Dumouchelle, 1998) and the revised parameter-estimation model, Great Miami River Basin regional study area, Ohio.

[units in m^3/d, cubic meters per day]

Stream reach	Streamflow gain or loss (1993)		
	Measured	Simulated (original)	Simulated (parameter estimation)
Great Miami River, Taylorsville Dam to Needmore Road	+0.481	–0.139	–0.191
Great Miami River, Needmore Road to Railroad	–0.983	–0.949	–0.752
Mad River, Huffman Dam to Harshman Road	–2.24	–1.55	–1.31
Little Miami River from Dayton-Xenia Road to Narrows Park	+0.439	+0.425	–0.489
Hebble Creek to Mad River	–0.008	–0.006	–0.011
Little Beaver Creek, Research Road to Factory Road	–0.062	+0.042	+0.040

The modified Beale measure is used to test linearity of a model, especially if the model's linear confidence and prediction intervals are to be used. The modified Beale's measure of this model (using the F-statistic of 2.1689) is 0.146, indicating the model is somewhat nonlinear with respect to the parameters. If Beale's measure is greater than 0.46, the model is nonlinear; if Beale's is less than 0.041, the model is effectively linear. These results are particularly applicable if this model will be used in predictive simulations where linear confidence intervals on predictions are to be used.

Model-Computed Water Budget

The water budget simulated by the calibrated parameter-estimation model (table 7.7) indicates less than one percent error in the steady-state-model water balance. Recharge to the modeled area is from losing stream reaches (38.9 percent of inflow), precipitation (38.8 percent of inflow), and downvalley ground-water underflow (22.3 percent of inflow). Discharge from the modeled area is to pumping wells (53.5 percent of outflow), gaining stream reaches (40.1 percent of outflow), and downvalley ground-water underflow (6.4 percent of outflow). The model-computed water balance is a reasonable approximation of the conceptual-model water balance.

Table 7.7. Water budget computed by the revised parameter estimation model for 1997–2001 average conditions, Great Miami River Basin regional study area, Ohio.

[m^3/d, cubic meters per day]

Water-budget component	Flow (m^3/d)	Percentage of inflow or outflow
Model inflow		
Downvalley flow into the modeled area	224,000	22.3
Rivers	391,000	38.9
Precipitation	390,000	38.8
TOTAL	**1,005,000**	**100**
Model outflow		
Downvalley flow out of the modeled area	64,100	6.4
Wells	538,000	53.5
Rivers	403,000	40.1
TOTAL	**1,005,100**	**100**

Simulation of Areas Contributing Recharge to Public-Supply Wells

The calibrated revised ground-water flow model was used to simulate areas contributing recharge for 60 public-supply wells and traveltimes from recharge areas to wells. The particle-tracking software MODPATH (Pollock, 1994) was used in conjunction with flux output from the revised flow model and a constant assumed effective porosity value of 0.2 to calculate flow paths and traveltimes. An effective porosity value of 0.2 is reasonable for the study area on the basis of previous work (Cunningham and others, 1994). A nested rediscretization method for particle tracking near wells (Spitz, 2001) was used for the analysis of contributing areas to identify flow paths for individual wells. A grid spacing of approximately 50 m was used for the rediscretization. Properties from the calibrated model were used for the finer grid. The model-computed areas contributing recharge represent advective ground-water flow and do not account for mechanical dispersion. Advection-dispersion transport simulations would likely yield larger areas contributing recharge than advective particle-tracking simulations because the effects of dispersion caused by aquifer heterogeneity would be included.

The areas contributing recharge are presented in figure 7.8, and several features of contributing areas are noteworthy.

- Areas contributing recharge can extend great distances from some wells.
- The areas contributing recharge and zone of contribution for wells with higher pumping rates are generally larger than those with lower pumping rates.
- Losing stream reaches coincide with several of the areas contributing recharge and likely affect the sizes of contributing areas.
- Zones of contribution often are similar to the areas contributing recharge, indicating that the primary source of water to those wells is water recharged at the water table.

Median simulated traveltimes from recharge areas to wells ranged from 21 days to 184 years; approximately 73.2 percent of the traveltimes were less than 25 years. Generally, traveltimes are shorter for shallow well screens and longer for wells screened in the lower part of the aquifer. For deeper wells, pathlines are longer and zones of contribution and areas contributing recharge are more distal from the well than those for shallower wells. Zones of contribution and areas contributing recharge mostly originate upgradient and upvalley from the wellhead. In some areas around Dayton, where multiple wells are completed in close proximity to each other, nearly all the water recharged to the valley is withdrawn by production wells.

Model Limitations and Uncertainties

The purpose of the original ground-water flow model for the Great Miami River Basin regional study area was to provide a better understanding of the flow system in the valley-fill deposits. The purpose of the revised model was to aid in determining contributing areas to public-supply wells and ground-water traveltimes. Both models simulate steady-state conditions. Water-level data and computed water budgets indicate the Great Miami River valley-fill aquifer in the study area was generally in steady-state equilibrium for 1997–2001. However, further calibration for transient conditions may be needed to accurately represent temporal changes in the system. Also, there may be areas where much more detailed geologic information may be necessary to define local flow paths and traveltimes. Because of the regional nature of the modeling effort, some generalizations, including how surface-water bodies (streams) were treated in the model, may adversely affect traveltimes, especially from wells near streams.

Computed areas contributing recharge and traveltimes through zones of contribution are based on the calibrated revised model and a constant assumed effective porosity value of 0.2 for all three model layers. In a steady-state model, changes to input porosity values do not change the area contributing recharge to a given well. Changes to input porosity values will change computed traveltimes from recharge to discharge areas in direct proportion to changes of effective porosity because there is an inverse linear relation between ground-water flow velocity and effective porosity and a direct linear relation between the traveltime and the effective porosity. For example, a one-percent decrease in porosity will result in a one-percent increase in velocity and a one-percent decrease in particle traveltime. A detailed sensitivity analysis of porosity distributions was beyond the scope of this study, although future work could compare simulated ground-water traveltimes to ground-water ages to more thoroughly evaluate effective porosity values.

The Great Miami River Basin regional ground-water flow model uses justifiable aquifer properties and boundary conditions and provides a reasonable representation of ground-water flow conditions in the study area for 1997–2001 average conditions. The model is suitable for evaluating regional water budgets and ground-water flow paths in the study area for the time period of interest but may not be suitable for long-term predictive simulations. This regional model provides a useful tool to evaluate aquifer vulnerability at a regional scale, to facilitate comparisons of ground-water traveltime between regional aquifer systems, and to guide future detailed investigations in the study area.

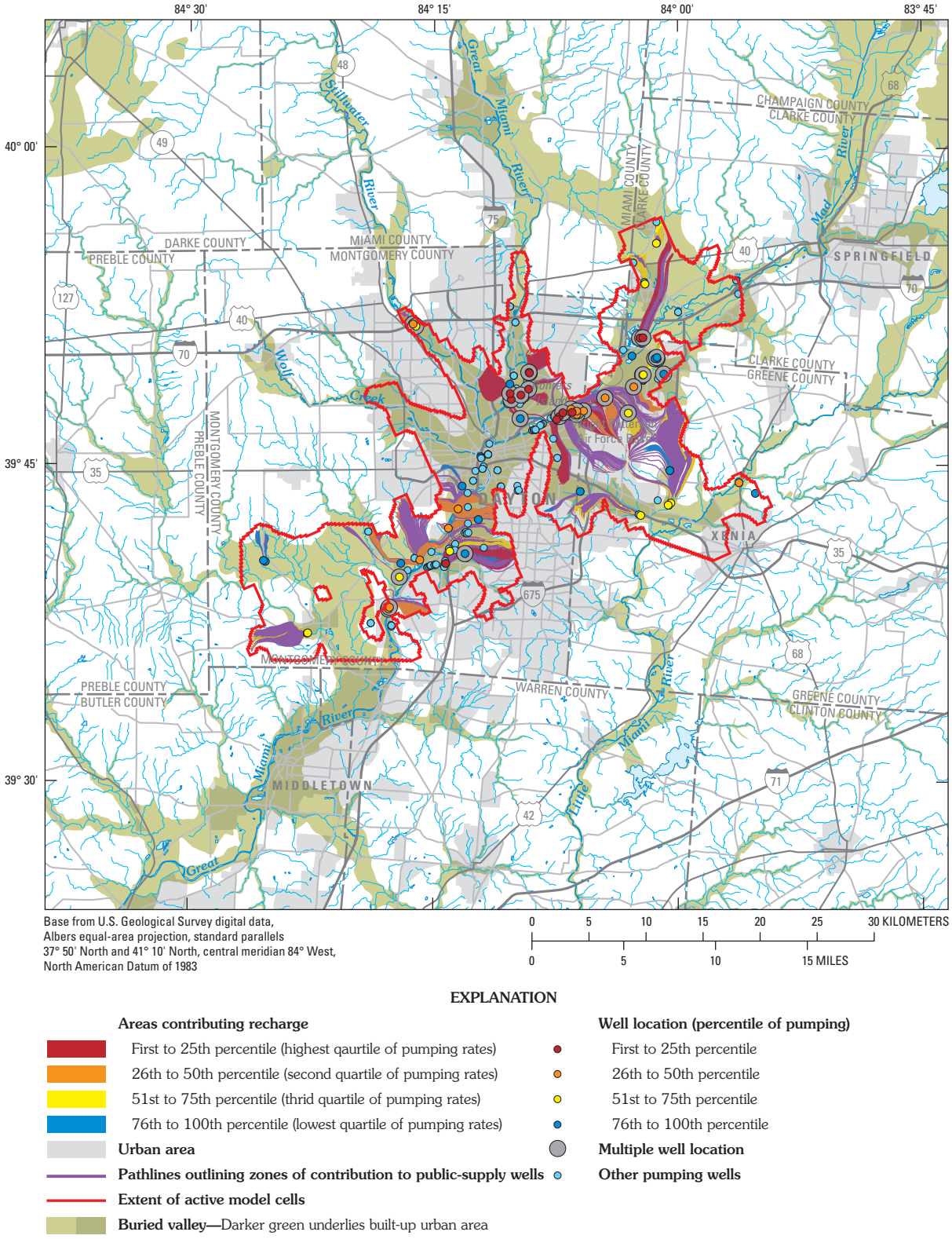

Figure 7.8. Model-computed areas contributing recharge for 60 public-supply wells, Great Miami River Basin regional study area, Ohio.

References Cited

Argus Interware, 1997, Argus Numerical Environments and Mesh Maker User's Guide: Jericho, N.Y., 463 p.

Barlow, P.M., and Dickerman, D.C., 2001, Numerical-simulation and conjunctive-management models of the Hunt-Annaquatucket-Pettaquamscutt stream-aquifer system, Rhode Island: U.S. Geological Survey Professional Paper 1636, 88 p.

Bradbury, K.R., Muldoon, M.A., Zaporozec, A., and Levy, J., 1991, Delineation of wellhead protection areas in fractured rocks: U.S. Environmental Protection Agency, EPA 570/9–91–009, 144 p.

Casey, G.D., 1994, Hydrogeology of the Silurian and Devonian carbonate-rock aquifer system in the Midwestern Basin and Arches Region of Indiana, Ohio, Michigan, and Illinois: U.S. Geological Survey Open-File Report 93–663, 14 p., 2 sheets, scale 1:1,000,000.

Casey, G.D., 1997, Hydrogeologic framework of the Midwestern Basins and Arches region in parts of Indiana, Ohio, Michigan, and Illinois: U.S. Geological Survey Professional Paper 1423–B, 46 p.

Cunningham, W.L., Sheets, R.A., and Schalk, C.W., 1994, Evaluation of ground-water flow by particle tracking, Wright-Patterson Air Force Base, Ohio: U.S. Geological Survey Water-Resources Investigations Report 94–4243, 11 p.

Debrewer, L.M., Rowe, G.L., Reuter, D.C., Moore, R.C., Hambrook, J.A., and Baker, N.T., 2000, Environmental setting and effects on water quality in the Great and Little Miami River Basins, Ohio and Indiana: U.S. Geological Survey Water-Resources Investigations Report 99–4201, 98 p.

DeSimone, L.A., Walter, D.A., Eggleston, J.R., and Nimiroski, M.T., 2002, Simulation of ground-water flow and evaluation of water-management alternatives in the Upper Charles River Basin, eastern Massachusetts: U.S. Geological Survey Water-Resources Investigations Report 02–4234, 94 p.

Dickerman, D.C., Kliever, J.D., and Stone, J.R., 1997, Hydrogeology, water quality, and simulation of ground-water development alternatives in the Usquepaug-Queen ground-water reservoir, Southern Rhode Island: U.S. Geological Survey Water-Resources Investigations Report 97–4126, 48 p.

Dickerman, D.C., Trench, E.C.T., and Russell J.P., 1990, Hydrogeology, water quality, and ground-water development alternatives in the lower Wood River ground-water reservoir, Rhode Island: U.S. Geological Survey Water-Resources Investigations Report 89–4031, 109 p.

Dumouchelle, D.H., 1998, Simulation of ground-water flow, Dayton area, southwestern Ohio: U.S. Geological Survey Water-Resources Investigations Report 98–4048, 57 p.

Dumouchelle, D.H., Schalk, C.W., Rowe, G.L., and deRoche, J.T., 1993, Hydrogeology, simulated ground-water flow, and ground-water quality, Wright-Patterson Air Force Base, Ohio: U.S. Geological Survey Water-Resources Investigations Report 93–4047, 160 p.

Eberts, S.E., and George, L.L., 2000, Regional ground-water flow and geochemistry in the Midwestern Basins and Arches Aquifer System in parts of Indiana, Ohio, Michigan, and Illinois: U.S. Geological Survey Professional Paper 1423–C, 103 p.

Environmental Systems Research Institute, 1987, ARC/INFO users guide: Redlands, Calif., Environment Systems Research Institute [variously paginated].

Fenneman, N.M., 1938, Physiography of Eastern United States: New York, McGraw-Hill, p. 449–536.

Gburek, W.J., Folman, G.J., and Urban, J.B., 1999, Field data and ground-water modeling in a layered fractured aquifer: Ground Water, v. 37, no. 2, p. 175–184.

Harbaugh, A.W., Banta, E. R., Hill, M.C., and McDonald, M.G., 2000, MODFLOW-2000, the U.S. Geological Survey modular ground-water model—User guide to modularization concepts and the ground-water flow process: U.S. Geological Survey Open-File Report 00–92, 121 p.

Harbaugh, A.W., and McDonald, M.G., 1996, User's documentation for MODFLOW-96, an update to the U.S. Geological Survey modular finite-difference ground-water flow model: U.S. Geological Survey Open-File Report 96–485, 56 p.

Harstine, L.J., 1991, Hydrologic atlas for Ohio—Average annual precipitation, temperature, streamflow, and water loss for 50-year period, 1931–1980: Ohio Department of Natural Resources, Division of Water, Water Inventory Report 28, 12 p., 4 sheets.

Hill, M.C., 1998, Methods and guidelines for effective model calibration: U.S. Geological Survey Water-Resources Investigations Report 98–4005, 90 p.

Hill, M.C., Banta, E.R., Harbaugh, A.W., and Anderman, E.R., 2000, MODFLOW-2000, the U.S. Geological Survey modular ground-water model—User guide to the observation, sensitivity and parameter-estimation processes and three post-processing programs: U.S. Geological Survey Open-File Report 00–184, 210 p.

Homer, C. C. Huang, L. Yang, B. Wylie and M. Coan, 2004, Development of a 2001 National Landcover Database for the United States: Photogrammetric Engineering and Remote Sensing, v. 70, no. 7, pp. 829–840, accessed Feb. 6, 2007, at *http://www.mrlc.gov/pdf/July_PERS.pdf*.

Kontis, A.L., Randall, A.D., and Mazzaferro, D.L., 2004, Regional hydrology and simulation of flow of stratified drift aquifers in the glaciated Northeastern United States: U.S. Geological Survey Professional Paper 1415–C, 156 p.

Lloyd, O.B., and Lyke, W.L., 1995, Ground-water atlas of the United States, segment 10—Illinois, Indiana, Kentucky, Ohio, and Tennessee: U.S. Geological Survey Hydrologic Investigations Atlas 730–K, 30 p.

McDonald, M.G., and Harbaugh, A.W., 1988, A modular three-dimensional finite-difference ground-water flow model: U.S. Geological Survey Techniques of Water-Resources Investigations, book 6, chap. A1 [variously paginated].

Melvin, R.L., Stone, B.D., Stone, J.R., and Trask, J.J., 1992, Hydrogeology of thick till deposits in Connecticut: U.S. Geological Survey Open-File Report 92–43, 49 p.

Morrissey, D. J., 1983, Hydrology of the Little Androscoggin River valley aquifer, Oxford County, Maine: U.S. Geological Survey Water-Resources Investigations 83–4018, 79 p.

Morrissey, D.J., Randall, A.D., and Williams, J.H., 1988, Upland runoff as a major source of recharge to stratified-drift aquifers in the glaciated Northeast, *in* Randall, A.D., and Johnson, A.I., eds., 1988, Regional aquifer systems of the United States–The northeast glacial aquifers: American Water Resources Association Monograph Series no. 11, p. 17–36.

Mullaney, J.R., and Grady, S.J., 1997, Hydrogeology and water quality of a surficial aquifer underlying an urban area, Manchester, Connecticut: U.S. geological Survey Water-Resources Investigations Report 97–4195, 40 p.

Norris, S.E., Cross, W.P., and Goldthwait, R.P., 1948, The water resources of Montgomery County Ohio: Ohio Water Resources Board Bulletin 12, 83 p.

Norris, S.E., Cross, W.P., and Goldthwait, R.P., 1950, The water resources of Greene County, Ohio: Ohio Department of Natural Resources, Division of Water Bulletin 19, 52 p.

Norris, S.E., and Spieker, A.M., 1966, Ground-water resources of the Dayton area, Ohio: U.S. Geological Survey Water-Supply Paper 1808, 167 p.

Orzol, L.L., and McGrath, T.S., 1992, Modifications of the U.S. Geological Survey modular, finite-difference, ground-water flow model to read and write geographic information system files: U.S. Geological Survey Open-File Report 92–50, 202 p.

Pollock, D.W., 1994, User's guide for MODPATH/MODPATH-PLOT, Version 3—A particle tracking post-processing package for MODFLOW, the U.S. Geological Survey finite-difference ground-water flow model: U.S. Geological Survey Open-File Report 94–464, accessed Feb. 6, 2007, at *http://water.usgs.gov/nrp/gwsoftware/modpath41/modpath41.html*

Randall, A.D., 1996, Mean annual runoff, precipitation, and evapotranspiration in the glaciated Northeastern United States, 1951–1980: U.S. Geological Survey Open-File Report 96–395, 2 plates.

Randall, A.D., 2001, Hydrogeologic framework of stratified-drift aquifers in the glaciated Northeastern United States: U.S. Geological Survey Professional Paper 1415–B, 179 p.

Randall, A.D., Francis, R.M., Frimpter, M.H., and Emery, J.M., 1988, Region 19, Northeastern Appalachians, *in* Back, W., Rosenshein, J.S., and Seaber, P.R., eds., Hydrogeology: Boulder, Colorado, Geological Society of America, The geology of North America, v. O–2, p. 177–187.

Rantz, S.E., and others, 1982, Measurement and computation of streamflow: U.S. Geological Survey Water-Supply Paper 2175, 2 v., 631 p.

Rogers, R.J., 1989, Geochemical comparison of ground water in areas of New England, New York, and Pennsylvania: Ground Water, v. 27, no. 5, p. 690–712.

Rowe, G.L., Shapiro, S.D., and Schlosser, P., 1999, Use of environmental tracers to evaluate ground-water age and water-quality trends in a buried-valley aquifer, Dayton area, southwestern Ohio: U.S. Geological Survey Water-Resources Investigations Report 99–4113, 81 p.

Schalk, C.W., 1992, Ground-water levels and flow in the vicinity of Wright-Patterson Air Force Base, Ohio, October-December, 1987: U.S. Geological Survey Water-Resources Investigations Report 92–4022, 1 sheet, scale 1:46,980.

Schmidt, J.J., 1986, Ground-water resources of Montgomery County: Ohio Department of Natural Resources, Division of Water, 1 sheet, scale 1:62,500.

Schmidt, J.J., 1991, Ground-water resources of Greene County: Ohio Department of Natural Resources, Division of Water, 1 sheet, scale 1:62,500.

Shapiro, A.M., Margolin, J.L., Dolev, S., and Ben-Israel, Y., 1997, A graphical user interface for the U.S. Geological Survey modular three-dimensional finite-difference ground-water flow model (MODFLOW-96) using Argus Numerical Environments: U.S. Geological Survey Open-File Report 97–121, 50 p.

Sheets, R.A., 1994, Contributing recharge areas of water-supply wells at Wright-Patterson Air Force base, Ohio: U.S. Geological Survey Water-Resources Investigations Report 94–4231, 35 p.

Sheets, R.A., Bair, E.S., and Rowe, 1998, Use of $^{3}H/^{3}He$ ages to evaluate and improve groundwater flow models in a complex buried-valley aquifer: Water Resources Research, v. 34, no. 5, p. 1077–1089.

Sheets, R.A., Darner, R.A., and Whitteberry, B.L., 2002, Lag times of bank infiltration at a well field, Cincinnati, Ohio, USA: Journal of Hydrology, v. 266, no. 3, p. 162–174.

Sheets, R.A., and Yost, W.P., 1994, Ground-water contribution from the Silurian/Devonian carbonate aquifer to the Mad River Valley, southwestern Ohio: Ohio Journal of Science, v. 94, no 5, p. 138–146.

Shindel, H.L., Mangus, J.P., and Frum, S.R., 2002, Ohio water resources data, water year 2002: U.S. Geological Survey Water-Data Report OH–02–1, 378 p.

Spitz, F.J., 2001, Method and computer programs to improve pathline resolution near weak sinks representing wells in MODFLOW and MODPATH ground-water-flow simulations: U.S. Geological Survey Open-File Report 00–392, 41 p.

Starn, J.J., Stone, J.R., and Mullaney, J.R., 2000, Delineation and analysis of uncertainty of contributing areas to wells at the Southbury Training School, Southbury, Connecticut: U.S. Geological Survey Water-Resources Investigations Report 00–4158, 53 p.

Tepper, D.H., Morrissey, D.J., and Johnson, C.D., 1990, Hydrogeology, water quality, and effects of increased municipal pumpage of the Saco River valley glacial aquifer: Bartlett, New Hampshire, to Fryeburg, Maine: U.S. Geological Survey Water-Resources Investigations Report 88–4179, 113 p., 6 pls.

Walton, W.C., and Scudder, G.D., 1960, Ground-water resources of the valley-train deposits in the Fairborn area, Ohio: Ohio Department of Natural Resources, Division of Water Technical Report 3, 57 p.

Warner, K.L., and Arnold, T.L., 2005, Framework for regional synthesis of water-quality data for the glacial aquifer system in the United States: U.S. Geological Survey Scientific-Investigations Report 2005–5223, 6 p.

Winston, R.B., 2000, Graphical user interface for MODFLOW, version 4: U.S. Geological Survey Open-File Report 00–315, 27 p.

Yost, W.P., 1995, Data on ground-water levels and ground-water/surface-water relations in the Great Miami River and Little Miami River valleys, southwestern Ohio: U.S. Geological Survey Open-File Report 95–357, 57 p.

Hydrogeologic Setting and Ground-Water Flow Simulation of the Eastern High Plains Regional Study Area, Nebraska

By Matthew K. Landon and Michael J. Turco

Section 8 of

Hydrogeologic Settings and Ground-Water Flow Simulations for Regional Studies of the Transport of Anthropogenic and Natural Contaminants to Public-Supply Wells—Studies Begun in 2001

Edited by Suzanne S. Paschke

Professional Paper 1737–A

U.S. Department of the Interior
U.S. Geological Survey

U.S. Department of the Interior
DIRK KEMPTHORNE, SECRETARY

U.S. Geological Survey
Mark D. Myers, Director

U.S. Geological Survey, Reston, Virginia: 2007

For product and ordering information:
World Wide Web: http://www.usgs.gov/pubprod
Telephone: 1-888-ASK-USGS

For more information on the USGS--the Federal source for science about the Earth, its natural and living resources, natural hazards, and the environment:
World Wide Web: http://www.usgs.gov
Telephone: 1-888-ASK-USGS

Any use of trade, product, or firm names is for descriptive purposes only and does not imply endorsement by the U.S. Government.

Although this report is in the public domain, permission must be secured from the individual copyright owners to reproduce any copyrighted materials contained within this report.

Suggested citation:
Landon, Matthew K., and Turco, Michael J., 2007, Hydrogeologic setting and ground-water flow simulation of the Eastern High Plains Regional Study Area, Nebraska, *section 8 of* Paschke, S.S., ed., Hydrogeologic settings and ground-water flow simulations for regional studies of the transport of anthropogenic and natural contaminants to public-supply wells—studies begun in 2001: Reston, Va., U.S. Geological Survey Professional Paper 1737–A, pp. 8–1 – 8–28.

Contents

Abstract 8–1
Introduction 8–1
Purpose and Scope 8–1
Study Area Description 8–1
Topography and Climate 8–4
Surface-Water Hydrology 8–4
Land Use 8–4
Water Use 8–4
Conceptual Understanding of the Ground-Water System 8–5
Geology 8–5
Ground-Water Occurrence and Flow 8–8
Aquifer Hydraulic Properties 8–9
Water Budget 8–9
Ground-Water Quality 8–10
Ground-Water Flow Simulations 8–11
Modeled Area and Spatial Discretization 8–11
Boundary Conditions and Model Stresses 8–13
Aquifer Hydraulic Properties 8–18
Model Calibration and Sensitivity 8–18
Model-Computed Hydraulic Heads 8–20
Model-Computed Water Budget 8–24
Simulation of Areas Contributing Recharge to Public-Supply Wells 8–24
Limitations and Appropriate Use of the Model 8–24
References Cited 8–26

Figures

Maps showing:

8.1. Location of the Eastern High Plains regional study area within the High Plains aquifer. 8–2
8.2. Topography, hydrologic features, and location of public-supply wells, Eastern High Plains regional study area, Nebraska. 8–3
8.3. Generalized hydrogeologic section showing ground-water flow and geochemical conditions, Eastern High Plains regional study area, Nebraska 8–8
8.4. Map showing oxidation-reduction conditions in wells screened in the confined part of the High Plains aquifer, Eastern High Plains regional study area, Nebraska 8–12

8.5. Graph showing changes in concentration of oxidation-reduction sensitive species in three York public-supply wells from 1996, prior to withdrawals for public water supply, and for 1997–2002, when municipal withdrawals occurred. 8–13
8.6. Map showing ground-water flow model grid boundary and selected boundary conditions in different model layers, Eastern High Plains regional study area, Nebraska. 8–14
8.7*A*. Hydrogeologic section showing hydraulic-conductivity zones and flux-boundary values for layers of calibrated ground-water flow model. 8–15
8.7*B*. Map showing hydraulic-conductivity and active-cell zones in layer 1 of calibrated ground-water flow model, Eastern High Plains regional study area, Nebraska. 8–16
8.8. Map showing distribution of recharge estimates used as ground-water flow model input, Eastern High Plains regional study area, Nebraska. 8–19
8.9. Graph showing relation between model-computed and measured hydraulic head, Eastern High Plains regional study area, Nebraska 8–20
8.10. Map showing model-computed potentiometric surface in layer 4 and observation points and residuals in all layers, Eastern High Plains regional study area, Nebraska 8–21
8.11. Graph showing relation between head residuals and measured hydraulic head, Eastern High Plains regional study area, Nebraska 8–22
8.12. Hydrogeologic section showing model-computed hydraulic heads through row 100 of calibrated ground-water flow model, Eastern High Plains regional study area, Nebraska. 8–22
8.13. Map showing model-computed areas contributing recharge and zones of contribution for 12 public-supply wells, Eastern High Plains regional study area, Nebraska. 8–25

Tables

8.1. Summary of hydrogeologic and ground-water quality characteristics for the High Plains aquifer and the Eastern High Plains regional study area, Nebraska.... 8–6
8.2. Average ground-water pumping rates for public-supply wells, 1997–2001, Eastern High Plains regional study area, Nebraska. 8–17
8.3. Model-computed water budget for 1997–2001 average conditions, Eastern High Plains regional study area, Nebraska. 8–23

Hydrogeologic Setting and Ground-Water Flow Simulation of the Eastern High Plains Regional Study Area, Nebraska

By Matthew K. Landon and Michael J. Turco

Abstract

The transport of anthropogenic and natural contaminants to public-supply wells was evaluated in a part of the High Plains aquifer near York, Nebraska, as part of the U.S. Geological Survey National Water-Quality Assessment Program. The aquifer in the Eastern High Plains regional study area is composed of Quaternary alluvial deposits typical of the High Plains aquifer in eastern Nebraska and Kansas, is an important water source for agricultural irrigation and public water supply, and is susceptible and vulnerable to contamination. A six-layer, steady-state ground-water flow model of the High Plains aquifer near York, Nebraska, was constructed and calibrated to average conditions for the time period from 1997 to 2001. The calibrated model and advective particle-tracking simulations were used to compute areas contributing recharge and traveltimes from recharge areas to selected public-supply wells. Model results indicate recharge from agricultural irrigation return flow and precipitation (about 89 percent of inflow) provides most of the ground-water inflow, whereas the majority of ground-water discharge is to pumping wells (about 78 percent of outflow). Particle-tracking results indicate areas contributing recharge to public-supply wells extend northwest because of the natural ground-water gradient from the northwest to the southeast across the study area. Particle-tracking simulations indicate most ground-water traveltimes from areas contributing recharge range from 20 to more than 100 years but that some ground water, especially that in the lower confined unit, originates at the upgradient model boundary instead of at the water table in the study area and has traveltimes of thousands of years.

Introduction

The Eastern High Plains regional study area for the transport of anthropogenic and natural contaminants to public-supply wells (TANC) is within the High Plains Regional Ground Water study unit of the U.S. Geological Survey National Water-Quality Assessment (NAWQA) program near York, Nebraska (fig. 8.1). The study area is in the High Plains aquifer, which is an important water source for agricultural irrigation and drinking-water supply throughout the region and for York, Nebraska.

Purpose and Scope

The purpose of this Professional Paper Chapter is to present the hydrogeologic setting of the Eastern High Plains regional study area. The chapter also documents the setup and calibration of a steady-state regional ground-water flow model for the study area. Ground-water flow characteristics, pumping-well information, and water-quality data were compiled from existing data to develop a conceptual understanding of ground-water conditions in the study area. A six-layer steady-state ground-water flow model of the High Plains aquifer near York, Nebraska, was developed and calibrated for this study to represent average conditions for the period from 1997 to 2001. The 5-year period 1997–2001 was selected for data compilation and modeling exercises for all TANC regional study areas to facilitate future comparisons between study areas. The calibrated ground-water flow model and associated particle tracking were used to simulate advective ground-water flow paths and to delineate areas contributing recharge to selected public-supply wells. Ground-water traveltimes from recharge to public-supply wells, oxidation-reduction (redox) conditions along flow paths, and presence of potential contaminant sources in areas contributing recharge were tabulated into a relational database as described in Section 1 of this Professional Paper. This section provides the foundation for future ground-water susceptibility and vulnerability analyses of the study area and comparisons among regional aquifer systems.

Study Area Description

The Eastern High Plains regional study area encompasses 388.5 km^2 and is located in east-central Nebraska around the city of York (fig. 8.2). Ground water in the study area is contained within Quaternary alluvial deposits that compose the High Plains aquifer in eastern Nebraska and Kansas. The study area was chosen because the aquifer is used extensively for public water supply, is susceptible and vulnerable

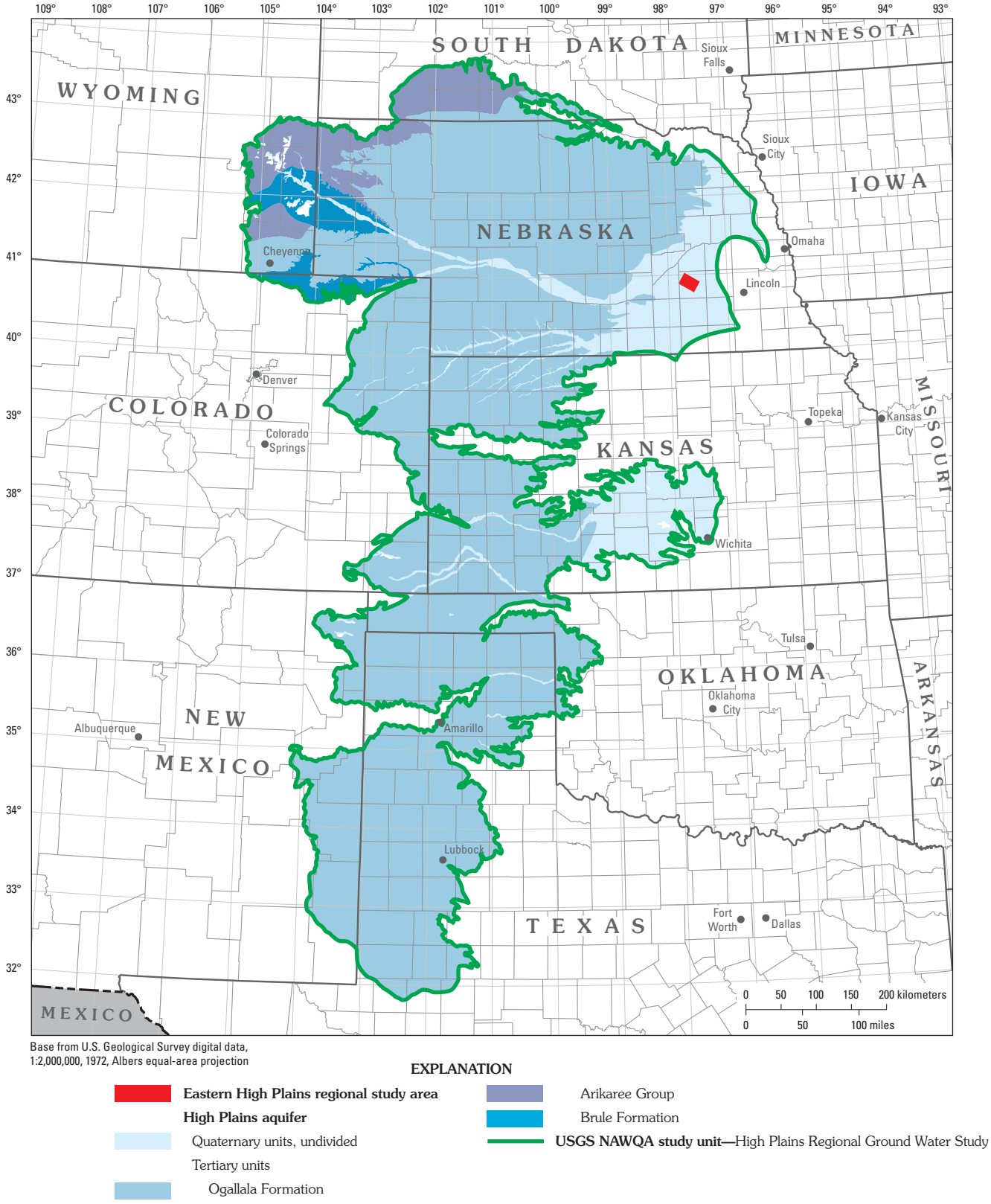

Base from U.S. Geological Survey digital data, 1:2,000,000, 1972, Albers equal-area projection

EXPLANATION

- **Eastern High Plains regional study area**
- **High Plains aquifer**
  - Quaternary units, undivided
  - Tertiary units
    - Ogallala Formation
    - Arikaree Group
    - Brule Formation
- **USGS NAWQA study unit**—High Plains Regional Ground Water Study

Figure 8.1. Location of the Eastern High Plains regional study area within the High Plains aquifer.

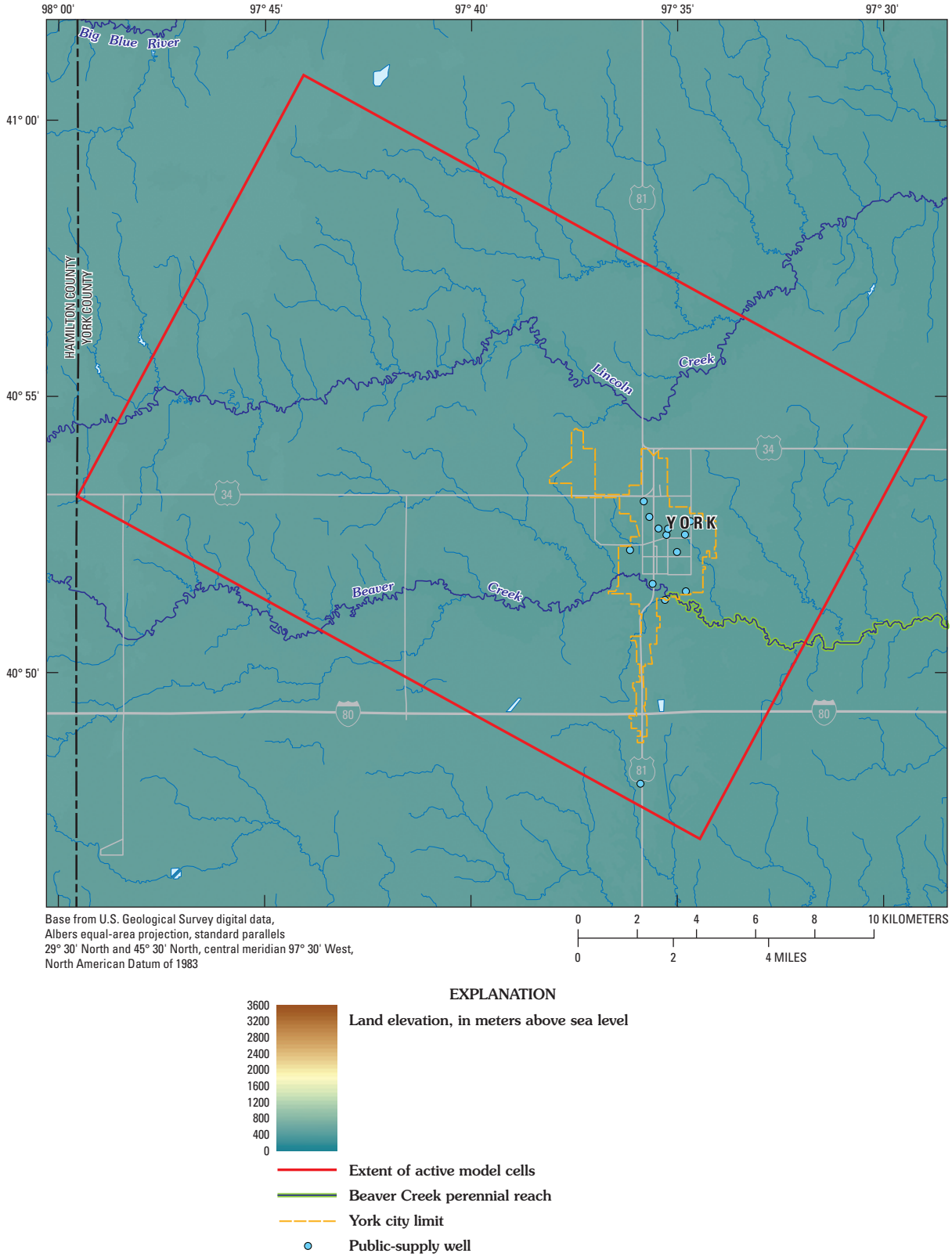

Figure 8.2. Topography, hydrologic features, and location of public-supply wells, Eastern High Plains regional study area, Nebraska.

to contamination, and is representative of the High Plains aquifer (table 8.1). The rectangular study area was selected to facilitate ground-water flow modeling of the region upgradient from and around York and coincides with the area between two ground-water flow lines from a regional ground-water flow-model (COHYST, 2001).

Topography and Climate

The Eastern High Plains regional study area is located within a mostly flat lying region of windblown silt (loess) with relatively little dissection by streams (fig. 8.2, table 8.1). The study area includes portions of the upper Lincoln and Beaver Creek Basins, tributaries to the Big Blue River. The topography is typical of the extensive upland areas of the High Plains with low relief.

Mean annual precipitation at York for 1950–2001 is 71.1 cm/yr (High Plains Regional Climate Center, 2003) with most of the precipitation falling during thunderstorms in the spring and fall (Verstraeten and others, 1998) (table 8.1). The High Plains generally has a middle-latitude dry continental climate with abundant sunshine, moderate precipitation, frequent winds, low humidity, and a relatively high rate of evaporation (Gutentag and others, 1984). Because evaporation rates usually exceed precipitation (table 8.1), there is little water available to recharge the aquifer (Luckey and Becker, 1999). Estimates of recharge rates from precipitation range from 0.1 cm/yr in parts of Texas to 15.2 cm/yr in areas of dune sand in Kansas and Nebraska (Gutentag and others, 1984); average rates are about 1.5 cm/yr based upon regional water budgets (Luckey and others, 1986; Dennehy and others, 2002). The High Plains in eastern Nebraska and central Kansas have a humid continental climate that has slightly greater precipitation and humidity than the dry continental climate of the remainder of the High Plains and is therefore likely to have greater recharge from precipitation (table 8.1) (Dugan and Zelt, 2000).

Surface-Water Hydrology

The High Plains aquifer is in hydraulic connection with the major river systems crossing the aquifer from west to east (Weeks and others, 1988). During low-flow periods, water in the rivers is almost entirely derived from ground-water discharge. However, the major rivers derive most of their flow from the Rocky Mountains to the west (Dennehy and others, 2002). Because evaporation rates exceed precipitation rates and topographic slopes are relatively flat, little water is available to produce surface-water runoff (Gutentag and others, 1984; Litke, 2001).

There are no naturally perennial streams in the Eastern High Plains regional study area other than the lower reaches of Beaver Creek near the southeastern edge of the study area. Flows in Beaver Creek east of York (fig. 8.2) are maintained by discharges from the York wastewater plant (6,500 m^3/d, 1997–2001 average) and York Cold Storage (2,700 m^3/d, 1997–2001 average), which pumps ground water for cooling in western York and discharges the water to Beaver Creek. Low-flow streamflow measurements on Beaver Creek near the southeastern edge of the study area reported by Fallon and McChesney (1993) average about 5,600 m^3/d. Subtracting the downstream measurement of 5,600 m^3/d from the sum of the upstream inflow (9,200m^3/d), implies a loss of about 3,600 m^3/d from Beaver Creek to the aquifer in the measured stream reach. Seasonally, flow in Beaver Creek may be greatest during the June through August irrigation season owing to irrigation return flows.

Land Use

Irrigated agriculture is the primary land use in the study area (85 percent of total land in the study area). Predominant crops in the study area, with their percentage of total land area in parentheses, are irrigated corn (50.0 percent); dryland corn (12.8 percent); irrigated soybeans (9.7 percent); dryland soybeans (5.6 percent); irrigated sorghum, alfalfa, and small grains (1.3 percent); and dryland sorghum, alfalfa, and small grains (3.9 percent) (Center for Advanced Land Management Information Technologies, 2000). The study area is within one of the most heavily irrigated parts of the High Plains aquifer (Thelin and Heimes, 1987; Qi and others, 2002). Irrigation well density in the study area is 2.0 wells/km^2 compared to an average of about 0.4 well/km^2 in the High Plains. Urban land uses, including commercial/industrial/transportation and low intensity, residential areas account for about 2.6 percent of the study area (U.S. Geological Survey, 1999–2000).

The population of the study area is approximately 9,400 (U.S. Census Bureau, 2003) with an average population density of about 24.2 people/km^2. The population of York is approximately 8,100 (U.S. Census Bureau, 2003), 86 percent of the total population in the study area. The only other community in the study area is Bradshaw (about 16 km west of York), with a population of approximately 330. Rural households account for about 10 percent of the population.

Water Use

Ground-water withdrawals for irrigation are the largest outflow from the ground-water system in both the High Plains aquifer and the Eastern High Plains regional study area (table 8.1). Irrigation withdrawals from the High Plains aquifer were about 72 million m^3/d in 1995 and accounted for 96 percent of withdrawals from the High Plains aquifer (Dennehy and others, 2002). The average withdrawal rate over the entire irrigated area of the High Plains aquifer (approximately 55,000 km^2) was about 39 cm/yr in 1995. In the study area, withdrawal rates for irrigation were estimated at 25.4 cm/yr for 1998 through 2002 on the basis of metered pumping reported to the Upper Big Blue Natural Resources District (NRD) in 50 to 150 wells per year (Rod DeBuhr, Upper Big

Blue Natural Resources District, written commun., April 15, 2003). Withdrawal rates for irrigation have changed through time with gradual decreases in withdrawal rates since the early 1980s because of increased irrigation efficiency, conversion of gravity irrigation systems to center pivot irrigation systems, and wetter climatic conditions than in the 1970s and early 1980s (Orville Davidson, Public Utilities Director, City of York, Nebraska, written comm., February 15, 2002).

Ground-water withdrawals for public-supply and industrial purposes account for less than 6 percent of withdrawals in both the Eastern High Plains regional study area and the High Plains aquifer (table 8.1). Ground water withdrawn from the High Plains aquifer is the source of drinking water for 100 percent of the population in the study area and 82 percent of the people in the area underlain by the High Plains aquifer (Dennehy and others, 2002). Public-supply withdrawals in the study area increased by about 4 percent per year during 1997–2001, and average public-supply withdrawals for 1997–2001 were about 15 percent greater than withdrawals for 1981–1996. Public-supply withdrawals fluctuate seasonally because of outdoor water use during the summer months. Average monthly withdrawals for May through September are about 65 percent greater than those for October through April for 1997–2001.

Withdrawals for commercial/industrial purposes slightly exceed those for public supply. Withdrawals for self-supplied domestic or livestock purposes were not quantified because they are considered negligible compared to other withdrawals (Upper Big Blue Natural Resources District, 1999).

Conceptual Understanding of the Ground-Water System

The conceptual model of ground-water flow for the Eastern High Plains regional study area was developed on the basis of data and interpretations of previous investigations including test-hole logs and hydrogeologic studies, water-level data, potentiometric maps, hydraulic-property measurements, measurements or estimates of pumping rates and irrigated areas, climatic data, and ground-water quality data. Average ground-water fluxes were estimated for 1997–2001.

Geology

The Quaternary-age sediments that compose the High Plains aquifer in the study area consist of heterogeneous, mostly fluvial deposits of sand, gravel, silt, and clay that form a layered sequence of unconfined and confined units with intervening confining units. About 70 geologic logs in the study area were assembled from test holes drilled by the Nebraska Conservation and Survey Division and the U.S. Geological Survey (Smith, 2000), wells drilled by the City of York (Orville Davidson, Public Utilities Manager, City of York, Nebraska, written commun., February 15, 2002), and registered wells (Nebraska Department of Natural Resources, 2002) that fully penetrated the High Plains aquifer. Inspection of the logs led to the conceptualization of a 6-layer system (fig. 8.3).

Layer 1 is mostly unsaturated loess (Keech and others, 1967; Swinehart and others, 1994) consisting of silty clay or clayey silt and ranging from 5 to 27 m thick with an average thickness of 16 m. The loess is thinnest in the valleys along Beaver and Lincoln Creeks, where a thin veneer of loess and soil overlies sand and gravel.

Layer 2 is sand and gravel with some discontinuous silt and clay. This layer is 6 to 43 m thick with an average thickness of 21 m and contains the coarsest gravels of all layers in the study area. Ground water in layer 2 is mostly unconfined, and the water table is at or just below the top of this unit. Depth to water ranges from 15 to 30 m below land surface. The sand and gravel deposits are sometimes fining downwards and contain abundant interbedded clays and silts, especially near the bottom of the unit. Layer 2 is continuous across the study area.

Layer 3 is predominantly clayey glacial till but includes silt layers where they directly underlie or overlie the clayey till. Cross sections by Keech and others (1967) indicate that thin silt layers adjacent to the glacial till are common. The glacial till has been interpreted as deposited by continental glaciers that advanced southward into eastern Nebraska; the western extent of these deposits is slightly to the west and south of the study area (Swinehart and others, 1994). Layer 3 is mostly continuous across the study area but is absent in a few locations in the southeastern portion. The thickness ranges from 0 to 35 m with an average thickness of 16 m, and the layer serves as a confining unit for the underlying sand of layer 4.

Layer 4 was assigned as the uppermost sand layer underlying the clayey till/silt. This fine to medium sand contains minor amounts of gravel and is considerably more homogeneous than layer 2. This upper confined sand thins in the northwestern one-half of the study area and is absent in some areas. Nearly all public-supply wells and many irrigation wells are fully screened across the layer 4 sand. The thickness ranges from 0 to 25 m with an average thickness of 11 m.

Layer 5 consists of clay and silt deposits underlying layer 4 but includes minor amounts of interbedded sand. Five public-supply wells are partially screened across layer 5. Layer 5 thins both at the southeast edge and in the northwestern half of the study area, where a bedrock high limits layer thickness. Layer 5 is heterogeneous, and the individual thin lithologic layers within it are probably not continuous over great distances. The thickness ranges from 0 to 32 m with an average thickness of 12 m.

Layer 6 consists of thinly interbedded fine to medium sand and silty clay. Most public-supply wells and some irrigation wells have screens that partially penetrate sand deposits in layer 6. Layer 6 has a spatial distribution of thickness similar

Table 8.1. Summary of hydrogeologic and ground-water-quality characteristics for the High Plains aquifer and the Eastern High Plains regional study area, Nebraska.

[m, meters; cm/yr, centimeters per year; %, percent; m^3/s, cubic meters per second, km^2, square kilometers; m/d, meters per day; mg/L, milligrams per liter; Kh, horizontal hydraulic conductivity; Kz, vertical hydraulic conductivity; NRD, Natural Resources District]

Characteristic	High Plains aquifer	Eastern High Plains regional study area
	Geography	
Topography	Flat to gently rolling with local relief of less than 90 m (Gutentag and others, 1984).	Mostly flat to gently rolling upland with shallow depressions; some stream valleys are incised into the uplands with local relief of less than 20 m.
Climate	Semiarid: mean annual precipitation 40 to 72 cm/yr from west to east; pan evaporation 150 to 270 cm/yr from north to south (Gutentag and others, 1984).	Subhumid; mean annual precipitation 68 cm/yr (High Plains Regional Climate Center, 2003); potential evapotranspiration 165 cm/yr (Gutentag and others, 1984).
Surface-water hydrology	Relatively low precipitation and slopes produce low runoff (0.1 to 6.1 cm/yr) (Hedman and Engel, 1989; Litke, 2001).	Ephemeral streams with relatively low runoff (3.3–4.5 cm/yr) (Hedman and Engel, 1989; Ma and Spalding, 1997); Beaver Creek is only perennial stream; flows maintained by municipal and commercial discharges.
Land use	Rangeland, 56%; agriculture, 41%; wetlands, forest, urban, water, and barren, 3% (U.S. Geological Survey, 1999–2000); irrigated lands, 12% (Qi and others, 2002).	Agriculture, 85%; rangeland, 8%, wetlands, forest, urban, water, and barren, 7% (U.S. Geological Survey, 1999–2000); irrigated lands, 61% (Center for Advanced Land Management Information Technologies, 2000).
Water use	Irrigation: 833 m^3/s, 39 cm/yr average application on 12% of area, 94% of total; Municipal: 18.5 m^3/s, 3% of total; Livestock: 9.7 m^3/s, 1% of total; Mining: 9.3 m^3/s, 1% of total; Industrial: 6.8 m^3/s, 1% of total (values calculated from Dennehy and others, 2002).	Irrigation: about 25 cm/yr withdrawal over 61% of study area, 1.89 m^3/s, 94% of total; Industrial: 0.08 m^3/s, 4% of total; Municipal: 0.05 m^3/s, 2% of total.
	Geology	
Surficial geology	Eolian loess overlying Quaternary alluvial and valley-fill deposits of the High Plains aquifer (Gutentag and others, 1984).	Heterogeneous, layered Quaternary deposits; loess overlying sand and gravel overlying clayey glacial till overlying fine sand overlying layered silt, clay, and sand.
Bedrock geology	Semiconsolidated Ogallala Formation (principal unit of High Plains aquifer) with heterogeneous sequences of sand, gravel, clay, and silt; Underlain by consolidated Tertiary, Cretaceous, Jurassic, Triassic, and Permian units (Gutentag and others, 1984).	Consolidated Cretaceous Carlile Shale and Niobrara Formation (Chalky Shale) underlie unconsolidated High Plains aquifer (Keech and others, 1967).

to layer 5. The thickness ranges from 0 to 48 m with an average thickness of 16 m.

The six model layers are underlain by the Carlile Shale of Late Cretaceous age in the southeastern two-thirds of the study area and the Cretaceous Niobrara Formation, consisting of chalky shale and chalk, in the northwestern one-third of the study area (Keech and others, 1967). The Cretaceous rocks are much less permeable than the sands and gravels of the High Plains aquifer and are considered the base of the High Plains aquifer (Gutentag and others, 1984). A bedrock high in the northwestern one-half of the study area results in thinning of the overlying Quaternary deposits to about one-half their thickness compared to similar deposits beneath York.

Table 8.1. Summary of hydrogeologic and ground-water-quality characteristics for the High Plains aquifer and the Eastern High Plains regional study area, Nebraska.—Continued

[m, meters; cm/yr, centimeters per year; %, percent; m^3/s, cubic meters per second, km^2, square kilometers; m/d, meters per day; mg/L, milligrams per liter; Kh, horizontal hydraulic conductivity; Kz, vertical hydraulic conductivity; NRD, Natural Resources District]

Characteristic	High Plains aquifer	Eastern High Plains regional study area
	Ground-water hydrology	
Aquifer conditions	Extent: 450,660 km^2, primarily bounded by erosional contacts; regionally unconfined, locally confined; saturated thickness: average 61 m, ranges 0 to 366 m; in hydraulic connection with major river systems crossing aquifer (Gutentag and others, 1984; Weeks and others, 1988; Dennehy and others, 2002).	Extent: 388.5 km^2, bounded laterally by approximate regional ground-water flow lines; unconfined and confined layers in aquifer (Keech and others, 1967); Saturated thickness: average 64 m, range 15 to 106 m; only perennial stream is artificially maintained by municipal and commercial discharges, primarily loses water to aquifer.
Hydraulic properties	Kh: average 18.3 m/d, range 0 to 91.4 m/d (Gutentag and others, 1984); Specific yield: average 15.1%, range 5 to 30% (Gutentag and others, 1984).	Kh unconfined: 41.5 m/d; Kh upper confined: 19.8 m/d; Kh lower confined: 4.8 to 6.9 m/d; Storage: Specific yield for unconfined, 0.01–0.3; storage coefficient for confined, $6 \times 10^{-6} - 2 \times 10^{-3}$ (Argonne National Laboratory, 1995; Upper Big Blue NRD, 1999).
Ground-water budget	Precipitation recharge: 0.1 to 15.2 cm/yr, average 1.5 cm/yr, 1 to 25% of precipitation (Gutentag and others, 1984; Luckey and others, 1986; Dugan and Zelt, 2000; Dennehy and others, 2002); Irrigation recharge: as much as 30 to 40% of applied (Luckey and others, 1986); Other inflow: canal and reservoir seepage (Luckey and others, 1986); Irrigation pumpage: average 39 cm/yr (Dennehy and others, 2002), consumptive irrigation demand, 20 to 53 cm/yr (Dugan and Zelt, 2000); Other outflow: discharge to streams (Luckey and others, 1986)	Precipitation recharge: 14.2 cm/yr, 20% of precipitation; Irrigation recharge: 6.4 cm/yr, 25% of irrigation pumpage; Stream seepage: 0.04 m^3/s; Irrigation pumpage: 25.4 cm/yr, 1.89 m^3/s; Industrial pumpage: 0.08 m^3/s; Municipal pumpage: 0.05 m^3/s.
	Ground-water quality	
Water chemistry	In areas unaffected by natural or anthropogenic contamination, primarily calcium bicarbonate waters with dissolved solids less than 517 mg/L, pH ranging from 7 to 8, median concentrations of dissolved oxygen greater than 5.4 mg/L; generally oxidizing conditions but some more reducing conditions occur locally (Dennehy and others, 2002).	Calcium bicarbonate waters with dissolved solids of 280 to 474 mg/L; pH ranges from 6.2 to 8.0; Oxygen reducing in unconfined to iron-reducing in lower confined; nitrate-to-iron reducing conditions in confined can locally become more oxidizing as a result of pumping.
Contaminants	Natural: salinity, iron, manganese, fluoride, radon, uranium, arsenic; Anthropogenic: nitrate, pesticides, salinity, carbon tetrachloride.	Natural: arsenic and uranium; Anthropogenic: nitrate, chlorinated solvents, carbon tetrachloride, pesticides.

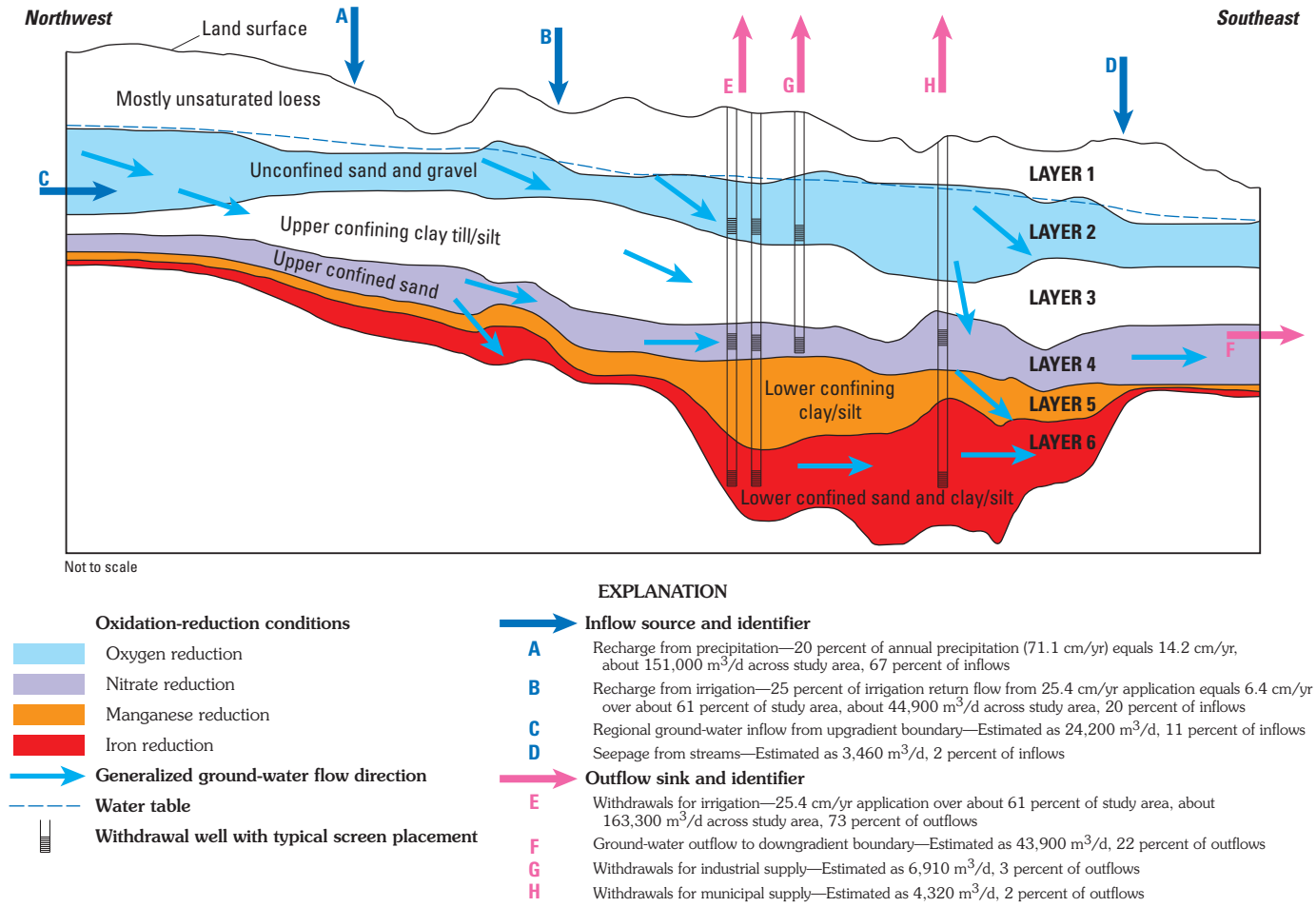

Figure 8.3. Ground-water flow and geochemical conditions, Eastern High Plains regional study area, Nebraska.

Ground-Water Occurrence and Flow

Unconfined and confined ground-water conditions occur in the Quaternary sediment layers as defined in the "Geology" section. Ground-water flow in the Eastern High Plains regional study area is predominantly from the northwest to the southeast with an average gradient of about 0.001326 (Johnson and Keech, 1959; Keech and others, 1967; Conservation and Survey Division, 1980; Verstraeten and others, 1998; Dreeszen, 2000). Quaternary sediment thickness, and therefore, aquifer saturated thickness increases near the center of the study area (fig. 8.3). Saturated thickness ranges from a minimum of 15 m in the northwestern part of the study area to a maximum of 106 m in the region near York, with an average of about 64 m. Ground water passing under the study area that is not withdrawn by pumping farther downgradient probably discharges into the West Fork of the Big Blue River about 24 to 32 km to the southeast. Exchanges of water between the High Plains aquifer and underlying Cretaceous units are considered negligible in comparison to other fluxes (Luckey and others, 1986).

Historical water-level data indicate the ground-water system was in a quasi-steady-state condition from 1997 through 2001. Winter water levels in observation wells generally fluctuated by less than 1.2 m from 1997 through 2001 and were similar to winter water levels prior to 1960, before substantial effects from ground-water withdrawals for irrigation occurred. During summer months, hydraulic heads in the confined aquifer decrease by as much as 15 m in response to irrigation withdrawals. After irrigation ceases in August or September, hydraulic heads in the confined aquifer increase sharply and then gradually recover until reaching stable maximum values during the following winter or spring. Thereafter, this annual cycle is repeated when irrigation withdrawals begin again in June. Over periods greater than 1 year, the effect of a single season cycle diminishes, and hydraulic heads in the late winter-early spring reflect climatic and water-use conditions over several preceding years.

Long-term ground-water hydrographs (U.S. Geological Survey Ground Water Site Inventory Data Base; Rod DeBuhr, Upper Big Blue Natural Resources District, written commun., April 15, 2003) indicate winter hydraulic heads around York decreased about 4.6 m from 1957 to 1982, increased about 4.6 to 5.2 m from 1983 to 1995, and were relatively stable from 1995 to 2001. The water-level history probably reflects the

effect of agricultural irrigation in the area. Pumping apparently exceeded recharge prior to 1982, but the conversion from gravity to sprinkler irrigation, improved irrigation efficiency, and slightly wetter climatic conditions during the 1980s and early 1990s resulted in smaller irrigation withdrawals, greater recharge, and rising water levels. Winter hydraulic heads in 2002 and 2003 decreased by more than 2 m in response to persistent drought conditions beginning in 2001.

Ground-water withdrawals from the confined sand layers induce large downward vertical gradients and flow (fig. 8.3). Comparison of hydraulic head in well clusters with wells screened in the unconfined and upper confined layers from 1957 to 1970 and from 1990 to 1994 shows heads in the confined layer are a maximum of 12.2 m lower than in the unconfined layer during the summer irrigation season. Heads in the confined layer are 0.3 to 2.7 m lower than in the unconfined layer during the fall, winter, and spring when irrigation withdrawals are absent. Seasonal water-level declines in response to irrigation withdrawals are larger in the confined layers than in the unconfined layer because storage coefficients are much smaller in the confined than in the unconfined layer. Hydrographs from a well cluster in north York showed that heads in the lower confined layer were 0.6 to 2.4 m lower than in the upper confined layer during 1983–2002 (U.S. Geological Survey Ground Water Site Inventory Data Base; Rod DeBuhr, Upper Big Blue Natural Resources District, written commun., April 15, 2003).

Many irrigation and some older public-supply wells are screened across both the unconfined and upper and lower confined layers of the aquifer. Those wells with multiple screened intervals and boreholes penetrating confining layers may provide pathways for water and contaminants to move to deeper parts of the aquifer. Active York public-supply wells are screened only in the confined part of the aquifer. Several wells with screens that partially penetrate the unconfined parts of the system were decommissioned in the last decade because of contamination with nitrate or trichloroethylene (Orville Davidson, Public Utilities Director, City of York, Nebraska, written comm., February 15, 2002).

Aquifer Hydraulic Properties

Horizontal hydraulic conductivity of the unconfined layer ranges from 41 to 122 m/d (Argonne National Laboratory, 1995). Results of a 5-day aquifer test just west of York indicate a horizontal hydraulic conductivity value of 41.5 m/d for the unconfined layer (Ma, 1996). Results of a 63-hour aquifer test in northern York indicate a range of horizontal hydraulic-conductivity values between 41 and 122 m/d for the unconfined layer (Argonne National Laboratory, 1995). Horizontal hydraulic-conductivity values for the confined layers were determined from one 24-hour aquifer test in the upper confined layer and two 24-hour aquifer tests in the lower confined layer (Layne Geosciences, Valley, Nebraska,, written commun., 1997). The horizontal hydraulic-conductivity value of the upper confined layer was 19.8 m/d, and horizontal hydraulic-conductivity values for the lower confined layer were 4.8 and 6.9 m/d. Thickness-weighted horizontal hydraulic conductivity for the entire thickness of the High Plains aquifer in the study area used in previous regional ground-water flow models was about 15 m/d (Luckey and others, 1986; COHYST, 2001). Horizontal hydraulic- conductivity values from the aquifer tests were used as initial estimates in the Eastern High Plains regional ground-water flow model.

Storage properties of the unconfined and confined layers were determined from aquifer tests in and around York and generally span a considerable range and have high uncertainties (table 8.1). Thickness-weighted average values of specific yield determined from interpretations of lithologic-log analysis reported by Gutentag and others (1984) indicate that specific yield in most of the study area is in the range of 10 to 20 percent.

Systematic estimates of vertical hydraulic conductivity, ratios of horizontal to vertical hydraulic conductivity, and porosity have not been made across the High Plains aquifer or in the study area. Chen and Yin (1999) summarize results from several aquifer tests in Quaternary or younger alluvial deposits along the Platte and Republican Rivers in Nebraska (north and south, respectively, of the study area), as having ratios of horizontal to vertical hydraulic conductivity ranging between 15 and 70. Values in this range were used as initial estimates for the Eastern High Plains regional ground-water flow model. Estimates of porosity for the various lithologic materials ranged from 0.2 to 0.4 based on specific-yield values presented by Gutentag and others (1984) and typical values reported by Zheng and Bennett (2002).

Water Budget

A conceptual water budget for the study area was developed and provided initial estimates of boundary fluxes for the ground-water flow model (fig. 8.3, table 8.1). Estimates of ground-water withdrawals and seepage from streams were reasonably well constrained. Withdrawals for irrigation per unit area are estimated as 25.4 cm/yr (see “Water Use”) over the irrigated part of the study area (61 percent) resulting in an estimated volumetric flux of 163,300 m^3/d. Withdrawals for industrial and public-supply purposes were known or estimated from historical records and were 6,910 m^3/d and 4,320 m^3/d, respectively. Seepage from streams to ground water (see “Surface-Water Hydrology”) was estimated as 3,460 m^3/d by subtracting measured low-flow stream discharge in Beaver Creek near the southeast end of the study area from commercial and wastewater discharges to Beaver Creek in York.

Ground-water inflows through the northeastern model boundary and outflows through the southwestern model boundary were estimated from Darcy’s equation (Freeze and Cherry, 1979). The Darcy’s equation calculation used a horizontal hydraulic-conductivity value of 61 m/d for the unconfined sand and gravel and 23 m/d for the confined sand,

an average regional hydraulic gradient of 0.001326 (Keech and others, 1967), and saturated-thickness values representative of the boundary. Hydraulic-conductivity values in the upper range of possible values were selected so the calculated boundary fluxes would be near the upper limits of any boundary-flux estimates. On the basis of data from nearby test holes, a saturated thickness of 19 m was assigned for the unconfined sand and gravel on the upgradient boundary, and saturated thicknesses of 33 m and 13 m were assigned for the unconfined sand and gravel and confined sand, respectively, on the downgradient boundary. The resulting calculated inflow on the upgradient boundary was 24,200 m^3/d, and the calculated outflow on the downgradient boundary was 49,300 m^3/d.

Areal recharge is the primary source of inflow to the ground-water system and typically has greater uncertainty associated with its estimation than other budget terms. Recharge estimates were constrained by the need to balance the inflow and outflows of the water budget. The assumption of a balanced water budget is justified by the quasi-steady-state condition of winter water levels during 1995–2001 and the similarity of these water levels to those prior to the late 1950s. Total recharge across the study area is about 196,000 m^3/d, assuming a balanced water budget. Recharge from irrigation return flows was assumed as 25 percent of withdrawals (25.4 cm/yr) or 6.4 cm/yr over the irrigated area for a volumetric flux of about 44,900 m^3/d. The assumed proportion of irrigation return flow is less than some historical estimates in the High Plains of 30 to 40 percent (Luckey and others, 1986) but reflect that irrigation efficiency has improved in the last 2 decades and that there has been considerable conversion of gravity irrigation to more efficient center-pivot irrigation in the study area. To balance the water budget, recharge from precipitation was assumed as 20 percent of annual precipitation or 14.2 cm/yr. Applied over the entire study area, this assumed recharge rate results in a flux of 151,000 m^3/d. The assumption of precipitation recharge as 20 percent of annual average precipitation is slightly higher than a previous recharge estimate of 15 percent of precipitation for the study area, based upon soil-water balance simulations (Dugan and Zelt, 2000), but is similar to values used in a previous local ground-water modeling study (Upper Big Blue Natural Resources District, 1999).

In the conceptual water budget (fig. 8.3), recharge accounts for about 87 percent of inflows, and withdrawals account for about 78 percent of outflows. Boundary inflows (11 percent of total) and outflows (22 percent of total) are lesser but important terms in the water budget. Conceptually, the dominance of recharge and withdrawals in the water balance indicates there should be considerable vertical and horizontal flow in the system between recharge areas and withdrawal wells, considering the relatively small size of the study area.

Ground-Water Quality

Sources of ground-water quality information in the study area include (1) samples collected as part of compliance monitoring of public-supply wells from the Nebraska Department of Health and Human Services (Ann Pamperl, Nebraska Department of Health and Human Services, Lincoln, Nebraska, written comm., January 15, 2002); (2) data from test wells drilled by the City of York (Orville Davidson, Public Utilities Director, City of York, Nebraska, written comm., February 15, 2002); (3) ground-water contamination investigations (Argonne National Laboratory, 1995); (4) regional ground-water quality investigations (Verstraeten and others, 1998); (5) data bases with compilations of historical data collected in the area (U.S. Geological Survey National Water Information System; University of Nebraska–Lincoln, 2000); and (6) samples collected from eight York public-supply wells for the NAWQA Source Water Quality Assessment (SWQA) program in October through December 2002. Of these sources, there are relatively few analyses with complete data with which to classify the oxidation-reduction (redox) state of the water. Moreover, many samples have been collected from wells with long screened intervals and large withdrawal rates such as irrigation or public-supply wells that may cause mixing of waters with different redox characteristics or have incomplete well-construction information so that the screened interval is not known. These factors limit the number of analyses useful for characterization of redox conditions.

The major-ion chemical data from City of York test wells, Argonne National Laboratory (1995), Verstraeten and others (1998), and SWQA data indicate ground water in the study area is of calcium-bicarbonate type water with dissolved-solids concentrations ranging from 280 to 474 mg/L with an average of about 364 mg/L (35 analyses). Values of pH are neutral ranging from 6.2 to 8.0 with an average of about 7.1 (151 analyses). Consistent spatial patterns of pH are not apparent from the available data.

Of the 124 sample results with sufficient data for redox classification, 98 of the samples were collected from the unconfined sand and gravel. Only one of the 98 samples had a dissolved-oxygen analysis (7.4 mg/L). All 98 samples had concentrations of nitrate-nitrogen greater than 0.5 mg/L, indicating the waters are likely in the range of oxygen- to nitrate-reducing waters.

Twenty-six samples with sufficient data for redox classification were collected from wells screened in the confined parts of the aquifer. Of these, 23 samples were collected from wells with unique locations: 10 were from public-supply wells, 12 were from test wells temporarily installed during exploratory drilling for public-supply wells by the City of York, and one was from a monitoring well. The spatial distribution of these

samples is limited to areas in or near York (fig. 8.4). The four oxygen-reducing samples were all collected from public-supply wells. Most of the samples from test or monitoring wells (7 of 12) were consistent with manganese- or iron-reducing conditions. At four of the locations with redox data in the confined aquifer, data were available from different depths. At all four locations, the water generally became more reduced with depth, becoming either iron or manganese reduced in the lowermost sample. Generally, the redox data indicate the unconfined parts of the aquifer are oxidized and the confined parts of the aquifer are reduced with some mixtures and oxidized waters. The occurrence of more mixed and oxidized waters from public-supply wells than in test or monitoring wells is consistent with the redox chemistry being affected by withdrawals from the wells.

Direct evidence of changes in redox status as a result of pumping is demonstrated by water-chemistry data from York public-supply well 97-1A, screened in the upper confined layer, and wells 97-1 and 97-2, screened in the lower confined layer (fig. 8.5). Samples collected in 1996 (prior to public-supply well operation) from nearby test wells with screen lengths similar to those of the public-supply wells indicated ground water in 97-1A was manganese reducing and water in the lower confined sand was iron reducing at 97-1 and manganese reducing at 97-2. No nitrate-nitrogen was detected in any of the three samples. After withdrawals from the three public-supply wells began in 1997, nitrate-nitrogen was detected in all three wells, and concentrations of iron, manganese, and arsenic decreased in wells 97-1 and 97-2. Sampling results in 2001-2002 indicate oxygen-reducing conditions at well 97-1A, manganese-reducing conditions at well 97-1, and oxygen- or nitrate-reducing conditions at well 97-2.

The changes in the public-supply wells to more oxidized conditions has two implications: (1) the redox data in large-capacity wells can be affected by the withdrawals and may not be representative of ambient chemistry in most of the confined aquifer, and (2) the reducing conditions in the confined aquifer are weakly poised and subject to change to more oxidized conditions in places in the aquifer. The persistence of iron-reducing conditions in two public-supply wells and manganese-reducing conditions in three public-supply wells indicates that redox conditions are not as changeable in response to withdrawals in all locations as in 97-1, 97-1A, and 97-2. The variability of redox conditions in public-supply wells may indicate spatial variations in the mineralogy, hydrogeology, and distribution of redox-sensitive dissolved constituents that influence the redox condition.

The time-series chemistry data from wells 97-1, 97-1A, and 97-2 indicate ambient redox conditions in the confined layers are primarily manganese or iron reducing, conditions become more reducing with depth, and redox conditions can change in response to withdrawals. The time-series data and the preponderance of evidence from other sites in the confined layers (fig. 8.4) indicate ground water in the confined layers is predominantly manganese or iron reduced and leads to the conceptual model shown in fig. 8.3.

Ground-Water Flow Simulations

A MODFLOW-2000 (Harbaugh and others, 2000) model was constructed to simulate ground-water flow in a 388.5-km^2 area of the High Plains aquifer near York, Nebraska. The model created for this study is discretized into rows, columns, and layers to represent the various hydrogeologic materials in the area, to simulate ground-water flow, and to delineate the areas contributing recharge to York public-supply wells. The flow model assumes steady-state conditions and represents average conditions for 1997–2001. Historical water-level data indicate the ground-water system was in a quasi-steady-state condition during 1997–2001 (see “Ground-Water Occurrence and Flow”). Most of the hydraulic-head data used to calibrate the model were collected in April 2001, and the values reflect average winter conditions for 1997–2001.

Modeled Area and Spatial Discretization

A previous regional ground-water flow model (COHYST, 2001) of a 26,936-km^2 area was used to select the model boundaries for this study. The Eastern High Plains regional ground-water flow model was aligned northwest to southeast at an azimuth of 117 degrees (fig. 8.6), which approximately corresponds to the regional flow direction on potentiometric maps from before 1953 (Johnson and Keech, 1959), 1964 (Keech and others, 1967), 1979 (Conservation and Survey Division, 1980), 1995 (Dreeszen, 2000), and 1996 (Verstraeten and others, 1998). The southeast model boundary is located closer to York than the northwest model boundary because ground-water flow is from the northwest, and areas contributing recharge to wells will likely extend toward the northwest. The northeastern and southwestern boundaries, approximately corresponding to lateral no-flow boundaries of two ground-water flow lines in the regional flow model, were selected far enough from York so as not to affect simulated flow paths to York public-supply wells.

Horizontal and vertical discretization was specified to yield representative simulation of ground-water flow and areas contributing recharge to public-supply wells while maintaining simplicity in model geometry. The flow model consists of 200 rows and 300 columns of square cells with dimensions of 82.57 m on each side. There are six model layers corresponding to the loess-unconfined, unconfined, upper confining, upper confined, lower confining, and lower confined units, as shown in the conceptual model (fig. 8.3).

Layer thicknesses are not uniform except for layer 1, which has a uniform thickness of 4.57 m. Layer 1 was specified with a relatively thin uniform thickness to better represent the interaction between Beaver Creek, which is simulated exclusively in layer 1, and the unconfined aquifer. The loess areas in layer 1 outside of the Beaver Creek alluvial valley go dry during the simulation. The remaining model layer thicknesses were interpolated from 71 driller’s logs in the study area, after assigning lithologies in the logs to the layers of

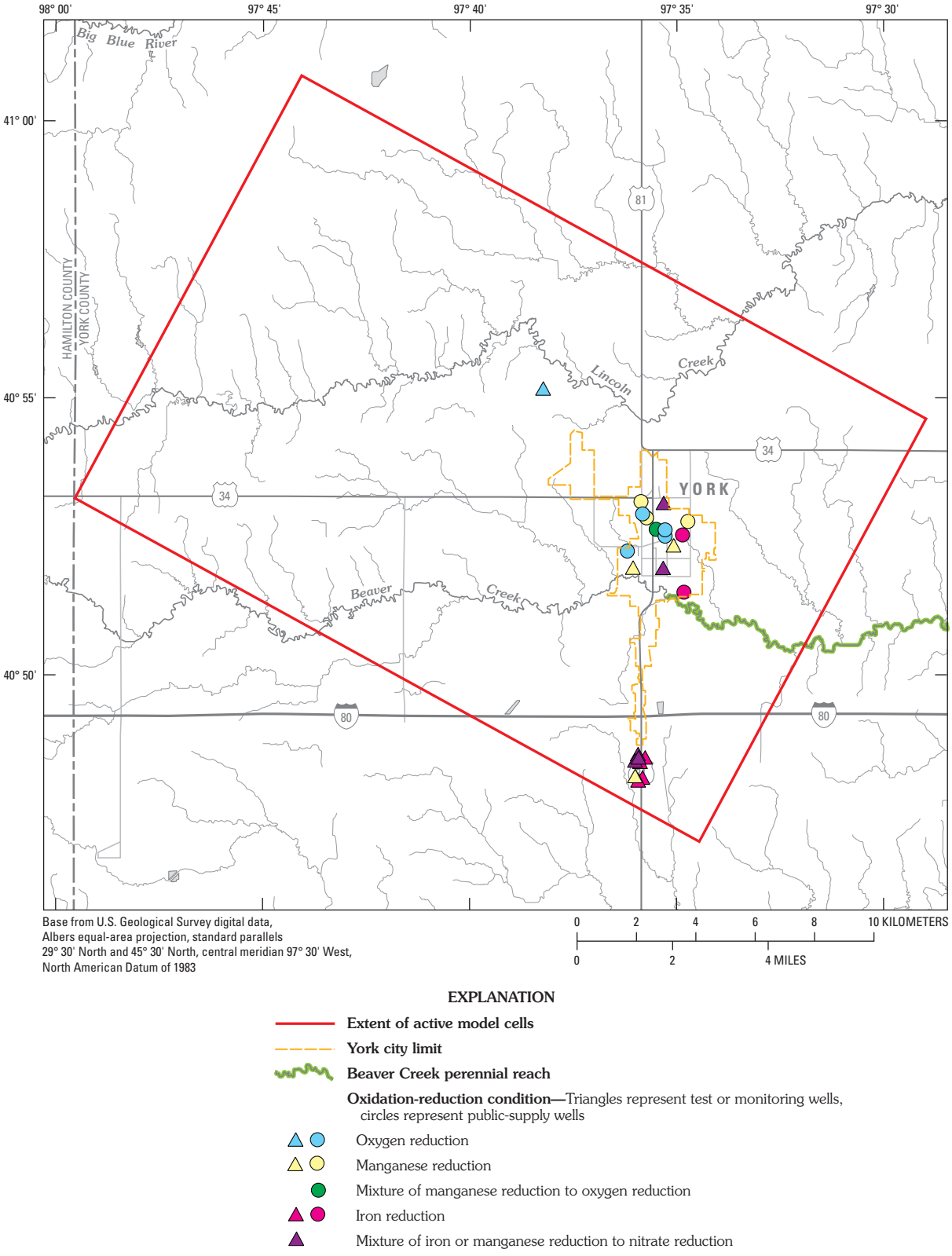

Figure 8.4. Oxidation-reduction conditions in wells screened in the confined part of the High Plains aquifer, Eastern High Plains regional study area, Nebraska.

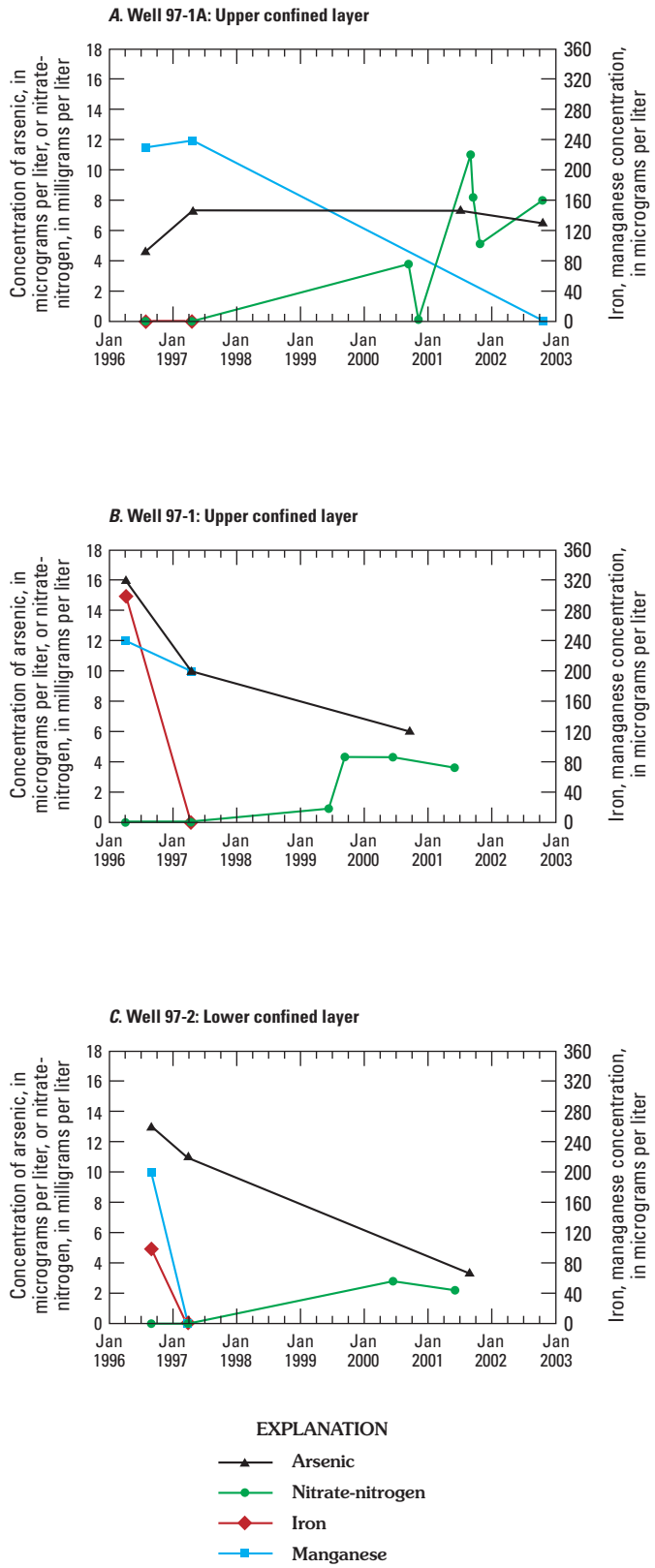

Figure 8.5. Changes in concentration of oxidation-reduction sensitive species in three York public-supply wells from 1996, prior to withdrawals for public water supply, and for 1997–2002, when municipal withdrawals occurred.

the conceptual model. Interpolations between geologic logs to develop hydrogeologic sections and three-dimensional stratigraphic models were done using the Department of Defense Groundwater Modeling System (GMS), version 4.0, developed by the Engineering Computer Graphics Laboratory at Brigham Young University. A minimum thickness of 0.3 m was assigned to model layers where layers were absent, which was primarily an issue for layers 4, 5, and 6. In general, the overall model thickness is smaller in the northwestern one-half of the modeled area than in the southeastern one-half to reflect changes in the bedrock topography (fig. 8.3).

Boundary Conditions and Model Stresses

The northeastern and southwestern model boundaries were specified as no-flow boundaries because they correspond to ground-water flow lines from the regional ground-water flow model. The northwestern (upgradient) and southeastern (downgradient) boundaries were initially specified-head boundaries by using heads telescoped to the model from the regional model and following the methods of Leake and Claar (1999). Following initial model simulations, the upgradient and downgradient model boundaries were changed from specified-head to specified-flux boundaries to more realistically represent ground-water underflow in the aquifer. Specifying flux rather than head along the boundaries allows head along the boundary to change with varying stress, which eliminates the artificial constraint of specified head.

Flux boundaries were specified for each of the primary water-bearing units on the upgradient and downgradient boundaries of the flow model. Flux boundaries were simulated using wells in each cell on the boundary for the unconfined, upper confined, and lower confined units, corresponding to layers 2, 4, and 6 (fig. 8.7). It is assumed that lateral inflow or outflow in the two confining layers is negligible. The flux boundaries are uniform along the boundary and unique for each water-bearing unit at the upgradient and downgradient boundaries. Initial boundary-flux estimates were based on conceptual-model estimates.

Anthropogenic stresses on the ground-water system include withdrawal for agricultural, industrial, and municipal needs. The MODFLOW Well package was used to simulate withdrawals from the aquifer. The locations of registered irrigation and industrial wells and data on potential irrigated area per well were available from a State of Nebraska data base (Nebraska Department of Natural Resources, 2002). The locations of public-supply wells were determined with a Global Positioning System and verified on street and topographic maps. Available well-screen elevations were used to assign withdrawal values to corresponding model layers. Withdrawal from wells without well-screen information was assigned to model layers considering nearby well-screen elevations and water use. For wells screened in multiple layers, the proportion of the total withdrawal assigned to each layer was determined from the ratio of an individual layer's transmissivity to the

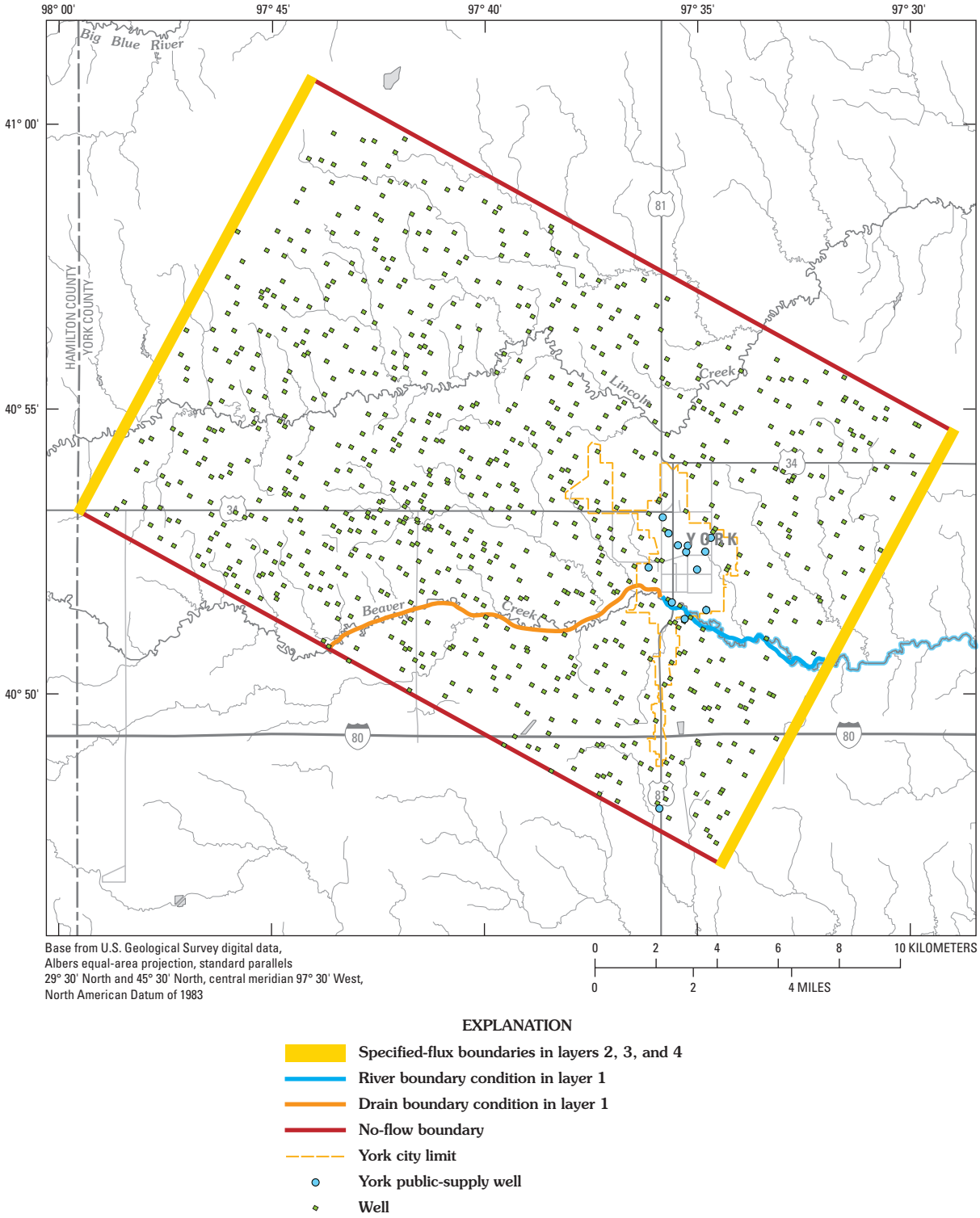

Figure 8.6. Ground-water flow model grid boundary and selected boundary conditions in different model layers, Eastern High Plains regional study area, Nebraska.

overall transmissivity. For example, the proportion of flow from layer 1 would be calculated as:

$$\frac{K_1 b_1}{\sum_{i=1}^{n} K_i B_i}$$

Where K_1 is the hydraulic conductivity of layer 1, b_1 is the saturated thickness of layer 1, K_i is the hydraulic conductivity of individual layer i, b_i is the saturated thickness of that layer, and n is the total number of layers.

A constant withdrawal rate of 25.4 cm/yr (see "Water Use") was multiplied by the estimated irrigated area to calculate the 1997–2001 average volumetric withdrawal rate for each irrigation well. For the 794 registered irrigation wells in the study area, the sum of the irrigated areas associated with each well record was considerably larger than the irrigated area in the study area indicated by a map of 1997 land use (Center for Advanced Land Management Information Technologies, 2000), a year with relatively normal climatic conditions. The irrigated areas listed in the well registration overestimate actual irrigated area because not all farmers irrigate all of the irrigable land each year. Consequently, the actual irrigated area per well was estimated by multiplying the potential irrigated area for each well by the ratio of the 1997 irrigated area from the 1997 land-use map to the sum of the irrigated areas from the well registration for the study area.

There were 14 public-supply wells active in York for all or most of 1997–2001 (table 8.2). Several public-supply wells have multiple screens that typically fully penetrate the upper confined sand (layer 4) and fully or partially penetrate the lower confined sand (layer 6). Six wells have screens in sand lenses that partially penetrate layer 5, the lower confining clay/silt. Three wells have screens that partially penetrate the unconfined sand and gravel, layer 2; two of these wells were shut down due to nitrate-nitrogen concentrations in excess of the EPA MCL of 10 mg/L during 2000–2001. Average 1997–2001 withdrawal rates were assigned for the steady-state simulations.

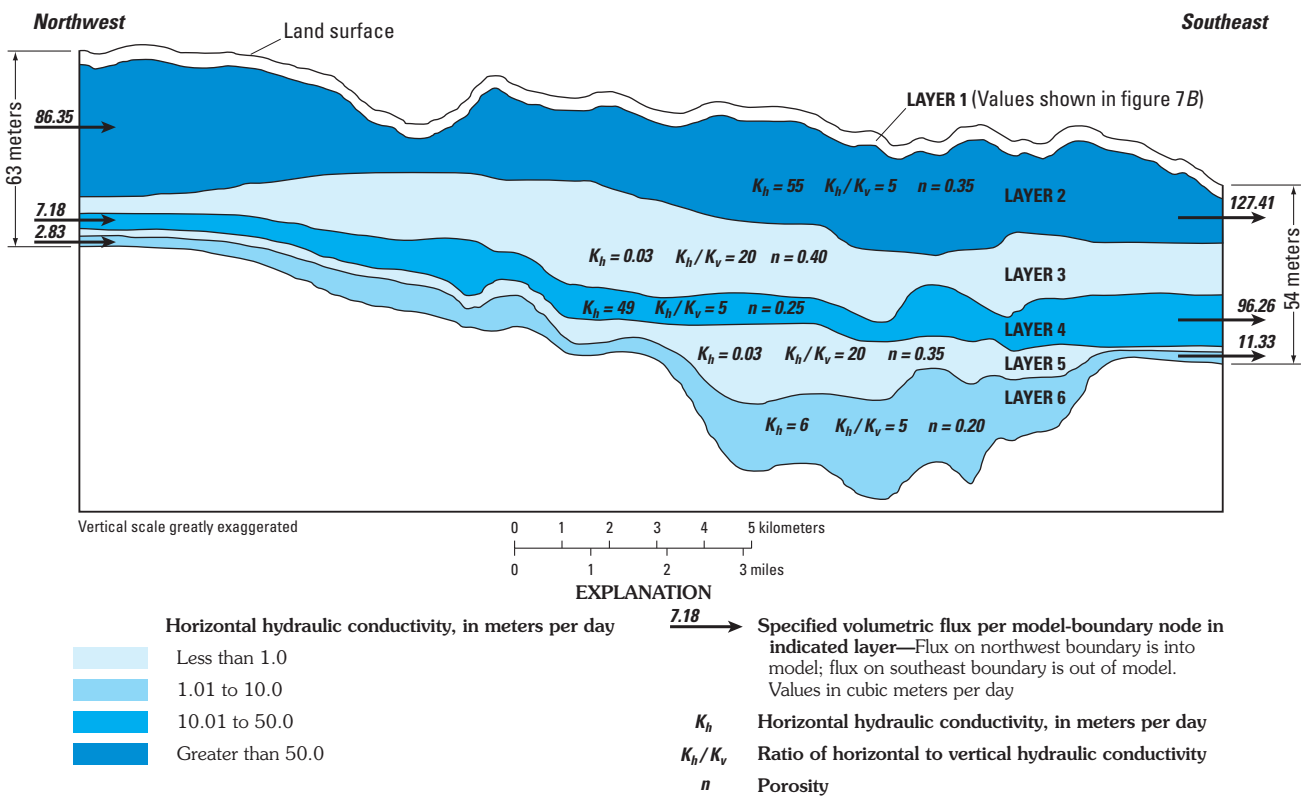

Figure 8.7*A*. Hydrogeologic section showing hydraulic-conductivity zones and flux-boundary values for layers of calibrated ground-water flow model.

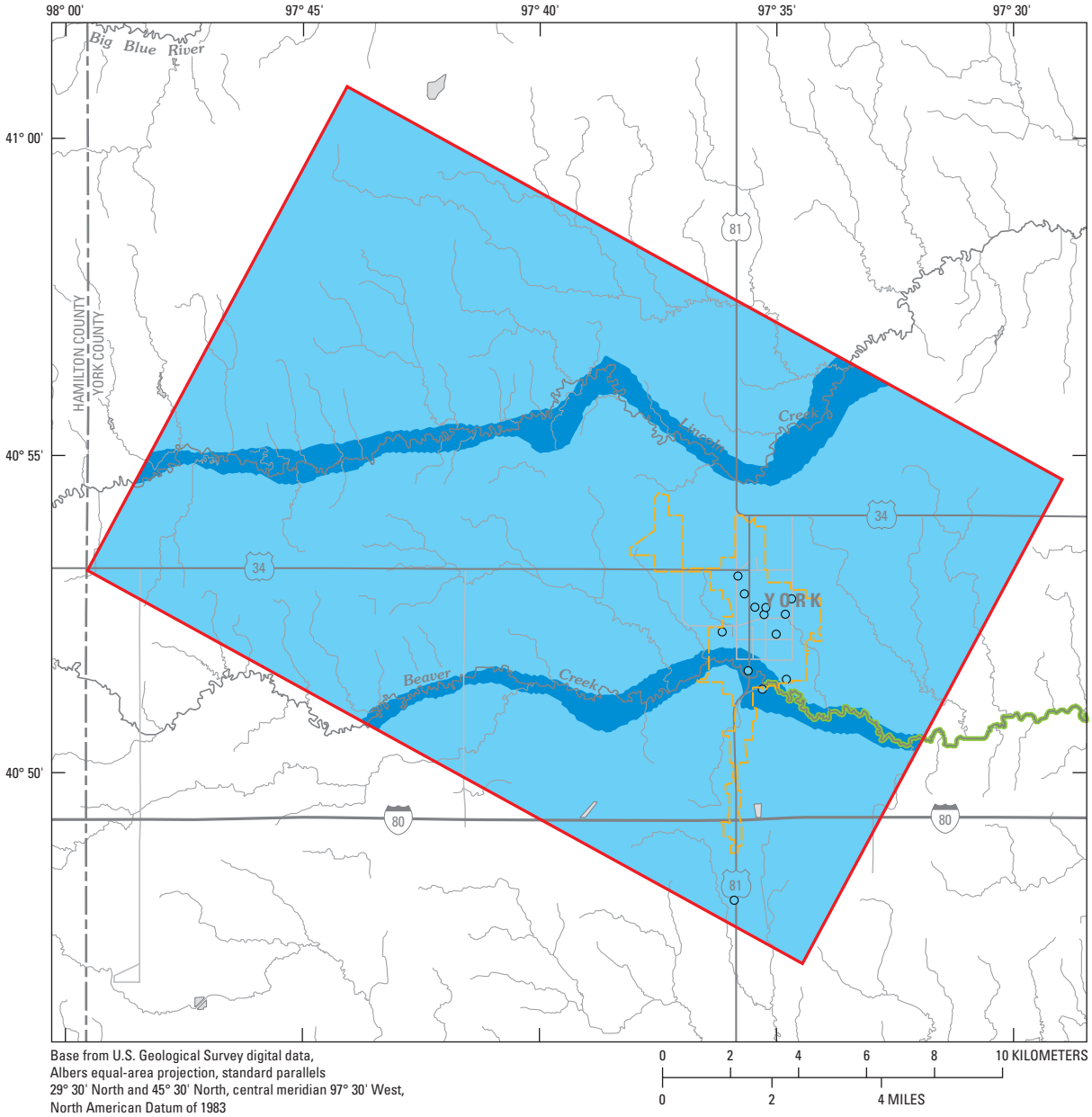

EXPLANATION

Horizontal hydraulic conductivity, in meters per day

Less than 1.00—K_h = 0.03; K_h/K_v = 20; n = 0.40

Greater than 50.01—K_h = 55; K_h/K_v = 5; n = 0.35

Extent of active model cells

York city limit

Beaver Creek perennial reach

York public-supply well

[K_h, horizontal hydraulic conductivity, in meters per day; K_h/K_v, ratio of horizontal to vertical conductivity; n, porosity]

Figure 8.7*B*. Hydraulic-conductivity and active-cell zones in layer 1 of calibrated ground-water flow model, Eastern High Plains regional study area, Nebraska

There were 10 commercial/industrial wells active in the study area, and most of the withdrawals were from 4 of the 10 wells. Withdrawal rates for commercial wells were estimated using values from the Upper Big Blue NRD (1999), or from the City of York, or by contacting commercial water users. The commercial/industrial wells were screened in layers 2, 4, and(or) 6.

Beaver Creek is the only continuously flowing stream in the modeled area (see "Surface Water Hydrology"), and flow in the creek results from municipal wastewater and commercial discharges in York. Downstream (southeast) from York, surface water in Beaver Creek seeps into the ground-water system, contributing about 3,630 m^3/d. Beaver Creek is simulated as a MODFLOW drain upstream from the York Cold Storage facility discharge (fig. 8.6). This part of the creek is dry except after rainstorms. Outflow to the drain is assumed to be zero during the steady-state simulation. The streambed-conductance factor is the product of the streambed hydraulic conductivity and the streambed width divided by the thickness of the streambed material. A 0.3048-m streambed thickness, a 3.048-m-wide stream channel, and a streambed hydraulic conductivity of 0.1 m/d were assumed, yielding a streambed-conductance factor of 1.0 m^2/d. The conductance factor was multiplied by the length of the stream reach in each drain cell to calculate the conductance (in m^3/d). Drain elevation was set as the estimated elevation of land surface. Four flow observations of zero were intermittently specified along the drain reach. The drain was included in the model as an aid in calibration rather than for its role in the water budget.

MODFLOW river cells represent Beaver Creek downstream from the York Cold Storage discharge to the southeastern model boundary to represent ground-water/surface-

Table 8.2. Average ground-water pumping rates for public-supply wells, 1997–2001, Eastern High Plains regional study area, Nebraska (Orville Davidson, Public Utilities Director, City of York, Nebraska, written commun., Feb. 15, 2002).

[m, meters; m^3/d, cubic meters per day]

Well name	Elevation of land surface (m)	Year of construction	Average withdrawal 1997–2001 (m^3/d)	Total length of well screens (m)	Well status	Actual screen placmement
48–1	501.40	1948	0.43	10.67	Shut down 2000*	2 screens partially penetrate layer 2
62–1	485.24	1962	9.53	35.66	Active	2 screens partially penetrate layer 2 and fully penetrate layer 4
68–1	499.87	1968	1,315.62	57.61	Active	2 screens fully penetrate layers 4 and 6
73–1	503.53	1973	535.68	71.63	Active	7 screens fully penetrate layer 4, partially layers 5 and 6
76–1	485.55	1976	123.98	21.34	Active	1 screen in layer 4
77–1	502.31	1977	239.84	60.96	Active	3 screens fully penetrate layer 4, partially layers 5 and 6
77–3	492.25	1977	276.63	43.28	Active	2 screens fully penetrate layers 4 and 6
77–4	489.20	1977	350.38	34.14	Active	2 screens fully penetrate layer 4 and partially penetrate 5 or 6
82–1	502.62	1982	465.93	59.44	Active	2 screens fully penetrate layer 4 and partially penetrate 5 and 6
82–2	502.92	1982	381.65	51.82	Active	3 screens fully penetrate layer 4 and partially penetrate 5 or 6
88–1	501.70	1988	1,646.23	44.20	Shut down 2001*	3 screen partially penetrate layers 2 and 5, fully penetrate 4
97–1	503.22	1997	278.25	25.73	Active	1 screen partially penetrates layer 6
97–1A	502.62	1997	230.55	20.12	Active	1 screen fully penetrates layer 4
97–2	502.92	1997	340.38	32.89	Active	2 screens partially penetrate layer 6

*Wells shut down because of nitrate contamination.

water interaction (figs. 8.6 and 8.7). The MODFLOW River package allows surface water to flow into the ground-water system where river leakage occurs and allows ground water to discharge to surface water near the southeastern edge of the study area where the stream becomes perennial. River conductance was calculated similar to drain conductance. A 0.3048-m streambed thickness, a 3.048-m-wide stream channel, and a streambed hydraulic conductivity of 0.8 m/d were assumed, yielding a streambed-conductance factor of 8.0 m^2/d. Stage was specified as 0.3048 m above the land surface. About one-half of the Beaver Creek leakage to the ground-water system is assumed to occur along the river reach within York where downward head gradients between the river and the aquifer are relatively large.

The upper model boundary consists of a water-table surface allowing inflow from recharge throughout the uppermost active model layer. A specified-flux boundary was used to simulate recharge to the ground-water flow system. Recharge was specified for the entire modeled area and was categorized as predominantly nonirrigated, gravity-irrigated, or sprinkler-irrigated agricultural land, urban land, or surface water. A recharge rate was specified for each of the following recharge zones, with percentage of total land area in parentheses: nonirrigated land 17.1 cm/yr (33 percent), gravity-irrigated agricultural land 22.8 cm/yr (33 percent), and sprinkler-irrigated agricultural land 20.6 cm/yr (28 percent), urban land 1.5 cm/yr (4 percent), and surface water 0 cm/yr (1 percent) (fig. 8.8). Initial estimates were values described in the conceptual model (see "Water Budget"). Urban recharge was assumed principally derived from leakage from the water-distribution system, and urban recharge from precipitation was considered negligible because of the large proportion of impervious area. For 1997–2001, the unaccounted water, the difference between water pumped and the water delivered, was 27,600 m^3/d (Orville Davidson, Public Utilities Director, City of York, Nebraska, written commun., June 6, 2003) or 12 percent of the annual pumping. Areal recharge in urban areas was therefore assumed equal to 27,600 m^3/d uniformly distributed across the urban area. Infiltration of surface water, with the exception of Beaver Creek, was considered insignificant; therefore, cells designated as "surface water" were given a value of zero recharge**.** The surface of the Carlile Shale and Niobrara Formation, underlying the High Plains aquifer in the study area, is represented as a no-flow boundary beneath the model.

Aquifer Hydraulic Properties

Aquifer hydraulic properties were assigned to model layers on the basis of lithology of the six layers of the conceptual model (figs. 8.3 and 8.7, table 8.1). Horizontal hydraulic- conductivity and vertical-anisotropy parameter values were incorporated into the model by using the Layer Property Flow Package (Harbaugh and others, 2000). Layer 1 of the flow model contains parameter zones representing the unconfined sand and gravel in the Beaver and Lincoln Creeks alluvial valleys and the more widespread silt and clay of the loess elsewhere (fig. 8.7*B*). Layers 2 through 6 were each assigned homogeneous values for hydraulic conductivity, vertical anisotropy, and porosity consistent with the predominant lithology based on the conceptual model. Final hydraulic-conductivity values were determined from model calibration.

Model Calibration and Sensitivity

Model calibration is the process by which model parameter values are adjusted within reasonable limits to minimize the difference between model-computed and measured heads and fluxes. Ground-water levels in 31 wells, mostly measured during the spring of 2001, and estimated fluxes from Beaver Creek into the aquifer were used as the basis of calibration. Every parameter used in the simulation was adjusted within reasonable limits until the differences between the model-computed and measured hydraulic heads were reduced to about 5.0 percent of the total head change across the study area. The final model was compared to measured hydraulic heads and estimated discharges in Beaver Creek to evaluate the calibration process.

The overall goodness of fit of the model to the observation data was evaluated using summary measures and graphical analyses. The root-mean-squared error (RMSE), the range of head and residuals, the mean residual, the standard deviation, and the standard-mean error of the residuals (SME), were used to evaluate the model calibration. The RMSE is a measure of the variance of the residuals and was calculated as:

$$RMSE = \sqrt{\frac{\sum_{i=1}^{N} (h_{meas} - h_{sim})i^2}{N}}$$

where h_{meas} is the measured hydraulic head, h_{sim} is the model-computed (simulated) hydraulic head, $(h_{meas} - h_{sim})$ is the head residual, and N is the number of wells used in the computation. If the ratio of the RMSE to the total head change in the modeled area is small, then the error in the head calculations is a small part of the overall model response (Anderson and Woessner, 1992).

The mean residual (R_{mean}) is computed as:

$$R_{mean} = \frac{\sum_{i=1}^{n} (h_{meas} - h_{sim})i}{N}$$

and its positive or negative sign indicates whether model-computed hydraulic heads were higher or lower than measured hydraulic heads, respectively.

The SME was calculated as:

$$SME = \frac{\sigma(h_{meas} - h_{sim})}{\sqrt{N}}$$

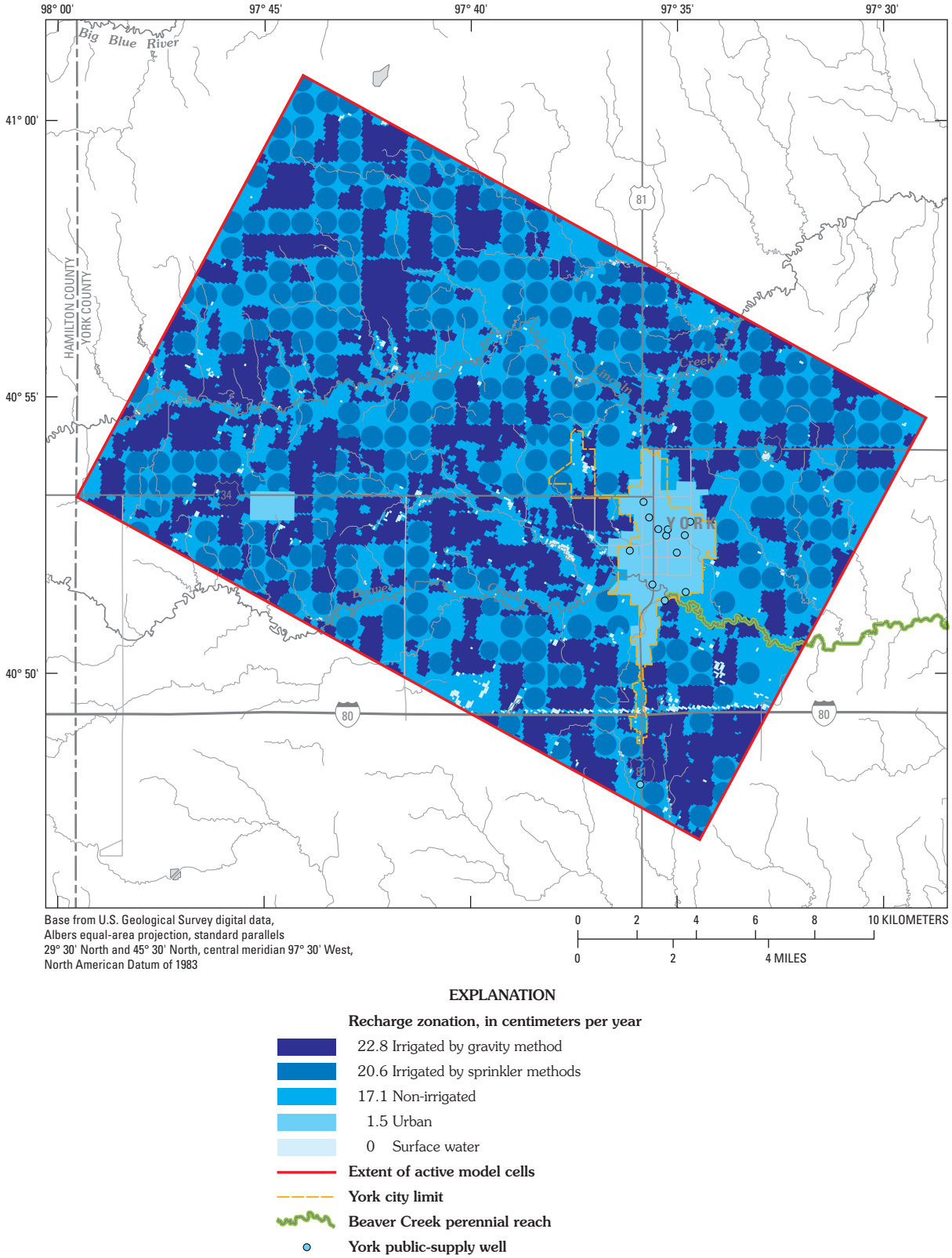

Figure 8.8. Distribution of recharge estimates used as ground-water flow model input, Eastern High Plains regional study area, Nebraska.

where $\sigma(h_{meas} - h_{sim})$ is the standard deviation of the residuals.

Model calibration continued until the mean residual and RMSE of the residuals for all model layers were minimized. The flow model was considered calibrated when the following criteria were satisfied:

1. Incremental changes in model parameters did not substantially reduce the RMSE (Hill and others, 2000) or other calibration statistics.
2. The RMSE of the entire model was less than approximately 5 percent of the total head change in the study area.
3. The simulated vertical gradients in two sets of nested wells were similar to the measured vertical gradients.
4. Simulated seepage to the High Plains aquifer from Beaver Creek was within one order of magnitude of the conceptual discharge of about 3,630 m^3/d.

The calibrated model is a simplified representation of a complex hydrogeologic system and inherently sensitive to some model parameters. The model is influenced by the uncertainty in the value of these parameters and in the dynamics of the boundary conditions. A sensitivity analysis characterizes the effect of model-parameter change on the model results. The model is considered sensitive to a model parameter when changes in the model parameter produce substantial changes in the model results. This type of analysis can be used to identify areas where additional hydrogeologic information is needed.

Sensitivity analysis was performed using MODFLOW-2000 and the sensitivity process (Hill and others, 2000). The calibrated steady-state model is nearly four orders of magnitude more sensitive to recharge than to any other type of parameter. The model also is sensitive to the hydraulic conductivity of layers 2 and 4 and the specified-flux boundaries. The model is relatively insensitive to the vertical anisotropy and the conductance factor of Beaver Creek.

Parameter values were changed within acceptable limits from initial estimated values to the final values during the calibration process. Most of the parameter changes before the change from specified-head to specified-flux boundaries were limited to the hydraulic conductivity of layers 2, 4, and 6; values in layer 2 yielding the best model fit at one point reached a value of about 150 m/d, about 3 times greater than values estimated from pumping tests. After the switch to the specified-flux boundary, hydraulic-conductivity values in all layers were changed to previously estimated values (see “Aquifer Hydraulic Properties”) resulting in a lower sum of square residuals and better vertical head distribution. Recharge values in the five zones were specified such that the total amount of recharge applied to the study area agreed with the conceptual model. Adjustments to the recharge distribution among the five recharge zones assumed gravity irrigation provided more recharge than sprinkler irrigation (Mustick and Stewart, 1992), irrigated land provided more recharge than nonirrigated land, urban land provided less recharge than agricultural lands, and surface-water areas provided no recharge (fig. 8.8). Although individual initial recharge parameters may have changed during the calibration process, the total recharge applied to the model remained essentially the same. After about 200 model runs, adjustments were made only to the most sensitive model parameters with most of the final adjustments occurring at the specified-flux boundaries.

Model-Computed Hydraulic Heads

The model-computed hydraulic heads in all model layers were in good agreement with ground-water flow directions and gradients indicated by previous regional investigations. A simple method of assessing model fit is to plot the model-computed hydraulic head values against the measured observations. For a perfect fit, all points should fall on the 1:1 diagonal line. Figure 8.9 presents a graph of the model-computed hydraulic heads plotted against measured hydraulic heads for the Eastern High Plains regional study area and indicates reasonable model fit. The mean residual for the entire model is -0.7 m, and residuals range from -3.6 m to 3.5 m (range of 7.1 m). The RMSE for the entire model is 1.66 m, which is about 5.4 percent of the 31-m range of head observations in the model, and the head residuals appear to be randomly distributed across the study area (fig. 8.10) at all values of measured head (fig. 8.11). The standard deviation of the residuals is 1.53 m, and the SME is 0.28 m. Individual layer calibration statistics vary, which is likely because most of the water-level measurements are located in layers 2 and 4, with only two water-level measurements in layer 6. Mean error and RMSE for layers 2, 4, and 6 are 0.53 m and 1.56 m, 0.15 m and 0.94 m, and 1.87 and 2.69, respectively. The sum

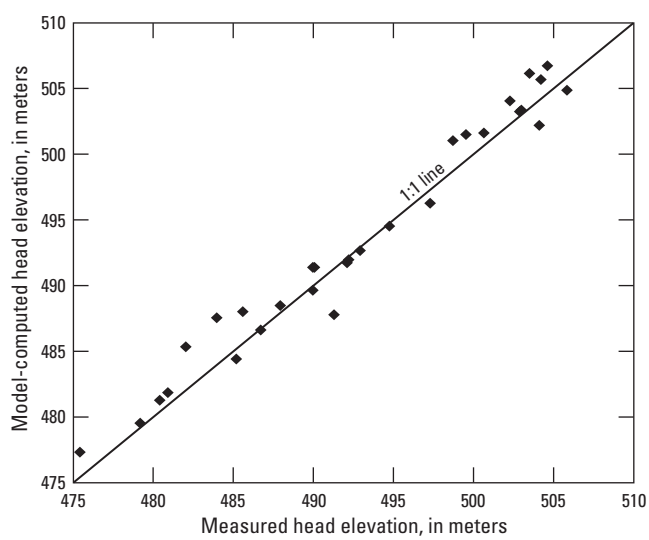

Figure 8.9. Relation between model-computed and measured hydraulic head, Eastern High Plains regional study area, Nebraska.

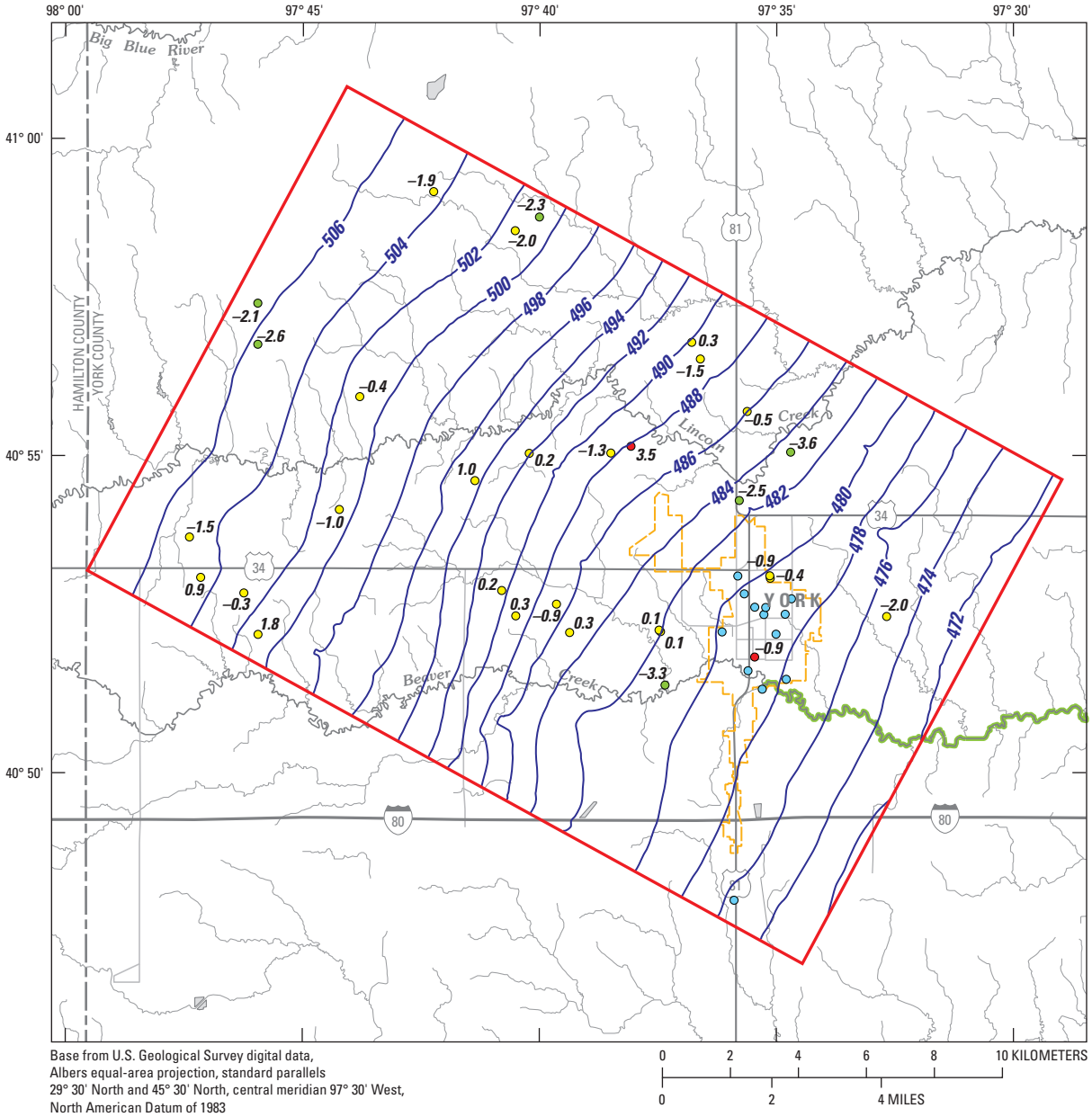

EXPLANATION

490 Elevation contour of model-computed potentiometric surface in model layer 4, in meters above sea level. Contour interal 2 meters

Observation well and residual head values (measured minus modeled), values in meters

3.5 Greater than 2

–0.3 2 to –2

–3.3 Less than –2

York public-supply well

Extent of active model cells

York city limit

Beaver Creek perennial reach

Figure 8.10. Model-computed potentiometric surface in layer 4 and observation points and residuals in all layers, Eastern High Plains regional study area, Nebraska.

of squared-weighted residuals for all heads in the model is 74.17 m, whereas the sum of squared-weighted residuals for all observations, including estimated Beaver Creek discharge, is 97.61 m. The reported correlation between the weighted residuals and normal order statistics is 0.950 (which is greater than the 5-percent significance level of 0.946), indicating the hypothesis that the weighted residuals are independent and normally distributed at the 5-percent significance level is valid (Hill, 1998).

The calibrated steady-state ground-water flow model calculates water levels and internal fluxes for each model cell. The simulated potentiometric surface in the upper confined unit (layer 4) and the simulated vertical distribution of head along row 100 in the model are shown in figs. 8.10 and 8.12, respectively. Simulation results indicate the direction of flow is predominantly from the northwest to the southeast, as expected from the conceptual model. The potentiometric surface of layer 2 in the area near Beaver Creek, indicates leakage from the reach of the creek downstream from York.

The magnitude and horizontal extent of vertical ground-water flow between model layers is greatest between the unconfined and upper confined layers (layers 2 and 4) (fig. 8.12, table 8.3). Although there are localized areas of vertical downward gradients between the upper confined and lower confined aquifers (layers 4 and 6) comparable to the gradients between layers 2 and 4, the typical head difference is about 1 m. The largest area of vertical downward movement is in and around the city of York between layers 2 and 4. The magnitude of the largest difference in simulated head between layers 2 and 4 is about 5 m.

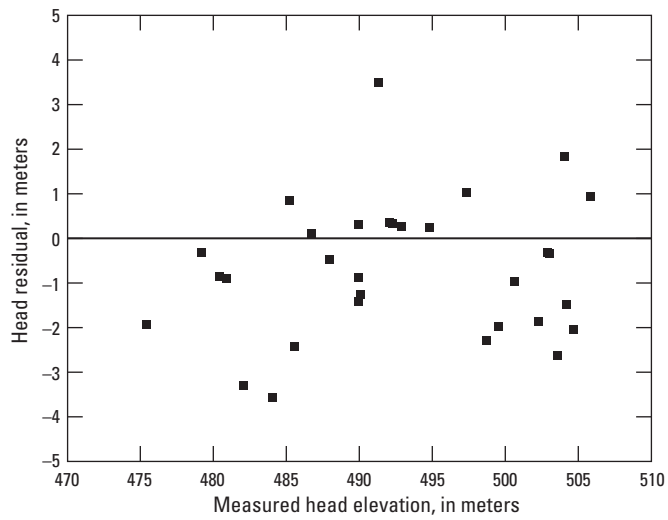

Figure 8.11. Relation between head residuals and measured hydraulic head, Eastern High Plains regional study area, Nebraska.

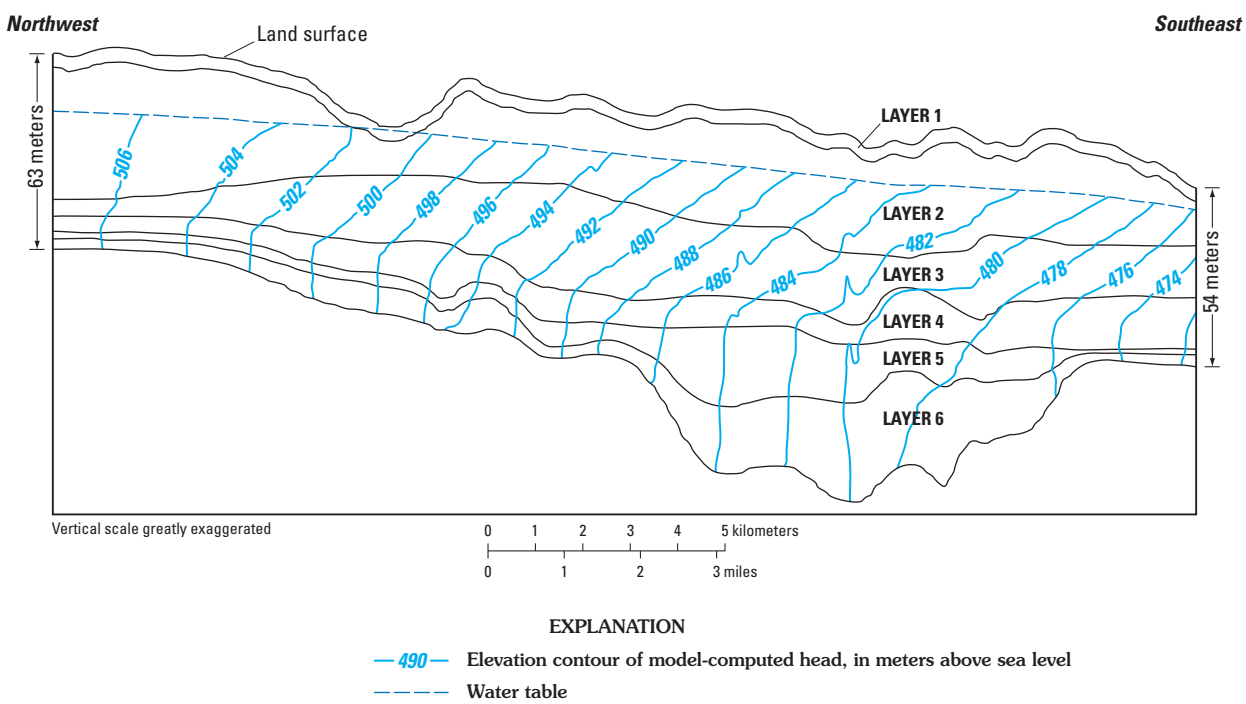

Figure 8.12. Hydrogeologic section showing model-computed hydraulic heads through row 100 of calibrated ground-water flow model, Eastern High Plains regional study area, Nebraska.

Table 8.3. Model-computed water budget for 1997–2001 average conditions, Eastern High Plains regional study area, Nebraska.

[m³/d, cubic meters per day; %, percent; <, less than; —-, not computed]

Water-budget component	Layer						Total	Percentage of inflow or outflow
	1	2	3	4	5	6		
Model inflow (m³/d)								
Upgradient constant-flux boundary	—	13,875	—	1,416	—	566	15,857	6.9
Recharge	14,431	189,932	—	—	—	—	204,363	89.3
Beaver Creek—downstream from York	8,780	—	—	—	—	—	8,780	3.8
Beaver Creek—upstream from York	—	—	—	—	—	—	—	—
Wells	—	—	—	—	—	—	—	—
Downgradient constant-flux boundary	—	—	—	—	—	—	—	—
SUBTOTAL (boundary fluxes)	23,211	203,807	—	1,416	—	566	229,000	100
INTERNAL FLUXES From:	—	—	—	—	—	—	—	—
Layer 1	—	25,436	—	—	—	—	25,436	9.4
Layer 2	2,206		103,509	—	—	—	105,715	39.1
Layer 3	—	287	—	95,385	—	—	95,672	35.3
Layer 4	—	—	4,350	—	19,428	—	23,778	8.8
Layer 5	—	—	—	995	—	16,255	17,250	6.4
Layer 6	—	—	—	—	2,667	—	2,667	1.0
SUBTOTAL (internal fluxes)	2,206	25,723	107,859	96,380	22,095	16,255	270,518	100
TOTAL (boundary + internal fluxes):	25,417	229,530	107,859	97,796	22,095	16,821	499,518	
Model outflow (m³/d)								
Upgradient constant flux boundary	—	—	—	—	—	—	—	—
Recharge	—	—	—	—	—	—	—	—
Beaver Creek—downstream from York	27.2	—	—	—	—	—	27.2	0.01
Beaver Creek—upstream from York	5.7	—	—	—	—	—	5.7	0.0
Wells	—	95,838	12,186	54,617	4,844	11,828	179,313	78.3
Downgradient constant-flux boundary	—	27,895	—	19,402	—	2,326	49,623	21.7
SUBTOTAL (boundary fluxes):	32.9	123,733	12,186	74,019	4,844	14,154	228,969	100
INTERNAL FLUXES To:	—	—	—	—	—	—	—	
Layer 1	—	2,206	—	—	—	—	2,206	0.8
Layer 2	25,436	—	287	—	—	—	25,723	9.5
Layer 3	—	103,509	—	4,350	—	—	107,859	39.9
Layer 4	—	—	95,385	—	995	—	96,380	35.6
Layer 5	—	—	—	19,428	—	2,667	22,095	8.2
Layer 6	—	—	—	—	16,255	—	16,255	6.0
SUBTOTAL (internal fluxes):	25,436	105,715	95,672	23,778	17,250	2,667	270,518	100
TOTAL (boundary + internal fluxes):	25,469	229,448	107,858	97,797	22,094	16,821	499,487	
INFLOW-OUTFLOW	-52	82	1.0	<-1.0	<1.0	0.0	31	
Percent discrepancy	-0.2%	0.04%	0.00%	0.00%	0.00%	0.00%	0.01%	

Model-Computed Water Budget

The calibrated model produces a detailed distribution of ground-water fluxes across cell faces and boundary conditions. The model-computed water budget indicates areal recharge from irrigation return flow and precipitation provides about 89 percent (14,431 m^3/d) of the total water flow into the modeled area (table 8.3). Inflow from the upgradient specified-flux boundary and ground-water seepage from Beaver Creek accounts for about 6.9 and 3.8 percent of model inflow, respectively. Simulated inflow from Beaver Creek in and below the city of York is 8,780 m^3/d. The model-computed water budget indicates that about 78 percent (179,314 m^3/d) of the model outflow is to wells, with the downgradient specified-flux boundary accounting for about 22 percent of the total outflow (49,623 m^3/d). A small outflow (0.01 percent) occurs along Beaver Creek near the southeastern boundary and at a topographic low near the middle of the simulated reach.

The simulated internal flux distribution indicates most of the water flows downward from the overlying layers to layer 4 with decreasing downward flow from layer 4 to layer 5 and from layer 5 to layer 6. Based on model results, a downward flux is persistent throughout the area. Overall, the difference between inflows and outflows throughout the entire modeled area was about 0.01 percent.

Simulation of Areas Contributing Recharge to Public-Supply Wells

The calibrated steady-state model was used to estimate the areas contributing recharge to selected public-supply wells in the city of York by using the MODPATH (Pollock, 1994) particle-tracking post processor. Output from the steady-state model is used in the MODPATH simulation to calculate the path of imaginary particles moving through the simulated ground-water system (Pollock, 1994). As MODPATH tracks the path of each particle, it also tracks the time required for the particle to travel along the path, yielding results both in direction and time, which is useful information when delineating areas contributing recharge to wells (Pollock, 1994). The model-computed areas contributing recharge represent advective ground-water flow and do not account for mechanical dispersion. Advection-dispersion transport simulations would likely yield larger areas contributing recharge than advective particle-tracking simulations because the effects of dispersion caused by aquifer heterogeneity would be included.

Along with output from the calibrated steady-state MODFLOW model, the MODPATH simulation requires specified porosity values to calculate ground-water flow velocities. Porosity values were assumed uniform within each layer (fig. 8.7) based on layer lithology, specific-yield values presented by Gutentag and others (1984), and typical porosity values listed in Zheng and Bennett (2002).

Results from the MODPATH simulations were used to delineate areas contributing recharge and zones of contribution to York public-supply wells (fig. 8.13). Because of the natural horizontal gradient from the northwest to the southeast across the study area, the areas contributing recharge extend northwest from the public-supply wells of York. Additional pumping upgradient from the public-supply wells affects the locations and orientations of the areas contributing recharge, as indicated by their occasionally irregular shapes. Traveltimes from the areas contributing recharge to wells range from 20 to more than 100 years. Based on particle-tracking results, some particles, especially those reaching screens in the lower confined unit, do not originate at the water table in the study area but track to the northwestern specified-flux boundary. These particles have estimated traveltimes of thousands of years. The zones of contribution to public-supply wells typically broaden until the area contributing recharge at the water table is reached then narrow as only a few deeper pathlines delineating the zones of contribution continue upgradient.

Limitations and Appropriate Use of the Model

The ground-water flow model for the Eastern High Plains regional study area was designed to delineate contributing areas to public-supply wells, to help guide data collection, and to support future local modeling efforts. Limitations of the ground-water flow model, assumptions made during model development, and results of model calibration and sensitivity analysis all are factors that constrain the appropriate use of the model and highlight potential future improvements.

The Eastern High Plains regional ground-water flow model simulates flow in the High Plains aquifer, assuming steady-state conditions. Although hydrologic conditions for the nonirrigation season from 1997 to 2001 appeared in a quasi-steady-state condition, hydrologic conditions during the late 1950s through the mid-1990s were not steady state. The effects of these deviations from steady-state conditions compared to the simulated ground-water fluxes and areas contributing recharge are difficult to predict without developing a transient model of the last several decades, which was beyond the scope of this study. Results of this steady-state model may not be representative of instances when hydrologic conditions are dissimilar to the assumed steady-state conditions. Seasonally transient stresses and vertical gradients of large magnitude that occur in the ground-water system during the irrigation season are not represented in the steady-state model. Public-supply withdrawals for 1997–2001 were greater than during earlier times, so the simulated areas contributing recharge and zones of contribution to public-supply wells using 1997–2001 average pumping in a steady-state model are likely larger than those that would be calculated for previous time frames. The 1997–2001 average areas contributing recharge and zones of contribution are therefore considered conservative (maximum) estimates of potential source areas for water reaching public-supply wells.

Recharge was estimated and its areal distribution was assigned on the basis of 1997 land use (U.S. Geological Sur-

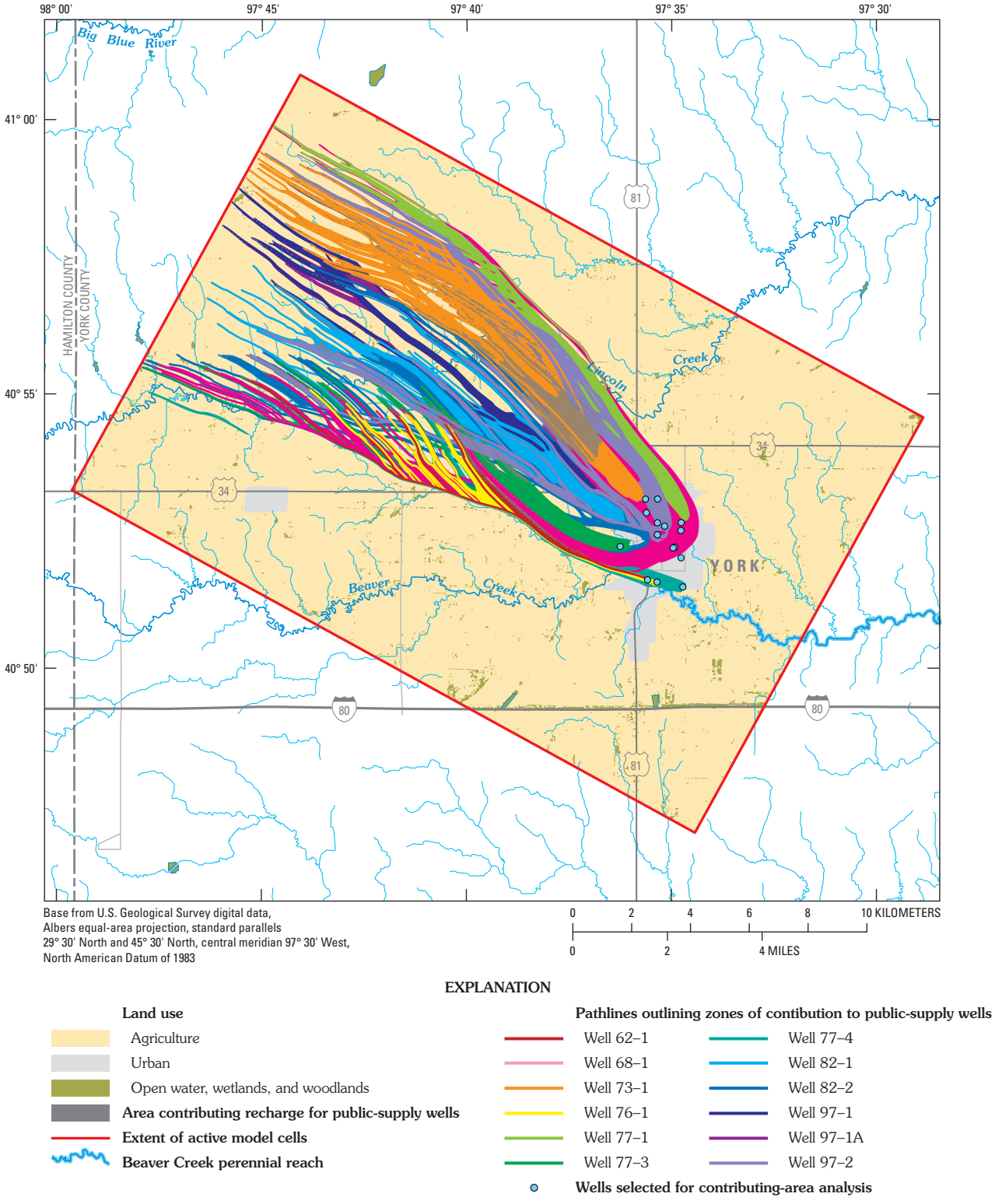

Figure 8.13. Model-computed areas contributing recharge and zones of contribution for 12 public-supply wells, Eastern High Plains regional study area, Nebraska.

vey, 1999–2000). Considering the significant sensitivity of the model to recharge values, the recharge distribution could be a significant, but presently unknown, source of error.

The ground-water flow model does not account for the heterogeneous nature of the High Plains aquifer but rather approximates all lithologies as being uniform throughout each layer. Heterogeneous aquifer complexity is beyond the scope of this study, but detailed mapping of aquifer lithology and layering would be appropriate for more site-specific modeling studies.

Computed areas contributing recharge and traveltimes through zones of contribution are based on a calibrated model and estimated effective porosity values. In a steady-state model, changes to input porosity values do not change the area contributing recharge to a given well. Changes to input porosity values will change computed traveltimes from recharge to discharge areas in direct proportion to changes of effective porosity because there is an inverse linear relation between ground-water flow velocity and effective porosity and a direct linear relation between traveltime and effective porosity. For example, a one-percent decrease in porosity will result in a one-percent increase in velocity and a one-percent decrease in particle traveltime. A detailed sensitivity analysis of porosity distributions was beyond the scope of this study, although future work could compare simulated ground-water traveltimes to ground-water ages to more thoroughly evaluate effective porosity values.

The Eastern High Plains regional ground-water flow model uses justifiable aquifer properties and boundary conditions and provides a reasonable representation of ground-water flow conditions in the study area for 1997–2001. The model can be used to better understand regional water budgets and ground-water flow paths in the study area for the time period of interest but may not be suitable for long-term predictive simulations. The model also proved helpful for understanding the vertical movement of water between various layers of the High Plains aquifer. This model provides a useful tool to evaluate aquifer vulnerability at a regional scale, to facilitate comparisons of ground-water traveltime between regional aquifer systems, and to guide future detailed investigations in the study area.

References Cited

Anderson, M.P., and Woessner, W.W., 1992, Applied ground-water modeling: Academic Press, Inc., New York, 381 p.

Argonne National Laboratory, 1995, Final phase II report—Expedited site characterization, York, Nebraska: Prepared for Community Credit Corporation, United States Department of Agriculture, April 1995.

Center for Advanced Land Management Information Technologies, 2000, Delineation of 1997 land use patterns for the Cooperative Hydrology Study in the Central Platte River Basin: University of Nebraska, Lincoln, Center for Advanced Land Management Information Technoligies.

Chen, X., and Yin, Y., 1999, Evaluation of streamflow depletion for vertical anisotropic aquifers: Journal of Environmental Systems, v. 27, no. 1, p. 55–70.

COHYST, 2001, Pre-groundwater development 1-mile groundwater flow model for the Eastern Model Unit: COoperative HYdrology STudy Technical Committee, May 2, 2001, 46 p., accessed June 26, 2006, at *http://cohyst.dnr.ne.gov/*

Conservation and Survey Division, 1980, Configuration of the water table 1979, 1:250,000 Lincoln and Nebraska City quadrangle, Nebraska: Conservation and Survey Division, Lincoln University of Nebraska, accessed June 26, 2006, at *http://csd.unl.edu/general/gis-datasets.asp*

Dennehy, K.F., Litke, D.W., and McMahon, P.B., 2002, The High Plains aquifer, USA—Groundwater development and sustainability, *in* Hiscock, K.M., Rivett, M.O., and Davison, R.M., eds., Sustainable groundwater development: Geological Society, London, Special Publication, 193, p. 99–119.

Dreezen, V. H., 2000, Configuration of the water table 1995, 1:250,000 Lincoln and Nebraska City quadrangle, Nebraska: Conservation and Survey Division, Lincoln University of Nebraska, accessed June 26, 2006, at *http://csd.unl.edu/general/gis-datasets.asp*

Dugan, J.T., and Zelt, R.B., 2000, Simulation and analysis of soil-water conditions in the Great Plains and adjacent areas, Central United States, 1951–80: U.S. Geological Survey Water-Supply Paper 2427, 81 p.

Fallon, J.D., and McChesney, J.A., 1993, Surface-water-quality assessment of the lower Kansas River Basin, Kansas and Nebraska—project data, November 1986 through April 1990: U.S. Geological Survey Open-File Report 93–51, 593 p.

Freeze, R.A., and Cherry, J.A., 1979, Groundwater: Englewood Cliffs, N.J., Prentice-Hall Inc., 604 p.

Gutentag, E.D., Heimes, F.J., Krothe, N.C., Luckey, R.R., and Weeks, J.B., 1984, Geohydrology of the High Plains aquifer in parts of Colorado, Kansas, Nebraska, New Mexico, Oklahoma, South Dakota, Texas, and Wyoming: U.S. Geological Survey Professional Paper 1400–B, 63 p.

Harbaugh, A.W., Banta, E.R., Hill, M.C., and McDonald, M.G., 2000, MODFLOW-2000, The U.S. Geological Survey modular ground-water flow model—User guide to modularization concepts and the ground-water flow process: U.S. Geological Survey Open-File Report 00-92, 121 p.

Hedman, E.R., and Engel, G.B., 1989, Flow characteristics for selected streams in the Great Plains subregion of the Central Midwest Regional Aquifer System and selected adjacent areas—Kansas and Nebraska, and parts of Colorado, Iowa, Missouri, New Mexico, Oklahoma, South Dakota, Texas, and Wyoming: U.S. Geological Survey Hydrologic Investigations Atlas HA–708, 3 sheets.

High Plains Regional Climate Center, 2003, National Weather Service surface observations and automated weather data network: accessed March 11, 2003 at *http://www.hprcc.unl.edu/data.htm*

Hill, M.C., Banta, E.R., Harbaugh, A.W., and Anderman, E.R., 2000, MODFLOW-2000, The U.S. Geological Survey modular ground-water flow model—User guide to the observation, sensitivity, and parameter-estimation processes and three post-processing programs: U.S. Geological Survey Open-File Report 00–184, 209 p.

Hill, M.C., 1998, Methods and guidelines for effective model calibration: U.S. Geological Survey Water-Resources Investigations Report 98–4005, 90 p.

Johnson, C.R., and Keech, C.F., 1959, Geology and ground-water resources of the Big Blue River Basin above Crete, Nebraska, with a section on chemical quality of water, by Robert Brennan: U.S. Geological Survey Water-Supply Paper 1474, 94 p.

Keech, C.F., Dreeszen, V.H., and Emery, P.A., 1967, Availability of ground water in York County, Nebraska: U.S. Geological Survey Water-Supply Paper 1839–F, 17 p.

Leake, S.A., and Claar, D.V., 1999, Procedures and computer programs for telescopic mesh refinement using MODFLOW: U.S. Geological Survey Open-File Report 99–238, 53 p.

Litke, D.W., 2001, Historical water-quality data for the High Plains Regional Ground-Water study area in Colorado, Kansas, Nebraska, New Mexico, Oklahoma, South Dakota, Texas, and Wyoming, 1930-98: U.S. Geological Survey Water-ResourcesInvestigations Report 00–4254, 65 p.

Luckey, R.R., Gutentag, E.D., Heimes, F.J., and Weeks, J.B., 1986, Digital simulation of ground-water flow in the High Plains aquifer in parts of Colorado, Kansas, Nebraska, New Mexico, Oklahoma, South Dakota, Texas, and Wyoming: U.S. Geological Survey Professional Paper 1400–D, 63 p.

Luckey, R.R., and Becker, M.F., 1999, Hydrogeology, water use, and simulation of flow in the High Plains aquifer in northwestern Oklahoma, southeastern Colorado, southwestern Kansas, northeastern New Mexico, and northwestern Texas: U.S. Geological Survey Water-Resources Investigations Report 99–4104, 35 p.

Ma, Li, 1996, Impact of artificial groundwater recharge at two Nebraska sites: Lincoln University of Nebraska, Ph.D. dissertation, 209 p.

Ma, Li, and Spalding, R.F., 1997, Herbicide persistence and mobility in a recharge lake watershed in York, Nebraska: Journal of Environmental Quality, v. 26, no. 1, p. 115–125.

Mustik, J.T., and Stewart, B.A., 1992, Irrigation technologies, *in* Kromm, D.E., and White, S.E., eds., Groundwater exploitation in the High Plains: Lawrence, University Press of Kansas, p. 110–144.

Nebraska Department of Natural Resources, 2002, Registered groundwater wells data base: accessed January–July 2002, at *http://nrcnt3.dnr.state.ne.us/wellssql/wellsindex.asp*

Pollock, D.W., 1994, User's guide for MODPATH/MODPATH-PLOT, Version 3—A particle tracking post-processing package for MODFLOW, the U.S. Geological Survey finite-difference ground-water flow model: U.S. Geological Survey Open-File Report 94–464, accessed Feb. 6, 2007, at *http://water.usgs.gov/nrp/gwsoftware/modpath41/modpath41.html*

Qi, S.L., Konduris, Alexandria, Litke, D.W., and Dupree, Jean, 2002, Classification of irrigated land using satellite imagery, the High Plains aquifer, nominal date 1992: U.S. Geological Survey Water-Resources Investigations Report, 02–4236, 35 p.

Smith, F.A., 2000, York County test-hole logs: Nebraska Water Survey Test-Hole Report No. 93, Conservation and Survey Division, Institute of Agriculture and Natural Resources, 60 p.

Swinehart, J.B., Dreeszen, V.H., Richmond, G.M., Tipton, M.J., Bretz, R., Steece, F.V., Hallberg, G.R., and Goebel, J.E., 1994, Quaternary geologic map of the Platte River 4° X 6° quadrangle, United States: U.S. Geological Survey Miscellaneous Investigations Series Map I–1420 (NK-14), 1 plate.

Thelin, G.P., and Heimes, F.J., 1987, Mapping irrigated cropland from Landsat data for determination of water use from the High Plains aquifer in parts of Colorado, Kansas, Nebraska, New Mexico, Oklahoma, South Dakota, Texas, and Wyoming: U.S. Geological Survey Professional Paper 1400–C, 38 p., 1 plate.

University of Nebraska–Lincoln, 2000, Quality-assessed agrichemical contaminant database for Nebraska ground water: A cooperative project of the Nebraska Departments of Agriculture, Environmental Quality, and Natural Resources and the University of Nebraska – Lincoln: accessed May 15, 2002 at *http://nrcnt3.dnr.state.ne.us/clearinghouse/index.asp*

Upper Big Blue Natural Resources District, 1999, A study of ground-water pumping for existing uses and proposed industrial development of the Heartland Fibers Processing Plant, York County, Nebraska: York, Nebraska, Upper Big Blue Natural Resources District, August 3, 1999, 32 p.

U.S. Census Bureau, 2003, 2000 Census of population and housing—population and housing unit counts: Washington, D.C., PHC–3–29, Nebraska,

U.S. Geological Survey, 1999-2000, National land cover data base: accessed June 26, 2006, at *http://edcwww.cr.usgs.gov/products/landcover.html*

Verstraeten, I.M., McGuire, V.L., and Heckman, K.L., 1998, Hydrogeology and subsurface nitrate in the Upper Big Blue Natural Resources District, Central Nebraska, July 1995 through September 1997: U.S. Geological Survey Water-Resources Investigations Report 98–4207, 81 p.

Weeks, J.B., Gutentag, E.D., Heimes, F.J., and Luckey, R.R., 1988, Summary of the High Plains Regional Aquifer-System Analysis in parts of Colorado, Kansas, Nebraska, New Mexico, Oklahoma, South Dakota, Texas, and Wyoming: U.S. Geological Survey Professional Paper 1400–A, 30 p.

Zheng, Chunmiao, and Bennett, G.D., 2002, Applied contaminant transport modeling (2nd ed.): New York, Wiley and Sons, 621 p.

Appendix 1. Database Dictionary for the Study of Anthropogenic and Natural Contaminants

TANC Database—TANC_STUDIES Table Data Dictionary A–2
TANC Database—SITES Table Data Dictionary A–4
TANC Database—WELL_INFO Table Data Dictionary A–6
TANC Database—RESULTS_RGNL Table Data Dictionary A–8
TANC Database—PARAMETERS Table Data Dictionary A–10
TANC Database—PUMPING_RGNL Table Data Dictionary A–11
TANC Database—ANCILLARY Table Data Dictionary A–13
TANC Database—CAREASUM_RGNL Table Data Dictionary A–15
TANC Database—CAREARDXPH_RGNL Table Data Dictionary A–22
TANC Database—CAREASRCE_RGNL Table Data Dictionary A–25

TANC Database—TANC_STUDIES Table Data Dictionary

[The TANC_Studies table stores descriptions of the TANC study areas]

STUDY_UNIT (USGS NAWQA Study Unit Code) Character; Width 4; **MANDATORY**
STUDY_UNIT is only served to the end user from the TANC Sites table

TANC_STUDY (TANC Study Identifier) Character; Width 12; **MANDATORY**
Each site for a study unit is given a code to identify the study unit,TANC, and the year the study unit was incorporated into the overall TANC study. The field is 12 characters wide so that an a, b, or c can be appended for study units with more than one TANC study area (nvbrtanc01a, nvbrtanc01b, sanjtanc01, hpgwtanc01)

SU_START_DATE (Study Unit Starting Date) Integer; Width 4
The year the study unit was started, or restarted in USGS NAWQA Cycle II

REGIONAL (Regional-Scale Investigation Flag) Boolean; Width 1; Yes (-1), No (0)
Indicates that the study unit conducted a TANC regional-scale investigation

LOCAL (Local-Scale Investigation Flag) Boolean; Width1; Yes (-1), No (0)
Indicates that the study unit conducted a TANC local-scale investigation

GENERAL_LOCATION (General Geographic Location) Character; Width 50
General geographic location of the TANC regional-scale investigation

SPECIFIC_LOCATION (Specific Geographic Location) Character; Width 50
Additional information on the specific geographic location of the TANC regional-scale investigation, if needed

AREA (Area of Regional-Scale Investigation) Real; Width 10; Decimal 2
Area of the regional-scale investigation, in square miles. This is the area of the regional ground-water flow model

AREA_SQUARE_KILOMETERS (Area of Regional–Scale Investigation, in Square Kilometers) Real; Width 10; Decimal 2
This is a calculated field (AREA multiplied by 2.59)

AQUIFER_LITH (Aquifer Lithology); Character; Width 4
Lithology(ies) of the aquifer simulated. For example, sand and gravel or limestone. Use USGS National Water Information System, Ground Water Site Inventory System (NWIS GWSI) C096 definitions (National Water Information System, Ground Water Site Inventory System *http://pubs.usgs.gov/of/2005/1251/pdf/gwcoding_Sect2-1.pdf accessed May 15, 2007)*

AQUIFER_TYPE (Aquifer Type Code); Character; Width 1
Aquifer type code for the aquifer simulated. Use NWIS GWSI [*C713*] definitions

PRINCIPAL_AQUIFER (USGS NAWQA Principal Aquifer); Character; Width 50
USGS NAWQA principal aquifer in which the TANC regional-scale investigation is located

LOCAL_AQUIFER_NAME (Aquifer Name); Character; Width 50
Local or study-unit name for the aquifer that is simulated in the TANC regional-scale investigation. If no local name, enter NA

PRINCIPAL_CATEGORY; Character; Width 50
Principal category of the aquifer being studied. (Values from the Ground Water Atlas of the United States *http://capp.water.usgs.gov/aquiferBasics/index.html*, accessed May 23, 2007)

HIERARCHICAL _CLASS_1; Character; Width 50
First level subdivision of the principal category of aquifer being studied. (Values are from the USGS Lexicon of Hydrogeologic Names in the United States, which were derived from the Ground Water Atlas of the United States *http://capp.water.usgs.gov/aquiferBasics/index.html*, accessed May 23, 2007)

HIERARCHICAL_CLASS_2; Character; Width 50

Second level subdivision of the principal category of aquifer being studied. (Values are from the USGS Lexicon of Hydrogeologic Names in the United States, which were derived from the Ground Water Atlas of the United States *http://capp.water.usgs.gov/aquiferBasics/index.html, accessed May 23, 2007)*

HIERARCHICAL_CLASS_3; Character; Width 50

Third level subdivision of the principal category of aquifer being studied. (Values are from the USGS Lexicon of Hydrogeologic Names in the United States, which were derived from the Ground Water Atlas of the United States *http://capp.water.usgs.gov/aquiferBasics/index.html*, accessed May 23, 2007)

HIERARCHICAL_CLASS_4; Character; Width 50

Fourth level subdivision of the principal category of aquifer being studied. (Values are from the USGS Lexicon of Hydrogeologic Names in the United States, which were derived from the Ground Water Atlas of the United States *http://capp.water.usgs.gov/aquiferBasics/index.html*, accessed May 23, 2007)

TANC Database—SITES Table Data Dictionary

[The Sites table, which is joined to tables in the greater USGS NAWQA Data Warehouse *http://infotrek.er.usgs.gov/traverse/f?p=NAWQA:HOME:822423385428597*, accessed May 15, 2007, stores information on sites included in the TANC study]

STUDY_UNIT (USGS NAWQA Study Unit Code) Character; Width 4; **MANDATORY**
USGS NAWQA Program study unit code. Used in conjunction with SITE_ID to create multiple-field primary key

SITE_ID (Station ID) Character; Width 24; **MANDATORY**
USGS NWIS GWSI (National Water Information System, Ground Water Site Inventory System, *http://pubs.usgs.gov/of/2005/1251/*, accessed May 15, 2007) Site ID [*C1*]. If a 15-digit Site ID is not available for a retrospective data site, SITE_ID can be the utility's short ID or a shortened version of STATION_NM. Must be unique within a given study unit. SITE_IDs for retrospective data collected from different depths at a single location also must be unique, but may be similar except for an ending depth added to the end of the ID (for example, CPT1A_92.5; CPT1A_110). SITES_RMKS field can be used to identify such sites related by depth. Used with STUDY_UNIT to create multiple-field primary key

STATION_NM (Local Number or Name) Character; Width 50
Name for sampling location, such as common name for a well or name of a well field if aggregate samples for a well field are stored. Commonly will match Station Name *[C12]* in GWSI database. May be the same as SITE_ID if no other local number or name is used

TANC_STUDY (Tanc Study Identifier) Character; Width 12; **MANDATORY**
Used to associate sites with year Study Unit was incorporated into TANC and separate sites from different study areas within a single Study Unit (sanjtanc01, nvbrtanc01a, nvbrtanc01b). TANC_STUDY codes are only served to the end user from the TANC_Studies table

SUCODE (USGS NAWQA Study Unit Network Code) Character; Width 50
Four-digit study unit abbreviation concatenated to USGS NAWQA network code. Multiple codes are allowed and must be separated by commas

STATE (State) Character; Width 2
Two-character State code. Not numeric State code

LAT (Latitude of Sampling Location) Real; Width 10; Decimal 2
Same as USGS NWIS GWSI field *[C9]*. Units of degrees, minutes, decimal seconds, no spaces. Horizontal datum must be NAD83. Latitude should be considered essential

LAT_DECIMAL (Latitude in Decimal Degrees) Real; Width 10; Decimal 6

LONG (Longitude of Sampling Location) Real; Width 10; Decimal 2
Same as USGS NWIS GWSI field *[C10]*. Units of degrees, minutes, decimal seconds, no spaces. Datum must be NAD83. Longitude should be considered essential

LONG_DECIMAL (Longitude in Decimal Degrees) Real; Width 10; Decimal 6
Longitude should be negative

COOR_METH (Method Used to Determine Lat / Long) Character; Width 1
Same as USGS NWSI GWSI field Lat/Long Method code *[C35]*. Valid values include–but are not limited to–D, DGPS; G, GPS; M, map; S, survey; U, unknown

ALTITUDE (Altitude of Land Surface) Real; Width 10; Decimal, 2
Similar to USGS NWIS GWSI *[C16]*. Units in feet above NGVD 29. NULL value is –9999

ALTITUDE_METERS (Altitude of Land Surface, in Meters Above NGVD 29) Real; Width, 10; Decimal, 2
This is a calculated field (ALTITUDE multiplied by 0.3048)

STA_TYPE (TANC Station Type Code) Character; Width 2
Valid values include USGS NWIS QWDATA (National Water Information System, Water Quality System, *http://pubs.usgs.gov/of/2006/1145/* accessed May 15, 2007) Table 11 *Station Type codes* (GW, well; used to identify sites that are composed of a single well. AG, aggregate ground water; used to identify sites where water from multiple wells has been blended by a water supplier. ME, meteorological). An additional code that is not a valid value for the NWIS database has been added to the TANC database. Specifically, BH, bore hole; used to identify sites where samples are collected but a well is not established (for example, hydropunch site or core hole not completed as a well). The BH code is equivalent to the combined C802 and C002 (X; test hole) fields in the NWIS GWSI database. (Note that the code CH is NOT used to identify core holes; rather, core samples are associated with a GW or BH STA_TYPE code and coded in the Results_Rgnl Table [Medium = 'E'] independently of site information)

SITE_USE (Primary Use of Site Code) Character; Width 2
Valid values are the same as those for the USGS NWIS QWDATA *Primary Use of Site code* Table 12 (C, standby; O, observation; R, recharge; T, test; U, unused; W, withdrawal of water; Z, destroyed)

WEB_FLAG (TANC Flag for Proprietary Data) Character; Width 1
P is stored if data from the site are proprietary and not available for release. All public-supply well sites (TANC database Well_Info table WATER_USE codes CWS, NTNCWS, TNCWS, and WS) should have proprietary data flags to prevent the accidental disclosure of precise well location

SITES_RMKS (Relevant Information or Remarks) Character; Width 100

TANC Database—WELL_INFO Table Data Dictionary

[The Well_Info table, which is joined to tables in the greater USGS NAWQA Data Warehouse, stores information on wells included in the TANC study. Sites in this table have TANC database Sites table STA_TYPE codes of GW (finished wells), BH (considered to be unfinished wells), or AG (site represents combined wells). Null values are coded for BH and AG sites where Well_Info table fields are not applicable]

STUDY_UNIT (USGS NAWQA Study Unit Code) Character; Width 4; **MANDATORY**
STUDY_UNIT is only served to the end user from the TANC Sites table

SITE_ID (Station ID) Character; Width 24; **MANDATORY**
Site ID. Entry must be identical to the Sites table entry. SITE_ID is only served to the end user from the TANC Sites table

PRIN_AQFR (USGS NAWQA Principal Aquifer) Character; Width 45
Valid values include the *19 USGS NAWQA principal aquifers*. Blank if not a principal aquifer

AQFR_TYPE (Aquifer Type) Character; Width 1
Valid values are the same as the USGS NWIS GWSI (National Water Information System, Ground Water Site Inventory System, *http://pubs.usgs.gov/of/2005/1251/*, accessed May 15, 2007) Aquifer Type codes *[C713]*

CONS_DATE (Date of First Construction) Integer; Width 8
Dates should be entered as YYYYMMDD. NULL value is -9999

CSNG_MAT (Casing Material) Character; Width, 1
Valid values are the same as USGS NWIS GWSI Casing Material codes *[C80].*

CSNG_DIAM (Casing Diameter) Real; Width 8; Decimal 2
Diameter of well casing, in inches. If more than one casing diameter exists, the largest diameter is recorded. NULL value –9999 is stored if the diameter is unknown

CSNG_DIAM_CENTIMETERS (Casing Diameter, in Cm) Real; Width 8; Decimal 2
This is a calculated field (CSNG_DIAM multiplied by 2.54)

T_OPEN_BLS (Top of Uppermost Open Interval) Real; Width 8; Decimal 2
Depth to top of uppermost open section, in feet below land surface. NULL is –9999

T_OPEN_METERS_BLS (Top of Uppermost Open Interval, in Meters Below Land Surface) Real; Width 8; Decimal 2
This is a calculated field (T_OPEN_BLS multiplied by 0.3048)

B_OPEN_BLS (Bottom of Lowermost Open Interval) Real; Width 8; Decimal 2
Depth to bottom of lowermost open section, in feet below land surface. NULL is –9999

B_OPEN_METERS_BLS (Bottom of Lowermost Open Interval, in Meters Below Land Surface) Real; Width 8; Dec. 2
This is a calculated field (B_OPEN_BLS multiplied by 0.3048)

NUM_OPEN (Number of Open Intervals) Character; Width 3

TOT_LENGTH_OPEN (Total Length of All Open Intervals) Real; Width 8; Decimal 2
Combined length of all open intervals, in feet. NULL value is –9999

TOT_LENGTH_OPEN_METERS (Total Length of All Open Intervals, in Meters) Real; Width 8; Decimal 2
This is a calculated field (TOT_LENGTH_OPEN multiplied by 0.3048)

GEN_LITH (Generalized Lithology) Character; Width 4
Single USGS GWSI code *[C96]* to generalize lithology of combined open/sample intervals

WELL_DPTH_BLS (Well Depth) Real; Width 10; Decimal 2
Units in feet below land surface. USGS NWIS GWSI field *[C28]*. NULL value is –9999

WELL_DPTH_METERS_BLS (Well Depth, in Meters Below Land Surface) Real; Width 10; Decimal 2
This is a calculated field (WELL_DPTH_BLS multiplied by 0.3048)

CAPACITY (Rated Pump Capacity) Real; Width 8; Decimal 2
USGS NWIS GWSI Rated Pump Capacity, in gallons per minute *[C268]*. NULL is –9999

CAPACITY_LITERS_PER_MINUTE (Rated Pump Capacity, in Liters per Minute) Real; Width 8; Decimal 2
This is a calculated field (CAPACITY multiplied by 3.785)

WATER_USE (TANC Water Use Code) Character; Width 6
Valid values include USGS GWSI National Water Use codes *[C39]* (DO, domestic; IN, industrial, IR, irrigation; LV, livestock) and one GWSI Primary Use of Water code (U, unused). A couple of codes that are not NWIS valid values have been added to accommodate TANC-specific project needs. CWS, community water system—public water system that provides water to the same population year round. Note that a public water system is one that provides piped water for human consumption to at least 15 service connections or serves an average of 25 people for at least 60 days each year as defined by the USEPA's Public Drinking Water Systems Programs *http://www.epa.gov/safewater/pws/pwss.html#pwsinfo*, accessed August 20, 2005; NTNCWS, nontransient noncommunity water systems—public water systems that serve at least 25 of the same people at least 6 months of the year and include schools, factories, and hospitals; and TNCWS, transient noncommunity water systems—systems that cater to transitory customers in nonresidential areas (campgrounds, motels, and gas stations). NWIS code CO (commercial) is used if it is not known whether a noncommunity water system is an NTNCWS or a TNCWS. If no information can be found other than that the well is for water supply, WS is used

POP_SERVED (CWS, NTNCWS, & TNCWS Populations Served) Character; Width 2
Code used to further qualify Public Water Systems. Valid values include VS, very small <500 served; S, small 501–3,300; M, medium 3,301–10,000; L, large 10,001–100,000; VL, very large > 100,000

DRILLERS_LOG (Hyperlink to .pdf of Driller's Log) Hyperlink
Intended for wells drilled specifically for the TANC study

WELL_INFO_RMKS (Relevant Information or Remarks) Character; Width 100
Good place for a study unit to code whether a CWS is screened across a confining unit

TANC Database—RESULTS_RGNL Table Data Dictionary

[The Results_Rgnl table stores information on concentrations or measurements associated with TANC regional-scale investigations. Entries are restricted to USGS NWIS QWDATA (National Water Information System, Water Quality System, *http://pubs.usgs.gov/of/2006/1145/,* accessed May 16, 2007) *Sample Type codes* 9, regular, and H, composite]

R_ID (Results ID) Integer; Width 10
Automatic sequence number used to serve as primary key for the Results_Rgnl table

STUDY_UNIT (USGS NAWQA Study Unit Code) Character; Width 4; **MANDATORY**
STUDY_UNIT is only served to the end user from the TANC Sites table

SITE_ID (Station ID) Character; Width 24; **MANDATORY**
Site ID. Entry must be identical to the Sites table entry. SITE_ID is only served to the end user from the TANC Sites table

DATE (Sample Date) Integer; Width 8; **MANDATORY**
Dates should be entered as YYYYMMDD

PCODE (Used to Uniquely Identify Parameter) Character; Width 7; **MANDATORY**
Code used to uniquely identify parameter, typically 5 digits. Additional information on parameters for which data exist in the TANC database can be found in the Parameters table. Null value –9999 will NOT be used

PNAME (Short Name for Parameter) Character; Width 30; **MANDATORY**
Entry must be identical to PNAME in the Parameters table

RESULT (Concentration or Measurement Reported) Real; Width, autoformat
Only 1 RESULT per PCODE per DATE for a given STUDY_UNIT / SITE_ID / MEDIUM combination can be stored for a site

REMARK_CODE (Info about the Magnitude [or Absence] of a Value) Character; Width 1
Valid values are the same as those for the USGS *NWIS QWDATA Remarks Code* Table 10 (Result Level) field

UNITS (Units for RESULT) Character; Width 27
Required units for each PCODE are specified in the TANC Parameters table

AGENCY (Source of Data) Character; Width 50
Collecting agency from which RESULTs were procured (for example, Ohio EPA or Ohio Department of Health). Valid agency descriptions, not codes from the *NWIS QWDATA Collecting Agency* list, are used where applicable. Separate entries for PCODE 00027 will not be coded

RETRO (Flag to Identify Result as TANC Retro Data) Character; Width 1
'R' is stored if the RESULT is part of the TANC retrospective data compilation. A blank is stored if the RESULT is not part of the retro compilation

MEDIUM (Code for Sample Medium) Character; Width 1; **MANDATORY**
6 (ground water), 7 (wet deposition), E (core material), F (interstitial water), $ (treated water supply). These are USGS *NWIS QWDATA Medium* codes

BEGIN_DPTH_BLS (Sample Beginning Depth) Real; Width 8; Decimal 2
Depth to top of sampled interval, in feet below land surface. Generally equal to top of screened interval for ground-water samples from wells. NULL is –9999

BEGIN_DPTH_METERS_BLS (Sample Beginning Depth, in Meters Below Land Surface) Real; Width 8; Decimal 2
This is a calculated field (BEGIN_DPTH_BLS multiplied by 0.3048)

END_DPTH_BLS (Sample Ending Depth) Real; Width 8; Decimal 2
Depth to bottom of sampled interval, in feet below land surface. Generally equal to bottom of screened interval for ground-water samples from wells. NULL is –9999

END_DPTH_METERS_BLS (Sample Ending Depth, in Meters Below Land Surface) Real; Width 8; Decimal 2
This is a calculated field (END_DPTH_BLS multiplied by 0.3048)

FILTERED (Flag to Indicate if Sample was Filtered) Character; Width 1
Y, sample filtered; N, sample not filtered; blank if unknown or not applicable

ANAL_METH (Analytical Test Method Number) Character; Width 20
Valid values include USGS NWIS method codes, USEPA test method numbers *http://www.epa.gov/epahome/index/*, accessed May 15, 2007, *Standard Methods for Examination of Water and Wastewater numbers* (Cleseri and others, 1998), ASTM method numbers *http://enterprise.astm.org/filtrexx40.cgi?index.frm*, accessed May 15, 2007. Insert EPA or SM or ASTM in all caps followed by blank space before actual number

DET_LIMIT (Detection Limit) Real; Width, autoformat
The larger of the reported MDL—method detection limit—OR the MRL—minimum reporting limit—OR the LRL—laboratory reporting level—OR the PQL—practical quantitation limit. Units should match the required units for the PCODE in the TANC Parameters table

RESULTS_RMKS (Relevant Information or Remarks) Character; Width 100
Good place to note type of treatment for treated water-supply samples, if known. Additional laboratory data qualifiers also could be stored here

Reference Cited

Cleseri, L.S., Greenberg, A.E., and Eaton, A.D., eds., 1998, Standard methods for the examination of waste and wastewater (20th ed.): Washington, D.C., American Public Health Association, 1220 p.

TANC Database—PARAMETERS Table Data Dictionary

[The Parameters table includes information on parameters that are included in the TANC study]

PCODE (Parameter Code) Character; Width 7; **MANDATORY**
Code used to uniquely identify parameter, typically 5 digits. Generally follows usage of the USGS NWIS QWDATA (National Water Information System, Water Quality System, *http://pubs.usgs.gov/of/2006/1145/*, accessed May 15, 2007) database as of November, 2006. Several PCODEs from USEPA's STORET database *http://www.epa.gov/storpubl/legacy/ref_tables.htm*, accessed August 20, 2005, that are not valid values for NWIS are included in the TANC database to accommodate miscellaneous retrospective data obtained from outside sources. Valid values for parameters not in NWIS are coded in the TANC database as the STORET PCODE or the closest NWIS PCODE followed by a '.u' for unofficial (for example, 81853.u, Trichloroethane, wu). Primary key for the Parameters table

PNAME (Short Name for Parameter) Character; Width 30; **MANDATORY**
Generally the 'Short Name' used in the USGS NWIS database as of November, 2006

R_UNITS (Required Units for Parameter) Character; Width 27
All results for a given PCODE must be converted to these required units before data are entered into the TANC database Results_Rgnl table

L_PNAME (Long Name for Parameter) Character; Width 175
'Long Name' in the November, 2006 parameters file for use in NWIS. More descriptive than the previous NWIS 'Long Name'. Can be used to differentiate between similar parameters in NWIS

MCL (Maximum Contaminant Level) Real; Width, autoformat
The highest level of a contaminant that is allowed in drinking water *http://www.epa.gov/safewater/mcl.html*, accessed May 15, 2007. MCLs are set as close to Maximum Contaminant Level Goals (MCLGs) as feasible using the best available treatment technology and taking cost into consideration. MCLs are enforceable standards. MCLs in the TANC database are stored in the same units as those specified for the parameter in the R_UNITS field

CAS_NUM (Unique Identifier for a Chemical Substance) Character; Width 12
Chemical Abstracts Service's unique numeric identifier in the CAS Registry *http://www.cas.org/EO/regsys.html*, accessed May 15, 2007, for a chemical substance. Each CAS Registry Number designates only one substance and has no chemical significance. CAS numbers can be used to acquire information about chemical substances and will be useful for retrieving results for all PNAMEs associated with a particular substance regardless of PCODE. CAS numbers are not relevant for parameters unrelated to a chemical substance, such as Flow Rate

PARAMETERS_RMKS (Relevant Information or Remarks) Character; Width 100
Includes info on how PCODEs from outside sources are mapped to NWIS PCODEs, where relevant

TANC Database—PUMPING_RGNL Table Data Dictionary

[The Pumping_Rgnl table stores information about ALL pumping centers simulated in each of the TANC regional ground-water flow models, including pumping centers with no chemistry or contributing-area data stored in the database. This table enables the rest of the data in the database to be placed into a broader context with respect to pumping. It is a standalone table because, in many instances, different well identifiers were used in the models and in the Sites table]

TANC_STUDY (Tanc Study Identifier) Character; Width 12; **MANDATORY**
Used to associate sites with year Study Unit was incorporated into TANC and separate sites from different study areas within a single Study Unit (sanjtanc01, nvbrtanc01a, nvbrtanc01b).

WELL_ID (Well ID) Character; Width 24; **MANDATORY**
Unique well identifier used in the regional ground-water flow model

SITE_ID (Station ID) Character; Width 24
Site ID. Entry must be identical to the Sites table entry. Stored only for wells where the relationship between the WELL_ID and the SITE_ID in the Sites table is known. Some wells may exist within the Pumping_Rgnl table and the Sites table, but not contain a SITE_ID entry in the Pumping_Rgnl table because the relationship between the model WELL_ID and the SITE_ID cannot be readily determined

MFPUMP (Pumping Rate from Flow Model) Real; Width 8; Decimal 2
Representative pumping rate for the period of study (for example, 1997–2001 for most studies begun in 2001). Yield of well, in gallons per minute. Used to generate the contributing area data in the CAreaSum_Rgnl, CAreaRdxpH_Rgnl, and CAreaSrce_Rgnl tables. Value will be identical to the value in the RATE field of the Ancillary table where the simulated pumping center represents an individual well, as opposed to multiple wells. Additional information on the pumping rate can be found in the MFPUMP_REMARK field

MFPUMP_LITERS_PER_MINUTE (Pumping Rate from Flow Model, in Liters per Minute) Real; Width 8; Decimal 2
This is a calculated field (MFPUMP multiplied by 3.785)

MFPUMP_REMARK (Information Related to Pumping Rate from Flow Model) Char; Width 100
Additional information on the representative pumping rate in MFPUMP field. Must identify the period represented by the pumping rate. Should also record whether the MFPUMP entry represents the most recent pumping value for the stated period (if pumping was fairly constant) or some other representative value, such as the median

SOURCE (Source of Pumping Data) Character; Width 100
Source of the pumping data incorporated in the regional ground-water flow model

CWS (Flag to Indicate if a Well IS a Community Water Supply Well) Integer; Width 1
‘1’ is stored for wells that are community water-supply wells; ‘0’ is stored for other types of supply wells, such industrial wells or irrigation wells

T_OPEN_BLS (Top of Uppermost Open Interval) Real; Width 8; Decimal 2
Depth to top of uppermost open section/top of screened interval, in feet below land surface. NULL is –9999

T_OPEN_METERS_BLS (Top of Uppermost Open Interval, in Meters Below Land Surface) Real; Width 8; Decimal 2
This is a calculated field (T_OPEN_BLS multiplied by 0.3048)

B_OPEN_BLS (Bottom of Lowermost Open Interval) Real; Width 8; Decimal 2
Depth to bottom of lowermost open section/screened interval, in feet below land surface. NULL is -9999

B_OPEN_METERS_BLS (Bottom of Lowermost Open Interval, in Meters Below Land Surface) Real; Width 8; Decimal 2
This is a calculated field (B_OPEN_BLS multiplied by 0.3048)

SIMULATED_T_OPEN_BLS (Top of Uppermost Simulated Open Interval) Real; Width 8; Decimal 2
Depth to top of uppermost simulated open section/top of screened interval, in feet below land surface. NULL is –9999

SIMULATED_T_OPEN_METERS_BLS (Top of Uppermost Simulated Open Interval, in Meters Below Land Surface) Real; Width 8; Decimal 2
This is a calculated field (SIMULATED_T_OPEN_BLS multiplied by 0.3048)

SIMULATED_B_OPEN_BLS (Bottom of Lowermost Simulated Open Interval) Real; Width 8; Decimal 2
Depth to bottom of lowermost simulated open section/screened interval, in feet below land surface. NULL is –9999

SIMULATED_B_OPEN_METERS_BLS (Bottom of Lowermost Simulated Open Interval, in Meters Below Land Surface) Real; Width 8; Decimal 2
This is a calculated field (SIMULATED_B_OPEN_BLS multiplied by 0.3048)

MF_COL (Column in Modflow Model) Integer; Width 5

MF_ROW (Row in Modflow Model) Integer; Width 5

MF_TOP_LAYER (Model Layer that Corresponds to the Top of the Screened Interval) Integer; Width 2

MF_BOT_LAYER (Model Layer that Corresponds to the Bottom of the Screened Interval) Integer; Width 2

RANK_ALL (Percentile Rank of All Wells) Real; Width, Autoformat
Percentile rank of pumping within a given study unit based on ALL simulated pumping centers in the regional ground-water flow model

RANK_CWS (Percentile Rank of All Wells) Real; Width, Autoformat
Percentile rank of pumping within a given study unit based on simulated community water-supply wells in the regional ground-water flow model

PUMPNG_RGNL_RMKS (Relevant Information or Remarks) Character; Width 100

TANC Database—ANCILLARY Table Data Dictionary

[The Ancillary table, which is joined back to tables in the greater USGS NAWQA Data Warehouse, stores ancillary data used to assist the TANC study team]

STUDY_UNIT (USGS NAWQA Study Unit Code) Character; Width 4; **MANDATORY**
STUDY_UNIT is only served to the end user from the TANC Sites table

SITE_ID (Station ID) Character; Width 24; **MANDATORY**
Site ID. Entry must be identical to the Sites table entry. SITE_ID is only served to the end user from the TANC Sites table

SWQA (Flag to Indicate Selected Use of Site) Integer; Width 1
'1' is stored for sites sampled as part of the NAWQA Source Water-Quality Assessment (SWQA) study. '2' is stored for sites where samples similar to SWQA study samples ('SWQA-like' samples) were specifically collected for the TANC study. '0' is stored for sites where neither SWQA nor SWQA-like samples were collected for use by the TANC study team

RDX_SWQA (Code to Indicate Redox Signature) Character; Width 6
Code to describe SWQA sample in terms of redox indicators. 'O2' is stored when sample has a signature consistent with oxygen reducing; 'NO3', consistent with denitrifying; 'MN', consistent with manganese reducing; 'FEHSO4', consistent with iron reducing high sulfate; 'FELSO4', consistent with iron reducing low sulfate. 'X' (miXed) is stored when sample contains evidence of two or more redox states; 'R#' (Range) is stored when redox indicators are missing from sample and redox signature can't be narrowed beyond a given range; # holds the number of redox indicator species used to describe redox (for example, R3; Nitrate, ferrous iron, and sulfate data are available). 'I' (Indeterminate) is stored where appropriate data are available but are not consistent with any of the above categories. Blank is stored if data are insufficient to describe redox. The TANC redox-classification system is the foundation for assigning redox codes

RDX_SWQAQ (X and R Redox Signature Qualifier) Character; Width 30
Code to further qualify samples for which an X or R# code is stored in the RDX_SWQA field. Valid values include any combination of the following redox codes: O2, NO3, MN, FEHSO4, FELSO4 separated by '/'. A '?' will identify redox states that can't be ruled out due to lack of data (for example, O2?/NO3?/; O2 data are missing and NO3 is present above the significance level)

BAL_RETRO (Charge Balance Flag for Retro Data Sample) Integer; Width 1
'2' is stored for sites where the representative retro data sample balances electrochemically within 10 percent; '1' is stored if the sample is not balanced; and '0' is stored if a charge balance was not or could not be calculated

RDX_RETRO (Code to Indicate Redox Signature) Character; Width 6
Code to describe representative retro data sample for the site in terms of redox indicators. 'O2' is stored when sample has a signature consistent with oxygen reducing; 'NO3', consistent with denitrifying; 'MN', consistent with manganese reducing; 'FEHSO4', consistent with iron reducing high sulfate; 'FELSO4', consistent with iron reducing low sulfate. 'X' (miXed) is stored when sample contains evidence of two or more redox states; 'R#' (Range) is stored when redox indicators are missing from sample and redox signature can't be narrowed beyond a given range; # holds the number of redox indicator species used to describe redox (for example, R3; Nitrate, ferrous iron, and sulfate data are available). 'I' (Indeterminate) is stored where appropriate data are available but are not consistent with any of the above categories. Blank is stored if data are insufficient to describe redox. The TANC redox-classification system is the foundation for assigning redox codes

RDX_RETROQ (X and R Redox Signature Qualifier) Character; Width 30
Code to further qualify samples for which an X or R# code is stored in the RDX_RETRO field. Valid values include any combination of the following redox codes: O2, NO3, MN, FEHSO4, FELSO4 separated by '/'. A '?' will identify redox states that can't be ruled out due to lack of data (for example, O2?/NO3?/; O2 data are missing and NO3 is present above the significance level)

QW (Flag to Indicate if Site HAS Water Quality Data) Integer; Width 1
'1' is stored for sites with water-quality data in the database

SOLIDS (Flag to Indicate if Site HAS Solid Phase Data) Integer; Width 1
'1' is stored for sites with solid phase data

C_AREA (Flag to Indicate if Site HAS Simulated Contributing Area) Integer; Width 1
Flag to indicate if site has contributing area data in the TANC database modeling tables (CAreaSum_Rgnl, CAreaRdxpH_Rgnl, and CAreaSrce_Rgnl). '1' is stored where data in the modeling tables represent the individual site; '2' is stored where data in the modeling tables represent multiple sites, including the individual site, and occurs when contributing areas were computed using combined pumping from more than one well in the same model grid block due to a lack of well-by-well location information

INSIDE_MODEL (Flag to Indicate if Site is IN Modeled Area) Integer; Width 1
'1' is stored for sites WITHIN the boundary of the regional ground-water flow modeled area. '0' is stored if the site is NOT within the regional ground-water flow modeled area

RATE (Representative Pumping Rate) Real; Width 8; Decimal 2
Representative pumping rate for the selected period of study (for example, 1997–2001 for most studies begun in 2001). Yield of well, in gallons per minute. May be based on the most recent value for the period, if pumping was fairly constant, or can be a median. The key here is to store what is most representative for the well/study area and to note what was done in the RATE_REMARK field. Generally consistent with pumping rates simulated in the regional ground-water flow model. Value will be less than the rate simulated in the corresponding model when the simulated pumping rate represents combined pumping from multiple sites (i.e., C_AREA flag of '2')

RATE_LITERS_PER_MINUTE (Representative Pumping Rate) Real; Width 8; Decimal 2
This is a calculated field (RATE multiplied by 3.785)

RATE_REMARK (Information Related to Representative Pumping Rate) Char; Width 100
Additional information on the representative pumping rate stored in the RATE field. Must include the period of time represented by the pumping rate

LOCAL_NETWORK (Flag to Indicate if Site IS Part of a TANC Local-Scale Sampling Network) Integer; Width 1
'1' is stored for sites that are part of a TANC local-scale sampling network

TANC_ANCILLARY_RMKS (Relevant Information or Remarks) Char; Width 100
Good place to store info related to the retro redox determination

Reference Cited

Chapelle, F.H., 2001, Ground-water microbiology and geochemistry (2nd ed.): New York, John Wiley and Sons, Inc., p. 291.

TANC Database—CAREASUM_RGNL Table Data Dictionary

[The CAreaSum_Rgnl table stores information on supply-well contributing areas from TANC regional-scale investigations. All fields summarize steady-state contributing areas for discharging supply wells that were computed by use of regional ground-water flow models and pumping data stored in the Pumping_Rgnl table]

STUDY_UNIT (USGS NAWQA Study Unit Code) Character; Width 4; **MANDATORY**
STUDY_UNIT is only served to the end user from the TANC Sites table

SITE_ID (Station ID) Character; Width 24; **MANDATORY**
Site ID. Entry must be identical to the Sites table entry. *SITE_ID is only served to the end user from the TANC Sites table*

AREA_CONTRIBUTING_RECHARGE (Area Contributing Recharge, In Square Feet) Real; Width; autoformat
Steady state 'area contributing recharge' to the simulated discharging supply well, in square feet, computed using pumping data stored in the Pumping_Rgnl table. Follows usage of the USGS Office of Ground Water (OGW Technical Memorandum No. 2003.02 *http://water.usgs.gov/admin/memo/GW/auto.html*, accessed May 15, 2007) and is the surface area on the three-dimensional boundary of the ground-water system that delineates the location of the water entering the ground-water system that eventually flows to the well and discharges

AREA_CONTRIBUTING_RECHARGE_SQUARE_METERS (Area Contributing Recharge, In Square Meters) Real; Width; autoformat
This is a calculated field (AREA_CONTRIBUTING_RECHARGE multiplied by 0.0929)

ZOC_AREA (Area of Zone of Contribution, In Square Feet) Real; Width, autoformat
Steady state 'areal extent of the zone of contribution' to the simulated discharging supply well, in square feet, computed using pumping data stored in the Pumping_Rgnl table. Follows usage of the USGS Office of Ground Water and is the projection of the three-dimensional volume of water flowing to the discharging well to a two-dimensional map [see AREA_CONTRIBUTING_RECHARGE for reference]

ZOC_AREA_SQUARE_METERS (Area of Zone of Contribution, In Square Meters) Real; Width, autoformat
This is a calculated field (ZOC_AREA multiplied by 0.0929)

ZOC_VOLUME *(Volume of Zone of Contribution) Real; Width, autoformat*
Steady state 'zone of contribution' to the simulated discharging supply well, in cubic feet. Follows usage of the USGS Office of Ground Water and is the three-dimensional volumetric part of the aquifer through which ground water flows to the discharging well from the area contributing recharge [see AREA_CONTRIBUTING_RECHARGE for reference]

ZOC_VOLUME_CUBIC_METERS (Volume of Zone of Contribution, In Cubic Meters) Real; Width, autoformat
This is a calculated field (ZOC_VOLUME multiplied by 0.02832)

TOTINFLOW (Simulated Inflow to Supply Well, In Cubic Feet Per Second) Real; Width, autoformat
Flow to supply well computed from forward tracked particles, in cubic feet per second

TOTINFLOW_CUBIC_METERS_PER_SECOND (Simulated Inflow to Supply Well, In Cubic Meters Per Second) Real; Width, autoformat
This is a calculated field (TOTINFLOW multiplied by 0.02832)

TTMIN (Minimum Traveltime) Real; Width, autoformat
Minimum traveltime along simulated particle pathlines that define the zone of contribution to the supply well, in years

TTMAX (Maximum Traveltime) Real; Width, autoformat
Maximum traveltime along simulated particle pathlines that define the zone of contribution to the supply well, in years

TT_LT10YR_PCT (Percent of Well Inflow <10 Years) Real; Width, autoformat
Percentage of inflow to the supply well that has a simulated traveltime less than 10 years

TT_LT20YR_PCT (Percent of Well Inflow <20 Years) Real; Width, autoformat
Percentage of inflow to the supply well that has a simulated traveltime less than 20 years

TT_LT30YR_PCT (Percent of Well Inflow <30 Years) Real; Width, autoformat
Percentage of inflow to the supply well that has a simulated traveltime less than 30 years

TT_LT40YR_PCT (Percent of Well Inflow <40 Years) Real; Width, autoformat
Percentage of inflow to the supply well that has a simulated traveltime less than 40 years

TT_LT50YR_PCT (Percent of Well Inflow <50 Years) Real; Width, autoformat
Percentage of inflow to the supply well that has a simulated traveltime less than 50 years

TT_LT60YR_PCT (Percent of Well Inflow <60 Years) Real; Width, autoformat
Percentage of inflow to the supply well that has a simulated traveltime less than 60 years

TT_LT100YR_PCT (Percent of Well Inflow <100 Years) Real; Width, autoformat
Percentage of inflow to the supply well that has a simulated traveltime less than 100 years

TT_LT200YR_PCT (Percent of Well Inflow <200 Years) Real; Width, autoformat
Percentage of inflow to the supply well that has a simulated traveltime less than 200 years

TT_GTE200YR_PCT (Percent of Well Inflow >= 200 Years) Real; Width, autoformat
Percentage of inflow to the supply well that has a simulated traveltime equal to or greater than 200 years

TIME_10TH (10th Percentile Traveltime, In Years) Real; Width, autoformat
10th percentile of the traveltimes associated with the simulated particle pathlines that define the zone of contribution to the supply well, in years

TIME_25TH (25th Percentile Traveltime, In Years) Real; Width, autoformat
25th percentile of the traveltimes associated with the simulated particle pathlines that define the zone of contribution to the supply well, in years

TIME_50TH (Median Traveltime, In Years) Real; Width, autoformat
Median of the traveltimes associated with the simulated particle pathlines that define the zone of contribution to the supply well, in years

TIME_75TH (75th Percentile Traveltime, In Years) Real; Width, autoformat
75th percentile of the traveltimes associated with the simulated particle pathlines that define the zone of contribution to the supply well, in years

TIME_90TH (90th Percentile Traveltime, In Years) Real; Width, autoformat
90th percentile of the traveltimes associated with the simulated particle pathlines that define the zone of contribution to the supply well, in years

TIME_MEAN (Mean Traveltime, In Years) Real; Width, autoformat
Mean of the traveltimes associated with the simulated particle pathlines that define the zone of contribution to the supply well, in years

DISTANCE_10TH (10th Percentile Distance Traveled) Real; Width, autoformat
10th percentile of the length of the simulated particle pathlines that define the zone of contribution to the supply well, in miles

DISTANCE_10TH_KM (10th Percentile Distance Traveled, In Kilometers) Real; Width, autoformat
This is a calculated field (DISTANCE_10TH multiplied by 1.6093)

DISTANCE_25TH (25th Percentile Distance Traveled) Real; Width, autoformat
25th percentile of the length of the simulated particle pathlines that define the zone of contribution to the supply well, in miles

DISTANCE_25TH_KM (25th Percentile Distance Traveled, In Kilometers) Real; Width, autoformat
This is a calculated field (DISTANCE_25TH multiplied by 1.6093)

DISTANCE_50TH (Median Distance Traveled) Real; Width, autoformat
Median of the length of the simulated particle pathlines that define the zone of contribution to the supply well, in miles

DISTANCE_50TH_KM (Median Distance Traveled, In Kilometers) Real; Width, autoformat
This is a calculated field (DISTANCE_50TH multiplied by 1.6093)

DISTANCE_75TH (75th Percentile Distance Traveled) Real; Width, autoformat
75th percentile of the length of the simulated particle pathlines that define the zone of contribution to the supply well, in miles

DISTANCE_75TH_KM (75th Percentile Distance Traveled, In Kilometers) Real; Width, autoformat
This is a calculated field (DISTANCE_10TH multiplied by 1.6093)

DISTANCE_90TH (90th Percentile Distance Traveled) Real; Width, autoformat
90th percentile of the length of the simulated particle pathlines that define the zone of contribution to the supply well, in miles

DISTANCE_90TH_KM (90th Percentile Distance Traveled, In Kilometers) Real; Width, autoformat
This is a calculated field (DISTANCE_90TH multiplied by 1.6093)

DISTANCE_MEAN (Mean Distance Traveled) Real; Width, autoformat
Mean of the length of the simulated particle pathlines that define the zone of contribution to the supply well, in miles

DISTANCE_MEAN_KM (Mean Distance Traveled, In Kilometers) Real; Width, autoformat
This is a calculated field (DISTANCE_MEAN multiplied by 1.6093)

VELOCITY_10TH (10th Percentile Velocity) Real; Width, autoformat
10th percentile of the velocities for the simulated particle pathlines that define the zone of contribution to the supply well, in miles per year

VELOCITY_10TH_ KILOMETERS_PER_YEAR (10th Percentile Velocity, In Kilometers per Year) Real; Width, autoformat
This is a calculated field (VELOCITY_10TH multiplied by 1.6093)

VELOCITY_25TH (25th Percentile Velocity) Real; Width, autoformat
25th percentile of the velocities for the simulated particle pathlines that define the zone of contribution to the supply well, in miles per year

VELOCITY_25TH_ KILOMETERS_PER_YEAR (25th Percentile Velocity, In Kilometers per Year) Real; Width, autoformat
This is a calculated field (VELOCITY_25TH multiplied by 1.6093)

VELOCITY_50TH (Median Velocity) Real; Width, autoformat
Median of the velocities for the simulated particle pathlines that define the zone of contribution to the supply well, in miles per year

VELOCITY_50TH_ KILOMETERS_PER_YEAR (Median Velocity, In Kilometers per Year) Real; Width, autoformat
This is a calculated field (VELOCITY_50TH multiplied by 1.6093)

VELOCITY_75TH (75th Percentile Velocity) Real; Width, autoformat
75th percentile of the velocities for the simulated particle pathlines that define the zone of contribution to the supply well, in miles per year

VELOCITY_75TH_ KILOMETERS_PER_YEAR (75th Percentile Velocity, In Kilometers per Year) Real; Width, autoformat
This is a calculated field (VELOCITY_75TH multiplied by 1.6093)

VELOCITY_90TH (90th Percentile Velocity) Real; Width, autoformat
90th percentile of the velocities for the simulated particle pathlines that define the zone of contribution to the supply well, in miles per year

VELOCITY_90TH_ KILOMETERS_PER_YEAR (90th Percentile Velocity, In Kilometers per Year) Real; Width, autoformat
This is a calculated field (VELOCITY_90TH multiplied by 1.6093)

VELOCITY_MEAN (Mean Velocity) Real; Width, autoformat
Mean of the velocities for the simulated particle pathlines that define the zone of contribution to the supply well, in miles per year

VELOCITY_MEAN_ KILOMETERS_PER_YEAR (Mean Velocity, In Kilometers per Year) Real; Width, autoformat
This is a calculated field (VELOCITY_MEAN multiplied by 1.6093)

PERM (Permeability, In Inches/Hour) Real; Width, autoformat
Flow-weighted average permeability of the soil in the area contributing recharge to the supply well, in inches/hour. Values from STATSGO Soil Characteristics for the Conterminous United States *http://water.usgs.gov/lookup/getspatial?muid*, accessed August 20, 2005

PERM_CM_PER_HOUR (Permeability, In Centimeters/Hour) Real; Width, autoformat
This is a calculated field (PERM multiplied by 2.54)

AWC (Available Water Capacity) Real; Width, autoformat
Flow-weighted average available water capacity of the soil in the area contributing recharge to the supply well, in inches per inch [see PERM for data reference]

OM (Organic Material) Real; Width, autoformat
Flow-weighted average organic material in soil in the area contributing recharge to the supply well, in percent by weight [see PERM for data reference]

SAND (Percent Sand) Real; Width, autoformat
Flow-weighted average percent sand in soil in the area contributing recharge to the supply well [see PERM for data reference]

SILT (Percent Silt) Real; Width, autoformat
Flow-weighted average percent silt in soil in the area contributing recharge to the supply well [see PERM for data reference]

CLAY (Percent clay) Real; Width, autoformat
Flow-weighted average percent clay in soil in the area contributing recharge to the supply well [see PERM for data reference]

HDG_A (Percent Soil in Hydrologic Drainage Group A) Real; Width, autoformat
Flow-weighted average percent soil in hydrologic drainage group A in area contributing recharge to the supply well [see PERM for data reference]

HDG_AC (Percent Soil in Hydrologic Drainage Group AC) Real; Width, autoformat
Flow-weighted average percent soil in hydrologic drainage group AC in area contributing recharge to the supply well [see PERM for data reference]

HDG_AD (Percent Soil in Hydrologic Drainage Group AD) Real; Width, autoformat
Flow-weighted average percent soil in hydrologic drainage group AD in area contributing recharge to the supply well [see PERM for data reference]

HDG_B (Percent Soil in Hydrologic Drainage Group B) Real; Width, autoformat
Flow-weighted average percent soil in hydrologic drainage group B in area contributing recharge to the supply well [see PERM for data reference]

HDG_BC (Percent Soil in Hydrologic Drainage Group BC) Real; Width, autoformat
Flow-weighted average percent soil in hydrologic drainage group BC in area contributing recharge to the supply well [see PERM for data reference]

HDG_BD (Percent Soil in Hydrologic Drainage Group BD) Real; Width, autoformat
Flow-weighted average percent soil in hydrologic drainage group BD in area contributing recharge to the supply well [see PERM for data reference]

HDG_C (Percent Soil in Hydrologic Drainage Group C) Real; Width, autoformat
Flow-weighted average percent soil in hydrologic drainage group C in area contributing recharge to the supply well [see PERM for data reference]

HDG_CD (Percent Soil in Hydrologic Drainage Group CD) Real; Width, autoformat
Flow-weighted average percent soil in hydrologic drainage group CD in area contributing recharge to the supply well [see PERM for data reference]

HDG_D (Percent Soil in Hydrologic Drainage Group D) Real; Width, autoformat
Flow-weighted average percent soil in hydrologic drainage group D in area contributing recharge to the supply well [see PERM for data reference]

SAND_10TH (10th Percentile Traveltime Through Sand, In Years) Real; Width, autoformat
10th percentile of traveltimes through sand along simulated particle pathlines that define the zone of contribution to the supply well, in years. Based on discretized lithologies as defined by study unit modelers

SAND_25TH (25th Percentile Traveltime Through Sand, In Years) Real; Width, autoformat
25th percentile of traveltimes through sand along simulated particle pathlines that define the zone of contribution to the supply well, in years. Based on discretized lithologies as defined by study unit modelers

SAND_50TH (Median Traveltime Through Sand, In Years) Real; Width, autoformat
Median of traveltimes through sand along simulated particle pathlines that define the zone of contribution to the supply well, in years. Based on discretized lithologies as defined by study unit modelers

SAND_75TH (75th Percentile Traveltime Through Sand, In Years) Real; Width, autoformat
75th percentile of traveltimes through sand along simulated particle pathlines that define the zone of contribution to the supply well, in years. Based on discretized lithologies as defined by study unit modelers

SAND_90TH (90th Percentile Traveltime Through Sand, In Years) Real; Width, autoformat
90th percentile of traveltimes through sand along simulated particle pathlines that define the zone of contribution to the supply well, in years. Based on discretized lithologies as defined by study unit modelers

SAND_MEAN (Mean Traveltime Through Sand, In Years) Real; Width, autoformat
Mean of traveltimes through sand along simulated particle pathlines that define the zone of contribution to the supply well, in years. Based on discretized lithologies as defined by study unit modelers

SLITCLAY_10TH (10th Percentile Traveltime Through Clay, Silt, or Till, In Years) Real; Width, autoformat
10th percentile of traveltimes through clay, silt, or till along simulated particle pathlines that define the zone of contribution to the supply well, in years. Based on discretized lithologies as defined by study unit modelers

SILTCLAY _25TH (25th Percentile Traveltime Through Clay, Silt or Till, In Years) Real; Width, autoformat
25th percentile of traveltimes through clay, silt, or till along simulated particle pathlines that define the zone of contribution to the supply well, in years. Based on discretized lithologies as defined by study unit modelers

SILTCLAY _50TH (Median Traveltime Through Clay, Silt, or Till, In Years) Real; Width, autoformat
Median of traveltimes through clay, silt, or till along simulated particle pathlines that define the zone of contribution to the supply well, in years. Based on discretized lithologies as defined by study unit modelers

SILTCLAY _75TH (75th Percentile Traveltime Through Clay, Silt, or Till, In Years) Real; Width, autoformat
75th percentile of traveltimes through clay, silt, or till along simulated particle pathlines that define the zone of contribution to the supply well, in years. Based on discretized lithologies as defined by study unit modelers

SILTCLAY _90TH (90th Percentile Traveltime Through Clay, Silt, or Till, In Years) Real; Width, autoformat
90th percentile of traveltimes through clay, silt, or till along simulated particle pathlines that define the zone of contribution to the supply well, in years. Based on discretized lithologies as defined by study unit modelers

SILTCLAY _MEAN (Mean Traveltime Through Clay, Silt, or Till, In Years) Real; Width, autoformat
Mean of traveltimes through clay, silt, or till along simulated particle pathlines that define the zone of contribution to the supply well, in years. Based on discretized lithologies as defined by study unit modelers

CARBONATE_10TH (10th Percentile Traveltime Through Carbonate, In Years) Real; Width, autoformat
10th percentile of traveltimes through carbonate along simulated particle pathlines that define the zone of contribution to the supply well, in years. Based on discretized lithologies as defined by study unit modelers

CARBONATE _25TH (25th Percentile Traveltime Through Carbonate, In Years) Real; Width, autoformat
25th percentile of traveltimes through carbonate along simulated particle pathlines that define the zone of contribution to the supply well, in years. Based on discretized lithologies as defined by study unit modelers

CARBONATE _50TH (Median Traveltime Through Carbonate, In Years) Real; Width, autoformat
Median of traveltimes through carbonate along simulated particle pathlines that define the zone of contribution to the supply well, in years. Based on discretized lithologies as defined by study unit modelers

CARBONATE _75TH (75th Percentile Traveltime Through Carbonate, In Years) Real; Width, autoformat
75th percentile of traveltimes through carbonate along simulated particle pathlines that define the zone of contribution to the supply well, in years. Based on discretized lithologies as defined by study unit modelers

CARBONATE _90TH (90th Percentile Traveltime Through Carbonate, In Years) Real; Width, autoformat
90th percentile of traveltimes through carbonate along simulated particle pathlines that define the zone of contribution to the supply well, in years. Based on discretized lithologies as defined by study unit modelers

CARBONATE _MEAN (Mean Traveltime Through Carbonate, In Years) Real; Width, autoformat
Mean of traveltimes through carbonate along simulated particle pathlines that define the zone of contribution to the supply well, in years. Based on discretized lithologies as defined by study unit modelers

SEDIMENTARY_10TH (10th Percentile Traveltime Through Sedimentary, In Years) Real; Width, autoformat
10th percentile of traveltimes through sedimentary rock along simulated particle pathlines that define the zone of contribution to the supply well, in years. Based on discretized lithologies as defined by study unit modelers

SEDIMENTARY _25TH (25th Percentile Traveltime Through Sedimentary, In Years) Real; Width, autoformat
25th percentile of traveltimes through sedimentary rock along simulated particle pathlines that define the zone of contribution to the supply well, in years. Based on discretized lithologies as defined by study unit modelers

SEDIMENTARY _50TH (Median Traveltime Through Sedimentary, In Years) Real; Width, autoformat
Median of traveltimes through sedimentary rock along simulated particle pathlines that define the zone of contribution to the supply well, in years. Based on discretized lithologies as defined by study unit modelers

SEDIMENTARY _75TH (75th Percentile Traveltime Through Sedimentary, In Years) Real; Width, autoformat
75th percentile of traveltimes through sedimentary rock along simulated particle pathlines that define the zone of contribution to the supply well, in years. Based on discretized lithologies as defined by study unit modelers

SEDIMENTARY _90TH (90th Percentile Traveltime Through Sedimentary, In Years) Real; Width, autoformat
90th percentile of traveltimes through sedimentary rock along simulated particle pathlines that define the zone of contribution to the supply well, in years. Based on discretized lithologies as defined by study unit modelers

SEDIMENTARY _MEAN (Mean Traveltime Through Sedimentary, In Years) Real; Width, autoformat
Mean of traveltimes through sedimentary rock along simulated particle pathlines that define the zone of contribution to the supply well, in years. Based on discretized lithologies as defined by study unit modelers

CRYSTALLINE_10TH (10th Percentile Traveltime Through Crystalline, In Years) Real; Width, autoformat
10th percentile of traveltimes through crystalline rock along simulated particle pathlines that define the zone of contribution to the supply well, in years. Based on discretized lithologies as defined by study unit modelers

CRYSTALLINE _25TH (25th Percentile Traveltime Through Crystalline, In Years) Real; Width, autoformat
25th percentile of traveltimes through crystalline rock along simulated particle pathlines that define the zone of contribution to the supply well, in years. Based on discretized lithologies as defined by study unit modelers

CRYSTALLINE _50TH (Median Traveltime Through Crystalline, In Years) Real; Width, autoformat
Median of traveltimes through crystalline rock along simulated particle pathlines that define the zone of contribution to the supply well, in years. Based on discretized lithologies as defined by study unit modelers

CRYSTALLINE _75TH (75th Percentile Traveltime Through Crystalline, In Years) Real; Width, autoformat
75th percentile of traveltimes through crystalline rock along simulated particle pathlines that define the zone of contribution to the supply well, in years. Based on discretized lithologies as defined by study unit modelers

CRYSTALLINE _90TH (90th Percentile Traveltime Through Crystalline, In Years) Real; Width, autoformat
90th percentile of traveltimes through crystalline rock along simulated particle pathlines that define the zone of contribution to the supply well, in years. Based on discretized lithologies as defined by study unit modelers

CRYSTALLINE _MEAN (Mean Traveltime Through Crystalline, In Years) Real; Width, autoformat
Mean of traveltimes through crystalline rock along simulated particle pathlines that define the zone of contribution to the supply well, in years. Based on discretized lithologies as defined by study unit modelers

TANC Database—CAREARDXPH_RGNL Table Data Dictionary

[The CAreaRdxpH_Rgnl table stores information on redox and pH conditions within supply well contributing areas from TANC regional-scale investigations. All fields describe the steady state 'zone of contribution' for discharging supply wells that were computed by use of regional ground-water flow models and pumping data stored in the Pumping_Rgnl table]

STUDY_UNIT (USGS NAWQA Study Unit Code) Character; Width 4; **MANDATORY**
STUDY_UNIT is only served to the end user from the TANC Sites table

SITE_ID (Station ID) Character; Width 24; **MANDATORY**
Site ID. Entry must be identical to the Sites table entry. SITE_ID is only served to the end user from the TANC Sites table

PCT_RDXUNK (Percentage of Water Entering Well from Unknown Redox Zone) Real; Width, autoformat
Percentage of simulated inflow to the supply well from areas defined by study unit modelers as having unknown redox conditions

PCT_O2NO3 (Percentage of Water Entering Well from O2NO3 Redox Zone) Real; Width, autoformat
Percentage of simulated inflow to the supply well from areas defined by study unit modelers as having O_2- or NO_3-reducing redox conditions

PCT_FESO4 (Percentage of Water Entering Well from FESO4 Redox Zone) Real; Width, autoformat
Percentage of simulated inflow to the supply well from areas defined by study unit modelers as having Mn-, Fe- or SO_4-reducing redox conditions

MAX_O2NO3 (Maximum Traveltime for a Particle Through O2NO3 Redox Zone, In Years) Real; Width, autoformat
Maximum time that any particle travels through areas defined by study unit modelers as having O_2- or NO_3-reducing conditions, in years

MAX_FESO4 (Maximum Traveltime for a Particle Through FESO4 Redox Zone, In Years) Real; Width, autoformat
Maximum time that any particle travels through areas defined by study unit modelers as having Mn-, Fe- or SO_4-reducing conditions, in years

FESO4_GT200_PCT (Percentage of Water That Spent Greater Than 200 Years in FESO4 Redox Zone) Real; Width, autoformat
Percentage of water that discharges to the supply well that is estimated to have spent greater than 200 years in areas defined by study unit modelers as having Mn-, Fe- or SO_4-reducing conditions

ZOC_O2NO3_PCT (Percentage of Zone of Contribution That Is In O2NO3 Redox Zone) Real; Width, autoformat
Percentage of zone of contribution that is associated with areas defined by study unit modelers as having O_2- or NO_3-reducing redox conditions

ZOC_FESO4_PCT (Percentage of Zone of Contribution That Is In FESO4 Redox Zone) Real; Width, autoformat
Percentage of zone of contribution that is associated with areas defined by study unit modelers as having Mn-, Fe- or SO_4-reducing redox conditions

TT_RDXUNK_PCT (Percentage of Total Traveltime Spent in Unknown Redox Zone) Real; Width, autoformat
Percentage of total traveltime associated with unknown redox zones

TT_O2NO3_PCT (Percentage of Total Traveltime Spent in O2NO3 Redox Zone) Real; Width, autoformat
Percentage of total traveltime associated with O_2- or NO_3-reducing redox conditions. Computed as O_2NO_3_MEAN/TIME_MEAN*100. O2NO3_MEAN is defined in this table (CAreaRdxpH_Rgnl); TIME_MEAN is defined in the TANC database CAreaSum_Rgnl table

TT_FESO4_PCT (Percentage of Total Traveltime Spent in FESO4 Redox Zone) Real; Width, autoformat
Percentage of total traveltime associated with Mn-, Fe- or SO_4-reducing redox conditions. Computed as FESO4_MEAN/TIME_MEAN*100. FESO4_MEAN is defined in this table (CAreaRdxpH_Rgnl); TIME_MEAN is defined in the TANC database CAreaSum_Rgnl table

O2NO3_10TH (10th Percentile Traveltime Through O2NO3 Zone, In Years) Real; Width, autoformat
10th percentile of the traveltimes through areas defined by study unit modelers as having O_2- or NO_3-reducing conditions along simulated particle pathlines that define the zone of contribution to the supply well, in years

O2NO3_25TH (25th Percentile Traveltime Through O2NO3 Zone, In Years) Real; Width, autoformat
25th percentile of the traveltimes through areas defined by study unit modelers as having O_2- or NO_3-reducing conditions along simulated particle pathlines that define the zone of contribution to the supply well, in years

O2NO3_50TH (Median Traveltime Through O2NO3 Zone, In Years) Real; Width, autoformat
Median of the traveltimes through areas defined by study unit modelers as having O_2- or NO_3-reducing conditions along simulated particle pathlines that define the zone of contribution to the supply well, in years

O2NO3_75TH (75th Percentile Traveltime Through O2NO3 Zone, In Years) Real; Width, autoformat
75th percentile of the traveltimes through areas defined by study unit modelers as having O_2- or NO_3-reducing conditions along simulated particle pathlines that define the zone of contribution to the supply well, in years

O2NO3_90TH (90th Percentile Traveltime Through O2NO3 Zone, In Years) Real; Width, autoformat
90th percentile of the traveltimes through areas defined by study unit modelers as having O_2- or NO_3-reducing conditions along simulated particle pathlines that define the zone of contribution to the supply well, in years

O2NO3_MEAN (Mean Traveltime Through O2NO3 Zone, In Years) Real; Width, autoformat
Mean of the traveltimes through areas defined by study unit modelers as having O_2- or NO_3-reducing conditions along simulated particle pathlines that define the zone of contribution to the supply well, in years

FESO4_10TH (10th Percentile Traveltime Through FESO4 Zone, In Years) Real; Width, autoformat
10th percentile of the traveltimes through areas defined by study unit modelers as having Mn-, Fe- or SO_4-reducing conditions along simulated particle pathlines that define the zone of contribution to the supply well, in years

FESO4_25TH (25th Percentile Traveltime Through FESO4 Zone, In Years) Real; Width, autoformat
25th percentile of the traveltimes through areas defined by study unit modelers as having Mn-, Fe- or SO_4-reducing conditions along simulated particle pathlines that define the zone of contribution to the supply well, in years

FESO4_50TH (Median Traveltime Through FESO4 Zone, In Years) Real; Width, autoformat
Median of the traveltimes through areas defined by study unit modelers as having Mn-, Fe- or SO_4-reducing conditions along simulated particle pathlines that define the zone of contribution to the supply well, in years

FESO4_75TH (75th Percentile Traveltime Through FESO4 Zone, In Years) Real; Width, autoformat
75th percentile of the traveltimes through areas defined by study unit modelers as having Mn-, Fe- or SO_4-reducing conditions along simulated particle pathlines that define the zone of contribution to the supply well, in years

FESO4_90TH (90th Percentile Traveltime Through FESO4 Zone, In Years) Real; Width, autoformat
90th percentile of the traveltimes through areas defined by study unit modelers as having Mn-, Fe- or SO_4-reducing conditions along simulated particle pathlines that define the zone of contribution to the supply well, in years

FESO4_MEAN (Mean Traveltime Through FESO4 Zone, In Years) Real; Width, autoformat
Mean of the traveltimes through areas defined by study unit modelers as having Mn-, Fe- or SO_4-reducing conditions along simulated particle pathlines that define the zone of contribution to the supply well, in years

PH_GT8_10TH (10th Percentile Traveltime Through pH>8 Zone, In Years) Real; Width, autoformat
10th percentile of the traveltimes through areas defined by study unit modelers as having pH greater than 8 along simulated particle pathlines that define the zone of contribution to the supply well, in years

PH_GT8_25TH (25th Percentile Traveltime Through pH>8 Zone, In Years) Real; Width, autoformat
25th percentile of the traveltimes through areas defined by study unit modelers as having pH greater than 8 along simulated particle pathlines that define the zone of contribution to the supply well, in years

PH_GT8_50TH (Median Traveltime Through pH>8 Zone, In Years) Real; Width, autoformat
Median of the traveltimes through areas defined by study unit modelers as having pH greater than 8 along simulated particle pathlines that define the zone of contribution to the supply well, in years

PH_GT8_75TH (75th Percentile Traveltime Through pH>8 Zone, In Years) Real; Width, autoformat
75th percentile of the traveltimes through areas defined by study unit modelers as having pH greater than 8 along simulated particle pathlines that define the zone of contribution to the supply well, in years

PH_GT8_90TH (90th Percentile Traveltime Through pH>8 Zone, In Years) Real; Width, autoformat
90th percentile of the traveltimes through areas defined by study unit modelers as having pH greater than 8 along simulated particle pathlines that define the zone of contribution to the supply well, in years

PH_GT8_MEAN (Mean Traveltime Through pH>8 Zone, In Years) Real; Width, autoformat
Mean of the traveltimes through areas defined by study unit modelers as having pH greater than 8 along simulated particle pathlines that define the zone of contribution to the supply well, in years

TANC Database—CAREASRCE_RGNL Table Data Dictionary

[The CAreaSrce_Rgnl table stores information on potential contaminant sources within supply-well contributing areas from TANC regional-scale investigations. All fields describe the steady state 'area contributing recharge' for discharging supply wells that were computed by use of regional ground-water flow models and pumping data stored in the Pumping_Rgnl table]

STUDY_UNIT (USGS NAWQA Study Unit Code) Character; Width 4; **MANDATORY**
STUDY_UNIT is only served to the end user from the TANC Sites table

SITE_ID (Station ID) Character; Width 24; **MANDATORY**
Site ID. Entry must be identical to the Sites table entry. *SITE_ID is only served to the end user from the TANC Sites table*

AREAL_RECHARGE (Percentage of Well Inflow from Areal Recharge) Real; Width, autoformat
Percentage of simulated inflow to the supply well from simulated areal recharge

SW_LEAKAGE (Percentage of Well Inflow from Surface Water Leakage) Real; Width, autoformat
Percentage of simulated inflow to the supply well from simulated surface-water features

MF_RECHARGE (Percentage of Well Inflow from Mountain Front Recharge) Real; Width, autoformat
Percentage of simulated inflow to the supply well from simulated mountain-front recharge

REG_INFLOW (Percentage of Well Inflow from Regional Inflow) Real; Width, autoformat
Percentage of simulated inflow to the supply well from lateral boundaries of the simulated aquifer

URBAN (Percentage of Well Inflow from Urban Areas) Real; Width, autoformat
Percentage of simulated inflow to the supply well from urban areas based on the enhanced National Land Cover Data (NLCDE), which is the National Land Cover Data (NLCD) for the period 1990-1995 enhanced with historical land use and land cover (GIRAS) data for the period 1970-1985 where problems with attribute miscoding and data coverage at quadrangle boundaries existed in the original NLCD *http://pubs.usgs.gov/ds/2006/240/#proc*, accessed August 20, 2005

AGRICULTURE (Percentage of Well Inflow from Agricultural Areas) Real; Width, autoformat
Percentage of simulated inflow to the supply well from areas that were agricultural in the early 1990's based on the enhanced National Land Cover Data (NLCDE) [see URBAN for a more complete data reference]

FOREST (Percentage of Well Inflow from Forested Areas) Real; Width, autoformat
Percentage of simulated inflow to the supply well from areas that were forested in the early 1990's based on the enhanced National Land Cover Data (NLCDE) [see URBAN for a more complete data reference]

RANGELAND (Percentage of Well Inflow from Rangeland/Shrubland Areas) Real; Width, autoformat
Percentage of simulated inflow to the supply well from areas that were rangeland/shrubland in the early 1990's based on the enhanced National Land Cover Data (NLCDE) [see URBAN for a more complete data reference]

BARREN (Percentage of Well Inflow from Barren Areas) Real; Width, autoformat
Percentage of simulated inflow to the supply well from areas that were barren in the early 1990's based on the enhanced National Land Cover Data (NLCDE) [see URBAN for a more complete data reference]

WETLAND (Percentage of Well Inflow from Wetland Areas) Real; Width, autoformat
Percentage of simulated inflow to the supply well from areas that were wetlands in the early 1990's based on the enhanced National Land Cover Data (NLCDE) [see URBAN for a more complete data reference]

WATER (Percentage of Well Inflow from Water Areas) Real; Width, autoformat
Percentage of simulated inflow to the supply well from areas that were water in the early 1990's based on the enhanced National Land Cover Data (NLCDE) [see URBAN for a more complete data reference]

URB_RES (Percentage of Well Inflow from Urban Residential Areas) Real; Width, autoformat
Percentage of simulated inflow to the supply well from areas that were urban residential in the early 1990's based on the enhanced National Land Cover Data (NLCDE). This is a subdivision of the URBAN field [see URBAN for a more complete data reference]

URB_COMIND (Percentage of Well Inflow from Urban Commercial/Industrial Areas) Real; Width, autoformat
Percentage of simulated inflow to the supply well from areas that were urban commercial/industrial in the early 1990's based on the enhanced National Land Cover Data (NLCDE). This is a subdivision of the URBAN field [see URBAN for a more complete data reference]

PERSONS2000 (People in Contributing Area from 2000 Census) Real; Width, autoformat
Estimated number of people in the contributing area from the 2000 census data based on the percentage of the census block within the simulated area contributing recharge. Census data obtained by the USGS NAWQA Program from *http://www.esri.com/data/download/census2000_tigerline/index.html*, accessed August 20, 2005

A_PERSONS2000 (People in Contributing Area from 2000 Census Adjusted by Urban Areas) Real; Width, autoformat
Estimated number of people in the contributing area from the 2000 census data based on the percentage of urban area within the census block in the simulated area contributing recharge. Census data obtained by the USGS NAWQA Program from *http://www.esri.com/data/download/census2000_tigerline/index.html*, accessed August 20, 2005; urban land use data from the NLCDE *http://landcover.usgs.gov/* , accessed August 20, 2005

HOUSES2000 (Houses in Contributing Area from 2000 Census) Real; Width, autoformat
Estimated number of houses in the contributing area from the 2000 census data based on the percentage of the census block within the simulated area contributing recharge [see PERSONS2000 for data reference]

A_HOUSES2000 (Houses in Contributing Area from 2000 Census Adjusted by Urban Areas) Real; Width, autoformat
Estimated number of houses in the contributing area from the 2000 census data based on the percentage of urban area within the census block in the simulated area contributing recharge [see A_PERSONS2000 for data reference]

PERSONS1990 (People in Contributing Area from 1990 Census) Real; Width, autoformat
Estimated number of people in the contributing area from the 1990 census data based on the percentage of the census block within the simulated area contributing recharge [see PERSONS2000 for data reference]

A_PERSONS1990 (People in Contributing Area from 1990 Census Adjusted by Urban Areas) Real; Width, autoformat
Estimated number of people in the contributing area from the 1990 census data based on the percentage of urban area within the census block in the simulated area contributing recharge [see A_PERSONS2000 for data reference]

HOUSES1990 (Houses in Contributing Area from 1990 Census) Real; Width, autoformat
Estimated number of houses in the contributing area from the 1990 census data based on the percentage of the census block within the simulated area contributing recharge [see PERSONS2000 for data reference]

A_HOUSES1990 (Houses in Contributing Area from 1990 Census Adjusted by Urban Areas) Real; Width, autoformat
Estimated number of houses in the contributing area from the 1990 census data based on the percentage of urban area within the census block in the simulated area contributing recharge [see A_PERSONS2000 for data reference]

PRVWAT1990 (Houses Served By Private Well in Contributing Area from 1990 Census) Real; Width, autoformat
Estimated number of houses served by a private well in the contributing area from the 1990 census data based on the percentage of the census block within the simulated area contributing recharge [see PERSONS2000 for data reference]

A_PRVWAT1990 (Houses Served By Private Well in Contributing Area from 1990 Census Adjusted by Urban Area) Real; Width, autoformat
Estimated number of houses served by a private well in the contributing area from the 1990 census data based on the percentage of urban area within the census block in the simulated area contributing recharge [see A_PERSONS2000 for data reference]

PRVSEW1990 (Houses Served By Private Sewer in Contributing Area from 1990 Census) Real; Width, autoformat
Estimated number of houses served by a private sewer in the contributing area from the 1990 census data based on the percentage of the census block within the simulated area contributing recharge [see PERSONS2000 for data reference]

A_PRVSEW1990 (Houses Served By Private Sewer in Contributing Area from 1990 Census Adjusted by Urban Area) Real; Width, autoformat
Estimated number of houses served by a private sewer in the contributing area from the 1990 census data based on the percentage of urban area within the census block in the simulated area contributing recharge [see A_PERSONS2000 for data reference]

BLT_B70 (Houses Built Before 1970) Real; Width, autoformat
Estimated number of houses built before 1970 in the contributing area from the 1990 census data based on the percentage of the census block within the simulated area contributing recharge [see PERSONS2000 for data reference]

A_ BLT_B70 (Houses Built Before 1970 Adjusted by Urban Areas) Real; Width, autoformat
Estimated number of houses built before 1970 in the contributing area from the 1990 census data based on the percentage of urban area within the census block in the simulated area contributing recharge [see A_PERSONS2000 for data reference]

BLT_7079 (Houses Built Between 1970 and 1979) Real; Width, autoformat
Estimated number of houses built between 1970 and 1979 in the contributing area from the 1990 census data based on the percentage of the census block within the simulated area contributing recharge [see PERSONS2000 for data reference]

A_ BLT_7079 (Houses Built Between 1970 and 1979 Adjusted by Urban Areas) Real; Width, autoformat
Estimated number of houses built between 1970 and 1979 in the contributing area from the 1990 census data based on the percentage of urban area within the census block in the simulated area contributing recharge [see A_PERSONS2000 for data reference]

BLT_8084 (Houses Built Between 1980 and 1984) Real; Width, autoformat
Estimated number of houses built between 1980 and 1984 in the contributing area from the 1990 census data based on the percentage of the census block within the simulated area contributing recharge [see PERSONS2000 for data reference]

A_ BLT_8084 (Houses Built Between 1980 and 1984 Adjusted by Urban Areas) Real; Width, autoformat
Estimated number of houses built between 1980 and 1984 in the contributing area from the 1990 census data based on the percentage of urban area within the census block in the simulated area contributing recharge [see A_PERSONS2000 for data reference]

BLT_8589 (Houses Built Between 1985 and 1989) Real; Width, autoformat
Estimated number of houses built between 1985 and 1989 in the contributing area from the 1990 census data based on the percentage of the census block within the simulated area contributing recharge [see PERSONS2000 for data reference]

A_BLT_8589 (Houses Built Between 1985 and 1989 Adjusted by Urban Areas) Real; Width, autoformat
Estimated number of houses built between 1985 and 1989 in the contributing area from the 1990 census data based on the percentage of urban area within the census block in the simulated area contributing recharge [see A_PERSONS2000 for data reference]

BLT_9099 (Houses Built Between 1990 and 1999) Real; Width, autoformat
Estimated number of houses built between 1990 and 1999 in the contributing area based on the percentage of the census block within the simulated area contributing recharge; difference between the 2000 and 1990 censuses [see PERSONS2000 for data reference]. Changes in census block boundaries between 1990 and 2000 may affect results [for example, negative values could result from changes in census block boundaries, or they could indicate that houses were vacated or destroyed]

A_BLT_9099 (Houses Built Between 1990 and 1999 Adjusted by Urban Areas) Real; Width, autoformat
Estimated number of houses built between 1990 and 1999 in the contributing area based on the percentage of urban area within the census block in the simulated area contributing recharge; difference between the 2000 and 1990 censuses [see A_PERSONS2000 for data reference]. Changes in census block boundaries between 1990 and 2000 may affect results [for example, negative values could result from changes in census block boundaries, or they could indicate that houses were vacated or destroyed]

ROADLENGTH (Length of Roads) Real; Width, autoformat
Total length of roads in the area contributing recharge, in feet. Data obtained by the USGS NAWQA Program from *http://www.esri.com/data/download/census2000_tigerline/index.html*, accessed August 20, 2005

ROADLENGTH_METERS (Length of Roads, In Meters) Real; Width, autoformat
This is a calculated field (ROADLENGTH multiplied by 0.3048)

TANKS_ALL (Underground Storage Tanks) Real; Width, autoformat
Number of underground storage tanks (gas stations, dry cleaners, unknown; leaking and not known to be leaking) in the area contributing recharge. Underground storage tank data are from Vista Information Solutions, Inc., San Diego, CA, and were retrieved by the USGS NAWQA Program by using the proprietary Starview 2.5.1 software and the June 1998 database. For tanks that did not have good location data, a probability that the tank would be in the contributing area was computed and then added to the number of tanks in the contributing area with more certain locations. Probabilities were computed by buffering the tank location in question with the radius of uncertainty provided in the dataset, overlaying the buffer on the simulated area contributing recharge, and dividing the area represented by the overlap of the buffer and contributing area by the total area of the buffer

TANKS_LEAKING_GAS (Leaking Underground Storage Tanks at Gas Stations) Real; Width, autoformat
Number of leaking underground storage tanks at gas stations in the area contributing recharge. Underground storage tank data are from Vista Information Solutions, Inc. For tanks that did not have good location data, a probability that the tank would be in the contributing area was computed and then added to the number of tanks in the contributing area with more certain locations [see TANKS_ALL for a more complete description and data reference]

TANKS_LEAKING_DRYCLEANER (Leaking Underground Storage Tanks at Dry Cleaners) Real; Width, autoformat
Number of leaking underground storage tanks at dry cleaners in the area contributing recharge. Underground storage tank data are from Vista Information Solutions, Inc. For tanks that did not have good location data, a probability that the tank would be in the contributing area was computed and then added to the number of tanks in the contributing area with more certain locations [see TANKS_ALL for a more complete description and data reference]

TANKS_LEAKING_UNKNOWN (Leaking Underground Storage Tanks at Unknown Facilities) Real; Width, autoformat
Number of leaking underground storage tanks in the area contributing recharge at facilities that are not known to be gas stations or dry cleaners. Underground storage tank data are from Vista Information Solutions, Inc. For tanks that did not have good location data, a probability that the tank would be in the contributing area was computed and then added to the number of tanks in the contributing area with more certain locations [see TANKS_ALL for a more complete description and data reference]

TANKS_UNDERGROUND_GAS (Underground Storage Tanks at Gas Stations not Known to be Leaking) Real; Width, autoformat
Number of underground storage tanks at gas stations in the area contributing recharge that are not known to be leaking. Underground storage tank data are from Vista Information Solutions, Inc. For tanks that did not have good location data, a probability that the tank would be in the contributing area was computed and then added to the number of tanks in the contributing area with more certain locations [see TANKS_ALL for a more complete description and data reference]

TANKS_UNDERGROUND_DRYCLEANER (Underground Storage Tanks at Dry Cleaners not Known to be Leaking) Real; Width, autoformat
Number of underground storage tanks at dry cleaners in the area contributing recharge that are not known to be leaking. Underground storage tank data are from Vista Information Solutions, Inc. For tanks that did not have good location data, a probability that the tank would be in the contributing area was computed and then added to the number of tanks in the contributing area with more certain locations [see TANKS_ALL for a more complete description and data reference]

TANKS_UNDERGROUND_UNKNOWN (Underground Storage Tanks at Unknown Facilities not Known to be Leaking) Real; Width, autoformat

Number of underground storage tanks in the area contributing recharge that are not known to be leaking at facilities that are not known to be gas stations or dry cleaners. Underground storage tank data are from Vista Information Solutions, Inc. For tanks that did not have good location data, a probability that the tank would be in the contributing area was computed and then added to the number of tanks in the contributing area with more certain locations [see TANKS_ALL for a more complete description and data reference]

FERTILIZER (Nitrogen in Fertilizer Applied) Real; Width, autoformat

Estimated amount of nitrogen in fertilizer applied to the area contributing recharge, in kilograms. Average based on 1990 through 1998 annual State- and county-level information on the tonnage of fertilizer product sales obtained by the USGS NAWQA Program from the Association of American Plant Food Control Officials (AAPFCO), University of Kentucky

MANURE (Nitrogen in Manure Applied) Real; Width, autoformat

Estimated amount of nitrogen in manure applied to the area contributing recharge, in kilograms. Average based on 1992 and 1997 animal populations *http://water.usgs.gov/lookup/getspatial?manure*, accessed May 15, 2007

Paschke, Suzzane S., ed.—**Hydrogeologic Settings and Ground-Water Flow Simulations for Regional Studies of the Transport of Anthropogenic and Natural Contaminants to Public-Supply Wells—Studies Begun in 2001**—Professional Paper 1737–A